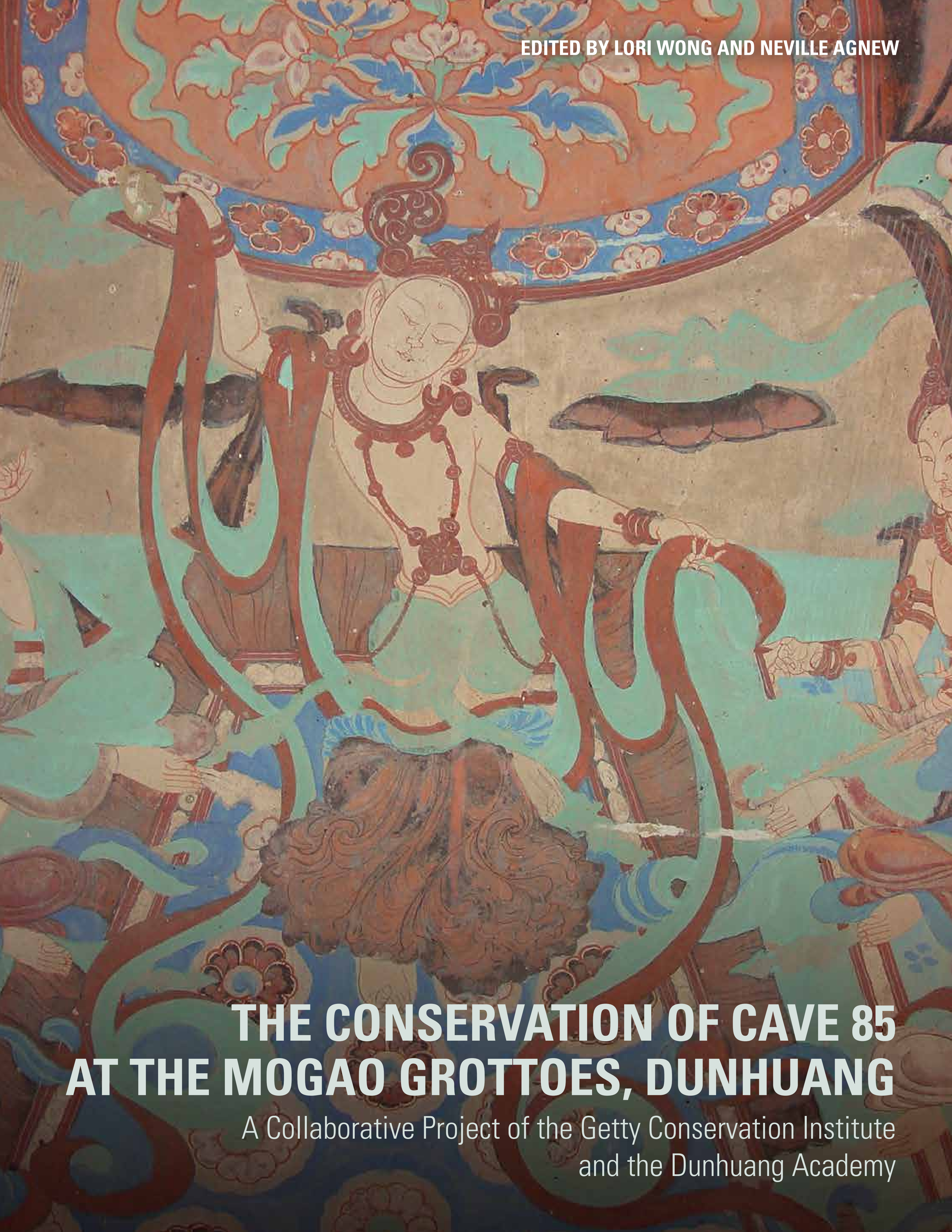

EDITED BY LORI WONG AND NEVILLE AGNEW

THE CONSERVATION OF CAVE 85 AT THE MOGAO GROTTOES, DUNHUANG

A Collaborative Project of the Getty Conservation Institute and the Dunhuang Academy

THE CONSERVATION OF CAVE 85 AT THE MOGAO GROTTOES, DUNHUANG

A Collaborative Project of the Getty Conservation Institute and the Dunhuang Academy

Panorama of the site showing the desert landscape and the grottoes in the distance.

The Getty Conservation Institute
Timothy P. Whalen, Director
Jeanne Marie Teutonico, Associate Director, Programs

The Getty Conservation Institute works to advance conservation practice in the visual arts, broadly interpreted to include objects, collections, architecture, and sites. It serves the conservation community through scientific research, education and training, model field projects, and the broad dissemination of the results of both its own work and the work of others in the field. And in all its endeavors, it focuses on the creation and dissemination of knowledge that will benefit professionals and organizations responsible for the conservation of the world's cultural heritage.

Published by the Getty Conservation Institute

Getty Publications
1200 Getty Center Drive, Suite 500
Los Angeles, California 90049-1682
www.gettypublications.org

Tevvy Ball, Project Editor
Catherine Lorenz, Designer
Suzanne Watson, Production Coordinator

Front cover: Detail of a wall painting depicting a dancer, on the south wall of Cave 85. Late Tang Dynasty.
Back cover: A view of the main chamber of Cave 85. Late Tang Dynasty.
Printed in USA

Library of Congress Cataloging-in-Publication Data

The conservation of Cave 85 at the Mogao Grottoes, Dunhuang : a collaborative project of the Getty Conservation Institute and the Dunhuang Academy / edited by Lori Wong and Neville Agnew ; with contributions by Chen Gangquan, Fan Yuquan, Fan Zaixuan, Su Bomin, Wang Wanfu, Wang Xudong, Neville Agnew, Martha Demas, Po-Ming Lin, Shin Maekawa, Francesca Pique, Stephen Rickerby, Michael Schilling, Lisa Shekede, Lori Wong.
pages cm
Includes bibliographical references.
ISBN 978-1-60606-157-2 (pbk.)
1. Mural painting and decoration, Chinese--Conservation and restoration--China--Dunhuang Caves. 2. Buddhist mural painting and decoration--Conservation and restoration--China--Dunhuang Caves. 3. Buddhist cave temples--Conservation and restoration--China--Dunhuang Caves. 4. Cultural property--Protection--China--Dunhuang Caves. 5. Dunhuang Caves (China)--Antiquities. I. Wong, Lori, editor of compilation. II. Agnew, Neville, 1938- editor of compilation. III. Getty Conservation Institute. IV. Dunhuang yan jiu yuan (China)
ND2849.D86C665 2013
755'.943095145--dc23

2013024811

THE CONSERVATION OF CAVE 85 AT THE MOGAO GROTTOES, DUNHUANG

A Collaborative Project of the Getty Conservation Institute and the Dunhuang Academy

Edited by Lori Wong and Neville Agnew

With contributions by

Chen Gangquan
Fan Yuquan
Fan Zaixuan
Su Bomin
Wang Wanfu
Wang Xudong
Neville Agnew
Martha Demas
Po-Ming Lin
Shin Maekawa
Francesca Piqué
Stephen Rickerby
Michael Schilling
Lisa Shekede
Lori Wong

THE GETTY CONSERVATION INSTITUTE
LOS ANGELES

Contents

Foreword

In 1987 China nominated its first six sites to the World Heritage List of UNESCO. Among these were the Mogao Grottoes near Dunhuang (hence also known as the Dunhuang Caves), situated along the ancient trading routes of the Silk Road in far northwestern China. It speaks to the national importance of this site that it was selected by the Chinese authorities for such recognition, together with the Forbidden City, the First Emperor's tomb at Xi'an, the Great Wall, Mount Tai, and the Peking Man site.

Since its earliest days, the Getty Conservation Institute (GCI) has undertaken collaborative conservation field projects in many parts of the world. Among the most successful and enduring of these has been our association with the Dunhuang Academy (DA), the organization formed to protect and study the site of Mogao. With its staff of several hundred professionals and its decades-long tradition of international cooperation, the DA is at the forefront of conservation and site management in China.

The GCI's continuous partnership with the DA, under successive agreements with China's State Administration of Cultural Heritage in the Ministry of Culture, dates from 1989. This has involved scientific research, conservation training and formal educational initiatives, site stabilization, master planning for the site, staff exchanges, and the Cave 85 project.

Cave 85, completed in 867, is one of the large caves at Mogao, and it contains many of the highest-quality wall paintings from the Late Tang dynasty. The Cave 85 project was initiated jointly by the DA and the GCI in 1997 to carry out several objectives: develop a model methodology for the conservation of wall paintings; solve, through analysis, research, and testing, a number of problems in the conservation treatment of the earthen-based wall paintings, which are ubiquitous at grotto sites in China and throughout central Asia; and provide training to DA staff in project planning, management, and implementation.

The conservation of Cave 85, along with the final components of the project—lighting, a raised platform for better viewing of the wall paintings, and bilingual interpretive panels that convey a conservation message—was completed in 2010. By combining resources and expertise, the DA and the GCI together achieved more than either might have accomplished alone. The project has been sustained through financial support from both institutions, each of which has benefited greatly from this remarkably fruitful collaboration.

I would like to thank Dunhuang Academy director Fan Jinshi and her staff, who have been steadfast supporters of our collaboration over the years and who count among our closest colleagues and friends. In addition, I would like to acknowledge and thank Neville Agnew, principal project specialist at the GCI, who has superbly led our work in China since 1989. I would also like to express my gratitude to Lori Wong, project specialist and wall paintings conservator, who was instrumental in the success of the Cave 85 project and the compilation of this volume, and consultant Po-Ming Lin, who over many years has helped bridge language and cultural gaps with professionalism and good humor.

It gives me pleasure to see the publication of the full report on the conservation of Cave 85, which has also been translated into Chinese and disseminated widely in China.

Timothy P. Whalen
Director
The Getty Conservation Institute

Acknowledgments

The Cave 85 project was undertaken as part of the long-term collaboration of the Dunhuang Academy (DA) and the Getty Conservation Institute (GCI). The conservation initiatives of the GCI in China fall under the aegis of the State Administration of Cultural Heritage (SACH). Deputy Director of SACH Zhang Bai and his successor, Tong Mingkang, have supported the collaboration wholeheartedly, and this is gratefully recognized. Other institutions, notably the Chinese Academy of Cultural Heritage (CACH), under former Director Wu Jia'an, and the Gansu Provincial Cultural Heritage Bureau, have assigned resources to the project and staff participation as team members.

The leadership of the DA, under Director Fan Jinshi, ensured the successful completion of the project through all of its phases, from 1997 to 2010, including the final period when the lighting, interpretive panels, and viewing platform were completed. Deputy Director Li Zuixiong and his successor, Wang Xudong, together with the directors of the DA's Conservation Institute, Su Bomin and Wang Wanfu, worked closely with the GCI, and Ma Xiwu and his staff provided essential administrative and travel facilitation for the GCI group. Many other Conservation Institute staff members participated in the project; they are listed in Appendix 2.A. In addition, Wang Huiming of the DA Archaeological Research Institute provided valuable information on the history and iconography of the cave, and guides from the Reception Department under Li Ping were also helpful with interpretation and advice regarding presentation of the cave to visitors.

Over the course of this long project, the relationship of the GCI with SACH and the DA was supported by GCI Director Tim Whalen and Associate Director Jeanne Marie Teutonico. We also thank our many colleagues at the GCI who in addition to the core team contributed to the Cave 85 project in various ways. Leslie Rainer participated in early field campaigns. Jim Druzik undertook research on the light stability of pigments and organic colorants and toward the end of the project tested LED light sources and advised on lighting the cave and long-term monitoring of the effects of light. Joy Mazurek conducted microbiological investigations, analyzed soluble salts, and worked with visiting DA staff, while David Carson and Eric Doehne undertook scanning electron microscopy and energy-dispersive X-ray spectrometry. Vincent Beltran performed processing of climate data. Cecily Grzywacz, consultant Jan Wouters, and visiting postdoctoral fellow Ana Claro undertook the initial research on organic colorants subsequently pursued at the DA. Alan Phenix assisted with cross-section mounting and interpretation. Herant Khanjian ran and interpreted infrared spectra. GCI intern Shuya Wei investigated migration of salts in rock and plaster. Valerie Greathouse and Kris Donovan helped with the project bibliography, and Rand Eppich was instrumental in putting together the graphic documentation. Gail Ostergren copyedited sections of the report text, and Anna Duer assisted with bibliographic references.

During the mid-project review convened by SACH, a group of experts offered useful critiques and suggestions. These experts are named elsewhere in this report. Sharon Cather of the Wall Painting Conservation Department at the Courtauld Institute of Art at various stages, including the mid-project review, provided constructive advice. Zheng Jun, formerly of the China National Institute for Cultural Property (now CACH), participated in early field campaigns and also took part in the mid-project review. We also thank our colleagues at the National Research Institute for Cultural Properties, Tokyo (NRICPT), for helpful discussions at Dunhuang, particularly Katsuhiko Masuda. Chikaosa Tanimoto generously shared environmental, hydrological, and thermographic data with the DA-GCI project team.

We are greatly indebted to Peter Barker, who contributed to the project as formal translator; consultant Debi van Zyl, for the design and layout of the report; and Kwo-Ling Chyi, who undertook the exacting task of translating this report into Chinese at the request of the DA. At the GCI, we would like to thank Cynthia Godlewski, who coordinated the publication of this volume. At Getty Publications, we would like to thank Tevvy Ball, con-sultant Sheila Berg, Catherine Lorenz, Suzanne Watxon and Dominique Loder.

Finally, the GCI's consultant Po-Ming Lin has been a key contributor to the project since its inception and to the partnership with the Dunhuang Academy. Special acknowledgment is his due.

Introduction

In the far northwest of China lie the Buddhist cave temples of the Mogao Grottoes, a World Heritage Site on the ancient Silk Road about 25 kilometers southeast of the trading entrepôt of Dunhuang. For a thousand years, from the fourth to the fourteenth century, Dunhuang thrived, enjoying unique status as an outpost guarding the westernmost regions of the Chinese empire, protecting trade and the flow of goods and knowledge between the heartland and regions to the west. It was along these trading routes that Buddhism percolated out of India into China proper and beyond. Over the course of a millennium, nearly five hundred cave temples were excavated and decorated along a mile of cliff face at Mogao. The earliest extant grotto dates to 366 C.E., and the last was made in the Yuan dynasty (1271–1368 C.E.). The renown of the cave temples spread across vast reaches of central Asia, east to the great capitals of China, and west through the Silk Road kingdoms toward the Mediterranean world.

As new shipping routes gradually supplanted the ancient overland tracks, China officially abandoned the Silk Road, and the Mogao cave temples fell into disrepair. Over time floods and earthquakes, among other natural phenomena, have caused deterioration of the beautiful and fragile wall paintings and sculpture, including flaking of the paint layer and progressive loss of adhesion between the conglomerate rock and the clay plaster. In 1997 the Getty Conservation Institute (GCI) and the Dunhuang Academy (DA), the organization responsible for the care and management of the site, began a project to address these problems. The project, focused on Cave 85, is a collaboration between the two institutions under the authorization of the State Administration of Cultural Heritage (SACH) within the Ministry of Culture of the People's Republic of China with responsibility inter alia for archaeological sites, monuments, and museums.

The Cave 85 project was born from an already successful collaboration between the GCI and the DA at the Mogao Grottoes, beginning in 1989, which focused on sitewide threats such as sand migration and accumulation, erosion and instability of the cliff face, and the effects of visitors on environmental conditions and led to a draft master plan for the site. Running parallel to this work has been the development of national guidelines for the conservation and management of cultural heritage sites in China, a joint undertaking between SACH, the GCI, and the Australian Heritage Commission. The guidelines were approved by SACH and authorized for dissemination in 2000 by China ICOMOS. Published under the title *Principles for the Conservation of Heritage Sites in China* (the China Principles), they have served as the basis for undertaking the conservation work in Cave 85.

Prior to this project, deterioration of the wall paintings at Mogao and in Cave 85 had not been studied in a way that allowed for the development of long-term conservation and maintenance solutions. As a result, deterioration has often recurred after conservation efforts, escalating in severity over time. Given that certain problems may never be completely eliminated, systematic and thorough study of deterioration and an understanding of the causes and mechanisms at work were essential for developing appropriate conservation interventions and preventive measures to reduce the rate of deterioration over the long term.

Cave 85, completed in 867, is among the larger caves at Mogao and contains some of the highest-quality wall painting of the Late Tang dynasty. Cave 85 was selected for study because the deterioration of its wall paintings—in particular, the widespread exfoliation of paint and plaster detachment from the bedrock—is representative of the problems found in many of the site's caves.

The Cave 85 project has achieved several objectives: development of a systematic methodology for the conservation of wall paintings through analysis, research, and testing and solution of a number of hitherto intractable problems at the site—with particular focus on the development and implementation of methods to conserve wall paintings on earthen supports. The knowledge gained from this project and the conservation methodologies developed can be applied to other caves at the Mogao Grottoes and at similar sites elsewhere along the Silk Road.

Historical Periods of Dunhuang

PERIOD	DATES
Sixteen Kingdoms	366—439
Northern Liang	420—439
Northern Wei	439—534
Western Wei	535—556
Northern Zhou	557—581
Sui	581—618
Early Tang	618—704
High Tang	705—781
Middle Tang	781—848
Late Tang	848—907
Five Dynasties	907—960
Song	960—1036
Western Xia	1036—1227
Yuan	1271—1368
Ming	1368—1644
Qing	1644—1911
Republic of China	1912—1949
People's Republic of China	1949—

Note: The dates may differ from traditional dynastic divisions of Chinese history. This table has been derived from two sources: Fan Jinshi and Liu Yongzeng, *Appreciation of Dunhuang Grottoes: A Selection of 50 Caves from the Mogao Grottoes, Yulin Grottoes and Western Thousand Buddha Grottoes* (Jiangsu Fine Arts Publishing House, a subsidiary of Phoenix Publishing & Media Group); and Tan Chung, ed, *Dunhuang Art: Through the Eyes of Duan Wenjie* (New Delhi: Indira Gandhi National Centre for Arts, Abhinav Publications, 1994), http://ignca.nic.in/ks_19004.htm.

Background
& Methodology

CHAPTER 1

Background of the Cave 85 Project

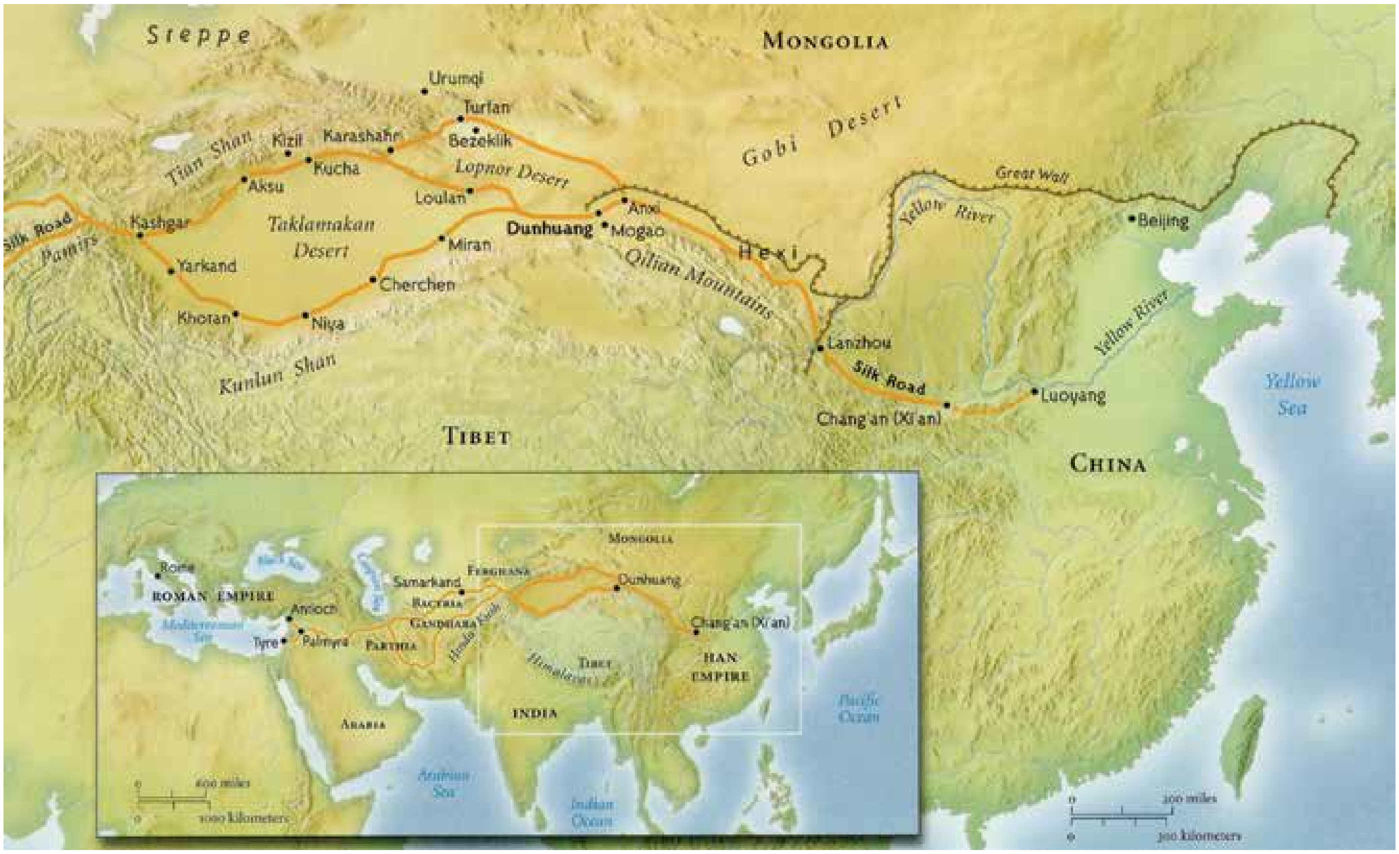

Fig. 1.1 The Mogao Grottoes are located 25 km southeast of Dunhuang. From Dunhuang to the east, the Silk Road (marked in orange) led to Chang'an (present-day Xi'an). To the west, it split into northern and southern routes around the Taklamakan Desert and on to central Asia, India, and ultimately the Mediterranean.

The Mogao Grottoes, a World Heritage Site since 1987 and one of the principal sites along the ancient Silk Road, are located near the town of Dunhuang in Gansu Province, northwestern China (fig. 1.1). Dating from the fourth to the fourteenth century C.E., the site contains 492 decorated Buddhist cave temples excavated into 1.6 km of cliff face (fig. 1.2). The site encompasses some 45,000 m^2 of wall paintings and over 2,000 polychromed sculptures, constituting the largest single body of Buddhist art in China (figs. 1.3, 1.4).

Among the world's significant cultural artifacts, the painting and sculpture of Mogao, together with the documents from the famed Library Cave, provide an unsurpassed record of the arts, music and architecture, science and technology, politics and law, and economic and military conditions in China over a thousand-year period. The Mogao Grottoes also provide an important historical record of the evolution and practice of Buddhism and Buddhist art in China during this long period.

Fig. 1.2 Panorama of the site showing the desert landscape and the grottoes in the distance.

Fig. 1.3 Details of the Mogao wall paintings in Cave 285 from the Western Wei dynasty (a) and Cave 61 from the Five Dynasties (b).

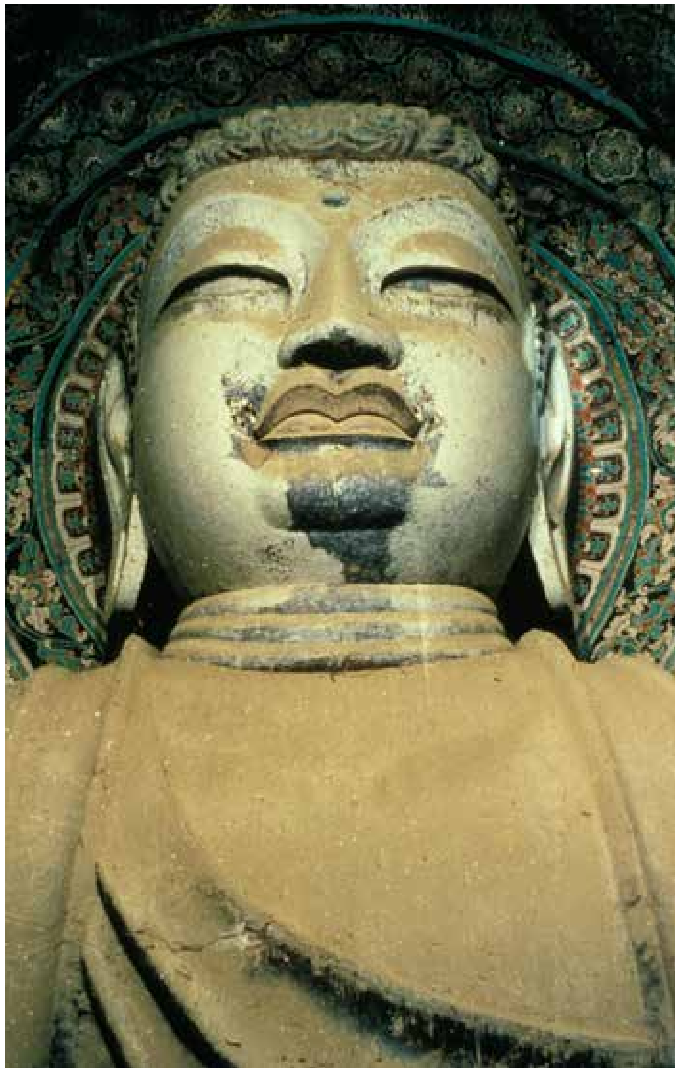

Fig. 1.4 The Great Buddha (26 m) of Cave 130 from the High Tang dynasty.

Fig. 1.5 During the first five years of collaboration, the project addressed site-related issues such as the problem of sand migration and accumulation in the grotto zone requiring a labor force of sweepers after a sandstorm.

The Collaboration

Under a collaborative agreement with China's State Administration of Cultural Heritage (SACH), the Getty Conservation Institute (GCI) and the Dunhuang Academy (DA)—the institution responsible for the care and management of the Mogao Grottoes—have been working together on the preservation of this site since 1989.[1] During the first five years of collaboration (1989–93), the project addressed site-related issues such as assistance with emergency stabilization of the overall site; investigation and research into the causes of deterioration, including sand migration and accumulation, erosion of the cliff, and treatment of thin-roof caves; and undertook environmental monitoring, documentation, and staff training (figs. 1.5, 1.6). This phase culminated in an international conference at Mogao in 1993, "Conservation of Ancient Sites along the Silk Road," which also commemorated the fiftieth anniversary of the Dunhuang Academy (fig. 1.7).

Subsequent to this early work was the development, with key involvement of the Dunhuang Academy, of national guidelines for the conservation and management of cultural heritage sites in China, published as *Principles for the Conservation of Heritage Sites in China* (the China Principles) (Agnew and Demas 2002). The China Principles respect and reflect Chinese traditions and approaches to conservation and comply with existing laws for the protection of cultural heritage (fig. 1.8). They were developed through a collaboration among three institutional partners—SACH, the GCI, and the Australian Heritage Commission (subsequently the Department of the Environment and Heritage). The China Principles are premised on a holistic approach to the preservation of heritage sites. Explicit in the process is the conviction that heritage sites have values that can be identified and stated and that the aim of conservation and management is to preserve those values unimpaired. The document was approved by SACH and issued by China ICOMOS (International Council on Monuments and Sites) in 2000.

After 1997, following the results of a comprehensive review and evaluation of the first phase of the DA-GCI project, the collaboration turned toward the conservation of wall paintings on earthen supports. Cave 85 was selected to meet specific conservation objectives set by the draft Mogao Master Plan

Fig. 1.6 In order to address the sand migration problem, a wind fence was constructed at the top of the cliff to prevent sand from migrating into the grottoes below.

for 2001–10 and to serve as one of two projects undertaken by SACH and the GCI for the application of the China Principles (China Architectural Design Academy et al. 2010).[2]

Notes

1. The Dunhuang Academy was established in 1944 as the Dunhuang National Art Research Academy.
2. The plan was initially developed by the DA and the GCI as part of this collaboration. It was later finalized by the Institute of Architectural History. Shuxiang Temple, Chengde, one of the Outlying Temples of the Imperial Mountain Resort of the Qing Dynasty Emperors in Hebei Province, is the second application project of the China Principles. This project, part of a larger initiative involving development of a master plan and visitor management strategy for the entire site, focuses on the conservation of Chinese classical architecture.

Fig. 1.7 The first DA-GCI international conference, "Conservation of Ancient Sites along the Silk Road," was held in 1993. The proceedings of the conference were published in 1997 (Agnew 1997).

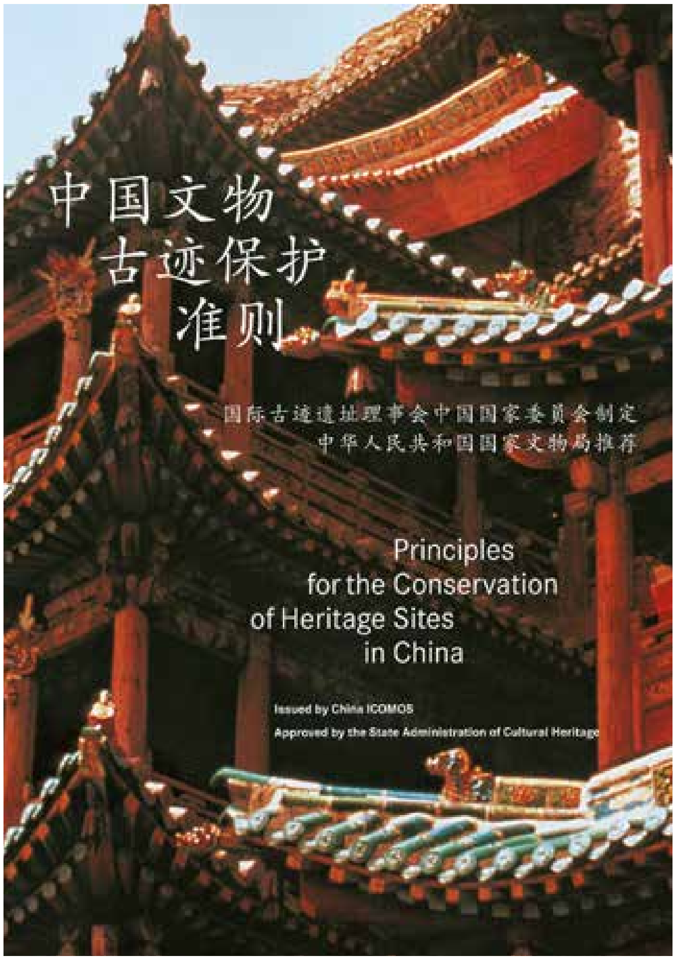

Fig. 1.8 The *Principles for the Conservation of Heritage Sites in China* was published in 2002.

CHAPTER 2

The Cave 85 Project

Fig. 2.1 Documentation and investigation of the wall paintings in Cave 85 at the start of the project.

Cave 85, a large Late Tang dynasty (848–906 C.E.) cave severely affected by deterioration phenomena typical of the site, was chosen jointly by the Getty Conservation Institute and the Dunhuang Academy as a model for the application of a rigorous methodology to develop and implement an overall conservation plan (fig. 2.1). The Cave 85 project (1997–2010) aimed to identify and understand, through investigation and research, the causes and mechanisms of deterioration of the wall paintings and sculpture in order to develop, test, and implement preventive strategies together with stabilization treatments to ensure long-term preservation.

Project Objectives

The specific objectives of the project were the following:

- Develop and implement a model process for the conservation of wall paintings and sculpture in Cave 85 following the China Principles;
- Conserve the wall paintings and sculpture without adversely affecting their authenticity or cultural values;
- Understand the causes and mechanisms of deterioration of the wall paintings and sculpture through research and investigation;

Fig. 2.2 Detail of the earthen paintings that decorate the walls and ceiling of the main chamber. Earthen-based paintings are generally less studied than lime-based paintings and therefore required significant research and testing as part of this project.

- Develop and implement preventive conservation measures to inhibit further deterioration and maintain the cave in stable condition;
- Make defined and measurable progress in solving the problems of wall painting deterioration at Mogao by improving techniques and materials for the conservation of wall paintings on earthen plaster;
- Develop and implement condition monitoring strategies;
- Improve methods of information management of the data collected;
- Train a new generation of wall painting conservators, conservation scientists, and documentation personnel at the DA;
- Present and interpret the conserved cave to visitors and convey a conservation message;
- Disseminate results of the project to extend knowledge and good conservation practice at other similar sites.

Project Challenges

Over a thousand-year period, from the fourth to the fourteenth century C.E. and encompassing nine dynasties, the cave temples of the Mogao Grottoes were hewn out of a cliff face of soft conglomerate rock. The cave walls were plastered with a mixture of clay, sand, and plant fiber, and the paintings were executed as line drawings in red and black ink on a ground layer covering the earthen plaster, then filled in with bright mineral pigments and, in some caves, finished with washes of organic colorants (fig. 2.2). For centuries, the paintings suffered deterioration of various kinds, from flaking of the paint to loss of cohesion between the conglomerate rock and the earthen plaster. The latter problem is the most serious, resulting in the detachment or separation of painted plaster from the support—a common problem at Mogao and other sites on the Silk Road. Large areas of the paintings have been lost, as detachment ultimately leads to the collapse of the plaster (fig. 2.3).

Fig. 2.3 The paintings have been severely affected by deterioration phenomena such as plaster detachment that led to the eventual collapse of a large area of plaster in Cave 85 in 1996. Understanding the causes of this deterioration and developing conservation solutions to preserve the paintings was one of the objectives of this project.

Deterioration of the wall paintings at the site had not been comprehensively studied in a way that would allow for the development of long-term conservation solutions. As a result, after previous conservation efforts deterioration often recurred and escalated in severity over time. Most previous research in the field of wall painting conservation—in particular the study of deterioration and treatment—has been on lime-based paintings. The paucity of research on earthen-based wall paintings compounded the conservation challenges at Mogao, necessitating in-depth investigation and testing. For this reason, the project placed heavier emphasis on the wall paintings than on the sculpture.

Fig. 2.4 Members of the Cave 85 conservation team from the Dunhuang Academy, Getty Conservation Institute, and Chinese Academy of Cultural Heritage.

Past causes of deterioration of the wall paintings have been both immediate and gradual: periods of flooding of ground-level caves, earthquakes, gradual physicochemical changes of the original materials, and deterioration caused by soluble salts in fluctuating humidity conditions. These persist today, flooding excepted. Systematic study of deterioration and determination of active phenomena, leading to an understanding of the causes and mechanisms at work, were therefore of first importance. Certain problems may never be completely eliminated; as a result, understanding the causes and processes—in particular the role of humidity and soluble salts—was the basis for developing conservation interventions and preventive measures to reduce the rate of deterioration over the long term.

Fig. 2.5 Delegates at the Second International Conference on the Conservation of Grotto Sites, Mogao Grottoes, 2004. The conference was jointly organized by
the DA and the GCI.

Project Approach

The philosophical and conceptual approach of the Cave 85 project is based on the China Principles and calls for a statement of the cultural values and significance of the cave in the context of the site as a whole (see chap. 10). Preservation of cultural significance is the ultimate objective of conservation and management actions and policy. The project adhered to accepted conservation principles, including minimal intervention, reversibility, retreatability, and compatibility. In accordance with this approach it was imperative that the paintings and sculpture in Cave 85 be conserved in situ and that treatment be based on diagnostic investigation, analysis and testing, and sustainable conservation practices.

The project was structured in five components—information gathering, assessments, testing and development, implementation, and monitoring (see chap. 3). The interdisciplinary project team, which included conservation, documentation, analytical, and environmental specialists, undertook detailed examination and recording of the wall paintings' condition, collection of information on the physical and conservation history of Cave 85, investigations into the paintings' composition and technique, quantitative analysis of the ionic species comprising the soluble salts, environmental monitoring of the climate inside and surrounding the cave, development and implementation of conservation interventions, and condition monitoring strategies.

In addition to the GCI and the DA (fig. 2.4), members of the Chinese Academy of Cultural Heritage (CACH) (formerly the China National Institute for Cultural Property) participated in the project, and conservators from several other sites in northwestern China intermittently participated as observers.[1] Two field campaigns, spring and fall, were held at Mogao each year throughout the course of the project. These were periods of joint work, exchange of information, and informal training. During interim periods GCI and DA team members worked separately, with regular communication, on agreed-upon tasks. Monthlong training of Dunhuang Academy staff took place annually at the GCI in areas of documentation, treatment testing, analytical instrumental analysis, and environmental investigation.

Project Results

Interim results of the project were presented at the Second International Conference on the Conservation of Grotto Sites, held at Mogao in 2004 (Agnew 2010) (fig. 2.5). Overall results are presented here in this final project report.

Cave 85 is representative of the remarkable artistic and historical heritage of the Mogao Grottoes and of its complex conservation problems. A structured, interdisciplinary approach, following the methodology of the China Principles, was effective in addressing the issues to ensure preservation of the cave's values and significance. Progress has been made toward detailed understanding of deterioration causes and mechanisms affecting the cave through the collaborative work of the team. This understanding and the conservation methodology developed have implications for other caves at the Mogao Grottoes and for other similar sites in China.[2]

Notes

1. A list of project participants is provided in Appendix 2.A.
2. A similar conservation methodology has been applied by the DA in the treatment of other caves at Mogao, notably Cave 98 (a similar, though larger, Five Dynasties cave).

CHAPTER 3

Project Methodology

Fig. 3.1 Flaking of the paintings is a recurrent problem in Cave 85. This area of the south wall had been treated in the 1970s.

In the past, conservation practice at the Mogao Grottoes was reactive and was focused on repair rather than addressing the causes or mechanisms of deterioration. Given the scale of the site and inadequate resources, this was the only feasible approach in the early days of the Dunhuang Academy. Consequently, some conditions—such as flaking and plaster detachment of the wall paintings—are recurrent, resulting in progressive deterioration and loss (fig. 3.1).

In order to address these problems, a methodology of investigation, assessment, and diagnosis to understand the causes, activation mechanisms, and rates of detrimental change of the wall paintings was undertaken in Cave 85. This important preliminary step was followed by the development and implementation of preventive interventions and stabilization treatments. The complexity of the deterioration processes and the sheer extent of wall paintings at Mogao warrant such a methodological approach and one that also favors preventive conservation. It is not possible to eliminate some causes of deterioration, thus efforts to slow decay need to be undertaken. Without such measures in place treatments will eventually fail and the paintings will continue to suffer loss. Therefore a sound conservation methodology is of great value and will have wide-reaching benefits for the conservation field in China.

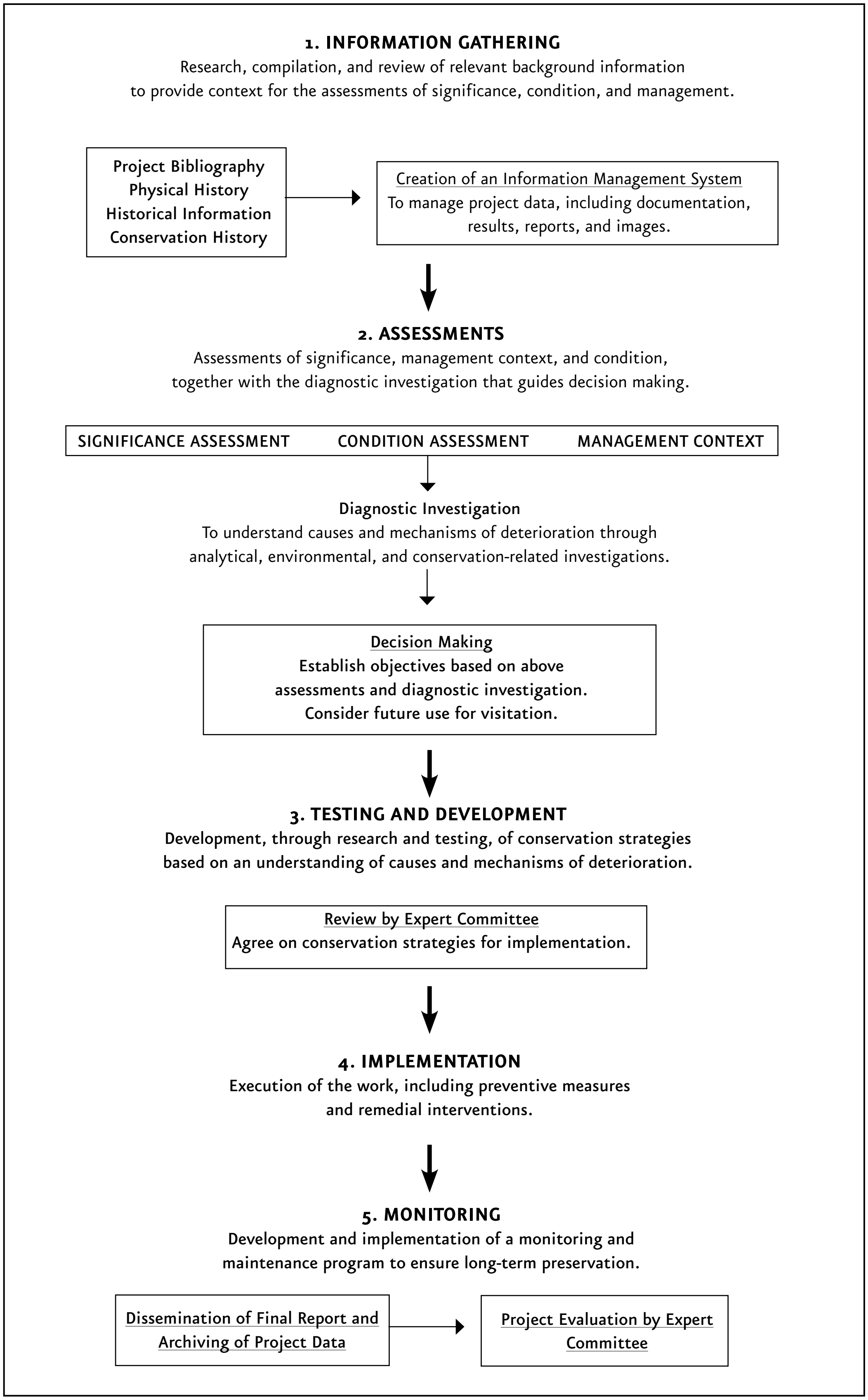

Fig. 3.2 Cave 85 project methodology and conservation process based on the *Principles for the Conservation of Heritage Sites in China*.

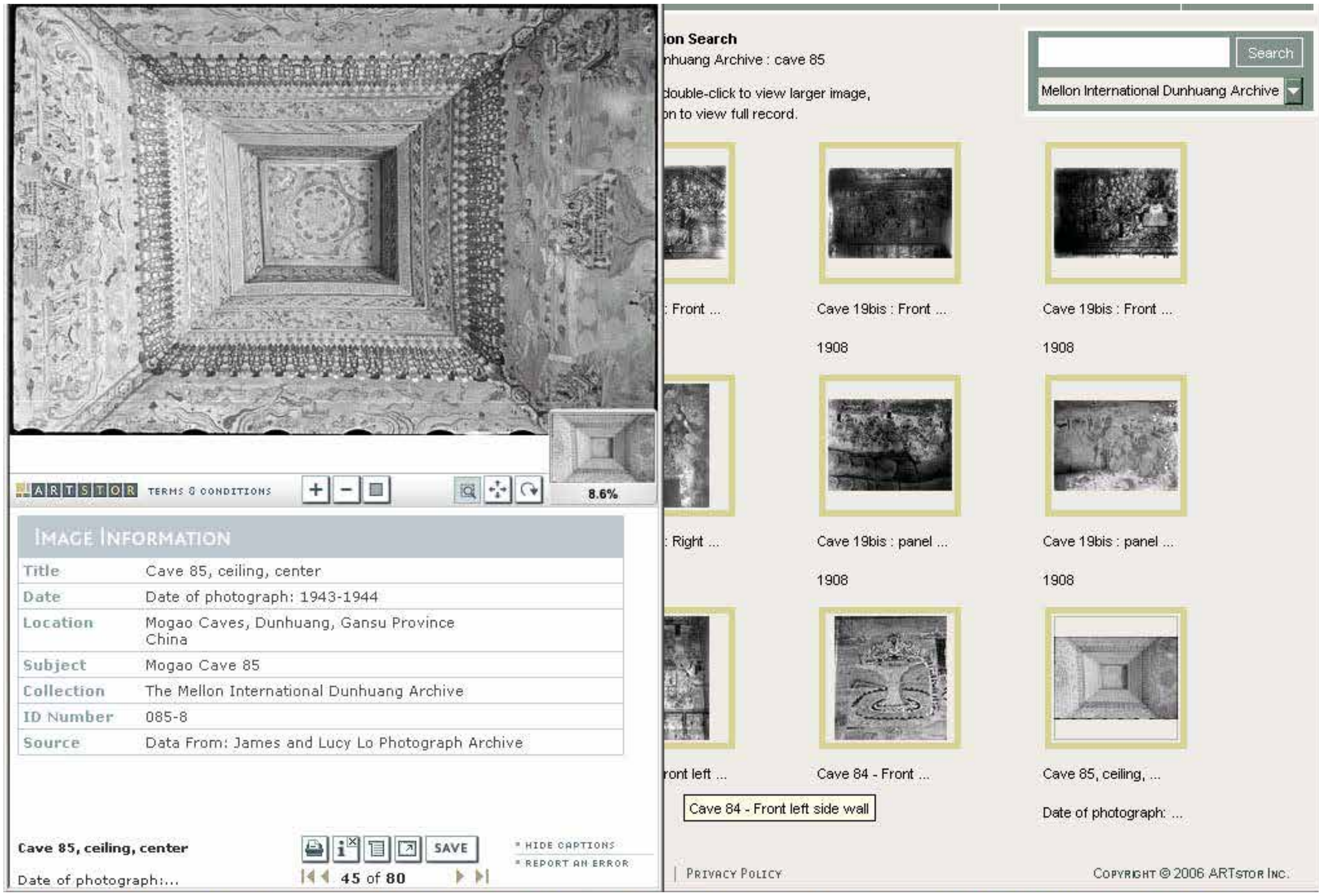

Fig. 3.3 As part of the information gathering component historical images were collected and studied. Images of Cave 85 from the James and Lucy Lo Photograph Archive were searched using ARTstor (www.artstor.org).

Conservation Planning Process

The conservation planning process for Cave 85 consisted of five components. These are described below and are summarized in figure 3.2.

Component 1: Information Gathering

This component involved research and compilation and review of background information relevant to Cave 85 for the assessments of significance, condition, and management context. An information management system was developed for systematic storage and retrieval of project data, including documentation, results, reports, and images (see chap. 4) and to allow quick access to data and sharing of information between teams.

Project Bibliography

Begun at the onset of the project with periodic updates throughout, the project bibliography comprises a review and compilation of all relevant literature on the site and on the wall paintings in Cave 85. This includes information on methods and materials used to make and to conserve the earthen-based paintings. The bibliography exists in hard copy and as a key-worded searchable ProCite database.

Background Information

In addition to bibliographic references, archival records, historical photographs, and oral and visual examination reports constituted the main sources for the information gathering stage of the project (fig. 3.3). The information compiled falls into the following general categories:

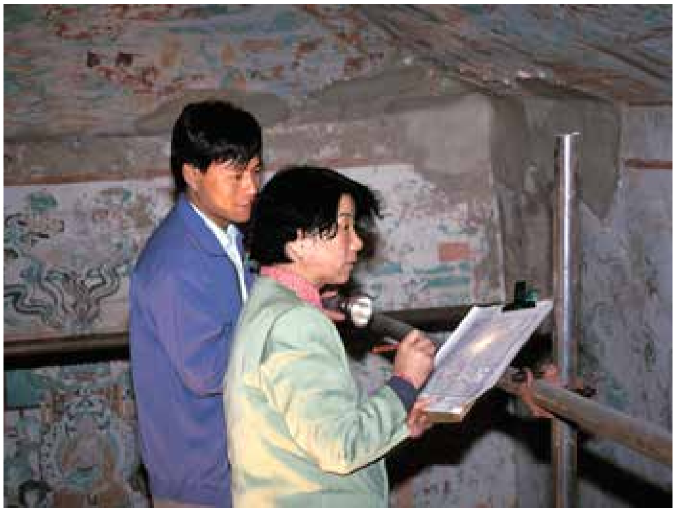

Fig. 3.4 As part of the assessment component, the condition of the wall paintings was studied and recorded.

Fig. 3.5 As part of the testing and development component, study of the causes and mechanisms of deterioration helped in developing conservation strategies.

- **Description of the site**: information on the history of Mogao as well as the geological context of the site (see chaps. 5, 6)
- **Description of Cave 85 and its wall paintings and sculpture:** information on cave construction, painting technology, art history, and iconography (see chap. 8)
- **Physical history of the site and Cave 85:** information on the physical history of the site and Cave 85, including historical photographs (see chap. 9)
- **Conservation history of the site and Cave 85:** information on previous interventions and general conservation practices at Mogao (see chap. 9)
- **Prior visitor use of Cave 85:** information on the preparation of the cave by the Dunhuang Academy for visitation and the dates it was open for visitation prior to the current conservation program.

Component 2: Assessments

The assessment component was central to the conservation process and included research and evaluation necessary to make decisions about the conservation and future use of the cave. This component required an understanding of the significance and values of the cave, the management context of the site itself, the condition of the wall paintings and sculpture, and a diagnostic investigation of the causes and mechanisms of deterioration. Agreement between project partners on these assessments was necessary as these documents served as the basis for subsequent decision making.

Significance Assessment

A significance assessment is an essential component of any project in order to ensure that the values and significance are preserved unimpaired. The Cave 85 significance assessment and the resulting statement of cultural values and significance took into consideration the artistic, historic, scientific, and contemporary social and economic values of the site as a whole and specifically of the cave itself. Preservation of authenticity and significance was the ultimate objective of the Cave 85 project, and it was therefore imperative to produce a clear and agreed-upon statement (see chap. 10).

Management Assessment

Management assessment involves identification of the factors, both positive and negative, that affect the management of the site. The management assessment for Cave 85 focused on understanding and evaluating the management structure of the Dunhuang Academy as the entity responsible for the preservation of the site, as well as current conservation practices at Mogao. This information was crucial to establishing a successful collaboration between the GCI and the DA in terms of the expertise, budget, and time needed for the completion and sustainability of the project.

Fig. 3.6 As part of the implementation component, stabilization of the wall paintings by injection grouting was undertaken.

Fig. 3.7 As part of the monitoring component, continued condition monitoring of the wall paintings will be necessary as the causes of deterioration—the soluble salts—have been reduced but not eliminated.

As a result of the assessment, training initiatives were organized to improve knowledge and practices of the Dunhuang Academy in the areas of conservation, scientific analysis, environmental science, and documentation (see chap. 11).

Condition Assessment

The condition assessment provided a comprehensive record and understanding of the condition of the wall paintings and sculpture through identification and documentation of the types and distribution of deterioration (fig. 3.4). This involved detailed visual and instrumental examination, a comprehensive photographic survey, graphic documentation in order to map the distribution and types of deterioration, and creation of an illustrated terminology to standardize the process of condition recording.

Deterioration phenomena observed in the cave included surface deterioration such as exfoliation, flaking, and "punctate" eruption of the paint layer and subsurface deterioration such as plaster detachment—phenomena that are also common in other caves at the site. Deterioration was markedly more severe toward the west and northwest (i.e., the rear) of the cave (see chap. 12).

Diagnostic Investigation

The aim of the diagnostic investigation was to understand the causes and mechanisms of deterioration of the paintings and sculpture (see chaps. 15, 16). This involved identification of active deterioration processes and testing of hypotheses of causes and mechanisms of deterioration. This was done through the study of original and added materials as part of the analytical investigation (see chap. 13) and monitoring of exterior and interior climatic conditions as part of the environmental investigation (see chaps. 7, 14).

Component 3: Testing and Development

Research and testing was undertaken to develop conservation strategies based on an understanding of the causes and mechanisms of deterioration (fig. 3.5). This work led to a conservation plan and a detailed program for its implementation, including strategies for sequencing and duration of activities and identification of human and material resource needs, as follows:

- Development and testing of preventive measures to mitigate deterioration by reducing the intrusion of exterior humid air into the cave and through treatment to reduce salt content in the earthen plaster in areas where grouting was done (see chap. 17);
- Establishment of treatment principles in order to develop remedial interventions to stabilize the painting, including research and testing of materials and methods, development of testing procedures, and evaluation of results.

Fig. 3.8 A review meeting with team members from the GCI and the DA was held at Mogao in preparation for a formal SACH project review.

Visitation policy and light susceptibility work in this component included:

- Development of a preliminary strategy for visitation to the cave as part of visitor management and cave carrying capacity studies undertaken for the grottoes;
- Laboratory research on effects of lighting on paintings and consultation with lighting engineers to develop options for lighting the cave;
- Development of a plan for presentation and interpretation of the cave to visitors (see chap. 19).

Component 4: Implementation

The implementation component included the execution of the conservation and visitation strategies. Preventive measures were instituted to reduce infiltration of exterior humid air into the cave by closing it during periods of rain and high relative humidity. Remedial interventions to stabilize the paintings and locally reduce soluble salt content were also undertaken (fig. 3.6). Principal remedial treatments included grouting for stabilization of detached plaster with an earth-based grout and fixing of flaking paint (see chap. 17).

Prior to application, test results for proposed treatments were reviewed on-site by an expert committee, a procedure required by the State Administration of Cultural Heritage before conservation work could begin.

Component 5: Monitoring

A condition monitoring program was developed for the long-term preservation of the cave after stabilization interventions. This was based on information collected during the diagnostic investigation. While condition monitoring is important for any conservation project, it is especially so when deterioration is still active and the causes of deterioration have been reduced but not eliminated. In the case of Cave 85, the principal cause of deterioration—soluble salts—is still present, and mitigation of their effects is based on environmental control. Completion of the conservation program in Cave 85 will be followed by regular condition monitoring and inspection of the paintings by the Dunhuang Academy (fig. 3.7) (see chap. 18).

Project Evaluation and Dissemination

Periodic evaluation of the project was conducted throughout the conservation process. The first, a midterm review of treatment testing for grouting by a panel of experts, was in April 2002.[1] Then, in October 2005, an internal project review meeting with DA and GCI team members was held in preparation for a formal SACH project review (fig. 3.8). The final archiving of project data and the dissemination of the results of the project through the present project report mark the completion of the conservation process in Cave 85.

Notes

1. The panel of assembled Chinese experts included Huang Kezhong, Zhang Zhiping, Wang Danhua, Lu Shuoling, and Ma Jiayu. Also present were Neville Agnew, Sharon Cather, Stephen Rickerby, Lisa Shekede, and Po-Ming Lin from the GCI; Zheng Jun from CACH; and Li Zuixiong, Wang Xudong, and Fan Zaixuan from the DA.

CHAPTER 4

Information Management

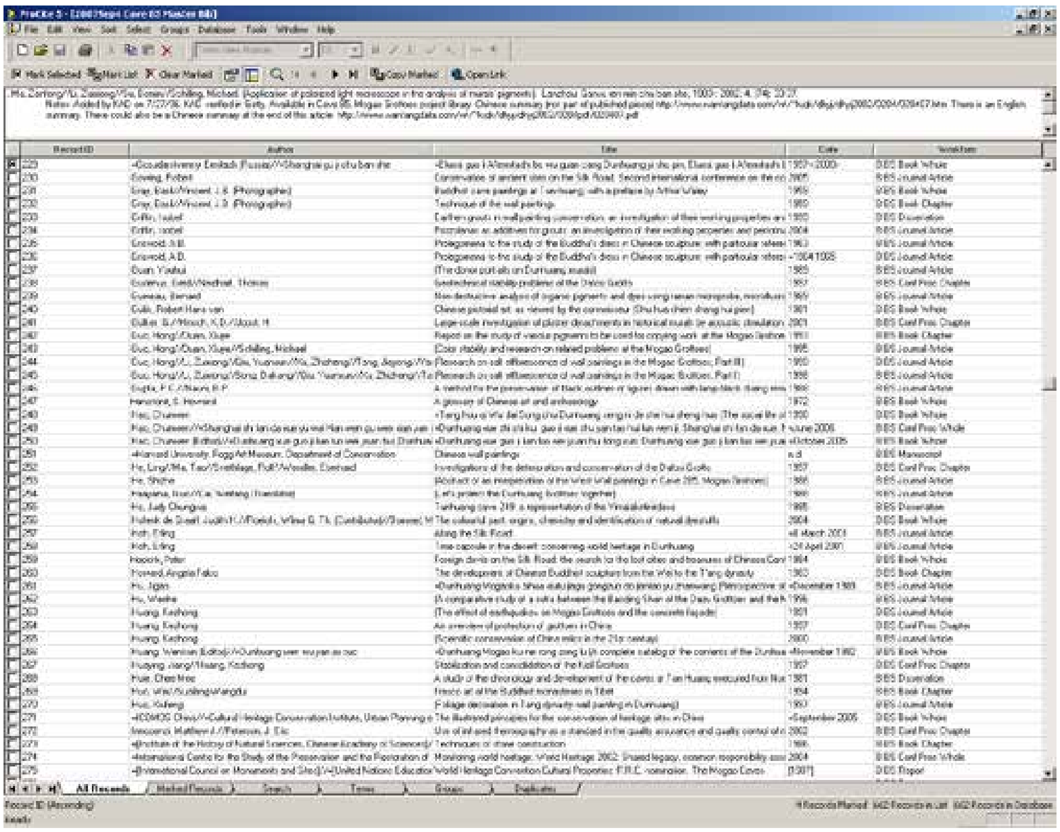

Fig. 4.1 A view of the project bibliography ProCite database.

The conservation project in Cave 85 (1997–2010) involved experts from many fields, including wall painting conservators, documentation specialists, photographers, environmental scientists, analytical chemists, geologists, historians, and translators. Each of these specialized disciplines generated large amounts of information, with team members from the Dunhuang Academy and the Getty Conservation Institute producing data in Chinese and English respectively.

The information produced included physical documents and photographs as well as considerable amounts of data in electronic form, consisting of text, data, photographic, and graphic files. Digital files were created using a range of software, including Microsoft Word, Excel, and PowerPoint programs; Autodesk AutoCAD; and Adobe InDesign, Photoshop, and Illustrator. In addition, thousands of digital images were generated in RAW, TIFF, and JPEG format. The amount of information has steadily increased throughout the project, with a steep rise beginning in 2003 with the transition from film to digital photography.

Because of the sheer volume and complex range of material generated by the project, methods for information management—the collection, organization, storage, retrieval, integration, manipulation, and presentation of multidisciplinary data—developed out of necessity and grew into a fundamental component of the overall project. The challenge was to establish a data management system that would facilitate work across

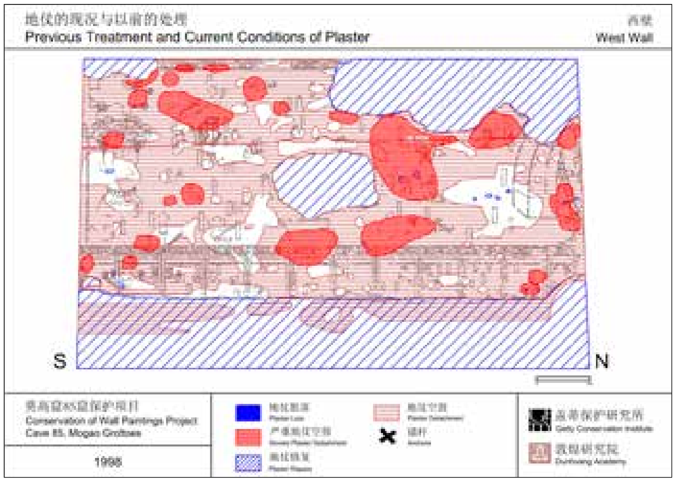

Fig. 4.2 The condition of the wall paintings was recorded on transparencies laid over photographs and then transferred into digital format as CAD drawings. This image shows the west wall of Cave 85 with areas of loss and plaster detachment indicated graphically.

Fig. 4.3 Example of a sample report that was created to manage information generated from the scientific investigation. The report includes a description of the sample, location, sampling rationale, and results of analyses.

disciplines by allowing access to information by team members and thereby promoting the integration and use of data, which was essential to guiding the project's work.

Types and Uses of Data

The information gathering, assessment, testing, and development, implementation, and monitoring components of the project generated many different types of information, ranging from bibliographic references to complex scientific data. The primary types of data amassed by the project are described here. The initial information gathering phase included collection of sources on the historical background of the site and the commissioning and construction of Cave 85 in the Late Tang dynasty, as well as art historical and iconographic research of the wall paintings and sculpture. The history of interventions was also compiled by consulting previous treatment reports and interviewing DA conservators. The resulting bibliography was specific to Cave 85 and relevant to paintings on earthen supports generally. As the project progressed the number of references grew; the final bibliography contains over seven hundred records (fig. 4.1).

Visual records were also collected to help reconstruct the physical history of Cave 85, including the earliest known photographs of the cave taken by the Russian expedition to the site in 1914–15 (see chap. 9). These photographs and those from other explorers and travelers who visited the Mogao Grottoes in the early twentieth century helped the project team understand the history of the site. In addition, photographs taken by the Dunhuang Academy (established in 1944) provide a detailed record of the first major interventions to the site and a comprehensive record of the condition of the site's wall paintings and sculpture over the years. Analysis of these images has been a key to understanding the processes and the causes of deterioration.

In addition, approximately five hundred photographic slides, both color and black-and-white, were taken as part of comprehensive documentation of the paintings at the start of the project. These photographs were used as base maps for graphic condition recording during the assessment component of the project. Condition was manually recorded on transparencies over the photographs and then transferred into digital format as CAD drawings (fig. 4.2). Supplementing the condition assessment, an illustrated terminology was created to standardize

Fig. 4.4 Documenting painted fragments uncovered during work on the altar base as part of a fragment archiving system.

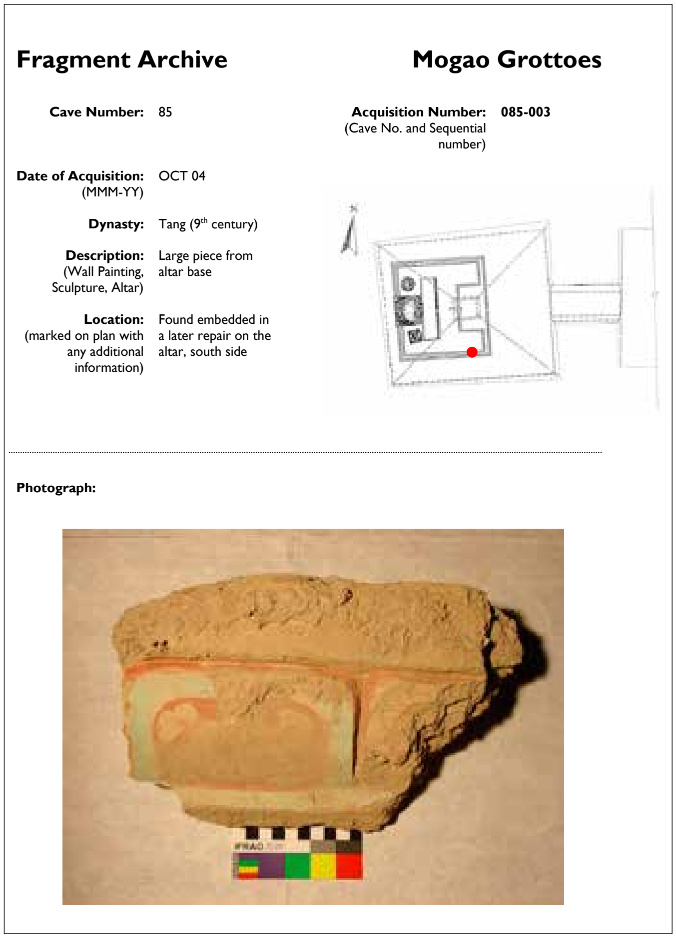

Fragment Archive **Mogao Grottoes**

Cave Number: 85

Acquisition Number: **085-003**
(Cave No. and Sequential number)

Date of Acquisition: (MMM-YY) OCT 04

Dynasty: Tang (9th century)

Description: (Wall Painting, Sculpture, Altar) Large piece from altar base

Location: (marked on plan with any additional information) Found embedded in a later repair on the altar, south side

Photograph:

Fig. 4.5 Example of a report that was created to archive individual fragments.

recording of condition and to show the severity of conditions recorded (see chap. 12).

Sampling was undertaken to characterize the original materials of the painting and to understand painting techniques, and each sample was individually documented and analyzed (see chap. 13). A report was created for each sample that included a description of the sample, its location, the sampling rationale, and results of the analyses. These reports served to disseminate the sampling results to both the conservation and analytical teams (fig. 4.3). The raw data resulting from each analysis were archived separately.

Environmental monitoring generated large quantities of data. This included years of data collected on exterior and interior conditions such as temperature, relative humidity, and rainfall accumulation and intensity (see chaps. 7, 14).

During the testing and development component, laboratory and in situ tests were documented. Research and testing of grout formulations were carried out for detached painted plaster, and some eighty grout formulations were tested (see chap. 17).

Following testing, treatments were implemented and documented using graphic documentation and photography. Original Tang-period painted fragments, uncovered during treatment on the altar base, were photographed, recorded, and inventoried as part of a fragment archiving system that was designed for this project (fig. 4.4). A report was created for each fragment, and the fragments were stored in the cave (fig. 4.5).

For future monitoring, areas were selected and recorded to create baseline documentation for use by the DA to assess any change of condition in the cave (see chap. 18).

Given the complexity of the deterioration mechanisms found in the wall paintings in Cave 85, information gathered from individual investigations can give an incomplete picture. Instead, data from multiple investigations should be integrated so that trends from various disciplines inform one another, providing a complete view of the data. For deeper meaning and context, data often also benefit from manipulation and visual presentation. As it is sometimes difficult to discern trends and draw conclusions from raw analytical and environmental data, the visual display of data can aid interpretation.

For example, as part of the diagnostic investigation of salts as the main cause of deterioration, a comprehensive salt survey was undertaken in which tiny micro-cores of plaster (from which painting had been lost) were carefully carved out of the upper 10 mm of plaster at selected locations throughout the cave (fig. 4.6). Forty-seven micro-cores, each at four or five incremental depths into the plaster strata, resulted in nearly two hundred samples. Quantitative analysis identified ions of soluble salts present, as well as their distribution. This investigation generated a large amount of raw data (fig. 4.7). To aid in interpretation, data were integrated and presented visually to correlate with condition by superimposition over the condition record. Each micro-core has a data table showing the main soluble ions divided by incremental depth. This type of plotting was done for all areas and clearly shows the enrichment of salts toward the rear (west) end of the cave (fig. 4.8) in comparison to the east end (fig. 4.9). It establishes a direct correlation between salt content of the plaster and deterioration of the wall paintings. Presenting the data visually allowed interpretation of the large amount of tabulated data generated from the micro-core sampling.

Fig. 4.6 Plaster micro-cores being sampled as part of a comprehensive salt survey. Each core was taken at four or five incremental depths into the upper 10 mm of the painting. The samples were quantitatively analyzed for ions of soluble salts present and their topographic and stratigraphic distribution throughout the cave.

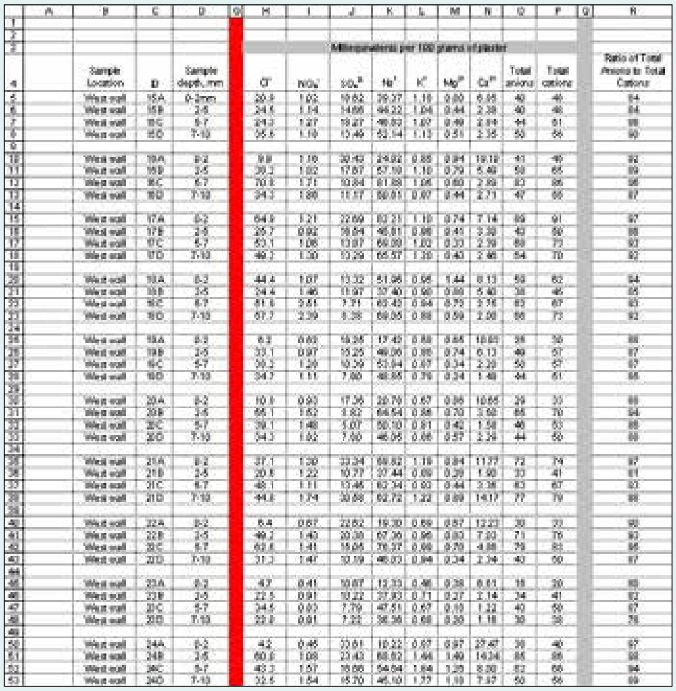

Fig. 4.7 Results of the salt survey in Cave 85 showing soluble ion content of the plaster micro-cores. In this raw form the data are difficult to interpret. Visually presented data correlates analytical results with condition (figs. 4.8, 4.9).

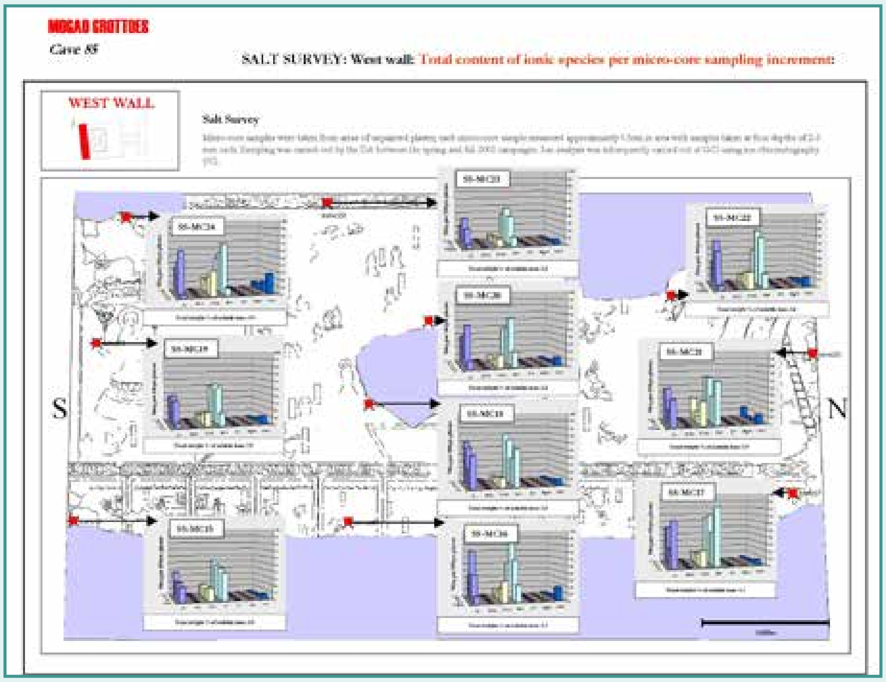

Fig. 4.8 Data from each micro-core were charted and superimposed over the CAD condition drawings to visualize enrichment of salts toward the rear (west) end of the cave and establish a direct correlation between salt content of the plaster and condition of the wall painting. This chart shows the west wall with high soluble ion content.

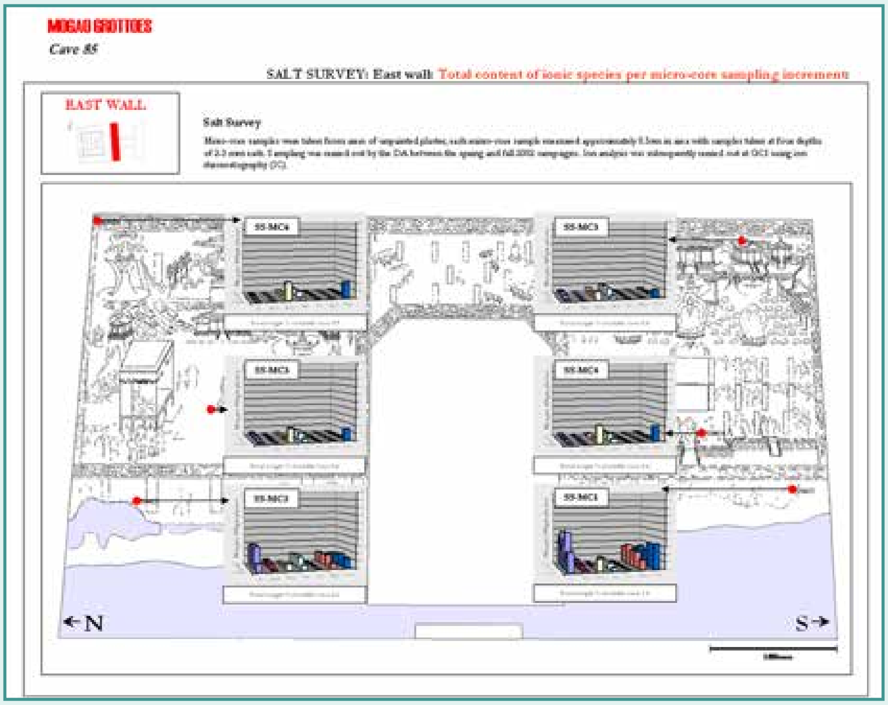

Fig. 4.9 Results of the salt survey on the east wall of Cave 85. The soluble salt content of these micro-core samples is significantly lower than those from the west wall.

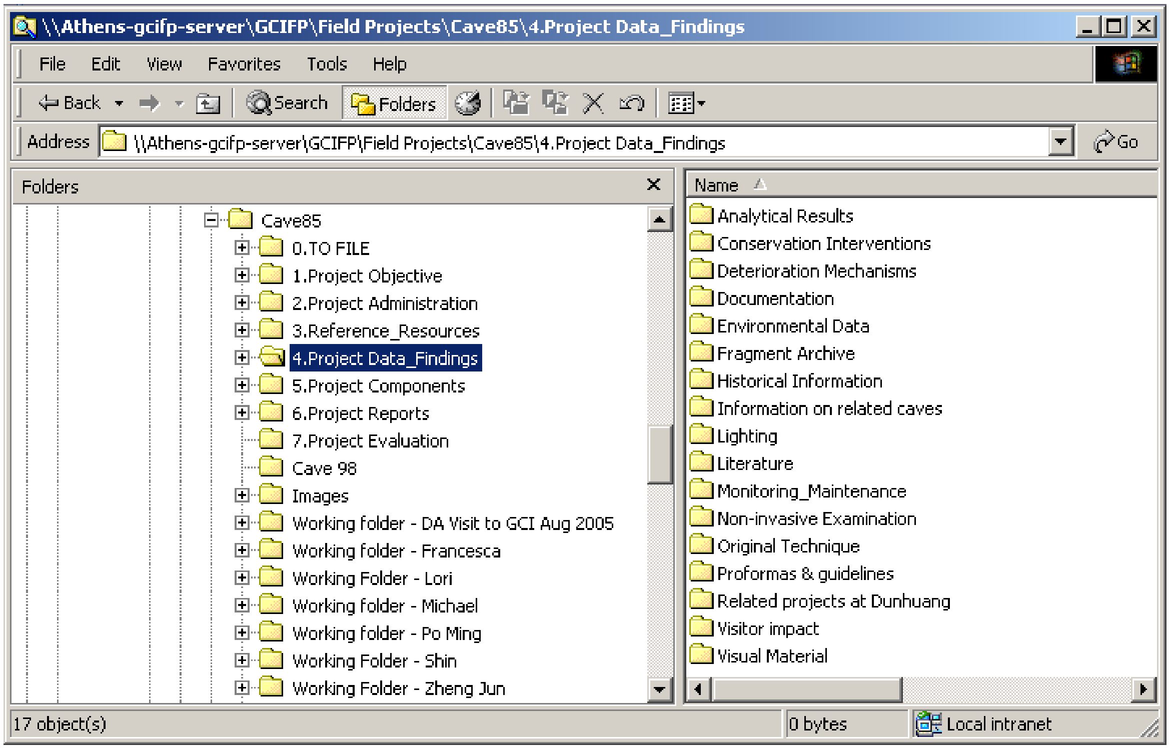

Fig. 4.10 The digital file organizational structure for the Cave 85 project.

An Information Management Strategy

Initially, the Cave 85 project lacked a comprehensive information management strategy. Owing to the multiyear duration of this project, with team members of different disciplines working in varied locations and in two languages, it became increasingly difficult and time consuming to locate and retrieve files and information. The lack of a standardized file naming protocol exacerbated the problem, as did the lack of centralized storage of files and a common file organizational structure. These circumstances led to wasted time and inefficiency. The decision to create an information management system came midway through the project. A protocol for receiving, storing, and sharing information was established; key to its implementation was the appointment of an information manager through whom all information would flow. Translation between the languages was also essential to the information flow.

The Cave 85 project information manager's responsibilities were as follows:

- **Data collection**: receiving and monitoring data;
- **File naming**: naming or renaming files following an agreed-upon convention (including a brief description of the content, metadata on the author, creation date, and file type);
- **Storage**: storing electronic files on a shared networked location accessible to all project team members, rather than on personal computers, and following an agreed-upon file organizational structure (fig. 4.10);
- **Data sharing**: communicating receipt and availability of project information to team members, including the creation of a parallel database and the identification of a counterpart information manager at the Dunhuang Academy, which allowed for the exchange of documents;
- **Retrieval**: locating files and directing team members to relevant information;
- **Maintenance**: maintaining and reorganizing the shared folder and keeping information current.

The Cave 85 project demonstrated the information management challenges generated by a complex, multiyear, interdisciplinary project involving a sizable team. The team's agreement to adopt a common information management system and appoint an information manager, who had responsibility for integration of data from different investigations, facilitated a successful approach to these challenges. Through the experiences gained from this project and the training of Dunhuang Academy team members, the process of managing the large body of data has had wider application for the conservation of other caves at the Mogao Grottoes.

Information Gathering

CHAPTER 5

The Mogao Grottoes

Early in the twentieth century, the ancient Buddhist grottoes of Mogao were referred to as Qianfodong, or Caves of the Thousand Buddhas. The name came from the legend of a monk's vision of a golden radiance in the form of a thousand Buddhas floating above one side of the valley. Later the grottoes became known as Mogaoku, or Peerless Caves, the name given to the site in the many inscriptions and documents found in the famous Library Cave (Cave 17). The site was inscribed on the World Heritage List in 1987 as the Mogao Caves. It is also referred to as the Dunhuang Caves or Grottoes (figs. 5.1, 5.2).[1]

Fig. 5.1 Overview of the site showing the southern section of the cliff face in the foreground marked by a line of trees with the northern grottoes visible in the distance. The Daquan River runs through the site in a northerly direction in front of the cliff face.

Fig. 5.2 The iconic Nine-Storey Pagoda of Cave 96, situated in the southern region of the cliff face, houses the largest Buddha statue at the site.

Geographic Location and Description

The site is located 25 km to the southeast of Dunhuang in Gansu Province, northwestern China, at the end of the Hexi Corridor, to the west of the Yellow River (see fig. 1.1).[2] Situated in a desert landscape, the grottoes lie on the southern edge of the Gobi Desert and are hundreds of kilometers to the east of the Taklamakan Desert in the Tarim Basin. Behind the cliff into which the caves are excavated are the Mingsha Dunes (Dunes of the Singing Sands), which face east toward the Sanwei (Three Peaks) Mountains. To the south lie the Qilian Mountains, the source of water from snowmelt that feeds the Daquan River running through the site in front of the cliff face. A wide valley and a line of poplar trees mark the course of the river.

The rock-cut caves are excavated along 1.6 km of cliff face that runs in a north-south direction (fig. 5.3). The cliff varies considerably in height from some 10 to 40 m; however, most of the caves are carved into the lower section of the cliff, where it is near-vertical and 18–23 m in height. The cliff is honeycombed with caves, excavated in some areas in as many as four levels and in a few cases even five levels.

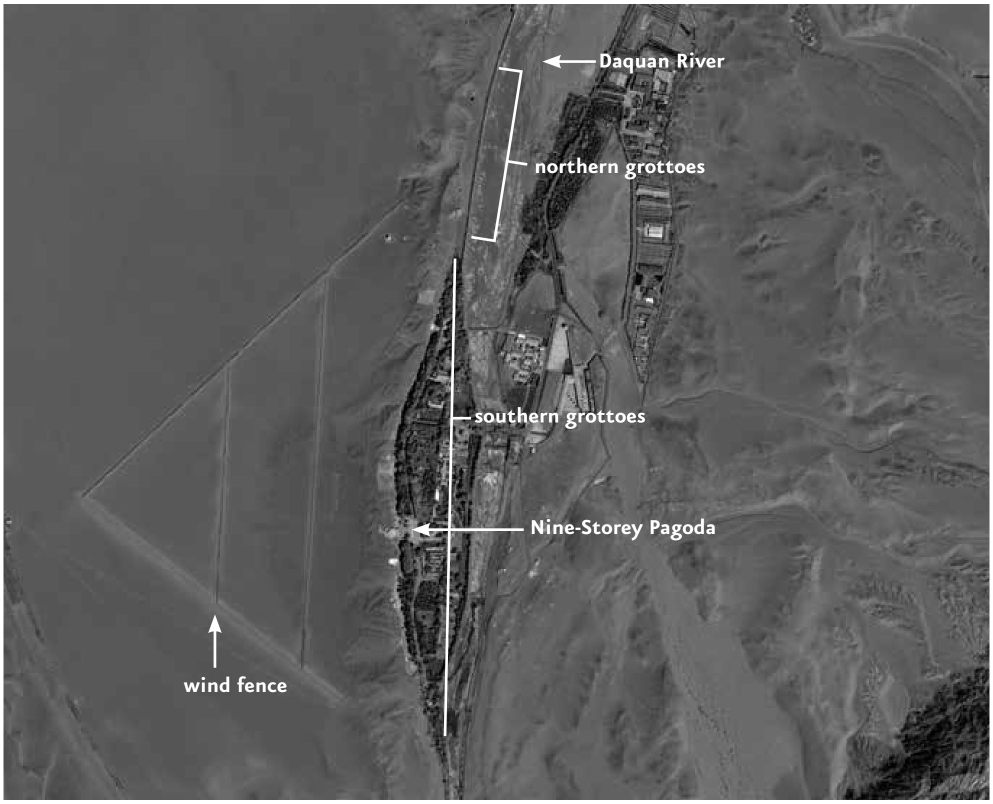

Fig. 5.3 The location of the northern and southern grottoes, the Nine-Storey Pagoda, the Daquan River, and the wind fence on top of the cliff (to reduce sand migration into the grotto zone) are marked on this satellite map of the site.

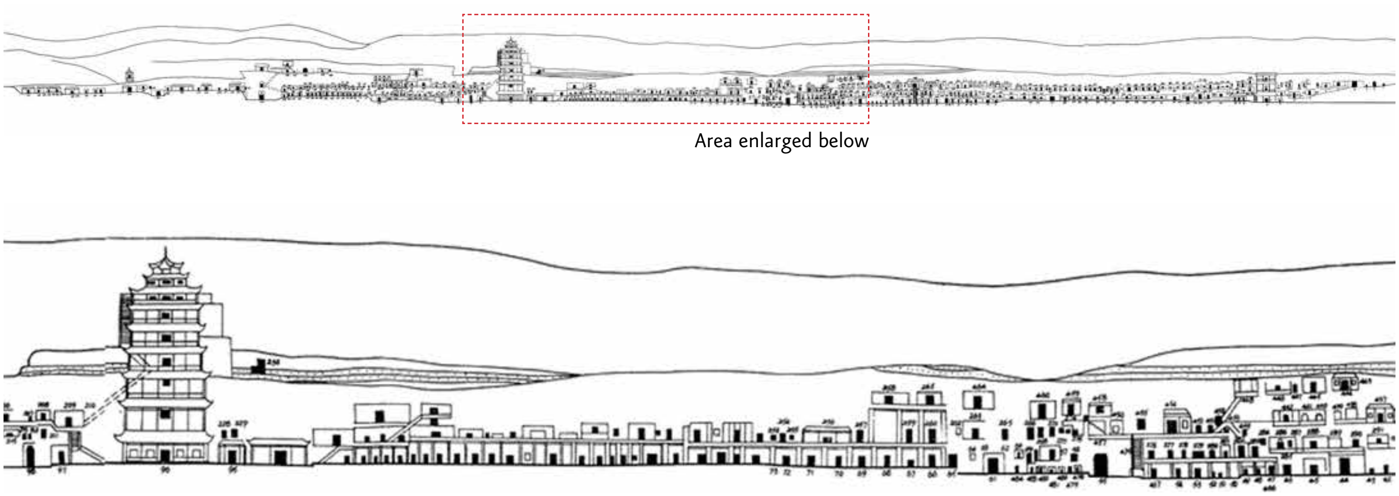

Fig. 5.4 The 735 rock-cut caves are excavated along 1.6 km of cliff face that runs in a north-south direction. This is an elevation of part of the southern grottoes where most of the decorated caves are situated.

Fig. 5.5 There are 248 caves in the northern section of the grottoes. Most are undecorated and were used as living quarters for meditation, storage, or burial. There is no modern concrete facade on this stretch of the cliff face, and many of the caves have no doors.

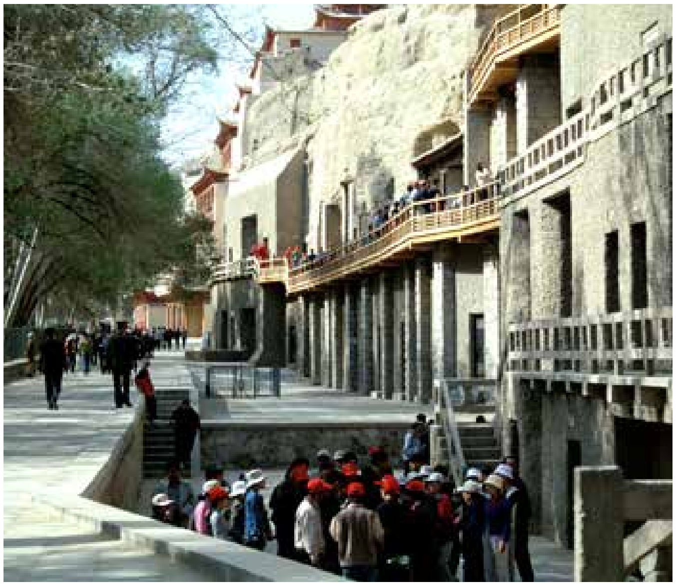

Fig. 5.6 Part of the southern section of the grottoes. The Nine-Storey Pagoda is visible in the distance.

The entire site consists of 735 caves, which are divided into a northern and southern section of the cliff face (fig. 5.4). The 248 caves in the northern section were used primarily as living quarters or for meditation, storage, or burial; all but five are undecorated (fig. 5.5). The 487 caves concentrated in the southern section of the cliff served as temples and meditation niches and were decorated with wall paintings and sculpture (fig. 5.6). The decorated caves, which between the northern and southern sections total 492 in number, contain some 45,000 m^2 of wall paintings on earthen plaster and over 2,000 polychrome statues sculpted in the same plaster on an armature of wooden sticks and bundled reeds. The site constitutes a gallery of Buddhist religious art built over a period of one thousand years from the earliest caves of the Sixteen States period (366–439 C.E.) through to the Yuan dynasty (1271–1368). The surviving paintings in these caves date from between 480 and 1250.

History

In the late fourth century the central Asian trade routes, later collectively known as the Silk Road, were China's main link with its western neighbors. Dunhuang, also known as Shazhou (Sand District), was an important oasis, cultural center, trading hub, and military outpost at the northwestern limit of the empire. Since 111 B.C.E., Dunhuang had been a garrison commandery, its location near to the westernmost extent of the Han dynasty Great Wall (Whitfield 1995). From Dunhuang to the east, the Silk Road led to Chang'an (present-day Xi'an), the ancient capital of the Han empire (206 B.C.E.–220 C.E.). To the west, the Silk Road split into the northern and southern routes skirting the Taklamakan Desert. As the last stop for caravans to stock up on provisions, Dunhuang, or Blazing Beacon, in reference to the many beacon towers that were used to signal enemy movement, controlled the flow of traffic between the East and the West. Not far from Dunhuang, two stations guarded the two branches of the route to the west, Yangguan (Yang Gate) guarding the southern branch and Yumenguan (Jade Gate) the northern branch. Dunhuang was to remain an important center in China's political, economic, and military life until the end of the Tang dynasty.

The Mogao Grottoes were founded in 366 C.E. by a wandering monk, Yue Zun, who was drawn to the tranquillity of the site and after seeing a vision of a thousand golden Buddhas, chiseled out the first cave. Soon after another monk, Fa Liang, added a second cave. The origin of the site is traced to these two monks.[3] The cliff, originally known as Miaoyan (Wonderful Cliff) and Xianyan (Precipice of the Immortals), already had a reputation as a sacred site. In the following thousand years,

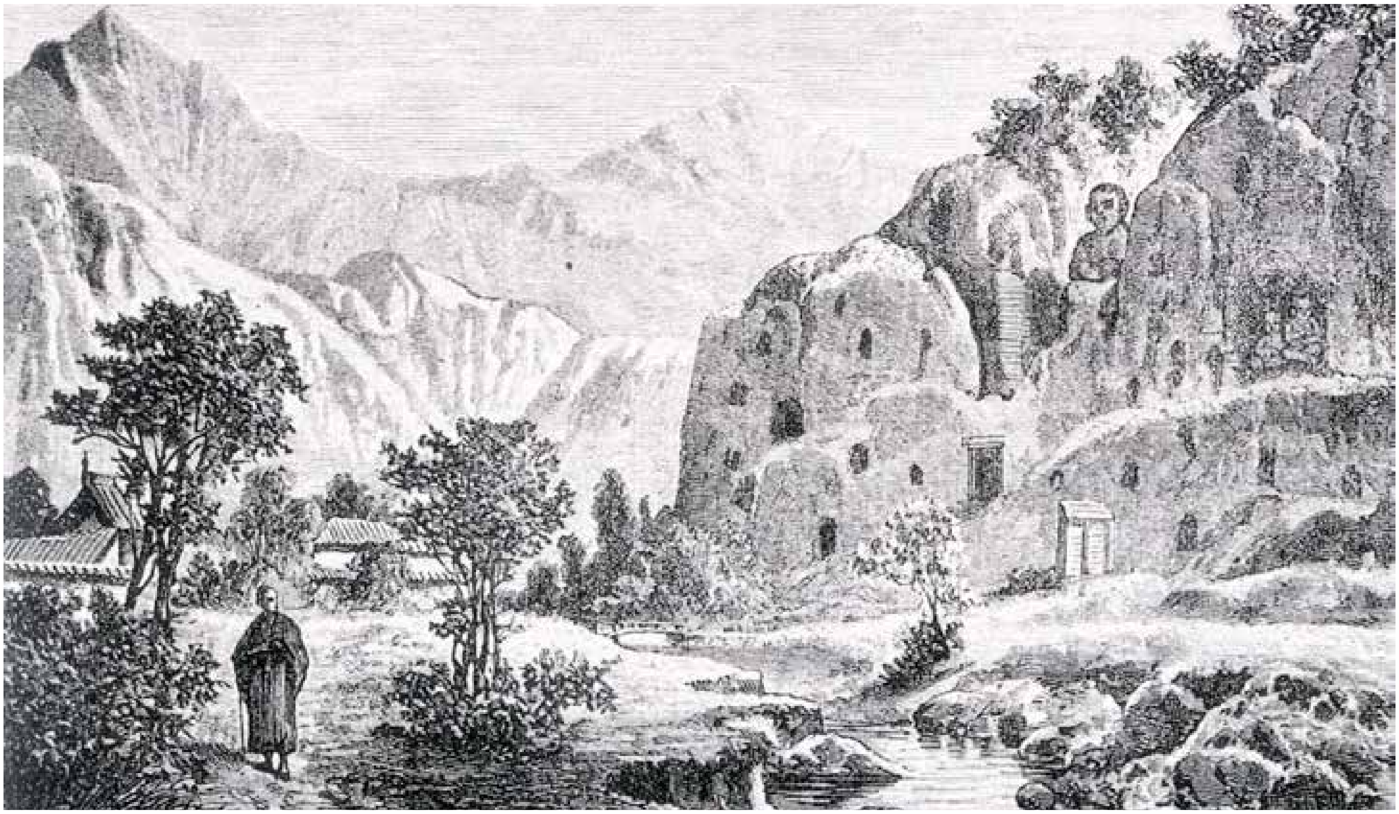

Fig. 5.7 A Hungarian, Lajos Lóczy, visited the site in 1878 and produced this engraving. The colossal Buddha of Cave 96 is depicted at right.

as many as one thousand caves were hewn from the cliff. An unknown number have been lost to earthquake and erosion over the centuries.

The site, because of its proximity to Dunhuang, became one of the most important religious centers along the Silk Road. Travelers would stop to give thanks or to pray for protection before or after their often hazardous journeys around the forbidding Taklamakan, and wealthy individuals from the local elite would sponsor the excavation and decoration of caves in order to achieve karmic merit. Over time the grottoes developed into an important monastery and center of Buddhist art and culture.

The Silk Road declined during the Ming dynasty (1368–1644), and China's westernmost borders contracted. Essentially, Dunhuang was abandoned by the empire until the mid-Qing dynasty (1644–1911), when China once again expanded its territory. The first known modern visitor from the West was the Hungarian Lajos Lóczy in the nineteenth century (fig. 5.7).

In 1900, what is now known as the Library Cave (Cave 17)—a treasure trove of documents and sutras written in various languages—was discovered by the Daoist monk and caretaker Wang Yuanlu (fig. 5.8). Wang sold many of these manuscripts to foreign explorers, sinologists, and treasure hunters for a pittance.[4] During the first two decades of the twentieth century, tens of thousands of items, including ancient manuscripts, silk paintings, mural paintings, and sculptures, were removed from the site (Ma 1995, 305) (fig. 5.9). The loss of so many important historical works led belatedly to a renewed interest in the site by Chinese authorities and scholars. The site suffered other depredations as well. For instance, in the early 1920s, following the Russian Revolution, the caves suffered damage when they were used as living quarters by White Russian émigrés.

The Dunhuang Academy, formerly known as the Dunhuang National Art Research Institute, was established by the Chinese government in 1944 as guardian of the site. The first director, Chang Shuhong, his successor, Duan Wenjie, and the present director, Fan Jinshi, are credited with instigating the overall plan of site stabilization, management, documentation, research, and publication at the site (Fan 1997).

In 1961, the State Council of the People's Republic of China listed the Mogao Grottoes as a nationally protected site—the same status accorded such other important cultural sites as the

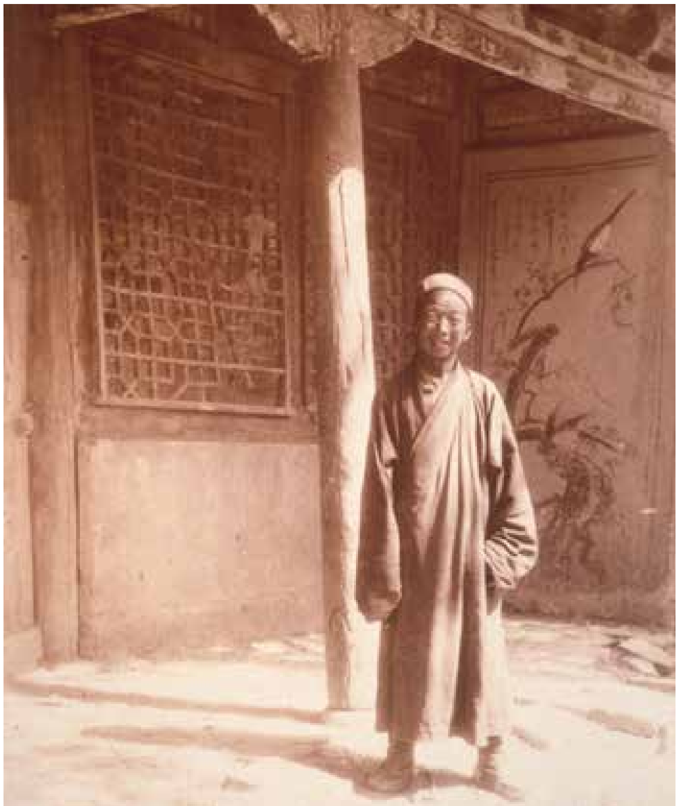

Fig. 5.8 Daoist priest and caretaker Wang Yuanlu shown in front of Cave 17, the famous Library Cave, discovered in 1900.

Fig. 5.9 The Library Cave was one of the greatest treasure troves of documents and sutras ever found.

Great Wall and the Forbidden City. It was subsequently included in the first list of sites for inscription on the World Heritage List after the country ratified the UNESCO Convention Concerning the Protection of the World Cultural and Natural Heritage on December 12, 1985. The Mogao Grottoes were formally inscribed on the list in 1987, confirming its outstanding universal value as a cultural and historic site (fig. 5.10).

Fig. 5.10 Official sign at the Mogao Grottoes indicating that the site was formally inscribed on UNESCO's World Heritage List in 1987.

Notes

1. The Mogao Grottoes is one of five Buddhist cave temple sites in the Dunhuang region. The others are the Western Thousand Buddha caves, the Eastern Thousand Buddha caves, the Yulin caves, and the Subei Wugemiao caves.
2. North latitude 40°02' and east longitude 94°48'; elevation 1,300 m.
3. From *An Account of Buddhist Shrines* (Mogaoku Fo Kan Ji) by Li Jun Xiu dated to 698 C.E., which recounts the earliest known activity at the site.
4. The Library Cave was walled up at the beginning of the eleventh century, possibly for fear that the contents would fall into the hands of invaders; the treasure remained hidden for nine hundred years. The foreigners who obtained works from Wang came from Britain, France, the United States, Russia, and Japan, and included, most notably, Aurel Stein, Paul Pelliot, Sergei Oldenburg, and Langdon Warner.

CHAPTER 6

Geology and Geomorphology

Issues of climate, geomorphology, and structural geology play a dual role in the survival and deterioration of the site. The desert environment of this part of the Hexi Corridor—the ancient geographic connection between China's heartland and the western regions—ensured preservation of the art. Oases like Dunhuang, fed by snowmelt from the Qilian Mountains to the south, the easternmost spur of the Himalayan massif, provided the water essential for settlement and agriculture. However, the area is also one of tectonic activity, and thus of seismic threat. Evidence of tectonic forces can be seen in the satellite image by the clearly demarcated faults that converge at the site and define the Sanwei Mountains (fig. 6.1; see also fig. 6.2).

Fig. 6.1 Large-scale satellite image of the Dunhuang region. The Mogao Grottoes are 25 km by road to the southeast of Dunhuang City, with the Sanwei Mountains to the northeast and east, the Mingsha Dunes to the west, and the Qilian Mountains to the south.

Geological Formation and Setting

The Sanwei basement gneiss has been upthrust in the area of the grottoes and juxtaposed to Pleistocene-epoch alluvial and pluvial deposits composed of conglomerate, gravel, and sand in excess of 200 m thick (Tanimoto et al. 2010, 191). These sediments, the Jiuquan formation, derived from the Qilian Mountains. The Mogao Grottoes are excavated into a cliff face composed of this soft conglomerate on the west bank of the Daquan River, which flows near the base of the cliff. To the immediate west of the grottoes, on the plateau above the cliff, large eolian crescent-shaped sand dunes, the Mingsha Dunes, overlie the conglomerate (fig. 6.3). These too can be seen in the satellite image, as can extensive sedimentary fan deposits from the Qilian and Sanwei Mountains.

The Mogao Cliff Face

The easily excavated conglomerate and the vertical cliff face undoubtedly were among the reasons for the choice of the site

Fig. 6.2 The fault between the recent conglomerate and the ancient Sanwei Mountains looking north (a). The Daquan River follows this fault running in a northerly direction. The Mogao Grottoes are identified by the cluster of trees in an otherwise barren landscape (b).

Fig. 6.3 The Gobi Desert extends several kilometers west of the site to the Mingsha Dunes.

in the fourth century; at the Western Thousand Buddha caves and Yulin Grottoes near Dunhuang similar suitable geological formations and topographical features are found. Certainly, in the Sanwei Mountains the rock is too hard for excavation; nor do vertical rock faces exist that would allow the creation of cave temples of the size and number found at Mogao. The cliff height varies from some 10 to 40 m along the 1,680 m length of the site (Sun 1997, 159); however, most of the caves are excavated into the lower section of the cliff, where it is vertical and 18–23 m high. Four groups of conglomerate formation exist; the caves, including Cave 85, are generally situated in the C and D layers (fig. 6.4).

Cementation of the coarse conglomerate is poor and therefore not suited for fine sculptural carving but allowed easy excavation of the caves. Consequently, the sculpture at Mogao was modeled from clay on wood and fiber armature rather than carved in stone as at other grotto sites such as Yungang in Datong, Shanxi Province, and Longmen in Luoyang, Henan Province.

Geological Threats

Weathering and Erosion

Poor cementation makes the conglomerate susceptible to weathering and erosion from wind and sand (fig. 6.5). Wind-driven sand from the Mingsha Dunes has abraded the upper levels of the cliff, in some instances cutting through the roof of caves, exposing the painting and sculpture to sand, rain,

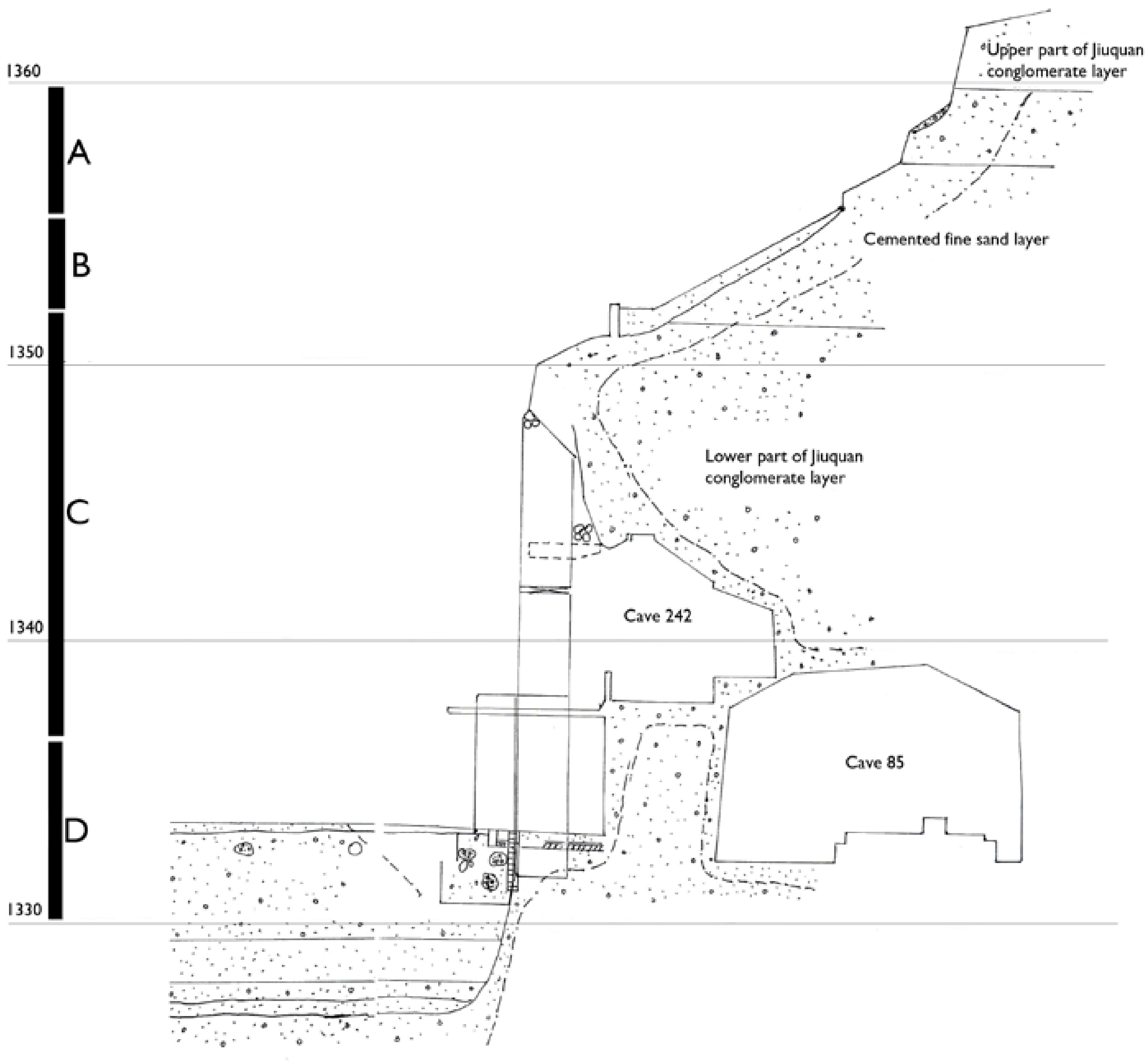

A Layer
6.8 m thick
cobbled conglomerate:
- gravel 81%
- sand 16%
- silt/clay 3%

average particle size: 15.7 mm
UCS = 100 kg/cm²

B Layer
2.0 m thick
siliceous sandstone including pebbles:
- gravel 16%
- sand 79%
- silt/clay 5%

average particle size: 0.17 mm
UCS = 126–160 kg/cm²

C Layer
14.5 m thick
cobbled pebble conglomerate:
- gravel 74-79%
- sand 19–24%
- silt/clay 2%

average particle size: 5.2-12.2 mm
UCS = 86–124 kg/cm²

D Layer
6.0 m thick
granular conglomerate (very pebbly):
- gravel 50–60%
- sand 35–45%
- silt/clay 5%

average particle size: 2.0–3.8 mm
UCS = 160–190 kg/cm²

Fig. 6.4 Four groups of conglomerate formation (A–D) are present within the cliff face. Most of the caves were carved into the lower section of the cliff where it is nearly vertical. The caves are generally excavated in the lower C and D layers, as Caves 242 and 85 are in this section. This drawing also shows construction detail of the concrete facade built in the 1960s to stabilize the cliff face and allow for the installation of security doors on all the decorated caves.

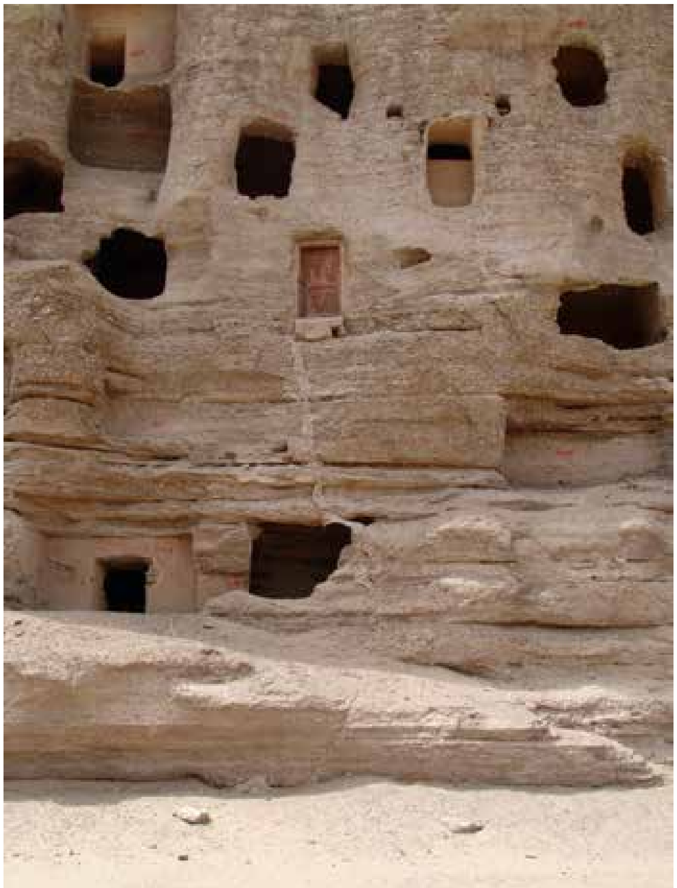

Fig. 6.5 Exposed conglomerate with interbedded lenses of friable sandstone in the northern section of the site. The meditation and habitation cells are mainly undecorated in this area. The poor cementation of the conglomerate making it susceptible to weathering and erosion is evident here.

and snow. The erosion rate of the cliff has been estimated to be 1 cm per annum.

Structural Cracks

Not only is the Pleistocene conglomerate structurally weak—it is geologically young and poorly cemented by calcareous minerals, clays, and silt, with variable amounts of soluble salts—but the cliff face displays extensive structural cracks, principally parallel to the face but also perpendicular and horizontal to it. Horizontal cracks follow bedding planes. There are two contributory causes for this phenomenon: the natural tendency of a cliff to develop cracks parallel to the face due to unconfined pressure stresses from the rock body and the proliferation of cave excavation over the centuries, which has weakened the remaining rock in excess of its structural capacity. This weakening, and the consequent grave threat of collapse, was early on recognized by the Dunhuang Academy and led to structural stabilization of the cliff, beginning in the 1950s, through construction of a concrete buttress facade (Sun 1997).

Structural rock cracks therefore predominate in areas of intensive excavation of caves, for example, in the central area of the site, where four levels of caves exist (Caves 448–443; and those below: 453–438, 449–290, and 49–44) (figs. 6.6, 6.7). Cave 85 by contrast, has only two caves above it (242 and 243), and has not been weakened by honeycombing to the same extent (see fig. 6.4). Cave 85, however, has lost its original entrance and most of the antechamber, presumably through collapse of the rock in previous times (see chap. 8).

Flood

The fan deposits, as shown in the satellite image (see fig. 6.1), provide striking visual evidence of the periodic floods that continue to threaten the ground-level caves of the site (and, incidentally, modern infrastructure on the floodplain to the north of the grottoes, notably the new railway station and airport). Burial of cave entrances by windblown sand from the dunes during the period of abandonment of the site between the Ming and mid-Qing dynasties resulted in wicking of moisture into the caves during flood and rain events (figs. 6.8, 6.9). Several times in the past three decades the Daquan River has flooded. In 1979, flood resulted in damage to the wall paintings in caves at the base of the cliff, and most recently, in June 2011, floodwater overflowed the banks of the river (Kuchitsu and Duan 1997) (fig. 6.10). Measures to protect the caves, principally by channeling the Daquan River, have long been implemented

Fig. 6.6 In some areas of the cliff face where caves are concentrated, there are three and four levels of excavated caves. The white box indicates the location of Caves 444, 439, 290, and 44, a particularly dense section of caves shown in fig. 6.7.

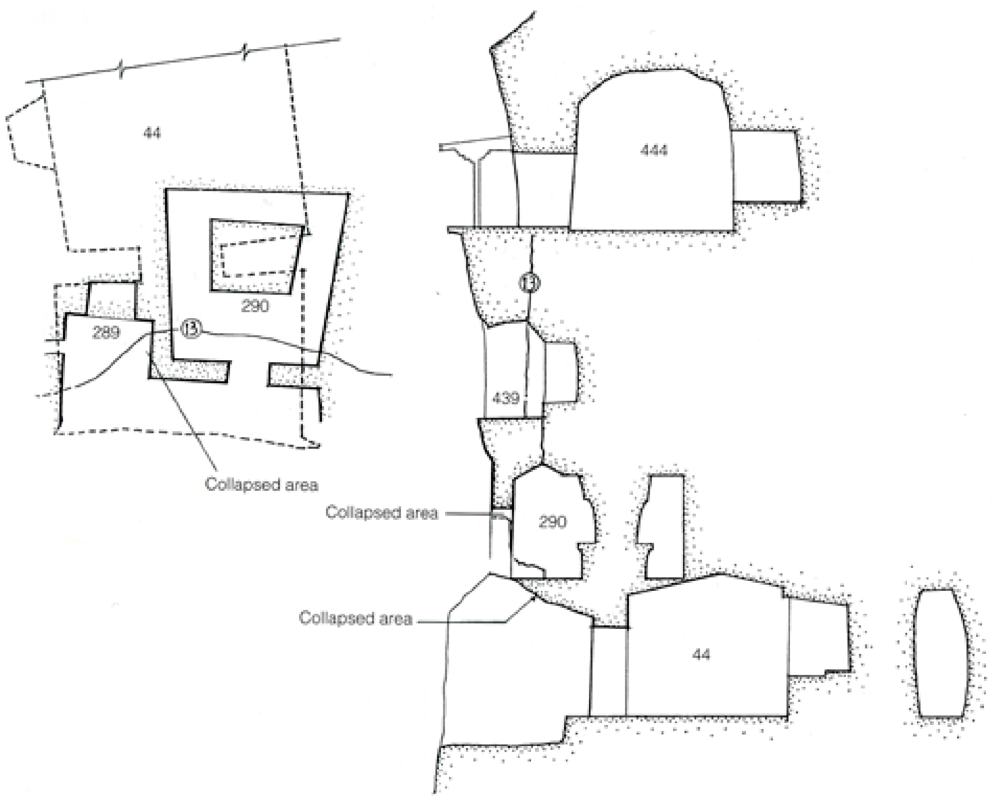

Fig. 6.7 Section of Caves 444, 439, 290, and 44 with areas of collapsed cliff face and structural cracks indicated. The excavation of Cave 44 during the Tang dynasty contributed to the collapse of the front part of Cave 290 and neighboring Cave 289. The structural crack, parallel to the cliff face, is marked with the number 13. (sun, 1997, 164).

Fig. 6.8 Windblown sand filled many of the cave entrances. Once wetted the sand often caused loss of painting at the base of the walls in decorated caves.

Fig. 6.9 Exposed conglomerate with soft sandstone layers at the base of the east wall of the main chamber of Cave 85 where the earthen plaster has been lost as a result of past flooding. White efflorescence is due to soluble salts.

by the Dunhuang Academy and are effective, but downstream infrastructure, such as the road to the site and the bridge, has been severely damaged.

Earthquakes

Seismic activity over the 1,600 years of the site's existence has resulted in great loss through the collapse of caves, themselves weakened by the honeycombing of the cliff face due to excavation with consequent development of structural weakness (Sun 1997) (see chap. 15).

Cave 85

Taking all the large- and small-scale factors into account when considering the overall preservation and conservation issues relative to Cave 85 has proven complex. It would seem that geological inhomogeneity of the conglomerate in the west wall of the cave may have facilitated the migration of water vapor (not liquid water) through the porous conglomerate to the surface, with accumulation of salts over time. Consequently, damage to the wall paintings and extensive separation of the painted earthen plaster from the underlying mother rock occurred. One cannot be sure that geological inhomogeneity, if it exists, is a contributor to the deterioration as the plaster is still intact (and thermal imaging to identify anomalies has not been successful), but elsewhere on the site, for example, where no facade or painted plaster exists, as in the northern section of the grottoes, it is apparent (fig. 6.11).

In summary, we see how the forces of nature, climate, geology, and land forms have all played significant roles in the history of the Mogao Grottoes. First, they have afforded the essentials for the founding of the site, the water necessary for the life of the monastic community, and mud and sand from the Daquan River for plastering the rough-cut caves in preparation for their painting. But, second, they have also been the source of damage: seismic, flood, wind and sand erosion, and soluble salts (mainly sodium chloride) derived from the alluvial sediments and the bedrock (see chaps. 15, 16).

Fig. 6.10 The Daquan River overflowing its banks in June 2011.

Fig. 6.11 Inhomogeneity of the conglomerate, which has led to preferential weathering and erosion, is visible in this section of the northern grottoes.

CHAPTER 7

Climatic Conditions

The climate of the Dunhuang region is arid, though sporadic periods of rain during the summer months and occasional snow in winter result in wide variations of temperature and humidity throughout the year: cold and dry in winter and hot and more humid in summer. The Köppen-Geiger system of world climate classification places Dunhuang in the cold desert (*BWk*) climate. The area is mostly sunny, with a light breeze throughout the year. However, dust storms and sandstorms are common in spring.

Climate Monitoring

Climate data at the Mogao Grottoes site have been collected since September 1989 using an autonomous weather station[1] installed on top of the cliff at the central part of the southern (decorated) grottoes area (latitude 40° 2' 14" N, longitude 94° 48' 15" E, elevation 1,320 m) (fig. 7.1). The station records air temperature (AT), humidity (RH), wind speed and direction, solar radiation, precipitation, and ground surface temperature every fifteen minutes. This chapter presents summaries of the data collected between 1990 and 2008.

Fig. 7.1 The weather station at the top of the cliff records air temperature, humidity, wind speed and direction, solar radiation, precipitation, and ground surface temperature every fifteen minutes.

Air Temperature

The site's annual average temperature was 11.3°C over eighteen years, from 1990 to 2008. Air temperature extremes reached −23.4°C in February 1991 and 39.9°C in July 1999 (fig. 7.2). Highest monthly mean temperatures annually were recorded in July, with the lowest reported in January. Monthly mean temperatures ranged from −15°C to −4°C in January and 24°C to 28°C in July. Larger temperature variations were recorded more often in winter than in summer. Daily averages ranged from −12°C in December and January to 28°C in June, July, and August. Diurnal temperature variations were from 10°C to 15°C, typical for a desert environment.

Humidity

The site is arid. Typically, relative humidity varies between 10% and 30% in summer and between 20% and 50% in winter (fig. 7.3). However, occasional high humidity, snow, and rain events (usually less than a few days) can cause spikes of relative humidity above 50%. Rain events are normally preceded and followed by periods of high humidity. Sometimes a weather system brings only humid air without measurable rainfall.

More of these humidity spikes are found in the summer months of June, July, and August. Otherwise, a typical daily variation is 10% to 30% RH (fig. 7.4). Due to normally short durations rain

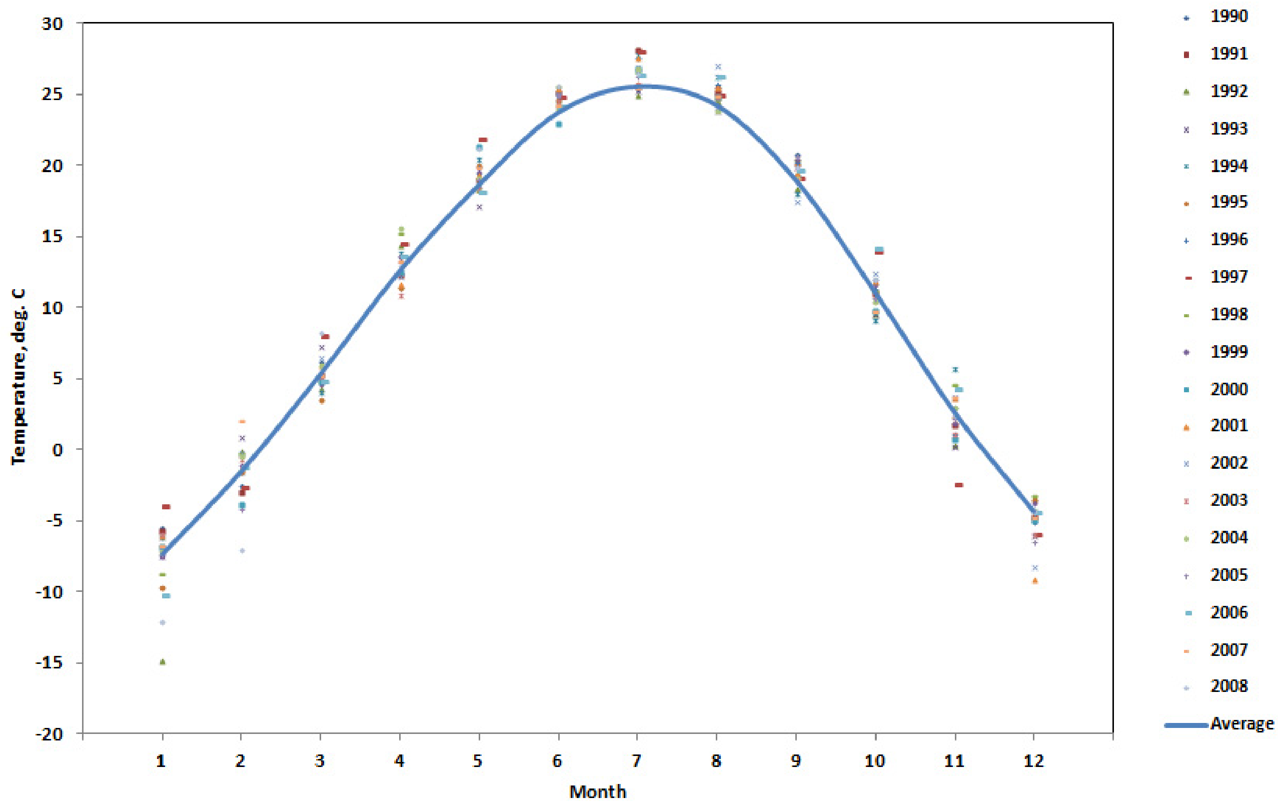

Fig. 7.2 Monthly average of site temperature between 1990 and 2008.

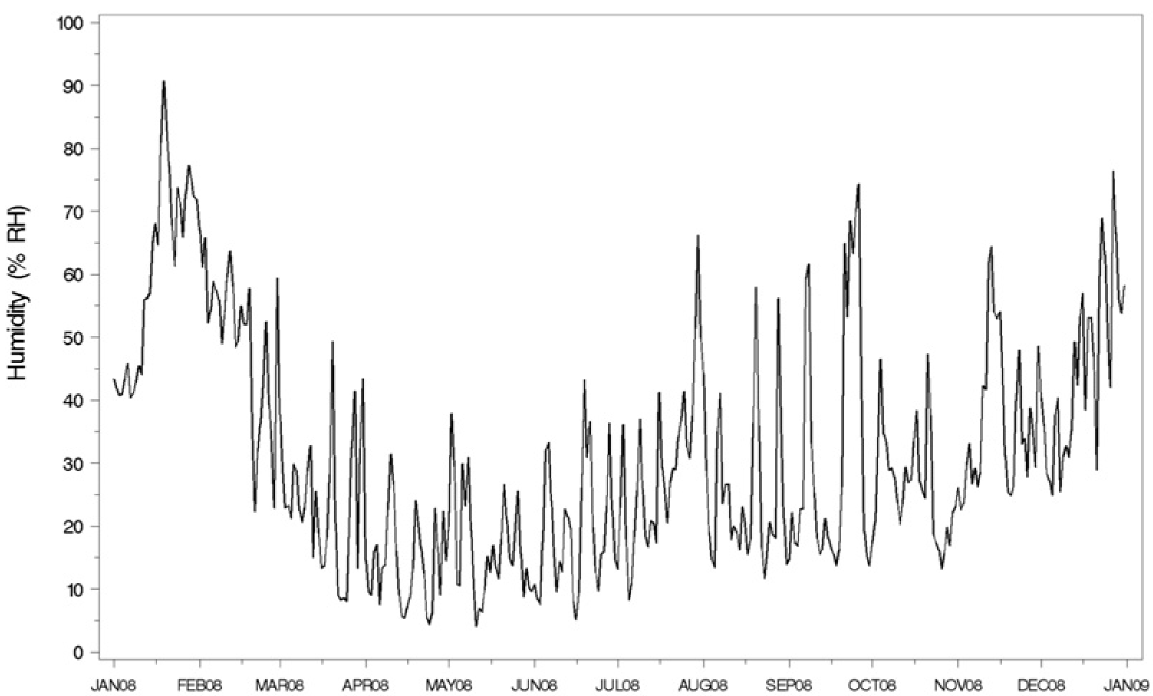

Fig. 7.3 Daily means of relative humidity in 2008 (a typical year).

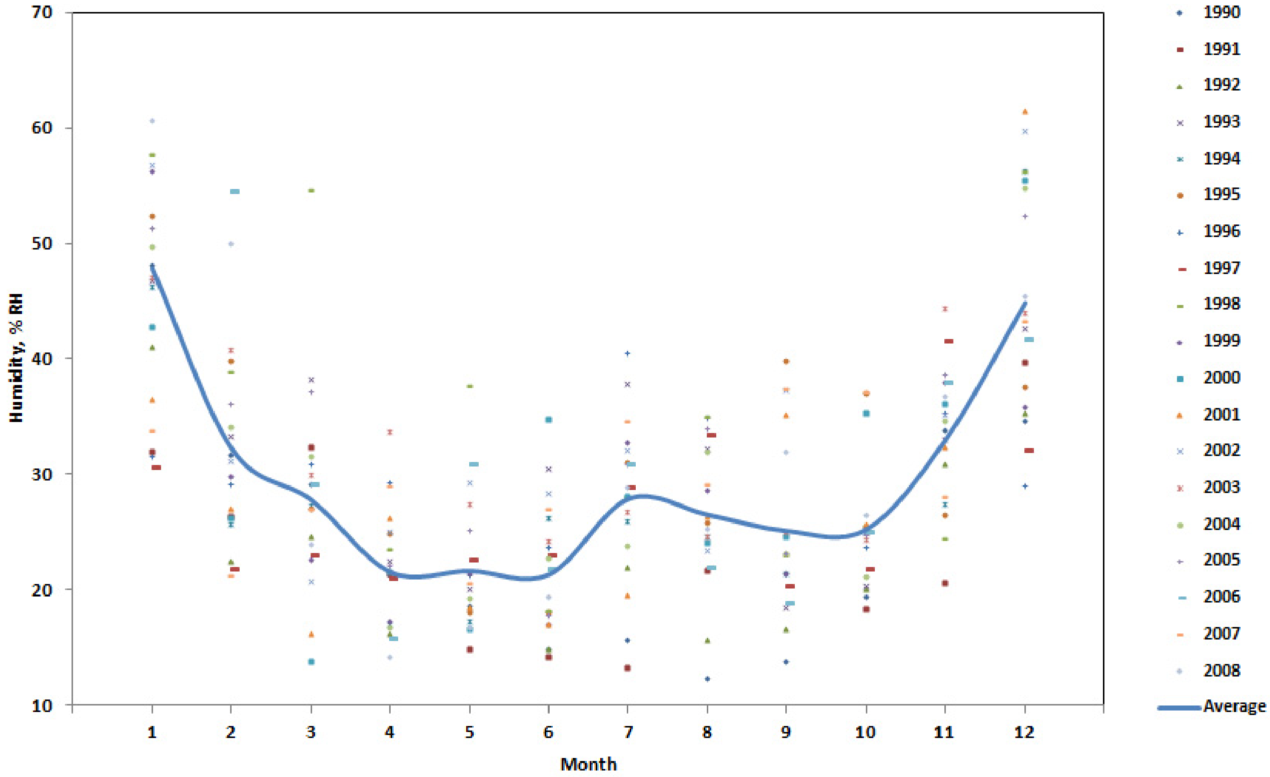

Fig. 7.4 Monthly average of site relative humidity between 1990 and 2008.

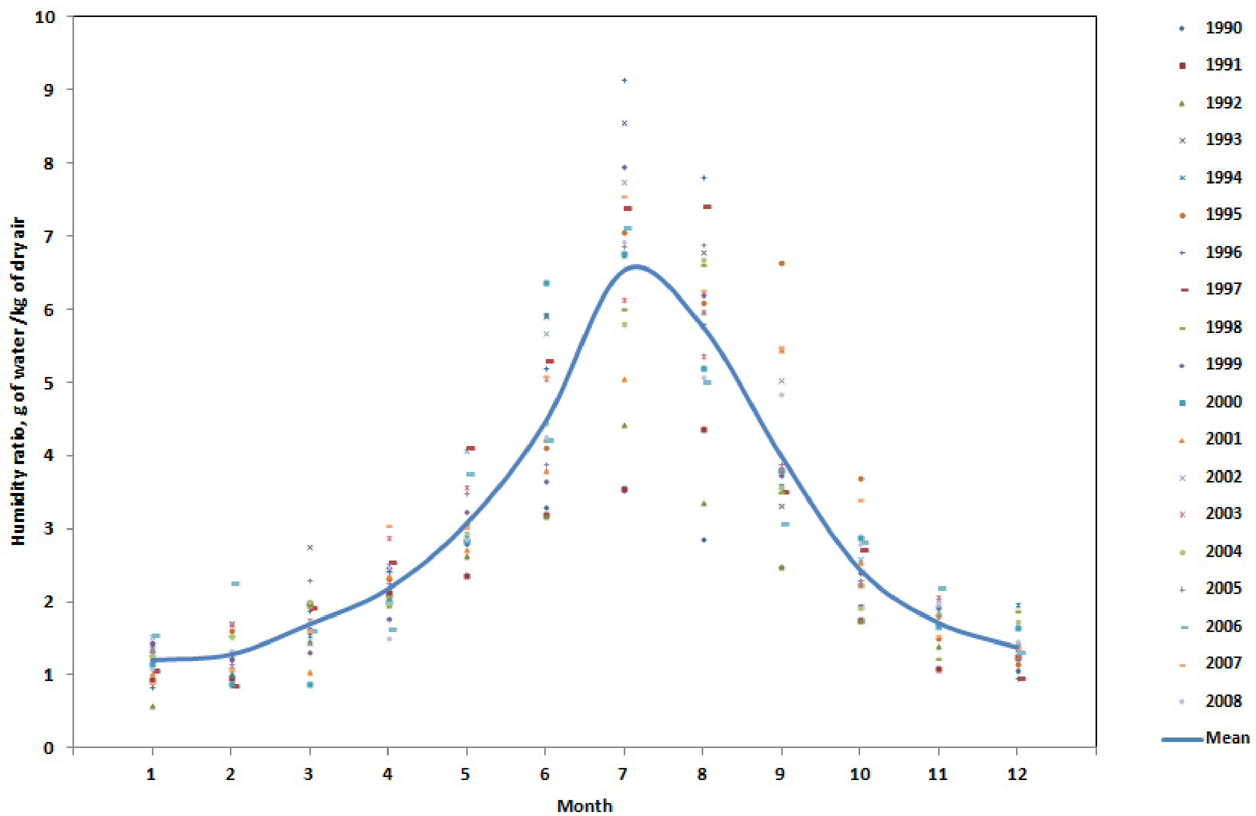

Fig. 7.5 Monthly average of humidity ratio (calculated from temperature and relative humidity) between 1990 and 2008.

Fig. 7.6 Summer rainfall approaching the site (a); visitors on a group tour in the rain (b).

events do not affect monthly means of the humidity, and the RH remains below 30%. However, when multiple or sustained rain events occur in a month, such as June and July 1993, September 1995, July 1996, and June 2000, monthly means can rise above 30% RH.

Relative Humidity and Humidity Ratio

Relative humidity is defined as the percent ratio of the amount of water vapor in the air to the saturation amount that the air can hold at a given temperature. Since saturation moisture exponentially increases with air temperature, relative humidity decreases when the air temperature rises and increases when the temperature falls. At the Mogao Grottoes, humidity of the outside air is higher in winter and lower in summer, as described in the previous section. However, this condition is reversed in the caves (see chap. 14). This can be explained by the temperature-humidity (psychrometric) relationship of air. In summer the average daytime condition of outside air is 30°C and 20% RH, and the cave's air temperature is approximately 18°C. The outside air infiltrates the cool cave, and the cooling process increases the humidity of air to 41%. In winter, typical outside air, −5°C and 50% RH, enters caves and is heated to 3°C. The heating process reduces the relative humidity to 4%.

When a psychrometric process is at constant temperature, relative humidity is a good measure of the moisture content of air. However, when temperature differences are involved, it is essential to use the actual moisture content of air rather than relative humidity. The amount of moisture contained in the air can be expressed as the humidity ratio (W) in grams of water per kilogram of dry air (g/kg).

The 19-year average of the humidity ratio shows the annual low at approximately 1 g/kg in January and February and the high at 6.6 g/kg in August (fig. 7.5). Variations are small in the winter months but significantly larger in the summer months due to occasional humid and rainy days in some years. The humidity ratio increased to 8–18 g/kg during summer rains, but these values normally returned to typical ones, 5–7 g/kg in less than 24 hours except in months with major rainfall, such as June 1993, July 1996, and June 2000. Monthly means of the humidity ratio ranged from 8.5 to 9.2 g/kg in those months.

Precipitation

The site's annual precipitation averaged approximately 32.9 mm between 1990 and 2008, while Dunhuang City reported 40.4 mm/year between 1937 and 1990 (www.worldclimate.com/). Precipitation occurred as snow during the winter

Fig. 7.7 A rare heavy snowfall. Northern grottoes area (a) and southern area with the Nine-Storey Pagoda visible (b).

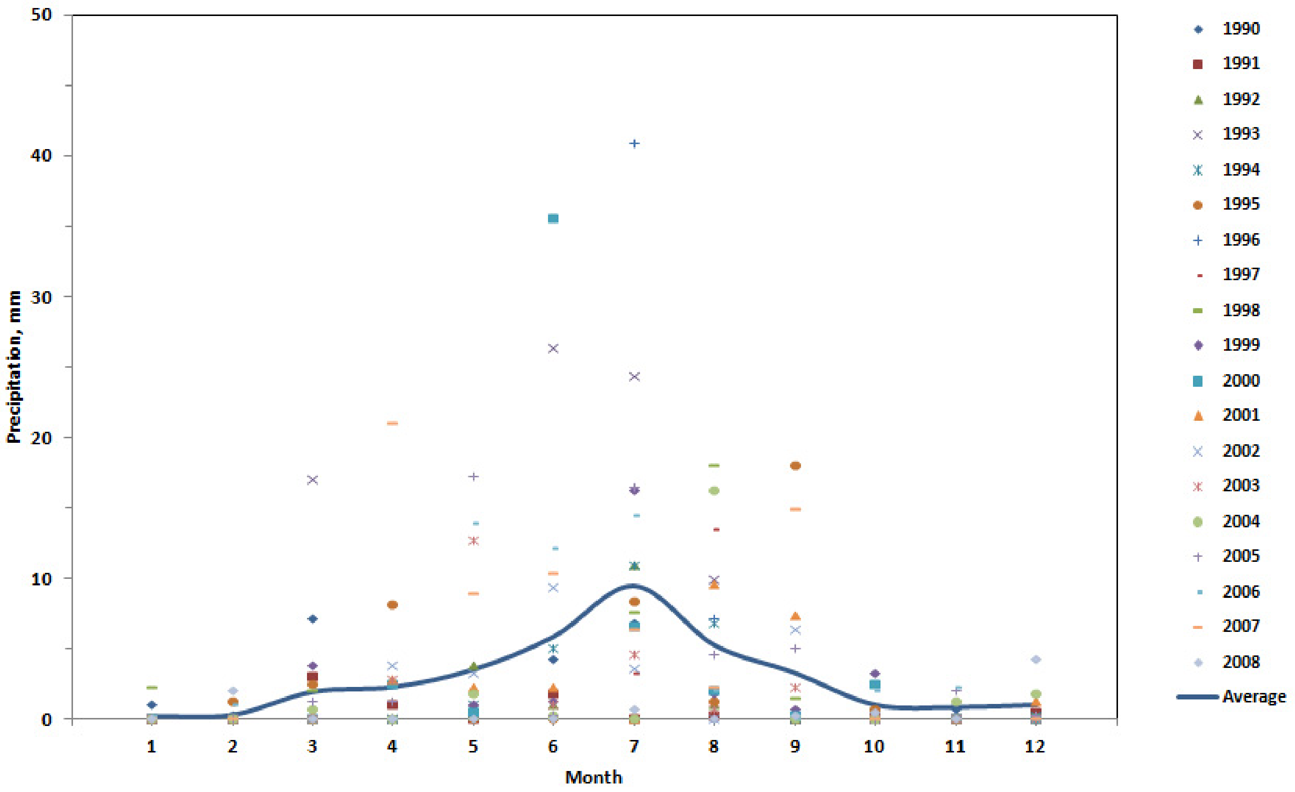

Fig. 7.8 Monthly totals of precipitation between 1990 and 2008.

YEAR	MONTH	DURATION (HR)	AMOUNT (MM)
1993	JUNE	25.50	23.1
	JULY	5.25	3.8
		17.75	20.3
1995	SEPTEMBER	72.00	18.0
1996	JULY	104.50	35.8
1998	AUGUST	46.00	15.5
1999	JULY	111.75	13.5
2000	JUNE	78.75	33.0
		5.25	3.8
2004	AUGUST	6.75	14.0
		2.75	2.3
2005	MAY	15.25	9.1
		12.25	8.1
	JULY	31.00	16.3
2006	APRIL	0.50	0.5
		4.00	7.9
		6.50	8.1
		5.25	4.6
	SEPTEMBER	6.25	4.8
		12.25	9.1

Table 7.1 Duration and Amount of Rainfall Recorded during Major Rain Events (1990–2008)

months and as rain for the remainder of the year (figs. 7.6, 7.7). Though generally low, there are significant variations from year to year: from 6.9 mm in 1991 to 78.5 mm in 1993.

Rain events are primarily concentrated in the summer months—June, July, and August (fig. 7.8). Monthly total rainfalls also varied greatly. Amounts exceeding the annual average were recorded twice, 40.9 mm in July 1996 and 35.6 mm in June 2000, over the 19-year period.

Normally, a rain event during summer lasts only a few hours. However, between 1990 and 2008 several sustained rain events were recorded (see table 7.1). The intensity of rainfall also varied significantly. For example, in June 1993, 23 mm fell over a 26-hour period; in July 1993, 20 mm fell over an 18-hour period; in July 1996, 20 mm fell over a 4-day period; and in June 2000, 33 mm fell over a 3-day period. Recently, in July 2011, 40 mm fell over a 15-hour period. Therefore, the amount of rainfall and the duration of rain may not coincide.

Wind Speed and Direction

The prevailing wind in the Dunhuang area is the Westerlies. The wind is stronger in winter. Weather systems as well as desert dust are transported by the wind from west to east. However, surface winds are caused by localized atmospheric pressure gradients generated by the daily solar heating and cooling of surrounding geographic features such as mountains and lower flat basins.

Mean wind speed at the site was 4.3 m/s between January 1, 1990, and December 31, 2008. Variations were minimal, and the annual means ranged only from 4.2 to 4.5 m/s. Yearly wind rose diagrams indicate the presence of a consistent south wind up to 8–9 m/s, and weaker winds, mostly less than 5 m/s, between the northeast and northwest (fig. 7.9). Occasional strong northeast winds reaching 15 m/s also occur. The strongest winds, approaching 20 m/s, were recorded from the east-east-south. The average daily wind speed was between 3.6 and 4.7 m/s throughout the year but calmer in October, November, and December and stronger and more variable in May and June, with occasional strong winds reaching 10–15 m/s and stormy winds 20 m/s (fig. 7.10).

Due to a large amount of solar cooling of the mountains north of the site, a south wind at about 4 m/s is normally consistent from late evening to midmorning (fig. 7.11). During the day the wind shifts to the north due to substantial solar heating of the same mountains but with seasonally varying speeds. The night-to-day wind transition occurs at about noon and 7 p.m. in January and 10 a.m. and 11 p.m. in July, coinciding with sunrise and sunset in respective seasons. These changes take place within an hour.

These consistent wind patterns drastically change to turbulent ones that include easterly and westerly components when weather systems, which often bring rain and snow, pass through the site. These stormy wind patterns produce a wind component vertical to the orientation of the cliff face.

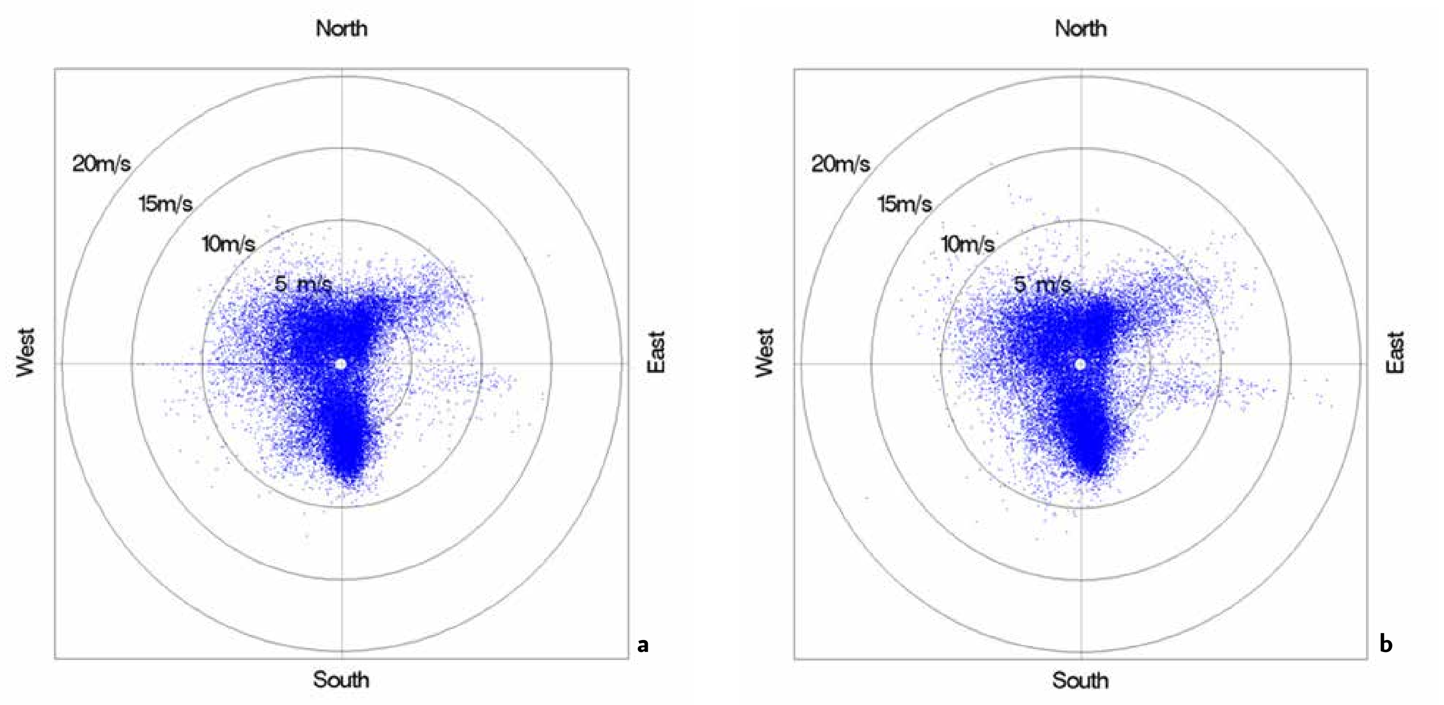

Fig. 7.9 Wind rose for two typical years at the site: 1998 (a) and 2005 (b). Each point represents a 15-minute average of the wind speed and direction.

Fig. 7.10 A dust storm on the road to the grottoes.

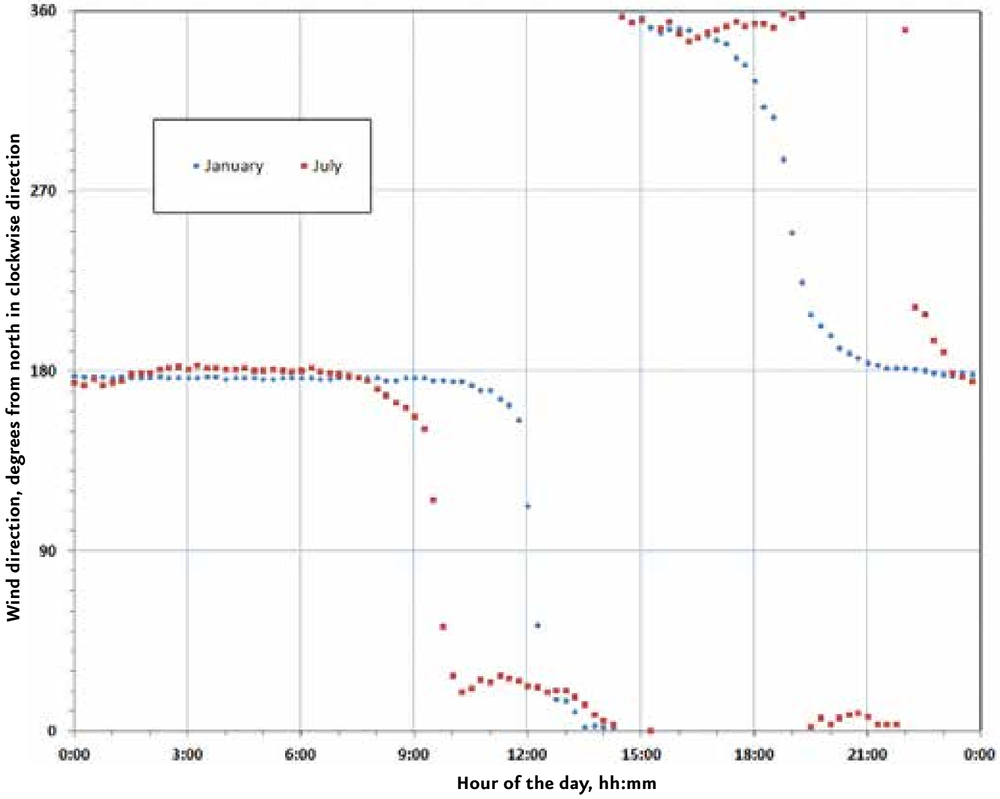

Fig. 7.11 Eighteen-year mean of 15-minute wind direction over a 24-hour period of a typical winter month (January) and summer month (July).

Solar Radiation

The site receives mean daily solar radiation (expressed as kilowatt-hour/m^2) with a maximum radiation of 7.06 in June and a minimum of 2.47 in January. These values indicate that most of the time the site has clear skies and receives full solar radiation (fig. 7.12).

Summary

Since its installation in September 1989, the DA-GCI autonomous weather station has been collecting climate data at the site. The low annual average temperature and precipitation confirmed the site climate as that of an arid cold desert according to the Köppen-Geiger climate classification. However, the moisture content of the air in summer months increases to approximately six times that of winter months. Highly variable rainfall in summer also produces an extended period of high humidity. Daily winds shift from north during the day to south at night, parallel to the cliff face of the site. However, the wind becomes turbulent in terms of both speed and direction during wind- and rainstorms.

Notes

1. The autonomous weather station, installed in September 1989 by the DA and the GCI, consists of environmental sensors mounted on a 2 m high metal tripod, Campbell Scientific Inc. (CSI) CR10X data logger, UHF radio telemetry device, and rechargeable battery with a photovoltaic panel. The sensors are Vaisala HMP 45°C temperature and relative humidity sensor, Licor LI200 solar radiation sensor, Texas Electronic 525 rain gauge, Met One 014 wind direction sensor, Met One 024 wind speed sensor, and Omega Engineering surface-mounting E-type thermocouple.

Fig. 7.12 Typical summer weather with clear (a) or partly cloudy (b) sky.

CHAPTER 8

Cave 85

Fig. 8.1 Cave 85, a ground-tier cave, lies just north of the Nine-Storey Pagoda in the southern section of the cliff face.

Cave 85 is situated midway along the 1.6 km cliff face, just north of the prominent Nine-Storey Pagoda that fronts Cave 96 and that houses the largest sculpture at Mogao—a 34.5 m high seated Maitreya Buddha (fig. 8.1). Cave 85 is a large, lower-tier cave.[1] Its entrance is 1.5 m below present-day ground level (Zhang 2000). What survives of the cave today comprises the partial remains of an antechamber, corridor, and main chamber with a truncated pyramid-shaped ceiling that is 6 m high at the walls, rising to approximately 13 m at the inset central ceiling panel (fig. 8.2).[2] During the Late Tang dynasty (848–907 C.E.), this type of cave architecture was common, as can be seen in Cave 16 of Mogao and Cave 25 of the nearby Yulin Grottoes.

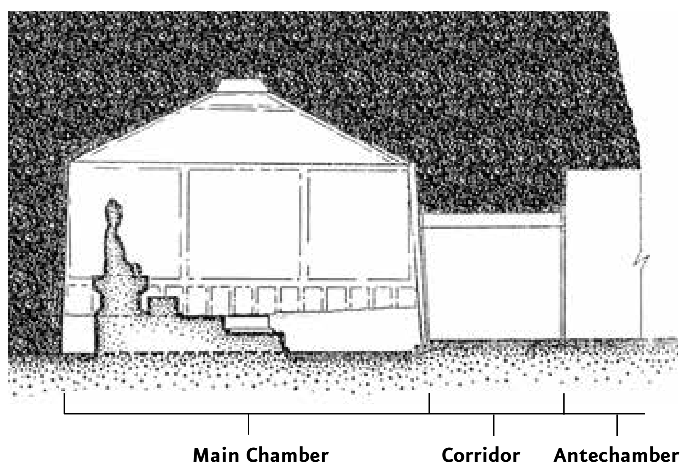

Fig. 8.2 Section of Cave 85 showing the main chamber with a truncated pyramidal ceiling, corridor, and partial remains of the antechamber.

The cave interior is decorated with 350 m^2 of wall paintings (fig. 8.3). The main scheme of painting is contemporary with the construction of the cave in the Late Tang dynasty. There are two later periods of localized redecoration from the Five Dynasties (907–60) and the Yuan dynasty (1271–1368). A polychrome sculpture group, also from the Late Tang, is situated on a large, horseshoe-shaped bed that rests on top of a larger, rectangular platform in the main chamber. The three sculptures were heavily restored at some point during the Qing dynasty (1644–1911) or Early Republic (1912–49).

Fig. 8.3 The walls and ceiling of Cave 85 are covered with 350 m² of painted plaster contemporary with the construction of the cave in the Late Tang dynasty. A heavily restored polychrome sculpture group, originally from the Late Tang, is situated on a large altar platform.

Prior to the current numbering system, Cave 85 was numbered 92 by Paul Pelliot in 1908 and 60 by Zhang Daqian in 1941–43 (fig. 8.4).[3]

History of the Cave

During the Tang dynasty (618–907) the Chinese empire expanded to its greatest extent—to be exceeded only one thousand years later in the Qing—and Mahayana Buddhism reached the summit of its popularity.[4] Decoration executed at the Mogao Grottoes during the Tang reflects the era's political power structure, economic prosperity, and cultural vitality, as well as the increasing importance of Buddhism, which attained new heights of elegance, refinement, and sophistication during this period (Murray 1994). Though remote from Chang'an (present-day Xi'an)—the cosmopolitan capital of the Tang—the decoration found at the Mogao Grottoes is thought to be strongly influenced by the art and religion of this city (Whitfield et al. 2000). Toward the end of the Tang dynasty, however, the influence and economic power of Buddhism came to be seen as a threat to the empire, and by 842–45 the government made attempts to suppress the religion through seizure of property and the forced secularization of monks and nuns.

The history of Dunhuang, located in the far western reaches of the Tang empire, differed slightly. Prone to attack from outside its borders, Dunhuang had fallen under Tibetan control by 781. It remained so until 848, when a local landowner, Zhang Yichao, led an uprising that expelled the Tibetans from the region and returned the area to Chinese rule. The period that followed was known as the Late Tang. Cave 85, with its wall

Fig. 8.4 Characters that read "Cave 60" are painted on the north wall of Cave 85's corridor. These are the remnants of the earlier Zhang Daqian numbering system.

Fig. 8.5 A statue of the high monk Hong Bian in the famous Library Cave (Cave 17).

painting and sculpture, was created during this period. Because of his deeds, Zhang Yichao was honored by the Tang emperor, Xuanzong (r. 846–59).[5] In 851, he was given jurisdiction over the eleven prefectures of the Hexi Corridor and named *jiedushi* (commander general) of the Guiyijun (Return to Allegiance Army). The army ruled this area until 1036 (Rong 1996).

According to the so-called Hong Bian stele, dated to the Tang dynasty and located on the west wall of the Library Cave (Cave 17), Zhang Yichao's actions were supported by the Buddhist high monk official of the time, Hong Bian. After the eviction of the Tibetans, Hong Bian was asked by Zhang Yichao to send one of his disciples, Wuzhen, to pay respects to the Tang emperor. The emperor acknowledged this gesture of loyalty by granting Hong Bian honorific titles (Li 1981). A statue of the famous monk is exhibited in the Library Cave (fig. 8.5).

Buddhism, already deeply rooted at Dunhuang, prospered further with the support of the Zhang family and the emperor. Nearly sixty caves were restored or constructed during the rule of the Zhang family, including Caves 9, 12, 94, 138 and Cave 85, all built to commemorate their meritorious deeds (Ma 1996). During the construction of Cave 85, Zhang Yichao's nephew, Zhang Huaishen, was the highest administrative official in the area, and therefore they were both depicted on the south wall of the corridor of the cave. The figures were painted over when the corridor was restored during the Five Dynasties. They are no longer visible in Cave 85.

Cave 85 was commissioned by Zhai Farong, who succeeded Hong Bian upon his death in 862 as the highest Buddhist official in the Dunhuang area. It was built to demonstrate the wealth of his family and to celebrate and commemorate his

Fig. 8.6 Document P.3720 from the Library Cave records the appointment of Wuzhen to the position of deputy monk in 862, inferring the promotion of Zhai Farong to chief monk. Zhai Farong commissioned Cave 85 in 862 to celebrate and commemorate this appointment. The document also details the erection of the Zhai family stele, which was originally placed in front of the cave but is now lost.

Fig. 8.7 Document P.4640 from the Library Cave is a copy of the inscription on the Zhai family stele. It records the start of construction of Cave 85 in 862 and its completion in 867.

Fig. 8.8 Zhai Farong (far left), the cave donor, is pictured with Chengqing and Chengqing's sons, Huaiguan and Huaien (partially lost), on the north wall of the corridor.

DATE	INTERVENTION
Late Tang dynasty (848–907)	Construction and decoration of Cave 85
Five Dynasties (907–60)	North and south walls of the corridor replastered and repainted; north side of the lower part of the east wall of the main chamber repainted with donor figures
	Construction of a wooden temple front
Yuan dynasty (1271–1368)	Construction of a second wooden temple front; antechamber replastered and repainted
Qing dynasty (1644–1911) or Republic of China (1912–49)	Replastering and repainting of the sculptures; Ananda statue remade

Table 8.1 Key Periods of Construction and Redecoration

appointment (Jin 1959). Documents found in the Library Cave were instrumental in establishing the history of Cave 85. For instance, document P.3720, now in the Pelliot collection of the Bibliothèque nationale de France, records the appointment of Wuzhen to the position of deputy monk in 862, inferring the promotion of Zhai Farong to chief monk, and also details the erection of a Zhai family stele in front of Cave 85 (fig. 8.6).[6] The stele was lost, but a copy of its inscription, as described by Wuzhen, was preserved in the Library Cave. This document, P.4640, now also in the Pelliot collection of the Bibliothèque nationale de France, records the start of construction on the cave in 862 and its completion in 867 (He 1980) (fig. 8.7).[7] Cave 85 was therefore completed in the exceptionally short period of only six years, testifying to the resources available for its construction. Zhai Farong died in 869, only three years after completion of the cave (see table 8.1).

Cave 85 was referred to as Zhai jiaku (Zhai family cave) in document MS322, "Name of Cave Niches where Buddhist Lanterns are to be Placed on the Eighth Day of the Twelfth Lunar Month," from the Library Cave and now held by the Dunhuang Academy (Wu 1959). Only a handful of caves at Mogao were built to serve as family temples. Caves 85 and 220 were the only two built by the Zhai family; they were maintained as family temples for generations (Ning 2004; Chen 2008).

There is a portrait of Zhai Farong on the north wall of the entrance corridor (fig. 8.8). It was originally accompanied by an inscription that no longer survives. Zhai Farong's brother Chengqing and Chengqing's sons, Huaiguan and Huaien, are also pictured (now partially lost) (Ma 1989). The identification of the people depicted is consistent with the information recorded from the Zhai family stele.

In the Five Dynasties, military power passed to the wealthy and powerful Cao family, which replaced the Zhangs as rulers of Dunhuang. The Cao family ruled for five generations and sponsored the decoration of some fifty-five caves at Mogao (Dunhuang wen wu yan jiu suo 1980–82, 180). During this period, the house of Cao established its own painting academy, employing the leading regional artists of the day (Whitfield et al. 2000, 85–87). The north side of the lower part of the main chamber's east wall was repainted with cave donors during this time, between 914 and 919 (Chen 2008, 206). The fifth figure to the north of the doorway is a portrait of Cao's eldest daughter, Lady Cao, now mostly lost. Her portrait also appears in neighboring Cave 98, constructed during the Five Dynasties, where the inscription indicates that she married into the Zhai family and died before the completion of the cave, in 924–25. The fourth figure to the north of the doorway is the niece of Zhang Yichao who married into the Zhai family. The first figure is the Buddhist monk Rijin, who was an official in Dunhuang when the area was under Tibetan occupation. Two layers of painting are visible in this area, the earlier presumably dating from the Late Tang (fig. 8.9).

In 924, Cao Yijin took over as commander general of the Return to Allegiance Army. Cave 85 was restored sometime between 924 and 931 by the grandchildren of Huaiguan and Huaien (Pan and Ma 1985, 26). The corridor was redecorated (replastered and repainted), and the portraits of the Zhangs were replaced by those of Cao Yijin with his sons and

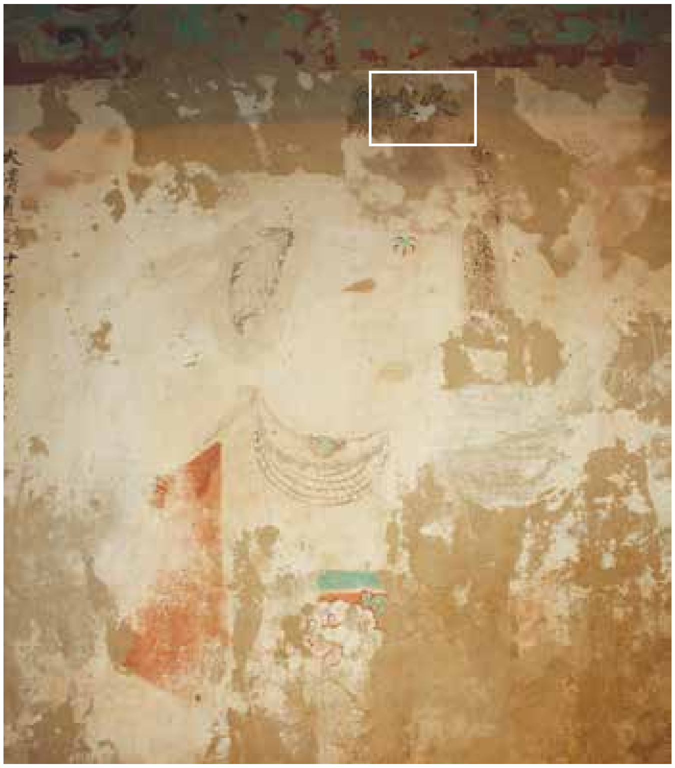

Fig. 8.9a In the Five Dynasties, the portrait of Zhang Yichao's niece was painted on the north side of the east wall of the main chamber.

Fig. 8.9b Remains of an earlier painting scheme are visible below the Five Dynasties paint layer. This is evidence of the repainting of this area during the Five Dynasties. Presumably, the earlier painting dates from the Late Tang.

attendants on the south wall (fig. 8.10). Traces of the earlier, presumably Late Tang painting is visible on the north wall of the corridor, west end (fig. 8.11).

The Cao family was responsible for construction of a wooden temple front at the entrance to the cave. Wooden temple fronts were customary, though few have survived (fig. 8.12). The foundations for the temple front, constructed of faced brick and decorated tiles, were discovered during archaeological excavations in the 1960s (figs. 8.13–8.17).[8] In 1280, during the Yuan dynasty, a new temple front was built within the confines of and on top of the previous Five Dynasties structure (Pan and Ma 1985).[9] Historical records indicate that a fire destroyed this structure; however, the date of the fire is unknown.

The west wall of the antechamber was replastered and repainted with the bodhisattvas Manjusri on the south and Samantabhadra on the north side. A yellow, seated Buddha is also present on the north wall. Evidence of earlier decoration, possibly from the Five Dynasties, is still visible on the north side of the west wall (fig. 8.18).

The details of work done in Cave 85 during the Qing dynasty and Early Republic are uncertain. It is thought that the central Sakyamuni Buddha and Kasyapa sculptures were replastered and repainted and the Ananda sculpture remade during this period.

The Paintings' Religious and Sociopolitical Significance

Cave 85 is significant for its rich, refined representation of seventeen Buddhist sutras. The art historian Julia K. Murray notes that these illustrations "gave visible form to the sometimes abstract concepts of the sutras and manifested the Buddha's teachings in splendid images" (Murray 1994, 129).[10] The paintings in Cave 85 represent the Pure Land school of Mahayana Buddhism, which places emphasis on rebirth of its followers in paradises ("Pure Lands") to ensure that they attain enlightenment in the next life. There are fourteen Buddhist sutras in the main chamber of Cave 85. Some of these sutras illustrate court scenes from the various heavens that feature the sovereign Buddha and his entourage in a paradise set among lavish, Tang-style architecture and landscapes (fig. 8.19). These large, central scenes are surrounded by a number of small vignettes set

Fig. 8.10 When Cave 85 was restored, sometime between 924 and 931, the corridor was completely replastered and repainted, and the portraits of Cao Yijin (far right) with his sons and attendants replaced those of the Zhangs on the south wall.

Fig. 8.11 One area on the north wall of the corridor shows traces of an earlier painting scheme below the later Five Dynasties paint and plaster layer. This is evidence that the corridor was replastered and repainted during the Five Dynasties, creating the paintings that are visible today.

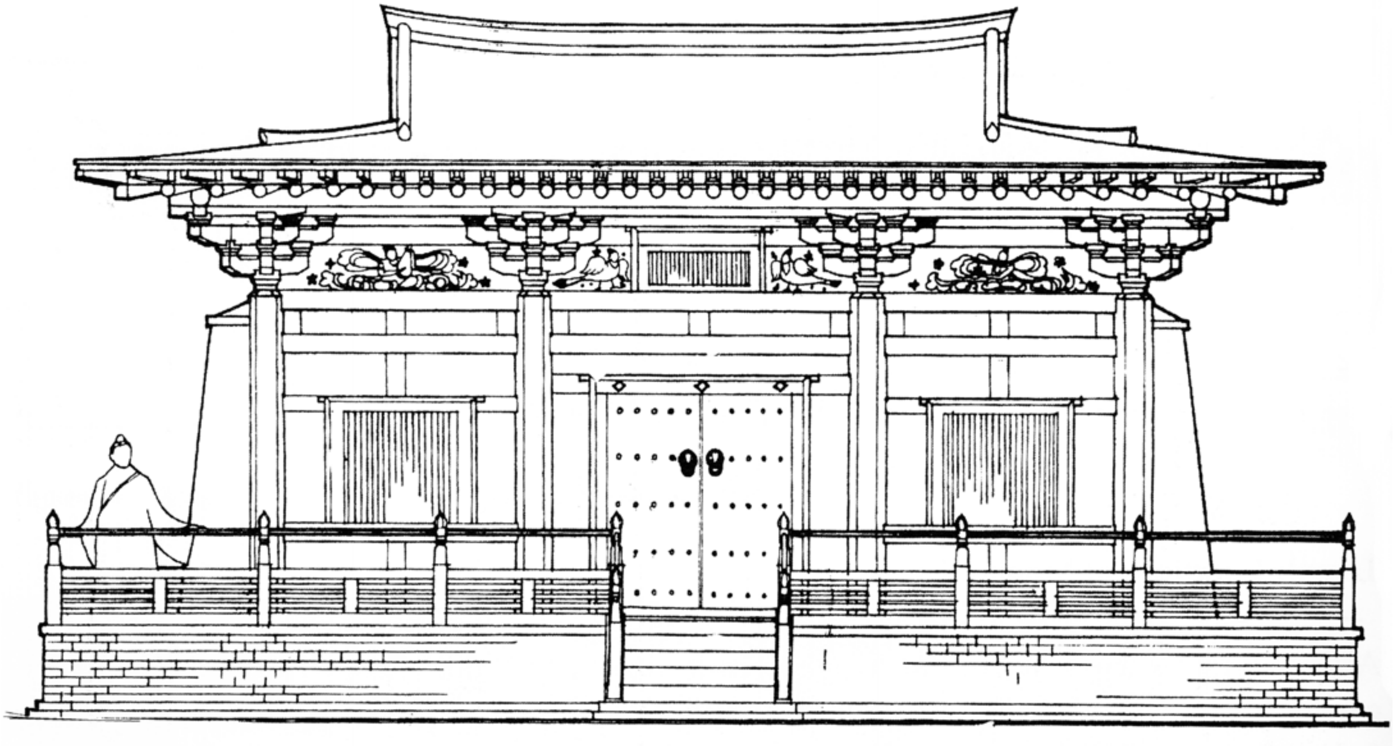

Fig. 8.12 Artist's rendering of a cave temple front. This example dates from the early Song dynasty (960–1063), slightly later than the Five Dynasties temple front of Cave 85. This rendering is based on archaeological investigation of Cave 53 and research by Xiao Mo (Xiao 1989) on other extant Song dynasty structures and historical documentation.

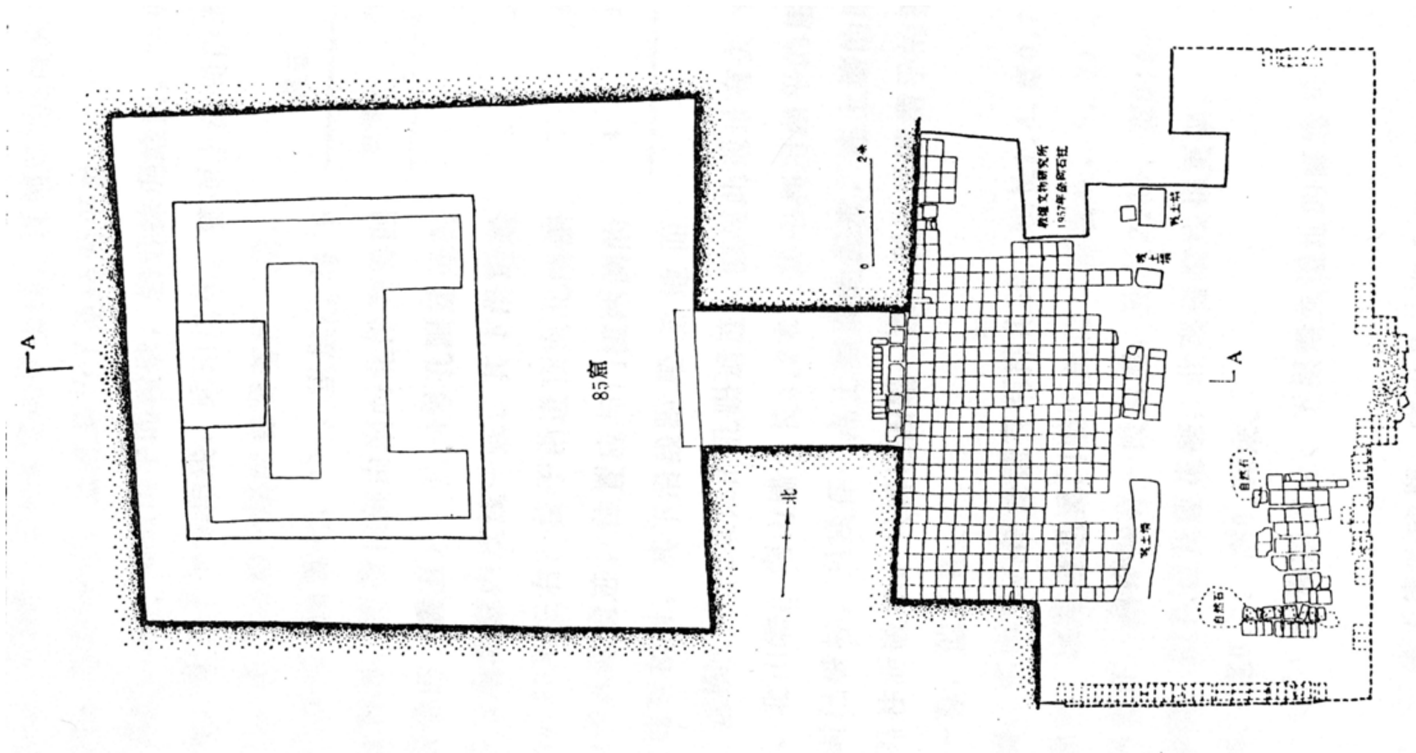

Fig. 8.13 Plan of Cave 85 based on archaeological investigation during the 1960s, which revealed the extent of the no longer extant Five Dynasties and later Yuan dynasty antechamber, platform, and temple front. The locations of found tiles are also pictured. (From Pan and Ma 1985, 24.)

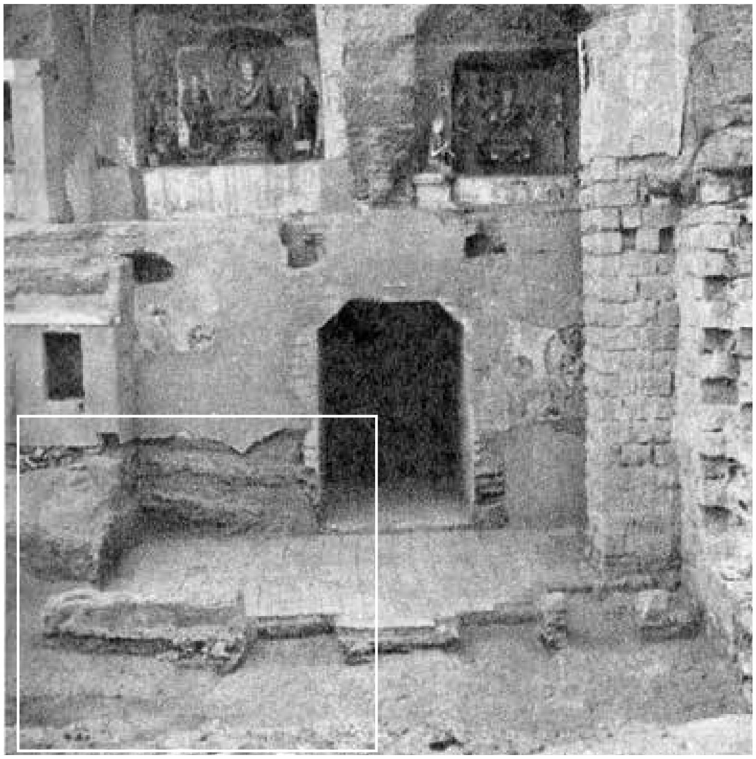

Fig. 8.14 Photograph taken during excavation in the 1960s showing the surviving tile flooring of the platform of the Yuan dynasty temple front. (From Pan and Ma 1985, vii.)

Fig. 8.15 The deteriorated tiles in the foreground show the Five Dynasties temple front platform. The later Yuan dynasty platform was laid over it. (From Pan and Ma 1985, vii.)

Fig. 8.16 Detail of the decorated floor tiles of the Yuan dynasty platform. (From Pan and Ma 1985, VIII.)

Fig. 8.17 One of the floor tiles from the later Yuan dynasty platform with the eight-petal lotus flower pattern found during excavation.

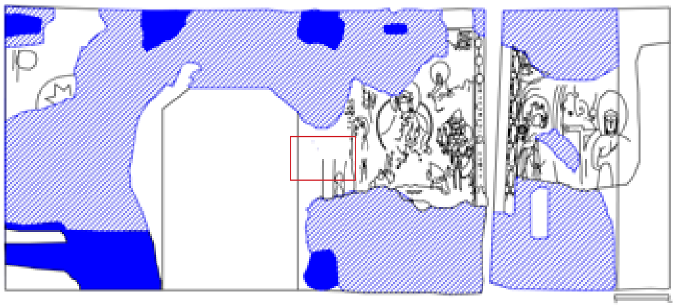

Fig. 8.18 Evidence of an earlier painting scheme is visible on the west wall of the antechamber below the later Yuan dynasty plaster and paint layer. Presumably, the earlier scheme is from the Five Dynasties and was covered over when the later Yuan dynasty temple front was constructed.

within an unbroken landscape and accompanied by cartouches containing sutra text to guide the practitioner through each narrative (Wu 1992). The use of cartouches, which were placed to highlight specific events and punctuate the narrative progression, became more common in the Mogao paintings after 850 (Murray 1994; Fraser 2004). The Suvarna-prabhasa Sutra, depicted in a cartouche on the east wall, features the most complete inscription of this sutra at Mogao (Shi 1990) (fig. 8.20). The appearance of multiple sutras on a single wall is evidence of the influence of Tibetan stylistic conventions during the occupation of Dunhuang (Whitfield et al. 2000). In earlier caves, it was common for a single sutra to occupy an entire wall, while in Cave 85 the north and south walls each depict three sutras (fig. 8.21).

“Screen paintings” were also popular during the period of the Late Tang and were used by monks as didactic tools to explain religious doctrine to practitioners. These scenes, meant to resemble folding screens, depict secular themes to make the messages of the more esoteric imagery in the upper registers of the wall accessible to the laity. In Cave 85, the Dama-muka Sutra is depicted in individual stories at the base of the north, south, and west walls (fig. 8.22). Some of these parables—such as the sea god testing the boatman, Gangata presenting seven treasures to the Buddha, the Vajra-devas, and Sandanika—are presented for the first time at Mogao in Cave 85.

The paintings in Cave 85 are among the highest-quality paintings of the Late Tang dynasty at Mogao. The Lankavatara Sutra on the east slope of the ceiling is generally considered among the masterpieces of Late Tang painting at Mogao (Wang 2010). The wall paintings in Cave 85 also include unique representations of sutras rarely depicted at Mogao, such as the Diamond Sutra, Suvarna-prabhasa Sutra, Lankavatara Sutra, Visesacinta-brahma-pariprccha Sutra, and Ghanavyuha Sutra.[11]

The sutra chosen to be depicted in a cave often reflected the sociopolitical climate of the time. The Late Tang followed a seventy-year period of Tibetan domination of the area, so sutras that illustrated stories of demons being subjugated and themes of righteousness overcoming evil, which expressed the victory of the return of the territory to Tang rule, were popular (Murray 1994). Two such choices are Sakyamuni’s defeat of the demon king Mara and the contest of powers between the Buddha’s disciple Sariputra and the heretic Raudraksha (also referred to as the Magic Competition). The Magic Competition sutra first appeared in the Late Tang on the west wall in Cave 85 (datable to 862–67; now mostly deteriorated) and became a popular theme, appearing in other caves through the 980s (figs. 8.23, 8.24). According to the art historian Sarah Fraser, “Once standardized, this competition remained virtually unchanged for 120 years” (Fraser 2004, 172, 180). Furthermore, the Battle of Sariputra and Raudraksha was depicted across the entire west wall. The special attention paid to this sutra indirectly reminds the viewer of both the recent victory over the Tibetans and the importance of preventing any future invasion by minority nations (Yin 2001, 11). This sutra appeared frequently during the rule of the Zhang and Cao families but disappeared entirely by the Western Xia (1038–1227), another period of minority rule.

Dunhuang was a mix of nationalities, including Tibetans, Uighurs, and Central Asian peoples, so the Han rulers of the Late Tang wanted to reemphasize their Chinese identity and reaffirm their political loyalty to the Tang emperor (Dunhuang wen wu yan jiu suo 1980–82, 190–91). The paintings became

Fig. 8.19 This image of the Amitabha Sutra on the center of the south wall shows the Buddha and his entourage in paradise.

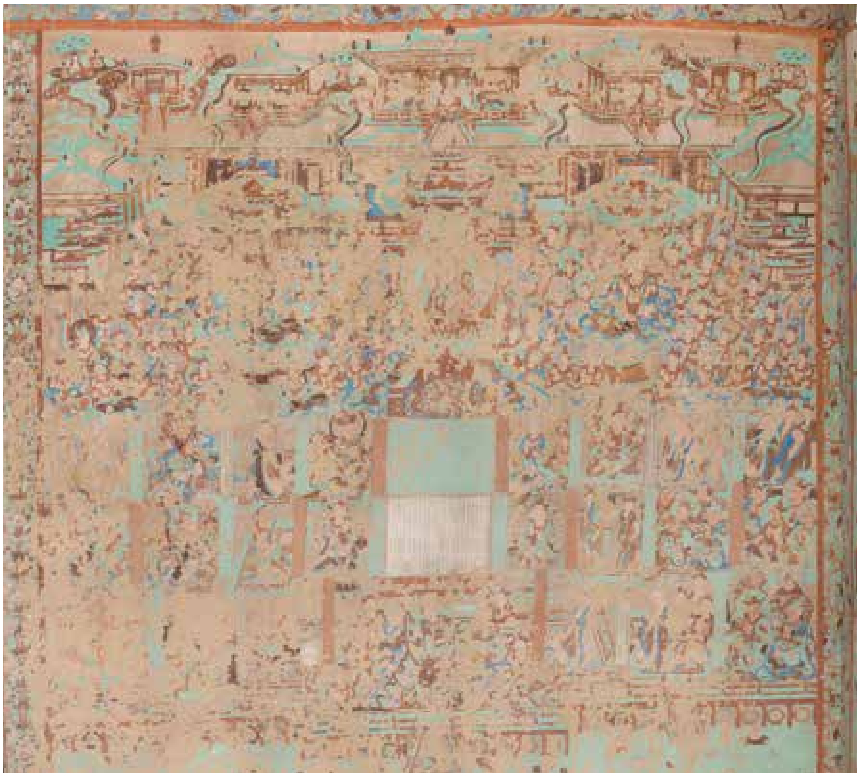

Fig. 8.20 The Suvarna-prabhasa Sutra, depicted in a cartouche on the east wall, features the most complete inscription of this sutra at Mogao.

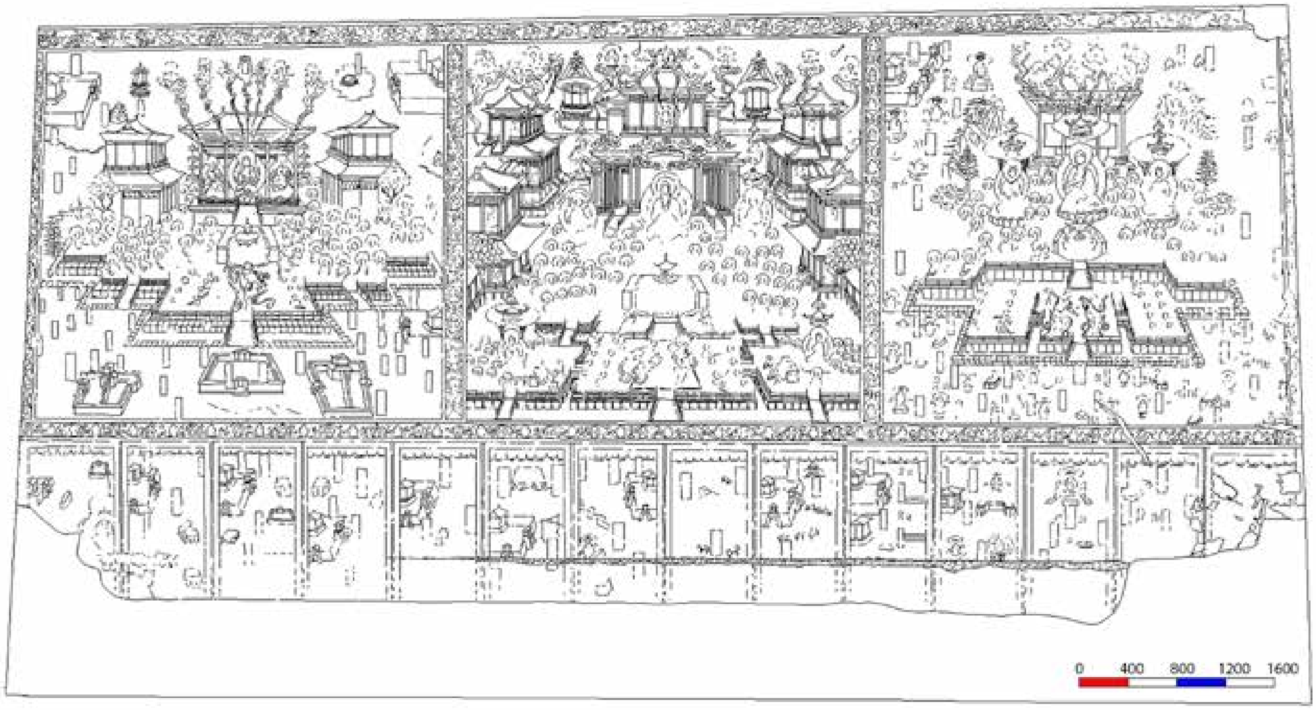

Fig. 8.21 A line drawing of the south wall showing three sutras depicted. The practice of depicting multiple sutras on one wall, rather than a single sutra across an entire wall, is attributed to Tibetan stylistic influence.

Fig. 8.22 The lower parts of walls in the main chamber are decorated with scenes from the Dama-muka Sutra that have been painted to resemble folding screens. Unfortunately, the lower portions of these scenes have suffered substantial deterioration related to flooding and wet sand banking up against the cave walls for extended periods.

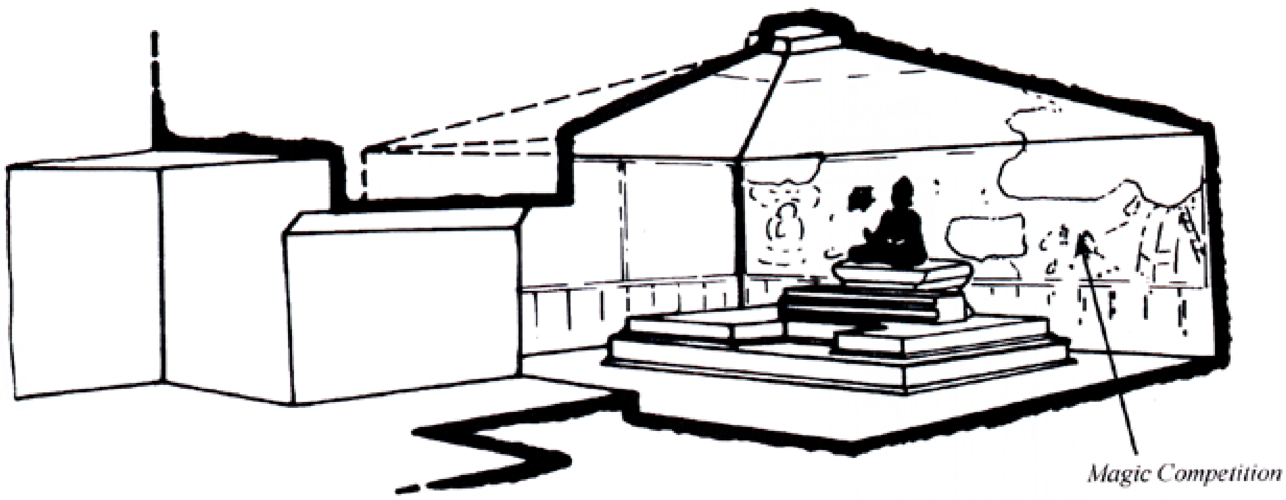

Fig. 8.23 The Battle of Sariputra and Raudraksha (also referred to as the Magic Competition) decorates the rear west wall of the main chamber. The scene has unfortunately suffered much deterioration and is now difficult to read.

Fig. 8.24 The Magic Competition, or Battle of Sariputra and Raudraksha, appears in other caves, including in a small niche of Cave 335 as seen in this drawing. The story depicts the contest of powers between Buddha's disciple Sariputra and the heretic Raudraksha. During the battle Raudraksha, despite successively transforming himself into a mountain, buffalo, pond, poisonous dragon, yellow-headed ghost, tree, and so on, is defeated time and time again by Sariputra, who also assumes other forms, including a warrior, lion, elephant, golden-winged bird, heavenly king, and strong wind. The story ends with Raudraksha's conversion to Buddhism.

Fig. 8.25 The Vimalakirti-nirdesa Sutra depicts the Debate between Vimalakirti and Manjusri watched by an audience of foreign kings and princes. Ordinarily, the Tibetan king would be depicted as a prominent figure in this story. Following the Tibetan occupation of Dunhuang in the mid-Tang, however, the Tibetan king is given less prominence and is shown together with other kings. In Cave 85, constructed in the Late Tang, the Tibetan king, depicted wearing a white robe with tiger skin collar (center), is presented among the other foreign rulers.

more Chinese in style. Some figures that were painted in caves during the Middle Tang—such as the Tibetan prince Zhanpu, a leader of princes from all nations in the narrative illustration of the Vimalakirti-nirdesa Sutra—were eliminated in later periods, as were depictions of Tibetan costume (fig. 8.25). Sutras were also selected that showed typical Chinese customs such as filial piety. The Bao Fumu Enzhong Jing (Sutra on Requiting the Great Kindness of Parents) on the east side of the south wall was a popular choice, presumably because it was one of the few Buddhist texts originating from within China (Murray 1994). With its focus on the virtue of filial piety, it was often symbolic of loyalty to the Tang emperor.

The painting of patrons or donors on the walls of cave corridors became widespread during the Tang period. Caves were constructed and used not only to express piety and adoration of the Buddha but also to fill a more secular social function. Cave 85 is one of the earliest examples where patrons were depicted in order to display the wealth and social rank of the family. Regional government officials were also depicted as honorary patrons (Wang 2010). The paintings of the cave benefactors are life-size and include painted inscriptions (some now lost) stating their official and imperial titles. Following the depiction of patrons in Cave 85 it became common in all large caves constructed or redecorated during this period for high officials to be included as honorary benefactors.

The Cave 85 paintings in addition provide a rich source of information on aspects of daily life and common customs in their depictions of, for example, a butcher shop, hunting scenes, a pottery factory, acrobats and magicians at the circus, market scenes, wedding scenes, farming, fights, and women applying makeup (fig. 8.26). Collectively, the paintings constitute what has been termed a pictorial encyclopedia of the Tang era that includes information on the weapons, costumes, musical instruments, tools, animals, and transportation of the period. The rich detail of these mundane scenes has long made these paintings an important resource, not just for art historians and religious scholars, but also for historians interested in all aspects of life along the Silk Road during the ninth century.

Notes

1. This size is based on the Dunhuang Academy classification system in which a large cave floor area is greater than 31 m^2.
2. This is often referred to as a coffer or caisson ceiling; in Chinese, as a *zaojing* (colorful well) (Fan and Sheng 2009, 155) or *tianjing* (well of heaven) (Whitfield 1995, 2:284). The overall shape of the ceiling was meant to imitate a tent. The painted hanging drapery decoration with tassels on the ceiling slopes also adds to this illusion.
3. Historical photographs sometimes use these previous cave numbering systems.
4. For ease of reading, Sanskrit diacritics have been omitted throughout this text.
5. Some of this information is drawn from historical and iconographic unpublished information about the site compiled by Dunhuang Academy tour guides at the request of Cave 85 project team members.
6. This manuscript has been digitized and is accessible online. See Pelliot chinois 3720, Gallica Digital Library, http://gallica.bnf.fr/ark:/12148/btv1b83025732.r=Pelliot+AND+3720.langEN (accessed 24 May 2010).

Fig. 8.26 This scene from the Lankavatara Sutra (Sutra on the Descent to Sri Lanka), on the east slope of the ceiling of the main chamber, shows a butcher cutting meat. Under the table, a sheep is tied waiting to be slaughtered. To the right, a hungry dog looks on expectantly. The paintings of Cave 85 show many aspects of daily life in the Tang period.

7. This manuscript has been digitized and is accessible online. See Pelliot chinois 4640, Gallica Digital Library, http://gallica.bnf.fr/ark:/12148/btv1b8304060b.r=pelliot+4640.langEN (accessed 24 May 2010).
8. Evidence of the flooring of the antechamber was recorded and then covered over during construction of the retaining walls and the new cliff facade as part of the stabilization work on the site in the 1960s.
9. It is unknown what happened to the earlier Five Dynasties temple front; it may have burned down or collapsed prior to the building of the Yuan dynasty replacement. The platform was seriously damaged during excavation, and the extent of it is therefore unknown.
10. Known as "Sutra transformations or tableaux" (*jingbian*) or "transformation images" (*bianxiang*), these depictions included scenes from parables organized sequentially in a landscape surrounding large central Buddha images (Murray 1994, 129).
11. This is according to unpublished information provided to project staff by official Dunhuang Academy guides.

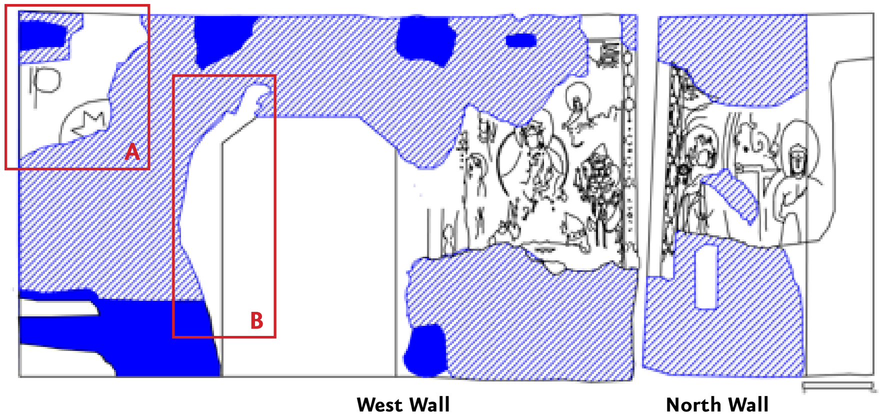

a

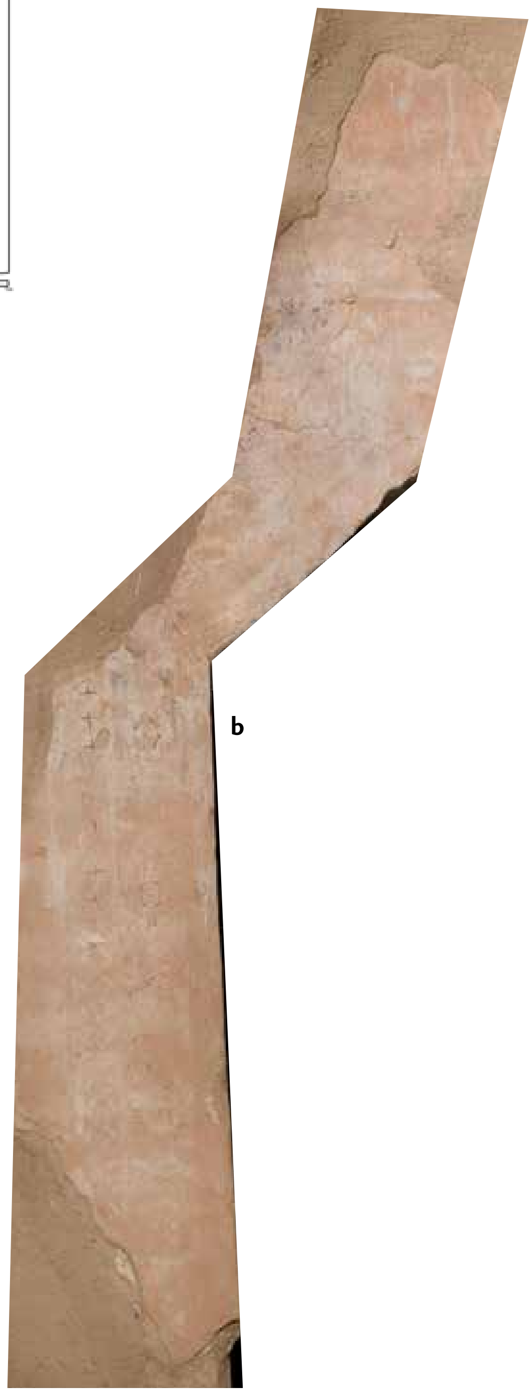

b

Fig. 8.27 Antechamber. West wall, south side: partial remains of the Samantabhadra Sutra from a period of redecoration during the Yuan dynasty (a, b).

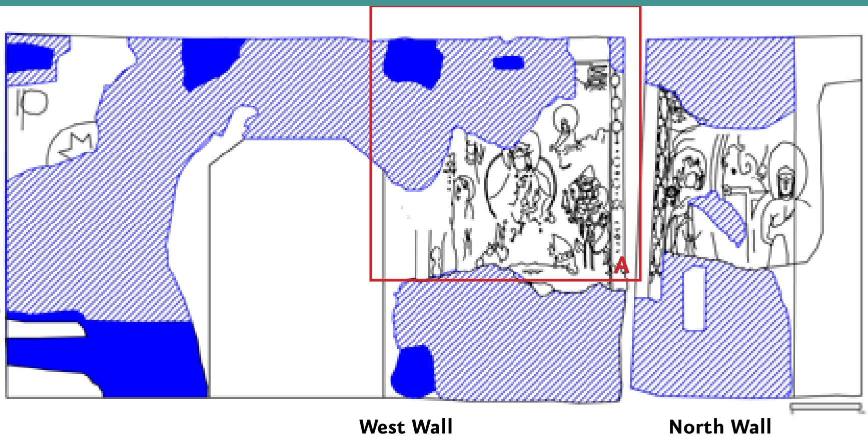

Fig. 8.28a Antechamber. West wall, north side: partial remains of the Manjusri Sutra from a period of redecoration during the Yuan dynasty. Traces of an earlier scheme of painting (possibly Five Dynasties) can be seen below the Yuan painting.

Fig. 8.28b Detail of the Manjusri Sutra showing raised relief decoration with metal foil.

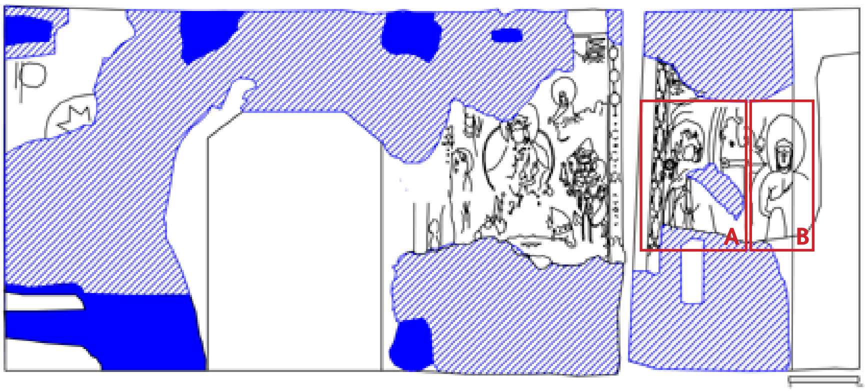

a

b

Fig. 8.29 Antechamber. North wall: partial remains of a yellow seated Buddha from a period of redecoration during the Yuan dynasty. The painting is now partially obscured by a supporting wall constructed as part of the modern cliff facade and walkways.

Fig. 8.30 Corridor. Paintings date from a period of redecoration during the Five Dynasties. Traces of an earlier scheme of painting (possibly Late Tang) exists below the Five Dynasties painting.

Fig. 8.31 Corridor. North wall: the monk Zhai Farong (far left), who sponsored the building of the cave, is pictured along with his brother Chengqing and Chengqing's sons, Huaiguan and Huaien (mostly lost).

Fig. 8.32 Corridor. South wall: Cao Yijin (far right) and two of his sons are pictured along with seven smaller figures originally thought to be attendants but now believed to be four young sons of Cao Yijin and three attendants (mostly lost).

Fig. 8.33a Corridor. Ceiling: a central seated Buddha surrounded by the thousand Buddha motif from the Bhadrakalpika Sutra.

Fig. 8.33b Corridor. North ceiling slope: decorative bands of the fourteen auspicious symbols.

Fig. 8.33c Corridor. South ceiling slope: decorative bands of the fourteen auspicious symbols.

a

b

c

Fig. 8.34 Main chamber. Central ceiling panel: a lion and lotus are surrounded by a series of decorative borders, including lotus, meander, fish scales or waves, curly leaf, and drapery or hanging valance patterns.

Fig. 8.35 Main chamber. North ceiling slope: the Avatamsaka Sutra (Flower Garland Sutra).

Fig. 8.36 Main chamber. East ceiling slope: the Lankavatara Sutra (Sutra on the Descent to Sri Lanka).

Fig. 8.37 Main chamber. South ceiling slope: the Saddharmapundarika Sutra (Lotus Sutra).

Fig. 8.38 Main chamber. West ceiling slope: the Paradise of Maitreya (Buddha of the Future).

Fig. 8.39 Main chamber. North wall: This wall contains three sutras, divided and framed by a decorative border of Buddhas. Scenes from the Visesacinta-brahma-pariprccha, Bhaisajyaguru (Medicine Buddha), and Ghanavyuha (Dense Array) Sutras were painted from east to west respectively. The lower section contains individual screen paintings (partially destroyed) telling stories from the Dama-muka Sutra (Sutra of the Wise and Foolish). The north wall contains fourteen individual stories.

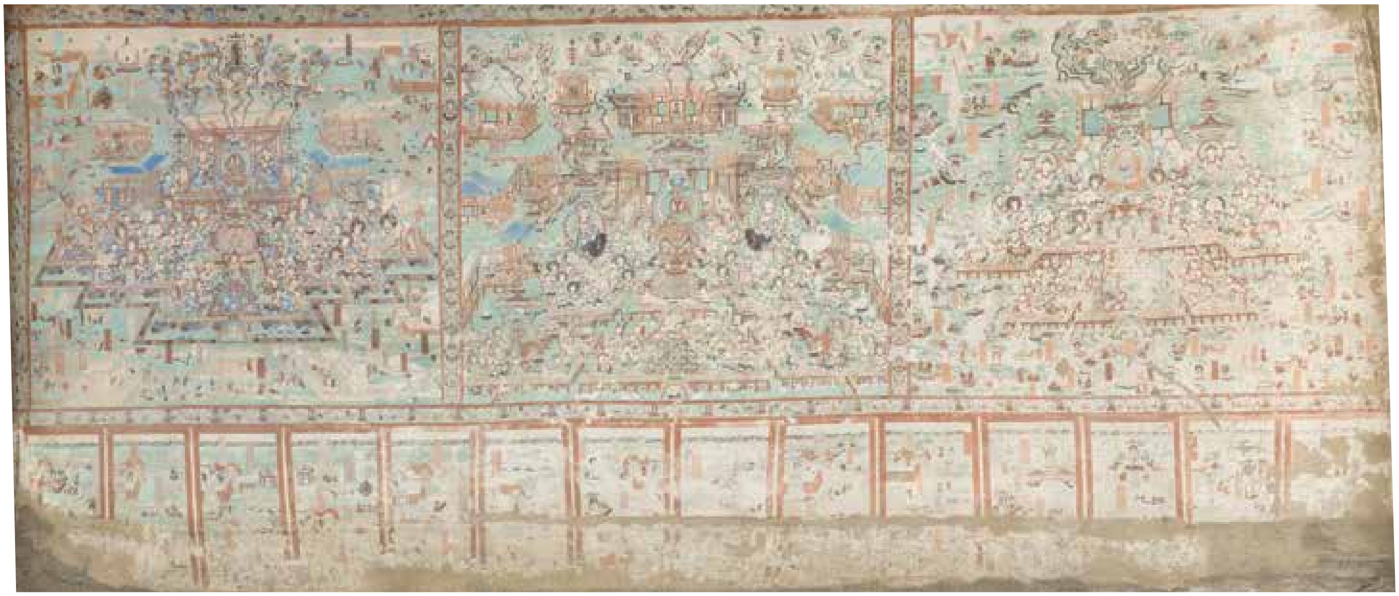

Fig. 8.40 Main chamber. South wall: This wall contains three sutras, divided and framed by a decorative border of Buddhas. Scenes from the Chinese Sutra on Requiting the Great Kindness of Parents (*Bao Fumu Enzhong Jing*) and the Amitabha and Diamond Sutras were painted from east to west respectively. The lower section contains individual screen paintings (partially destroyed) telling stories from the Dama-muka Sutra (Sutra of the Wise and Foolish). The south wall contains fourteen individual stories.

Fig. 8.41 Main chamber. East wall: The wall contains two sutras, the self-sacrifice story from the Suvarna-prabhasa Sutra (Sutra of Golden Light), painted above the doorway with a portion of the text to the south; and the Vimalakirti-nirdesa Sutra (Debate between Vimalakirti and Manjusri), which was painted to the north and south sides of the doorway. The lower section contains donor figures. Six figures, including three female donors and three Buddhist monks, were painted on the north side of the door, two now partially destroyed. These donors were repainted during the Five Dynasties. To the south of the door are ten (possibly eleven) figures. These figures are smaller in size than those on the north side and may therefore date to the Late Tang. Only five of these figures are still visible, the rest now destroyed. The figures include Buddhist nuns from Puguang temple (Chen 2008, 205).

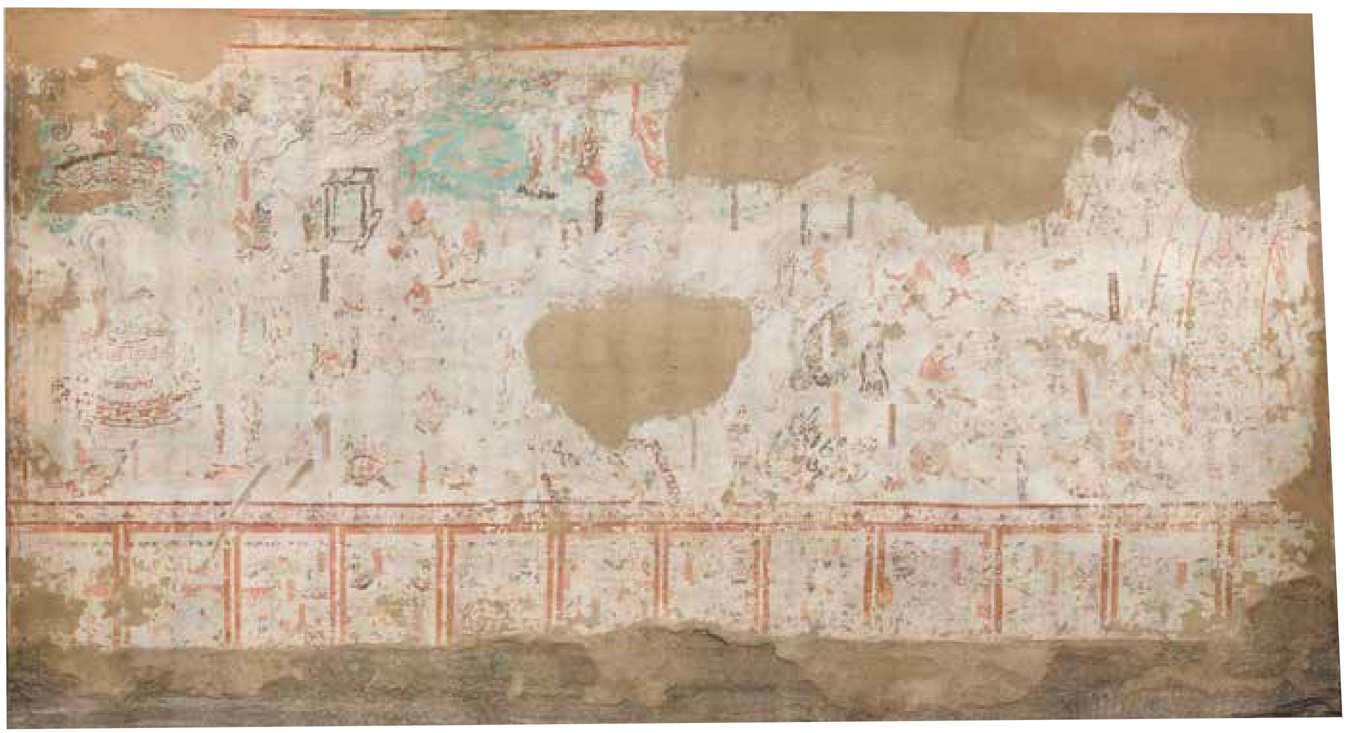

Fig. 8.42 Main chamber. West wall: A large, severely deteriorated depiction of the Magic Competition between Sariputra and Raudraksha covers the entire upper register of the wall. The lower section contains individual screen paintings (partially destroyed) telling stories from the Dama-muka Sutra (Sutra of the Wise and Foolish). The west wall contains twelve stories.

Fig. 8.43 Main chamber. A polychrome sculpture group that includes a central seated Sakyamuni Buddha flanked by the standing figure of Kasyapa (older disciple) to his left and Ananda (young disciple) to his right. The central Sakyamuni figure sits cross-legged on a large decorated pedestal, while the two side figures stand on smaller pedestals. The sculpture group resides on a large, horseshoe-shaped bed that sits on an even larger, rectangular stepped central platform. The entire altar platform was both sculpted and painted; lotus flowers, lions, and heavenly kings are still visible. A raised altar, which now obstructs the pedestals of Kasyapa and Ananda, is thought to be a later addition from the Five Dynasties on which five additional figures would have stood. There are depressions on the raised altar indicating the former location of these figures, now lost.

Fig. 8.44 Main chamber: Sakyamuni Buddha.

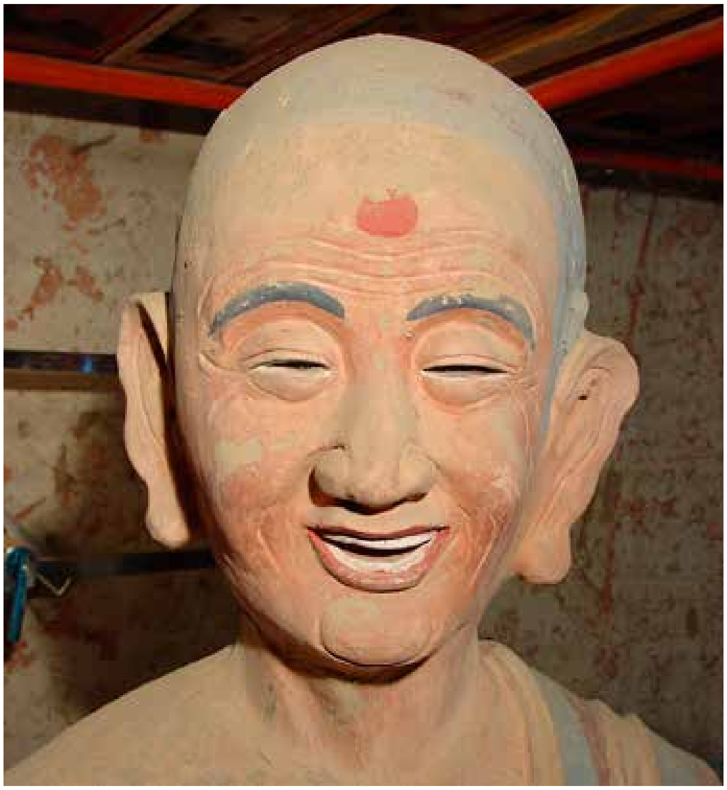

Fig. 8.45 Main chamber: Kasyapa (older disciple).

Fig. 8.46 Main chamber: Ananda (young disciple).

CHAPTER 9

Physical and Conservation History

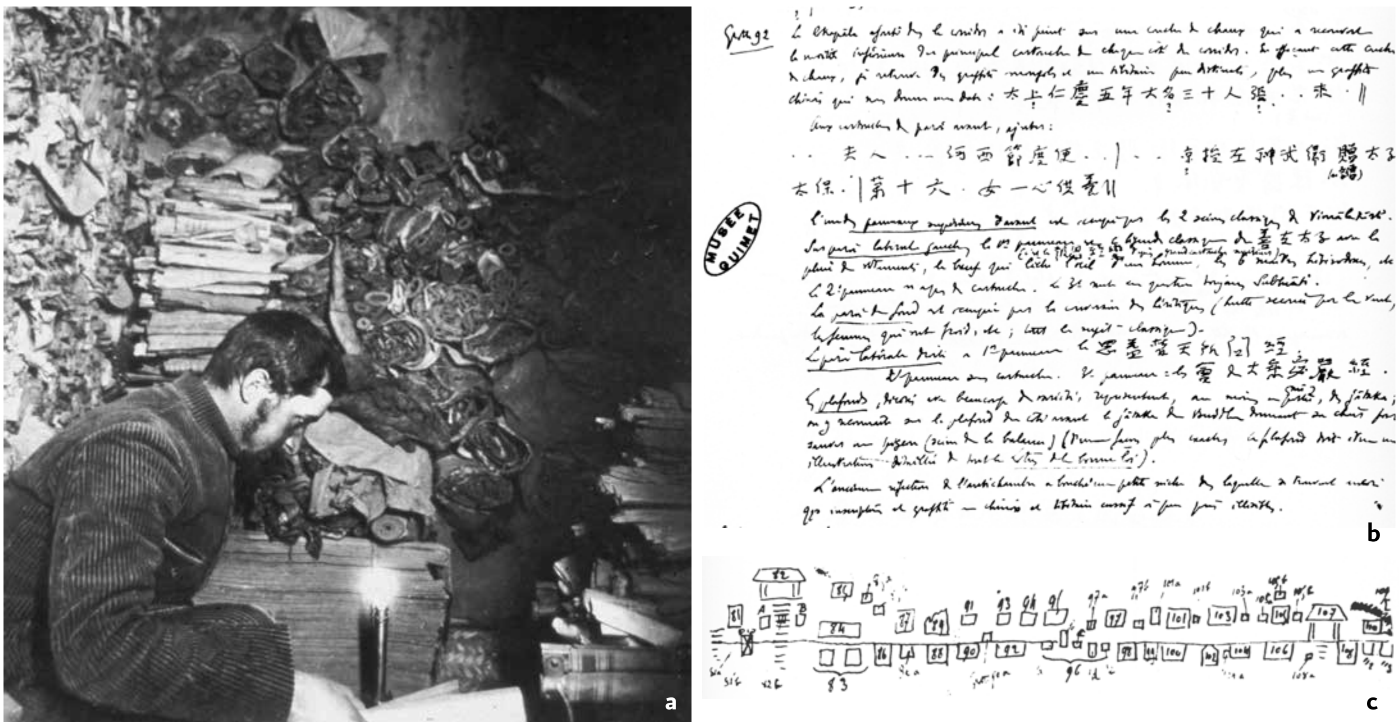

Fig. 9.1 The French sinologist Paul Pelliot visited Dunhuang in 1908. Pelliot is shown examining manuscripts in the Library Cave (a). Pelliot produced copious notes on individual caves (b) as well as sketches and drawings, including these for Cave 85 (c). Note: In Pelliot's cave numbering system, Cave 85 was numbered 92. His archives are now housed at the Musée Guimet in Paris.

Information that could shed light on the history of Cave 85 was collected and studied to understand past and current deterioration. Research included compiling a physical history of the site and cave to highlight events that may have contributed to the deterioration of the wall paintings and sculpture. A conservation history of the site and cave was also compiled to facilitate understanding of past conditions and previous interventions and conservation treatments.

Information Sources

The wealth of existing documentation, in particular the large number of historical photographs, provides a valuable resource for illustrating the history of the site and the cave (see table 9.1). Information was amassed from the archives of the early explorers to the site; they included Marc Aurel Stein in 1907, Paul Pelliot with photographer Charles Nouette in 1908, and Sergei Oldenberg with photographer Samuil Martynovich Dudin in 1914–15.[1] These early travelers produced copious notes, drawings, and photographs that now provide a record of the condition of the site, the caves, and their wall paintings and sculpture at the time (fig. 9.1).

Additional researchers visited the site around the time of the establishment of the Dunhuang National Art Research Institute

Fig. 9.2 As part of their archives the Conservation Institute of the Dunhuang Academy has a documentation book for every cave where information on condition and past treatment is recorded. Shown here is the documentation book for Cave 85.

Fig. 9.3 Cracks and fissures are visible in the eroded cliff face, while sand buries parts of the entrances of lower-tier caves in a 1907 view taken during Aurel Stein's first visit to Mogao.

in 1944 (renamed the Dunhuang Research Institute of Cultural Relics in 1950 and later the Dunhuang Research Academy). These included Shi Zhangru, a Taiwanese archaeologist, who spent three months recording and photographing the caves in 1942; James and Lucy Lo, who documented the caves over an eighteen-month period between 1943 and 1944; and Irene Vongehr Vincent, an American who was born and lived in China and visited Dunhuang in 1948.

The Dunhuang Academy itself has a large collection of prints and negatives dating to the early 1950s and continuing to the present day.[2] Also as part of its archive, the Conservation Institute of the Dunhuang Academy has a documentation book for each of the decorated caves that contains observations on condition, descriptions of previous conservation treatments, and photographs (fig. 9.2). The recollections of longtime Dunhuang Academy staff members, including senior conservators who retain knowledge of conservation work undertaken decades ago, are another valuable source of information.[3]

Physical History of the Site

The earliest images from the first part of the twentieth century show the general neglect and abandonment of the site and the erosion and collapse of parts of the cliff face that exposed wall paintings and sculpture to the elements (figs. 9.3–9.5). Cracks and fissures are visible in the rock of the exposed cliff face, and the lower-tier caves are shown partially buried by sand and debris.

The lower caves of the site are also thought to have flooded throughout its history. Historical photographs show the Daquan River, situated close to the cliff, overflowing its banks (fig. 9.6).[4] There is clear evidence of wet sand banking up against the wall paintings in many of the lower-tier caves, which resulted in loss of painting at the base of walls and a zone of moisture-induced deterioration above this area (fig. 9.7). Flood control measures were put in place in the 1960s and have since prevented flooding at the site; however, flash floods still periodically occur (the last in June 2011), causing the river to overflow its banks.

Dunhuang is located in a seismic zone. Seven earthquakes are reported to have occurred between 1927 and 1960 (Sun 1997, 159–60). None of these were severe, but the frequency of their occurrence was potentially damaging to the grottoes and may be responsible for losses apparent in wall paintings and sculpture (see chap. 15).

The wall paintings have also suffered damage from human activity in the caves. For instance, photographs show evidence of the caves being used by locals for worship (incense and offerings are visible on the altars) during the early twentieth century. In

EXPLORER/PHOTOGRAPHER	DATE	DESCRIPTION OF PHOTOGRAPHS	LOCATION OF HOLDINGS AND REFERENCES
Aurel Stein (1862–1943)	1907	55 photographs documenting 16 caves	Images held at the British Library. Accessible through the International Dunhuang Project: http://idp.bl.uk.
Paul Pelliot (1878–1945) with photographer Charles Nouette (1869–1910)	1908	300 photographs documenting 100 caves	Images held at the Musée Guimet. Accessible through Artstor: www.artstor.org. Images published in *Grottes de Touen-houang: carnet de notes de Paul Pelliot: inscriptions et peintures murales* (Pelliot 1981).
Sergei Oldenburg (1863–1934) with photographer Samuil Martynovich Dudin (1863–1929)	1914–15	2,000 photographs documenting the exterior cliff face and the interiors of 150 caves	Images held at the State Hermitage Museum of Russia. Images published in *Eluosi guo li Ai'ermitashi bo wu guan cang Dunhuang yi shu pin* (Gosudarstvennyĭ Ėrmitazh [Russia] 1997–2005).
Shi Zhangru (Shih Chang-Ju)	1942	Photographs of cave interiors taken over a three-month period	Images published in *Section and Plan Measurements of the Mogao Grottoes, Field Project Report No. 3* (Shi Zhangru 1996).
Joseph Needham (1900–1995)	1943	Photographs of exterior of caves	Images held at the Needham Research Institute. Accessible through www.nri.org.uk/JN_wartime_photos/cft.htm.
James (Luo Jimei) (1902–87) and Lucy Lo (Luo Fang) (b. 1921)	1943–44	2,590 photographs taken over an eighteen-month period. A system of mirrors and cloth screens was devised to bounce light along the corridors of the caves to illuminate the paintings and sculptures.	Images part of the Lo Archive held at Princeton University. Accessible through Artstor: www.artstor.org.
Irene Vongehr Vincent (1920–91)	1948	Photographs documenting the early interventions to the site	Images published in *The Sacred Oasis* (Vincent 1953).
Dunhuang Academy		Photographs documenting cave interiors and the exterior cliff face as stabilization work was being undertaken	Images held by the Dunhuang Academy Digital Information Center.
		Photographs from the Dunhuang Academy documentation book compiled for each cave	Cave documentation books held by the Conservation Institute of the Dunhuang Academy.
		Photographs documenting the archaeological excavations of the cave temple fronts	Images held by the Dunhuang Academy Digital Information Center. Images published in *Mogao ku ku qian dian tang yi zhi* (Ruins Frontal Buildings Added to Mogao Grottoes) (Pan and Ma 1985).
Dunhuang Academy/ Mellon/ Northwestern University		High-resolution color digital images of cave interiors	Images held by the Dunhuang Academy Digital Information Center. Accessible through Artstor: www.artstor.org.

Table 9.1 Photographic Sources

Fig. 9.4 The site as photographed by Charles Nouette in 1908 looking north shows the erosion of the cliff face and overgrown trees. Some of the caves have wooden ladders to provide access to upper levels.

Fig. 9.5 The site as it appeared to the Russian expedition in 1914–15. This view is taken looking south with the Nine-Storey Pagoda at right and the Daquan River flowing through the site at left.

Fig. 9.6 Irene Vongehr Vincent photographed sitting by the banks of the Daquan River in 1948 (a). The northern grottoes are just visible across the river in the distance. Image of the Daquan River with high water in June 2000 (From Pan and Fan 2003.) (b). Since the 1960s flood control measures have prevented serious flooding of the site.

1920–21, over nine hundred White Russian refugees were stationed in some of the caves where they built beds out of earth and left graffiti and soot blackening on the painted walls from fires (Fan 1997, 12) (fig. 9.8).

Interventions at the Site

In the late nineteenth and early twentieth century, the first interventions at the site were carried out by the Daoist priest Wang Yuanlu (1850–1931). He repaired and repainted a large number of the sculptures and created new sculpture where loss or destruction had occurred. These new creations are easily identifiable as their technical expertise and artistic and aesthetic values are low. It is possible that restoration work was also carried out on the wall paintings at this time or in the middle Qing, but this was on a limited basis, and the exact extent of work is unknown.

Interventions during the early twentieth century also included clearing of the lower-tier caves of sand and debris and providing access to upper-tier caves via wooden walkways. Wooden doors may also have been installed in some of the caves at this time to provide protection.

The main period of repair and improvement at the site began after the founding of the Dunhuang National Art Research Institute in 1944. Initiatives aimed at improving security and preservation included enclosing the grotto zone with a fence, closing more of the caves with wooden doors, connecting the caves with walkways, and providing security guards. Irene Vongehr Vincent's 1948 photographs are the first to show the results of these efforts, with wall paintings reinforced with plaster repairs (fig. 9.9). In addition, the institute developed a new cave numbering system and completed a written description of the site and an inventory of the caves' contents (Fan 1997, 13).

In the 1950s, the Dunhuang Research Institute of Cultural Relics embarked on a full-scale stabilization project of the grottoes, resulting in the reinforcement of 570 m of cliff face and 358 caves (fig. 9.10). Given the extent of the site and its problems, this work took three decades to complete (Sun 1997, 159). Interventions included construction of a concrete facade on the cliff face to prevent further erosion, filling of structural cracks in the cliff, erection of stone pillars to support overhanging rock, construction of concrete stairs and walkways to access upper-tier caves, restoration of the surviving wooden temple

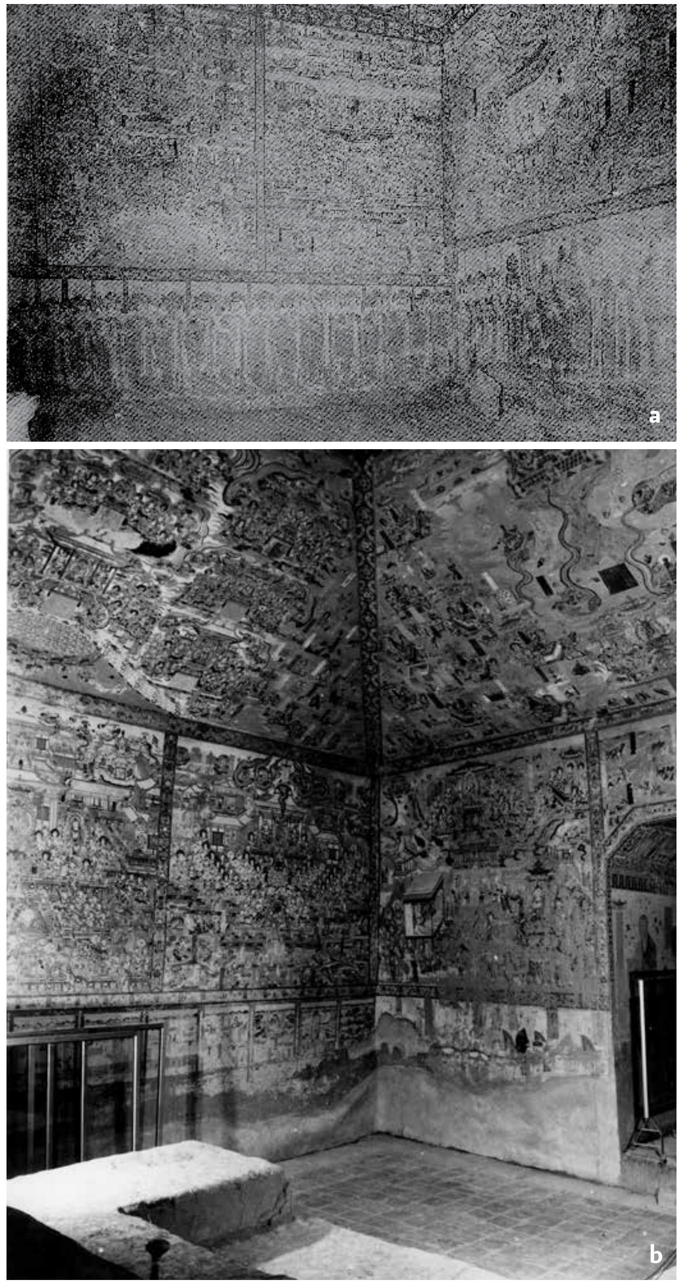

Fig. 9.7 Detachment of plaster is typical where bases of walls have been exposed to wet sand. The interior of Cave 61 (a), another ground-level cave, shows areas of detached painted plaster at the base of the wall in a 1908 photograph by Charles Nouette. Similar deterioration at the base of the walls in Cave 85 can be seen in the 1989 photograph (b) of the northeast corner of the main chamber.

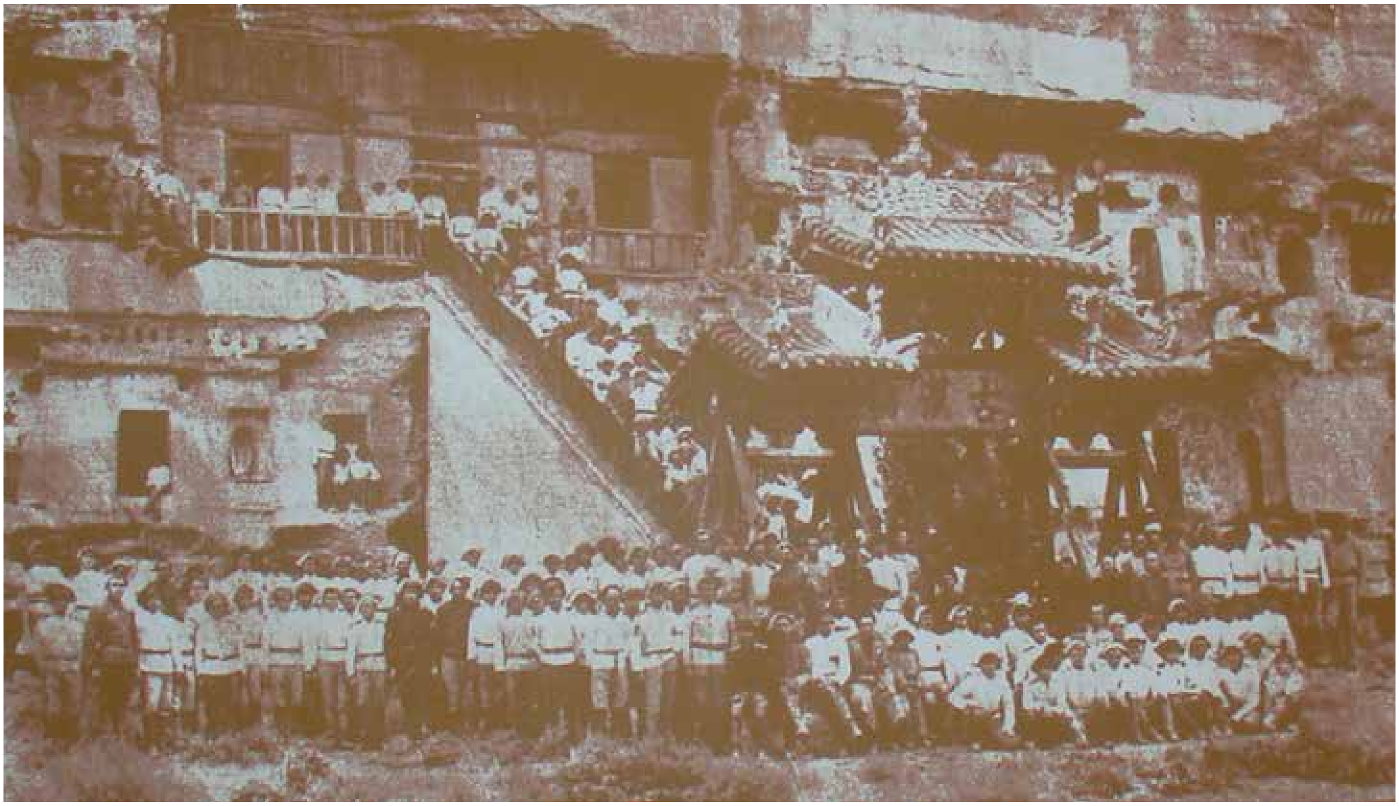

Fig. 9.8 Over nine hundred White Russians were stationed in the caves in 1920–21. They left graffiti and soot blackening on the walls of some of the caves.

Fig. 9.9 Image of the site taken by Irene Vongehr Vincent in 1948 showing the early efforts to improve preservation and security of the caves.

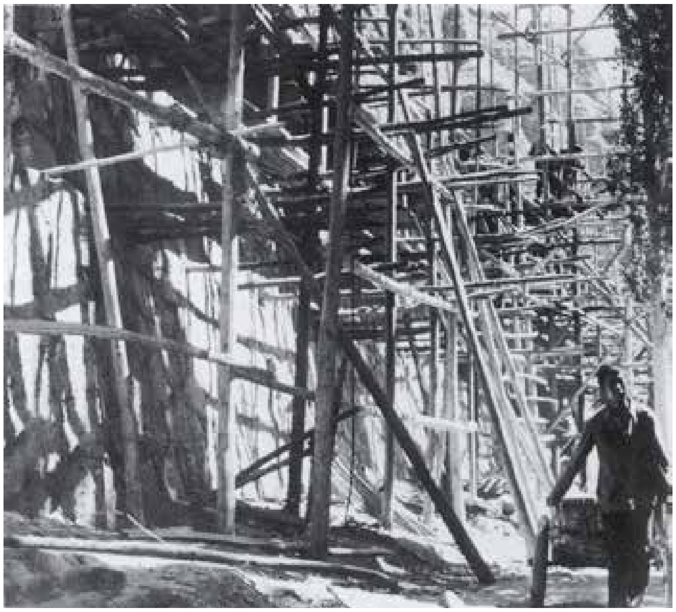

Fig. 9.10 Beginning in the 1950s, full-scale stabilization of the grottoes resulted in the reinforcement of the cliff face and caves. This work took three decades to complete.

Fig. 9.11 Earliest known photograph of Cave 85, taken by the Russian expedition led by Sergei Oldenburg to the Mogao Grottoes in 1914–15.

Fig. 9.12 Russian expedition image from 1914–15 showing the south wall of the corridor and the loss of painting at the base of the wall.

fronts, and construction of a small brushwood windbreak fence at the top of the cliff as a trial to reduce windblown sand. Some of the cave interiors were renovated with cement floors, and sculpture and wall paintings were stabilized. Interventions to the wall paintings included anchoring areas of detachment with metal cross-braces and filling large lacunae with earthen plaster repairs (Fan 1997, 13–14; Sun 1997).

During the late 1960s, synthetic conservation materials—namely, acrylic emulsions (polyvinyl acetate and alcohol)—were introduced and utilized as adhesives and consolidants for treating the wall paintings and sculpture in many of the caves. Use of these materials continues today.

In the 1980s, the site was opened to visitors and measures were taken to protect the art in visited caves. Security systems and glass screens were installed and cement tile floors were laid in preparation for visitors. From 1986 to 1989, wooden doors were removed and aluminum louver security doors were installed at each cave entry.

At this time, the Dunhuang Academy also began collaborations with various foreign institutions to address unresolved problems at the site. Between 1989 and 1993, the Dunhuang Academy partnered with the GCI to address sitewide stabilization issues (Agnew and Huang 1997). Activities included sand and dust control and stabilization of the thin rock ceilings of upper-tier caves. As part of the project, a wind fence was designed and installed on the plateau above the grottoes in fall 1990 (see figs. 1.5, 1.6). The synthetic fabric windbreak fence reduced the wind speed by 50% and cut down sand deposition at the grottoes by 62% (Ling et al. 1997, 213). In 1992, the synthetic fence was supplemented with a wind fence of desert-adapted plants native to northwestern China. A drip irrigation system was designed and installed to support these plants (Lin et al. 1997, 228–29).5 To further reduce dust deposition in the caves, filters were installed on entrance doors. The system was found to significantly reduce airborne particulates.

Erosion of the cliff over time has resulted in thinning of the rock ceilings of upper-level caves, which in some cases led to

Fig. 9.13 The earliest known photographs of the main chamber were taken by James and Lucy Lo in 1943–44. Large losses of painted plaster are clearly visible on the west wall and altar platform. The sculpture has already been restored.

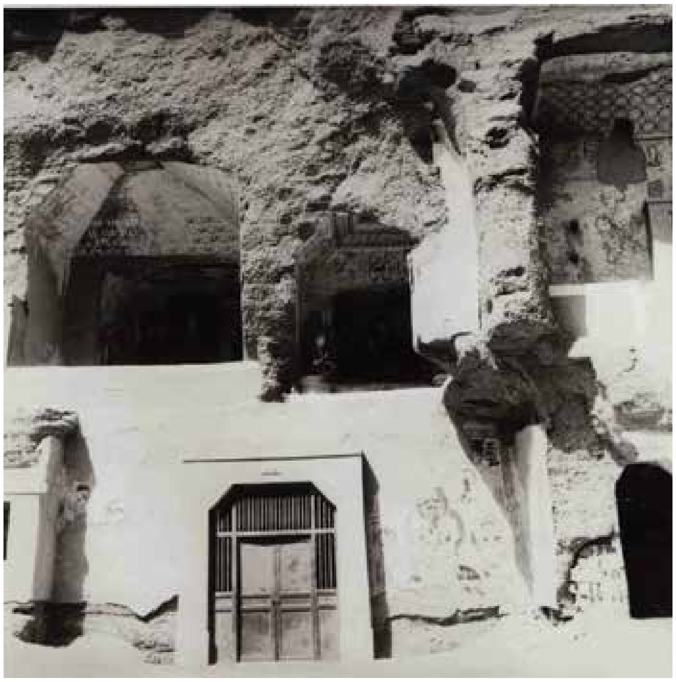

Fig. 9.14 Cave 85 showing a doorway constructed at the corridor entrance. The date of the installation of this door is not known.

partial collapse. Seismic activity may have accelerated this process. A technique for strengthening the remaining rock ceilings was devised using a composite layer of a geosynthetic mat and a geomembrane (Agnew et al. 1999). Surface sand on top of the composite material was then consolidated with potassium silicate to create a natural appearance, and areas within the cave were plastered over.

Physical History of Cave 85

The earliest known photograph of the exterior of Cave 85, taken by the Russian expedition (led by Sergei Oldenburg) to Mogao in 1914–15, provides a sense of the condition of the cave at that time (fig. 9.11). Taken some fifty years before the construction of the modern cliff facade, it shows sand accumulation in the cave entrance and a tree growing close to the cliff in what was once the antechamber. The cave has no door, and only part of the antechamber survives, with wall paintings visible on the west wall. Another photograph from this period shows the south wall of the corridor (fig. 9.12). Images of both the antechamber and the corridor show extensive losses to the paintings and areas of exposed conglomerate at the base of the walls.

The next photographs of Cave 85, from the James and Lucy Lo archive, date from 1943–44. These black-and-white photographs are the first known images of the main chamber (fig. 9.13).[6] The sculptures are already restored, and the wall paintings in the main chamber have the same losses at the base of the walls as seen in the earlier Oldenburg photographs, most likely from wet sand banking up against them for long periods. There are also large losses of plaster in the upper areas of the west wall, on the west slope of the ceiling, and on the altar platform. Paint loss is also apparent across the entire west wall. A wooden door was later installed at the entrance to the corridor (fig. 9.14).

A photograph taken by Irene Vongehr Vincent in 1948 shows the exterior of the cave and new plaster fills around the surviving areas of painting in the antechamber (fig. 9.15). This is the first photograph documenting stabilization work to the cave wall paintings. A series of images were also taken by the Dunhuang Academy in the 1960s documenting cliff stabilization work around Cave 85 as it was carried out (figs. 9.16–9.20).

Concrete tiling was installed in 1986 on top of an existing cement floor that was laid in 1959. The current aluminum louver door with vents was installed in 1987, the same year that Cave 85 was opened to the public. Protective glass screens (on wheels) were also placed in front of the walls in 1985 in preparation for the cave being opened to the public. A steel grid door was added at the entrance for extra security in 1999 (fig. 9.21).

Interventions to Wall Paintings and Sculpture in Cave 85

The sculpture in Cave 85 was restored during the Late Qing or Early Republic period, possibly by Wang Yuanlu. The altar platform was repaired sometime after 1944 by the Dunhuang Academy.[7] The wall paintings underwent two major periods of treatment by the Dunhuang Academy in the 1940s and 1970s (see table 9.2).[8] These interventions included both surface and subsurface treatments such as fixing of flaking paint and surface consolidation and in-depth treatments such as plaster repairs of areas of loss and securing detaching plaster. Treatments during the 1970s dealt with recurring problems, which reappeared approximately twenty-five to thirty years after the previous intervention (in the 1940s). The continuation of these problems indicates failure to successfully address the causes of deterioration.

Surface and Subsurface Treatments to Wall Paintings

In 1963 the Dunhuang Academy recorded severe paint flaking and disruption of plaster in Cave 85. Black-and-white photographs from 1973 show extensive flaking on the east wall (fig. 9.22). Comparison of a photograph of the east wall from 1943–44 with the same area in 2009 shows significant loss of paint layer (fig. 9.23). In 1974 the east wall and the western end of the main chamber were treated with acrylic emulsion, which was both injected behind paint flakes and applied as a surface consolidant (fig. 9.24). According to the Dunhuang Academy roughly 186 m^2 of wall painting were treated in this manner.

Twenty-five years later, in summer 1999, following a period of prolonged rainfall, severe exfoliation and losses of the painted surface occurred at the western end of the cave in an area that had been treated in 1974. The Dunhuang Academy initially carried out emergency treatment using polyvinyl acetate (PVAc). This treatment was discontinued in fall 1999, and instead a slurry of clay and distilled water was used in areas where paint had been lost or was lifting and the earthen plaster was friable as a result of salts (fig. 9.25).

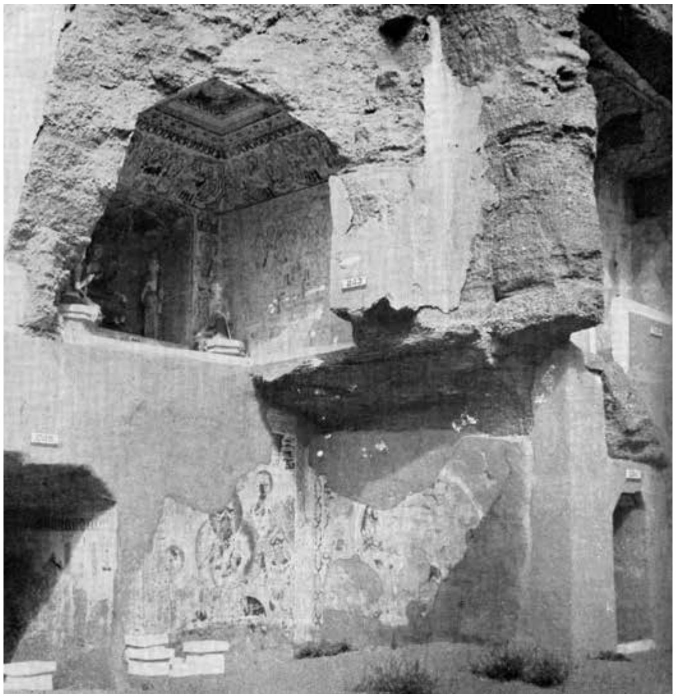

Fig. 9.15 Cave 85 as photographed by Vincent in 1948 showing plaster repairs on the west and north walls of the antechamber. This is the earliest image showing stabilization work on the wall paintings.

In-Depth Treatments to Wall Paintings

Photographs from the late 1940s and 1950s show plaster fills in areas of flood damage along the base of the walls in the corridor as well as in the antechamber (fig. 9.26). The cave documentation book also records treatment at this time on the corridor ceiling and the base of the walls in the main chamber and in upper areas at its western end. These repairs were carried out between 1944 and 1948.

By 1974 a new loss had appeared on the west ceiling slope of the main chamber, which was then filled with a hard, gray-colored plaster (figs. 9.27, 9.28). Sometime after 1974 another loss occurred in the south corner of the west slope (fig. 9.29). This loss corresponded to the location of a repair filled in the 1940s. Most recently, in 1996, another loss occurred on the west slope.

Fig. 9.16 Cave 85 in the early 1960s showing construction of a stabilizing wall to support overhanging areas of conglomerate. The door at the entrance to the corridor has been removed.

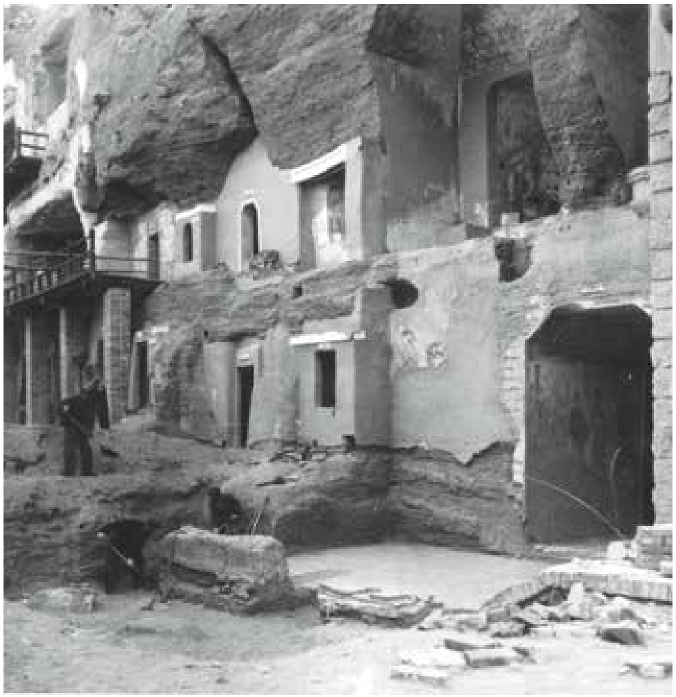

Fig. 9.17 Cave 85 during archaeological investigation in 1963. The original floor level, the extent of the antechamber, and the foundations of the Five Dynasties and Yuan dynasty temple front platforms were found at this time.

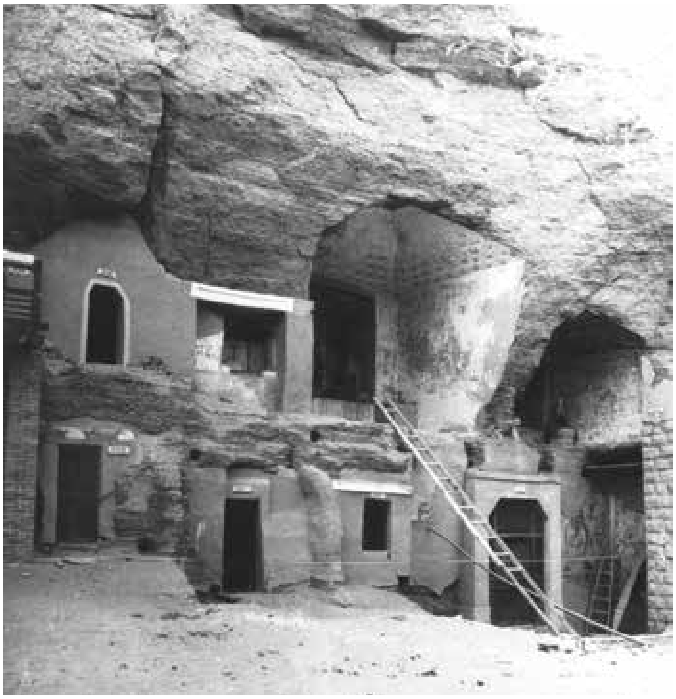

Fig. 9.18 Cave 85 in the 1960s showing the addition of a second wooden door. A ladder is positioned to access the caves above.

Fig. 9.19 Cave 85 sometime between 1963 and 1965 showing the walkways under construction.

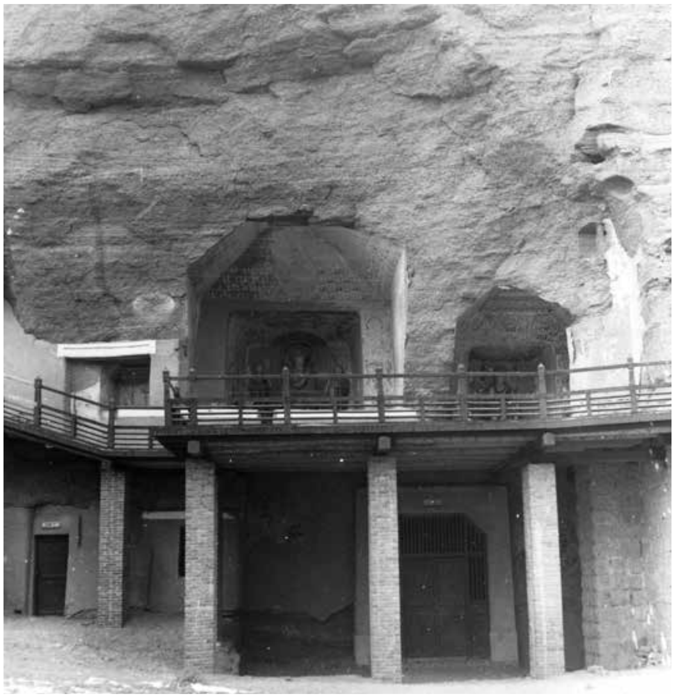

Fig. 9.20 Cave 85 in 1965 after the walkways have been completed. The wooden door is visible at the entrance to the corridor, but the antechamber is still exposed to the elements. An area of painting on the west wall of the antechamber is just visible below the walkway and to the left of the door.

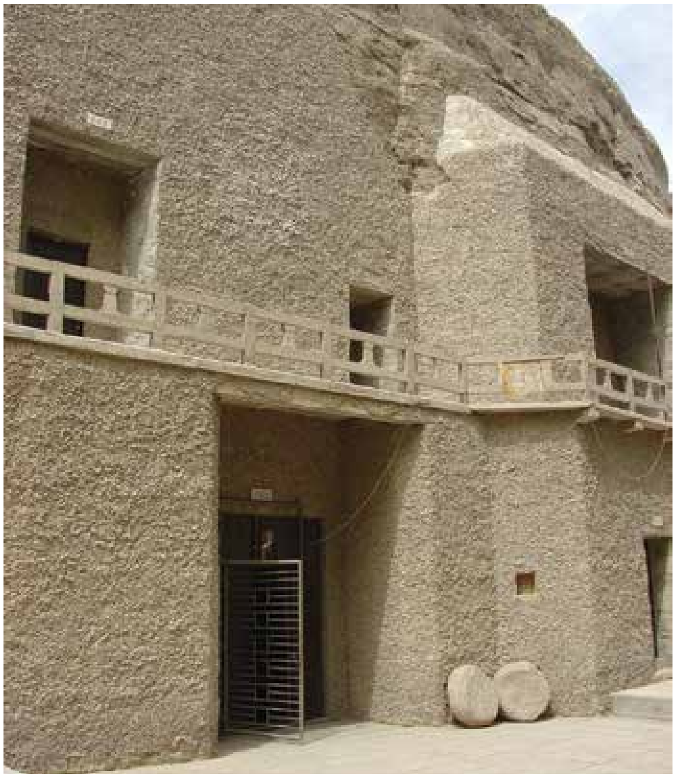

Fig. 9.21 Cave 85 today showing the modern facade that now encloses the antechamber and the aluminum louver and metal grid doors.

DATE	INTERVENTION	LOCATION WITHIN CAVE	MATERIALS/METHOD OF APPLICATION
PERIOD 1			
1944–48	Plaster fills	Main chamber: around lower portion of all walls,* upper areas of the west wall, and on west ceiling slope Corridor: lower portions of north and south walls and ceiling	Earth and straw plaster covered by a hard skim coat, possibly containing cement or lime
	Plaster fills	Antechamber: lower and upper portions of north and west walls	Earth and straw plaster without hard skim coat
PERIOD 2			
1974	Reattachment of flaking paint	Main chamber: west end of the south and north walls, west wall, west slope, and portions of east wall Entrance corridor: portions of south and north walls	Fixing of paint flakes with a mixture of 1.5% polyvinyl alcohol (PVA) and 2% polyvinyl acetate (PVAc) emulsion (1:4) injected behind paint flakes and lightly pressed back with brushes, metal spatulas, and cotton balls covered with silk Consolidation of surface with a mixture of 2% PVA and 3% PVAc emulsion (1:4), sprayed on
	Surface consolidation	Main chamber: entire west wall	1% PVA and 1.5% PVAc emulsion (1:4), sprayed on
	Plaster fills	Main chamber: west slope	Plaster, possibly lime-based
	Anchoring of detached wall paintings	Main chamber: on east wall (1 anchor), north wall (2), and west slope (2) Corridor: ceiling (5)	Metal anchors (8) painted to match surrounding areas of painting; transparent Plexiglas cross-braces (2) on north wall

Table 9.2 Summary of Previous Conservation Interventions to the Wall Paintings in Cave 85

*These plaster fills were removed in 1999 by the Dunhuang Academy.

Fig. 9.22 A 1973 image of severe paint flaking on the north side of the east wall of the main chamber.

Fig. 9.23 Photographic documentation indicates severe paint loss on the east wall of the main chamber. Compare the north side of the east wall in 1943–44 (a) to a photograph taken in 2009 (b).

Fig. 9.24 A gun was used to apply adhesives to fix areas of flaking paint in the early treatment of the wall paintings at the site.

Fig. 9.25 Severe exfoliation and loss of painted surfaces occurred in Cave 85 following a period of prolonged rainfall in an area previously treated in the 1970s at the western end of the main chamber (a). A slurry of clay and distilled water was used, injected by pipette, to readhere lifted layers (b).

In addition to the repairs, large areas of detached plaster were stabilized in 1974 by pinning the painted plaster using anchor-braces mounted on long steel rods (fig. 9.30). Ten anchors were installed throughout the cave. The anchors were unfortunately an imperfect solution to plaster detachment as they caused damage to the painting during installation and created stress on surrounding areas, which leads to cracking and eventual loss of plaster over time. The plaster loss that occurred on the west slope in 1996 was located next to a metal anchor installed in 1974 (fig. 9.31).

Summary

The recurring nature of conditions in Cave 85 following previous treatment indicated that the cause of deterioration was still present. The Dunhuang Academy attributed the deterioration to moisture present at the base of the walls and lack of ventilation in the cave. As a result an iron grid door was installed at the entrance of the cave to allow for the door to be kept open to provide ventilation while maintaining security. At this time the plaster fills from the 1950s along the base of the walls in the main chamber were removed, leaving the conglomerate exposed in order to increase evaporation of any moisture in the wall.

The DA-GCI project determined that the moisture problem in the cave was actually related to the entry of water vapor from the exterior during periods of rain and high humidity and that installation of a new, tight-fitting door to reduce air intrusion—rather than to encourage ventilation as previously thought—would be most beneficial. It was recommended that this door be kept closed at all times but particularly during and after rain and periods of high humidity (see chaps. 15, 17).

Fig. 9.26 This 1957 image shows a large plaster repair at the base of the south wall of the corridor. Comparison with the Russian expedition photograph taken in 1914–15 (see fig. 9.12) indicates that the paintings have also been cleaned.

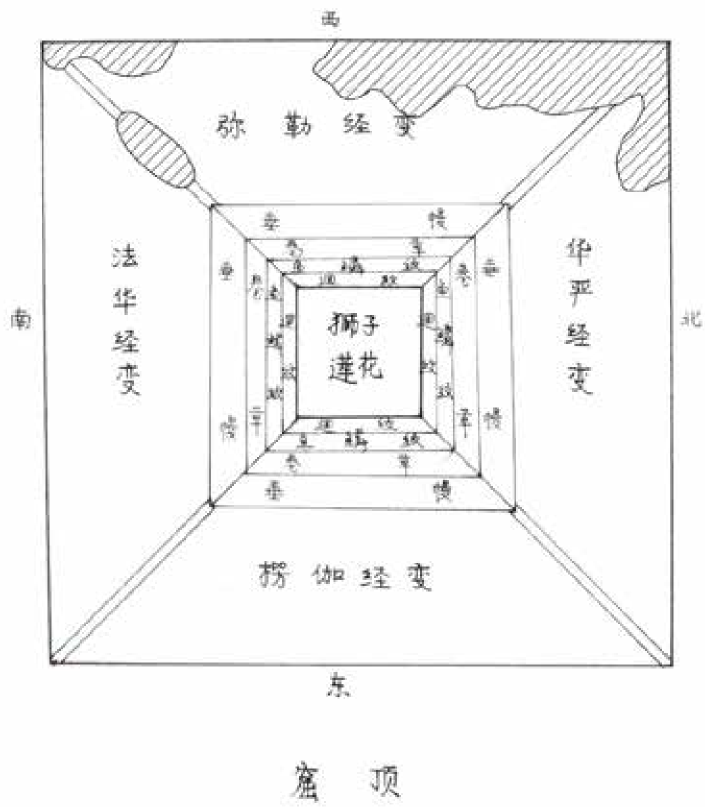

Fig. 9.27 Graphic documentation from the Cave 85 documentation book records plaster fills in 1974. A new area of loss not previously noted on the west slope is recorded for the first time (see fig. 9.28).

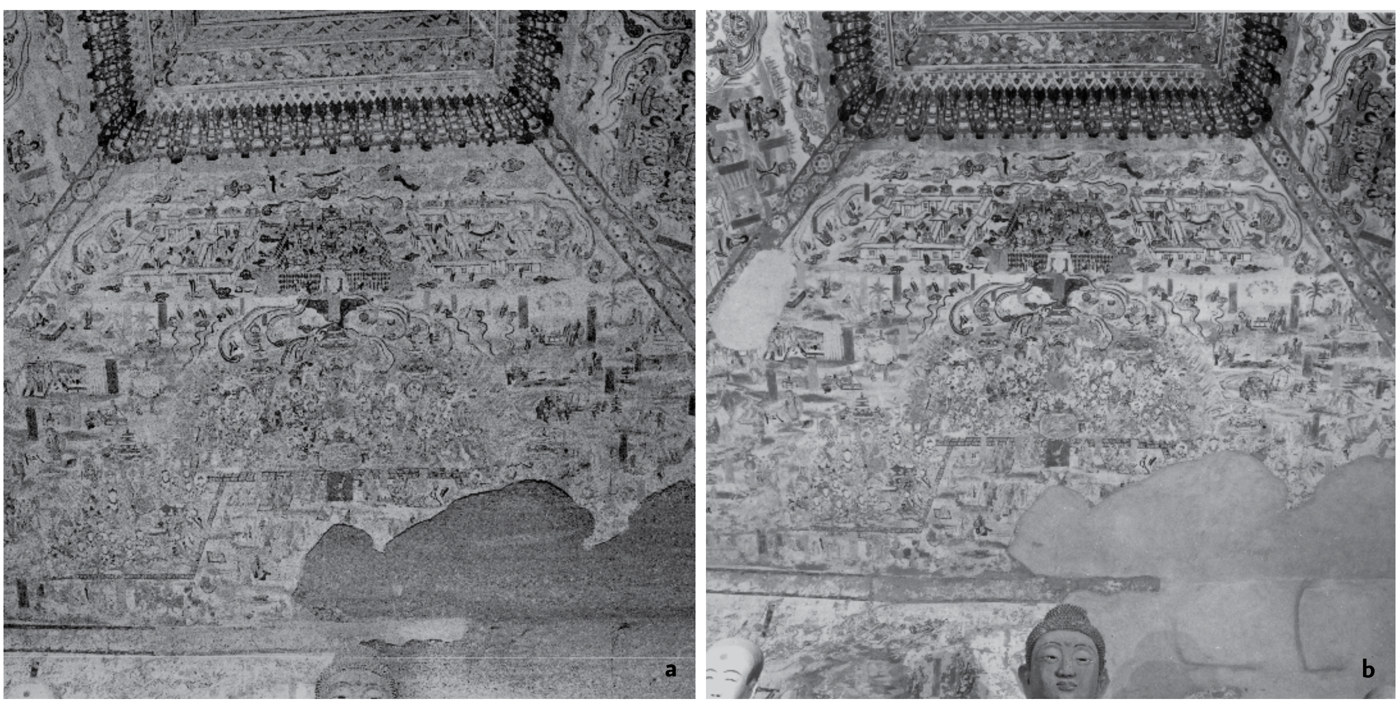

Fig. 9.28 Loss and repair over time can be analyzed using photographs. The west ceiling slope as photographed in 1943–44 (a) and in 1987 (b). The losses shown in 1943–44 have been filled, but a new oval-shaped plaster repair that is whiter in color and looks to be composed of different materials is visible in the 1987 image. Both periods of repair are recorded in the 1974 graphic documentation (fig. 9.27).

Fig. 9.29 Image showing deterioration in the upper southwest corner of the main chamber. A new loss has occurred in this area since the plaster repairs were recorded in 1974.

Fig. 9.30 In the 1970s the Dunhuang Academy used anchor braces to secure an area of detaching plaster. The process consisted of drilling a hole through the plaster and into the conglomerate. A rod was inserted and a metal or Plexiglas cross-anchor bolted on top, bracing the plaster back to the conglomerate. Metal crosses were painted to match the surrounding decoration. It is possible that the metal and Plexiglas anchors represent two different periods of treatment, although there is no record of this. This photograph is not of Cave 85.

Fig. 9.31 Loss of painted plaster from the west slope in 1996 near a metal anchor installed in 1974.

Notes

1. For a complete account of explorers who traveled to Dunhuang, see the Collection pages of the International Dunhuang Project (IDP) website (http://idp.bl.uk/pages/collections.a4d). The IDP is an international collaboration aimed at providing information and images of more than 100,000 manuscripts, paintings, textiles, and artifacts from Dunhuang and other Silk Road sites.
2. The Dunhuang Academy's photographic archive is currently being digitized.
3. These recollections are unpublished.
4. The completion of flood control measures for the site is one of the specific conservation objectives of the draft 2001–10 Mogao Master Plan (China Architectural Design Academy et al. 2010).
5. The Institute of Desert Research in Lanzhou selected the plants. The irrigation drip fence was designed by Po-Ming Lin, consultant of the Getty Conservation Institute.
6. The Lo Archive at Princeton University contains 2,590 black-and-white negatives of the caves taken in 1943–44. This collection can be viewed online at the Mellon International Dunhuang Archive (www.artstor.org/info/collections/mida.jsp).
7. The Lo Archive photograph from 1943–44, which shows the altar platform before restoration, is the earliest known image of the platform.
8. This was recorded in the Cave 85 documentation book and verified by project team members through oral communication with Li Yunhe, former head of the Conservation Section of the Conservation Institute, Dunhuang Academy.

Assessments

CHAPTER 10

Statement of Cultural Values and Significance

Fig. 10.1 A view of the Mogao Grottoes, which were inscribed on the World Heritage List in 1987.

The significance assessment is an essential part of any heritage conservation project. The identification and resulting statement of cultural values and significance is used to guide decision making throughout the course of a project in order to ensure that the values and significance of a site are conserved unimpaired.[1] This is a fundamental precept of the China Principles (Agnew and Demas 2002) and other international heritage conservation and management guidelines. The significance assessment for Cave 85 included identification of historic, artistic, scientific, and contemporary social and economic values of the site as a whole and of the cave itself. Further, these values were important in relation to future use of the cave for public visitation.[2]

In summary, the essential points in the cultural values and significance statement for Mogao and Cave 85 are presented here.

The Site

- The Mogao Grottoes—one of the world's significant cultural artifacts—was listed by the State Council of the People's Republic of China as a nationally protected site in 1961 and was inscribed on the World Heritage List in 1987 (fig. 10.1).
- The geographic location of Mogao at the crossroads of cultures from the East and West ensured its prominent

Fig. 10.2 Rolled up manuscripts from the Library Cave in the corridor of Cave 16.

Fig. 10.3 The paintings in Cave 85 are an important pictorial record of Late Tang dynasty life in China that includes information on musical instruments, as seen in these details from the south wall of the main chamber.

place in history as one of the most important historical and cultural sites on the Silk Road.

- The grottoes afford a unique record of the introduction, evolution, and practice of Mahayana Buddhism and Buddhist art in China.
- The grottoes, as the oldest, best-preserved, most richly endowed, and largest collection of Buddhist art in China, provide an unparalleled overview of one thousand years, from the fourth to the fourteenth century C.E., of Chinese Buddhist mural painting and sculpture.
- Documents from the famous Library Cave (Cave 17), discovered in 1900, together with the wall paintings continue to be studied by scholars around the world (fig. 10.2).
- The paintings and sculpture constitute a valuable historical record of the arts and music, architecture, science and technology, politics and law, and economic and military situations of the times (fig. 10.3).
- The setting in a desert landscape has a high aesthetic and natural value (fig. 10.4).
- The site is of cultural and religious significance to the local community and to national and international visitors.
- The grottoes offer educational and research value to various professional communities.
- Economic stimulus to the local community in Dunhuang and Gansu Province is generated by tourism. An estimated 350,000 visitors visit the grottoes yearly (fig. 10.5).[3]

Fig. 10.4 The desert landscape of the Mogao Grottoes is of high aesthetic and natural value.

Cave 85

Historic Values

- Cave 85 took only six years to complete (862–67 C.E.), testament to the many resources available for its construction.
- Cave 85 reflects an interesting period of history from the Middle to the Late Tang, following the Tibetan occupation of Dunhuang (781–848). The choice of sutras depicted in Cave 85 reflects the sociopolitical climate of the time, illustrating stories of righteousness overcoming evil, which expressed joy over the territory's return to Tang rule. Two such stories include Sakyamuni's defeat of the demon king Mara and the contest of powers between the Buddha's disciple Sariputra and the

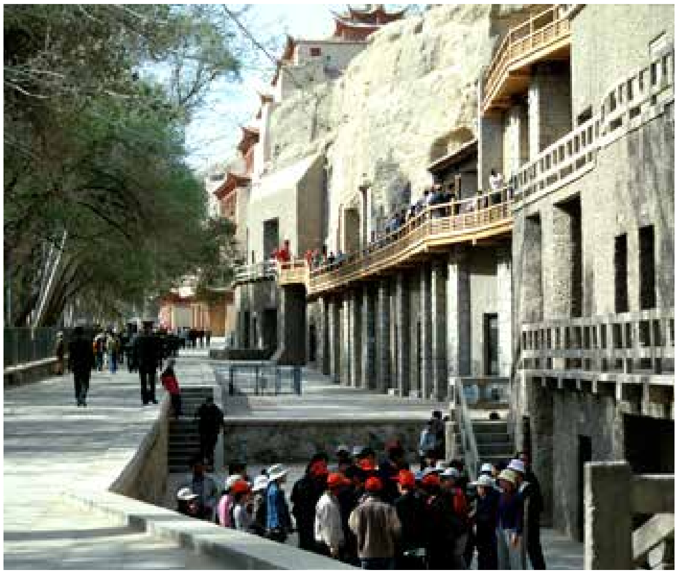

Fig. 10.5 Tourism at the site provides economic benefits to the local community and to Gansu Province.

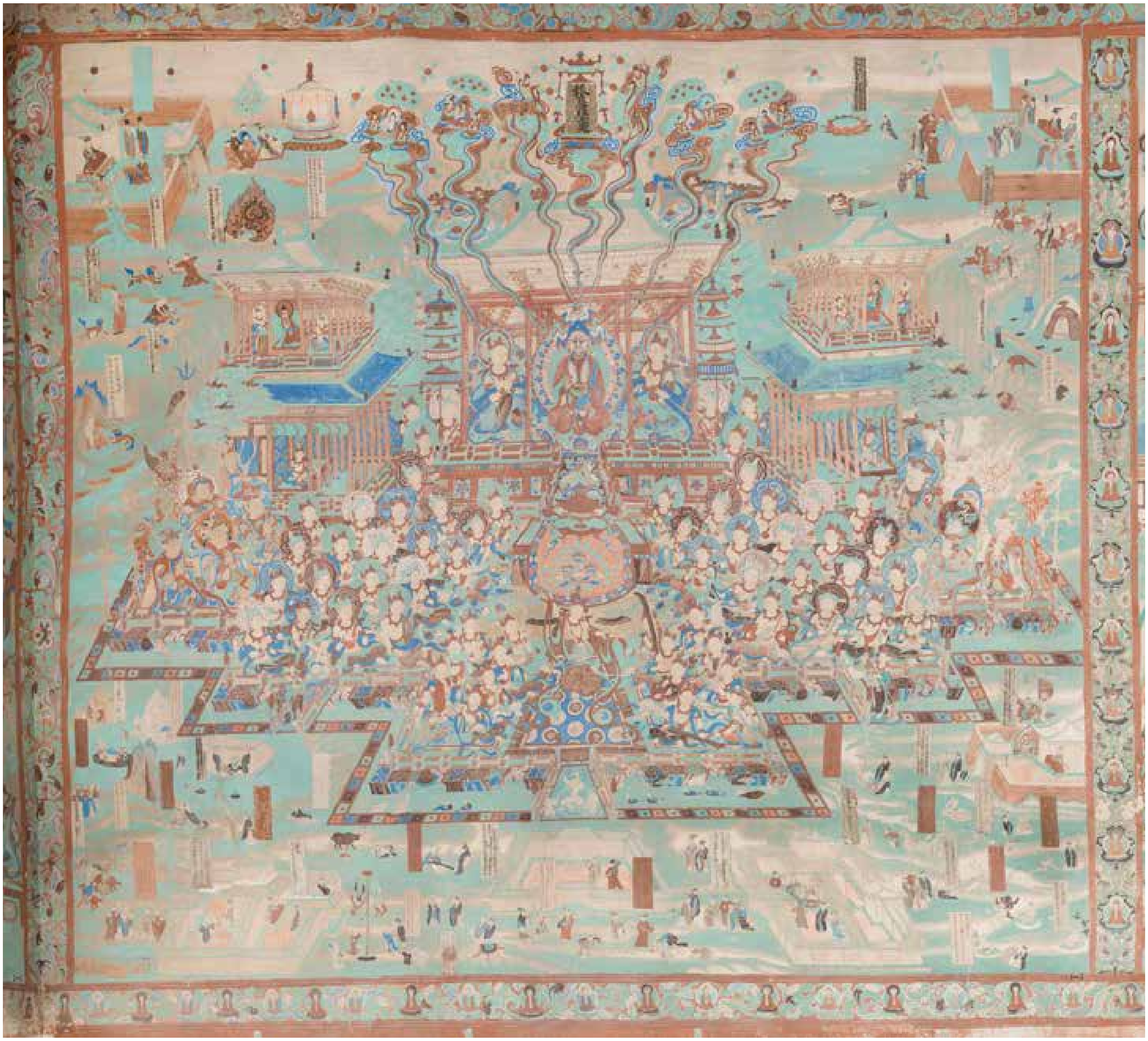

Fig. 10.6 The Sutra on Requiting the Great Kindness of Parents (*Bao Fumu Enzhong Jing*) on the east side of the south wall of Cave 85 shows typical Chinese customs such as filial piety. During the Late Tang, Dunhuang's population was a mix of various nationalities, including Tibetans, Uighurs, and Central Asian peoples. The depiction of Chinese sutras during this period was an intentional effort to reemphasize Chinese identity.

heretic Raudraksha (also referred to as the Magic Competition) depicted in the main chamber of the cave. These stories first appeared across an entire wall in the Late Tang in Cave 85 and became a popular theme thereafter, appearing in other caves through the 980s.

- Dunhuang was a mix of various nationalities (including Tibetans, Uighurs, and Central Asian peoples) during the Late Tang. The Han rulers wanted to reemphasize their Chinese identity and reaffirm their loyalty to the Tang emperor. As a result, the paintings became more Chinese in style, with sutras selected that showed typical Chinese customs such as filial piety. The Sutra on Requiting the Great Kindness of Parents (Bao Fumu Enzhong Jing) on the east side of the south wall of Cave 85 is one such example (fig. 10.6).
- Documents found in the Library Cave, now in the Pelliot collection of the Bibliothèque nationale de France, were instrumental in establishing the history of Cave 85.[4] For example, document P. 4640 references the construction of Cave 85 and provides information on the Zhai family, which commissioned the cave.
- Cave 85 was one of a few caves commissioned by the high-ranking official Zhai Farong to demonstrate the wealth and social status of the Zhai family and to celebrate and commemorate his appointment as the highest-ranking monk in the Hexi area. Portraits of Zhai Farong and his family appear on the north wall of the corridor (fig. 10.7).
- The cave was one of nearly sixty caves restored or constructed during the rule of the Zhang family in the Late Tang period to commemorate their meritorious deeds. Zhang Yichao was the commander general of the Return to Allegiance Army, which ruled the Dunhuang area from 851 to 1036. Cave 85 was constructed during this time, and portraits of Zhang Yichao and his nephew, Zhang Huaishen, were depicted on the south wall of the corridor. These figures were painted over when the corridor was restored during the Five Dynasties period and are no longer visible.
- The cave includes portraits of the Cao family, which ruled Dunhuang during the Five Dynasties and sponsored the restoration of some fifty-five caves at Mogao. Cao Yijin and his family are pictured on the south wall of the corridor. Lady Cao, daughter of the regional high official who sponsored the construction of Cave 98, is depicted on the east wall of the main chamber.

Fig. 10.7 Cave 85 was built by the Zhai family to commemorate the appointment of Zhai Farong as the highest-ranking monk in the Hexi area. A portrait of Zhai Farong is found on the north wall of the corridor.

- Cave 85 is one of the first caves at Mogao to depict life-size donor portraits of both the cave benefactor and high officials of the area.
- The paintings provide information about aspects of daily life and common customs in their depictions of, for example, a butcher shop, hunting scenes, a pottery factory, acrobats and magicians, market scenes, wedding scenes, farming, fights, and women applying makeup. The paintings comprise what has been termed a pictorial encyclopedia that includes information on the weapons, costumes, musical instruments, tools, animals, and transportation of northwestern China in the late ninth century (fig. 10.8).
- The use of cartouches, which were placed to highlight specific events and punctuate the narrative progression, became more common in the Mogao paintings after 850 and are prominently featured in Cave 85 (fig. 10.9).
- The Suvarna-prabhasa Sutra, depicted on the east wall

Fig. 10.8 The paintings are a pictorial encyclopedia of life during the Late Tang dynasty. They include scenes from daily life, such as a man throwing a pot on a wheel (a) and acrobats performing (b). Both images are from the Lankavatara Sutra on the east ceiling slope of the main chamber.

Fig. 10.9 Text cartouches, used to help the narrative progression of the sutras depicted, became more common in paintings at Mogao after 850 C.E. They are plentiful in the paintings in Cave 85, as seen in this detail from the south wall.

Fig. 10.10 The Lankavatara Sutra on the east ceiling slope of the main chamber is a masterpiece of Late Tang painting at Mogao.

of the main chamber, illustrates the most complete inscription of this sutra found at Mogao.

- The cave contains sutras rarely depicted at Mogao, including the Diamond Sutra, Suvarna-prabhasa Sutra, Lankavatara Sutra, Visesacintabrahma-pariprccha Sutra, and Ghanavyuha Sutra. In addition, sutras that had already been depicted in other caves were further elaborated with additional detail and substories in Cave 85.
- The appearance of multiple sutras on a single wall is evidence of Tibetan stylistic conventions during the occupation of Dunhuang. Cave 85 is one of the earliest caves to exhibit this influence: its north and south walls each contain three sutras. In earlier caves, it was common for only a single sutra to occupy an entire wall.
- The cave is one of only a handful of caves at Mogao built to serve as a private family temple. The Zhai family built two: Cave 85 and Cave 220.

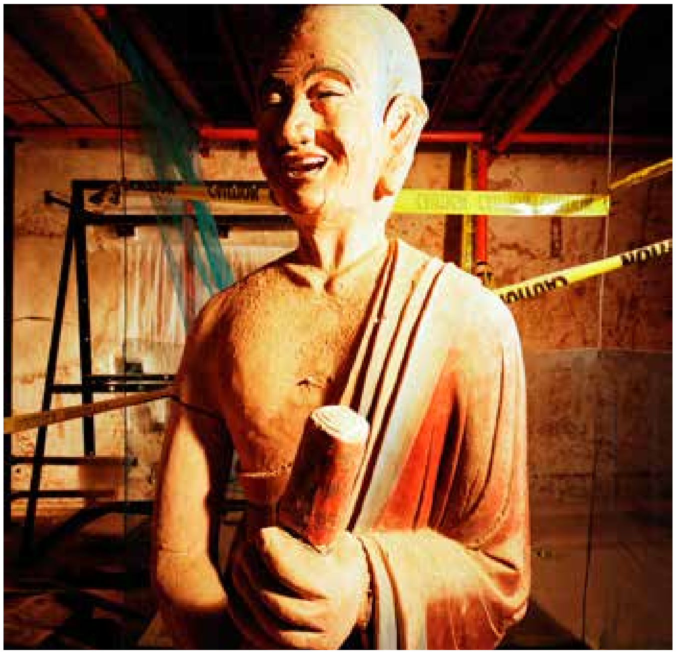

Fig. 10.11 The Kasyapa, though restored during the Late Qing or Early Republic, still retains some original Late Tang features. The scroll carried by this figure is identified as the Diamond Sutra by its inscription. The image shows the statue before conservation treatment during the current project.

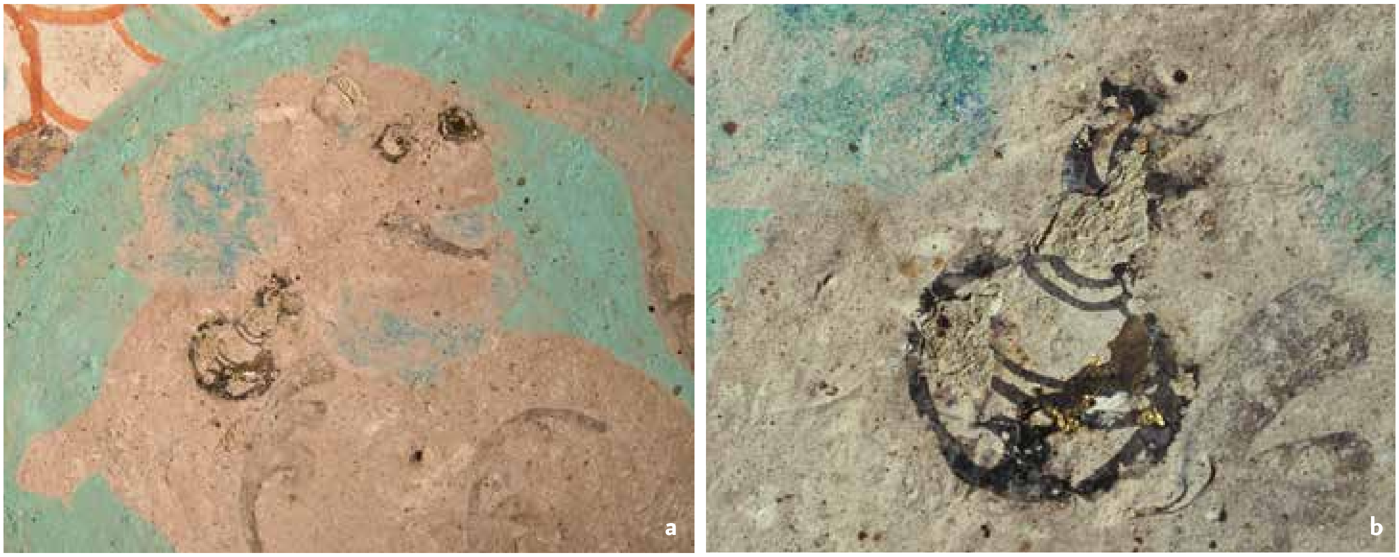

Fig. 10.12 Small amounts of gold were found surviving on the lion on the central ceiling panel (a), including on the eyes and bell (b).

Fig. 10.13 The Yuan dynasty painting in the antechamber has raised relief decoration with metal foil.

Artistic Values

- The painted decoration in the main chamber of Cave 85 from the Late Tang period (848–907) is of the finest quality. The paintings include representation of seventeen sutras of the Buddha. The Lankavatara Sutra on the east slope of the ceiling is generally considered among the masterpieces of Late Tang painting at Mogao (fig. 10.10).
- Despite the restoration of the sculpture (most likely undertaken by the Daoist monk Wang Yuanlu in the Late Qing dynasty or Early Republic period) the central statue of Sakyamuni (seated in an unusual pose, with his left leg crossed over his right) and the figure of Kasyapa retain some original Late Tang features and painting. This sculpture holds a scroll identified as the Diamond Sutra by its inscription (fig. 10.11). Only the figure of Ananda was completely replaced during the restoration.
- The paintings and sculpture provide information on painting technology from the Late Tang dynasty, including both materials and application methods. Gold was found on the eye of the lion on the central ceiling panel and on the altar platform of the main chamber (fig. 10.12).
- The areas of overpainting in the corridor and lower part of the east wall of the main chamber provide information on painting technology during the Five Dynasties, including the use of stencils, as seen in the corridor.
- Fine quality overpainting survives in the antechamber from a period of redecoration in the Yuan dynasty. This painting has metal foil attachments and raised relief decoration (fig. 10.13).

Scientific Values

- Analysis of pigments, organic colorants, and binding media may yield information on sources of materials, trade routes, and ancient technology.
- Identification of organic colorants in the wall paintings is among the first recorded instances of their use at Mogao.
- Information on the technology of the Late Tang dynasty may be inferred from the wall paintings, and in certain instances there is the possibility of correlation with information from documents in the Library Cave.
- Study of changes to the wall paintings provides information on the cave environment and is of relevance to the conservation of other caves at Mogao and at similar sites on the Silk Road.

Contemporary Social Value

- Cave 85 is a large cave with high visitation potential because of its manifold values. Recently reopened to special visitation, the cave offers interpretive material that explains these values and the work of the project, communicating a message of conservation.
- The Cave 85 project has the potential to become a model for international collaboration leading to best practice conservation at other similar sites on the Silk Road and throughout China.

Notes

1. Much of what is included here is based on the significance statement prepared for the master plan for the conservation and management of the Mogao Grottoes (China Architectural Design Academy et al. 2010).
2. Cave 85 was previously open to visitors but was closed during the GCI-DA conservation project. The cave reopened to special visitation in 2011.
3. This is based on an average of the visitor numbers from 1997 to 2010.
4. Digitized versions of these documents are accessible at http://gallica .bnf.fr/.

CHAPTER 11

Management Context

An assessment of the management system of the Mogao Grottoes, under the authority of the Dunhuang Academy (and ultimately China's State Administration of Cultural Heritage within the National Ministry of Culture), was undertaken at the start of the project to establish the necessary measures and improvements required to ensure a successful collaborative conservation project in Cave 85 between the Dunhuang Academy and the Getty Conservation Institute. The main operational partner of the GCI for the Cave 85 project has been the Dunhuang Academy's Conservation Institute, itself a nationally recognized scientific research entity specialized in wall painting and earthen architecture conservation (fig. 11.1).

Fig. 11.1 Members of the conservation team at work in Cave 85. The team is composed of Dunhuang Academy and Getty Conservation Institute staff and consultants.

The Dunhuang Academy

The Dunhuang Academy began in 1944 as a unit established to study and protect the site.[1] Over the past six decades the DA has been increasingly effective in the management and conservation of the site. Since 1979, it has built a management team and established a visitor reception department, a conservation institute, an art institute and art historical research and archives, a security department, and maintenance and grounds sections. The DA has authority over two other sites in the region: the Yulin Grottoes and the Western Thousand Buddha Grottoes. Today the Dunhuang Academy is widely regarded as an organization of national importance because of its expertise in management and conservation research and application (fig. 11.2).

Fig. 11.2 The main Conservation Institute building of the Dunhuang Academy at the Mogao Grottoes.

The Dunhuang Academy has also effectively collaborated over the long term with international organizations. Through these collaborations its Conservation Institute has expanded its expertise and scientific capabilities to the extent that it is called upon increasingly to undertake projects for other sites in China, notably in the Xinjiang and Tibet Autonomous Regions.

Fig. 11.3 The Getty Conservation Institute in Los Angeles.

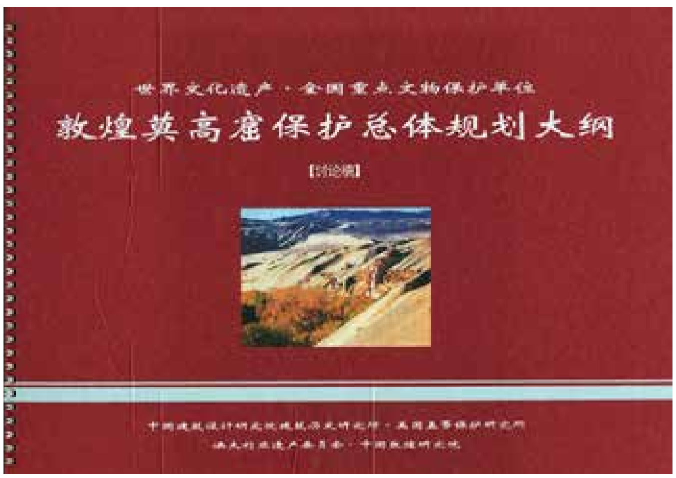

Fig. 11.4 The Mogao Master Plan, issued in 2010.

The Getty Conservation Institute

The Getty Conservation Institute, a program of the J. Paul Getty Trust, began operation in 1985 to advance conservation practice in the visual arts (fig. 11.3).[2] Since its inception, the GCI has engaged in a program of model field projects, scientific research, educational activities, documentation, and dissemination of information through publications, conferences, workshops, and public programs. It has conducted international field projects in Asia, Africa, North and South America, and Europe.

Advancing conservation practice is the organizing principle for all of the GCI's work—which includes identifying activities that improve the way conservation treatments are carried out, pursuing research that expands conservation knowledge, and increasing access to information on conservation subjects. The GCI's activities continue to emphasize scientific research into the nature, decay, and treatment of materials; educational initiatives for the conservation professional; model field projects designed to advance conservation practice internationally; and the dissemination of information through both traditional publications and electronic means.

Context of the Partnership

China has well-codified heritage laws (revised in 2002), as well as regulations and ordinances governing heritage sites. A master plan for the Mogao Grottoes was drafted over a number of years by the Dunhuang Academy, the Getty Conservation Institute, and the Australian Heritage Commission (China Architectural Design Academy et al. 2010). This document was compiled in accordance with both legally binding requirements and the *Principles for the Conservation of Heritage Sites in China* (Agnew and Demas 2002), issued by China ICOMOS. The draft master plan was subsequently incorporated by the DA, working with a certified planning institution (a legal requirement for master plans at nationally important sites), into an official and legally binding document (fig. 11.4).[3]

The Cave 85 project was identified as an objective in the master plan, and adhered to the precepts of the China Principles, which are themselves based on the imperative to preserve the identified values of a site (see chap. 10). The Mogao Master Plan also provided the framework for the management of the

Fig. 11.5 A mid-project evaluation was undertaken in 2002 by a panel of experts.

Cave 85 project by the Dunhuang Academy and the Getty Conservation Institute throughout the course of the project.

Cave 85 Project Management

Management of the Cave 85 collaborative project was structured on joint decision making based on clearly stated and agreed-upon objectives and responsibilities. Continuity of the project's momentum required good communication between the partner organizations, managers, and team members and was key to both effective forward planning for the field campaigns and regular data exchange. Biannual field campaigns of two to eight weeks' duration were undertaken for site work, with research, testing, and data exchange occurring between the spring and fall campaigns according to an established schedule. Translation between Chinese and English (especially time-consuming for written documents) depended on having skilled interpreters as team members. Since team members from both institutions were committed to other projects that frequently demanded time away from Cave 85 work, problems of continuity, completion of assignments, and so on arose from time to time. These were managed by periodic review and discussion.

Project Evaluation

Formal project evaluations were built into the design of the overall project plan. These included a two-day mid-project evaluation, as mandated by SACH, undertaken at Mogao by some eight senior professionals from SACH and other sites in China (fig. 11.5). The evaluation meetings, attended by team members from the Dunhuang Academy and the GCI, comprised presentations on every component of the project. Review of progress and proposed interventions (notably grouting of detached areas of wall painting with concurrent extraction of soluble salts) was undertaken in Cave 85 itself. The meeting produced a favorable report, with constructive recommendations for additional testing, such as determination

Fig. 11.6 Informal training was conducted during each field campaign in areas of analytical investigation, documentation, environmental monitoring, and wall painting conservation.

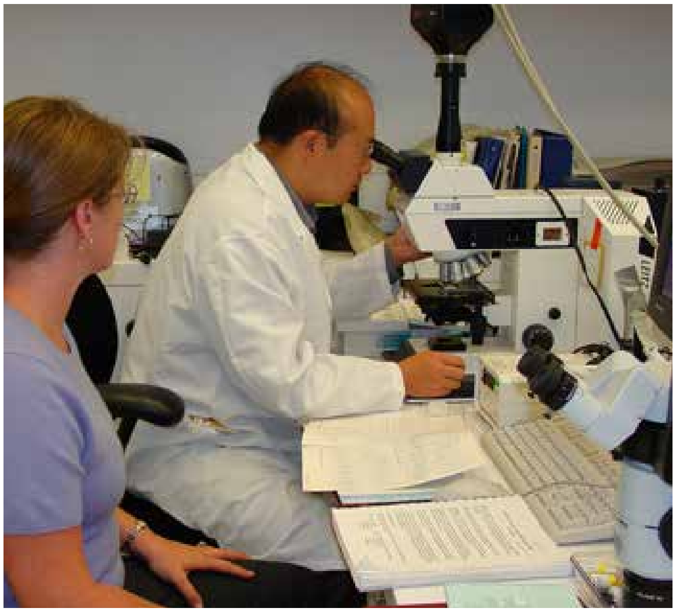

Fig. 11.7 Scientists from the GCI and the DA using polarized light microscopy to look at paint samples from Cave 85.

of the shear strength between the proposed grout formulation and the conglomerate rock.

A final evaluation by SACH will be based on the present report, which will be translated into Chinese by the Dunhuang Academy and disseminated widely within China.

Research and Training

Among the objectives of the Cave 85 project were to enhance the capabilities of the DA's conservation staff through research and training, thereby strengthening their management and application capacities over the long term. The project addressed these components in several ways: the formation of core joint teams to focus on documentation, analysis, environmental monitoring, and wall painting conservation; and informal and formal training (fig. 11.6). Informal training during campaign work served to inculcate the methodological approach and also involved annual periods of work experience in Los Angeles at the GCI's facilities on a rotational basis for DA team members (fig. 11.7). Later, the need for formal training led to an agreement between the DA and Lanzhou University to offer a master's-level degree in wall painting conservation. This has been supported by the GCI and the Courtauld Institute of Art, with instruction undertaken principally by Courtauld personnel and consultants (figs. 11.8, 11.9). As part of the formal training, in situ fieldwork was conducted in Cave 260 (fig. 11.10). A further objective of the project, supported by management of the DA, was to involve personnel from other similar sites in China so as to disseminate the fundamentals of the methodology from the beginning of the project. Intermittent participation of personnel from sites in Xinjiang and Tibet occurred.

Project Resources

Both project partners contributed resources in the form of staff expertise, funding, and consultants under the consecutive three-year agreements between the State Administration of Cultural Heritage and the GCI that spanned two decades. Given the high cost of undertaking a project of long duration in a remote region, the contribution from SACH and the DA to the GCI's internal travel, accommodations, and meals during field campaigns was critical to the sustenance and ultimate success of the collaboration.

In conclusion, the goals and objectives of the project were satisfied through a collaborative management structure that was well supported by the partner institutions.

Fig. 11.8 Representatives from the Dunhuang Academy, the Getty Conservation Institute, the Courtauld Institute of Art, and Lanzhou University meet to discuss the master's-level program in wall painting conservation.

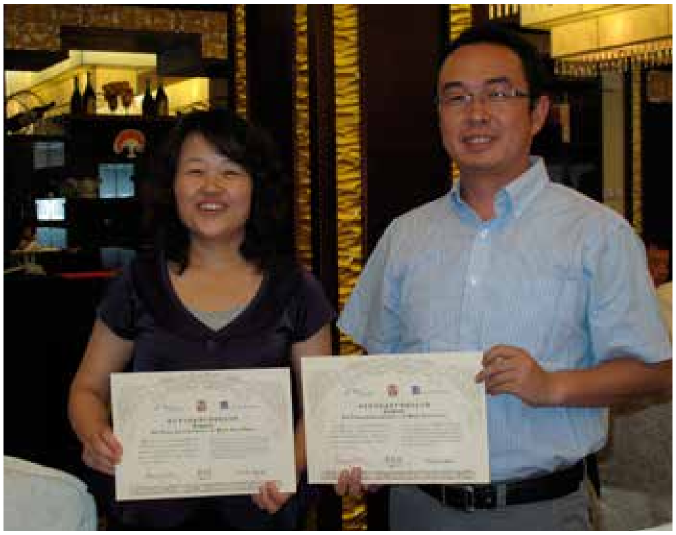

Fig. 11.9 Two graduates from the first MA course in wall painting conservation are pictured with their course certificates.

Fig. 11.10 As an important component of the MA course in wall painting conservation, students take part in in situ exercises. Here students from both Lanzhou University and the Courtauld Institute of Art are being trained in the use of a hyper-spectral imaging camera.

Notes

1. The Dunhuang Academy's website (in Chinese) can be accessed at www.dha.ac.cn.
2. The Getty Conservation Institute's website can be accessed at www.getty.edu/conservation/.
3. The certified planning institute is the Architectural History Research Institute of China Architectural Design Academy. The master plan for the Mogao Grottoes was finalized in 2010.

CHAPTER 12

Condition Assessment

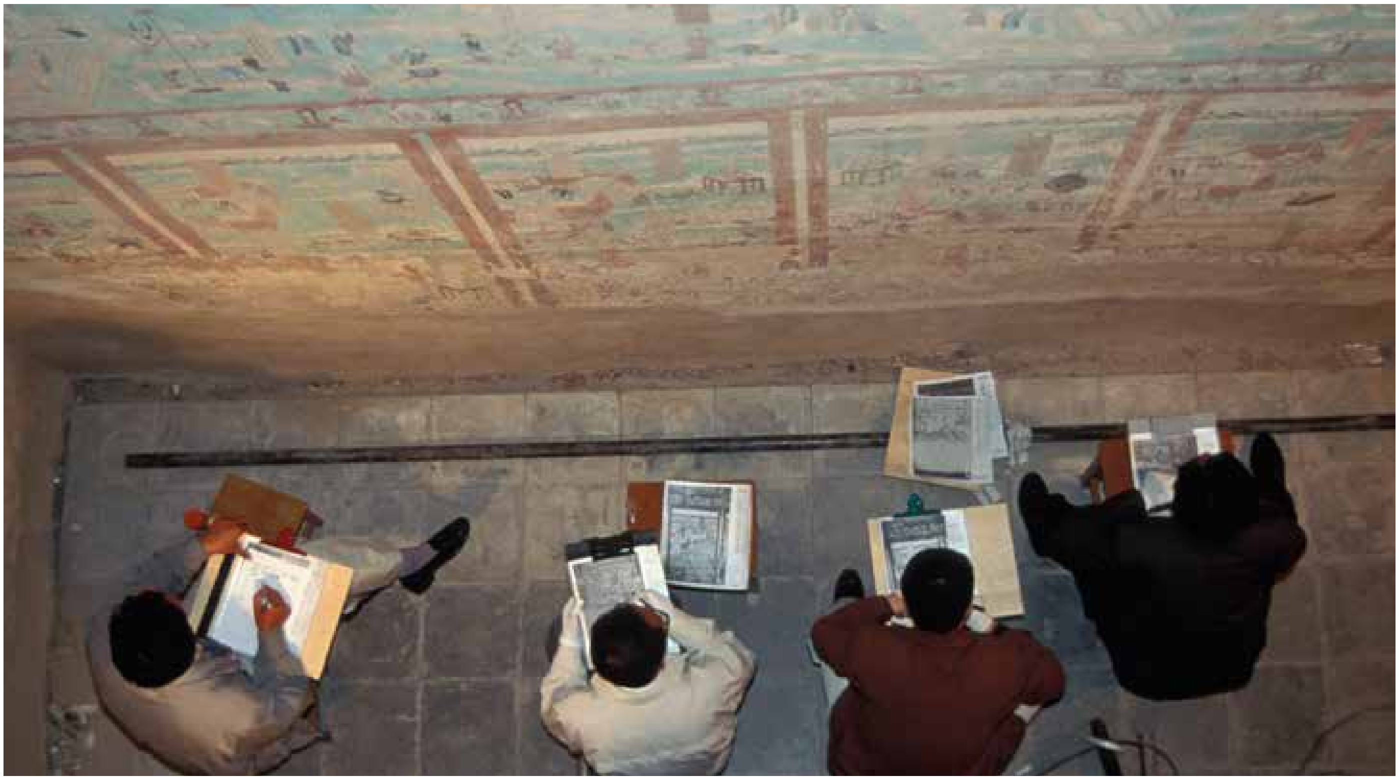

Fig. 12.1 Condition recording in Cave 85 at the base of the south wall of the main chamber.

Condition assessment in wall painting conservation is the collection and interpretation of data that provides information on physical condition, or state of preservation, at a given time (Wong 1997, 1–2). In particular, it is concerned with aspects of observable deterioration and establishing the occurrence of change over time. Documentation in this context includes any recorded information relevant to these aims (archival photographs, graphic documentation, written records of historical conditions, scientific data, and treatment reports).

The condition assessment of Cave 85 focused on the wall paintings in the main chamber, as a means of clarifying the nature of the principal forms of deterioration (fig. 12.1). Other aspects of condition could not be fully determined. For instance, although the condition of the rock is of fundamental importance, it is concealed by plaster, which limits effective assessment. The conditions of the sculpture and platform are considered separately at the end of this chapter. As discrete constructs in the cave—and having been heavily restored in past times—the sculpture and platform are largely isolated (except at the base) from the mother rock and show different patterns of deterioration from those in the main chamber wall paintings. For similar reasons, the condition of the entrance corridor and antechamber is considered only briefly. While sharing many types of deterioration with the main chamber, both these areas have been subject to different physical conditions owing to external exposure in the past.

Fig. 12.2 Semi-rectified photography was undertaken by positioning a camera at a fixed distance of 140 cm from the wall surface.

For discussion of the condition of the wall paintings in the main chamber, a number of factors are considered: definition of the objectives and uses of the condition assessment; overview of condition documentation components and procedures; summary of the constraints affecting condition documentation and assessment; summary of the nature, extent, and distribution of the observable deterioration phenomena; and evaluation and interpretation of all the accumulated information.

Objectives and Uses of Condition Assessment

Condition assessments can be undertaken to serve multiple purposes that include conservation, management, and investigation objectives. In Cave 85 it fulfilled conservation needs: to establish hypotheses about the nature and rate of deterioration, prioritize aspects of treatment, produce a record of condition before treatment, serve as a guide when undertaking treatment, and provide a record of treatment materials and methods. The condition assessment also served management purposes with the basis for risk assessment in order to prioritize conservation requirements; to identify specific treatment needs including duration of work, number of conservators required to perform the work, materials, and costs; to provide a record for developing a long-term plan for future assessment and monitoring; and to facilitate communication about the care necessary for the paintings. For investigation purposes, condition assessment was used to indicate the nature and distribution of deterioration, to help diagnose causes of deterioration, to determine whether other specialist investigations might be required, to record the effects of past treatments, and to assess the success or failure of materials and methods used.

Components and Procedures

Condition documentation in Cave 85 comprised compilation of historical documentation, overall photography, physical and conservation histories, graphic documentation, a three-dimensional model, and condition terminology.

Information was compiled on circumstances and events that have had an impact on the cave and its painting, including dates, nature, and extent of conservation interventions and treatments, in order to provide information on rates of change (see chap. 9). Information consulted included photographs, illustrations, written documentation, and oral history collected during the information gathering stage. This archival material served to illustrate general and specific changes that had affected the site and the cave (e.g., loss of the cliff frontage and subsequent exposure of the paintings at the cave entrance).

Semi-rectified photographs (using a camera positioned at a right angle and at a fixed distance of 140 cm from the wall surface) were taken both in black-and-white and color of the entire painted surface to provide a pretreatment record of the cave (fig. 12.2). This comprised 532 photographs of areas each measuring 85 × 110 cm, with a 30% overlap between images. A gray scale and color bar were included in the photograph, and each image was labeled with date, wall orientation, and wall section (see Appendix 12.A: Documentation Area Grid References) (fig. 12.3). A set of black-and-white and color photographs is archived at the Dunhuang Academy. A set of color images is also archived at the GCI.

Graphic documentation comprised manual graphic recording undertaken in the cave at a scale of 1:5 of visible deterioration and damage phenomena using black pens on semitransparent sheets overlaid on black-and-white photographic prints (20 × 28 cm) as base maps (fig. 12.4). To show overall patterns, selected deterioration phenomena were then transferred to measured line drawings using AutoCAD® represented by the wall and ceiling slope surfaces at 1:20 scale (see Appendix 12.B: Graphic

Fig. 12.3 Examples of the documentation photographs taken at the start of the conservation project. Each photograph is of an area of wall painting measuring 85 × 110 cm.

Documentation—Previous Treatment and Current Conditions of Plaster) (figs. 12.5, 12.6). A 3D model was constructed to help visualize the distribution of deterioration in Cave 85 (fig. 12.7).

Constraints on Condition Documentation and Assessment

For all wall paintings, the process of recording and assessing condition poses a number of problems. Principally, the ability to record damage and deterioration phenomena accurately is limited by the physical size of wall paintings and by their irregular surfaces. Traditional forms of condition recording involve reducing three dimensions to two, with inevitable loss of accuracy. Wall paintings are also typically composed of multiple layers, and deterioration may occur within and between them. Deterioration conditions are therefore often concealed and inaccessible. Typically, in most wall paintings a multiplicity of conditions arise from different deterioration phenomena.

Each of these issues represented challenges in Cave 85, one of the larger caves at Mogao with approximately 350 m^2 of surviving painted plaster. Condition recording was therefore a difficult undertaking, involving coordinating and standardizing the work of the team. An illustrated terminology was created to establish a common understanding among team members and thereby ensure consistency. The terminology includes an agreed-upon term and definition in both English and Chinese for each condition phenomenon and is illustrated with photographs (fig. 12.8). The glossary helped to establish objectivity in a normally subjective recording process in order to standardize both the recording and the subsequent interpretation of condition records.

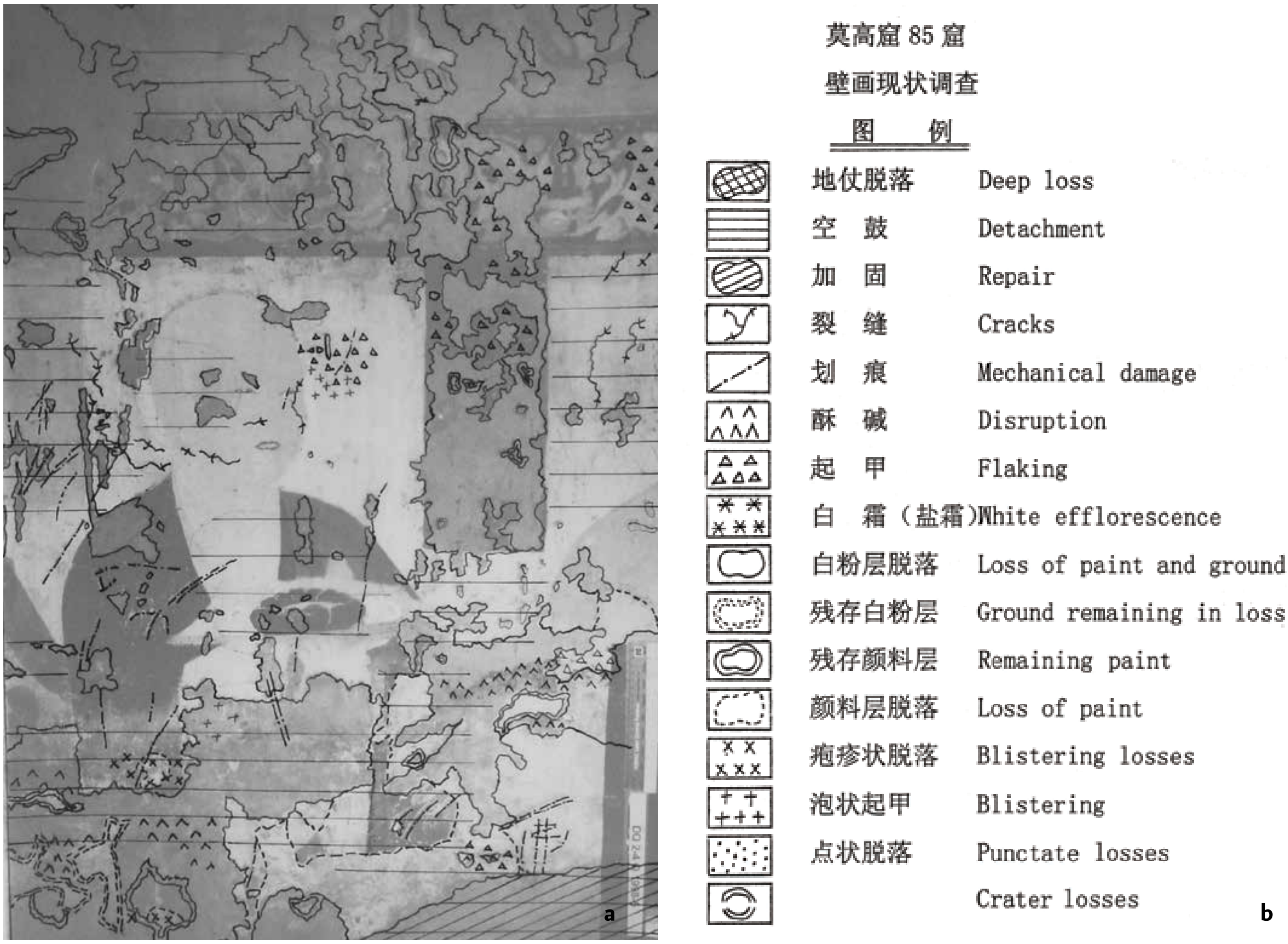

Fig. 12.4 Manual graphic documentation was done on photographic base maps such as this example from the east wall (a). The graphic documentation legend used for condition recording (b).

Fig. 12.5a Measured line drawings of the wall paintings were created by Li Weitang of the Dunhuang Academy to serve as base maps for graphic condition recording (a, b).

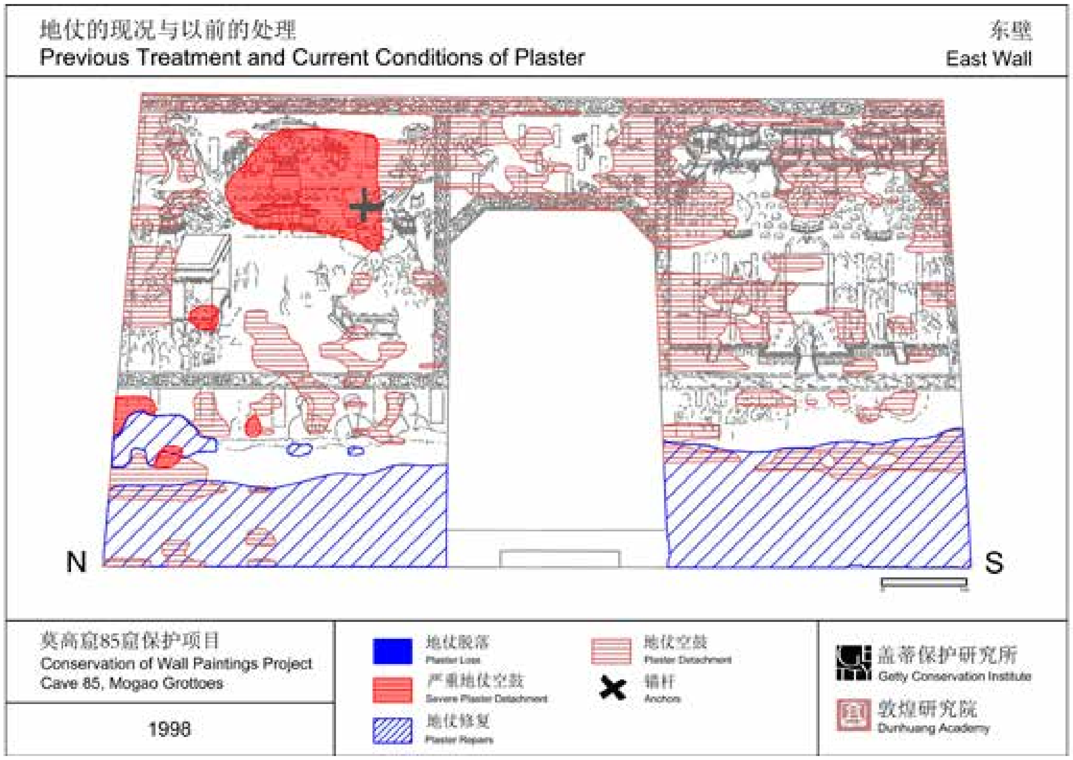

Fig. 12.6 The manual documentation was transferred to measured line drawings in order to show general patterns of deterioration. This example shows previous treatments and current conditions of the painted plaster on the east wall of the main chamber.

Fig. 12.7 A 3D cave model was constructed and graphic condition documentation was superimposed in order to show patterns of deterioration throughout the cave. The solid yellow indicates areas of loss; the hatched red, areas of stable plaster detachment; and the solid red, areas of severe plaster detachment.

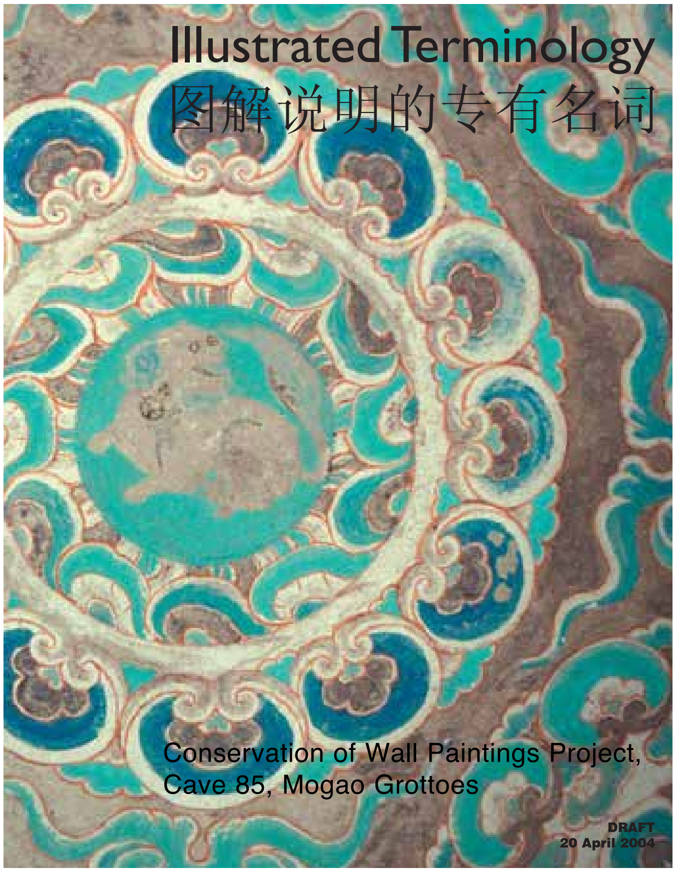

Fig. 12.8a Cover of the illustrated terminology of conditions in Cave 85.

Fig. 12.8b Example from the Illustrated Terminology showing plaster detachment.

Fig. 12.9 Concealed conditions such as plaster detachment are difficult to assess. Gentle tapping of the surface of the wall painting was used to detect voids and roughly map their extent.


Fig. 12.10 Though the modern facade conceals much of the condition of the underlying rock (a), a crack is visible above Cave 85 (b). However, it does not seem to be adversely affecting the cave.

The plaster surface in the cave is markedly irregular, and was an important condition to record and assess. Issues dealing with detachment and areas of collapse of the plaster layers from the conglomerate were a focus of the conservation program. Understanding the implications of plaster detachment and irregularity was therefore key to assessing short- and long-term risks and to formulating treatment.

A related problem was assessment of concealed conditions within the stratigraphy of the wall painting. While areas of voids could be approximately mapped, their volume, the separation gap between the plaster and the rock, the nature and condition of the supporting rock, and other related issues (e.g., structural risks) could not be fully assessed. A range of nondestructive instrumental techniques have been used in wall painting conservation to record and to some extent quantify these problems, but none has been entirely successful.[1] To a large degree, the conditions and risks created by plaster detachment in the cave could not be accurately measured. Tapping was the most reliable means of detecting and measuring the extent of voids between painting and rock (fig. 12.9).

While plaster detachment was the principal focus of the conservation program (because of the risk of collapse), the wall paintings of the cave also show a range and complexity of other deterioration phenomena. These reflect the role of soluble salts in deterioration and the complex painting technology (see chap. 13), which comprises multiple layers and materials (plasters, ground, sealants, pigments and colorants), many of which are water-sensitive or water-soluble. The interaction of these heterogeneous materials with a number of deteriogens (soluble salts, humidity, light) has produced a multiplicity of deterioration effects (paint flaking, exfoliation, disruption, color change, etc.) (see chap. 15). These factors complicated the condition recording and assessment.

Faced with these constraints, condition recording in the cave was rationalized to provide information on phenomenological categorization of observable aspects of deterioration and damage and topographical mapping of the visible types and distribution patterns of deterioration and damage.

Fig. 12.11 Incidents of mechanical damage such as accidental scratches (a) and graffiti (b) are localized and few in number.

Structural Condition of Cave

It is difficult to assess the geotechnical structural condition of the cave because the original plasterwork conceals most of the rock and the facade and exterior walkways, constructed in the 1960s, obscure most external evidence on the cliff face. The following points are based on historical evidence. For the site as a whole, photographs from the beginning of the twentieth century illustrate the effects of shearing of the cliff face, with many caves having lost all or part of their antechambers as a result of rock collapse and erosion. A photograph of the exterior of Cave 85 before the facade and walkways were built in the 1960s shows the antechamber exposed to the elements, with only the west and north walls remaining (see chap. 9). The same photograph shows a perpendicular rock fissure in the vicinity of Cave 85. This crack is still visible today, though no adverse effect on the stability of the cave has been detected (fig. 12.10).

In summary, while the structural condition of the cave appears to be stable, it is clear that the rock has a tendency to shear parallel to the cliff, as is often the case with cliffs composed of sedimentary rocks. A number of other caves at the site are transected by extensive rock cracks. The risk today, particularly from seismic activity, is obviously greater where cracks already exist in the cliff face (Sun 1997, 160) (see chap. 6).

Summary of Deterioration Phenomena in Cave 85

Although the cave has been affected by various types of damage (vandalism, graffiti, scratches), these are localized and relatively few in number (fig. 12.11). In contrast, deterioration is widespread and is characterized by its complexity. Deterioration was therefore the principal focus of the condition assessment.

The main types of deterioration fall broadly into two categories: in-depth deterioration, principally relating to plaster detachment, plaster cracks, and plaster disruption (fig. 12.12); and surface and subsurface deterioration relating to paint and ground layers and upper plaster, including phenomena such as flaking, blistering, exfoliation, "punctate" loss, crater eruptions, and color change (mineral pigment alteration and organic colorant fading) (fig. 12.13). These conditions are defined in the illustrated condition terminology (see Appendix 12.C).

In-depth deterioration comprises areas of "stable" plaster detachment (i.e., areas of plaster separation from the rock not considered at risk of imminent collapse) found throughout the cave and areas of "unstable" plaster detachment (i.e., a condition of imminent risk of loss of the full painting stratigraphy). Plaster detachment was found to increase in severity on a southeast to northwest axis (on both walls and ceiling slopes) toward the rear

Fig. 12.12 In-depth deterioration includes such conditions as plaster detachment, as seen in this example from the west wall (a). A wooden press was used to support a large and fragile area of plaster detachment before the start of conservation work (b).

Fig. 12.13 Surface and subsurface deterioration includes such conditions as exfoliation, as seen in this example from the northwest corner. Exfoliation is defined as combined lifting of the paint layer, ground, and some fine plaster. It is associated with the loss of cohesion of the plaster below the paint and ground layers.

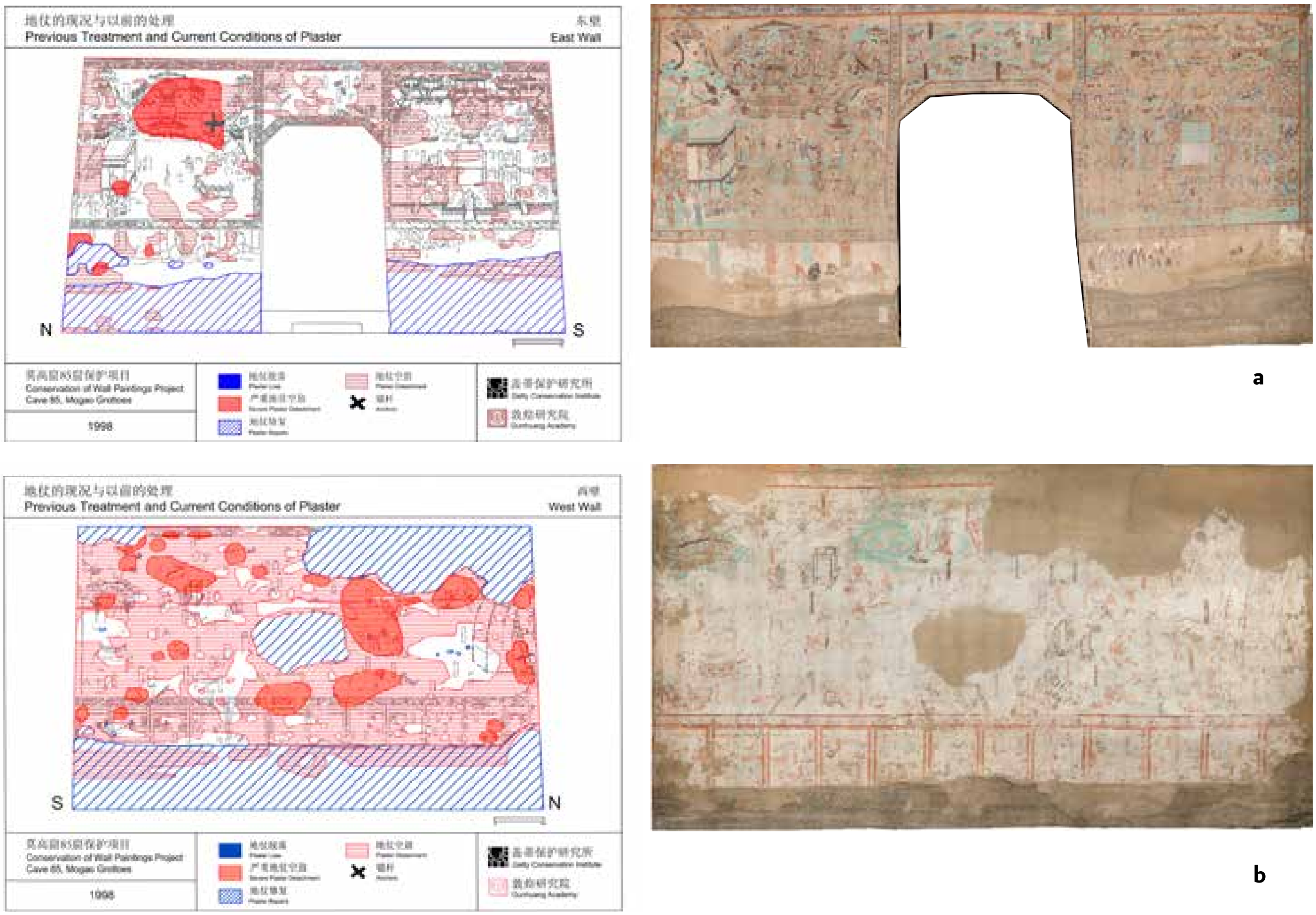

Fig. 12.14 There is an east-west distribution of deterioration, with the condition worsening toward the rear, west end of the cave. The graphic documentation shows areas of stable detachment (light red hatching) throughout, but the east wall (a) exhibits far fewer areas of unstable detachment (solid red) and loss (blue hatching) than the west wall (b).

a b

Fig. 12.15 A striking difference in condition can also be seen between the east (a) and west (b) ceiling slopes. Both surface and subsurface deterioration is visible on the west slope, while the east slope is in excellent condition.

(west end) of the cave. Unstable plaster detachment was most severe at the upper northwest corner of the cave, where approximately 70% of the 57 m^2 of plaster on the west wall was separated from the rock conglomerate; the east end had noticeably less plaster detachment, except for a large area on the north side of the east wall (fig. 12.14). Surface and subsurface deterioration likewise increased in severity on a southeast to northwest axis (on both walls and slopes) toward the rear of the cave (figs. 12.15, 12.16). In summary, all forms of observed deterioration progressively worsen in both severity and extent toward the west end of the cave, with a concentration in the northwest corner.

In addition to the above deterioration phenomena, color change—namely mineral pigment alteration and organic colorant fading—occurs extensively (fig. 12.17). These phenomena also display distinctive distribution patterns, though they are not entirely predictable. For organic colorant fading, there is a clear east to west axis of worsening condition (i.e., colorants are most faded where light from the entrance occurred, most likely during the long period of abandonment of the site when the structure fronting the cave was lost and rock collapse occurred). Distribution patterns of pigment alteration are more complex and relate to other phenomena (types of pigments used and their application, interaction with other pigments, presence of salts, possible alkalinity, and humidity). Much pigment alteration therefore is randomly distributed. Nevertheless, pigment alteration also occurs toward the west end of the cave and can be visually related to the presence of salts, in common with other surface and subsurface deterioration phenomena (see chaps. 15, 16).

Among the numerous uses and objectives of condition assessment, its main purpose is to establish hypotheses about the nature and rate of deterioration. For Cave 85, the nature and topographic distribution of the main observed conditions—plaster detachment and paint exfoliation—suggested deterioration mechanisms associated with salts and relative humidity. Data relating to the physical history of the cave also suggested that these conditions were a problem of long-standing duration. This information from the condition assessment helped to focus subsequent investigations, including an extensive salt survey. Findings also complemented those of environmental monitoring in determining the risks to the cave from the climate at the site.

Notes

1. Techniques include: 3D laser scanning and modeling for documenting spatial deformations (see, e.g., Casciu et al. 2000, 208–19); ultrasonic pulse vibration and measurement (see, e.g., Gosálbez et al. 2006, 492–97); and infrared thermography (see, e.g., Grinzato et al. 1994, 257–74) and laser speckle interferometry.

Fig. 12.16 Detail of musicians from the south wall of the main chamber. There is a striking difference in surface survival of paint between the painting at the east end (a) versus the painting at the west end (b) of the cave.

Fig. 12.17 There is an east to west gradation of color change throughout the cave. This example shows both organic colorant fading and mineral pigment alteration between the east (a) and west (b) ceiling slopes. Note the richer coloring of the east wall lotus flower versus the west wall, which indicates fading of organic colorants; and the horizontal blue bands of the east wall that appear green on the west (with only faint traces of blue surviving), which shows azurite alteration into a green copper chloride pigment.

Antechamber

The antechamber and entrance corridor wall paintings have been exposed over the years (at least since the Russian expedition of 1914–15 and likely much longer based on photographic evidence from that time). These areas are further differentiated from the main chamber by having been repainted: the entrance corridor was replastered and repainted during the Five Dynasties, and the antechamber was replastered and repainted in the Yuan dynasty (see chap. 9).

General types of deterioration in the antechamber and entrance corridor include plaster separation on the corridor ceiling; various forms of surface and subsurface deterioration (flaking paint, blistering, and loss); and color change (mineral pigment alteration and organic colorant fading). Types of damage include abrasion due to blown sand in the entrance; complete loss of plaster at the base of the walls due to moisture damage from wet sand; and various types of graffiti (antechamber: fig. 12.18; corridor, north wall: fig. 12.19; corridor, south wall: fig. 12.20; corridor, ceiling: fig. 12.21).

a

Fig. 12.18 Before the construction of the modern facade the wall paintings in the antechamber were exposed to the elements (see fig. 9.11). (a) A detail of the west wall of the antechamber taken in 1908. Wall paintings from the west and north walls of the antechamber are visible in the Needham photograph from 1943 (b) and in 2009 (c).

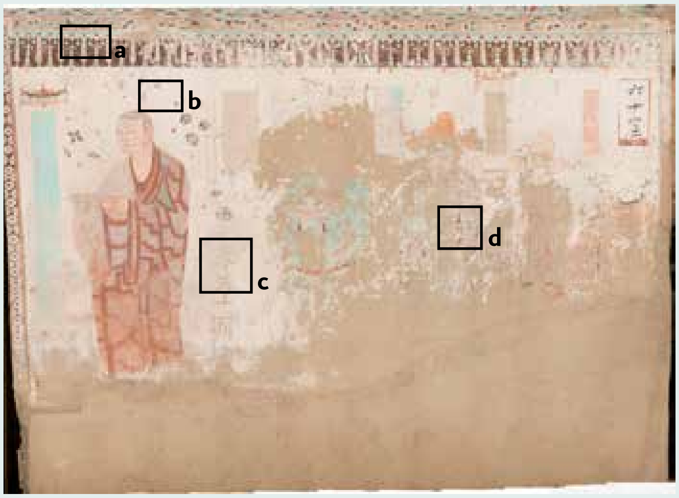

Fig. 12.19 The north wall of the entrance corridor was also exposed for many years. Windblown sand and periods of flooding caused loss of painted plaster at the base of the wall and abrasion of the painted surface that worsens in condition toward the cave entrance (right side of the image). Conditions at the start of the project included
(a) Flaking and loss of the paint layer;
(b) Blistering of the paint layer;
(c) Graffiti;
(d) Surface abrasion.

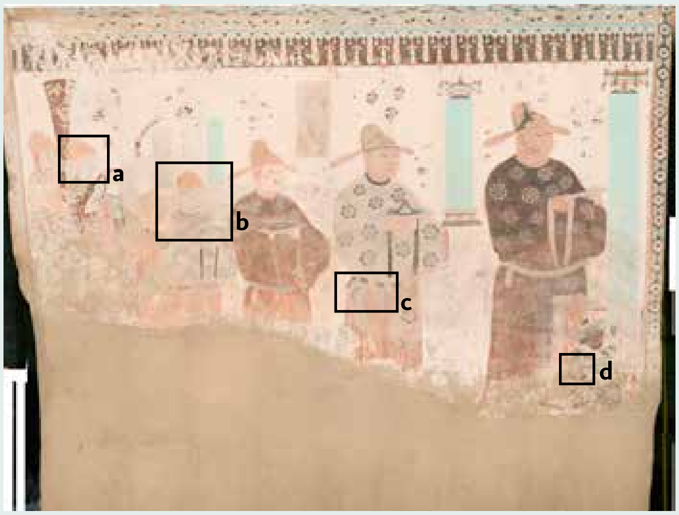

Fig. 12.20 The south wall of the entrance corridor was also exposed for many years. Windblown sand and periods of flooding caused loss of painted plaster at the base of the wall and abrasion of the painted surface that worsens in condition toward the cave entrance (left side of the image). Conditions at the start of the project included
(a) Paint flaking and loss;
(b) Surface abrasion and smearing (possibly intentional to destroy paintings);
(c) Gray veil on surface (possibly from moisture exposure);
(d) Plaster loss.

Fig. 12.21 The ceiling of the entrance corridor was also exposed for many years, resulting in loss of painted plaster and surface abrasion that worsens in condition toward the entrance of the cave (top of far left image). Conditions at the start of the project included
(a) Detachment of painted plaster (the four metal anchors that were inserted in the 1970s were removed during the current conservation project);
(b) Drying cracks, as well as more recent cracking from stresses in the painted plaster caused by insertion of the metal anchors;
(c) Salt pustules on the face of one of the small Buddhas.

In almost all of the caves at Mogao, the polychrome statues were constructed from earthen plaster modeled over armatures consisting of wood and bundles of reeds to provide internal support. The Cave 85 sculpture group was heavily restored in the Late Qing or Early Republic period. Importantly, much of the Tang sculpture and polychromy still survive, though concealed: large parts of the Sakyamuni Buddha and Kasyapa were replastered and repainted, and the statue of Ananda was completely re-created.


a

Owing to its history of conserving sculpture, the Dunhuang Academy undertook treatment of the sculpture (including structural stabilization) after a condition assessment was carried out by both the GCI and the Dunhuang Academy (see Appendix 10.D). Results of the assessment are presented here in summary.

Despite their history of damage, deterioration, and inept past restoration, the statues are in fair condition overall (Sakyamuni Buddha: fig. 12.22; Sakyamuni Buddha base: fig. 12.23; Kasyapa: fig. 12.24; Ananda: fig. 12.25). The main phenomena affecting them can be categorized as follows: structural tilting of whole sculpture (Kasyapa); failure of internal armatures at junctures (e.g., between shoulder and arm) and at unsupported features (e.g., outstretched arms), resulting in plaster cracking and risking loss of sculptural parts; minor damage to and losses of sculptural features, especially at junctures and extremities (e.g., elbows, necks, ears, noses, hands, fingers); and failure of restoration surface treatments, including flaking of repainting and peeling of paper applied to disguise cracks and damage.


b


c


d

Fig. 12.22
(a) Sakyamuni Buddha, originally constructed in the Late Tang and restored in the Late Qing or Early Republic period;
(b) Rear of Sakyamuni Buddha;
(c) Hole in back (it is unclear what the purpose of this hole was);
(d) Back of head of Buddha showing original and repaired areas, now cracking;
(e) Detail of original hair of Buddha, some areas now lost;
(f–h) Minor damage and losses of sculptural features, especially at junctures and extremities (right shoulder, right finger, and nose).

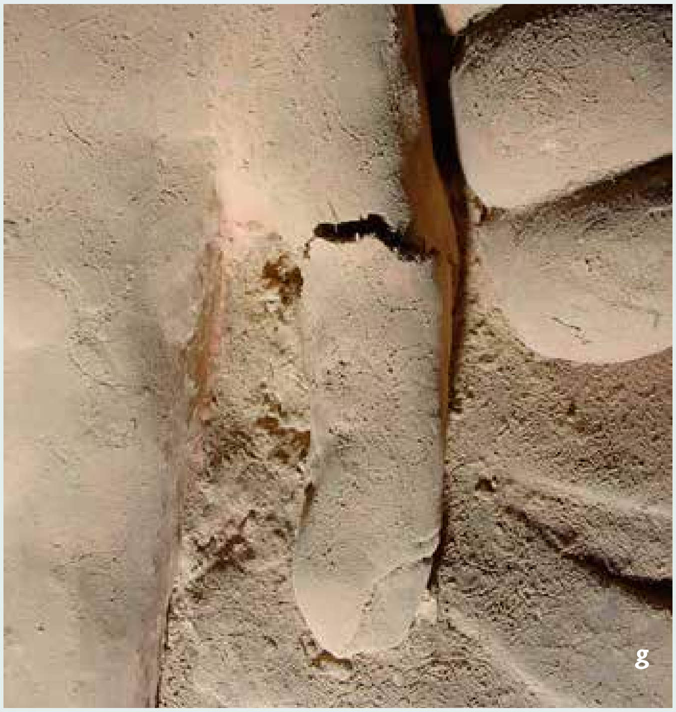

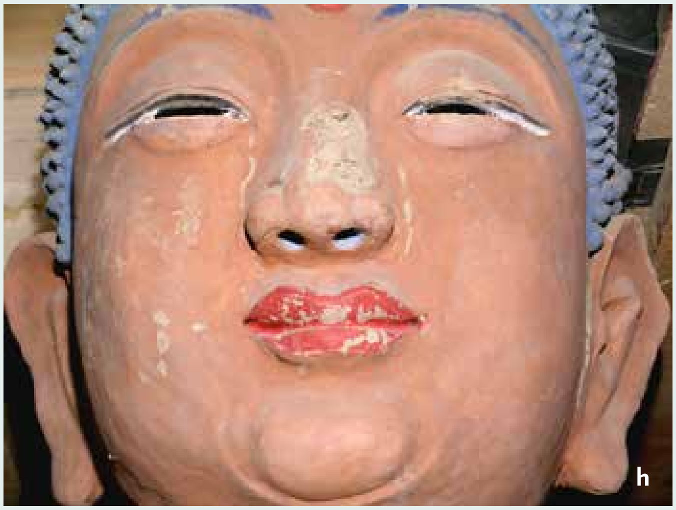

Fig. 12.23
(a) Sakyamuni Buddha base showing loss of the lotus molded decoration and disruption of the painted plaster;
(b) Losses in the base have been previously repaired;
(c) Punctate loss caused by salt activity;
(d) Flaking of gilded areas;
(e) Disruption of the painted plaster;
(f) Graffiti.

Fig. 12.24
(a) Kasyapa (older disciple), originally constructed in the Late Tang, was restored in the Late Qing or Early Republic period;
(b) Paint flaking and loss;
(c) Cracking of plaster scroll;
(d) Failure of internal armatures at junctures of right arm has resulted in plaster cracking, and risks loss of sculptural parts;
(e) Structural tilting of whole sculpture.

Fig. 12.25
(a) Ananda (young disciple), completely remade during the Late Qing or Early Republic period;
(b) Plaster cracking and loss in neck;
(c) Paint loss;
(d) Structural tilting of whole sculpture.

Platform

The altar platform, built on a core of the original conglomerate with earthen brick additions, has been previously restored (fig. 12.26). Compared to platforms in other caves it is in poor condition. It exhibits the same conditions as the wall paintings at the west end of the main chamber, including punctate loss, flaking of the paint layer, and powdering and disruption of the plaster. Traces of painted relief decoration still survive, but most have been lost. The platform has probably endured repeated periods of flooding and exposure to wet sand together with the wall paintings at the base of the walls. Large losses occur at the edges and corners of the base, and the lotus flower decoration was broken in areas. Exposed conglomerate and mudbrick were visible in areas of loss. Fragments of the original Tang-period painted base uncovered during conservation work had been incorporated during previous repairs as blocks for reconstructing the shape of the base.

Horseshoe-shaped Bed

This structure, atop the altar platform, was severely abraded on its upper surface (fig. 12.26). The east and north faces had severe paint and ground loss, exposing the fine plaster and in some areas the conglomerate below. The west face was deteriorated and the conglomerate exposed in two locations.

Fig. 12.26
(a) Detachment of areas of original and repair plaster;
(b) Plaster loss exposing conglomerate;
(c) Abrasion and loss of painted decoration on horseshoe-shaped bed;
(d) During treatment of the platform and bed original Late Tang painted fragments were uncovered. The fragment had been reused as repair blocks for reconstructing the shape of the base.

Raised Bed

The raised bed is a later addition thought to date from the Five Dynasties (fig. 12.27). It exhibits punctate loss, flaking of the paint layer, and powdering and disruption of the plaster.

Fig. 12.27
(a) Raised bed (indicated by black box);
(b) Loss;
(c) Powdering and disruption of plaster layers caused by salt activity;
(d) Detail of painted plaster in an area of salt deterioration.

Findings & Implementation

CHAPTER 13

Original Materials and Techniques

The study of painting technology—the identification and characterization of the materials constituting the painting and its support and the methods used—provides information that is fundamental to good conservation practice and that contributes to the scientific and historic values of the cave (see chap. 10). It also provides essential information on the physical and chemical stability of materials, their vulnerability to change, and their response to conservation interventions. This knowledge affords insight into the probable causes of deterioration phenomena and helps to distinguish between original and added materials (see chaps. 9, 15). Crucially, it guides conservation interventions in the use of appropriate and compatible materials (see chap. 17).

Fig. 13.1 A hyper-spectral imaging camera was used to investigate materials and techniques of the paintings.

Investigation in Cave 85 relied heavily on in situ visual examination of the wall paintings (Shekede et al. 2010), utilizing powerful light sources, magnification tools, the MuSIS™ HS hyper-spectral imaging camera,[1] and UV-induced fluorescence[2] and IR photography (figs. 13.1, 13.2).[3] These noninvasive means of visual examination provided a focused direction for a systematic program of sampling and instrumental analysis (Schilling et al. 2010).[4]

Fig. 13.2 Examination under ultraviolet illumination provided information on the presence of organic materials such as colorants and coatings.

Understanding the sophisticated painting technology in Cave 85 was challenging due to the aged and deteriorated nature of the paintings, the presence of acrylic emulsions from past treatments, and the limited knowledge from primary source documents of Late Tang painting materials and techniques. Analytical capabilities and standards for identifying these materials, other than pigment analysis, were generally absent. Nonetheless, the project presented an unparalleled opportunity to study the materials and techniques of the Late Tang dynasty. The results provide a detailed knowledge of the structure and materials of the paintings.

Fig. 13.3 An unfinished cave from the northern grottoes shows that caves were excavated from the top down.

Mural Painting Workshops

Historical production of mural paintings at the Mogao Grottoes has been studied by scholars. A government-supported painting academy was begun under the rule of Cao Yijin (r. 914–35) and his son Cao Yuanzhong (r. 944/45–74) during the Five Dynasties (Fraser 2004). The number of caves with similar sutras painted during the period of the Late Tang and the Five Dynasties is evidence of a systematized production of murals and a highly organized artists' workshop where painters worked alongside scribes and sculptors, each belonging to their respective artisan guild or workshop.

It is clear from variations in painting quality and style that different hands were at work in Cave 85, with many of the most important elements of the scheme executed with skill and precision and others displaying very rough-and-ready application. There is also evidence that colors—at least those forming the basic paint palette—were applied sequentially, most likely by divided labor. These features reflect a workshop hierarchy, for which there is also a substantial documentary record. At the start of the Tang dynasty, mural painting was the focus of religious artistic expression, and the names of a number of renowned artists engaged in mural painting have been preserved (Clunas 1997, 46). At Mogao, too, artists enjoyed unprecedented respect and prosperity. Wall painting production was organized within the structure of a painting academy, which was responsible both for the management of materials (presumably including procurement and manufacturing) and for the organization of labor (Fraser 2004, 27, 34). Lists of artisans, or *jiangren*, and a painting master, or *huashi*, in a Tang dynasty document from Turfan testify to the hierarchical nature of the painting academy in which up to seven ranks of personnel may have been employed in the execution of a commission (Fraser 2004, 31–34).

Excavation of Caves

The cave temples were excavated into the cliff face composed of conglomerate rock. The rock is easy to work, and tool marks, evidence of the use of hammers and chisels, are visible in some caves (see fig. 13.23). Caves were excavated from the top down, as can be seen in an unfinished cave on the northern end of the cliff (figs. 13.3).

During excavation of Cave 85, a large platform of conglomerate rock was retained to form the altar base for the sculpture group at the rear end of the main chamber. The upper parts were then built up with mud brick, and wooden frames and molded lotus petal earthen blocks were added to complete the form.[5] Mud bricks were also used to frame the doorway opening at the western end of the corridor.

Plastering of the Walls

After the cave temples were excavated, the walls were plastered and smoothed over with layers of earthen plaster. A coarse plaster was applied first to the rough-hewn walls, the thickness of which is quite variable (5–30 mm) due to the irregular surface of the underlying conglomerate. Over this, a fine plaster was applied at 4–5 mm in thickness (fig. 13.4).

Examination of plaster joins using raking light indicates that the walls were plastered first, apparently in a clockwise direction, as a distinct vertical overlap can be seen where the plaster is thicker, for example where the plaster from the south wall overlaps onto that of the east in the southeast corner. The slopes were plastered next, with an overlap of 30–40 cm extending down onto the walls. It is possible that large areas of the cave were plastered at once with little drying time between applications. Earthen plasters, as opposed to lime plasters, maintain significant plasticity while drying, allowing for areas to be

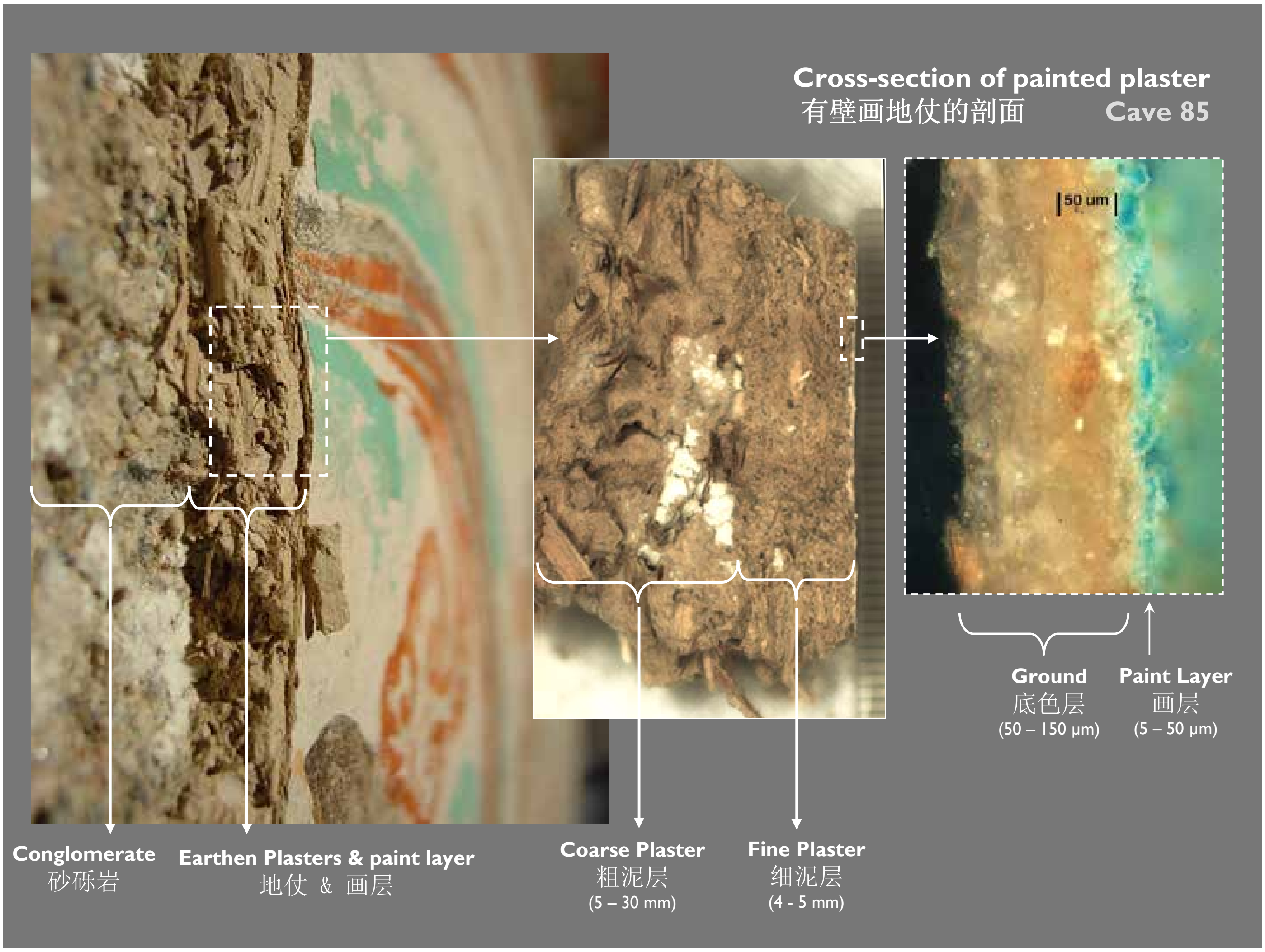

Fig. 13.4 Stratigraphy of the painted plaster comprises coarse and fine plaster layers followed by ground and paint layers.

progressively plastered with joins smoothed over or "feathered" to create a seamless plastered area. Trowel marks showing the working and smoothing of the plaster are visible (fig. 13.5). However, in other areas it can be seen that plaster joins were not smoothed over (fig. 13.6).

The final plaster layer was allowed to dry, then checked and adjusted before painting commenced. It is clear that such caution was necessary, as ancient plaster repair patches were found on the upper west wall of the main chamber (fig. 13.7). These repairs were required in areas where the conglomerate support was friable and unable to provide a good base for the plaster to adhere. Small drying cracks also formed in the plaster, but these were allowed to remain. Subsequent paint layers can clearly be seen to have been applied over them (fig. 13.8).

The earthen component of the plasters was found to contain the same mineral range and silt:clay ratio as the alluvial sediment of the Daquan River.[6] Evidently, this locally available deposit was the primary component of the plaster (fig. 13.9). Alluvium was mixed with river water, local desert sand, and vegetable fiber to increase tensile and cohesive strength, reduce density and shrinkage, and retard drying, thereby improving adhesion and minimizing cracking.

The bulk analysis of the coarse and fine plasters found 36% sand, 45% silt, and 19% clay.[7] The sediment from the Daquan River was found to contain 1% sand, 71% silt, and 28% clay. Recalculation of the plaster in Cave 85 without the added sand is an almost exact match to the components of the riverbed sediment: 0% sand, 70.3% silt, and 29.7% clay.

Fig. 13.5 Trowel marks in the plaster are visible in this area of the east slope in incident (a) and raking (b) light.

Fig. 13.6 An overlapping plaster join on the east wall.

Fig. 13.7 Ancient repair on the west wall indicates a problem with plastering.

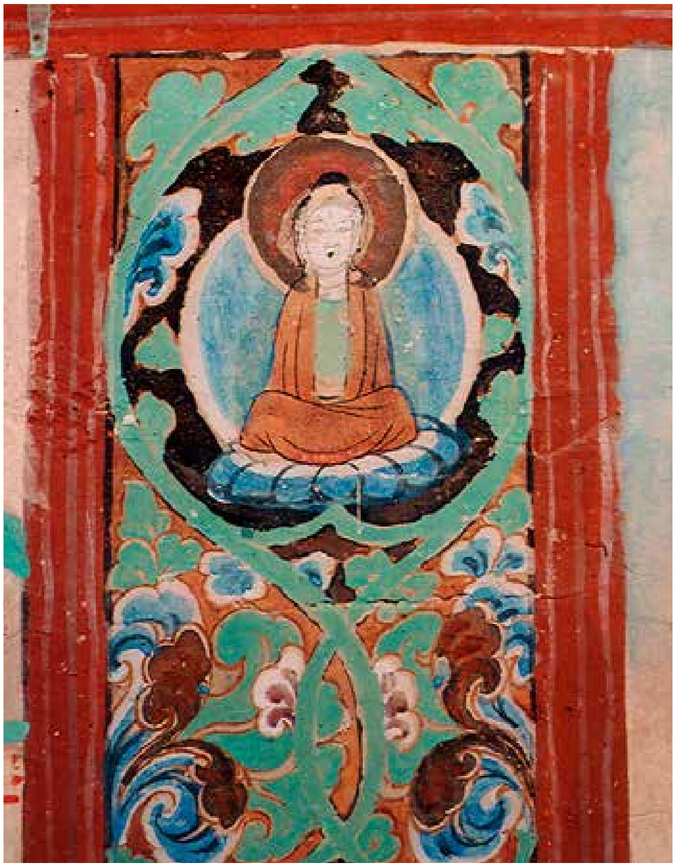

Fig. 13.8 Small drying cracks are visible below the seated Buddha in this area of painting on the south wall. The paint goes into the cracks, indicating that they formed during drying of the plaster before the paint was applied.

Fig. 13.9 Alluvial sediment from the Daquan River is the primary component of the original plaster. It is still used today for repair plasters. It is washed and dried before use (a, b).

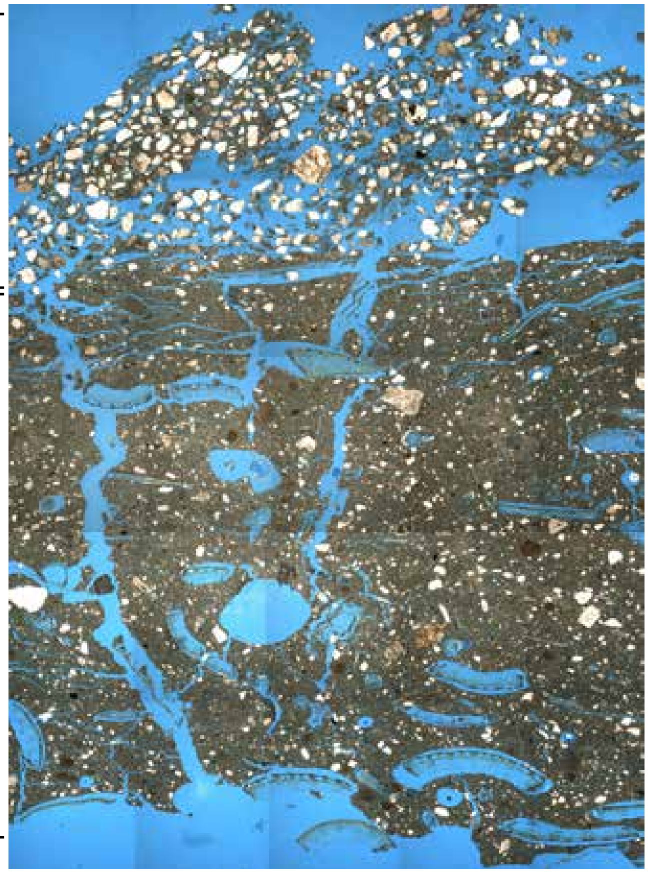

Fig. 13.10 Blue-dyed epoxy-mounted thin section of fine and coarse plaster layers.

Examination of a thin section of the two plaster layers shows a high concentration of sand in the fine plaster layer with a particle size distribution concentrated in the 100 μm diameter range. In contrast, the coarse plaster has less sand and a concentration of particles in the 50 μm diameter range (figs. 13.10, 13.11).

Natural plant fibers, including hemp and other unidentified organic material (possibly wood and straw), are visible in the coarse plaster (Bukantis 2002; Bisbing 2006) (fig. 13.12).[8] The fine plaster contains extremely fine strands of a beaten untreated bast fiber that was identified as hemp (figs. 13.13, 13.14).[9] Beaten hemp has been noted in other Tang dynasty plasters at Mogao (Duan et al. 1993, 307), and its use is consistent with the Song dynasty *Treatise on Architectural Methods*, or *Yingzao Fashi*, which documents sand, earth, and beaten hemp fiber as the main constituents of plaster (Yu 1988, 29).[10] Examination of the painting in raking light sometimes shows the imprint of these fibers visible just below the paint layer, but generally the fineness of the fibers in the upper plaster allowed for the surface to be troweled to an extremely smooth finish (fig. 13.15).

Ground

In preparation for the paint a ground was applied over the fine plaster. Literary sources on Chinese painting technique refer to the use of an alum (potassium aluminum sulfate, $KAl(SO_4)_2 \cdot 12\ H_2O$) and glue sealant, or "size," applied over the fine plaster to prepare the surface for the ground and paint layers.[11] The alum component makes the size water resistant and helps to give it a viscous consistency. This would have been applied as a solution that could easily penetrate into the fine plaster. However, the thinness of this resulting layer and the natural presence of aluminosilicates in the earthen plaster make an enriched aluminum layer difficult to detect through analysis.

Nevertheless, as alum is water soluble it could provide sulfate ions for precipitation with the calcium-rich earthen minerals of the plaster to produce gypsum ($CaSO_4 \cdot 2\ H_2O$). A number of samples from Cave 85 showed a gypsum deposition layer between the fine plaster and the ground of varying thickness

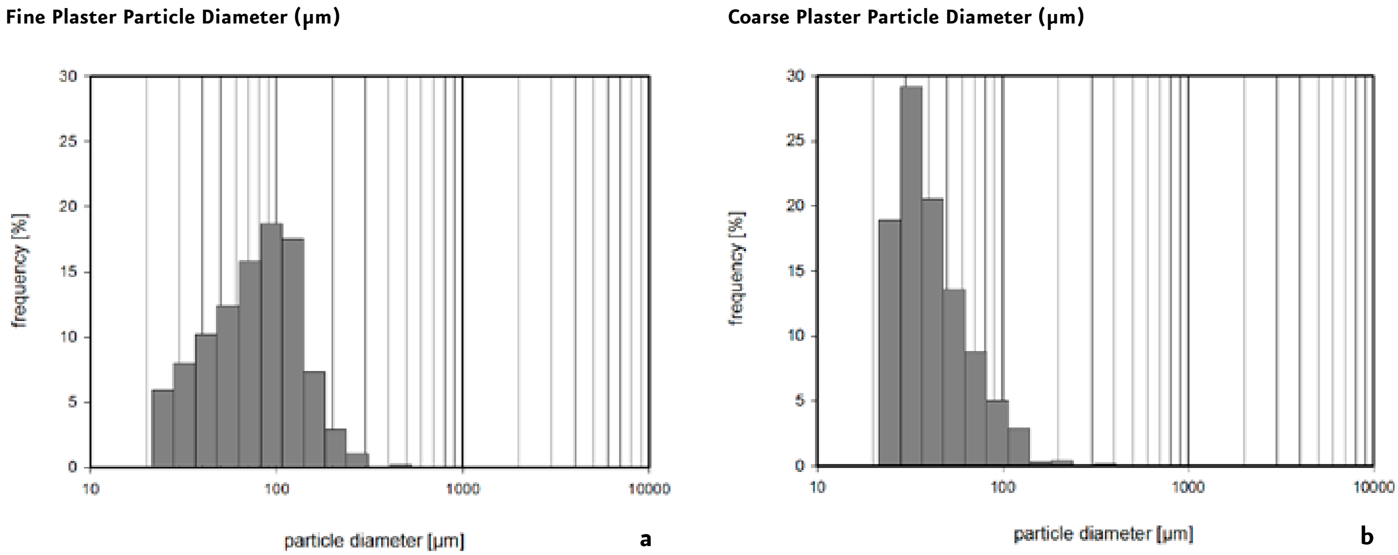

Fig. 13.11 Particle size analysis of fine and coarse plaster layers. The upper, fine plaster has a concentration of sand particles in the 100 µm range (a). The lower, coarse plaster has less sand and a finer particle range concentrated in the 50 µm range (b).

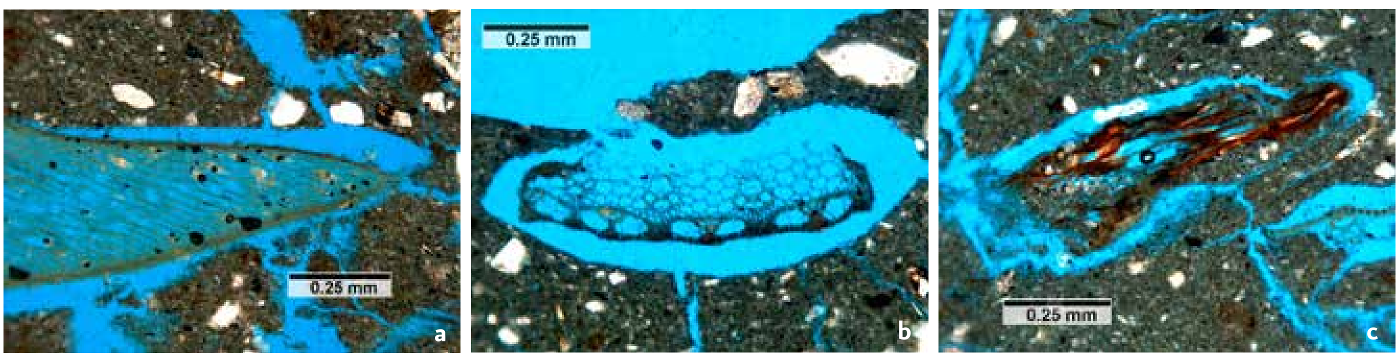

Fig. 13.12 A variety of organic fibers (hemp, straw, and wood) were added to the coarse plaster and are visible in thin section (a, b, c).

Fig. 13.13 Plant fibers isolated from the plaster for identification (a) under magnification (b) and in section (c).

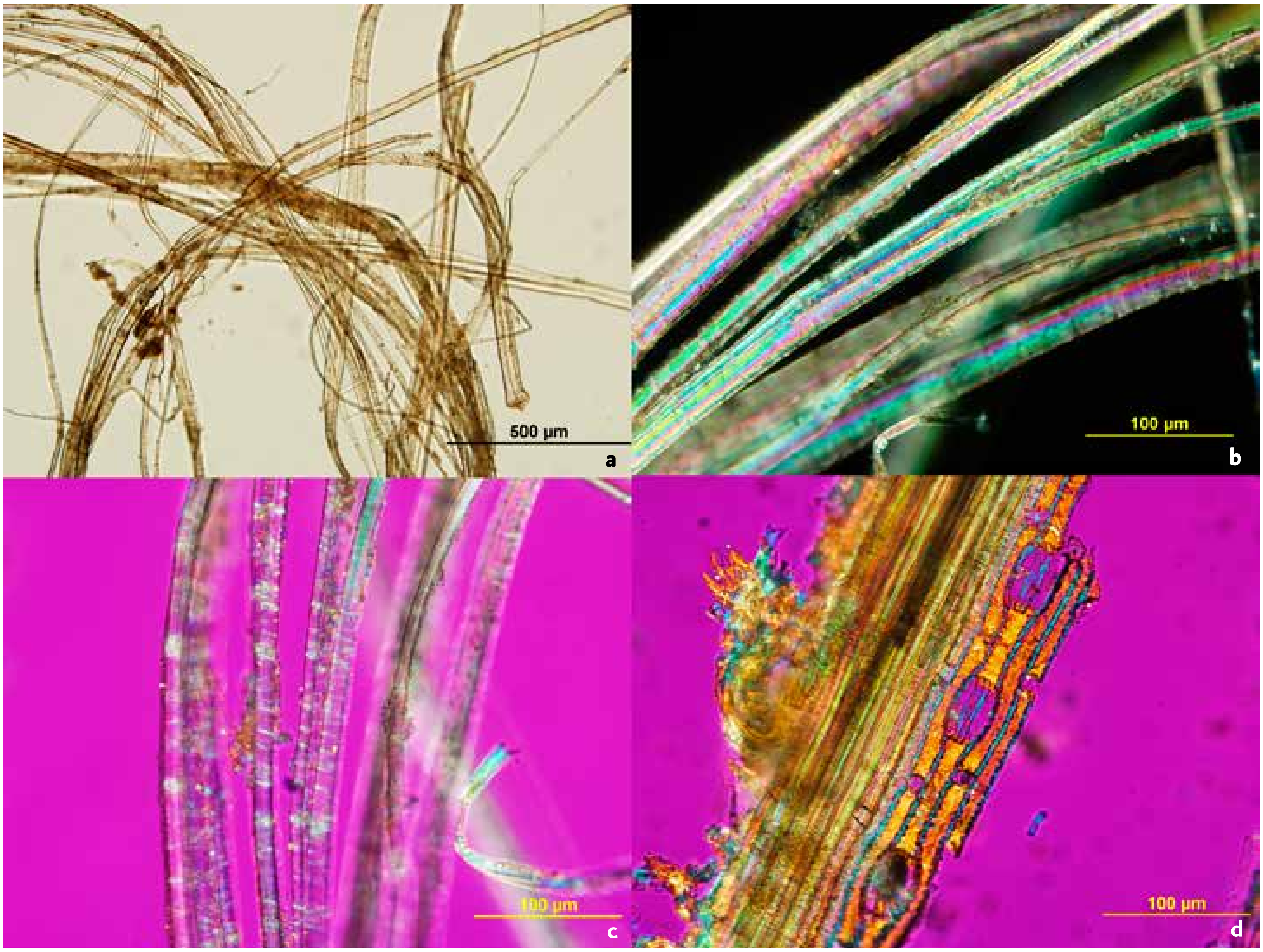

Fig. 13.14 Photomicrographs of plant fibers from the upper and lower plaster layers. Natural plant fiber bundles from the fine upper plaster layer shown under single-polar illumination (a) and under crossed-polar illumination (b). Fibers are oriented perpendicular to the polarizer with a first-order compensator inserted. The faint blue coloration in this orientation is a feature of positive (z-twist) natural fibers (c). Natural plant fiber fragments from the coarse lower plaster layer appear more like tubular cereal grass. The fragments have serrated cells and what appear to be leaf stomata (d).

Fig. 13.15 A large plant fragment can be seen protruding through the paint layer on the east wall. Occurrences such as this are rare as the fine plaster is normally troweled to a smooth finish.

identified by XRD and ESEM-EDX elemental maps. The presence of calcium and sulfate ions is the most direct evidence for the presence of an alum sealant layer applied on the fine plaster beneath the ground (fig. 13.16).

Raking light examination of the painted surface indicated that the ground was applied as a wash, with drips visible (fig. 13.17). Cross-section examination showed that the ground layer varies widely in thickness (20–300 µm). Calcium carbonate ($CaCO_3$), talc (hydrated magnesium silicate, $Mg_3Si_4O_{10}(OH)_2$), and mica were identified as the main components of the ground by XRD. It is possible to distinguish sheets of mica, calcite, and other minerals in cross section (fig. 13.18). ESEM-EDX elemental maps of a cross section of the painting show the ground rich in magnesium from the talc (fig. 13.19).[12]

The ground in Cave 85 was originally tinted. This can still be seen at the eastern end of the cave where the paintings are less deteriorated and the ground is pinkish beige in color. In contrast, the ground at the western end of the cave, where deterioration is concentrated, is stark white, indicating that the color may have been lost (fig. 13.20). This application of a colored ground provided a delicately tinted background for the entire painting scheme. Cross-section examinations of samples with colored grounds show a corresponding UV-induced fluorescence of this layer (fig. 13.21). The ground may have also functioned as a sealant, much the same as the alum and glue sealant, separating the fine plaster from subsequent paint layers to minimize color "bleeding" and to create a smoother, less porous surface for execution of the line drawing.

GC/MS analysis for protein and carbohydrate content was carried out on three samples of ground (see table 13.2). A colored ground sample from the east end of the south wall, sample 85NQ01PE11, had a 2.6% carbohydrate composition, which correlates with fruit gum and/or plant mucilage, and a 0.12% amino acid profile, which could also indicate the presence of fruit gum. It did not contain hydroxyproline, a typical indicator for animal glue. Results of white ground from a deteriorated area at the west end of the south wall, sample 85NQ01PE12, had only 0.75% carbohydrates, possibly due to the loss of organic material. The third sample, BP00PE9, also white ground but from a highly deteriorated area on the north wall, had a carbohydrate content of <0.1%, which is considered insignificant. The 0.12% amino acid profile did not provide a good correlation coefficient with a proteinaceous binder.[13] Based on these three samples, polysaccharides are present in the ground, indicating the presence of plant gum or mucilage and/or deteriorated plant fibers. There was no indication from these samples of the presence of animal glue.[14] Although organic colorants may also contain glycosidic components it is unlikely that a correlation can be established between colorants and carbohydrates.

Setting-Out Technique

In the preface to his work *The Record of the Classification of Ancient Painters*, the fifth of the "Six Principles of Chinese Painting" expounded by the Chinese writer and art critic Xie He (ca. 475 C.E.)—"dividing and planning, positioning and arranging" (Yu 1988, 19)—testifies to the importance placed on conceptualization of the artistic work. A number of preparatory drawings dating to the ninth and tenth centuries preserved among the Library Cave documents provide unique insight into this process (Fraser 2004). These rough working drawings, some containing technical and logistical instructions, range from schematic large-scale designs for entire portions of wall decoration to detailed studies of individual scenes (Fraser 2004, 49). The main use of the former would have been to allocate positions to themes and vignettes selected from a number of well-known possibilities (fig. 13.22).

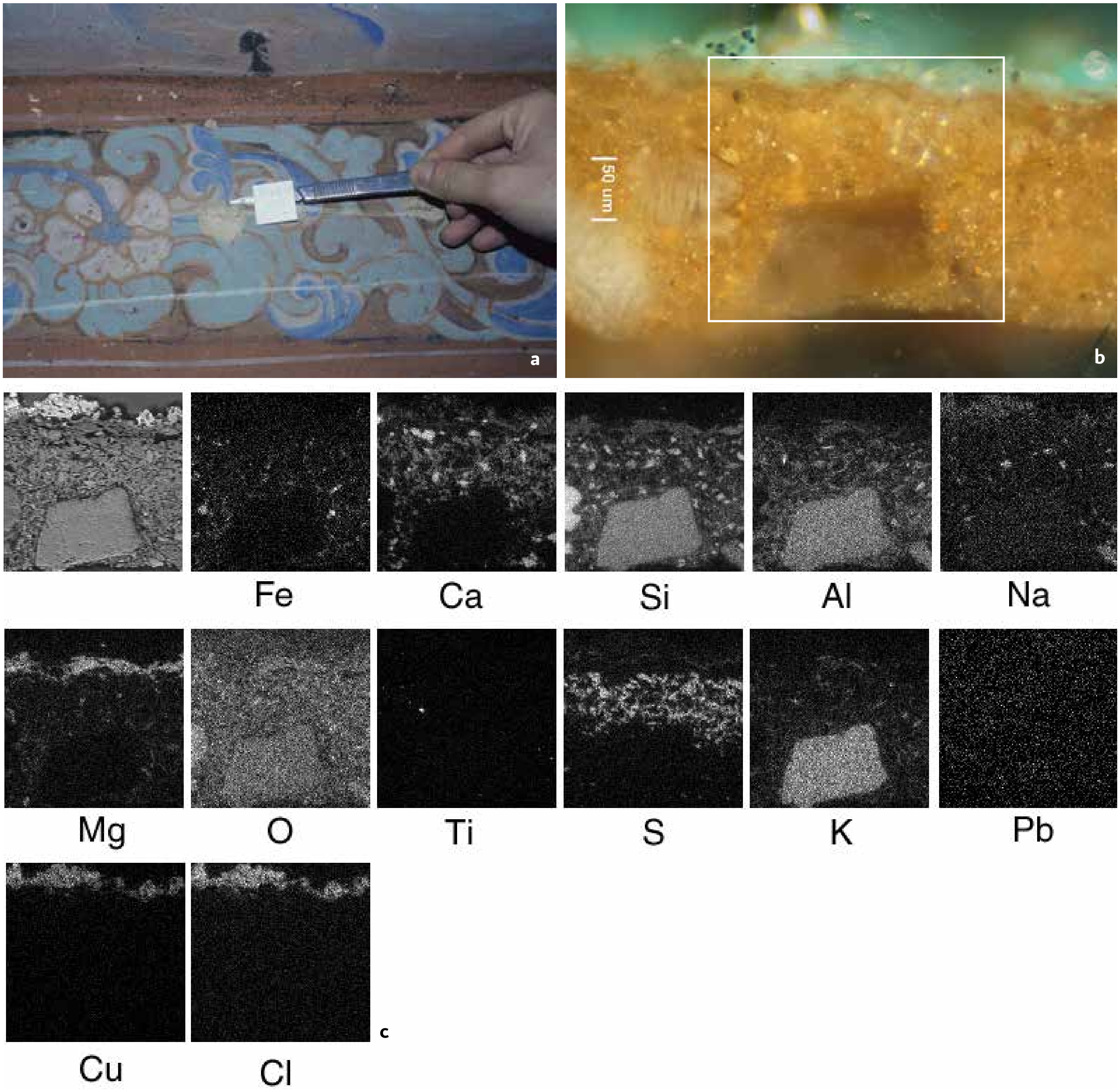

Fig. 13.16 Cross section of paint sample (85DQ00PE) from the east wall was examined by ESEM-EDX (a, b). Copper and chloride were present in the blue-green paint layer (most likely atacamite); below this is a thin layer of magnesium (~10-20 μm), a marker for talc in the ground layer, followed by the fine plaster (the trapezoidal large fragment in this layer may be a potassium feldspar such as orthoclase). On the fine plaster is a thick (~70 μm) layer of sulfur coincident with calcium (c). In the absence of XRD identification it is likely from the element maps that this is gypsum and could therefore be an indication of an alum sealant layer applied to the fine plaster, the alum having provided the sulfate ions for precipitation with the calcium-rich earthen minerals of the plaster to produce gypsum.

Fig. 13.17 Incident (a) and raking (b) light images of a musician on the south wall. Note the brushstrokes and vertical drips showing that the ground was applied as a liquid.

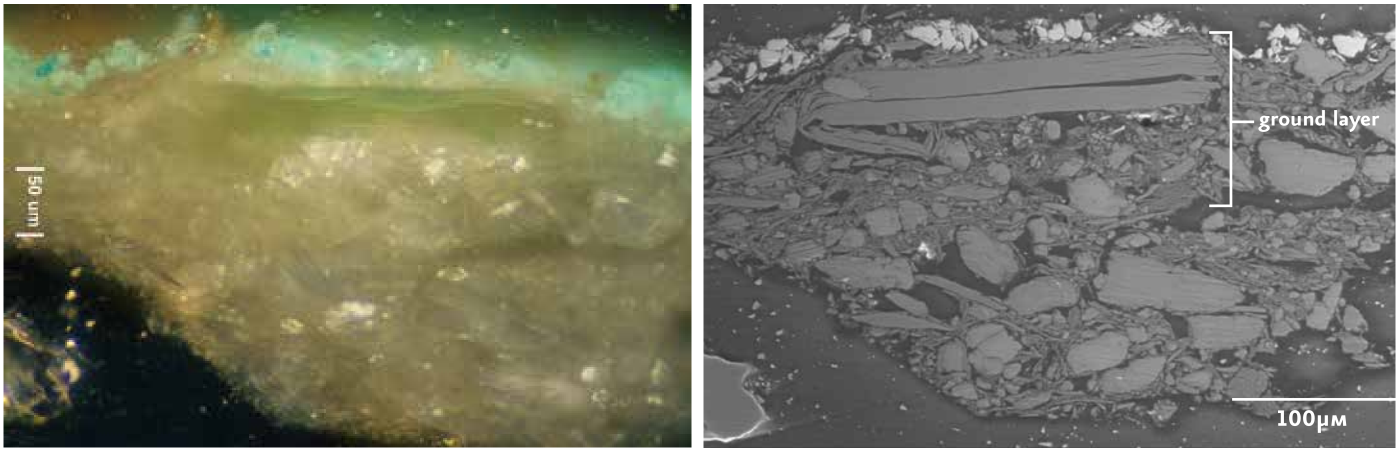

Fig. 13.18 A large sheet of mica is visible in the ground of sample 85NQ98PE3 from a green area on the south wall. Polished section (a) and backscattered electron image of section (b).

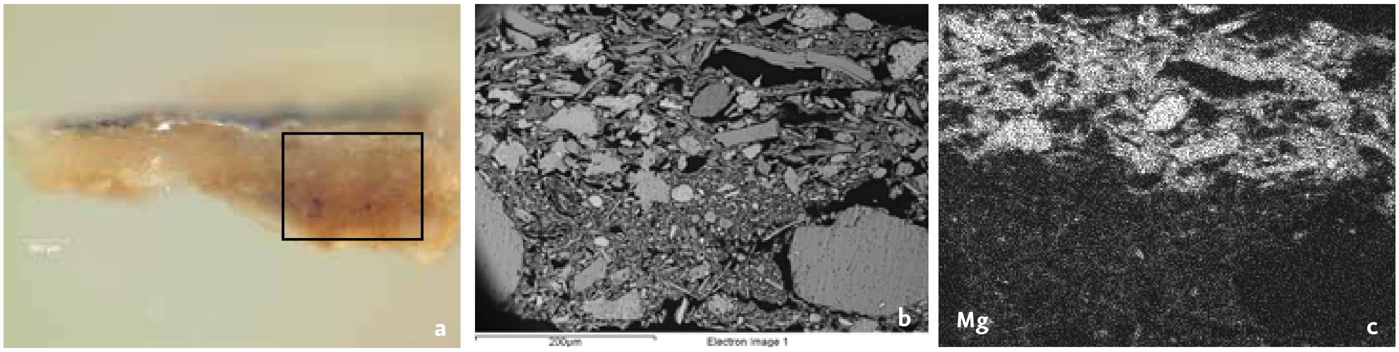

Fig. 13.19 Sample MOG.85.F03.S05 from the south wall has a thick ground layer (~200 µm)(a). The backscattered electron image includes the ground and fine plaster (b). The ground can be easily identified by the presence of magnesium in the talc in the elemental map for magnesium (c).

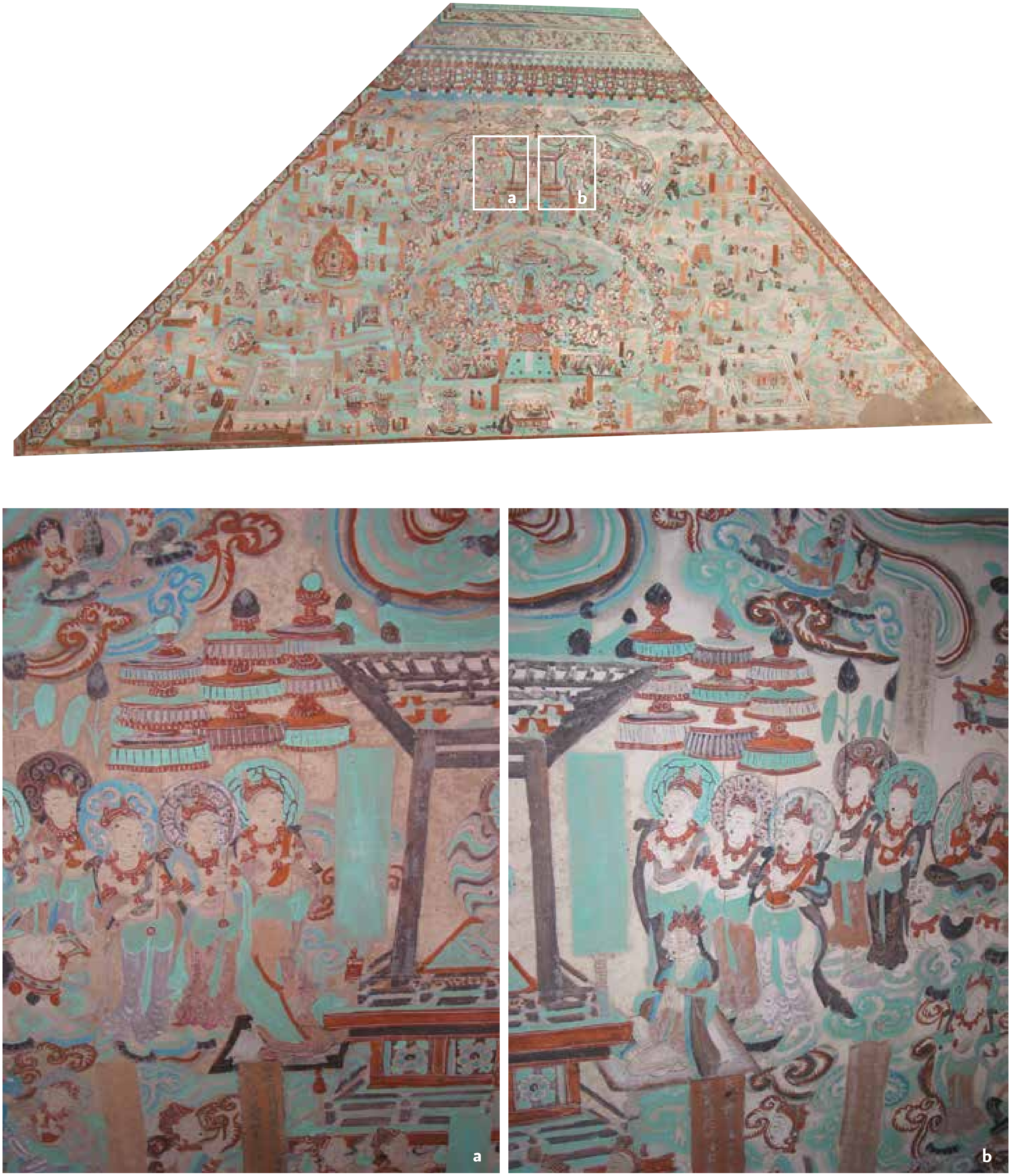

Fig. 13.20 A pinkish beige tinted background wash is visible on the ground of the east side of the south slope (a). In contrast, the same area on the west side of the south slope has a white background (b).

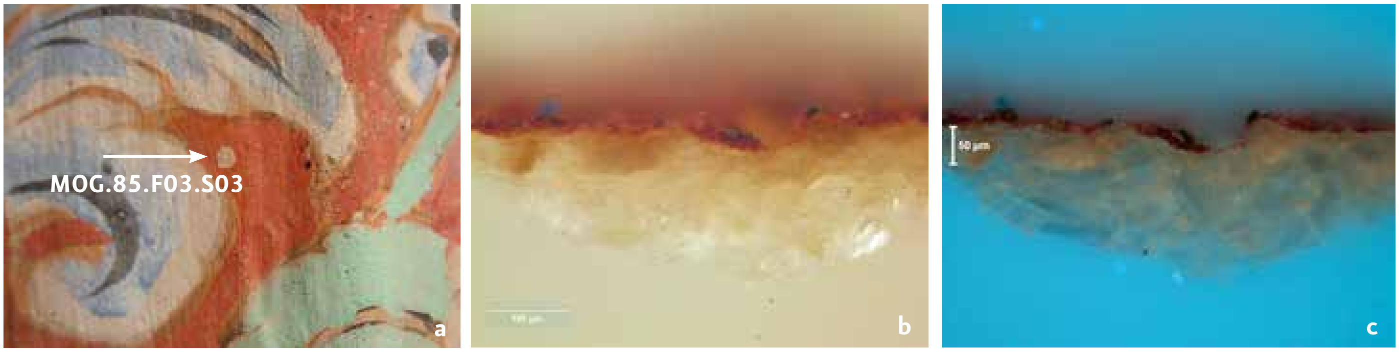

Fig. 13.21 A sample of the red paint layer from the east wall (MOG.85.F03.S03) shows fluorescence of the ground, possibly indicating the presence of a tinted organic wash. Polished cross section in incident light (b) and under UV illumination (c).

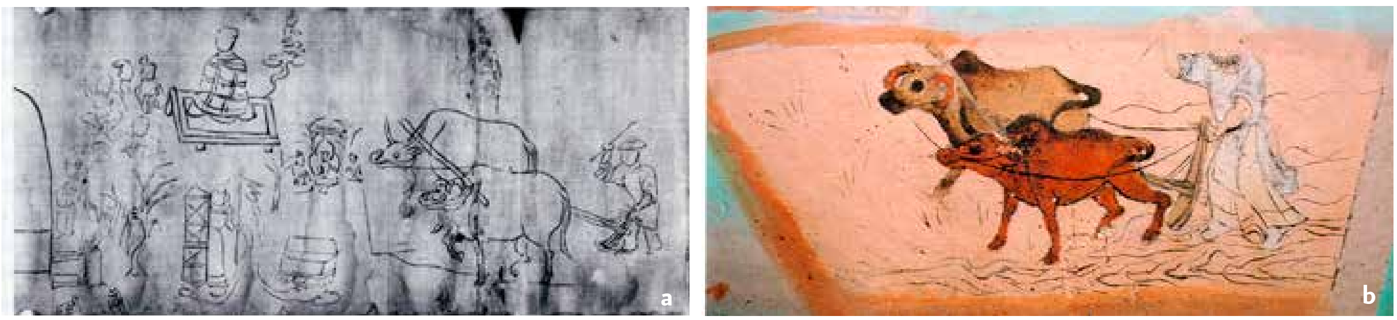

Fig. 13.22 Ink sketches of Maitreya's Paradise (a). Late ninth or tenth century. Image from the south slope of Cave 85 (b).

The ink sketches on paper were an important first stage of the mural process (Fraser 2004, 228). The sketches have a spontaneous quality that indicates the freehand drawing technique used: "The artist quickly draws, [and] the sketch becomes a visual notation and translation of how he envisages painting large surfaces in a systematic way" (Fraser 2004, 226); "Many of the Dunhuang drawings are notations and jottings in which the organization, but not the details, of a composition is provided." Freehand sketching was considered a valuable skill in a wall painting atelier (Fraser 2004, 51).

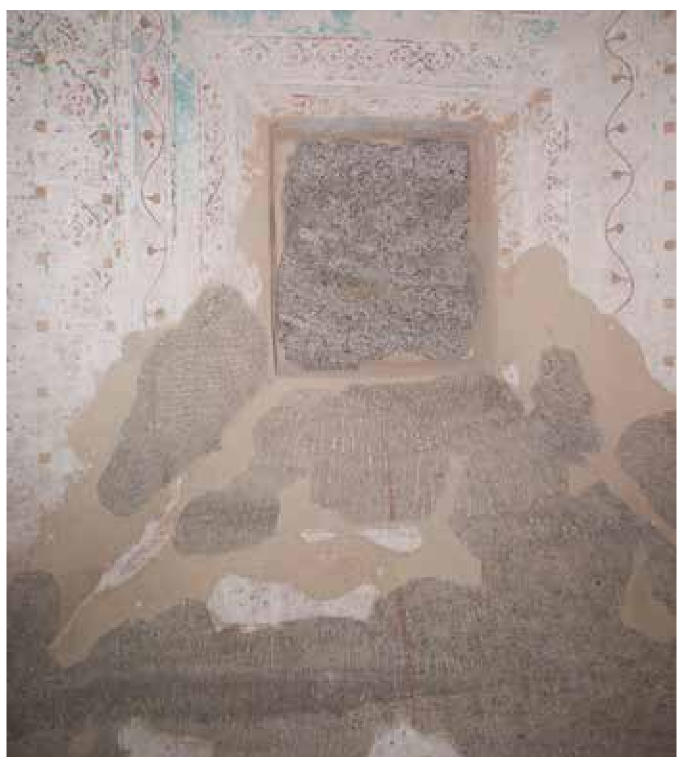

Fig. 13.23 A red line was painted on the west slope of Cave 256 as an early setting-out mark. Chisel marks are also visible on the conglomerate.

The red paint lines on the exposed conglomerate seen in Cave 256 appear to be early setting-out lines to help guide and plan the excavation of the rock and the application of plaster (fig. 13.23). To transfer the roughly executed sketches to the plastered walls, major horizontal and vertical lines were applied on the ground probably by the use of plumb lines, straightedges, and snapped lines, and although little evidence of their use can be detected in Cave 85, there is evidence for the setting out of compositional details. Direct straight-edge incisions—characterized by thin, sharp, deep lines—were used to delineate

Fig. 13.24 Fine straight-edge incisions provide guides for the painted design on the central ceiling panel.

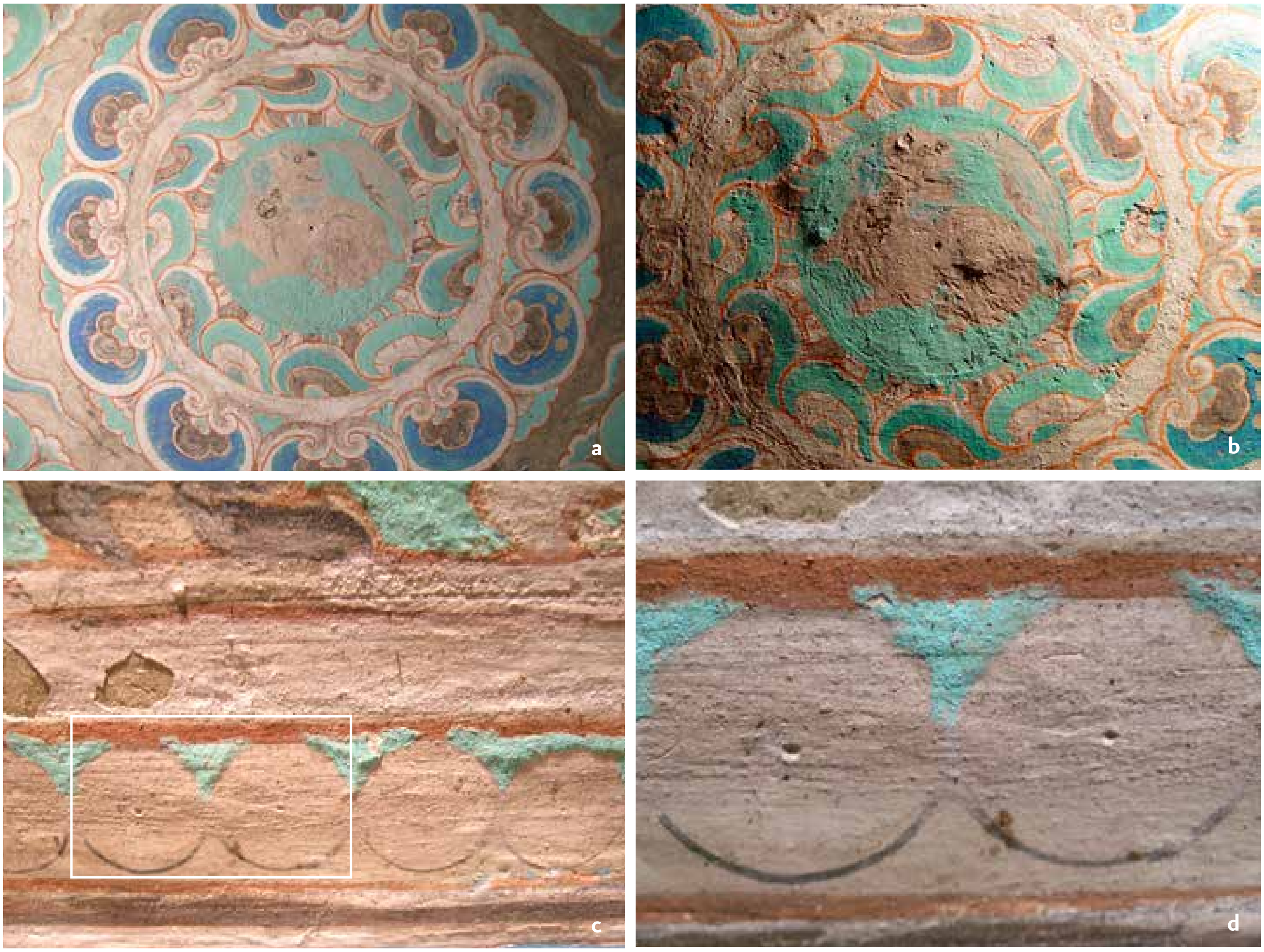

Fig. 13.25 Compass points are found in the central ceiling panel (a, b) and on the "beaded pearl" decorative border (c, d).

the spacing of the "beaded pearl" design of the ceiling panel, to set out text cartouche outlines, and to form guidelines for the texts themselves (fig. 13.24). Compass points can be seen for setting out halos, mandorlas, and the beaded pearl decoration on the ceiling (fig. 13.25).

Although cartoons are known to have been used during the Tang dynasty, and a number of paper pouncing cartoons from the period survive from the Library Cave cache (Fraser 1996), it is clear from measurements taken of repeat motifs in foliate borders that cartoons were not used in Cave 85 (fig. 13.26). Despite this, the more extensive use of cartoons cannot be ruled out, as evidence of pounces, like most of the other preparatory evidence, may simply have been covered over by successive paint layers. There is evidence of stencils used in Cave 85 but only in the corridor paintings that date to the Five Dynasties period (fig. 13.27).

The paintings most likely combined a range of planned preparatory techniques such as preliminary sketches, pounces, or guide marks with a free, creative, and improvisational hand.

Fig. 13.26 Pounce P4517.2. Ink on paper with perforations. Ninth or tenth century. There is no evidence of pounces having been used in Cave 85.

Ink Line Drawings

Delicate and detailed line drawings were executed using dilute black ink (fig. 13.28).[15] In some instances these line drawings are now hidden under paint layers, though with ultraviolet illumination and/or infrared examination these lines can sometimes still be clearly seen (fig. 13.29). Red line drawings were also added to provide extra detail and to emphasize the lines of important figures (fig. 13.30). These lines were executed with a confident and skilled hand by the most senior member of the painting workshop (Barnhart et al. 1997). It is thought that the master painter created outlines, while the apprentices filled in the color—a technique known as "outline-and-fill" or "plain-line painting" (Yu 1988, 26).

Paint Layers: Inorganic Pigments and Organic Colorants

Much of the existing information on the materials and techniques of Chinese wall painting focuses on inorganic pigment identification. Mineral pigment findings in Cave 85 were consistent with other technical studies of the Mogao wall

Fig. 13.27 Papercuts found during the archaeological investigations of the northern grottoes could have been used as stencils (a). (From Peng and Wang 2000.) Evidence of stencil use can be found in the corridor of Cave 85 (b); raking light on corridor paintings shows leaves and flowers (c, d).

Fig. 13.28 Skilled line drawing using black ink of an elephant on the south wall.

Fig. 13.29 When line drawings are covered by inorganic pigments, they are sometimes visible using IR illumination and can be recorded as IR-reflected photographs. In this example the drawing of the wicker chairs is visible in IR even though covered by a wash of a copper-based green pigment (a, b).

	PIGMENT [CHEMICAL COMPOSITION]	ANALYTICAL METHOD*	REPRESENTATIVE SAMPLES
INORGANIC PIGMENTS			
Blues	• Azurite [$Cu_3(OH)_2(CO_3)_2$]	XRD	MOG.85.F03.S04
Greens	• Atacamite [$Cu_2Cl(OH)_3$] • Malachite[2] [$CuCO_3$•$Cu(OH)_2$]**	XRD XRD ESEM-EDX	MOG.85.F03.S16 MOG.85.F03.S04 MOG.85.F03.S01
Reds	• Red lead [Pb_3O_4] • Vermilion [HgS]*** • Red iron oxide (containing hematite) [Fe_2O_3]	XRD XRD XRD	85NQ97P13/P1/P3 MOG.85.F03.S16 85NQ97P14/P15 MOG.85.F03.S03/S08 MOG.85.F03.S03
Yellows	• Orpiment [As_2S_3]	ESEM-EDX	MOG.85.F03.S29 MOG.85.F04.S02
Whites	• White lead [$PbCO_3$ and $Pb_3(CO_3)_2 \cdot (OH)_2$]	XRD	MOG.85.F03.S11
Blacks	• Carbon black [C]	PLM	MOG.85.F03.S04
ORGANIC COLORANTS			
Blues	• Indigoid	HPLC-PDA-MS	MOG.85.S05.S02
Reds	• Lac dye • Unknown red colorant	HPLC-PDA-MS	MOG.85.S05.S01 MOG.85.S05.S03 MOG.85.F03.S23
Yellows	• Genistein, a colorless compound often present in flavonoid dyes • Unknown yellow colorant	HPLC-PDA-MS	MOG.85.F03.S21 MOG.85.F03.S23

Table 13.1 Pigments and Colorants Identified in Cave 85

Notes:

*XRD results are reported here when available. The presence of some mineral species, for example, orpiment, was deduced by ESEM-EDX elemental mapping for sulfur and arsenic.

**Malachite was found only on the east wall and corridor of Cave 85. In other areas of the cave malachite was not found but atacamite was.

***It is unclear whether naturally occurring cinnabar or an artificially produced pigment was used in Cave 85. Either is possible; dry-process vermilion, achieved by combining mercury and sulfur, is likely to have originated in China and is known to have been developed at a very early date (Li 1948, 133–34).

paintings (Guo 1997; Wainwright et al. 1997).[16]
Analysis identified pigments derived from naturally occurring mineral deposits including calcite, orpiment, atacamite,[17] azurite, and red iron oxide and occasionally malachite. Pigments obtained through chemical and other processes include carbon black, lead white, red lead, and vermilion, which were almost certainly locally manufactured (Wang 2003, 56).[18]

Chinese sources describe extensive use of organic colorants together with mineral and synthetic inorganic pigments (Yu 1988). For example: "Through ceaseless invention and improvement, from the Sui and Tang dynasties on, vegetable pigments, chemically produced pigments, and mineral pigments were combined for use. For example, rouge laid on over cinnabar becomes somewhat redder, cinnabar washed over indigo becomes more purple, and a light application of rattan yellow over malachite turns it to a delicate shade of green. These colors washed over drawn and painted objects are plant and mineral pigments used in combination to produce 'mixed colors' and 'multiple-mixed colors'" (Yu 1988, 31).

Visual examination of the paintings in Cave 85, including UV-induced fluorescence examination, suggested the widespread use of organic colorants. This is not the first time organic colorants have been detected on the wall paintings at Mogao. The chemist Rutherford J. Gettens (1900–1974) at the Fogg Museum, Harvard University, in the 1930s, using simple microchemical tests, suspected the presence of indigo in samples brought back by Langdon Warner.[19]

A wide range of organic colorants are known to have been available to Tang dynasty artists, but until recently their use has been associated almost exclusively with painting on paper and silk, and investigations into their use in Mogao wall paintings have been omitted from almost all technical studies (see Appendix 13.A: Literary Evidence to Support the Use of Organic Colorants in Chinese Painting during the Tang Dynasty).

Identification of organic colorants on wall paintings is notoriously difficult. Use of UV illumination can help to show layers of organic materials that are today barely perceptible in visible light. However, this provides information only on the topographic distribution of fluorescent materials thought to be organic in nature (several inorganic compounds also fluoresce); it is not possible to specify whether fluorescence is due to a binder, an organic pigment, a surface coating, a treatment

Fig. 13.30 Exquisite red line drawing of a central dancing figure on the south wall.

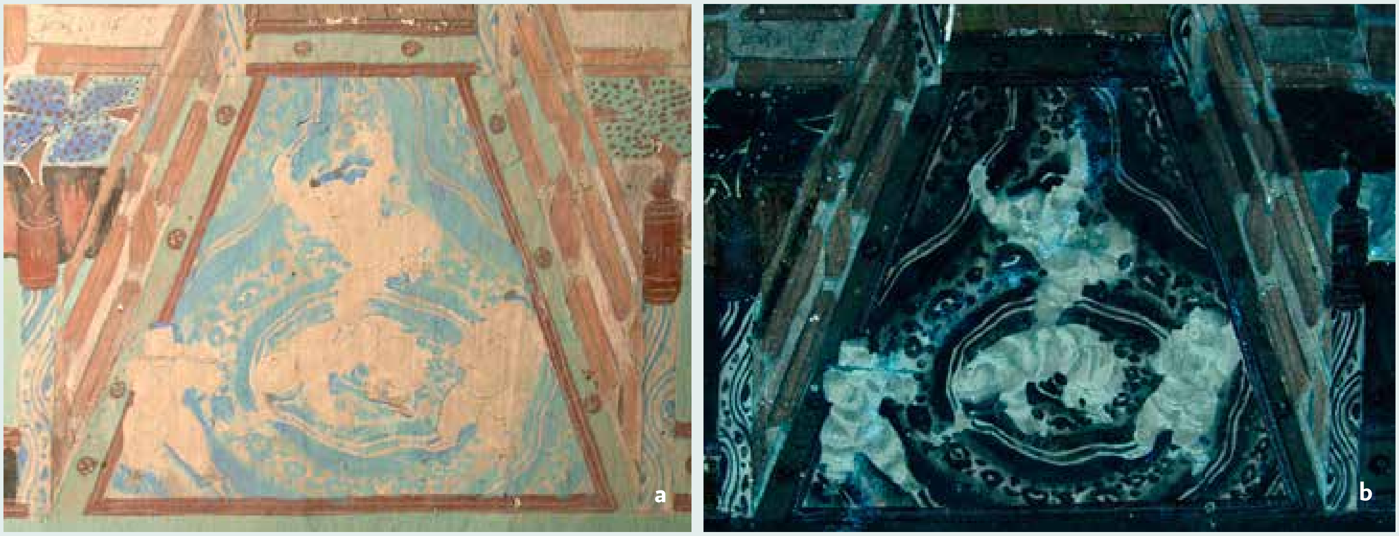

Fig. 13.31 The rosy flesh tones of the chubby boy acrobats are no longer discernible in visible light (a). They were achieved using organic glazes, but these can now be seen only with UV-induced fluorescence imaging (b).

Fig. 13.32 Red UV-induced fluorescence such as on the pedestal of the central Buddha from the south wall can be a good indicator of the presence of red organic colorants (a, b). Spectroscopic measurements of UV-induced fluorescence of organic binders (such as oil, glue, and casein) show maximum emission in the region of 450 nm (blue). Red and yellow inorganic pigments (such as red and yellow ochre) absorb visible light in the blue region, creating a weak response to UV examination. In contrast, spectroscopic measurements of red organic colorants show a strong fluorescence in the region of 700 nm (red) (Verri, Clementi, et al. 2008; Verri et al. 2005).

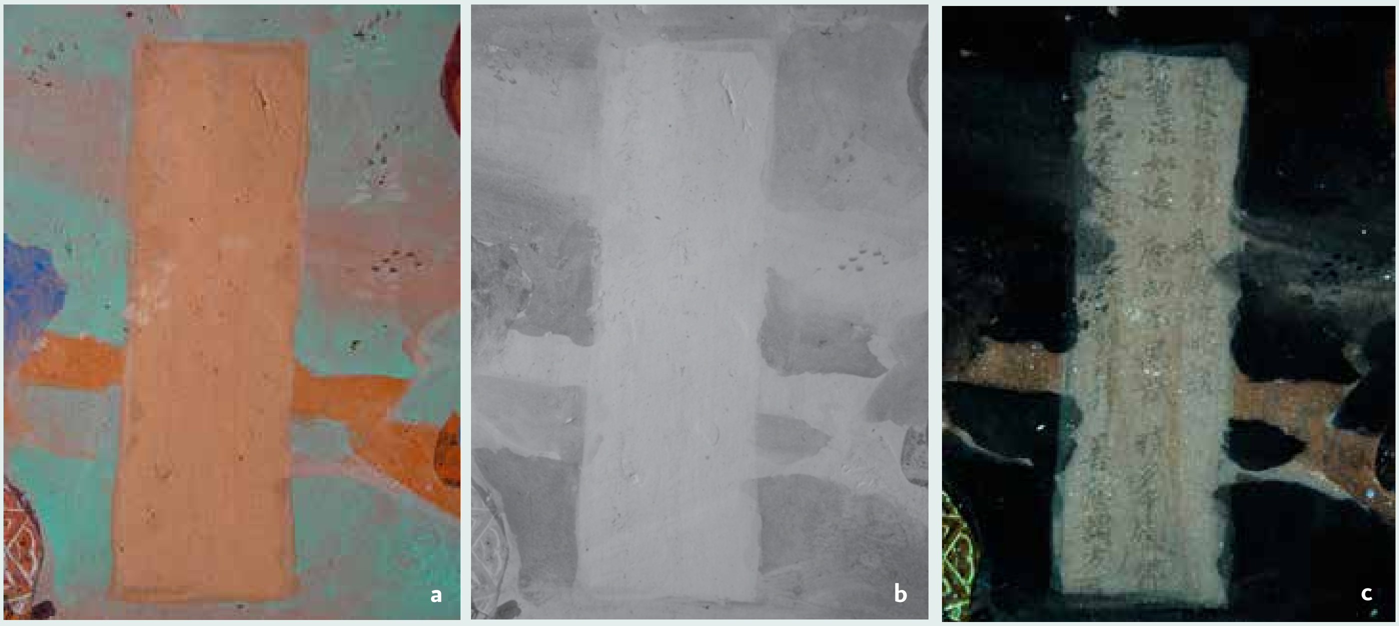

Fig. 13.33 Text cartouche on the south slope in visible (a), infrared reflected (b), and UV-induced fluorescence (c) imaging. Due to discoloration of an upper layer the black ink characters on the cartouche are no longer visible. However, under UV the cartouche can clearly be read. The local auto-absorption of fluorescence by the black ink makes the characters visible.

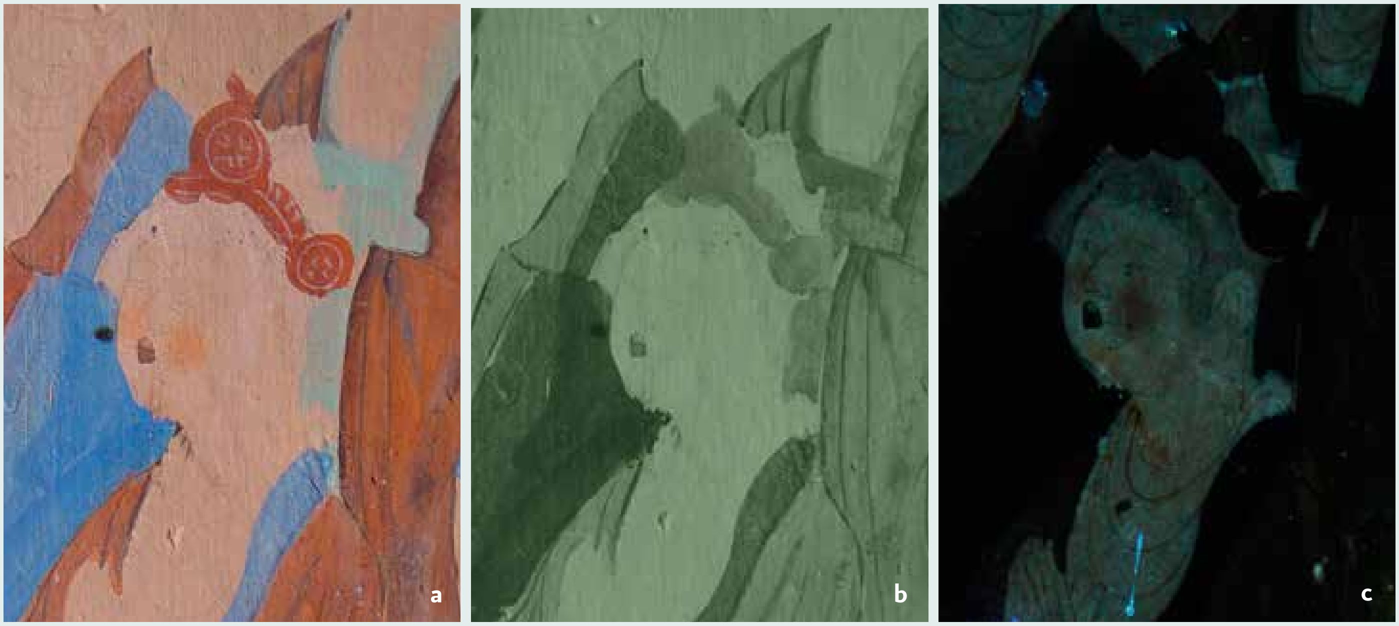

Fig. 13.34 The black ink line drawings of the figure are hard to see in visible light (a) and infrared reflected (b) imaging but are clearly seen under UV-induced fluorescence (c).

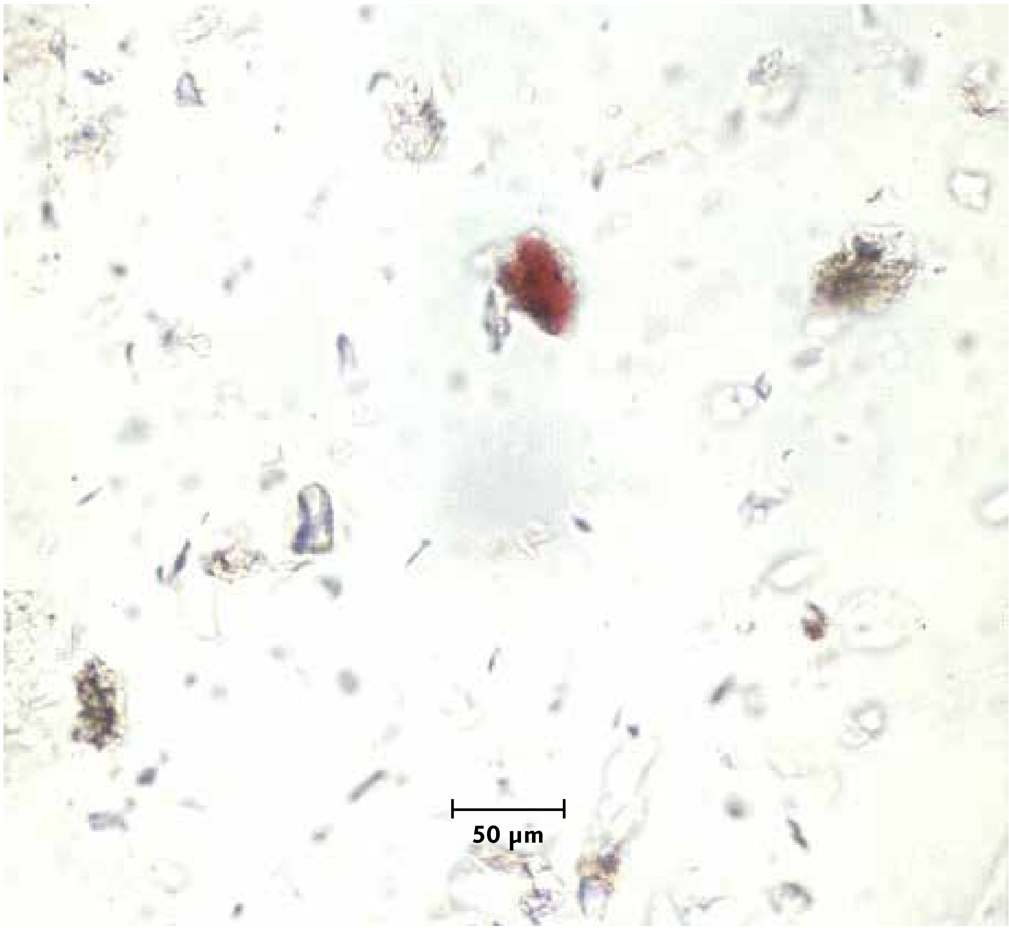

Fig. 13.35 Polarized-light microscopy of a cranberry red paint sample (85JXNB98PE11) from the ceiling is amorphous and shows no crystalline material.

material, or a combination of one or more of these.[20]
Analysis and identification of organic colorants using a range of analytical instrumentation also proved to be difficult. Examination of samples from an area of cranberry red paint from the ceiling using polarized-light microscopy (PLM) showed no crystalline material but rather transparent, amorphous cranberry red deposit on calcite particles and bound in a medium-rich layer (fig. 13.35).

Samples were also tested using high-performance liquid chromatography–photodiode array–mass spectrometry (HPLC-PDA-MS), a technique used for identifying organic dyes and pigments present in artifacts (Wouters 1985, 1994; Grzywacz and Wouters 2005). Lac dye was identified in plum-colored samples MOG.85.S05.S01 and MOG.85.S05.S03 (fig. 13.36). Sample MOG.85.S05.S02 from a bright red area detected an indigoid (fig. 13.37). Sample MOG.85.F03.S21, taken from a translucent brown area, was found to contain genistein, a colorless compound often present in flavonoid dyes (fig. 13.38). This is likely an organic yellow colorant but from a still unidentified plant species. Traces of at least two different yellow organic colorants can be seen in Cave 85. The first is a dark, rich, glossy yellow-brown organic glaze, used mainly in the depiction of clouds, as in sample MOG.85.F03.S21, and a much paler, dull yellow, traces of which have been detected in architectural detailing such as brickwork and roof tiling at the east end of the south wall (fig. 13.39). Both may be considerably altered from their original appearance, and it is likely that the latter was originally a much stronger color and may well have been much more widely used in the cave than is now apparent.[21] Thus, the test results confirmed the presence of organic colorants in the wall paintings, but absolute identification of a greater range of colorants was unsuccessful.[22]

Detection and identification of traditional Chinese organic colorants with scientific instrumentation presents a challenge

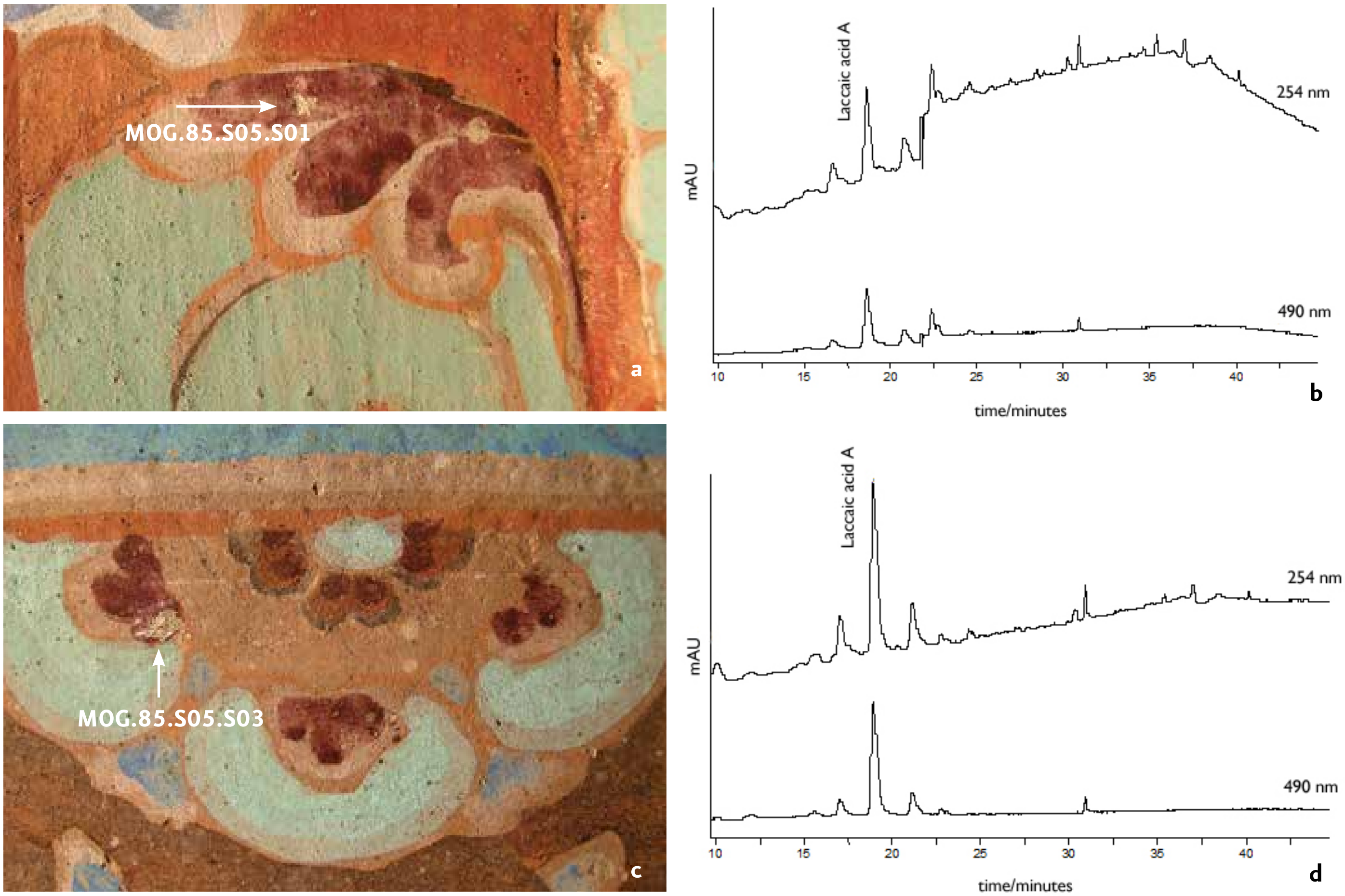

Fig. 13.36 Lac dye was identified in two samples using HPLC-PDA-MS: MOG.85.S05.S01 (a, b) and MOG.85.S05.S03 (c, d).

not only because many of the biological sources used to create them have not been well studied but also because in the case of organic paints concentrations of these colorants are low compared with inorganic pigments and binding media. Much less is known of these colorants than of the dye and organic pigment sources used in Europe and the Americas.

These problems were investigated as part of a collaborative scientific research project on Asian organic colorants conducted by the GCI and the Dunhuang Academy (2006–10).[23]

Painting Technique

The general sequencing of paint applications involved first the rough blocking in of a narrow range of stable and relatively common colors. A dull red (red iron oxide) was used for landscape elements, architecture, garments, flesh, animals, and scene and register divisions; a pale green (atacamite) was used for garments, foliage, and landscape elements; and black (carbon black) was used for some halos, garments, and floral border decorations.

A much broader palette of colors was used for subsequent layers, from which a wide variety of different effects were obtained. Pigments were used singly or in combination, as thin washes or in impasto, ground to different particle sizes, combined with organic colorants, and modulated by glazing with organic paint washes. Mistakes were sometimes made and then painted over, or a change in decoration occurred (fig. 13.40).

The thickness of the paint layer therefore varies considerably between 5 and 150 µm depending on the area. For example, two areas of red vary considerably. The bright pink-red robes of a figure, sample MOG.85.F03.S23, have a thick paint layer (~100 µm) composed of coarsely ground vermilion and red

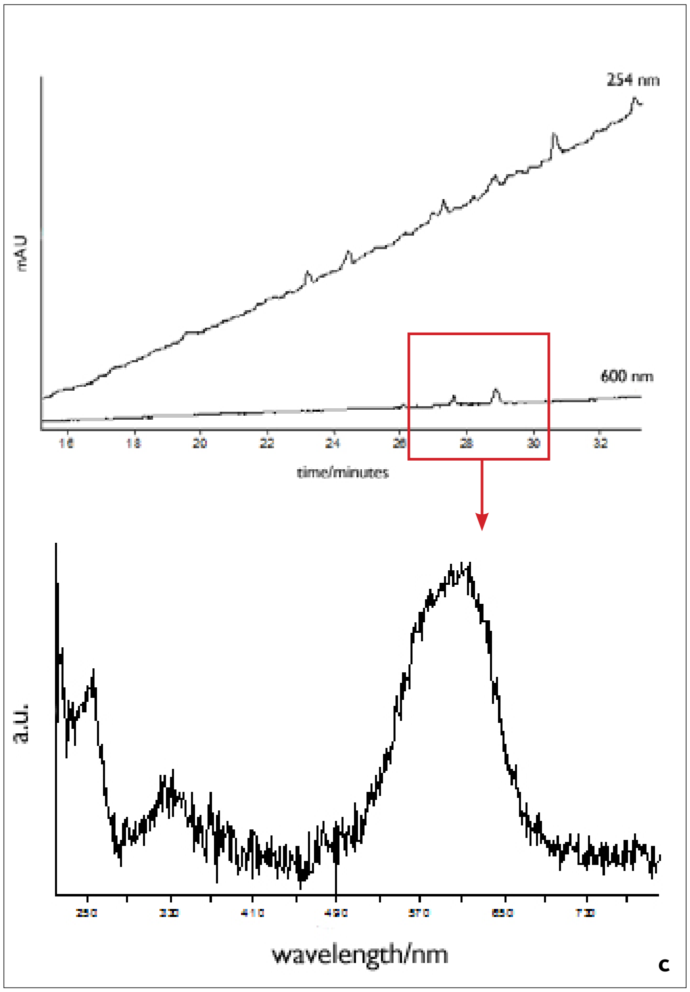

Fig. 13.37 A blue organic material was identified in sample MOG.85.S05.S02 similar to indigo and classified as an indigoid (a, b, c). The blue organic colorant was mixed with coarsely ground vermilion and some iron oxide and lead white to produce a bright pinkish red color.

Fig. 13.38 Sample MOG.85.F03.S21 from a translucent brown area on the cloud (a) that fluoresced under UV (b) was found to contain genistein, a component of an organic yellow. The actual colorant was not identified.

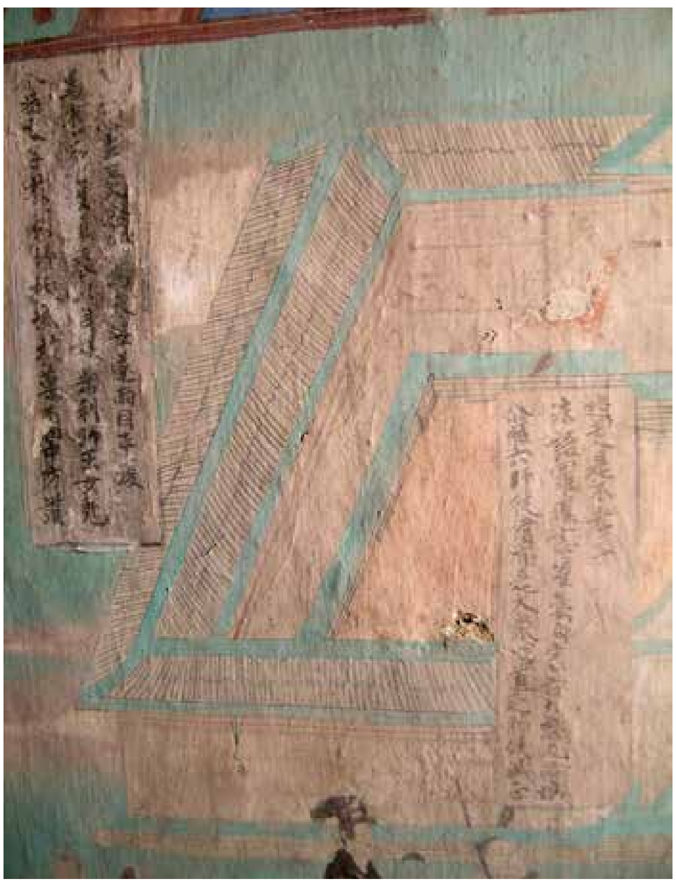

Fig. 13.39 Though only traces of yellow are still visible, a pale, dull yellow would have covered architectural features such as brickwork and roof tiling, as in this area on the south wall. A sample (MOG.85.F03.S05) taken from a similar area showed a few pale yellow translucent particles sparsely distributed in a matrix of fine colorless particles under magnification. ESEM-EDX analysis did not indicate As, Pb, and Fe in the paint layer and therefore eliminated the presence of common yellow mineral pigments. An organic yellow was therefore suspected but could not be identified.

Fig. 13.40 A cartouche on the east slope was modified by painting over the top and bottom portions with green paint.

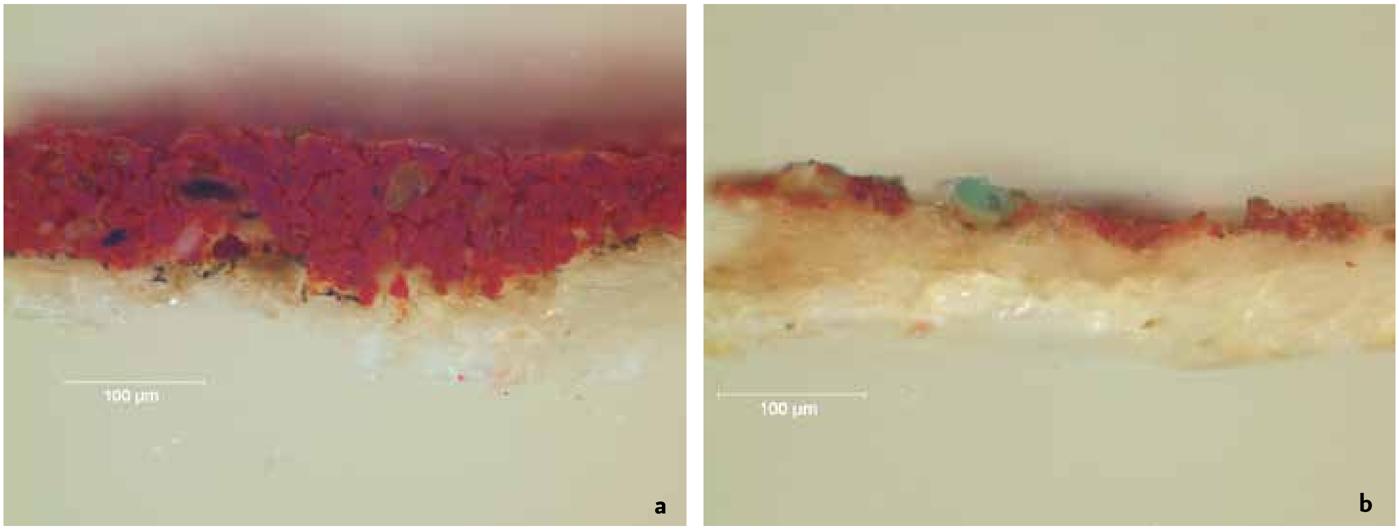

Fig. 13.41 The thickness of paint layers differs considerably. Sample MOG.85.F03.S23 has a thick paint layer (~100 µm) (a), while sample MOG.85.F03.S28 is much thinner (10–30 µm) (b). Both samples are from red painted areas.

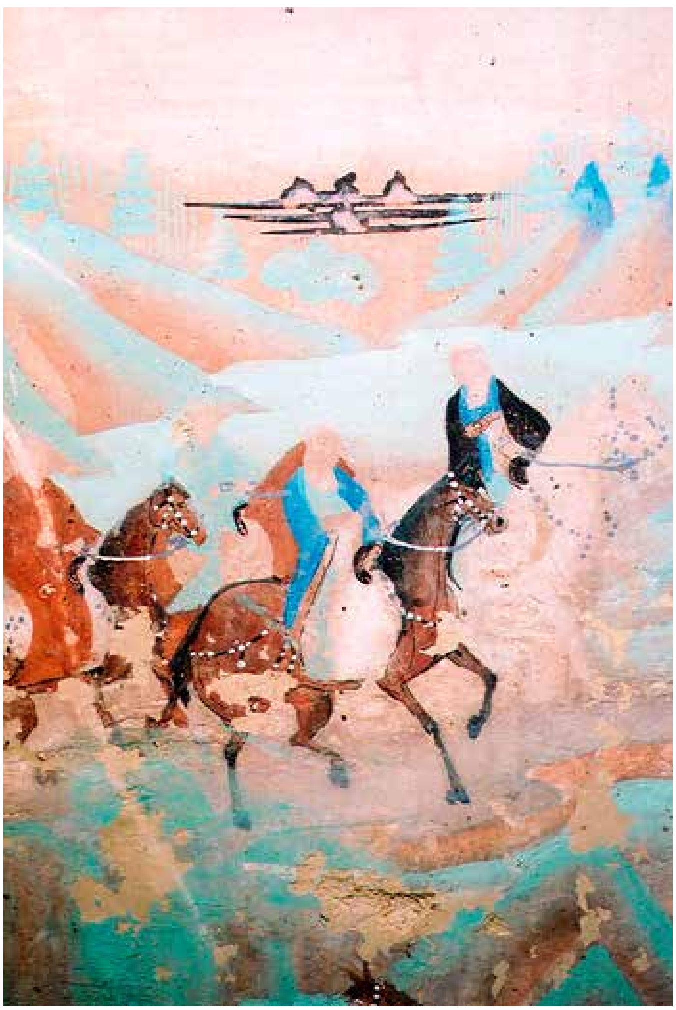

Fig. 13.42 Blending of greens and blues is used to create the mountainous landscape in this scene from the east wall. The vivid depiction of horses also demonstrates the high artistry of these paintings.

lead with a red organic surface application (fig. 13.41).[24] Other areas of red, such as sample MOG.85.F03.S28, from a ceiling border decoration, are of composition similar to the previous sample but applied much more thinly (10–30 µm).

Consummate skills are displayed in the blending of colors on the wall using what is sometimes referred to as the "boneless method" (Yu 1988, 52). In this technique—used primarily for the depiction of objects of multiple hues and indistinct outlines—color is not confined by preliminary outlining and is applied in multiple washes of varying translucency and color nuance. Extremely sophisticated effects are achieved in Cave 85, for example, in landscape painting. Thin washes are blended to create blurred textures and subtle variations of color and are used to great effect to provide an illusion of aerial perspective and misty mountain scenery. This "blue-and-green," or *qinglü shanshui*, landscape painting represents a high point in Tang dynasty painting (Zhuang and Nie 2000, 46) (fig. 13.42). Also noteworthy is the vivid depiction of horses, achieved by layering applications of tinted background color, iron oxides, organic reds, azurite blue, and atacamite green.

One of the subtlest and most inventive uses of color is achieved by exploiting variations in the optical properties of certain mineral particles when they are ground to different sizes. Larger particles produce deep, intense, and lustrous colors that can be applied in thick, opaque layers, while progressively smaller particle sizes produce paler colors that can be applied more thinly. This exploitation of the optical properties of different grades of pigment particle size has a long history in China, having been observed in Qin dynasty wall paintings in Shaanxi Province (Liu 1980, 98–99).

In Cave 85 up to three different grindings of atacamite, azurite, and vermilion can be discerned both by the intensity of the color and by the texture of the paint layers.[25, 26] For example, in the depiction of brocade fabrics, a thin wash of finely ground pigment (either azurite or atacamite) is applied as the background color, and then the pattern is picked out in a richly colored impasto composed of larger particles of the same pigment (fig. 13.43). The light, delicate greens of tree bark, branches, and leaves—especially the pale gray-greens of willow—are vividly realized by layering finely ground grades of atacamite (fig. 13.44).

While the practice of grading pigments according to particle size was not unknown in the West, this was done solely to separate particles by quality, and the exploitation of particle size to achieve subtle nuances of hue was never learned by Western artists.[27] Thus, the coarsest, most intensely colored pigment particles were always the most highly prized in the Occident, whereas in China the finest grindings—which allowed more refined brushwork and produced more delicate colors—were equally if not more highly valued.

Given the technique of layering of pigments, a sizing or fixative may have been used between layers to prevent the problem of unintentional color bleeding from one layer into the next (Yu 1988, 18). This was used commonly by Chinese painters working on paper and silk. In Tang Liuru's (Tang Yin's) *Painting Manual* of the Song dynasty a painting was put through "three sizings and eight washes." "In nearly all types of Chinese painting…an alum solution is employed to fix the colors. If a painting has several layers of color applied, a light alum solution should be spread on, separating each or every other layer, especially the bottom layer of color. This is done in order to prevent the pigments underneath from spreading when the other colors are applied over them" (Yu 1988, 18). "If a layer of cinnabar is put down first—no matter what concentration of glue it contains—and if no alum solution is applied, then when a heavy or light layer of rouge is washed over it, the cinnabar can begin to spread and to become mixed with the rouge. If alum is applied, the cinnabar will remain fixed no matter what kind of wash is applied over it" (Yu 1988, 18).

An ESEM-EDX elemental map of three samples from the foliage border on the south end of the east wall shows a calcium and sulfur overlap occurring within the paint layer as discussed previously (see Ground section) (fig. 13.45). The presence of the mineral gypsum, confirmed in two of these samples by

Fig. 13.43 A coarse grade of atacamite green superimposed on a finer grade in the depiction of brocade.

XRD, could possibly indicate the application of an alum solution used as a fixative.[28] This is the third suspected use of alum in the painting, in addition to its use as a sealant layer on the fine plaster and on the ground. It is possible that it was common practice to apply this material at regular stages throughout the mural painting process.

Binding Medium

Pigments were mixed with organic binding media, and it is evident from the thinness of most paint layers—even those containing very coarsely ground particles—that the medium-to-pigment ratio must have been high. While this enabled mineral pigments to be applied as semitranslucent glazes, thereby greatly extending the range of obtainable effects, it also made paint susceptible to run and drip, much evidence for which can be seen in Cave 85 (fig. 13.46).

Previous studies of binding media on Mogao wall paintings identified collagen-based proteinaceous materials such as animal glue in the majority of the caves studied from the Northern Liang (420–439) to the Yuan (1271–1368) dynasty (Li 1993, 108–17).[29] The amino acid compositions of the remainder of the samples correlated broadly with fruit gums and mucilage in the form of glycosides (Li 1995).[30]

GC/MS analysis undertaken during the Cave 85 project also

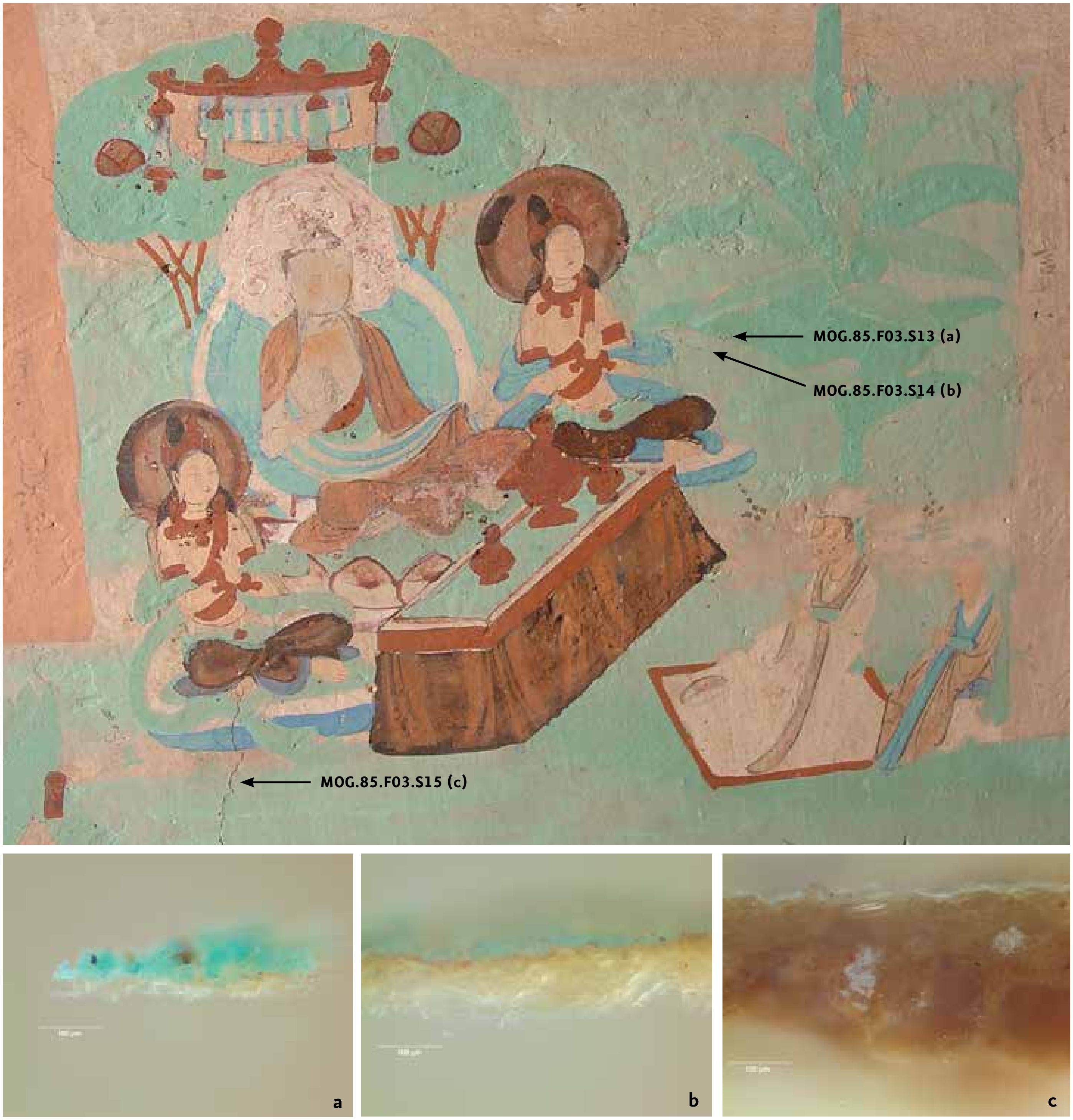

Fig. 13.44 Three gradings of green have been used to create the willow tree and background of a scene on the north wall. Sample MOG.85.F03.S13, the darkest green, is coarsely ground (a), sample MOG.85.F03.S14 is medium ground (b), and sample MOG.85.F03.S15 is finely ground (c).

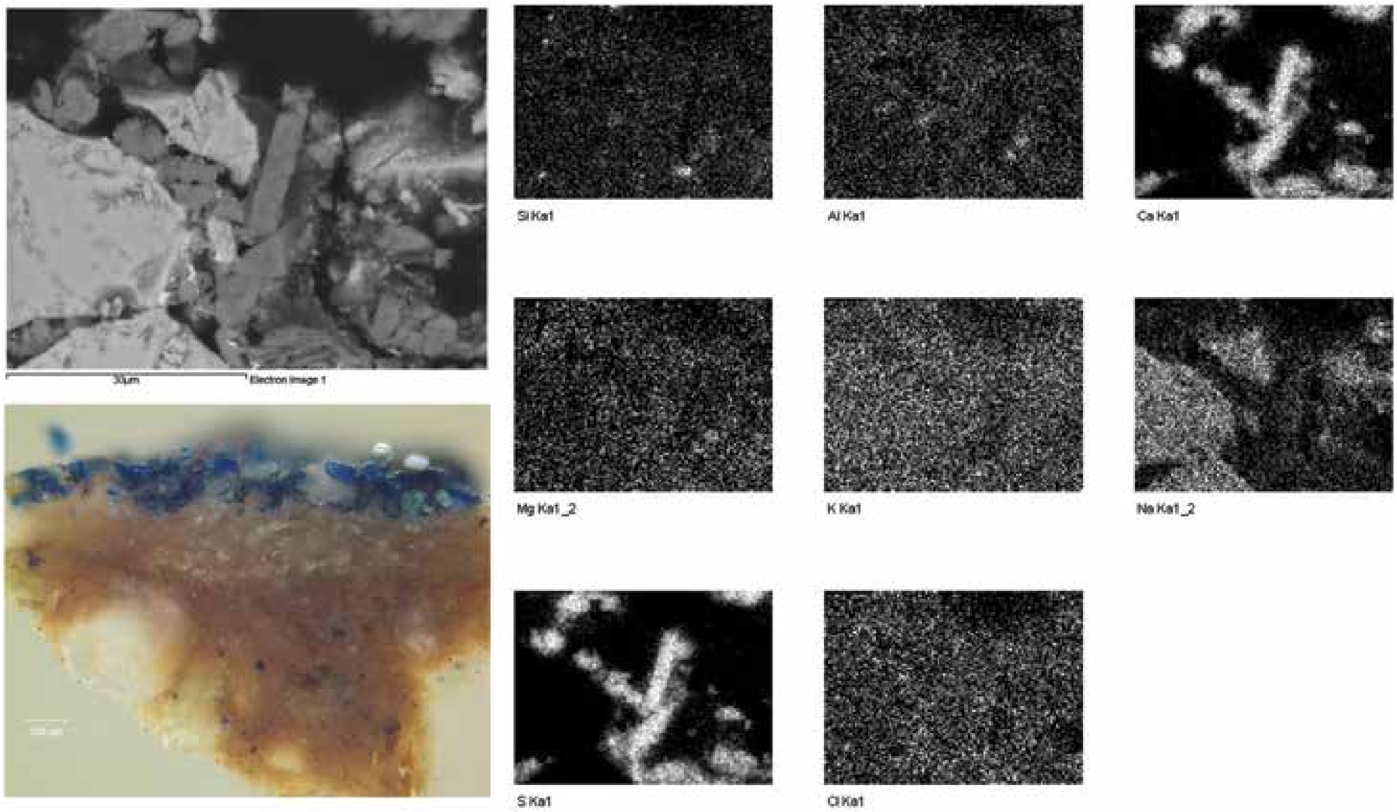

Fig. 13.45 Backscattered electron image and elemental maps of a detail of sample MOG.85.F03.S04 show small crystals of calcium and sulfur in the paint layer. The presence of gypsum crystals could be an indication of the application of an alum solution used as a fixative between paint layers, the water soluble alum providing the sulfate ions for precipitation with calcium to produce gypsum.

found animal glue as the most extensively used paint medium.[31] Samples with a total amino acid content equal to or above 0.1% by weight were analyzed for best correlation coefficient and provided a best match with collagen, an indication of the use of animal glue as a binder.[32]

Samples including paint layers suspected to contain organic colorants, based on both visual examination and UV-induced fluorescence, had significantly higher carbohydrate content (between 0.4% and 1% weight percent of sugars) as compared to paints with only inorganic pigments (which typically have 0.1% by weight). For example, sample JXDB00P1, an organic red from the ceiling panel, has 0.77% carbohydrates and 5.9% amino acid content, while sample MOG.85.F03.S29, an inorganic red from the south slope, had carbohydrate content below 0.1% (the detection limit of the instrument) and 0.8% amino acid.

A larger number of samples were tested for carbohydrates than for amino acids: twenty-six paint samples were tested for carbohydrates, while fourteen were analyzed for amino acids (see

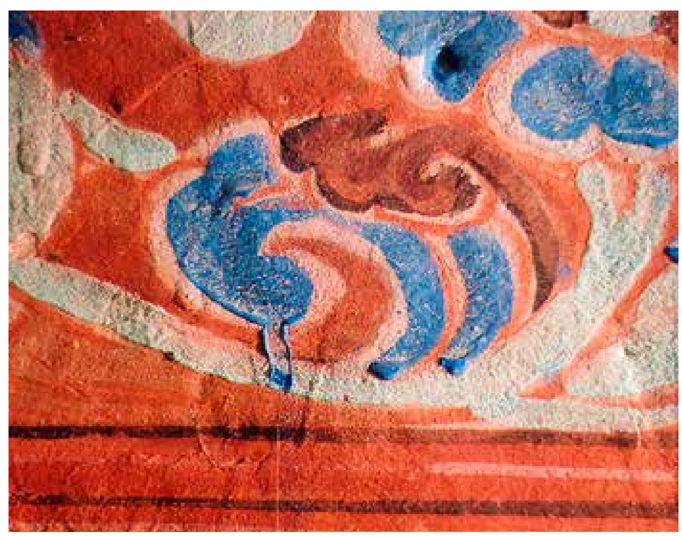

Fig. 13.46 Drips and run marks of paint are a common occurrence in the paintings.

Sample	Description	Weight % Amino Acids	Normalized Mole Percentages							Weight % Sugars	Normalized Weight Percentages of All Carbohydrates								
			Ala	Val	Ile	Leu	Gly	Pro	Hyp		Rham	Fuc	Rib	Arab	Xyl	Mann	Fruct	Glu	Gal
JXDB00P1	Organic red	5.9	13	5.7	4.0	6.6	61	7.8	1.8	0.77	0.7	0.4	0	5.4	2.2	1.8	17	69	4.3
YDNQ01PE14	Gray	2.6	21	12	9.3	18	22	11	6.7	0.76	0.5	0	0	2.1	64	1.1	0	30	2.4
MOG.85.F03.S29	Dark red	0.8	14	3.1	2.7	3.5	44	18	15	<0.1									
MOG.85.F03.S24	Brown-resinous	0.7	16	8.8	7.3	8.2	21	19	20	0.40	10	1.0	0	41	6	4.0	4	26	10
DQ00PE16	Red and ground	0.4	17	3.7	2.9	4.9	31	25	16	0.23	0	0	0	2.5	3.2	0	35	58	0.6
MOG.85.F03.S25	White	0.4	20	6.6	4.3	5.7	35	18	11	<0.1									
MOG.85.F03.S22	Pink	0.4	15	3.6	2.7	3.7	41	16	19	<0.1									
MOG.85.F03.S08	Red	0.4	17	5.9	5.1	6.1	45	12	9.3	<0.1									
JXNB01PE13	Discolored ceiling	0.39	19	3.6	2.0	4.1	48	15	8.6	0.12	1.1	0	0.5	2.7	1.6	2.2	16	73	3.2
MOG.85.F03.S17	Brown	0.3	16	9.6	6.9	10	40	13	4.2	<0.1									
DQ00PE15	Blue and ground	0.22	20	6.1	4.1	7.6	26	18	18	0.10	0.4	0	0	7.2	7.0	0	22	60	3.3
NQ01PE11	Colored ground	0.12	24	7.6	5.5	12	38	12	0.0	2.6	0	0	0	5.4	18	0	0	71	6.2
BP00PE9	White	0.12	14	7.0	7.5	13	13	28	18	<0.1									
MOG.85.F03.S20	White	0.1	19	8.9	5.6	10	26	15	16	<0.1									
Collagen	Mean data	84	16	3.0	1.8	3.7	47	17	12.4										
Whole Egg	Mean data	46	22	17	13	22	15	11	0.0										
Microbe	Cave 85	13	22	14	16	17	23	7	0.3	16	0	0	0.7	0.6	1.2	16	0.2	22	59
Gum Tragacanth	Iranian Kurdistan									68	3.2	3.7	0	50	13	0	0	17	13
Mucilage	Cucumber									52	0.6	0	1	3	2	0.3	36	52	6
Apricot Gum	Mogao									70	1.0	0	0	40	7.0	4.0	0	2.0	46
Gum Arabic	England									59	22	0.1	0	36	0	0	0	0.2	41
DP98PE12	Shiny brown									8.4	1.5	2.9	0.6	20	9.5	2.4	19	25	19
PLATXQ98P2	Amber 'resin'									4.1	7.3	4.5	2.7	9.7	6.9	4.5	1.5	45	18
NP98P9	Red									2.2	0	0.1	0	3.3	44	13	3.5	33	2.5
NQ01PE12	White ground									0.75	0	0	0	21	0	0	0	79	0
DP98PE13	Beige									0.23	1.2	0	0.6	6.7	3.7	1.8	47	31	7.9
JXNB98PE11	White and earth									0.23	0	0	0	2.2	2.2	0	32	63	0.7
NPOOPE4	Red, ground and earth									0.21	0.6	0.5	0	3.6	3.7	2.1	25	59	5.4
PLATXQ98P2	Red and ground									0.21	16	1.2	1.5	15	7.3	4.7	10	22	22
XQ98PE2	Red									0.20	3.7	0	0	8.9	16	4.4	21	40	6.7
NQ98P4	Red and ground									0.17	2.4	0	0	7.2	78	7.2	0	0	4.8
DQ98PE3	Beige and earth									0.12	0.4	0.1	0	8.2	5.0	0	7.3	75	3.4

Table 13.2 Summary of Results of GC/MS Amino Acids and Carbohydrates Quantitative Analysis

table 13.2). Results showed that many of the paint samples contained various amounts of polysaccharides such as those found in plant gums, honey, plant mucilages, and sugars. Apricot gum and *Eremurus* sp. mucilage have been reported in literature as binding media in Central Asian art (Birstein 1975), and fruit gums would have been locally available (fig. 13.47). However, as wall painting samples may be composed of several materials that can contribute to the overall carbohydrate composition, including, for example, plant mucilage in the ground, plant gum medium in the paint, and an organic colorant applied on top, it is usually not possible to specify where plant gums and mucilages were used. In addition, degradation of plant fibers in the plaster can produce mannose, a sugar commonly found in plant gums and mucilages, which would bias data interpretation. Moreover, inorganic pigments, especially copper-based ones, can interfere with the hydrolysis and derivatization sample preparation for GC/MS and can also complicate data interpretation; similarly alum can create such constraints.[33]

Gold

Gold foil was used in Cave 85 but very sparingly, being reserved for small details such as in the center of the ceiling panel where gold is found on the eyes and bell of the lion. The use of gold is also found on the base of the central Sakyamuni Buddha statue (fig. 13.48).

Fig. 13.47 Analytical results indicate that many of the paint samples contain polysaccharides such as those found in local plant gums.

Fig. 13.48 Gold foil was used for small details such as the eyes of the lion on the base of the central Sakyamuni Buddha statue.

Fig. 13.49 The central ceiling panel has a surface coating that was applied as a thin wash (a). This coating is clearly visible under UV-induced fluorescence (b), particularly as part of the ceiling (on the "beaded pearl" decoration) was missed during application.

Surface Coating

Areas of the painting such as the central ceiling panel appear to have a surface coating used as a finishing layer. This type of coating was applied as a thin wash. The coating is clearly visible under UV-induced fluorescence, indicating that it is an organic material (fig. 13.49). It is possible that organic coatings were used throughout the cave to fix, enrich, and saturate underlying layers such as on text cartouches and on figures, but analysis has not provided conclusive results, and this requires further investigation.

Summary

A systematic approach to technical investigation was pursued during the Cave 85 project by bringing together analytical results, information from historical Chinese treatises, and utilizing visual, noninvasive examination and imaging technologies. This chapter brings into focus the subtlety and complexity of the Cave 85 paintings, furthering understanding of the links between painting technology and patterns of deterioration. This study has helped to clarify many aspects of Cave 85 painting technology, but it has also highlighted how limited our knowledge remains. A number of intriguing phenomena have come to light during the project that have so far eluded interpretation but that are certainly worthy of further study.

Fig. 13.50 The figures are constructed of earthen plaster applied to an armature of wood or bundled reeds held together with a desert plant known as feather grass, *jiji cao* (*Achnatherum splendens*). The plaster was built up in layers starting with a thick, coarse, fiber-containing plaster followed by a fine plaster and ground and paint layers. In Cave 85, some of the original Tang dynasty polychromy is still visible beneath later restoration (the example shown is not from Cave 85). (From Gao and Giès 1998.)

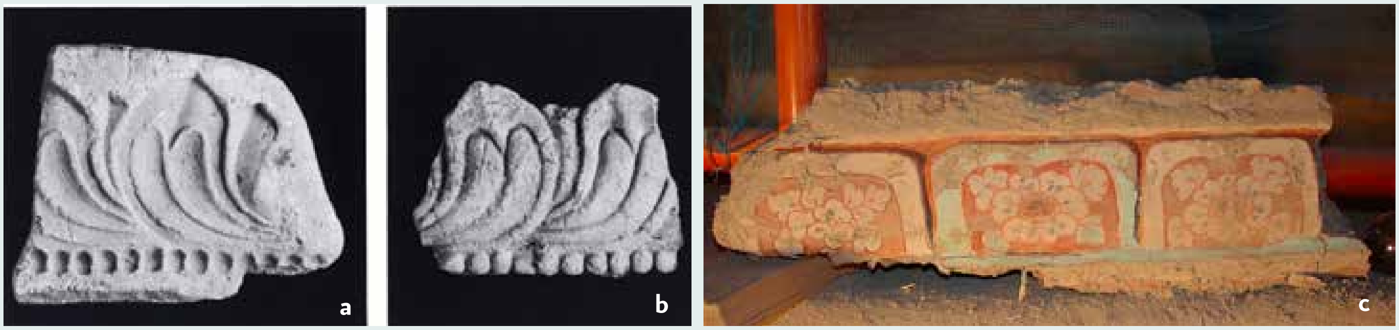

Fig. 13.51 A fifth- to sixth-century stucco mold excavated from Khādalik (a, b). Similar molds may have been used during the Tang period to create sculpted altar platforms and statuary bases. A piece of the platform in Cave 85 (c).

Fig. 13.52 A circa sixth-century stucco mold for molding spiral curls of hair excavated from Khādalik (a, b). Some of the original Late Tang spiral curls survive on the Sakyamuni Buddha in Cave 85 (c, d).

Notes

1. MuSIS™ HS, produced by Forth Photonics, is a hyper-spectral camera featuring imaging spectroscopy and spectrometry in a spectral range from 370 nm (UV) to 1,000 nm (near-infrared). The spectral resolution ranges from 10 nm (for visible or near-infrared) to 20 nm (for both visible and near-infrared). More than 30 spectral bands plus a color reference image can be acquired in less than one minute. From the collected images, spectra can be obtained and per-point spectral and color analysis can be performed through a graphical user interface.
2. Ultraviolet-induced fluorescence imaging is a commonly used technique for the characterization and identification of painting materials such as organic binders and organic colorants. Images were taken with a Sony DSC-F828 camera fit with a UV KV418 Schott filter to block UV-reflected radiation. Lights (produced by IFAC-CNR in Florence) equipped with two UV lamps with DUG11 Schott filters that remove visible light were positioned perpendicular to the wall painting surface. Photography was undertaken in absolute darkness to avoid parasitic visible light.
3. Infrared reflected light (IRR) images were captured using tungsten lights (650–1,000 watts) positioned perpendicular to the surface. An infrared R72 Hoya filter was used on the camera and the "night shot" mode selected in order to disable the IR blocking filter.
4. Noninvasive examination and imaging of the painted surface when paired with focused sampling and analysis reduces the number of samples needed. Graphic documentation of sampling locations can be found in Appendix 13.B.
5. An earthenware mold in the shape of a lotus petal was found during excavations in Cave 464 (Peng and Wang 2000). Although this cave dates from the Yuan dynasty (1279–1368), similar molds would probably have been used for three-dimensional platform and statuary base decoration during the Tang period.
6. Minerals identified by XRD are listed in decreasing order of abundance. Alluvial sediment of the Daquan River: quartz, calcite, plagioclase feldspar, dolomite, illite, chlorite, illite/smectite. Cave 85 plaster: quartz, dolomite, calcite, orthoclase feldspar, plagioclase feldspar, illite, chlorite, illite/smectite.
7. The plaster sample analyzed was collected from the upper southwest corner of the main chamber.
8. The fibers in the coarse plaster layer are tubular cereal grass showing serrated cells and what appear to be stomata. A vegetable fiber, most likely straw, but analysis was unable to confirm identification of the species (Bisbing 2006).
9. The fibers were oriented perpendicular to the polarizer with a first-order compensator inserted, and the faint blue colorization in this orientation is a feature of positive z-twist of natural fibers (Schilling et al. 2010).
10. Hemp is known to have been locally available (as it is today), and plasterers working at the grotto site were partially paid in hemp oil (Whitfield 1999, 210).
11. The clay surface itself had to be covered before painting by three to four layers of a binder made from alum mixed with glue. Lu (1956, 15–17) gives proportions—50 g of glue to 100 g of alum to 1.25 kg of water, varying with the season—but he does not provide any dates or sources for the introduction of this technique (Yu 1988, 29).
12. Because magnesium is present in talc it was used as a marker in ESEM-EDX elemental maps to identify the location of the ground layer in paint cross sections.
13. Hydroxyproline was found in sample BP00PE9, but the 0.26 correlation coefficient did not match with animal glue.
14. These results are based on a limited number of samples of ground analyzed. Other samples of ground were analyzed but included the paint layer and were run as bulk analysis. The amino acid profiles for these samples usually contained hydroxyproline, which correlates with collagen, indicating the presence of an animal glue binder in the paint layer. Further investigation of the ground is necessary to confirm these results. See the Binding Medium section in this chapter for more information.
15. The preparation of ink during the Tang dynasty was a lengthy and complex procedure in which lamp black made from pine wood or vegetable oils such as tung oil was combined with glue and a range of other materials to impart luster and to prolong shelf life (Li 1948, 119–32).
16. The Dunhuang Academy scientists have a long and well-established history in the area of inorganic pigment identification using XRD and XRF to study the Mogao wall paintings. As part of the Cave 85 project, the analytical capabilities of the Dunhuang Academy were expanded through the acquisition of a research-quality transmitted polarized-light microscope and the training of scientists in its use for pigment identification and cross-section examination.
17. Atacamite, a copper chloride hydroxide, was first used at Mogao in the Northern Liang dynasty (397–439 C.E.) (Wang and Wang 1999, 141–43). Synthetic atacamite has been produced since the Early Tang dynasty (Piqué 1997, 352–53). In Cave 85, copper chloride hydroxide is present both as an original pigment and as an alteration product.
18. Needham 1976 contains a list of chemical substances, pigments, and materials from *Chi Ni Tzu*, also known as *Fan Tzu Chi Jan*, a book attributed to the fifth-century administrator, wealthy merchant, and alchemist Fan Li (Needham 1976, 33; *Origins of Alchemy*, 15).
19. From unpublished notes by Gettens held at Harvard University Art Museum's Straus Center for Conservation and Technical Studies.
20. The interpretation of fluorescence imaging is complex and is connected with the physical and chemical interactions among materials in the paint layers. Paint layers are commonly composed of a fluorescent organic material (binder and/or colorant) and a nonfluorescing inorganic pigment. When irradiated with ultraviolet radiation, the light emitted by fluorophore moieities present in the organic material undergoes several types of interactions, in particular scattering and absorption by neighboring pigmented particles and auto-absorption. As a result of scattering and absorption phenomena, the emission spectrum and color is deformed according to the physical properties of the surrounding pigmented particles. This can lead to shifts of the emission maxima and/or the formation of apparent new emission bands. The extent of the modifications to the emission spectra, caused by auto-absorption and selective absorption phenomena, may lead to erroneous characterization or identification of fluorescent materials (Verri, Comelli, et. al 2008).
21. The conspicuous absence of yellow in the majority of Mogao's Tang dynasty wall paintings is in sharp contrast to their abundant presence in Tang paintings on silk and paper.
22. Further characterization of organic materials can be achieved by other noninvasive methods, including point analysis with fiber optic fluorescence spectroscopy (FOFS) and mid-FTIR. These tools were not used in Cave 85.
23. For more information see http://www.getty.edu/conservation/our_projects/science/asian/index.html.
24. Wang Gai and Ze Lang both describe the application of washes of "rouge"

(possibly from safflower) over vermilion. Although both are writing in the Qing dynasty, they are evidently drawing on earlier traditions of the application of an organic red used over mineral pigments (Yu 1988, 65).

25. The simplest method of separating different grades of pigments was by "levigation" or "elutriation" in water following grinding, a process advocated for the grading of cinnabar in the seventeenth-century treatise *T'ien kung k'ai wu* (Li 1948, 133–34). However, more complex methods are described in earlier literature, involving repeated grinding, suspension of the ground material in glue mixed with water, and repeated decanting to separate the lighter, suspended particles floating on the surface from heavier, settled particles (Yu 1988, 5). The process differs slightly between pigments.
26. Up to five different grades could be obtained, providing an enormous range of color and texture nuances (Guo and Duan 1993, 304).
27. See Cennini regarding ultramarine: the first blue produced during processing was of the deepest and richest hue and regarded as of superior quality, while the last produced—a pale gray-blue called ash blue—was much less highly valued (Cennini 1960, 37–38).
28. Given the limited number of samples this requires further investigation.
29. These studies used high-performance liquid chromatography (HPLC) to analyze the amino acids in acid hydrolysates of 2 mg paint samples.
30. Proteins are polymers of amino acids, whereas plant gums contain glycoproteins, i.e., proteins that contain oligosaccharide chains covalently bonded to their polypeptide side-chains. Accordingly, proteins such as animal glue are entirely made up of amino acids, whereas the amino acid content of plant gums falls within the range of 0.2 to 5% by weight. It is therefore possible to identify both classes of paint binding media on the basis of amino acid composition. Correlation coefficients were determined to allow comparison of the sample data to data from reference materials in order to identify the binding medium. Li Shi of the Dunhuang Academy successfully identified animal glue in most samples analyzed, and in the remainder he concluded that a fruit gum could have been used. However, in actual practice, the process of identifying fruit gum is problematic because of the vast number of plant species that produce gumsThe HPLC data were reinterpreted for protein and plant gum identification. From a review of the amino acid molar ratio data it is evident that animal glue was used exclusively in Cave 263 (Northern Wei: 439–534 C.E.), Cave 427 (Sui: 581–618 C.E.), Cave 57 (Early Tang: 618–712 C.E.), Cave 272 (Northern Liang: 421–39 C.E.) and Cave 172 (High Tang: 712–81 C.E.). In the other caves animal glue was used in the vast majority of cases, but a few paint samples did not correlate strictly to animal glue. This may be due to the low concentration of binding medium present or because these colors contain organic colorants or were applied with plant gum media.
31. Paint samples (in the submilligram range) were prepared for quantitative gas chromatography–mass spectrometry (GC/MS) analysis following protocols developed for identification of protein and polysaccharide binding media in easel paintings (Schilling 2005). Procedures involve an acid hydrolysis step to depolymerize the media, followed by chemical derivatization to produce volatile analytes suitable for GC. Proteinaceous binding media were identified on the basis of amino acid composition (Schilling and Khanjian 1996a, 1996b), and plant gums on the basis of carbohydrate composition (Schilling 2005). Compositional data were evaluated using correlation coefficients and principal component analysis, which are two common statistical evaluation tools (Schilling and Khanjian 1996b; Colombini et al. 1998).
32. Amino acids may be present in more of the samples except that the concentration may be at or below the detection limit of the GC/MS method, which ordinarily is 0.02% by weight per 200 µg paint samples. For example, samples from deteriorated areas of painting generally had amino acids concentrations below detection limits.
33. Protein identification by GC is difficult in the presence of high concentration of inorganic species. Pigments—typically inorganic ones—may interact with the medium forming strong complexes. For example, copper ions in pigments such as azurite and atacamite have a great affinity for the complex formation with amino acids. It is therefore much harder to identify in a quantitative manner the protein content in the presence of copper-based pigments, such as the case in Cave 85 (Gautier and Colombini 2007).

CHAPTER 14

Environmental Conditions

An environmental investigation was undertaken to determine the interior microclimatic conditions of Cave 85, including the surface and subsurface of wall paintings in order to understand the role that moisture has played in the ongoing deterioration of the paintings and sculpture. Hygrometric analyses of salt mixtures as well as wall plasters in Caves 85 and 98 (which have similar deterioration) determined the conditions necessary for the prevention of deterioration of the wall paintings in these caves and similar caves at the site. Research and analysis were carried out to investigate possible sources of moisture, in both liquid and vapor form, through monitoring of the environment in bedrock and long-term monitoring of cave microclimatic conditions (fig. 14.1). Further study was also undertaken on the potential impact of visitation and the influence of the site climate on the microclimate of the caves.

Fig. 14.1 Environmental monitoring station being installed in the antechamber in Cave 85.

Moisture through Bedrock

The Daquan River runs south to north through the site and today is situated approximately 160 m from the cliff face. The riverbed maintains a small stream throughout the year, though in summer months it can be nearly dry. The river floods on rare occasions; the last reported floods that overflowed the channel were in 1979 and in June 2011. However, with flood control measures now implemented, water does not reach the caves and is instead diverted away from the site. Flooding is therefore no longer considered a potential source of liquid moisture in the caves and elsewhere.

A visual inspection of Cave 85 did not indicate any obvious signs of liquid water infiltration other than loss of painted plaster at the floor level (due to historical flooding) to varying heights of up to 1 m. To confirm this, the following possible sources of moisture were considered:

Fig. 14.2 Holes were drilled in areas of repair plaster (left). A plastic casing tube was inserted with silicone filler to seal possible air leakage from the space between the hole and the casing (center). An air temperature and relative humidity sensor was placed in the casing and its lead end was plugged using a rubber plug to seal off the cave air (right).

- Capillary rise of groundwater or water vapor through bedrock;
- Subterranean migration of irrigation water and/or water vapor from the garden in front of the caves;
- Infiltration of rainwater and/or water vapor through fissures in the conglomerate.

To investigate sources of water in bedrock, temperature (T) and relative humidity (RH) sensors (structural humidity sensors) were installed at 10 cm and 30 cm depths into the cave walls and floor (fig. 14.2).[1] Values of temperature and relative humidity were recorded daily or weekly between May 1998 and December 2000 (fig. 14.3).

Temperature and relative humidity sensors registered a saturation reading (100% RH) if free (unbound) water was present. Probes were positioned to monitor two depths in the east and west walls and to assess north-south variations of moisture in the cave floor (fig. 14.4).

Capillary Rise of Groundwater through Bedrock

The water table was found to be 30 m below ground level from a well existing at the site. Given this significant depth, the occurrence of capillary rise of groundwater into the cave was considered unlikely (Maekawa et al. 2010). Monitoring results were used to determine whether ground and rock moisture plays a role in deterioration in the cave.

Wall Moisture

The following discussion focuses on results of sensor readings in the west wall. Values were recorded at 0.8 m (#10), 3 m (#11), and 4 m (#12) from the floor at 10 cm depth; the west side of the sloped ceiling at 10 cm depth (#13); and 30 cm depth at 0.8 m from floor (#20) (fig. 14.5). At 10 cm depth, the temperature and humidity varied from 4–6°C and 20–30% RH in winter to 17–18°C and 40–60% RH in summer. Throughout the year, humidity at locations closer to the cave floor was higher than that at higher locations. However, the temperature was lower at locations closer to the floor: #12 was 5–6 % RH lower and 1.5°C warmer than #10 throughout the year. Therefore, the higher relative humidity values at lower locations were the effect of lower temperatures, and the humidity ratios at different heights were virtually the same. There was no vertical humidity variation on the west wall.

Sensors positioned at 30 cm depth reported higher and more stable humidity (50% RH in spring and 60% RH in summer) than those at a 10 cm depth. However, all variations followed the trend of seasonal changes of the cave air, indicating the cave air's influence on the subsurface environment, depending upon depth. The humidity ratio of the cave air ranged from 1.0 g/kg in February to 7.5 g/kg in August. In the west wall it ranged from 1.5 g/kg (3°C and 28% RH) in February to 7.5 g/kg (18°C and 50% RH) in August; and from 3.5 g/kg (5°C and 55% RH) to 7.5 g/kg (15°C and 60% RH) at 10 cm and 30 cm depths, respectively. These results confirm that the moisture content of the cave air influenced that in the cave rock to at least a depth of 30 cm.

Two possibilities can be considered from the above observations: (1) the bedrock is humidified or conditioned to 7.5 g/kg in summer, and the moisture is partially removed from the rock by the cave air during the dry winter; or (2) a source of moisture exists in the deep bedrock (which could be groundwater), with water vapor being transferred by diffusion from the deep bedrock to the surface and to the outside throughout the year. More moisture removal takes place in winter as the air is significantly drier than the rock. Less moisture is removed from the rock in summer as the site air contains more moisture.

The significantly lower humidity ratio at 10 cm in comparison to that at 30 cm depth in winter indicates the moisture is being transferred from the bedrock to the cave air in winter. The shallower 10 cm depth contains less moisture because of the stronger influence of the normally drier cave air.

Floor Moisture

Seasonal variations of humidity at various locations and depths of the cave floor were recorded throughout the year at 10 cm depth (fig. 14.6). Highest values (68–72% RH) were recorded at the southeast corner (#5) and the lowest (55–62%) at the antechamber (#6) and the west end of the main chamber (#3). The humidity was 65% in winter and 70% in summer, and the humidity ratio was 2.5–3.0 g/kg in winter and 6.5–7.5 g/kg in summer at other locations (#1, #2, and #4). All readings were consistently higher (30% RH higher in winter and 10% higher in summer) than those of the walls at the same depth throughout the year. Seasonal variations were about 5% throughout the floor. The relative humidity was higher (82–87%) at 30 cm depth, with the west end always higher than the east end of the main chamber floor; however, seasonal variations were reduced to less than 5%.

Higher humidity, as well as humidity ratio, found at greater depths in walls and floor indicates the presence of a moisture source at depth in the bedrock. Water vapor diffuses from the deep bedrock conglomerate to the cave walls, then to the cave air. The cave air continuously exchanges with the outside air. Higher humidity in the floor compared to that in the walls suggests that the concrete floor tiles, 5 cm thick, may be acting as a vapor retardant, reducing moisture transfer from the floor to the cave air.

Similar monitoring was undertaken in Cave 98, which is comparable to Cave 85 in its ground-level location, its large size and geometry, and type and distribution of deterioration,[2] in order to investigate the humidity profile along the depth of the west wall and to determine if liquid moisture can be found at depth in the

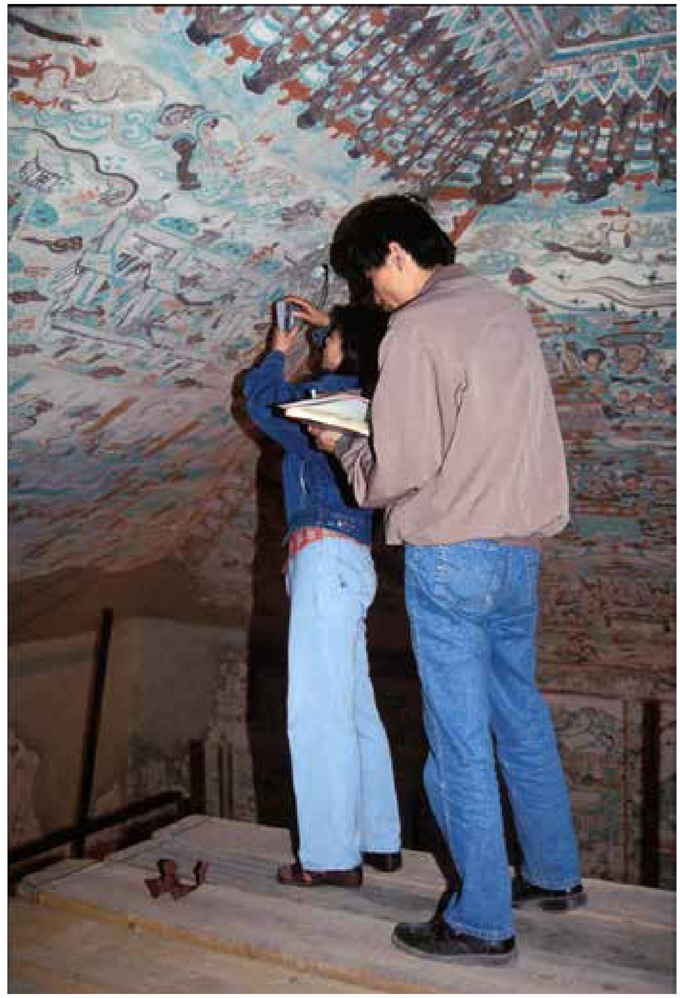

Fig. 14.3 Collecting conglomerate rock humidity and temperature data from the ceiling slope.

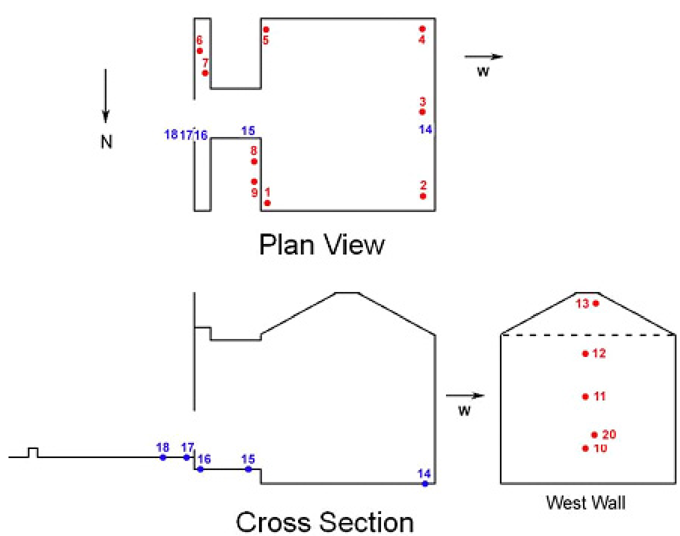

Fig. 14.4 Locations of temperature and relative humidity sensors in walls and floor.

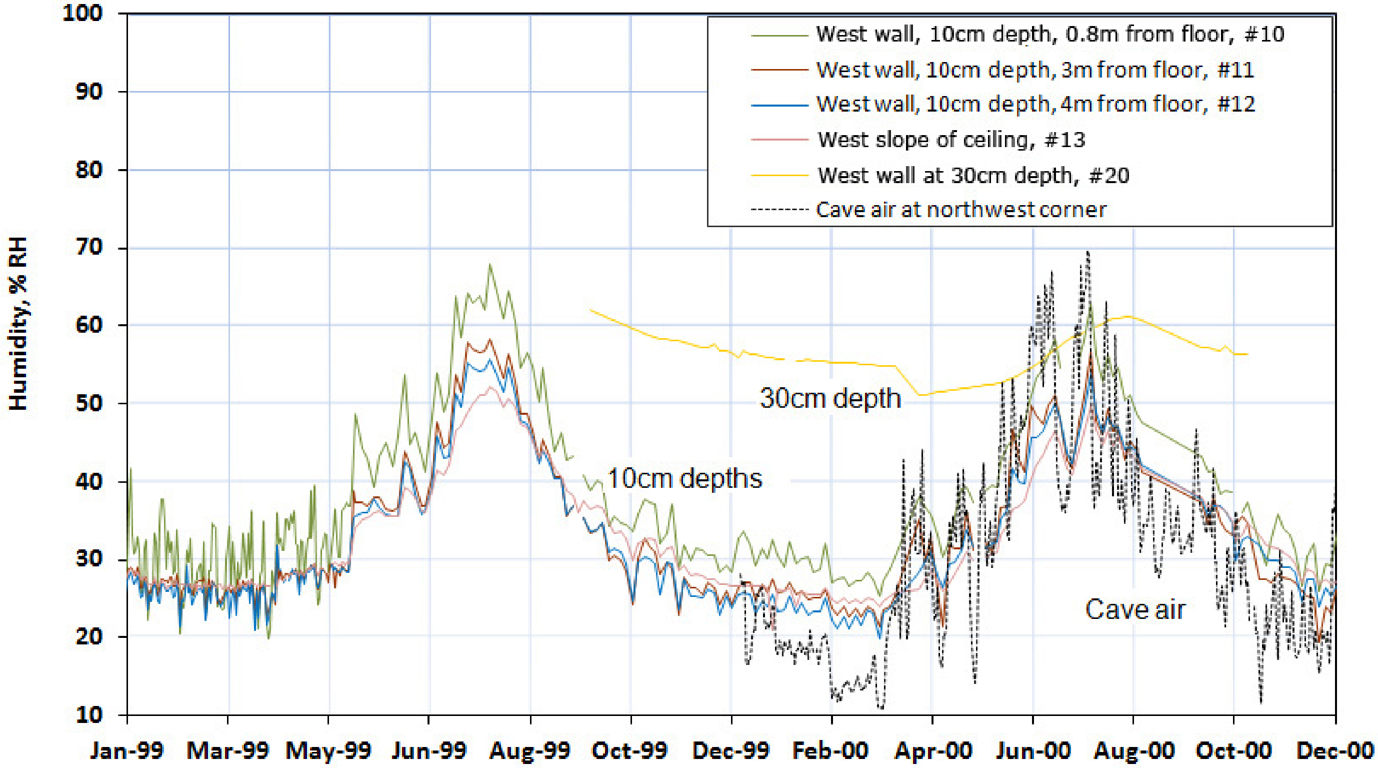

Fig. 14.5 Humidity in the bedrock conglomerate of the west wall.

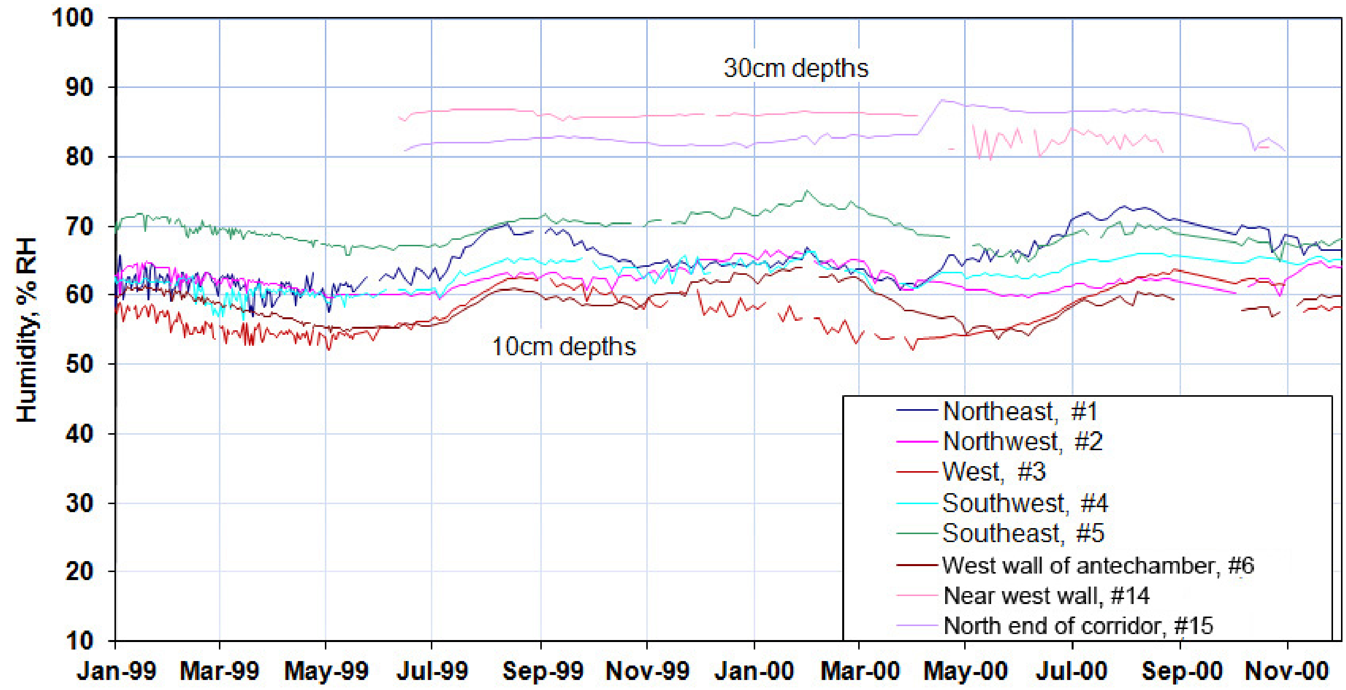

Fig. 14.6 Humidity in the bedrock floor at 10 cm and 30 cm depths.

Fig. 14.7 In Cave 98, similar to Cave 85 in its size, location, and pattern of deterioration, five air temperature and relative humidity sensors, separated and thermally insulated and hygrically sealed from each other, were mounted at 10, 30, 60, 85, and 125 cm positions on a steel rod (left). The rod was inserted into bored 10 cm diameter holes in the walls (center). Sensor readings were recorded weekly (right).

bedrock conglomerate. Cave 98 was chosen because it was possible to drill deeper holes (to a depth of 125 cm) into the bedrock than in Cave 85. Probes measuring T and RH at five different depths (10 cm, 30 cm, 60 cm, 85 cm, and 125 cm) were installed in the west wall (probe locations were 1.5 m above floor level and 0.5 m from the north and south walls) and near the western end of the floor (figs. 14.7, 14.8). Weekly measurements were recorded.

The temperature in the bedrock varied from 5.2 to 14.8°C, 6.1 to 14.2°C, 6.9 to 13.8°C, 8.0 to 13.3°C, and 8.5 to 12.9°C at 10 cm, 30 cm, 60 cm, 85 cm, and 125 cm depths, respectively. These variations were significantly less than those of the surface and the cave air. Based on these temperature profiles we estimated that an annually stable temperature of approximately 9.5°C occurs at 3 m depth of the bedrock. Seasonal variations of the humidity of the cave's microenvironment affected the rock humidity up to about 60 cm depth (fig. 14.9). At 125 cm depth 100% RH occurred (although no liquid water was found) throughout the monitored period. The humidity ratio was 8.7 g/kg, which is 1.2 g/kg higher than that of the cave air in summer. RH was above 75% at depths greater than 60 cm and lower than 65% at depths less than 30 cm throughout the monitored period. These results showed a moisture content gradient that decreased toward the surface of the cave walls. This indicated that water vapor is transported by diffusion from deep within the porous conglomerate bedrock to the cave surface, then to the cave air. Soluble salts, principally sodium chloride, are in solution at about 60 cm depth in the bedrock where the RH is 70%. The water vapor gradient transports soluble salts and enriches their concentration at the wall (see chap. 16).

Subterranean Migration of Irrigation Water from Garden in Front of Caves

Flood irrigation has been used at the site to water poplar trees in front of the eastern face of the cliff that shade the walkways (fig. 14.10). The irrigation trench is located approximately 15 m from Cave 85. The area in front of the grottoes was irrigated for 130–150 days per year, mainly in summer. During the initial investigation wet sand was found under the concrete walkway tiles between the garden and the entrance to the cave. In order to investigate the extent of moisture seepage from irrigation, five clusters of temperature and RH probes were installed in the floor in a line running from the west wall of the main chamber to outside the cave entrance (see fig. 14.4, sensor locations #14, #15, #16, #17, and #18).[3]

Sensor readings of 100% RH with a humidity ratio larger than 17 g/kg between the outside of the cave and just inside the cave entrance (sensors #16, #17, and #18) verified the wet condition of the sand during the summer irrigation period, as well as the non-irrigation period in winter (fig. 14.11). However, liquid water only extended to just inside the cave entrance. The moisture dissipated before reaching the entrance of the corridor (#15) as well as at the west wall (#14) at the 30 cm depth, which maintained 82–87% RH. Therefore, it is unlikely that the wall paintings even in the antechamber and corridor have been affected by moisture from irrigation. Furthermore, relative humidity levels in the cave floor remained the same after the flood irrigation practice was replaced with a drip irrigation system in 2000, indicating that irrigation of the garden does not affect the wall paintings in the caves. Wet sand was no longer

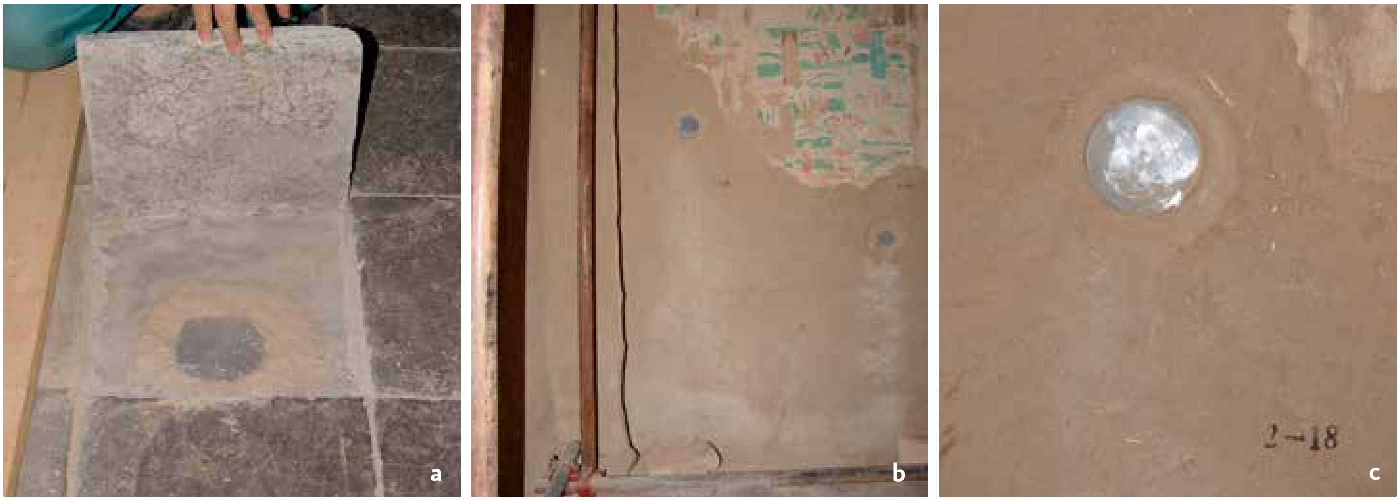

Fig. 14.8 Subfloor (a) and subsurface monitoring holes (shown plugged) for rock moisture monitoring in Cave 98 (b, c). Holes were drilled through modern repair plaster where paint had been lost.

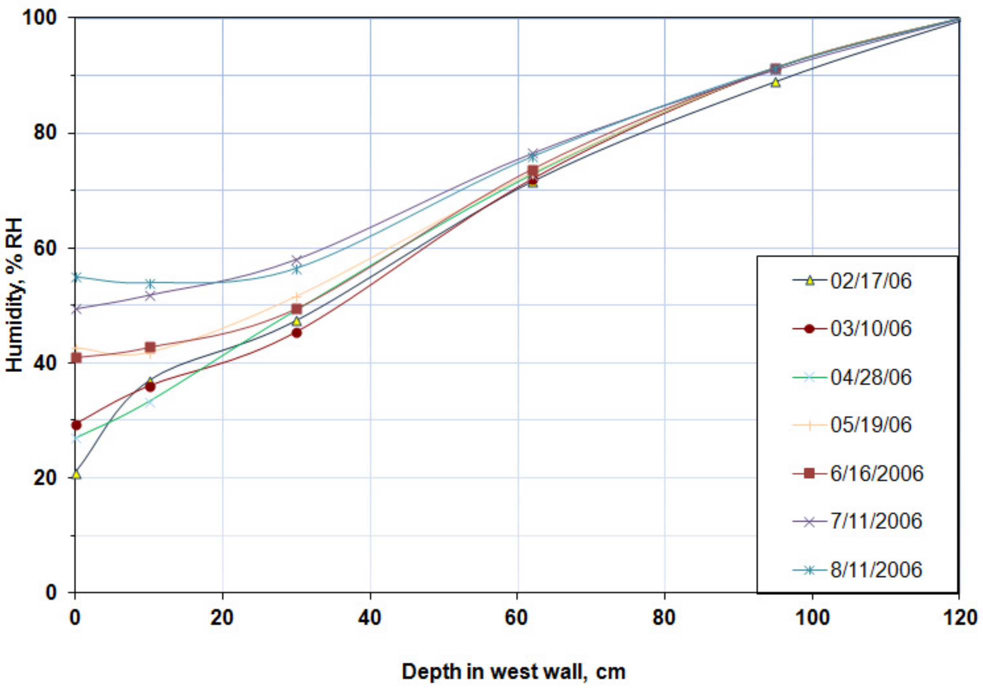

Fig. 14.9 Humidity profiles in the bedrock of the west wall of Cave 98.

Fig. 14.10 Flood irrigation was previously used to water trees along the walkway in front of the caves.

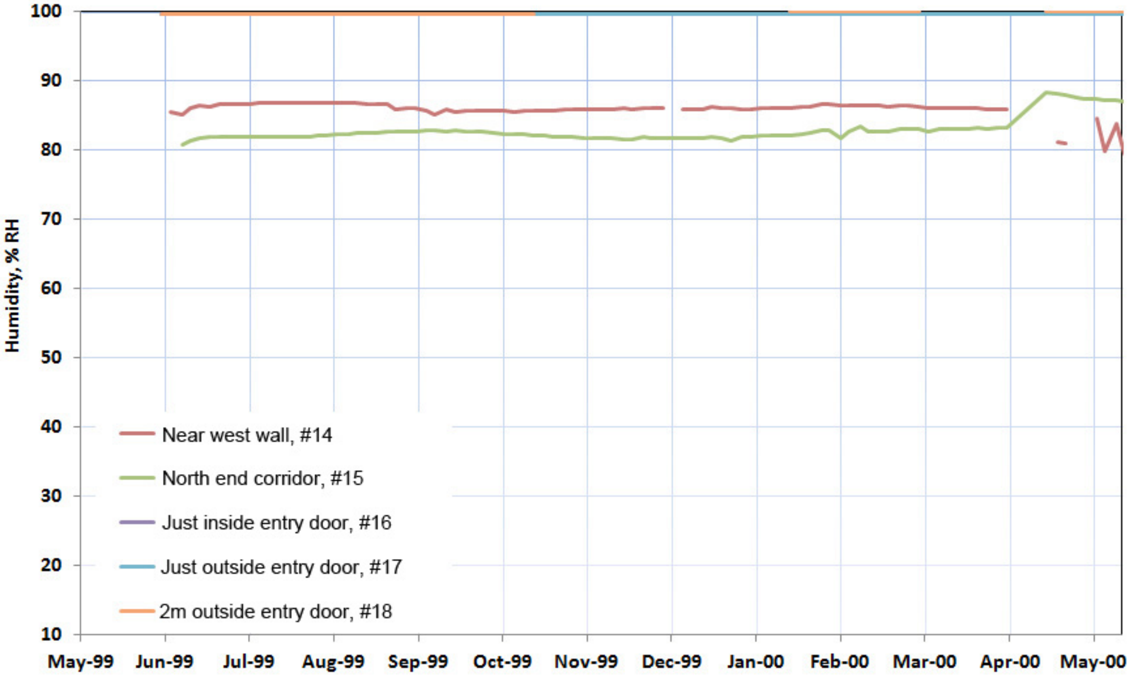

Fig. 14.11 Humidity at various locations in the cave floor between the outside of the entrance and near the west wall.

MONITORING PERIOD	OBJECTIVES
DECEMBER 1992–APRIL 1998 (DUNHUANG ACADEMY)	Characterization of microclimate when cave was open to self-guided visitation (entrance doors were open during operational hours).
MAY 1998–APRIL 2001 APRIL 2001–APRIL 2005 (GCI/DUNHUANG ACADEMY)	More detailed characterization of microclimate focusing on the west wall deterioration when cave was closed to visitation but periodic conservation work was carried out. Detailed characterization of microclimate to understand the east to west gradation of worsening deterioration of the wall paintings when cave was closed to visitation but periodic conservation work was carried out.
JUNE 2005–DECEMBER 2009 (GCI/DUNHUANG ACADEMY)	Characterization of microclimate when cave has been closed to general visitation (entrance doors have been closed at all times).

Table 14.1 Periods of Environmental Data Collection

observed under the paved walkway after the change in irrigation method.

Infiltration of Rainwater through Fissures in the Conglomerate

Cave 85, a ground-level cave, is situated 25 m below the top of the cliff. Given this distance, the rate of rainwater seepage through the conglomerate[4] is estimated at 3 m per day (Tanimoto et al. 2005). However, the generally low rainfall at the Mogao Grottoes makes rainwater infiltration through rock fissures an unlikely source of liquid moisture.[5] In addition, the values of RH measured in the walls do not vary drastically with rain events. Therefore, infiltration of rainwater through fissures in the conglomerate is not likely to any significant extent in Cave 85.

Infiltration of Humid Outside Air and Other Moisture Sources

Environmental monitoring was carried out to determine whether humid air was a source of moisture within the cave and to measure how well the cave functioned as a hygrical and thermal buffer from the site climate. Implications of the environmental conditions for the preservation of the cave are important given the role of soluble salt activity in the deterioration of the wall paintings.

A temperature and humidity sensor was first placed in Cave 85 and also in surrounding caves in December 1993 to characterize the environment. Environmental monitoring was expanded with multiple sensors in Cave 85 in May 1998 and continued. Environmental monitoring was divided over time into three periods with different objectives (see table 14.1).

In the following section, discussions are provided on

- General microclimate;
- Microclimate during specific monitoring periods;
- Condensation;
- Natural ventilation;
- Efficacy of the second (internal) door; and
- Impact of visitation.

General Microclimate of Cave 85

Monthly means of the air temperature at the center of Cave 85 were measured during the entire monitored period (fig. 14.12). Annually highest monthly mean temperatures were recorded in August, with the lowest reported in January. Monthly mean temperatures ranged from 5°C in January to 18°C in August. Larger temperature variations were recorded more often in winter than in summer, similar to the site climate (see chap. 7).

Annually highest monthly mean humidity values were recorded in July, with the lowest occurring in February, which is the opposite of the annual trend of the site climate (fig. 14.13). Monthly mean humidity values ranged from 21% in February to 49% RH in July. Larger variations were recorded more often in summer months than in winter, also the opposite of the site climate trend. Major rain events, such as in July 1993 and July 1996, affected monthly means and resulted in 61% and 57% RH, respectively.

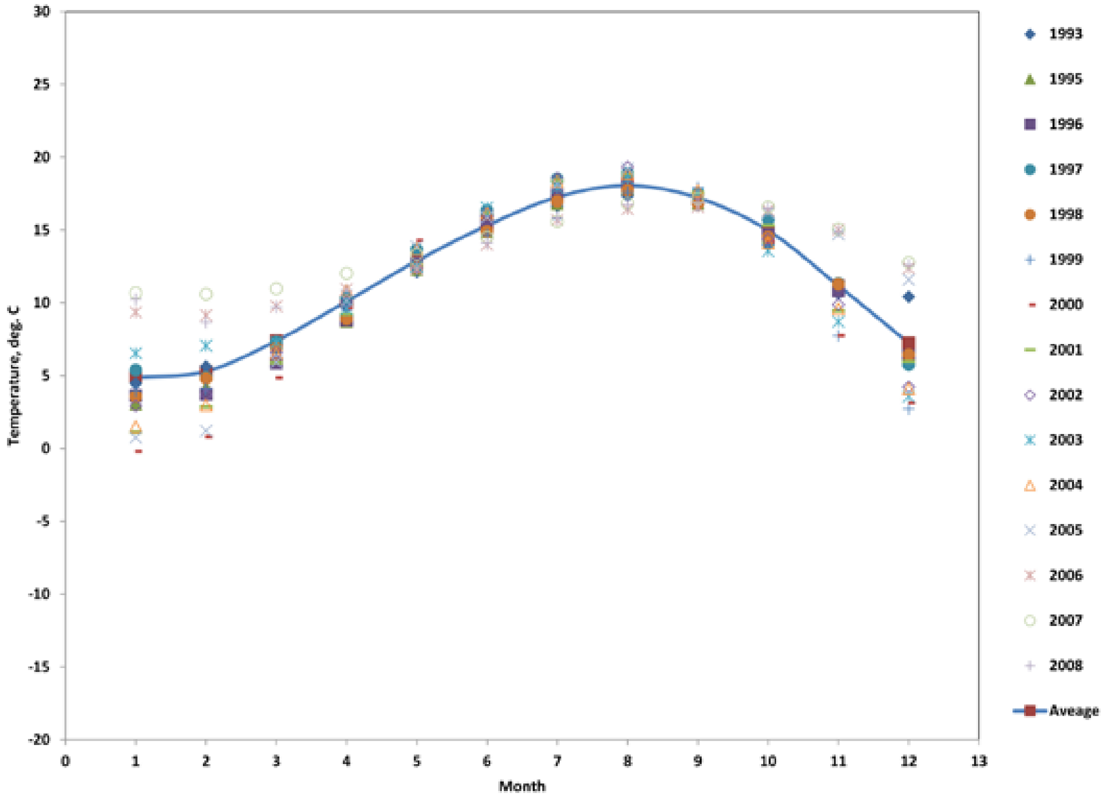

Fig. 14.12 Monthly averages of air temperature between 1993 and 2008.

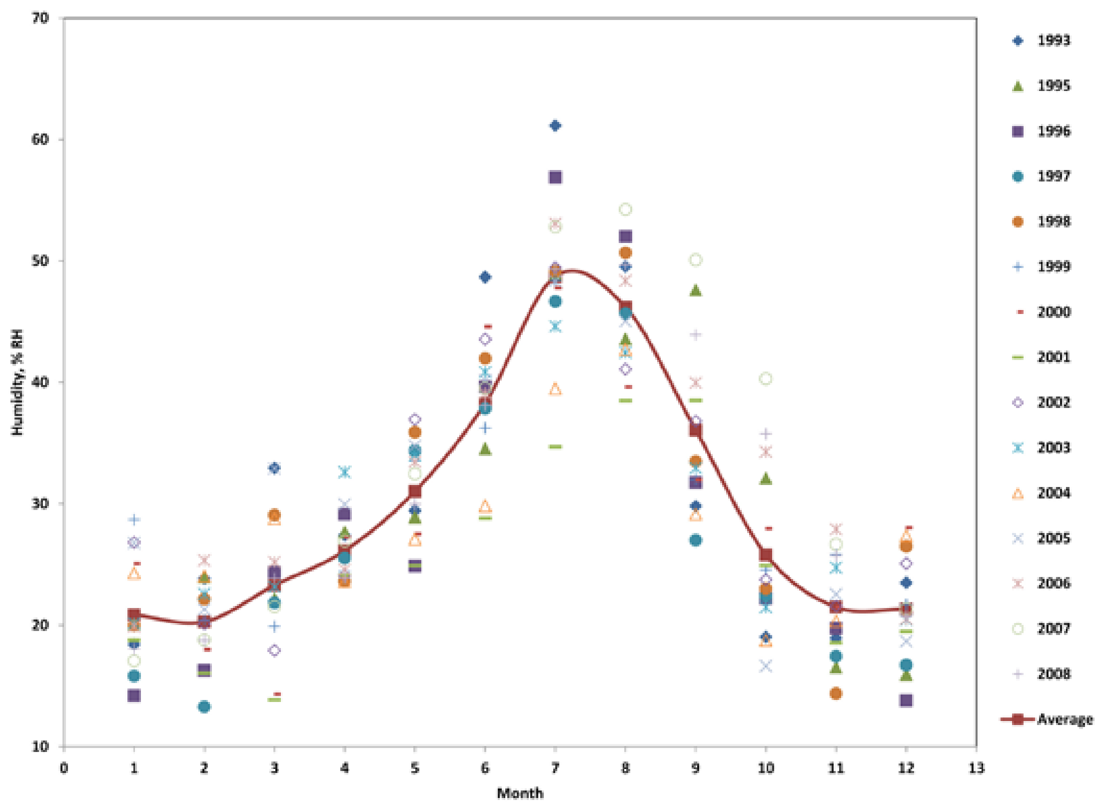

Fig. 14.13 Monthly averages of relative humidity between 1993 and 2008.

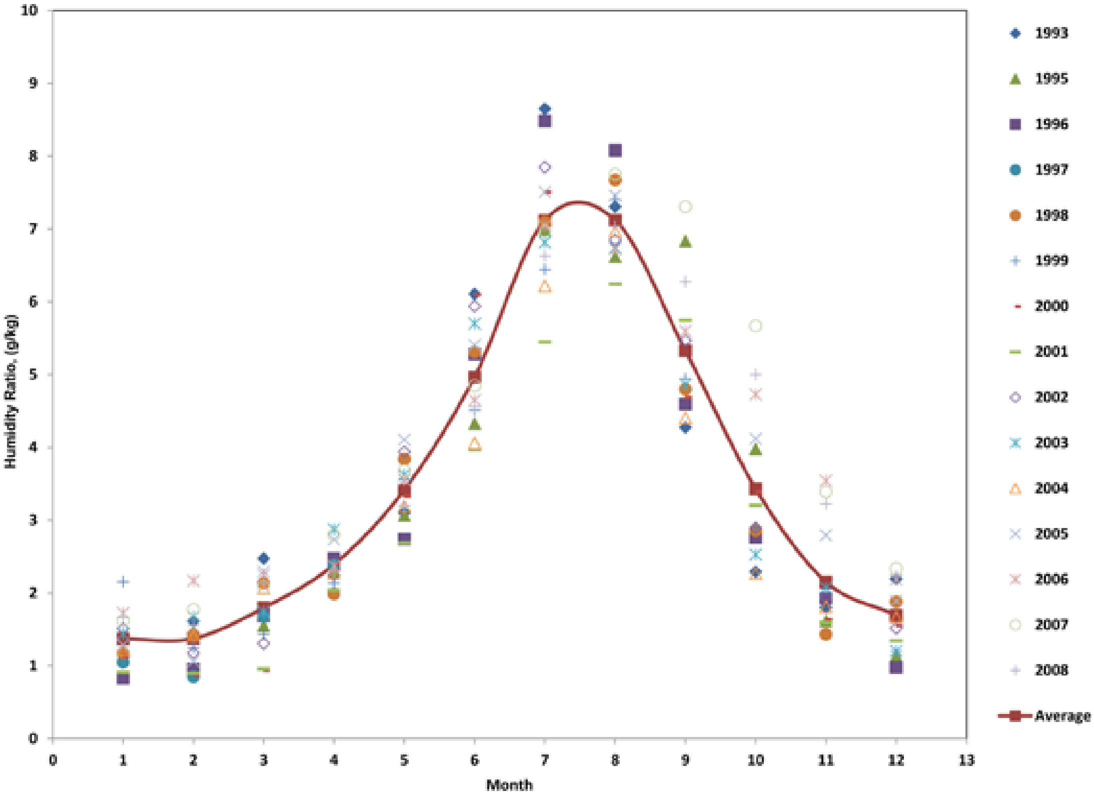

Fig. 14.14 Monthly averages of humidity ratio between 1993 and 2008.

As described in chapter 7, the amount of moisture contained in the air can be expressed as the humidity ratio. This parameter provides a useful means of comparing moisture content of the air inside and outside the caves, as large temperature differences exist between the two environments. Unlike the dissimilarity between annual variations of humidity at the site (see fig. 7.4) and in Cave 85 (fig. 14.13), both the values and the annual trends of humidity ratios between the environments (see fig. 7.5, fig. 14.14) are similar. An annual low of approximately 1.4 g/kg in January and February and a high of 7.1 g/kg in July and August were observed. Variations were small in winter months; however, they were significantly large in summer months due to occasional humid and rainy days for particular years, again similar to the humidity ratio of the site. Major rainfall events in July 1993 and 1995 resulted in monthly means of 8.7 and 8.1 g/kg, respectively.

Microclimate of Cave 85 during Specific Monitoring Periods

Microclimate When Cave Was Open to Self-Guided Visitation (December 1992–April 1998)

During this period Cave 85 was open to visitors through a system of self-guided tours. Entrance doors were open throughout the day. Temperature and humidity data indicate significant periods of high humidity corresponding to rain events and producing a humidity ratio greater than 12–13 g/kg in the cave (fig. 14.15) (see Appendix 14.A).

Comparison of the outside humidity ratio to that in the cave during the 1992–98 period shows that for the most part the cave interior retains moisture (as shown in the large number of data points observed above the line in fig. 14.16). Humid air above 10 g/kg in summer can deliquesce the salt mixture in Cave 85 (see chap. 16). Highly humid outside air (humidity ratio larger than 10 g/kg) infiltrated the cave and produced high humidity conditions during this period. One such event took place between July 15 and August 2, 1996, resulting in the collapse of an area of wall painting from the ceiling.

Microclimate When Cave Was Closed to Visitation but While Conservation Work Was Ongoing (May 1998–April 2005)

The DA-GCI collaborative project in Cave 85 began in May 1998. An environmental monitoring station was installed in the cave to conduct a detailed study of the cave environment (see fig. 14.1). During the period of monitoring, temperature and humidity were measured at three locations in the cave:

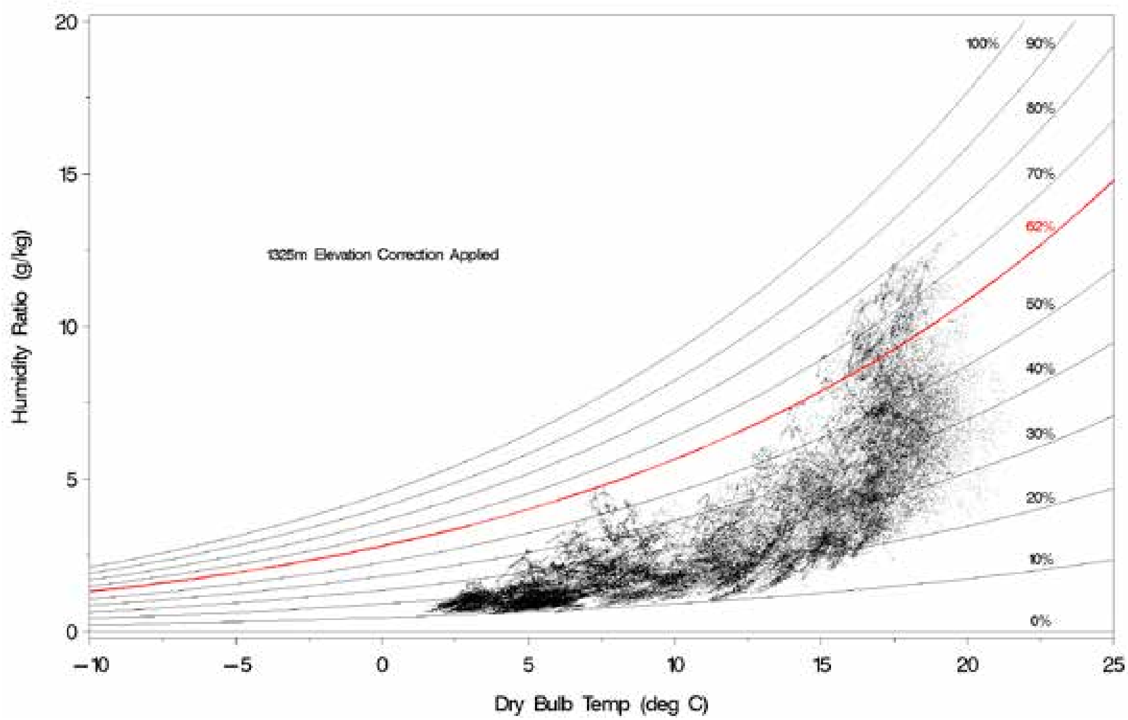

Fig. 14.15 Temperature and humidity data during the period of self-guided tours (December 1992–April 1998) plotted on a psychrometric chart. Each dot corresponds to a set of air temperature and relative humidity data recorded every 15 minutes. The red line indicates 62% RH, above which uptake by salts of humidity from the air begins. A significant number of points above the red line indicate periods of high humidity inside the cave due to the entrance door being kept open.

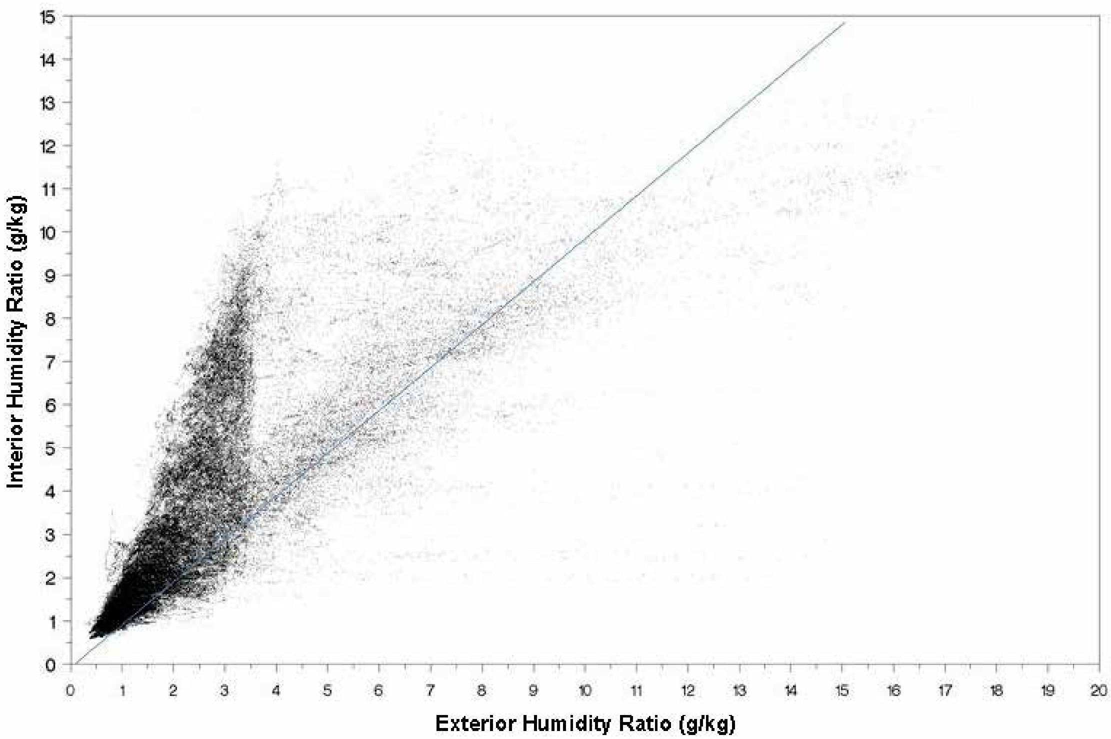

Fig. 14.16 Comparison of humidity ratios inside Cave 85 and outside. The blue line corresponds to the outside and inside values being the same. Data points above the line indicate moisture retention by the cave (i.e., the outside air is significantly drier).

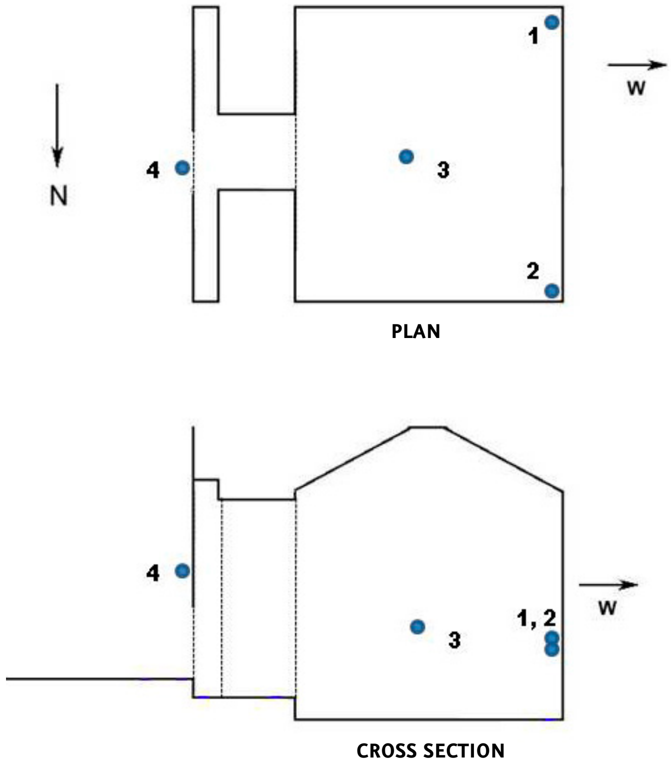

Fig. 14.17 Sensor locations during the monitoring period May 1998–April 2001.

the center of the cave; the northwest and southwest corners of the main chamber at approximately 1 m from the floor; and outside the cave entrance, where a probe was placed. Surface temperature (ST) probes were placed midway up the walls in the northwest and southwest corners (fig. 14.17).

In May 1998 Cave 85 was closed to visitors and the entrance doors generally kept shut. Although the cave doors have louver vents, they provide protection against infiltration of humid air when they are closed. The temperature and humidity at the center of the cave during this period are plotted on a psychrometric chart (fig. 14.18). After the installation of scaffolding and start of conservation work in the cave, the entrance doors were probably often left open in winter, following Dunhuang Academy policy to "air" the cave. This resulted in greater infiltration of cold outside air and lower temperatures than during the 1992–98 period and also resulted in similar temperature variations as before but with both the minimum and maximum reduced 3–4°C. Diurnal temperature variations ranged only from less than 0.8°C in winter to 1.5°C in summer. The relative humidity ranged from less than 8% in January and February to 40–70% in June, July, and August. Humidity values less than 10% RH together with lower temperatures than the previous period were probably due to open door conditions during winter months as shown by the temperature. Again, rain events in summer months caused the humidity to rise from 40% RH to 70% RH in the cave depending on the length and intensity of rain. The maximum monthly humidity ratio averaged 1.4 g/kg in February and 6.8 g/kg in July, peaking to as high as 10 g/kg during summer rain events, though with the values normally returning to typical summer values within 24 hours. These showed a significant reduction from the previously monitored period.

A focus of monitoring was to understand the conditions of the west wall where deterioration was the greatest. Though fewer high humidity events were reported during this period than the previous one, there were still occasions when the outside humidity was found to influence the interior microclimate, which reached 62% RH and higher. This is explained by the door being left open when conservation work was under way. However, the number of events with above 62% RH conditions was significantly reduced from the 1992–98 period, and conditions above 75% RH were not recorded at all.

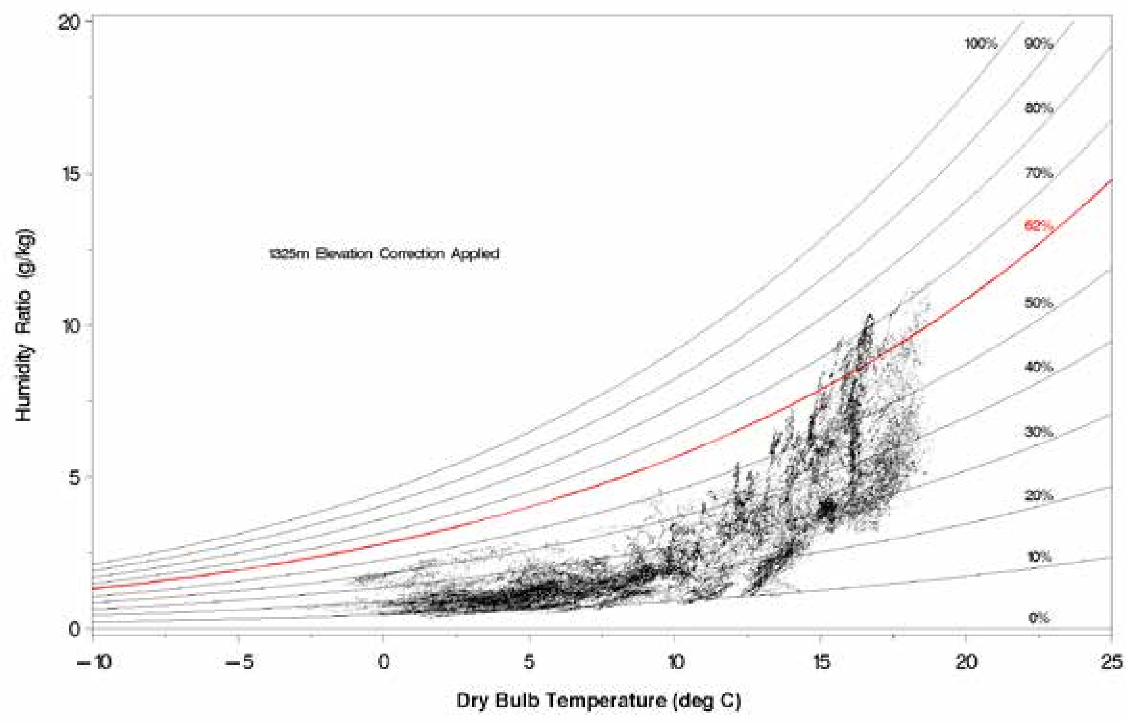

Fig. 14.18 Temperature and humidity data at the center of the cave plotted on a psychrometric chart (May 1998–April 2005). Compared to fig. 14.15 (December 1992–April 1998) the number of data points above 62% is reduced as the cave was closed to visitation and the door generally kept closed. Conditions above 75% were not recorded at all.

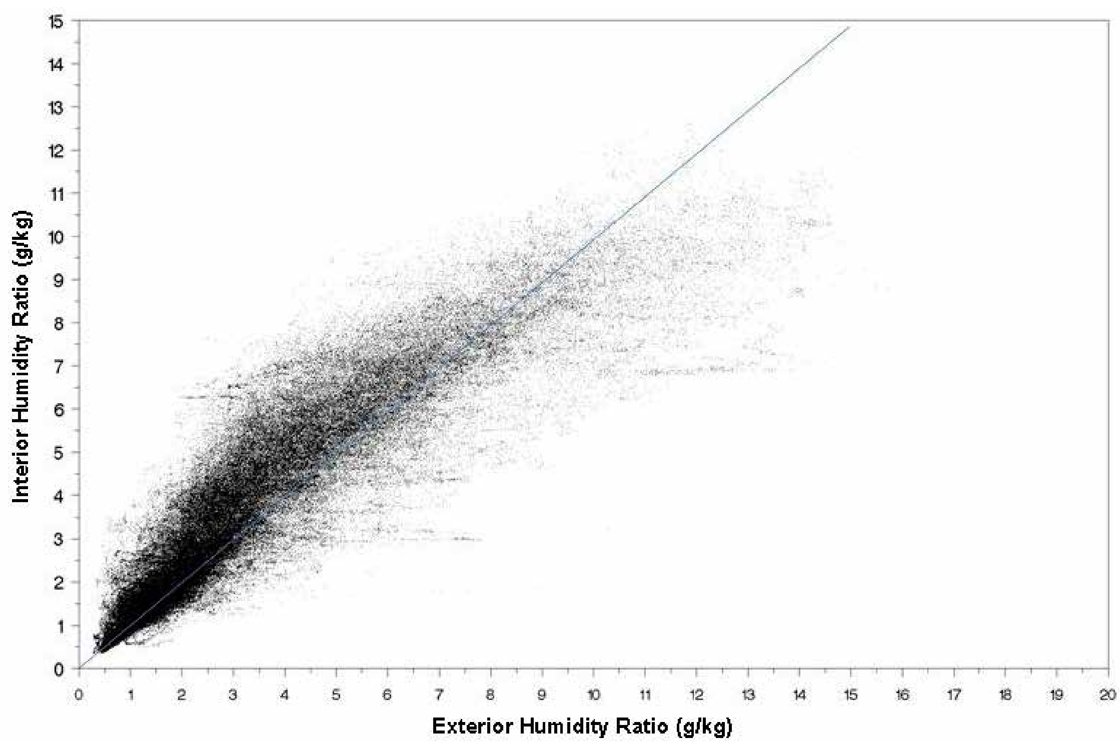

Fig. 14.19 Comparison of humidity ratios inside Cave 85 and outside during the 1998–2005 period.

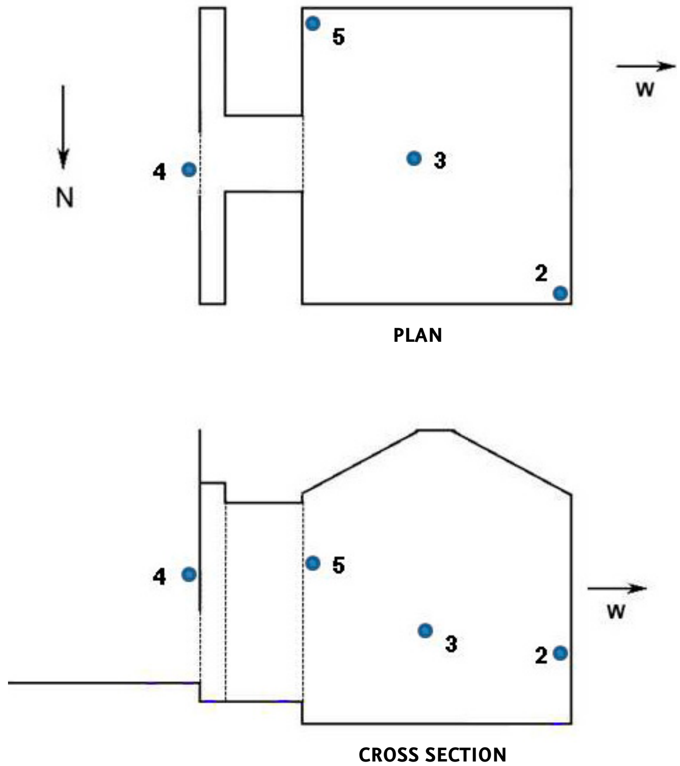

Fig. 14.20 Sensor arrangements for the monitoring period from April 2001 to December 2009.

Comparisons of the outside humidity ratio to that in the cave during the 1998–2005 period show that the majority of values above 10 g/kg are below the blue line, indicating that the conservation work did not have much impact on the cave environment and that the moisture content of the cave air was similar to that of the outside air for the most nonrainy days (fig. 14.19). The entrance doors were probably left open when conservators were working in the cave. However, the doors were mostly closed during rain and infiltration of humid air was limited.

Investigation into the East-West Gradation of Worsening Deterioration (April 2001–April 2005)

In late April 2001 sensors were rearranged to further investigate possible climatic zones within the cave in an attempt to explain the general patterns of deterioration in the main chamber, with a southeast to northwest gradation of worsening deterioration, and to better understand the influence of the site climate on the cave interior. Sensors were repositioned to the southeast and northwest corners measuring temperature, humidity, and surface temperature, and additional sensors were placed near the door to measure the external environment (fig. 14.20).

During the 2002–4 period, the average temperature of the southeast corner was 0.6–0.9°C cooler than the northwest corner due to cooler winter site temperatures, and the standard deviation of the temperature at the southeast corner was up to 1.5°C higher, indicating slightly higher temperature variations than the northwest corner due to proximity to the entrance (see table 14.2). For humidity, both the southeast and northwest corners had similar annual averages, minimums, and standard deviations. However, slightly higher maximum values were recorded at the northwest corner.

Results show that the west side is warmer in winter and cooler in summer than the east side of the cave. This translates to lower relative humidity in winter and higher relative humidity in summer, respectively. The east side is more affected by the outside climate variations as it comes closer to the entrance. However, the difference between the two zones is likely too small to explain variations in deterioration between the west and east sides in the closed door condition.

YEAR	AVERAGE		STANDARD DEVIATION		MAXIMUM		MINIMUM	
	TEMPERATURE °C	RH%	TEMPERATURE °C	RH%	TEMPERATURE °C	RH%	TEMPERATURE °C	RH%
2002	12.3/11.7	31/31	4.4/5.9	14/12	19.3/20.3	69/69	3.8/0.7	9/9
2003	12.7/12.0	29/29	3.9/5.1	11/10	22.3/21.7	65/62	5.7/1.7	9/9
2004	12.4/11.5	25/26	5.6/6.2	10/10	22.7/21.4	64/67	1.0/-3.9	8/6

Table 14.2 Comparison of Air Temperature and Relative Humidity at the Northwest and Southeast Corners of the Main Chamber (2002–2004)

Note:
Data are presented as northwest corner/southeast corner, respectively.

Microclimate of Closed Cave with No Conservation Work (April 2005–December 2009)

With conservation work in the cave completed, the cave remained closed to general visitors. This third period of monitoring aimed to further investigate the undisturbed closed cave environment. Only special guests and visitors were allowed to enter the cave during this period. Winter temperatures were higher than 7.5°C, and summer temperatures did not exceed 18.5°C (fig. 14.21). Annual temperature variations were significantly reduced, while the minimum humidity in winter increased to 15% RH. Although the maximum was 74% RH, data above 20% RH were sparse and only two isolated events were recorded in which the entry doors were left open during rainy days. The majority of conditions remained at less than 62% RH. Other entries on less humid summer days caused the cloud of data above 18°C between the 30% and 62% RH lines.

During the 1998–2005 period the moisture content of the cave air did not always follow that of the outside air, although it varied between 1.2 and 8.0 (values above 8.0 are due to visitation) throughout the year (fig. 14.22). The data from this period show that closed entry doors for most of the time segregated the environment of the cave from that of the humid exterior.

Climate comparison of the northwest and southeast corners of the cave shows, as expected, that the exterior climate had a greater effect on areas closer to the cave entrance, such as the antechamber, corridor, and east wall of the main chamber, as found during the previous period (2001–5) (fig. 14.23). The west wall was least affected by the outside climate and therefore was coldest in summer and warmest during winter. This difference may be attributed to the air circulation pattern as well as the different thermal inertia between the east wall and the west wall. Therefore, relative humidity in the eastern part of the cave is likely to remain lower, even after rain events. In addition, smaller caves on either side of Cave 85 may play a role in lowering the thermal inertia.

In late summer the maximum temperature difference between the center of the cave and the west wall was approximately 1°C, corresponding to 4% higher relative humidity values. However, the temperature difference between the south and north walls was lower, typically less than 0.5°C, translating into less than a 2% RH difference. These temperature and relative humidity variations among cave walls of the main chamber are likely too small to have caused the gradation of deterioration between the southeast and northwest areas.

Statistical summaries of air temperature and relative humidity at the northwest and southeast corners of the cave during the 2006–8 period show the annual average as well as minimum temperatures rose a few degrees and standard deviations and maxima reduced by a few degrees from the previous, 2002–4, period (see table 14.3). Relative humidity had similar changes, except for annual maxima, which had higher values than the previous period. During this period, the southeast corner had higher annual average, minimum, and maximum temperatures than the northwest corner. And standard deviations were larger at the northwest corner than the southwest corner. For the relative humidity, both the southeast and northwest corners had virtually identical statistical values during the period, with the exception of the annual maximum.

Because the cave was closed it maintained a more constant climate than during the previous period when conservation work was being carried out. This meant cooler and drier conditions

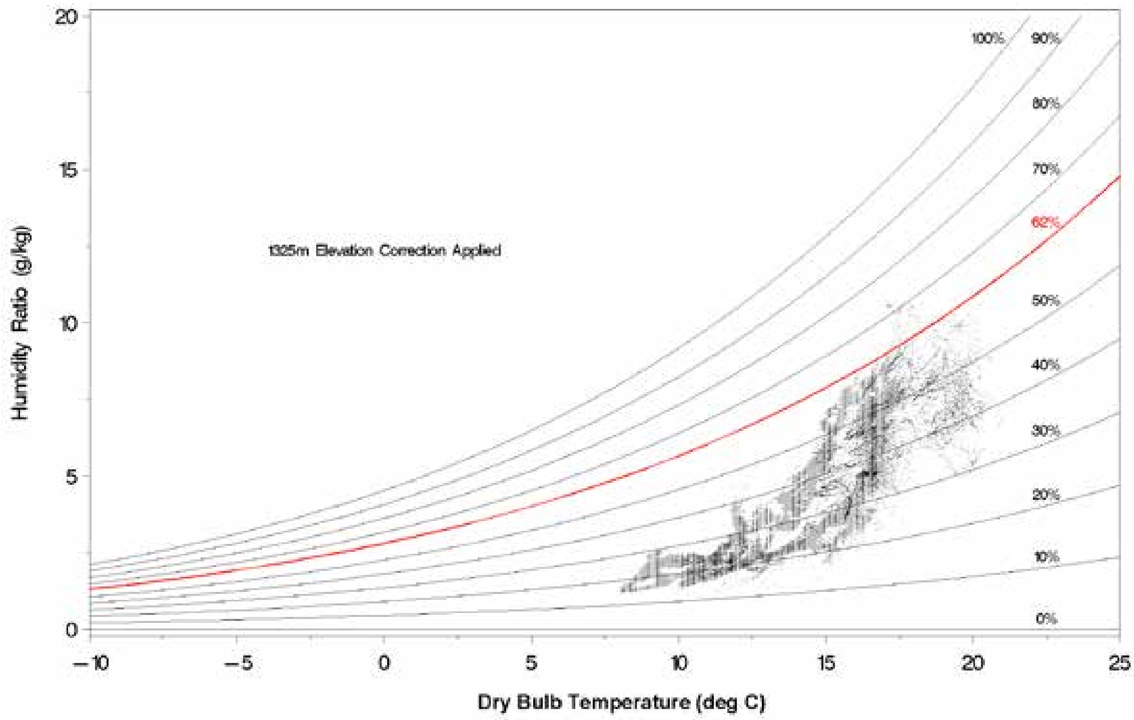

Fig. 14.21 Temperature and humidity during 2005–9 plotted on a psychrometric chart. Compared with figs. 14.15 and 14.18 there are very few data points above 62% RH as the cave door was kept closed.

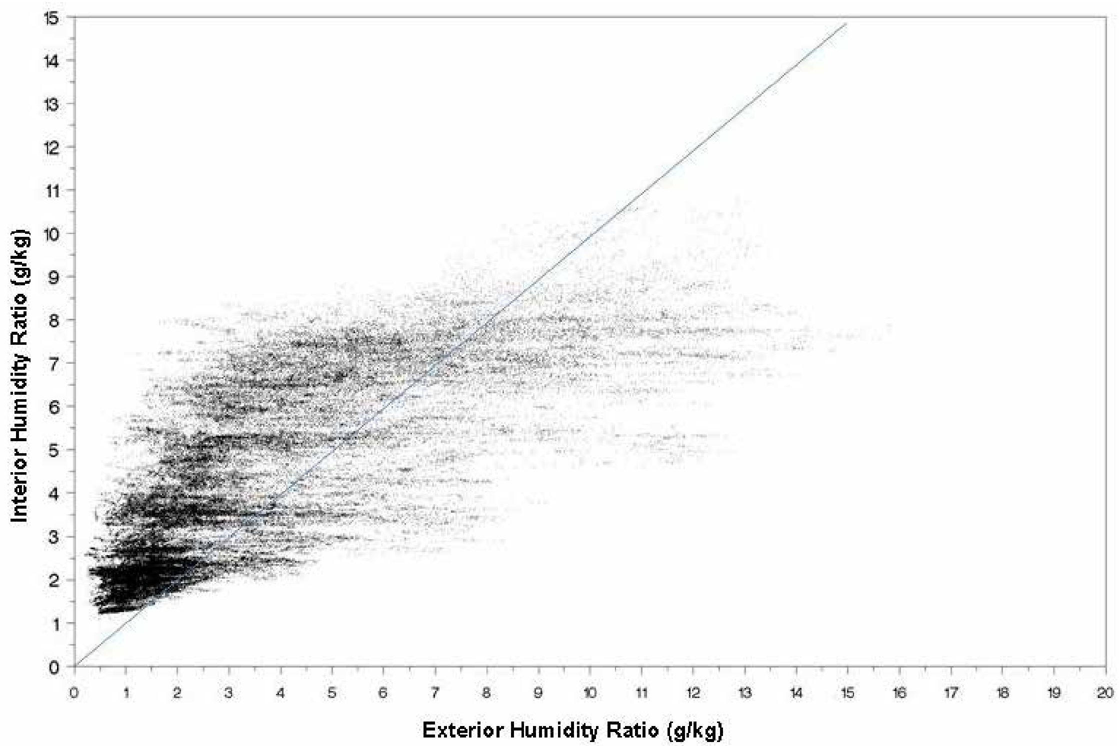

Fig. 14.22 Comparison of humidity ratios between inside the cave and outside. The dense data cloud, which was found along the equivalent line during the 1998–2004 period, has diffused to both right and left of the blue line, indicating that the moisture content of the cave air did not always follow that of the outside air, although it varied between 1.2 and 8.0 g/kg (values above 8.0 are due to visitations) throughout the year. Values above 9 g/kg are all below the equivalent line, confirming that closed entry doors isolated quite effectively the cave environment from that of the humid outside.

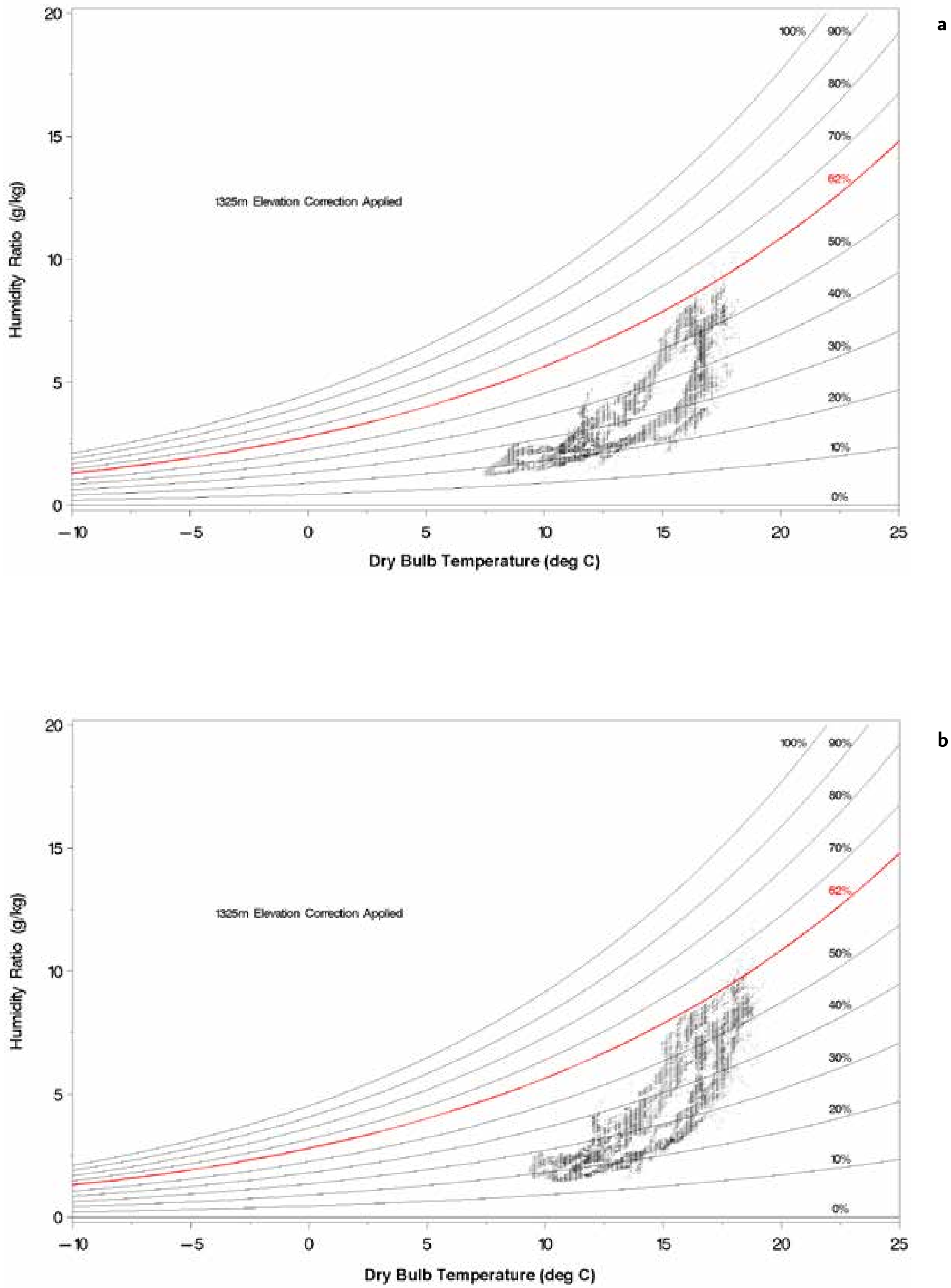

Fig. 14.23 Comparison of temperature and humidity data collected at the northwest (a) and southeast (b) corners of the main chamber (2005–9).

YEAR	AVERAGE		STANDARD DEVIATION		MAXIMUM		MINIMUM	
	TEMPERATURE °C	RH%	TEMPERATURE °C	RH%	TEMPERATURE °C	RH%	TEMPERATURE °C	RH%
2006	13.1/13.5	33/33	3.1/2.6	10/11	18.3/19.0	61/65	7.5/9.3	17/15
2007	13.7/14.7	34/35	2.6/2.5	13/14	18.4/19.8	70/74	9.3/10.8	15/15
2008	13.0/14.3	32/32	3.0/2.5	12/12	18.0/19.2	68/74	7.4/10.0	11/14

Table 14.3 Comparison of Air Temperature and Relative Humidity at the Northwest and Southeast Corners of the Main Chamber (2006–2008)

Note:
Data are presented as northwest corner/southeast corner, respectively.

in summer and warmer and more humid conditions in winter. Higher maximum relative humidity values than the previous period were a combined result of isolated visitation on humid days and cooler cave temperature in summer. During 2006–8, for an unknown reason, the southeast of the cave was warmer and more stable than the northwest during the winter. However, the cave climate is within a stable and uniform range; consequently the climate variation within the cave was small and not a contributing factor to the observed variations in deterioration of the wall paintings.

Condensation

Consideration was given to possible condensation on wall surfaces, especially in late spring and early summer when the walls are significantly cooler than the outside air and warm and humid outside air enters the cave. Water vapor condenses on a cold surface if the dew point temperature of the air is higher than the surface temperature. However, this was shown not to be the case.

Since physical detection of surface condensation is difficult in caves, an equivalent relative humidity of the cave air at wall surfaces was calculated. Relative humidity is a condition of air, so a solid surface cannot have relative humidity. However, surface humidity conditions can be expressed using the water activity number, which is an equivalent relative humidity. First, values of the humidity ratio (moisture content of the air) were calculated from sets of air temperature and relative humidity. The equivalent relative humidity was then calculated from the humidity ratio and the wall surface temperature. If the equivalent relative humidity value were to exceed 90% the inception of condensation in micro-pores of the walls may be assumed, as condensation in small pores occurs before 100% RH is reached. Maxima of equivalent relative humidity values calculated at various wall surfaces between 1998 and 2008 occurred during rain events in summer months, June, July, and August, or in September, and durations were short, especially in 2006 and later (see table 14.4). The entrance doors have been closed since conservation work was completed in the cave in 2005, resulting in 2–4°C cooler wall temperatures in summer than those of previous years when infiltration of outside summer air warmed wall surfaces. Cooler walls caused equivalent relative humidity values to reach 80% during sporadic visitations on highly humid days. These are documented in high equivalent relative humidities evaluated at various surfaces in 2007 and 2008. However, the highest value was 80% RH and thus too low for condensation on the wall surfaces.

Natural Ventilation

The above results led to awareness that an important factor is the rate of exterior air infiltration into the cave. During the summer, the outside warm air enters the cave and is cooled by cave air and walls. Cooled air is heavier, and a downward circulation develops in the main chamber and the air flows from the main chamber in the lower half of the corridor to the entrance and the outside. This induces outside air to flow into the cave through the top half of the entrance and corridor, and a continuous air exchange develops between the cave and the outside.

Infiltration rates are most influenced by the doors, as one would expect. Cave air can freely exchange with the outside when the doors are wide open; with the doors closed, however, ventilation is restricted to the fabric-filtered louvers of the doors and gaps in the bulkhead. This results in an order of magnitude smaller rate

YEAR	WEST WALL (SOUTHWEST CORNER)	WEST WALL (NORTHWEST CORNER)	WEST WALL (NEAR TOP)	BASE OF CENTRAL STATUE	EAST WALL (NORTH OF DOORWAY)	EAST WALL (SOUTH OF DOORWAY)	SOUTH WALL	NORTH WALL
1998	73	75		71			70	77
1999	74	76		70			61	70
2000	76	78		77				
2001		68	69	68	64	69	67	70
2002		63	73	73	70	72	72	75
2003		64	63	63	60	63	63	65
2004		70	63	64	60	64	63	65
2005			70	71	67	70	73	72
2006		68	65	67	63	65	61	67
2007		78	77	79	72		78	79
2008		78	77	80	70		79	80

Table 14.4 Annual Maximum of Equivalent Humidity (%RH) at Various Wall Surfaces (1998–2008)

than with open doors. Among major factors affecting the rate of natural ventilation, such as architectural configuration of the cave and wind conditions, is the temperature difference between the cave walls and the outside air. In summer, walls remain at less than 18°C, while the outside temperature can elevate to mid-30s°C. This large temperature difference drives a high rate of natural ventilation. However, the outside temperature can drop to below 20°C during periods of overcast sky, humid air, and rainfall. Due to the small difference between the cave air and the outside air in this condition, the natural ventilation rate is reduced to between a half and a quarter of that of a hot day.

To measure the air change rate, a tracer gas, sulfur hexafluoride (SF_6) or carbon dioxide (CO_2), is released into the cave, and the rate of dilution, as a result of natural ventilation, is measured using a trace gas analyzer (fig. 14.24). The concentration of the tracer gas is recorded as a function of elapsed time from the start of the measurement. The rate of the concentration decay is converted into air change rate (see Appendix 14.B). Four large ground-level caves (Caves 55, 61, 100, and 108), all architecturally similar to Cave 85, were measured on sunny days in May 2001. Air change rate measurement of Cave 85 was not performed due to the presence of scaffolding, which restricted air circulation in the cave. Measurements were undertaken using CO_2 as the tracer gas and with cave doors both opened and closed (see table 14.5). With the doors open, air infiltration rates were between 2 and 4 air changes per hour (ACH); with doors closed ACH rates were an order of magnitude lower, 0.1–0.2 ACH. As described earlier, air infiltration is mainly driven by the temperature difference between the cave interior and the exterior: the larger the difference, the higher the infiltration rate. During the summer, interior temperatures ranged between 16 and 20°C, while the outside temperature was normally in the 30s°C during the day and in the 20s°C at night. After 4–5 air changes, the inside and outside reaches equilibrium. This could occur in 4–8 hours depending on the ACH of the particular cave.

The outside humidity ratio increases from the normal average value of 6.5 g/kg to 12–13 g/kg during rain events. With a cave infiltration rate of 2–4 changes per hour, infiltration of humid outside air is the equivalent of having 160 to 80 visitors respectively in Cave 85 during that period. This finding again suggests that the moisture levels in large caves are predominantly influenced by the outside climate and the cave's air infiltration rate and not by the moisture produced by visitors (Maekawa et al. 1997).

Fig. 14.24 Conducting air change measurements outside Cave 35 using CO_2 as the tracer gas.

CAVE NUMBER	ESTIMATED VOLUME OF MAIN CHAMBER (m3)	AIR CHANGE RATE (ACH) (number of air changes/hour)	
		DOOR OPEN	DOOR CLOSED
55	1000	2.1	0.1
61	1500	3.3	0.2
100	500	3.6	0.1
108	600	3.4	0.2

Table 14.5 Air Change Rate Measurements of other Large Caves at Mogao

CAVE NUMBER	AIR CHANGE RATE (ACH) (number of air changes/hour)		
	DOOR OPEN	DOOR CLOSED	DOOR CLOSED (with plastic sheeting placed behind door)
29	12.0	0.2	0.1
108	3.4	0.2	0.1

Table 14.6 Comparisons of Air Change Rates with Entry Doors Open, Closed, and Sealed

Fig. 14.25 The cave entrance has an aluminum louvered door with an outer barred security gate (a). On the interior, the louvers are covered with filters (b).

Efficacy of the Second (Internal) Door

Analyses of the salt mixture found in Cave 85 and the microclimate of the cave pointed to infiltration of the humid outside air as the cause of wall painting deterioration. At that time, it was recommended that entrance doors be closed during highly humid outside conditions to minimize infiltration. However, the doors have two louvered panels at the top and the bottom, and gaps exist at the bulkhead (fig. 14.25). There was concern that these openings would permit the infiltration of outside air. To counter this, an additional sliding door was installed in fall 1999 at the west side of the antechamber (fig. 14.26).

We were not able to quantify the efficacy of the second door. It did not show improvement of drier conditions compared to the closed primary doors, probably because the door was not consistently kept closed. The reduction of the air change rate from open door to closed door condition is an order of magnitude, while the reduction from the secondary door was much less. Results of air change rate measurements conducted in Cave 29 (medium size) as well as Cave 108 (large size) with entry doors open, doors closed, and doors closed with an additional large plastic sheet behind them to simulate the second door show that air change rates were reduced by one to two orders of magnitude by closing the entrance doors (see table 14.6). In a few measurements, the presence of the plastic sheet reduced the air change rate by an additional 50%. Therefore, in Cave 85, the louvre openings and poorly fitted bulkheads require sealing to provide adequate protection against air exchange during periods of extended high humidity.

Impact of Visitation

Visitors have an impact on the conditions of a cave since doors remain open while they visit and their bodies release moisture. The effects of visitation on various caves' microclimates have been reported (Maekawa et al. 1997; Agnew et al. forthcoming). In brief, results showed stronger effects of the outside climate, rather than the presence of visitors, on the climate of a moderately visited open cave than that of a closed cave. This means that the cave humidity increased when the outside was humid and decreased when the outside was hot and dry. However, the temperature always increased as a result of visitation. Highly visited caves typically have monthly averages

Fig. 14.26 A prefabricated sliding door between the antechamber and the main chamber was fitted in 1999 to reduce intrusion of humid air. Its efficacy was difficult to determine, most likely because the door was not consistently kept closed.

of humidity ratio 0.7 to 1.0 g/kg over those of moderately visited caves and about 1.5 g/kg over those of closed and sealed caves. These are equivalent to increases of 5–7% and less than 10% RH.

Summary

Liquid water was not found during the current investigation in the main chamber of Cave 85. However, this does not rule out past sources of water, such as flooding of the Daquan River. In the centuries of abandonment, windblown sand filled entranceways and caused rain- and floodwater to be wicked into the cave. Many lower-tier caves show a rising level of plaster loss where wet sand or standing water had banked against the walls. Also, treatment such as extensive plaster repairs throughout the cave no doubt provided the introduction of a significant amount of water at various periods.

The climate data from the Mogao Grottoes site as well as microclimate data in Cave 85, supplemented with environmental monitoring from other caves, were used to identify sources of moisture that could cause the humidity to reach higher than 67% RH, the critical value for deliquescence established in the laboratory on extracted salts from the cave wall. Allowing for a 5% increase due to cooler wall temperature in summer months, a not to be exceeded value of 62% RH was decided upon. The following conclusions apply specifically to Cave 85 but more generally to other caves as well.

- No visible sign of liquid water infiltration was found in the cave, except for evidence of past flooding.
- Flood irrigation of the trees in front of the grottoes does not affect the humidity in the cave and thus also does not cause damage to the wall paintings.
- Saturated conditions (100% RH) exist in the bedrock deeper than 1 m in the west wall and in the floor. This indicates a source of moisture in deep bedrock. The humidity gradient with depth provides the transport mechanism for salts from the bedrock to the west wall. This condition was documented in Cave 98, with similar deterioration of the west wall.
- Cave walls (at less than 10 cm depth) remain below 50% RH in normal climate. However, surface humidity

can exceed 62% if humid outside air enters the cave through open doors during humid or rainy periods.

- Climate variations occur seasonally and diurnally in the caves; however, they are generally below the critical relative humidity at which salt-related deterioration occurs.
- Moisture released by high numbers of visitors increases the humidity in caves; however, this is only significant in smaller caves and those with extremely high numbers of visitors, such as Caves 16 and 328.
- Results demonstrate that when open to visitation Cave 85 and other caves allow a higher rate of air exchange with the outside, and therefore the interior conditions closely follow those of the outside. Changes in the outside humidity cause the humidity inside the cave to vary from 10% RH in winter to as high as 50% RH in summer. But the occasional extended humid or rain event during summer months causes the interior to exceed 62% RH several times per year. These conditions activate the principal deterioration mechanism—deliquescence and recrystallization of salts.
- Caves with salt-related deterioration should remain closed to visitation during rainy periods in summer.
- Real-time monitoring of RH and a warning system in susceptible caves such as Cave 85 are recommended.
- Cave doors require better sealing to prevent intrusion of external humid air.

Notes

1. All holes were drilled in areas where repair plaster replaced lost original painted plaster using a 1.6 cm diameter rotary masonry bit. RH and T probes, designed for monitoring dryness of structural concrete, were placed in each drilled hole at 10 cm and 30 cm depths. The holes were then sealed with neutral cure silicone filler and a rubber plug to eliminate the influence of the cave air. Readings were taken manually.
2. The moisture content at all areas of the conglomerate along the cliff face is unlikely to be the same because of fractures in the rock, intersections with fault planes, lenses of sandstone with different water-vapor permeability, and areas of greater porosity, where the conglomerate is inhomogeneous, allowing more rapid diffusion of water vapor (Agnew et al. 2010).
3. Floor sensors #16, #17, #18 were placed 10 cm into the sand below floor level. Floor sensors #14 and #15 were placed at 30 cm depth into the bedrock through the floor tile in the cave.
4. Percolation through conglomerate is difficult to assess at any point along the cliff, as it is dependent not only on the permeability of the rock but also on the number and size of nearby caves and cracks or fissures.
5. Rainwater infiltration has occurred in a few upper-tier caves where erosional thinning and collapse of the ceiling rock has occurred.

CHAPTER 15

Diagnostic Investigation

The diagnostic investigation identified factors responsible for deterioration in Cave 85 and aimed, through analytical and environmental research, to understand the causes, activation mechanisms, and processes involved (see chaps. 13, 14). This understanding is an essential step in the conservation process in order to develop measures to reduce causes of deterioration and to design and implement appropriate and compatible interventions for the stabilization and long-term preservation of the wall paintings and sculpture (see chap. 17) (fig. 15.1).

Phenomenological identification and categorization with topographical mapping of observable types of deterioration and damage formed the basis of the condition assessment, which in turn was needed to determine the causes and activation mechanisms of deterioration (see chap. 12). Information from the physical history and past conservation treatment in the cave was taken into account during the condition recording. This information allows for past deterioration to be distinguished from ongoing deterioration and for hypotheses regarding their causes and activation mechanisms to be made (see chap. 9). Research then confirmed or negated the hypotheses or pointed to the need for further investigation. The range and complexity of deterioration in Cave 85 made the diagnostic investigation challenging, and despite lengthy research some questions are not fully answered. In these cases, the limitations of our understanding and the need for further investigation are indicated. Discussion is focused on the wall paintings in the main chamber of the cave.

Fig. 15.1 An area of detached plaster collapsed from the west ceiling slope in 1996. Plaster detachment is the most serious threat in Cave 85. Understanding the causes and mechanisms of this ongoing deterioration to prevent further loss of painting was the main focus of the diagnostic investigation.

Over the centuries the Late Tang dynasty paintings in the cave suffer from deterioration of various kinds broadly falling into two categories: in-depth deterioration, including plaster layers; and surface and subsurface deterioration, including paint, ground, and upper plaster layers. In-depth conditions include detachment, disruption, and cracking. Surface and subsurface deterioration includes flaking, exfoliation, punctate loss, crater

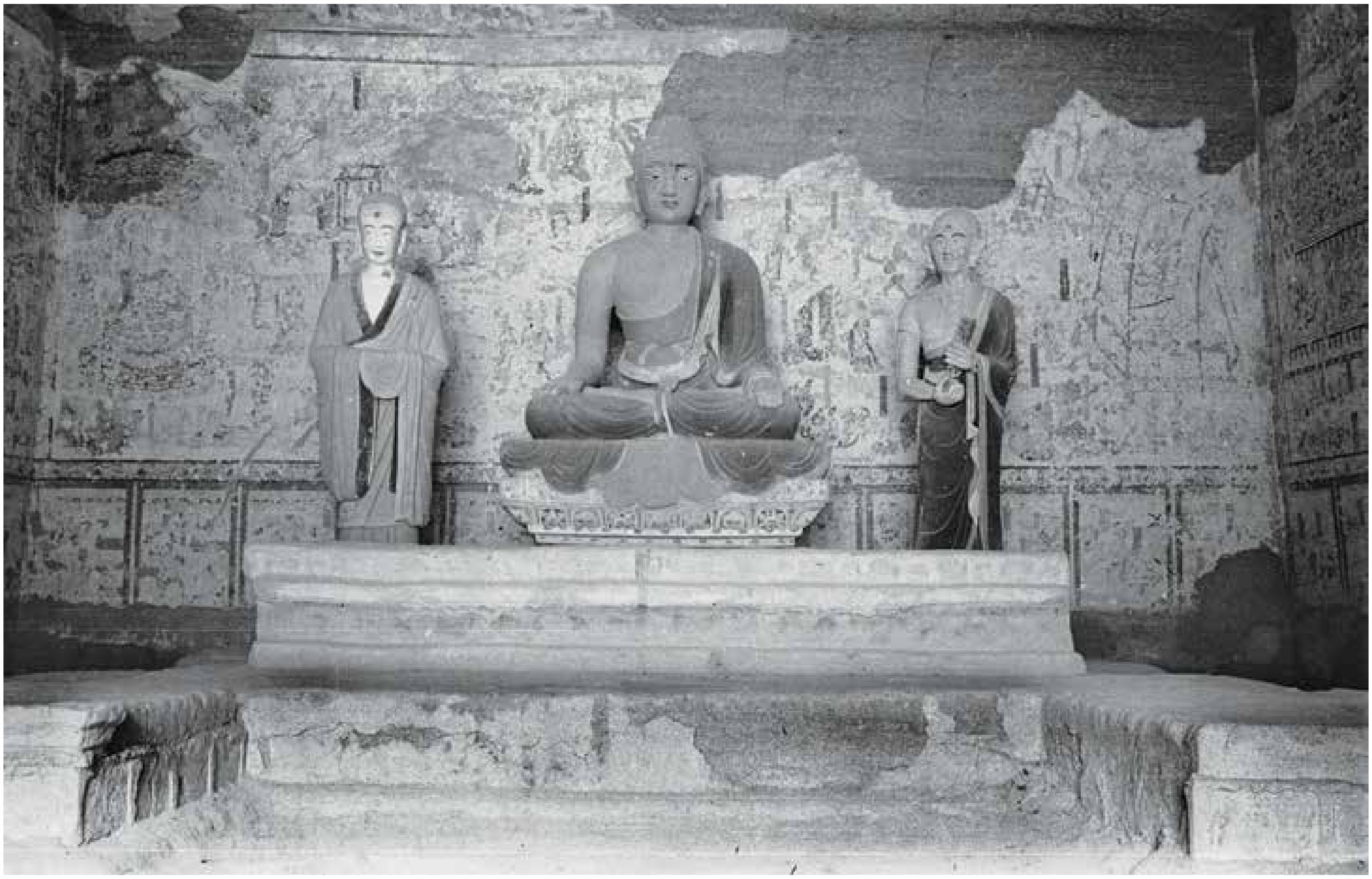

Fig. 15.2 Plaster losses have occurred toward the rear, west end of the cave in the upper southwest and northwest corners, as seen in this photograph from the 1940s.

eruptions, and color change (mineral pigment alteration and organic colorant fading) (see figs. 12.12, 12.13).

The condition assessment showed that detachment of the painted plaster, concentrated toward the rear or west end of the cave, was the most serious problem. Severe plaster disruption and exfoliation were similarly distributed. The bulk of the research discusses the causes and mechanisms of these forms of deterioration. Conditions that occur on a limited scale, not considered a current or serious risk to the painting, are discussed only in summary.

In-Depth Deterioration

Over time, plaster loss has occurred both at the base of the cave walls and on the west wall and west ceiling slope, particularly in the upper northwest and southwest corners (fig. 15.2).

Loss at the base of the walls is found in many other ground-level caves that have suffered periodic flood damage. Complete loss of painting at the base of the walls is attributed to floodwater and to wet sand buildup against the walls over prolonged periods. Flood control measures were put in place in the 1960s. Since then there has been only one flood event, which occurred in 1979 when unusually heavy rain caused water from the Daquan River to overflow its banks and enter some of the ground-level caves (Kuchitsu and Duan 1997, 247). Floodwaters from a 2011 storm did not reach the caves.

The rate of plaster loss through collapse in the upper parts of the west end of the cave was assessed from recorded instances of loss and the history of interventions intended to address these problems (see chap. 9). The available evidence indicated a progressive and alarming history of plaster detachment and loss occurring at the west end of the cave. Losses in the wall paintings were first filled in the 1940s and then again in 1974. Repeated treatment indicates a continuing problem, including enlargement of existing areas, as well as new ones. Since 1974, additional plaster losses have occurred in the upper southwest

Fig. 15.3 Cave 94 is another large cave that, like Cave 85, has severe plaster detachment and loss of painting at its rear west end.

corner of the cave, and in 1996 an area of painted plaster from the west slope collapsed (see fig. 15.1).

Plaster Detachment

Plaster detachment, defined as a loss of adhesion (i.e., separation) between the lower coarse plaster and the conglomerate, is widespread throughout the cave. The condition assessment identified areas of stable plaster detachment (i.e., areas not at imminent risk of collapse) distributed throughout the cave, while extensive areas of unstable plaster detachment increased toward the northwest of the cave. This problem of plaster detachment is found in many other caves at Mogao. One such example is Cave 94 where substantial losses have also occurred (fig. 15.3).

Various factors are suggested—singly or in combination—as causes for the observed plaster detachment and loss. These include original methods and materials of construction, earthquake, and soluble salts.

Original Methods and Materials of Construction

At the time the cave was plastered, variable keying and poor bonding of the wet earthen plaster to irregular and friable conglomerate may have resulted in poor adhesion. Shrinkage and contraction of the plaster upon drying would have caused additional detachment from the rock. Laboratory testing showed up to 21% linear shrinkage upon drying of a clay and fiber mixture of composition comparable to the original plaster.[1]

The original plastering of the cave was undertaken in large sections, with joins occurring at junctures between walls and slopes. Detachment is concentrated in these areas of adjacent and partly overlapping plaster layers, including, in particular, the upper southwest and northwest corners of the cave where much loss of original plaster has occurred. Another example is a large area of plaster detachment on the north side of the east wall. This area corresponds with the location of a plaster join, multiple trowel marks suggesting that the original plasterers had difficulty getting the plaster to adhere. A network of ancient

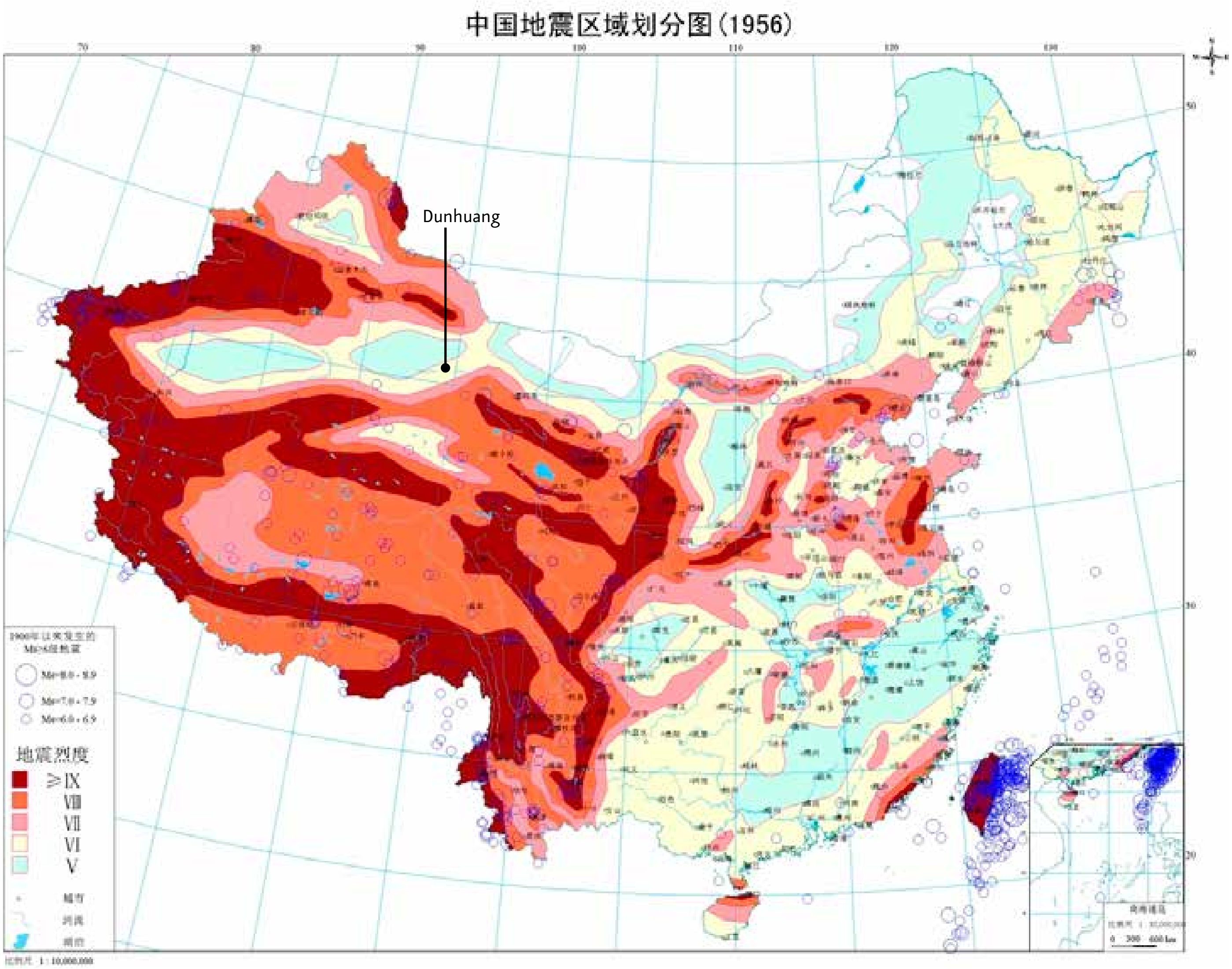

Fig. 15.4 Seismic intensity map of China (1956). Dunhuang is a degree 6 seismic region (map scale 1:10,000,000; depicts both the epicenters of earthquakes higher than magnitude 6.0, from the year 1900 to 1956, and the seismic speed rating as colored zones).

cracks indicates that there were likely problems of plaster shrinkage as well (see chap. 13).

These conditions resulting from the original plastering probably account also for the many areas of stable plaster detachment found throughout the cave. However, these areas, as the word *stable* suggests, do not necessarily indicate immediate risk. Indeed, it appears that in most cases the detachment occurred soon after plastering, and conditions have since remained essentially static. Indicators of what can be termed stable plaster detachment in the cave include static historical cracks identifiable because paint is carried over them and plaster deformation that shows bulging of the plaster having occurred during drying rather than subsequently.

Earthquakes

Dunhuang is a degree 6 seismic region according to the national classification of seismic intensity zones (Sun 1997, 159) (fig. 15.4). Seven earthquakes are reported to have occurred between 1927 and 1960 (Sun 1997, 159–60). None of these were high on the Richter scale, but the frequency of their occurrence is a latent danger to grottoes excavated in close proximity to one another and in areas where rock fractures exist. Tectonic evidence of faulting and seismic analyses and earthquake predictions indicate that there could be an earthquake of 6.5 to 7.0 on the Richter scale in the Hexi Corridor area of Gansu Province in the future (Fan 1997, 16). In response to this danger, mechanical-type strain gauges were installed along major crevices in the cliff face to monitor their stability (Huang 1991). A seismometer was set up to record activity, analyze shaking susceptibility of the cliff and reinforcement structures, and evaluate earthquake hazard in the area (Yao et al. 1993).

Soluble Salts

As is well known, soluble salts cause serious deterioration of stone and earthen materials when activated by moisture in either liquid or vapor form. Hygroscopic salts can contribute to detachment and collapse of the paintings by cycles of crystallization and dissolution at the interface between the plaster and the conglomerate—effectively pushing off the plaster—or by deterioration of the conglomerate itself, leading to friability and spalling of the rock behind the plaster. The large area of painted plaster that collapsed from the west slope in 1996 had white crystalline material both on the back of the fallen fragments and on the surface of the exposed conglomerate (fig. 15.5). Sodium chloride was identified by XRD as the main component of the white material. A description of the analytical and

Fig. 15.5 White material was observed on the conglomerate following the loss of painted plaster from the west ceiling slope in 1996. Sodium chloride was identified.

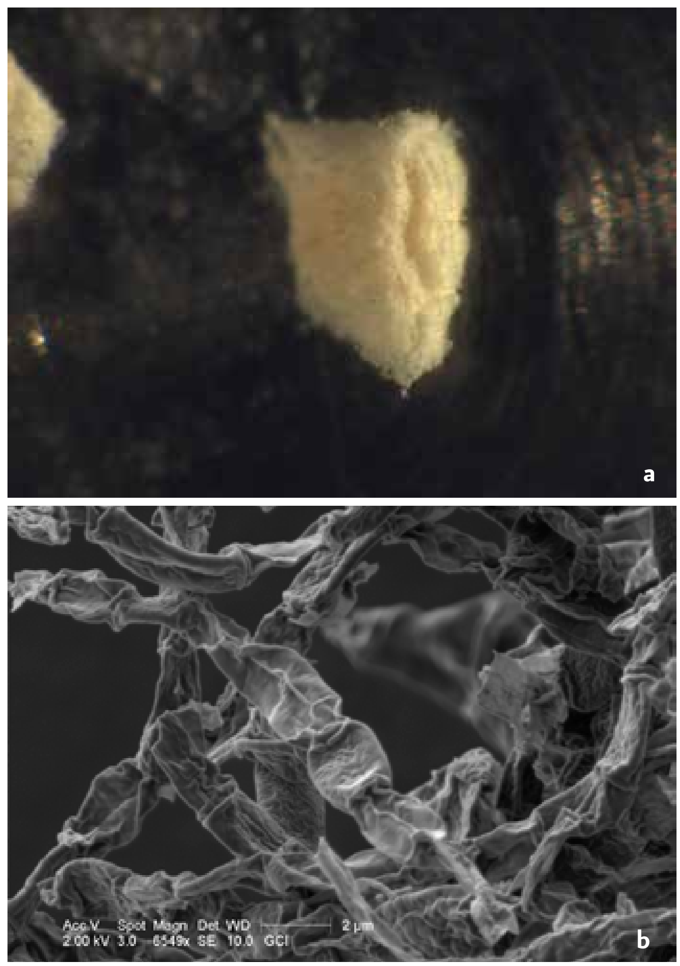

Fig. 15.6 In addition to sodium chloride, filamentous bacteria and fungi were found in the white material on the surface of the conglomerate. Shown under magnification (a) and a backscattered electron image (b). This was the only area of the cave where microorganisms were observed and which therefore were not considered to be a cause of the plaster detachment.

Fig. 15.7 ESEM-EDX elemental maps of Na, Cl, and S from plaster sample 85BQ99E3 from the upper west side of the north wall shows NaCl present along cracks. No sulfur is present.

b

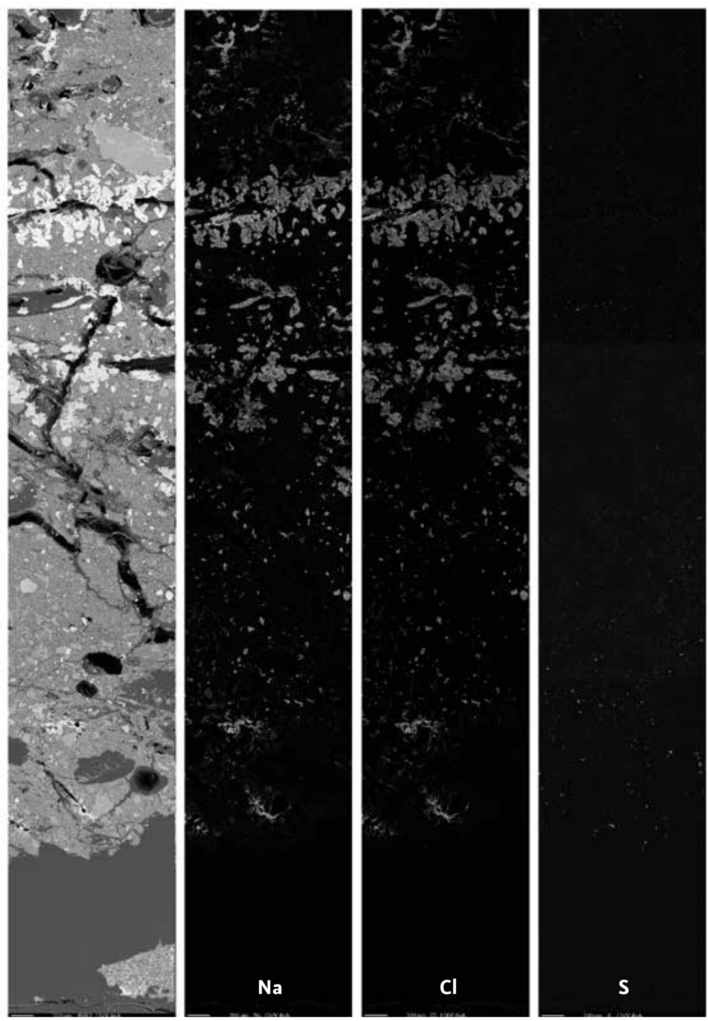

environmental investigation of the role of salts and moisture in the deterioration of the wall paintings is given in chapter 16, "Salt-Induced Deterioration."

Interestingly, a large amount of white material was found in addition to the white efflorescence on the back of the collapsed fragment and also within the plaster stratigraphy (fig. 15.6). Microscopically, it resembled a white powdery cotton-like material found in another cave, Cave 98, where DNA analysis revealed it to be composed of a micro-colony of several different kinds of bacteria and fungi. The most abundant and viable organism was identified as *Acremonium* spp., which is a common fungus found in plant debris and soil. As this was found in only one area of Cave 85 it is not considered to be a cause of the detachment.

Plaster Disruption

Plaster disruption, defined as loss of cohesion in the plaster, typically occurs around repairs at the base of the walls and at the west end of the cave. The disruption of the plaster is undoubtedly caused by soluble salts.

Samples of disrupted plaster from the base of the walls and a vertical profile on the north wall were collected and mounted in cross section to examine the stratigraphic distribution of salts by ESEM-EDX. The elemental distribution maps showed sodium and chloride. Sample 85BQ99E3 shows NaCl present in cracks and voids, suggesting its movement in solution and crystallization at interfaces (fig. 15.7).

A salt sample from an area of disrupted plaster at the base of the south wall (sample 85NQ9802) was analyzed by PLM and found to contain both Na_2SO_4 and NaCl. This composition corresponds to other salt samples taken from plaster repairs at the base of the wall in a nearby location (sample 85NQ9801). Disruption of the plaster is caused by the repeated crystallization and deliquescence of the salt. For further discussion on the mechanisms of salt deterioration see chapter 16.

Surface and Subsurface Deterioration

Surface and subsurface deterioration with a similar distribution to that seen for plaster detachment and disruption was found on a southeast to northwest axis on both walls and ceiling slopes, with increasing severity toward the northwest of the cave. There is a progressive worsening of condition of the painted surface especially but not exclusively at the rear of the cave. Though not as severe as the losses caused by plaster detachment, comparison of current condition with historical photographs showed losses occurring, though gradually, over time (see fig. 9.23).

There are important distinctions to be made between types, rates, and distribution patterns of surface and subsurface deterioration, though these are not always easy to reconstruct or to explain.

Flaking

Flaking, defined as the lifting and fragmenting of the ground and/or paint layers, was found on only a limited scale in Cave 85 (fig. 15.8). However, historical photographs document severe and widespread flaking that was treated in 1974 by the Dunhuang Academy (see fig. 9.22). This treatment was undertaken using vinyl emulsions (PVAc and PVA) on the west wall and slope, the west portions of the south and north walls and slopes, and portions of the east wall (see chap. 9).

Since the 1974 treatment, little flaking recurred on the east wall, but toward the west end of the cave another form of flaking—referred to as exfoliation or disruption flaking—was observed (discussed in the next section). It can be inferred that the flaking that occurred on the east wall was therefore different from that at the west end of the cave. Although it is not possible to determine the precise causes and activation mechanisms of this flaking, it may be related to differing painting technique[2] or past circumstances that only affected the east side of the cave (e.g., greater exposure to the frequent influence of the exterior environment). As the flaking had only very limited recurrence recorded during the condition assessment, it is not considered progressive. Flaking is a common condition seen in many of the caves at Mogao.

Exfoliation

The problem of exfoliation, defined as the combined lifting of the paint layers, ground, and upper plaster, is a more serious form of flaking affecting not only the paint and ground layers but also the upper plaster layer. It occurs in areas of plaster

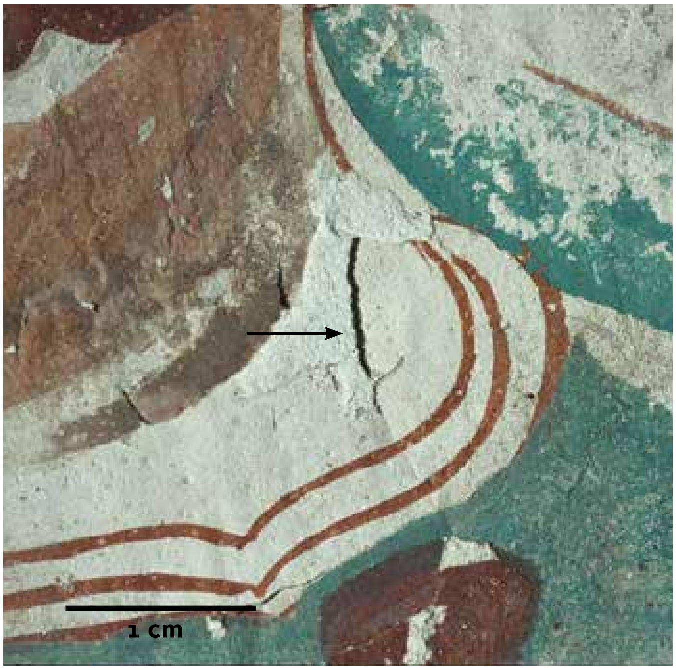

Fig. 15.8 Flaking is lifting of paint and ground layers. Only limited areas of flaking were found following treatment in the 1970s by the Dunhuang Academy. Instead, the more severe form of flaking known as exfoliation was observed toward the west end of the cave.

Fig. 15.9 Exfoliation is a more serious form of flaking that occurs in areas of salt activity where the fine plaster below the paint and ground layers has lost its cohesion (disruption).

disruption and is also referred to as "disruption flaking." Typically, it has been associated with soluble salt activity and past surface treatment of the wall paintings with vinyl emulsion. Exfoliation is a condition that occurs in other caves at Mogao, such as Cave 98 (Guo et al. 2010).

In 1999, following a period of summer rain, exfoliation and disruption occurred at the west end of Cave 85, resulting in substantial loss of original material (fig. 15.9).[3] Monitoring of fallen paint flakes and plaster on the floor was undertaken to assess the material lost over time (fig. 15.10).[4] Paper sheets were placed on the floor along the west wall and the western ends of the south and north walls to collect fallen paint flakes and plaster. The material was then weighed to quantitatively estimate loss. The bulk of fallen material was found in the middle section of the west wall and the western end of the north wall. Debris from the north wall typically was lost from its upper parts. The rest of the areas monitored had only minor loss.

These areas were previously treated in 1974 for flaking. Analysis of paint flakes from the base of the walls found 16–18% (by weight) of polyvinyl acetate (PVAc) (Schilling 2000) (figs. 15.11, 15.12).[5] Analysis also identified Na_2SO_4 and NaCl salts.

Surface deterioration at the west end of the cave increased in nature and extent after the first recorded treatment in 1974. Key to understanding this process is the connection between salt-related deterioration caused by changes in RH and treatment materials and their apparent excessive use.

During a period of heavy rain in July 1999, 10 mm of rain fell over a two-day period. The RH data indicated sustained high RH, 75% or higher, for approximately four days between 11 July and 15 July 1999.[6]

Post-1974 exacerbated deterioration is interpreted as follows: PVAc and PVA treatments consolidated the paint, ground, and upper fine plaster layers, creating a moisture vapor barrier that significantly reduced porosity and restricted movement of salts to the surface and thereby pushing the interface of salt-related deterioration deeper into the painting stratigraphy. Soluble salts, trapped below the surface, crystallized and caused powdering of the ground and fine plaster layers. Cohesive paint, having been consolidated with vinyl emulsions, tended to be lost as large flakes. Thus, the treatment for flaking in the 1970s

Fig. 15.10 Paper sheets were placed at the base of walls to collect fallen material following the 1999 summer rain. The area pictured is the southwest corner (a, b). The bulk of the fallen material, comprising paint flakes and disrupted, powdery plaster, was found in the middle part of the west wall and the western end of the north wall (c).

Fig. 15.11 PVAc was identified in fallen paint flakes. Beading of water on the painted surface showed that a moisture barrier was formed following the consolidation of paint, ground, and upper fine plaster layers in the 1970s.

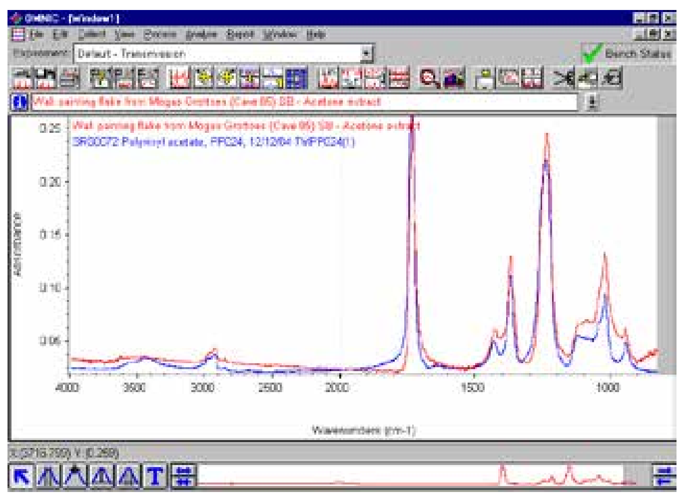

Fig. 15.12 FTIR spectra of a paint flake (red) and polyvinyl acetate reference (blue); 16–18% (by weight) of PVAc was measured in fallen paint flakes collected at the base of the wall.

Fig. 15.13 "Punctate" loss is characterized by tiny pointlike losses in the paint layer, as shown in this detail from the west end of the north wall. This form of deterioration is found only at the west end of the cave.

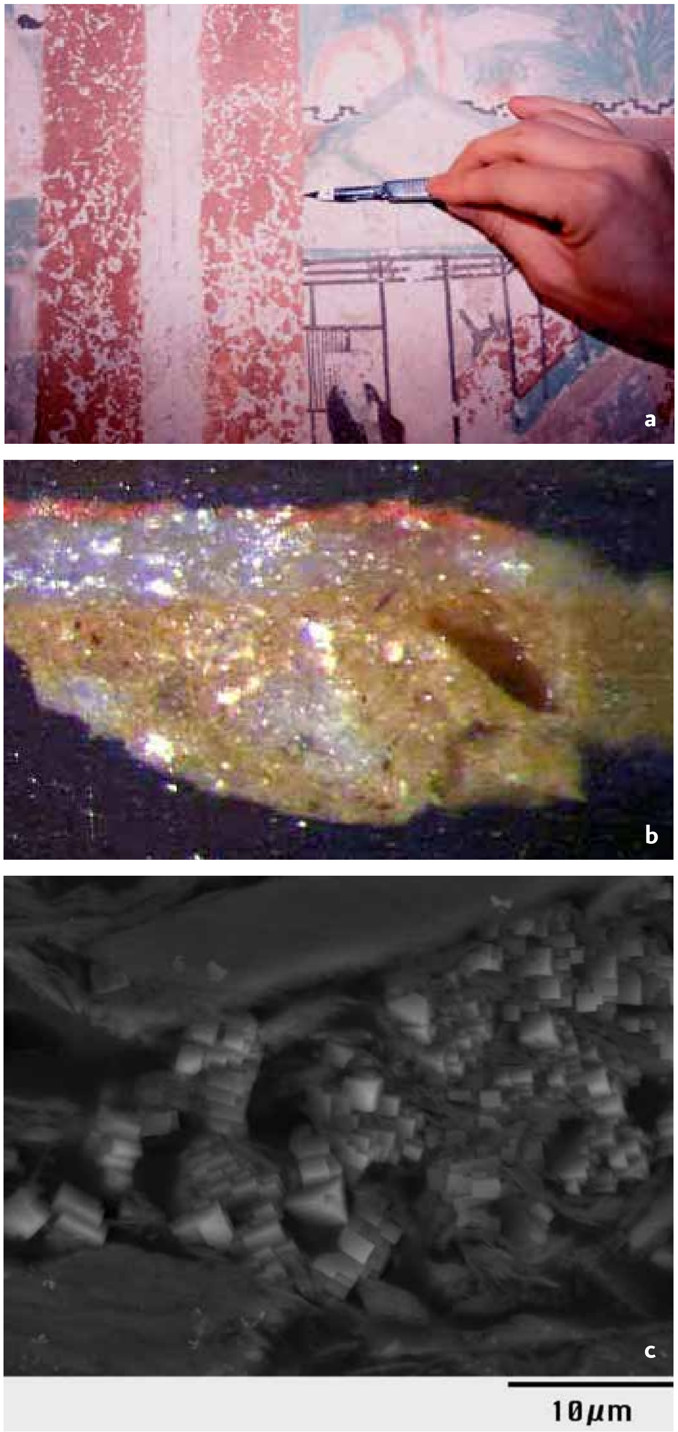

Fig. 15.14 Sample 85NQ98PE2 was taken from an area of red paint with punctate loss at the west end of the south wall (a). A polished cross section of the sample (b) and a backscattered electron image of the section shows NaCl crystals pushing up the paint layer resulting in pointlike losses in the paint layer (c).

later led to renewed deterioration that occurred in worsened form. For further discussion and testing to confirm mechanisms of salt deterioration, see chapter 16.

Punctate Loss

Punctate loss is defined as small rounded losses (less than 1 mm in diameter) of the paint and ground layers, which occurs at the west end of the cave. It was given the name "punctate loss" because of its appearance as tiny dots of loss in the paint layer (fig. 15.13). Punctate loss can be seen in other caves at Mogao and typically coincides with areas that exhibit other types of salt-related deterioration such as disruption and exfoliation. This type of surface deterioration occurs within paint and ground layers and is interpreted as follows: when relative humidity is high salts deliquesce and migrate through the plaster and recrystallize just below the paint layer. The salt crystals that form break through the paint and cause tiny round losses.

ESEM-EDX was used to examine a painting cross section (sample 85NQ98PE2) taken from a dark red stripe on the south wall exhibiting incipient punctate loss. In this sample, cubic crystals can be seen between the red paint layer and the ground, in some areas breaking through the paint layer. Elemental analysis of these crystals confirmed the presence of sodium and chloride, indicating NaCl (fig. 15.14).

Significantly, areas of painted plaster that were not detached from the conglomerate generally exhibited more surface deterioration than areas of plaster that were detached. This may be because salts had continued to migrate from the conglomerate into the plaster. In areas where the plaster was detached, salts instead crystallized within the void, generally at the interface between the rock and the plaster, and consequently placed such areas at risk of collapse.

It is possible that the original binding media, organic colorants or a surface coating, may have acted as a barrier trapping salts below the paint layer. If this is the case, it could explain why punctate loss appears to favor certain colored areas such as reds (see fig. 15.13). In addition, the thickness of the paint layer may have played a role in the ability of salts to crystallize. The thinner the layer, the easier it is for salts to break through and to form punctate losses.

Fig. 15.15 Example of an area of crater eruption and loss. The crystal at the center of the crater was identified as gypsum. The crater may be caused by anhydrite, present as an impurity in the earthen plaster, which then hydrated to gypsum, leading to a volume increase and the loss of painted plaster.

It is unclear whether this condition is still active and a continuing risk to the paintings. Given that large areas of the painted surface were consolidated with vinyl emulsion, restricting the ability of salts to move through the painting stratigraphy, it is possible that in areas where the paint layer has been consolidated the risk of punctate loss occurring is now low. However, as noted previously, use of vinyl emulsions led to more extensive deterioration and loss within a period of less than 30 years.

Crater Eruption and Loss

Crater eruptions are defined as bulges (from 0.5 cm to 1 cm in diameter) in the paint, ground, and fine plaster layers containing small inclusions that occasionally break through the surface and lead to crater-shaped losses (fig. 15.15). This is an unusual condition mainly localized in the west ceiling slope of the cave. It is not commonly observed in other caves at Mogao.

The centers of two craters on the west slope were sampled and analyzed by ESEM-EDX and XRD. Coincident clusters of calcium and sulfate ions indicated that the principal mineral compound is gypsum (calcium sulfate, $CaSO_4·2\ H_2O$). Crater formation may be associated with a process of volume change when earthen plaster containing anhydrite as an impurity transforms into gypsum, causing a significant increase in volume.[7]

Fig. 15.16 Color change is visible in these two images from the east (a) and north (b) ceiling slopes. Note the different appearance of the background color where an organic colorant wash on the ground survives on the east slope but has faded or been lost on the north slope.

Color Change

Color change is a form of deterioration that includes both alteration of mineral pigment and fading of organic materials (colorant and binder) (fig. 15.16). Color change is difficult to assess given the complexity of the painting technique in Cave 85 (see chap. 13) and the inability to know what the original painting looked like. Research was undertaken to understand the original appearance of the painting and how it has changed and to determine current risks of further color change (Druzik 2010). Previous research has also been conducted by the Dunhuang Academy in this area (Tang and Sun 1988). This information will influence decisions on the presentation of the wall paintings and sculpture, including recommendations for safe levels of lighting to enhance the visitor experience in the cave (see chap. 19).

Inorganic Pigment Alteration

Lead Alteration

Lead-based pigments, lead white ($(PbCO_3)_2 \cdot Pb(OH)_2$) and red lead, minium ($Pb_3O_4$), have been found in Cave 85 and in many other caves at Mogao (Li and Michalski 1989; Li 1992; Shen et al. 1990). Visual examination of the paintings indicated areas of alteration of these lead pigments into dark brown lead oxide (plattnerite, PbO_2). This well-known alteration process has been the subject of previous investigations, including studies conducted on the Mogao wall paintings. The studies indicate moisture, alkalinity, light, and oxidizing agents as factors influencing this alteration (FitzHugh 1986; Giovannoni et al. 1990; Gettens et al. 1993). In Cave 85, the rate at which lead pigments are altering is difficult to determine with the historical photographic documentation that exists—much of it in black-and-white.

Lead White Alteration

The darkening of lead white is common to the wall paintings at Mogao. In Cave 85 it is visible throughout and is not confined, as with other types of deterioration, to the cave's west end. Observations suggest that the proximity of green copper chloride pigments may contribute to the darkening phenomenon. An example of this can be seen in the thin white vertical lines on the "tassel" decoration in the upper portion of the ceiling slopes (fig. 15.17). The white lines, painted in lead white, were applied over several bands of different colors. Depending on which color the line overlaps, the lead white has preferentially altered. This is most noticeable over the band of green copper chloride pigment, where the line has darkened; over other colored bands it appears unaltered. This is also seen under UV-induced fluorescence where the white line fluoresces over all colored bands, except over the green where the altered line appears black.

Typically, lead white was applied thickly, such as the small white dots on the "pomegranate" decoration on the east slope. Sample MOG.85.F03.S11 taken from this area consists of a white dot applied over a layer of green (fig. 15.18). This white dot is partially altered, again seemingly influenced by the lower layer of green copper chloride pigment. Optical microscopy at low magnification of the cross section shows the upper part of the paint layer still unaltered and white in color (0.1 mm) while the lower portion has altered to a dark brown color (0.4 mm). ESEM-EDX elemental analysis confirmed the presence of lead throughout the entire paint layer. The backscattered image showed the unaltered lead white portion, typically composed of a mixture of lead carbonate (cerussite, $PbCO_3$) and hydrocerussite ($Pb_3(CO_3)_2(OH)_2$) denser than that of the altered compound, lead oxide (PbO_2). This difference in density is probably due to the volume change of the crystal form of altered versus unaltered lead. The "bubbles" visible on the surface of the sample may possibly suggest that the alteration, which involves the production of water and carbon dioxide gas, occurred while the paint was drying.

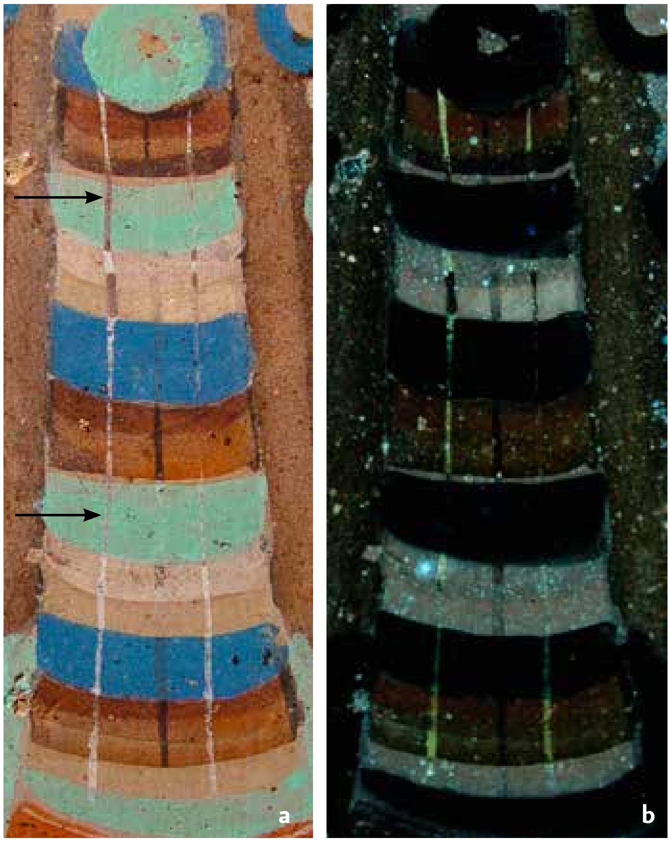

Fig. 15.17 Lead white alteration can be seen in the thin white vertical lines on the tassel decoration on the east ceiling slope. Depending on which color the white line overlaps, the lead white has altered or remained unaltered. Applied over the green copper chloride pigment in particular, the line has preferentially darkened; over other pigments the line is unaltered or only partially altered (a). Under UV-induced fluorescence the white line fluoresces yellow over all colored bands apart from the green (b).

Red Lead Alteration

From visual examination the darkening of red lead is less evident than that of lead white and does not seem to be affected by the presence of green copper chloride pigments.

Minium transformation into plattnerite can be seen in sample MOG.85.F03.S17, when compared with sample MOG.85.F03.S16, an unaltered area of red lead (figs. 15.19, 15.20). Both samples were taken from similar areas of painting. ESEM-EDX elemental analysis showed the presence of lead in the paint layers of both samples, but visible light examination of the cross sections indicated that the alteration was only occurring in sample MOG.85.F03.S17. The reason one area shows alteration and the other does not is unknown.

Light exposure tests on sample MOG.85.F03.S28 from an area of red paint from the ceiling showed that vermilion and red lead are still prone to darkening (Druzik 2010, 460–61) (see table 15.1).

Azurite Alteration

Tang dynasty painting is characterized by a blue and green palette that often alternates in repeating design motifs. In the eastern end of Cave 85, where the paintings survive in good condition, several areas are colored with azurite ($Cu_3(CO_3)_2(OH)_2$), whereas at the western end of the cave, where the paintings are deteriorated, the same colored designs are now lost and appear primarily green. It is thought that this difference in color is due to the alteration of blue azurite into a green copper pigment.

The conversion of azurite into green copper-based pigments has been shown to be caused by environmental conditions, alkalinity, and the availability of chloride ions (Dei et al. 1998; Kerber et al. 1972; Naumova et al. 1994). Investigation of soluble salts has shown the enrichment of sodium chloride at the west end of

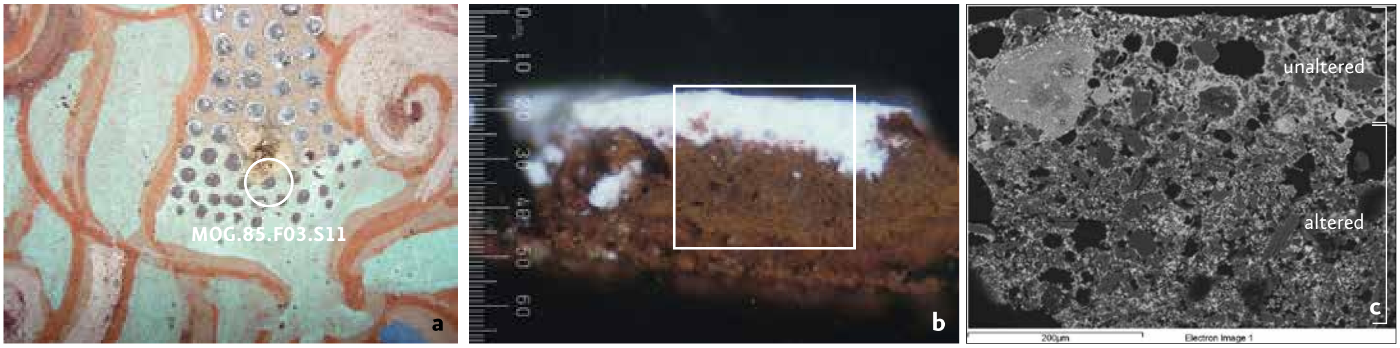

Fig. 15.18 Sample MOG.85.F03.S11 from an area of lead white over green copper chloride pigment (a). The polished cross section shows the paint layer partially altered and only the upper part still unaltered (b). The backscattered electron image shows that the unaltered portion appears denser than that of the altered compound (c).

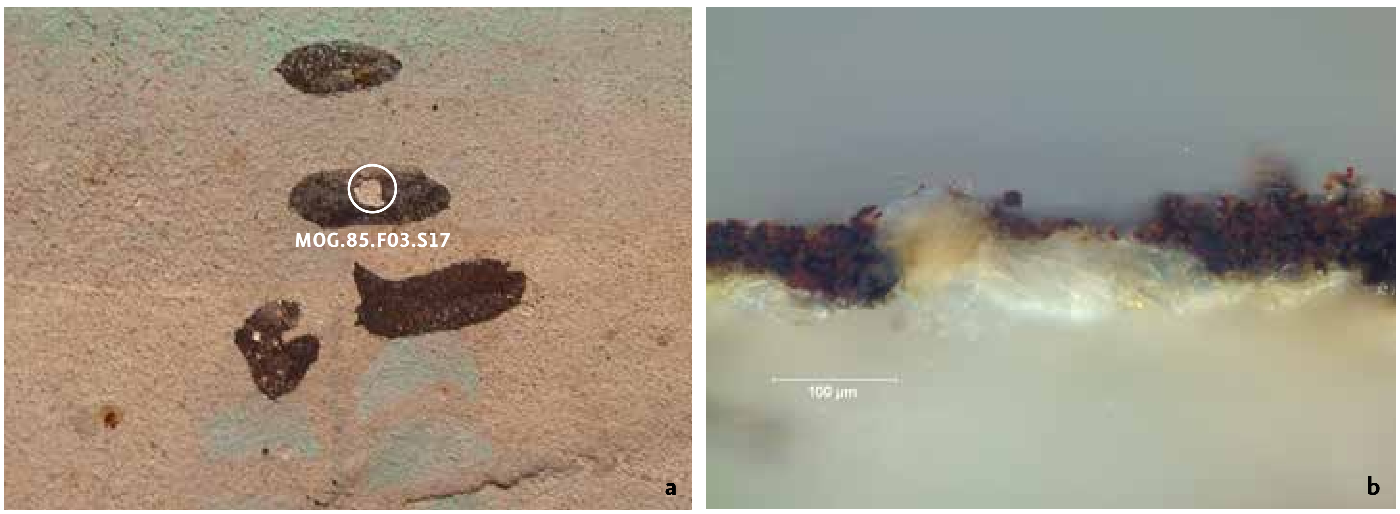

Fig. 15.19 Red lead alteration into plattnerite is visible in sample MOG.85.F03.S17 from the east slope (a). Polished cross section shows blackening of the once-red layer (b).

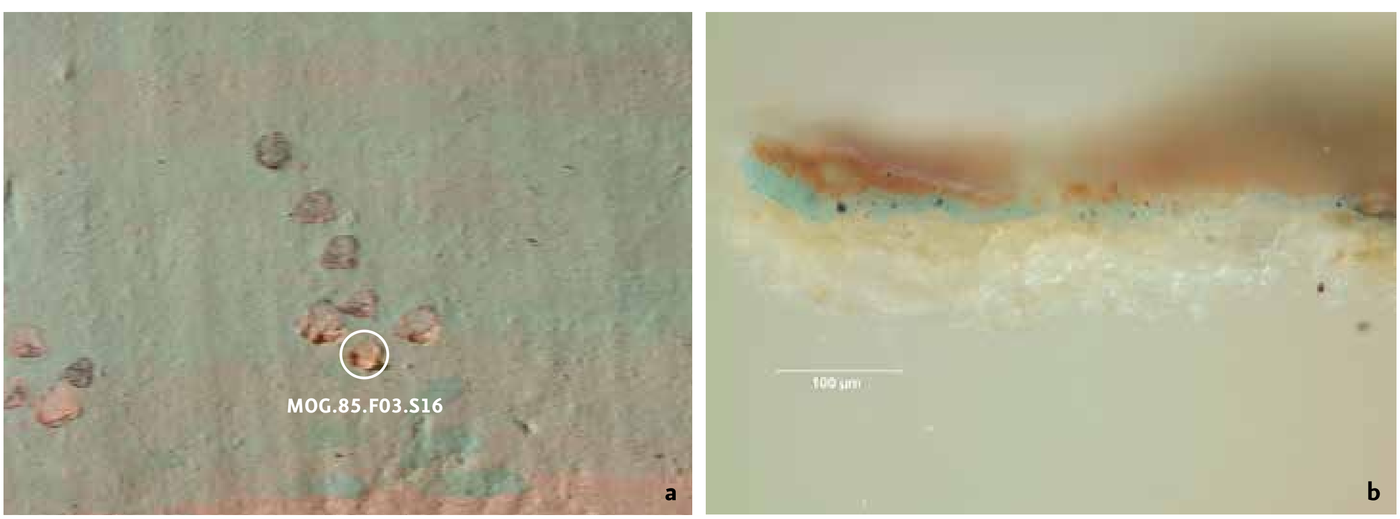

Fig. 15.20 Sample MOG.85.F03.S16 from the north wall is an unaltered area of red lead (a). Polished cross section shows the layer still red without alteration over a copper chloride green paint layer (b).

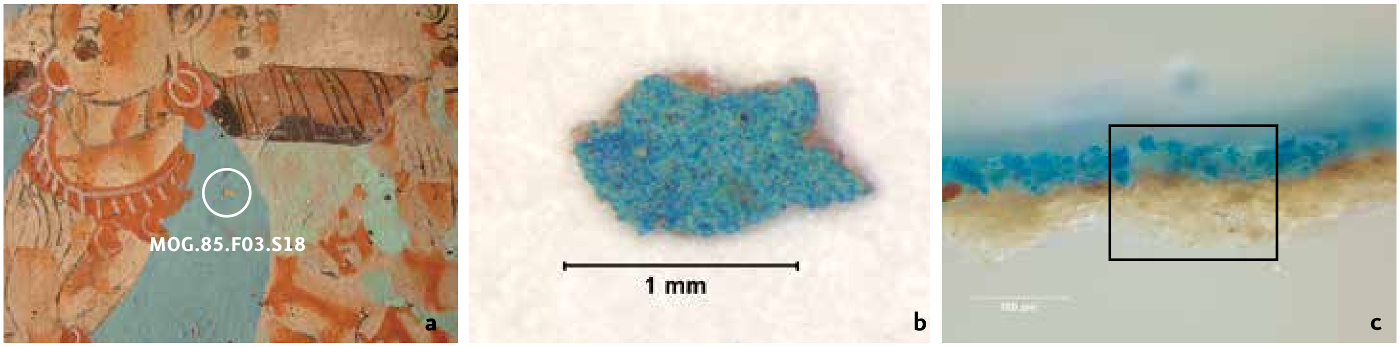

Fig. 15.21 Location of partially altered azurite sample (MOG.85.F03.S18) from the east slope (a). The unmounted sample under magnification appears mainly blue with some green (b) and the polished cross section shows azurite particles with blue unaltered centers (c).

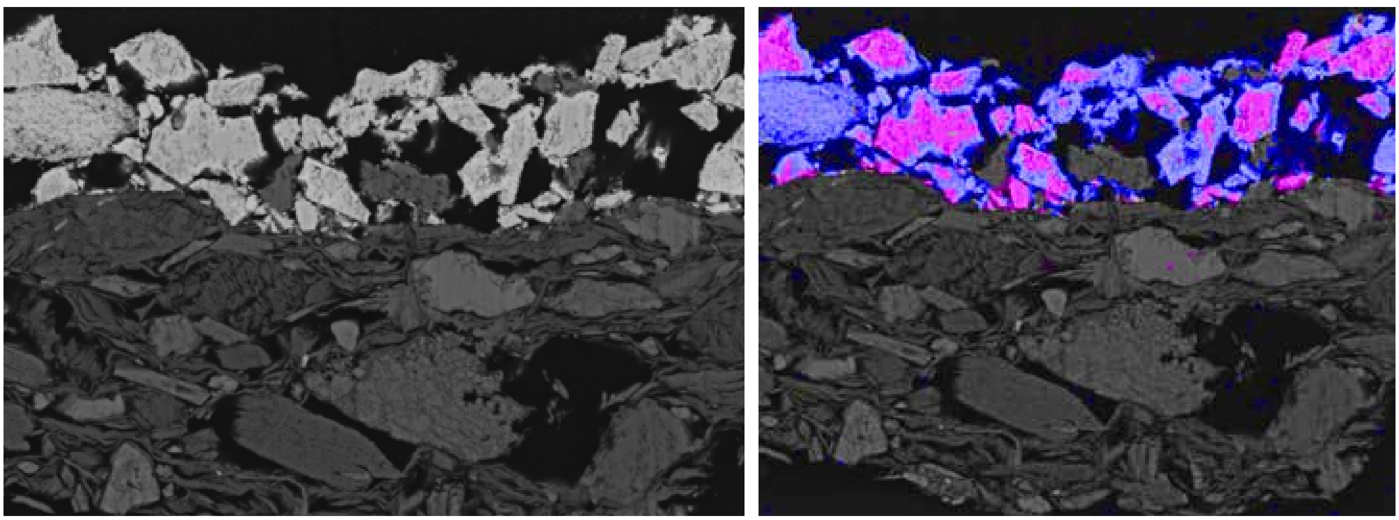

Fig. 15.22 Only the outer edges of sample MOG.85.F03.S18 have transformed into a green copper chloride pigment. Backscattered electron image of section (a) and an ESEM X-ray phase map of the same section shows Cl-enrichment in blue and Cu-enrichment in pink (b). The centers of many of the particles are still Cu-rich, indicating that the transformation from azurite to copper chloride happens from the outside in.

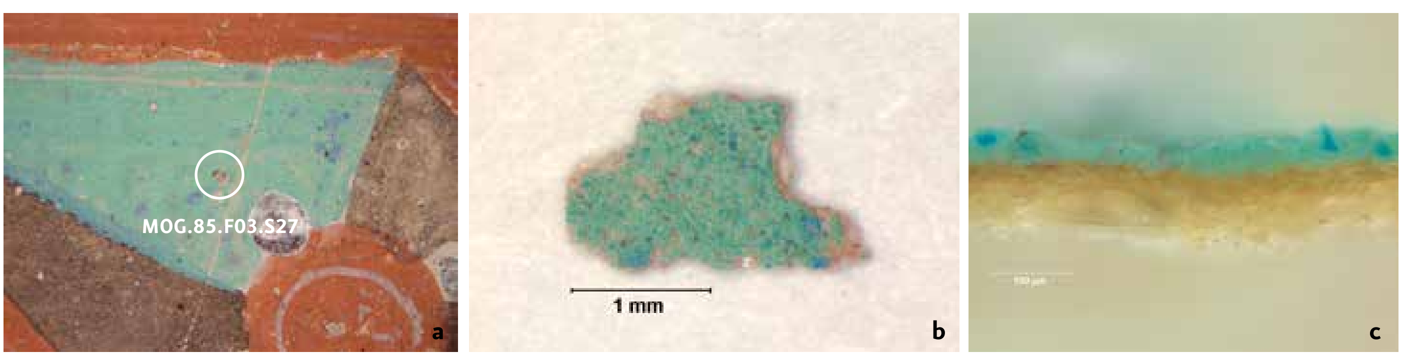

Fig. 15.23 Location of an almost entirely altered azurite sample (MOG.85.F03.S27) from the west ceiling slope (a). The unmounted sample under magnification appears more green than blue (b), and the polished cross section shows little blue remaining (c).

SAMPLE NUMBER	DESCRIPTION	ΔE^*_{94} (30 MIN)	ΔE^*_{94} (60 MIN)	RESULTS
MOG.85.F03.S01	East wall, southeast corner. Plum-colored organic lake over ground.	0.4	—	Possible Change ≥BW3
MOG.85.F03.S02	East wall, southeast corner. Dark plum-colored pigment over ground.	0.5	0.45	Possible Change ≥BW3
MOG.85.F03.S19	South wall, east side. Pink-colored organic colorant suspected. No Fe, Hg, or Pb.	0.2	0.2	No Detectable Change
MOG.85.F03.S21	South wall, east side. Brown translucent color. Possible mix of yellow organic colorant with vermilion (SEM-EDX).	0.6	0.7	Possible Change ≥BW3
MOG.85.F03.S27	Ceiling panel, west side. Green layer. Azurite transformation to a green copper pigment suspected.	0.1	0.2	No Detectable Change
MOG.85.F03.S28	Ceiling panel, east side. Red lead and vermilion (SEM-EDX).	1.7	2.6	Definite Change =BW2–3
ISO BW1	ISO Blue Wool #1 Standard	5.5	8.1	
ISO BW2	ISO Blue Wool #2 Standard	2.9	4.0	
DETECTION LIMIT		0.4	0.6	

Table 15.1 Summary of Light Sensitivity of Paint Samples from Cave 85

the cave, which corresponds to the pattern of alteration of azurite. However, pH tests undertaken on twenty plaster samples using Merck indicator strips found a range from 6.5 to 7.5 with an average of 6.9, indicating that the plaster is not alkaline and therefore unlikely to contribute to the conversion.

The alteration process occurs on blue crystals of azurite from the outside in. This is illustrated in a cross section of sample MOG.85.F03.S18 from an area on the east slope where the blue has only partially altered (fig. 15.21). The particles have blue centers with green edges. ESEM-EDX elemental maps of copper and chlorine show a progressive inward transformation of the blue azurite particles into green copper chloride (fig. 15.22).

In sample MOG.85.F03.S27 the azurite conversion process is even more progressed (fig. 15.23). The area sampled appears almost entirely green with only traces of blue remaining. In cross section only a few remaining azurite crystals are visible at the center; the rest have been completely converted into green. ESEM maps show concentrations of copper and chlorine in the paint layer.

Light exposure tests on sample MOG.85.F03.S27 from an area of green identified as azurite transformation showed no color change as it is not typically a light-sensitive pigment (Druzik 2010, 460) (see table 15.1).

Orpiment Alteration

In several areas of the cave, there is a brownish gray color that appears to be altering into white. On the upper part of the ceiling slopes small bells hanging from the tassel decoration illustrate the various phases of this conversion from brownish gray into white. The bells on the east slope appear white with black line drawing and a thin gray-colored wash on top (~5 μm thick) (fig. 15.24). By contrast the bells from the north slope

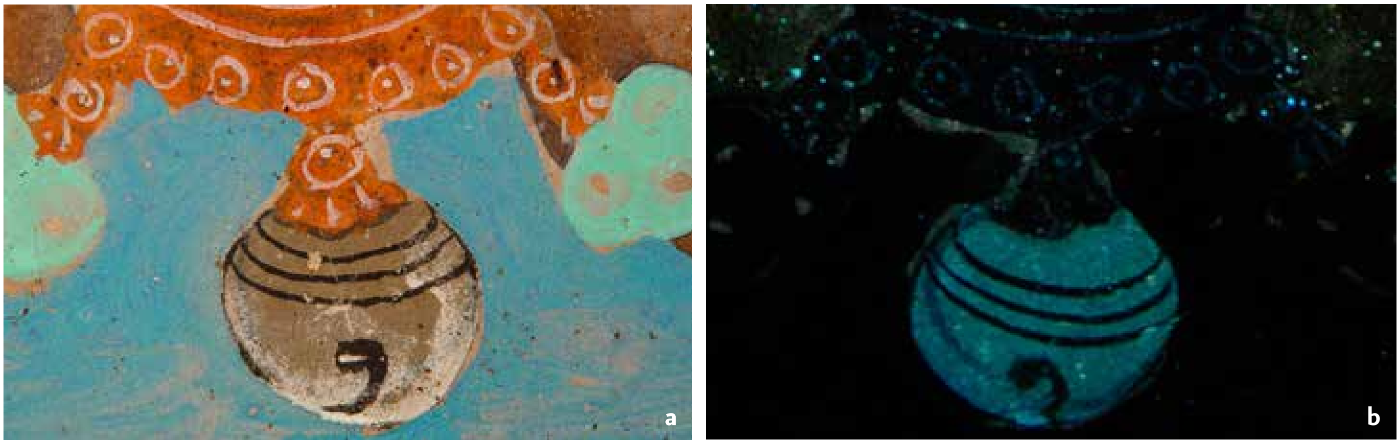

Fig. 15.24 Sample MOG.85.F03.S10 was taken from a bell on the east ceiling slope. The bell has a thin brownish gray wash with black line drawing (a). Under UV-induced fluorescence the organic-containing wash fluoresces blue (b).

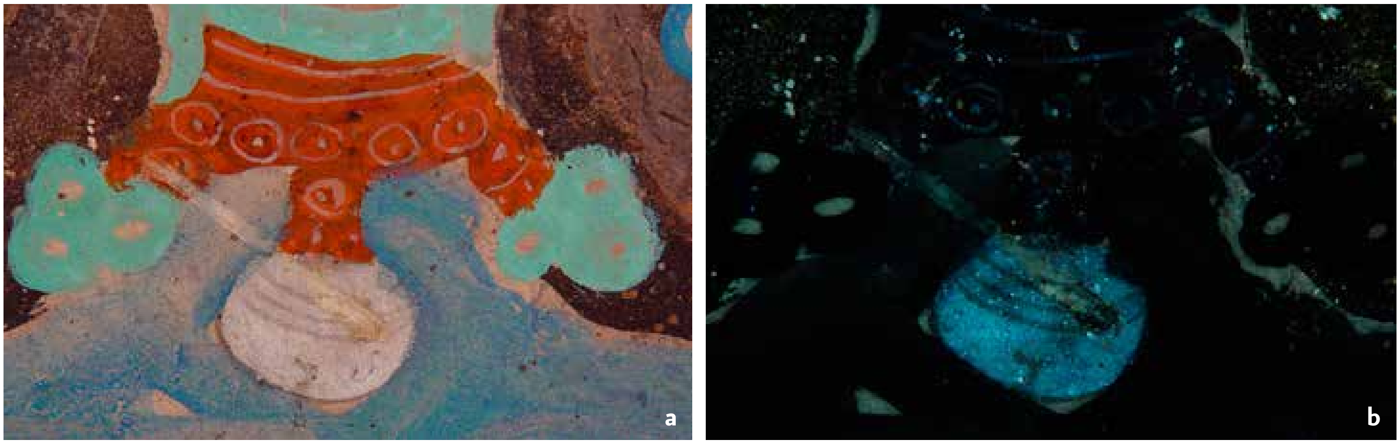

Fig. 15.25 Sample MOG.85.F03.S09 was taken from a bell on the north ceiling slope. The bell appears white with faint black line drawing (a). Under UV-induced fluorescence the bell fluoresces blue, indicating an organic-containing material on the surface similar to sample MOG.85.F03.S10 (b).

appear all white with the black line drawing only barely visible, though under UV illumination the lines can still clearly be read (fig. 15.25). Also under UV, both the altered and unaltered bells exhibit a strong UV-induced fluorescence in the blue region, suggesting the presence of a similar fluorescing compound on both bells. This fluorescence is also visible in cross section despite the thinness of this paint layer.

Cross sections from the bell decoration on the east slope, sample MOG.85.F03.S10, and from the north slope, sample MOG.85.F03.S09, both show a very thin paint layer, indicating that it is most likely an organic-containing wash (figs. 15.26, 15.27). The black line drawing is also visible in both sections.

The composition of the thin gray wash was not identified. A white spongy material on the painted surface was also observed in areas that exhibit the conversion into white. The fluffy material is thought to correspond to the presence of round amorphous globules, which can be seen in cross section, typically found within the ground layer and/or above the surface of the paintings.[8] The morphology of these globules and their position within the painting stratigraphy seem to indicate that they have expanded and pushed the paint layer upward. The cross section of sample MOG.85.F03.S09 and the elemental maps show the globules are rich in arsenic (fig. 15.28). These globules are not present in sample MOG.85.F03.S10 (unaltered area) where no arsenic was detected.[9]

The presence of arsenic in the altered areas suggests an alteration of an arsenical pigment, such as orpiment or realgar. In Cave 85, yellows are conspicuously absent, though orpiment was identified in two samples and has been documented in

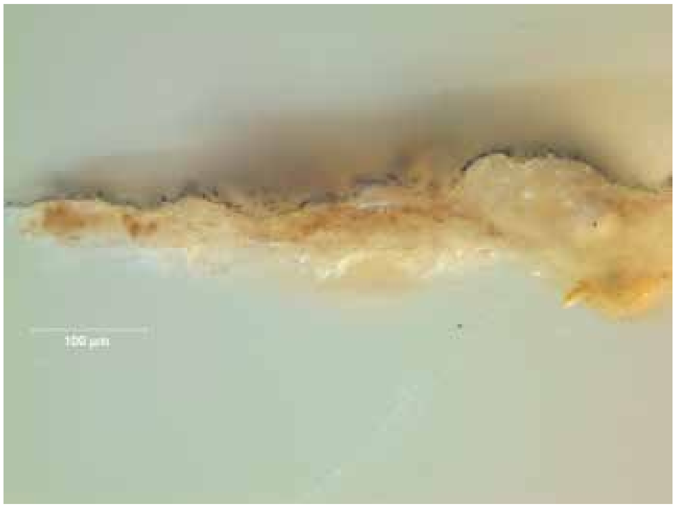

Fig. 15.26 Polished cross section of sample MOG.85.F03.S10 has only a thin paint layer that could be an organic colorant–containing wash.

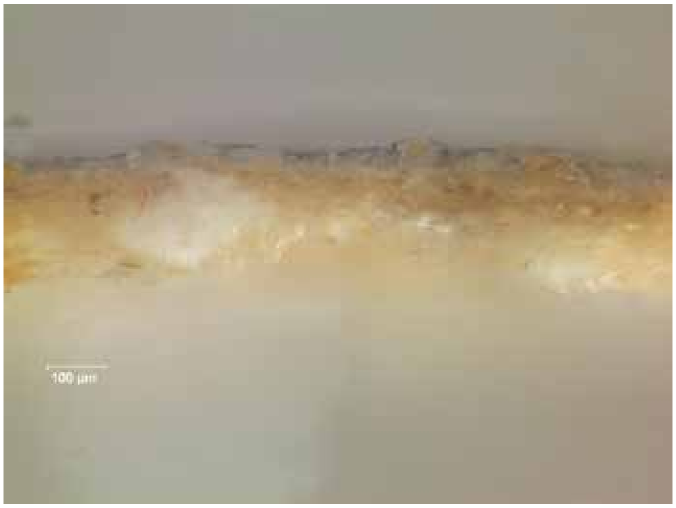

Fig. 15.27 Like the previous image, sample MOG.85.F03.S09 also has only a thin wash. Notably, this sample has large globules (100 µm) thought to be associated with the alteration of the brownish gray wash to white. These globules can be seen in the ESEM X-ray phase maps (fig. 15.28).

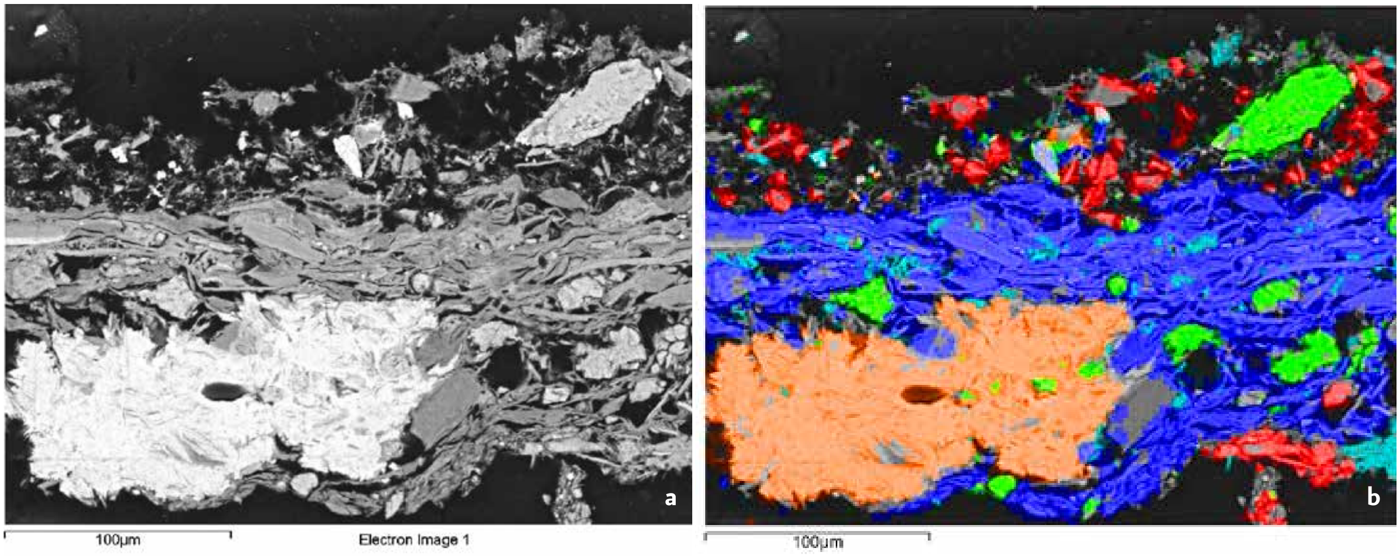

Fig. 15.28 Backscattered electron image of sample MOG.85.F03.S09 showing large globules (a). The ESEM X-ray phase map (b) shows arsenic enrichment in the globules (orange). It is thought that the sample may have contained orpiment that has transformed into arsenic trioxide.

several comparable Chinese wall paintings.[10] Under certain conditions, orpiment can transform into white arsenic trioxide (As_2O_3). Exposure to light, ozone, and heat is known to affect the rate and extent of the reaction (FitzHugh 1997; Walker 1999; Wallert 1984). However, the absence of arsenic in sample MOG.85.F03.S10 does not support this theory, and further study is required in this area.

Organic Material Alteration

In addition to the inorganic pigment alteration described above, organic materials including binding media, organic colorants, and surface coatings are susceptible to alteration, deterioration, or loss. Again, the distribution pattern of deterioration is concentrated toward the west end of the cave.

One example is the difference in ground color from the east to the west end of the cave. The east end ground is pinkish beige in color, while the west end ground is stark white (see fig. 13.20). This effect has also been observed in other caves at Mogao and also at the Yulin Grottoes. The phenomenon is well illustrated on the south wall of Cave 85 where the paintings on the eastern side still exhibit the colored ground while the western side is white, possibly indicating fading or deterioration of an organic colored wash (see chap. 13).

Examination of cross sections of samples taken from colored (85NQ01PE11) versus uncolored (85NQ01PE12) areas of ground from the south wall both fluoresced under UV indicates remaining traces of an organic wash even in areas where no color remains (fig. 15.29). ESEM-EDX analysis showed no difference in the inorganic and mineralogical composition of the two samples, further supporting the possibility that fluorescence is due to an organic colorant.

GC/MS analysis indicated the presence of carbohydrates in both samples but in much higher quantities in the colored ground, sample 85NQ01PE11, with a 2.6% carbohydrate composition which correlates with fruit gum and/or plant mucilage and a 0.12% amino acid profile which could also indicate the presence of fruit gum (see table 13.2). It did not contain hydroxyproline, a typical indicator for animal glue. Results of the white ground, sample 85NQ01PE12, had only 0.75% carbohydrates, possibly due to the loss of organic material. In general, organic materials, both polysaccharides and proteins, were low, often below detection limit, in samples from the deteriorated west end of the cave. It is therefore likely that the organic materials have deteriorated, visible as loss of the colored ground.

Oxidation of organic materials can lead to fading of colorants as well as the deterioration and loss of binders and coatings. Factors that contribute to this deterioration include light, alkalinity, salts, moisture, and the presence of copper pigments.[11] Preliminary color fading, using a microfadometer, was carried out on paint samples from Cave 85 thought to contain organic colorants (Whitmore 1999). Samples MOG.85.F03.S01 and MOG.85.F03.S02 from a plum-colored area showed borderline change, while MOG.85.F03.S09 had results below the detection limit and MOG.85.F03.S21 showed no light sensitivity, indicating that the organic pigments, if originally present, are no longer at risk of fading (Druzik 2010) (see table 15.1).

Summary

Over the centuries the Late Tang dynasty paintings in Cave 85 have suffered from deterioration of various kinds through exposure at some point when the cave facade at the entrance was lost; flooding of the base when the Daquan River overflowed its banks, resulting in complete loss of the painted plaster to a height of one meter from the floor; and cyclical dissolution and crystallization of hygroscopic salts, which has led to detachment and collapse of the painted plaster, plaster disruption, and exfoliation and the gradual loss and alteration of pigments and colorants.

The most serious and ongoing of these conditions are those associated with soluble salt activity concentrated toward the west end of the cave. The difference between the west and east ends is striking. The west end has suffered much loss due to the higher concentrations of salts present, affecting both in-depth and surface conditions, while the east end remains stable.

The findings of the diagnostic investigation were crucial for the development of conservation treatments in the cave and for striving to prevent further deterioration (see chap. 17).

Fig. 15.29 Location of sample 85NQ01PE11 from an area of colored ground on the east side of the south wall (a) and sample 85NQ01PE12 from an area of white ground on the west side of the south wall (b).

Notes

1. Testing was undertaken in 1999 by the Dunhuang Academy Conservation Team.
2. Flaking was also observed to be concentrated in areas of plaster joins where the plaster is generally thicker. Large areas of flaking and some detachment occur at the interface between the plaster joins on the west and north walls.
3. During this episode the east side of the cave remained stable and unchanged.
4. Undertaken by the Dunhuang Academy 1999–2000. Results presented in the report, "Results of Painting Flakes collected on the Cave 85 Floor," 16 February 2000.
5. Samples of the adhesives polyvinyl acetate emulsion (PVAc) and polyvinyl alcohol resin (PVA) that are used in conservation treatments at Mogao were tested at the GCI. Using pH paper wetted with de-ionized water, the pH of the PVAc was found to be between 5 and 6. An FTIR spectrum of a dried film of the PVAc emulsion closely matched a standard reference spectrum of PVAc. Likewise, the spectrum of PVA from Mogao matched closely a reference spectrum of PVA.

   A gravimetric procedure was used on white paint sample 85XQ98PE2 (18%) and red paint sample 85XQ98PE2 (16%). Paint flakes were weighed and treated with 1-methyl-2-pyrrolidinone, a solvent effective in extracting dried PVAc but much less effective in dissolving PVA. The solution was then dried and the amount of resin calculated as a percent of the sample weight. FTIR analysis performed on the clear film extracted from the paint flakes confirmed that the resultant material is PVAc.
6. During this period the monitoring station in Cave 85 lost power. However, a Japanese monitoring station set up in Cave 98 provided comparable data to the climate in Cave 85.
7. Lime-based wall paintings can also show similar deterioration caused by poorly slaked lime containing calcium oxide (CaO) that hydrates and carbonates, causing a significant volume increase and the formation of crater losses.
8. The formation of "aggregations" has been reported in the alteration of realgar, a naturally occurring orange-red arsenic sulfide, into pararealgar. The conversion process involves a volume change that causes the degraded pigment to become friable and powdery and liable to dissociate from the painted surface (Green 2001, 46). This alteration phenomenon, caused primarily by light, is well studied (Douglass et al. 1992).
9. Globules were also found in samples of an altered cartouche from the south wall exhibiting the same type of alteration (MOG.85.F03.S25).
10. Orpiment has been found at Mogao (Guo 1997; Xu et al. 1983) and the Yungang Grottoes at Datong (Piqué 1997). Orpiment is a known pigment in China. One of the best-known sources of orpiment was a deposit in the far southeastern part of what is now Gansu Province (Schafer 1955, 76). There is little evidence of realgar's use as a pigment because it lacks brilliance and tends to disintegrate into a mixture of orpiment and arsenlite (Schafer 1955, 79).
11. Copper ions ($Cu2^{+}$) can act as a catalyst in the oxidation and hydrolysis of carbohydrates, especially in alkaline conditions.

CHAPTER 16

Salt-Induced Deterioration

The diagnostic investigation identified soluble salts, activated by humidity, as the principal cause of deterioration in Cave 85 (see chap. 15). Research was therefore undertaken to understand the processes of salt enrichment and deterioration in order to develop conservation interventions to stabilize the paintings and mitigate further deterioration (see chap. 17).

Salts, Water, and Deterioration

Moisture and soluble salts can cause great harm (fig. 16.1). Though the mechanisms by which salts cause deterioration are not entirely understood, it is generally agreed that it is due to mechanical disruption by forces exerted during a phase change of the salts—typically crystallization from an aqueous solution or due to a hydration state change.[1] Hygroscopic salts in porous materials cause deterioration through cycles of this deliquescence and recrystallization or where volume variation in particular salts also occurs (Pühringer 1983). There is still a poor understanding of what happens within porous materials and what the thermohygrometric conditions actually are, their rate of change and what the influence of past conditions and treatment might be on present behavior (Cather 2003).[2]

Fig. 16.1 Salts are responsible for the loss of surface painted decoration on the west wall of Cave 85.

Identification of Salt Species

Analysis of samples of white crystalline efflorescence from the base of the east wall in Cave 85, both behind and on the surface of the 1940s plaster repairs, in an area of previous flood damage, found 82% sulfates, 18% chlorides, and 0.3% nitrates by ion chromatography. Sodium chloride (NaCl) and sodium sulfate ($NaSO_4$) were then identified by X-ray diffraction (XRD) (fig. 16.2). Sodium chloride was also identified by XRD from efflorescence collected from the surface of the conglomerate on the west ceiling slope, following collapse of an area of painted plaster in 1996. Traces of sulfates were also found in this sample using sulfate test strips[3] and a barium chloride test for sulfate.[4]

The presence of soluble salts at the Mogao site has been reported also in other studies. Salt investigation undertaken by the Tokyo National Research Institute of Cultural Property and the Dunhuang Academy in two caves, 194 and 53, found sodium chloride in Cave 194, an upper-tier cave, and calcium sulfate (gypsum, $CaSO_4 \cdot 2\ H_2O$) in Cave 53 (Kuchitsu and Duan 1993), located at ground level. No sodium chloride was reported in Cave 53 (Kuchitsu and Duan 1997, 246).[5] This is different from the data from Cave 85, also a ground-level cave, where sodium chloride is the main salt (other than at floor level where the cave had flooded and sulfate predominated) that has been identified throughout.

Fig. 16.2 A salt sample was taken from the conglomerate behind a plaster repair in Cave 85 (a). XRD results (b) identified sodium sulfate and sodium chloride. Sodium chloride is the primary salt in the cave.

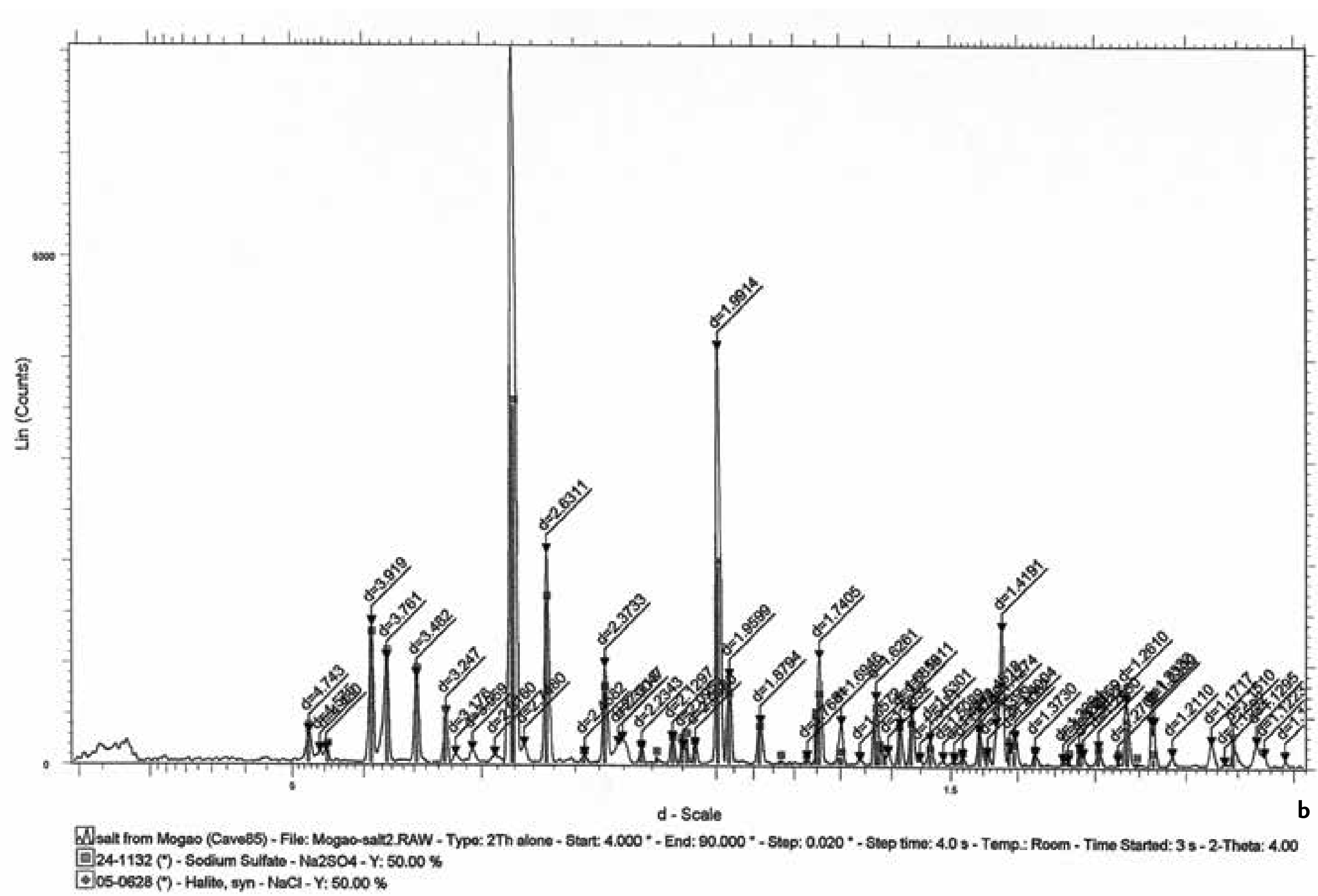

Investigation of Salt Profile

Investigation of the salt distribution in Cave 85 consisted of core sampling of both the conglomerate and the clay plaster. Though invasive in nature, coring provided stratigraphic information. Less invasive aqueous extraction methods were also tried; however, results depended on the method of extraction, the nature of the porous substrate, and the solubility of the salts being extracted. Aqueous extraction also does not provide any stratigraphic information and is weighted in favor of more soluble ions. Aqueous extractions have further limitations in Cave 85 because the painting is composed of water-sensitive and in some cases water-soluble materials, including gum and glue binding media and clay containing plaster.[6] Identification of salts through solid samples can provide a useful range of data; however, solid salt species identified are a consequence of the prevailing thermohygrometric conditions and may differ as conditions change (Cather 2003).

Analysis of soluble ionic species in core samples was undertaken using ion chromatography in the laboratory[7] or on site using ion-specific test strips and a chloride ion–specific electrode. After identification of sodium chloride as the predominant salt species in the cave, the equivalent amount of NaCl was stochiometrically calculated using results from the chloride ion–specific electrode. Microequivalents per gram were reported (mass % divided by molecular weight and charge of ion) (fig. 16.3).

Fig. 16.3 Analysis of samples was undertaken using a chloride ion–specific electrode at the Dunhuang Academy scientific laboratory. Ion chromatography was also used on samples brought back to the GCI.

Salt Distribution in Conglomerate

Information on salt content in the conglomerate was limited to areas of plaster loss where core drilling was possible, generally at the base of the walls in the flood zone.

Sixteen macro-cores (12.5 mm diameter) were taken along the base of the walls, all below 2 m from floor level (fig. 16.4). Each core was sampled in four depth increments of 10 cm, and the chloride and sulfate profiles of the rock material were measured.[8] The soluble components of samples were extracted with water, and ion-specific test strips were used to estimate the content of chloride and sulfate. In general, results showed enrichment of chloride and sulfate content at the surface up to 10 cm. Moreover, the salt content in the west wall conglomerate greatly exceeded that of the three other walls (see Appendix 16.A).

Macro-cores were also taken in Cave 98, a cave with a similar distribution of deterioration. Chloride ions were found as the predominant component (see chap. 14).

Salt Distribution in Plaster of Cave 85

Micro-core sampling of the plaster provided a topographic and stratigraphic distribution of salt in the upper 10 mm. Forty-seven micro-core samples were taken throughout the main chamber, in areas where the paint layer was lost, in four increments (approximately 0–2, 2–5, 5–7, 7–10 mm) (fig. 16.5). The increments roughly correspond to the layers in the painting stratigraphy, including the ground, the fine plaster, and part of the coarse plaster (fig. 16.6).

Results exhibited an expected trend of higher salt enrichment toward the west end of the cave on a northwest to southeast axis, matching the overall pattern of deterioration observed during the condition assessment for both in-depth and superficial deterioration.[9] The soluble salt content in the plaster (expressed in weight percent of sodium chloride per 100 g of plaster) was highest on the west wall and on the west end of the

Fig. 16.4 Core samples were taken of the conglomerate at the base of the wall (a, b). Samples were then weighed and analyzed for soluble ion content (c).

north wall between 2% and 3.9% (fig. 16.7). The west end of the south wall also had high values but generally less than 3%. The soluble salt content was lowest on the east wall and on the east end of the north and south walls, with values less than 1% (fig. 16.8) (see Appendix 16.B).

Sodium and chloride made up the highest percentage of the total soluble salt content of the samples. Results showed that the profile for chloride closely mirrors that of sodium, again indicating that the major species in the cave is sodium chloride.

Soluble ion content was plotted by sampling increments on the east and west walls (see Appendix 16.C). The general trend showed chloride and sodium profiles lower at the surface (0–2 mm) and highest at the second increment (2–5 mm). This indicated enrichment of NaCl below the surface in the fine plaster and roughly corresponding to the interface between the coarse and fine plaster layers.

Sulfate ion content of the micro-cores was overall lower but was still present in increasing amounts toward the west end of the cave, generally in the upper 0–2 mm. Sulfate ion was also found in high percentages at the base of the walls. Interestingly, a low concentration of sulfate was also found at the 0–2 mm increment in four micro-core samples taken on the east wall. Though overall ion content is very low on this wall, the sulfate amounts are higher than the amounts of sodium and chloride. Though conjecture, the presence of sulfate may be attributable to original technique and could relate to the possible use of alum as a sealant on the ground or plaster (see chap. 13).

Comparison with Caves 61 and 98

Because the caves are excavated into the bulk of the mother rock and the west walls are the primary surface of evaporation, they have a far larger potential reservoir of salts than the east walls, which form the outer face of the caves. One would therefore expect the west walls of caves to show greater deterioration than the east walls. Comparative salt distribution studies were carried out in Caves 61 and 98, two ground-level caves of similar size and date that have also previously flooded and suffered total loss of painted plaster to a height up to about 1 m from the floor (see table 16.1). Caves 85 and 98 both exhibit the same types and distribution of deterioration at their west ends. Cave 61, however, has survived in better condition, with severe salt-related deterioration generally confined only to the base of the walls where

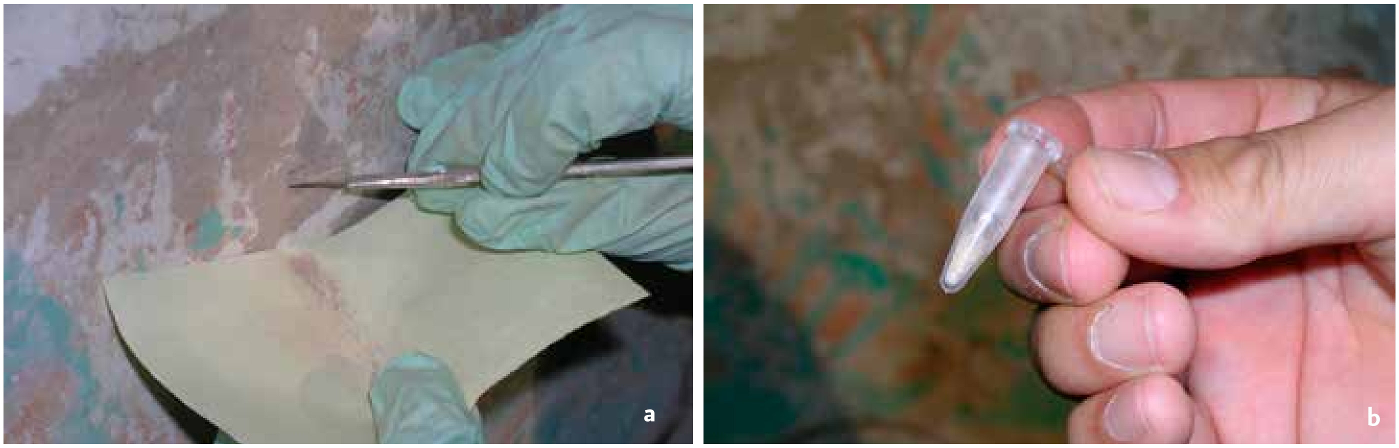

Fig. 16.5 Micro-cores of the plaster were taken using a scalpel at different incremental depths to get a salt profile (a, b).

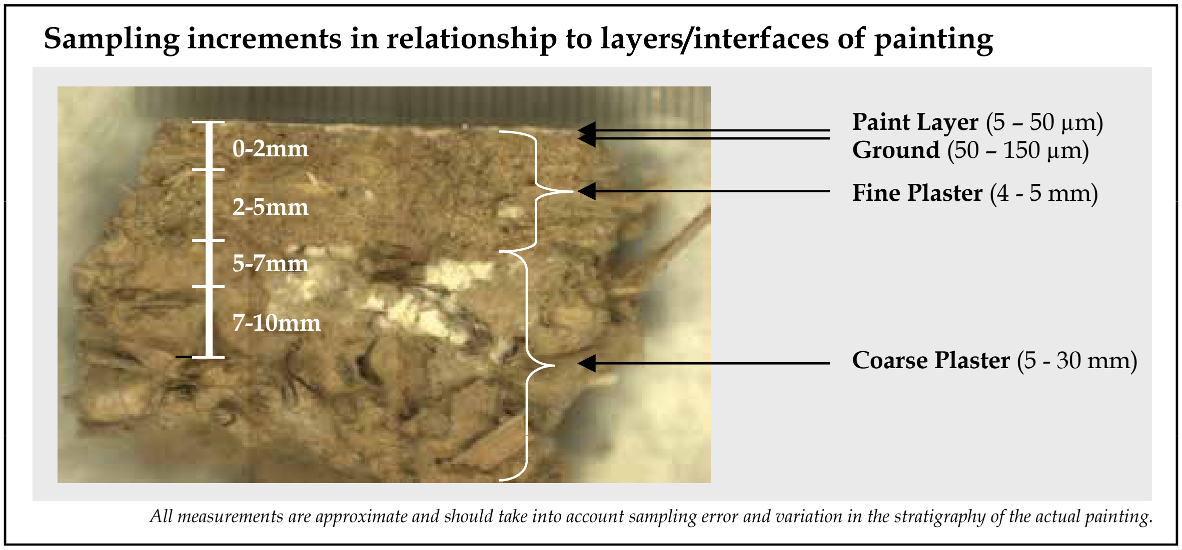

Fig. 16.6 Diagram of the painted plaster showing layers and interfaces in relation to actual micro-core sampling increments.

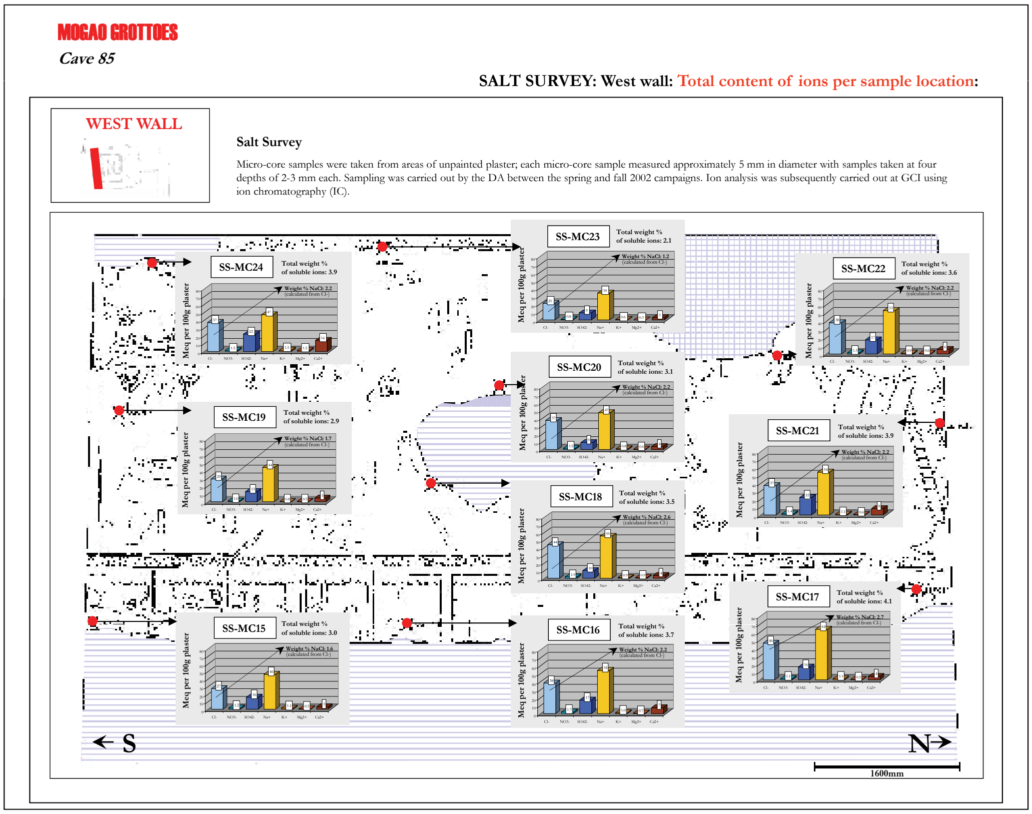

Fig. 16.7 Total ion content was highest on the west wall and the west end of the north wall, between 2.0% and 3.9%.

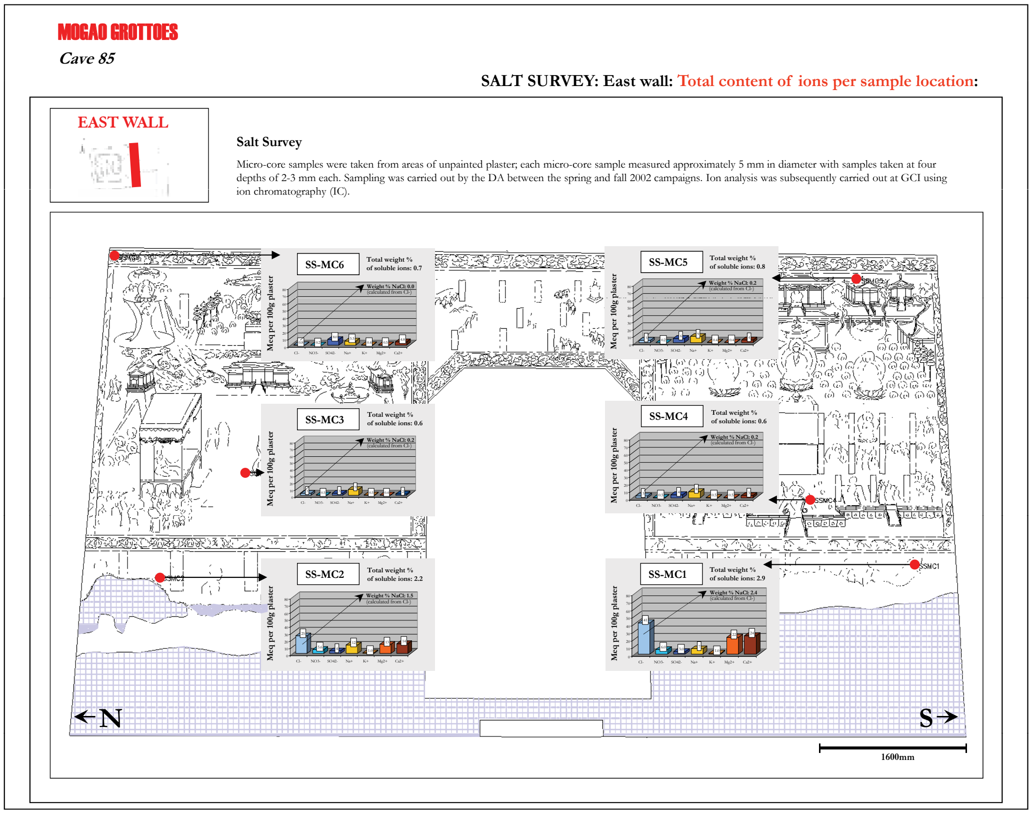

Fig. 16.8 Total ion content was lowest on the east wall and on the east end of the north and south walls, with values less than 1%.

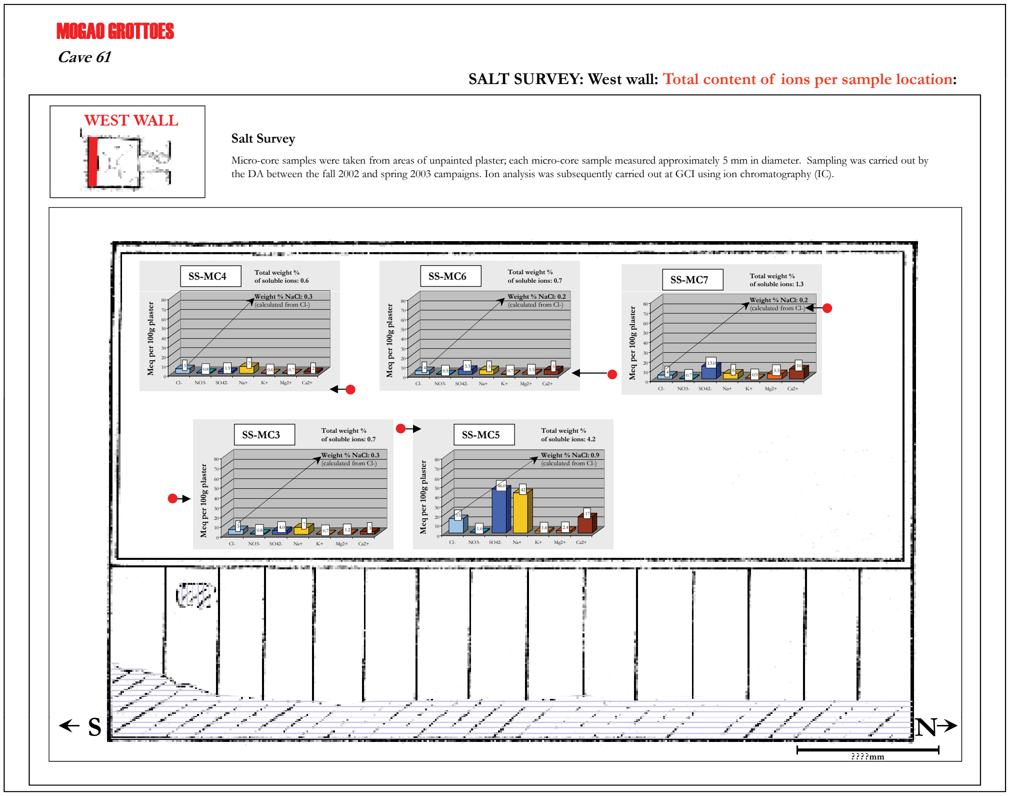

a

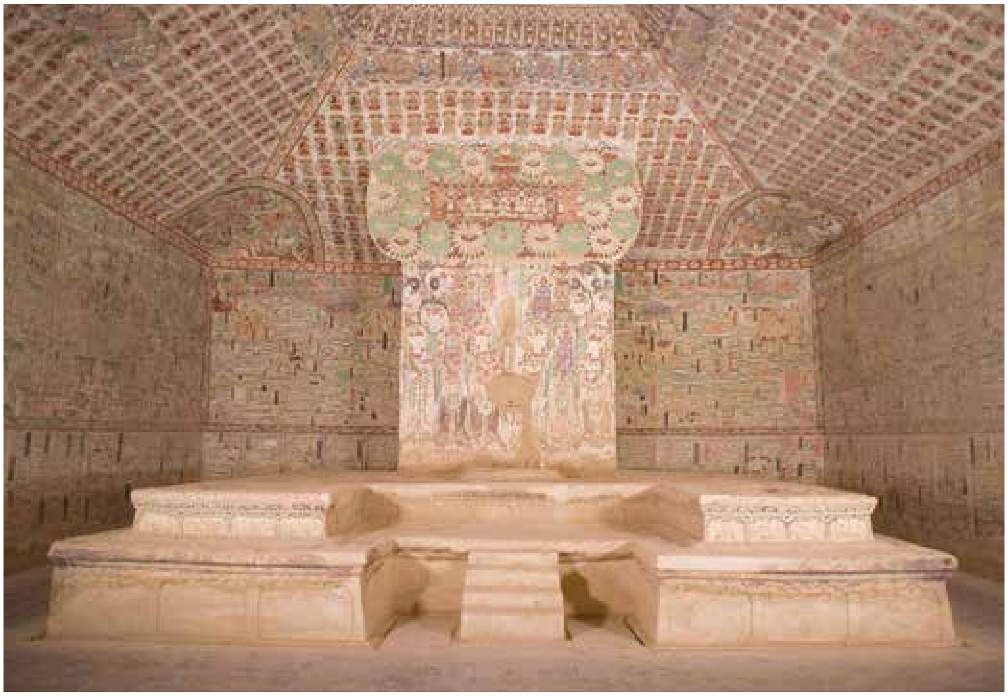
b

Fig. 16.9 The total ion content in Cave 61 is low, between 0.2 and 0.3 weight % NaCl, with no enrichment of salts at the west wall (a). Correspondingly, the west wall does not show the same salt-induced deterioration as in Cave 85 (b).

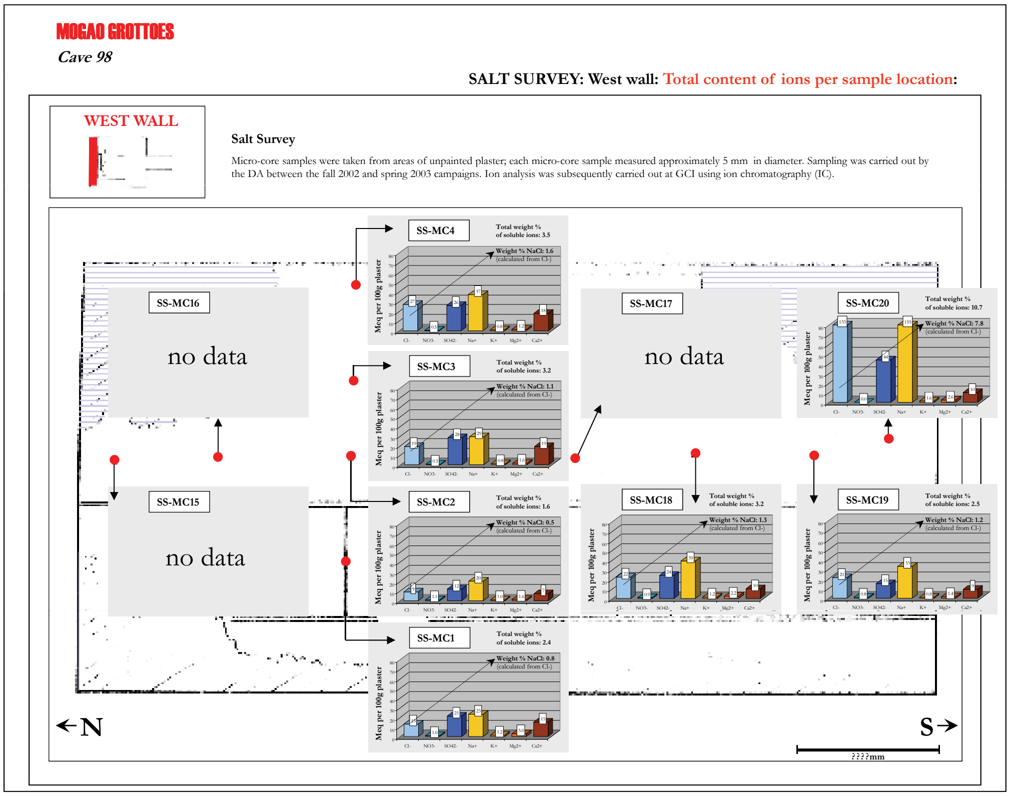

Fig. 16.10 The west wall of Cave 98, like Cave 85, has significantly higher values of soluble ions than the east wall and compared to the west wall of Cave 61. It also suffers from the same types and distribution of deterioration as Cave 85.

flooded. The resulting plaster salt profiles showed a significant difference in the concentration and distribution of soluble salts between Cave 61 and Caves 85 and 98. In Cave 61 the soluble ion content was low, between 0.2 and 0.3 weight % NaCl, and there was not a higher concentration of salts at the west end. In Caves 85 and 98 much higher values of soluble ions were found, with significant increase toward the west end (figs. 16.9, 16.10) (see Appendixes 16.D, 16.E).

The differences may be best accounted for in terms of geological inhomogeneities. Caves 85 and 98 possibly have more fractured rock and stratigraphic differences such as highly porous sandstone lenses intercalated with the conglomerate than Cave 61 (Agnew et al. 2010) (see chap. 6).

Source of Soluble Salts

Possible sources are

- Conglomerate;
- Flooding of the Daquan River or use of river water in the original plastering of cave walls;
- Mud from the Daquan River used in the original plastering of cave walls.

Conglomerate at the site contains varying quantities of sodium chloride, sodium sulfate, magnesium sulfate, calcite, and gypsum, depending on the area, and is believed to be the main source of salts in Cave 85.[10]

Salts may also have been introduced during periods of past flooding of the Daquan River. The river water was found to contain high levels of soluble ions and sulfates in particular (Chen 2008, 133; Duan 1988, reproduced in Kuchitsu and Duan

	CAVE 61	CAVE 85	CAVE 98
DYNASTY	Five Dynasties	Late Tang	Five Dynasties
DATE OF CONSTRUCTION	947–51	862–67	915–25
TIER/LEVEL	Lower	Lower	Lower
CAVE SIZE	Large	Large	Large
CONDITION SUMMARY	• Large loss in the southeast corner of ceiling • Losses along base of the wall to a height of 0.40 m from past flood	• Southeast to northwest axis of worsening deterioration with a concentration toward the west end of the cave • Large plaster losses at west end of cave, as well as plaster disruption and areas of detachment • Losses along base of the wall to a height of 1 m from past flood	• Concentration of deterioration at the west end of the cave • Large plaster losses at west end of cave, as well as plaster disruption and areas of detachment • Losses along base of the wall to a height of 0.50 m from past flood
TOTAL NUMBER OF MICRO-CORE SAMPLES	10 micro-core samples	47 micro-core samples	20 micro-core samples
WEIGHT % NaCl (calculated from Cl^- ion)	Very low throughout the cave 0.2–0.4% (excluding MC5 from the west wall, which at 0.9% is possibly an error) (see Appendix 16.D)	Higher on the west wall: 2.1% versus 0.2% on the east wall (excluding SS-MC2 and SS-MC1, which have unusually high values given their location in the flood zone) (see Appendixes 16.B and 16.C)	Higher on the west wall: 1.1% versus 0.2% on south and east walls (excluding SS-MC20 from the west wall, which at 7.8% is possibly an error) (see Appendix 16.E)

Table 16.1 Comparison of Cave 85 with Caves 61 and 98

1997), which would account for the concentration of sulfates at the base of the walls (see table 16.2).

Salts are also present in the mud from the Daquan River used to plaster the cave walls. Salts collected from the riverbed were analyzed and compared with salts from the exposed conglomerate at the base of the wall in Cave 85. Results show a similar distribution, with high sulfate content, followed by chlorides and scant nitrate, which roughly matches that found in the river water (see table 16.3).

Behavior of Hygroscopic Salts

Deliquescence Determination of Salt Mixtures

At standard conditions for temperature and pressure, pure NaCl starts absorbing water vapor when the relative humidity reaches 75%, the equilibrium relative humidity, RHeq, for this salt.[11] For salt mixtures, as is the case in Cave 85, the situation is more complex (Price 2000). Salt mixtures will deliquesce at values below the RHeq of individual pure species (Price and Brimblecomb 1994; Bionda 2004). This lowering of the RHeq affects phase transitions and increases rates of deliquescence and recrystallization because environmental RH would tend to vary more over the lower critical value of the mixture.

Isotherm of Salt Mixture from Cave 85

Moisture uptake of a material can be measured by placing it in a sealed chamber whose relative humidity is maintained at a fixed value and constant temperature. The material is periodically weighed until its equilibrium weight is reached. The isotherm of the material is produced by repeating the process for several relative humidity values.

An isotherm of salts from the ceiling of Cave 85 was determined. Weight increases were measured in an electronically controlled environmental chamber maintained at 59%, 64%, 69%, 71%, and 73% RH, at 20°C. From the experiment it was

SAMPLES	Cl^- (mg/l)	NO_3^- (mg/l)	SO_4^{2-} (mg/l)
DAQUAN RIVER WATER (DUAN 1988)	463.19	3.46	824.20
DAQUAN RIVER WATER (CHEN 2008)	418.41	0.55	721.89

Table 16.2 Analysis of Water from the Daquan River

ANALYTE	SALTS COLLECTED FROM THE DAQUAN RIVERBED (WEIGHT%)	SALTS COLLECTED FROM BEHIND REPAIR PLASTER AT BASE OF WALL IN CAVE 85 (WEIGHT%)
CHLORIDE	40%	18%
SULFATE	59%	82%
NITRATE	0.8%	0.3%

Table 16.3 Comparison of Salts Collected from the Daquan Riverbed and Salts from Cave 85 (salt analysis was undertaken using ion chromatography by West Coast Analytical Services)

determined that either a major hydration or deliquescence occurred between 64% and 69% RH. To accurately determine the relative humidity of the transition, the salt mixture was sent to Surface Measurement Systems (Allentown, PA) for establishing its isotherm using Dynamic Vapor Sorption (DVS) equipment.[12] The sample was tested between 60% and 75% RH with increments of 0.5% RH. The resulting isotherm shows percent mass increase starting at 67% RH, the transition RH for this salt mixture (fig. 16.11). The slope exponentially increases above 67% RH as the relative humidity increases.

Images of the salt mixture taken during DVS isotherm measurements show that at 65% RH all sample particles appear to be dry; at 70% RH water droplets begin to form around some of the salt particles; and at 73.1% RH particles are enlarged due to the formation of water around them (fig. 16.12). Thus, the increase of moisture uptake recorded at 67% RH is due to deliquescence.

The above measurements indicate that the salt mixture in the cave will begin to deliquesce once the relative humidity of the cave air adjacent to the wall or within cave walls reaches 67% RH; and the deliquesced salt mixture will recrystallize when the relative humidity returns to less than 67% RH.

Ionic Species Plots and Salt Crystallization Software Programs

Salt mixtures were also analyzed using software modeling programs that attempt to predict the salt species (and their relative amount) that would be in crystal form at different values of relative humidity based on theoretical calculations of salt phase transitions. The ionic concentration of a plaster micro-core from the west wall (sample 18A) and rich in salts was examined with a program called RUNSALT that is based on the ECOS thermodynamic model for the prediction of the behavior of salt mixtures under changing climatic conditions (Price 2000).[13]

The results are plotted as amount of substance (mol) versus RH (%). Starting from RH values above 73% no species exist in crystal form. As RH decreases, at 73% both halite (sodium chloride, NaCl) and thenardite (sodium sulfate, Na_2SO_4) start to precipitate. NaCl completely crystallizes between 73% and

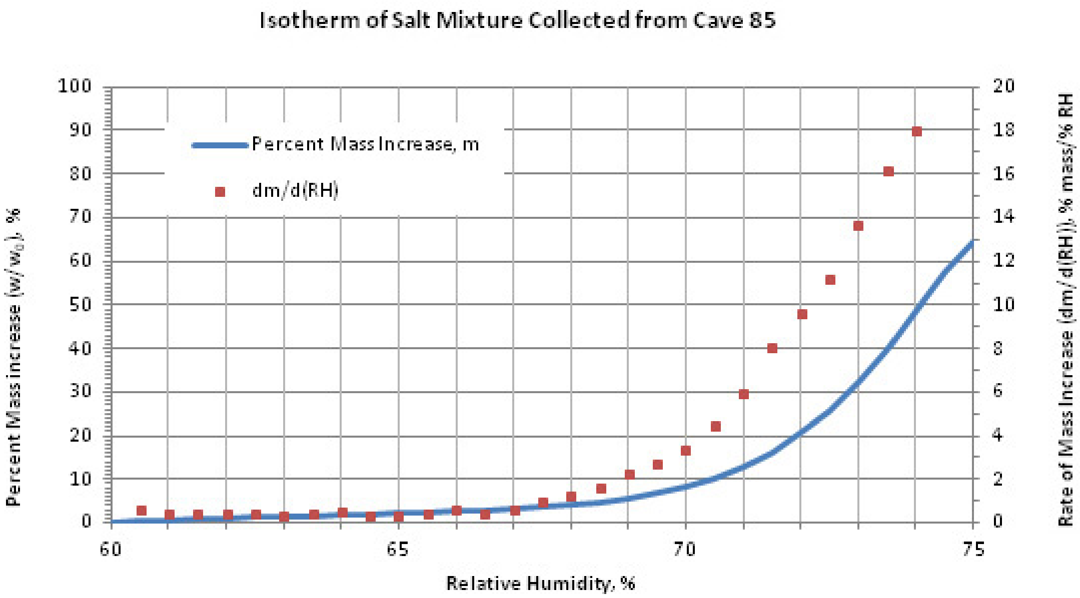

Fig. 16.11 Isotherm by Dynamic Vapor Sorption (DVS) of salt mixture collected from the ceiling of Cave 85. The slope of the percent mass increase or moisture absorption (blue line) is nearly linear for the RH range less than 67% RH. The linear region is confirmed by the constant value of its first derivative, dm/d(RH), plotted on the same graph. In this region, multiple layers of water molecules cover the salt particle. However, the slope starts to increase at 67% RH, which is confirmed by an increase of the dm/d(RH) value. This is an indication of the transition RH of the salt. The slope exponentially increases with RH above 67%.

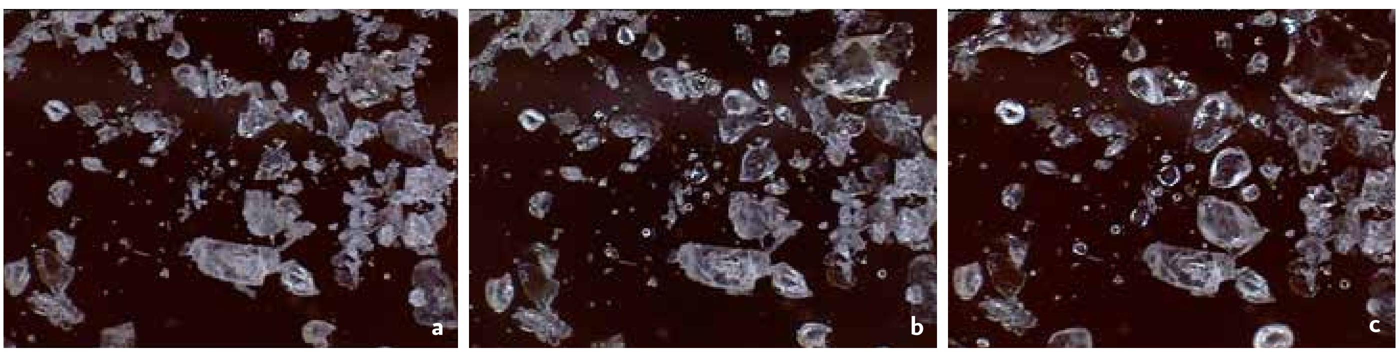

Fig. 16.12 Images of the salt mixture from the ceiling of Cave 85 during DVS isotherm measurement at 65% RH (a), 70% RH (b), and 73.1% RH (c). The crystals begin showing deliquescence at 70% RH with noticeable increase at 73.1% RH.

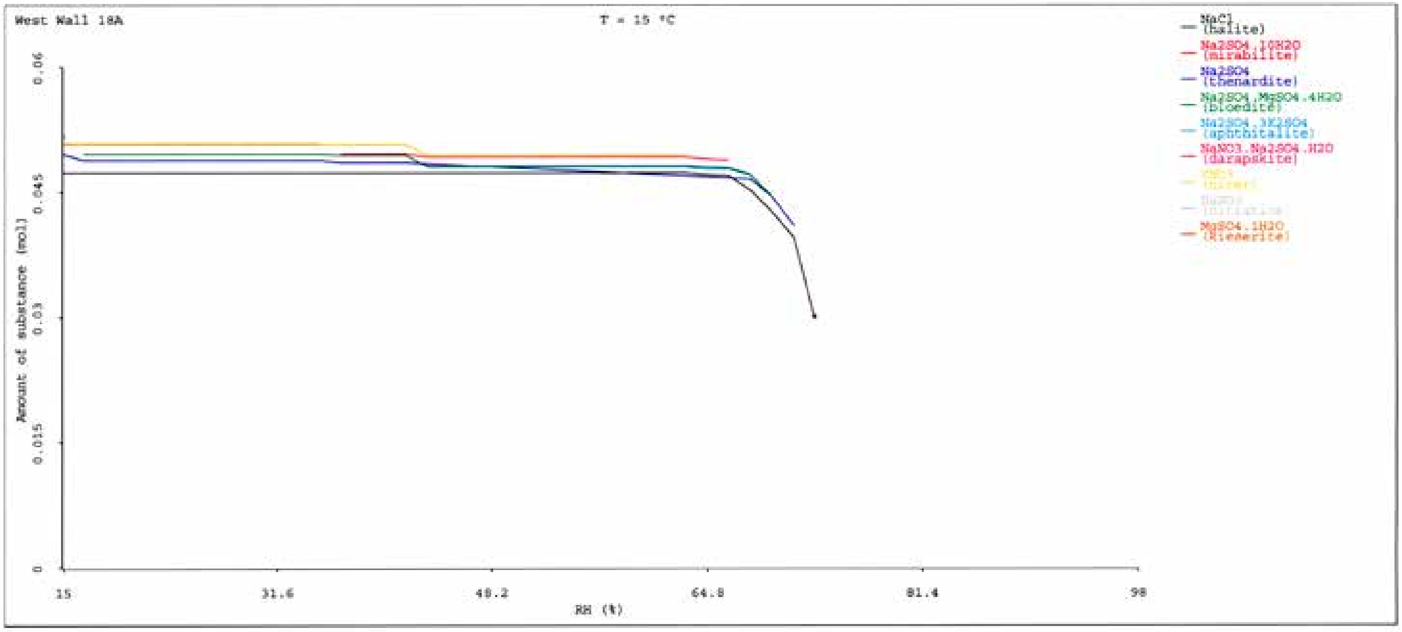

Fig. 16.13 Results of a thermodynamic model for the prediction of the behavior of salt mixtures under changing environmental conditions (using the program RUNSALT) of a plaster micro-core from the west wall (sample 18A) that is rich in salts. These theoretical calculations illustrate the variety of species that can form from a salt mixture as relative humidity changes.

65% RH. The sulfates are somewhat more unstable, and as the environment dries other types of double sulfates, such as aphthitalite (nonhydrated sulfate of sodium and potassium, $Na_2SO_4 \cdot 3\ K_2SO_4$) and bloedite (hydrated sulfate of sodium and magnesium, $Na_2SO_4MgSO4 \cdot 4\ H_2O$), are formed as well. The diagram indicates at low relative humidity (below 45%) the formation of very hygroscopic salts such as niter (potassium nitrate, KNO3) or kieserite (magnesium sulfate, $MgSO_4 \cdot H_2O$) (fig. 16.13).

These are only theoretical calculations, but they illustrate the variety of species that can form from a salt mixture as humidity changes. In the presence of multiple salt species, several humidity equilibria are possible. The dissolution in turn allows for other species that are less soluble to form.

Therefore the theoretical determination of a safe humidity value at which no salt phase changes would occur is difficult; instead this value was determined gravimetrically as a function of relative humidity (RH) and temperature (T), as previously described (Agnew et al. 2010). Ideally, RH and T fluctuations should be kept to a minimum and a stable environment maintained (see chap. 17).[14]

Salt Movement through the Conglomerate and Plaster

In solution, salts can migrate through the porous structure of a wall painting until the ambient RH falls below the RHeq when the salt recrystallizes. Historically, mobilization of salts in Cave 85 may have begun during the original plastering of the walls in the ninth century. Possible prewetting of the walls with river water in preparation for the application of the wet plaster would have solubilized salts in the conglomerate. The plaster would then act as a poultice as it dried to extract dissolved salts in solution from the rock.

Typically, salts originating from the conglomerate migrate in solution to the surface of the cave walls as the water evaporates, leading to enrichment at the surface of cave walls. In time, the salts recrystallize and depending on where they are within the stratigraphy of the painted plaster cause different forms of deterioration. Salts accumulate and recrystallize at the interface between the plaster and the conglomerate, both where separation might already exist and where adhesion is good and also within the plaster itself or at the interface between plaster and paint and ground layers.

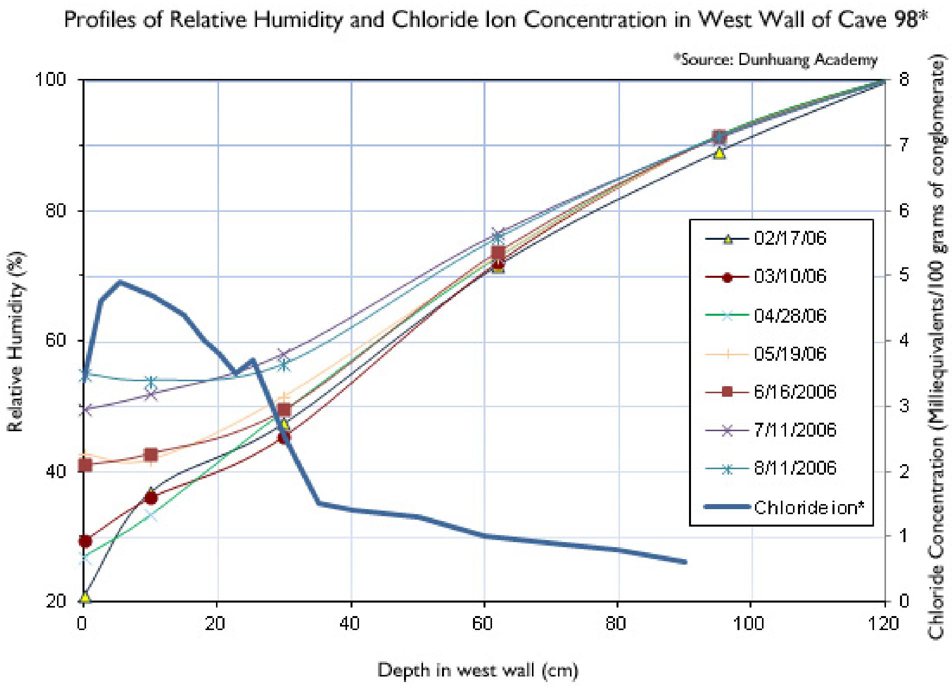

Fig. 16.14 Salt accumulation at the surface and subsurface in the conglomerate in Cave 98.

In desert climates, however, in the absence of direct evidence of water seepage, the mechanism whereby salts enrichment occurs at and near the wall surface seems not to be definitively understood. The actual process of salt enrichment suggested is transport of salts in solution through capillary condensation and migration of solution to the surface, where a zone of enrichment occurs as the water evaporates. In Cave 98 accumulation of salt in the conglomerate is due to the phenomenon of salt "creep" (fig. 16.14). This process is the proposed mechanism for salt accumulation in caves such as 98 and 85 via the intrusion of meteorological moisture and its adsorption by the plaster and rock during periods of high and sustained humidity. Pühringer (1983, 2002b) has proposed a possible mechanism for water vapor–induced migration of soluble salts in porous substrates during atmospheric humidity cycling. This is based on his explanation of the phenomenon of salt creep (Ginell 2005). Over the millennium since the caves were created these two processes abetted each other, leading to the accumulation of salt. Laboratory studies show that salt migration to the evaporative surface occurs driven by a humidity differential. Once enrichment has occurred at the plaster to rock interface and in the plaster meteorological humidity cycles dominate as the active mechanism of deterioration.

Tests were undertaken to understand and confirm the model proposed for the possible migration of salts to the surface of cave walls through the conglomerate and plaster over time within the climatic condition measured in Cave 85. Sodium chloride migration experiments were conducted in which samples of conglomerate and sandstone (approximately 25 mm thick, roughly square) were embedded around four sides in wax and sealed onto a glass container (fig. 16.15). The samples had a paste of NaCl applied to the undersurface and were then cycled between two environmental chambers, one at "high" RH (75–85%) and the other at "low" RH (33–43%).[15] The sample was kept in each chamber until equilibrated (when the inside RH was equal to the RH of the chamber). An RH paper strip was positioned inside the jar to determine when equilibrium was reached. Cycling continued until salts were observed on the surface of the rock conglomerate (Schilling 2001).

It took only five complete cycles for salts to appear on the upper surface of the conglomerate. Sandstone samples, while equilibrating more rapidly than the conglomerate, showed a salt distribution throughout the body of the sample but without the appearance of salt on the upper surface (fig. 16.16). The difference in salt profile between conglomerate and sandstone confirms that pore characteristics play a role in transporting salt.

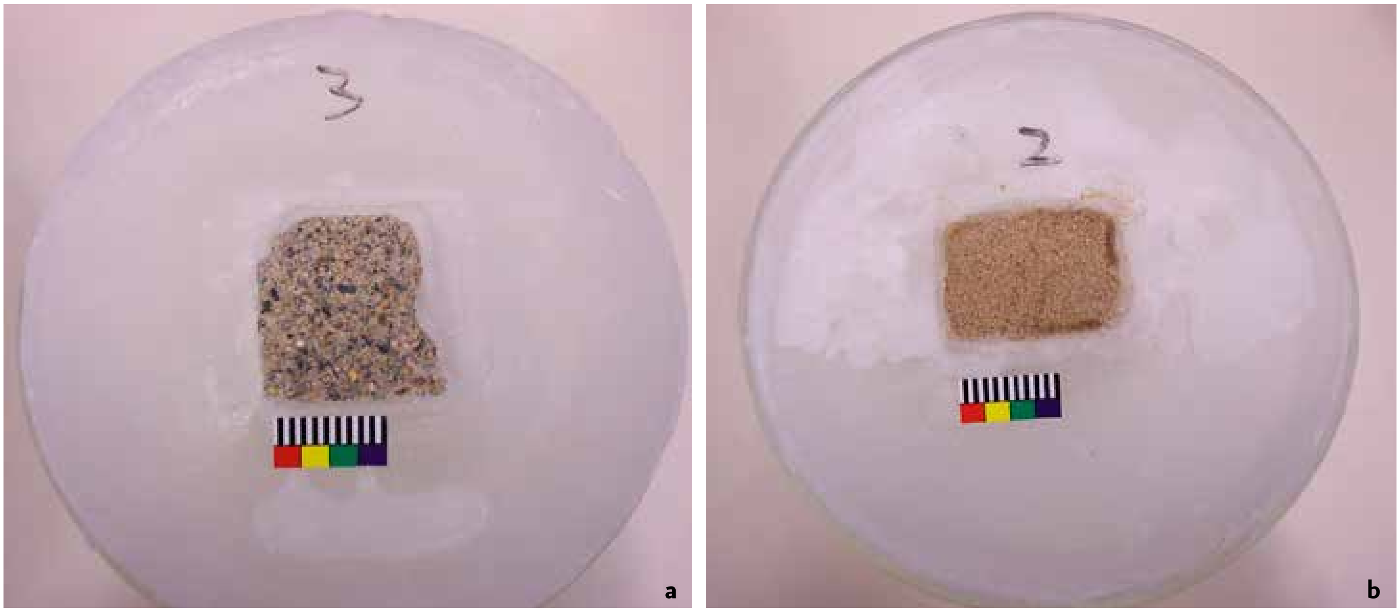

Fig. 16.15 Sodium chloride migration experiments were conducted in which samples of conglomerate (a) and sandstone (b) (approximately 25 mm thick, roughly square) were embedded around four sides in wax and sealed onto a glass container. The samples had a paste of NaCl applied to the undersurface and were then cycled between two environmental chambers, one at "high" RH (75–85%) and the other at "low" RH (33–43%). The cycling continued until salts were observed on the surface of the conglomerate.

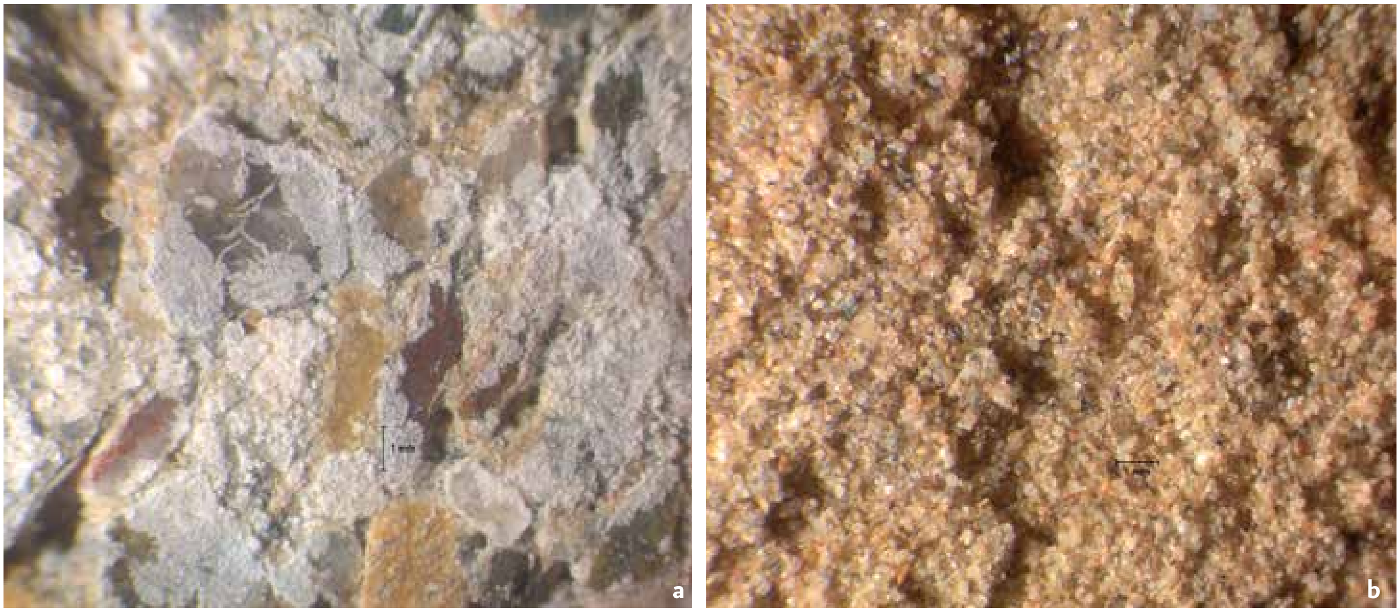

Fig. 16.16 Sodium chloride crystallization on the upper surface of conglomerate (a). Note salt creep around edges of larger grains. In the sandstone sample salt distribution was found throughout the body of the sample, but no crystallization was observed on the surface (b).

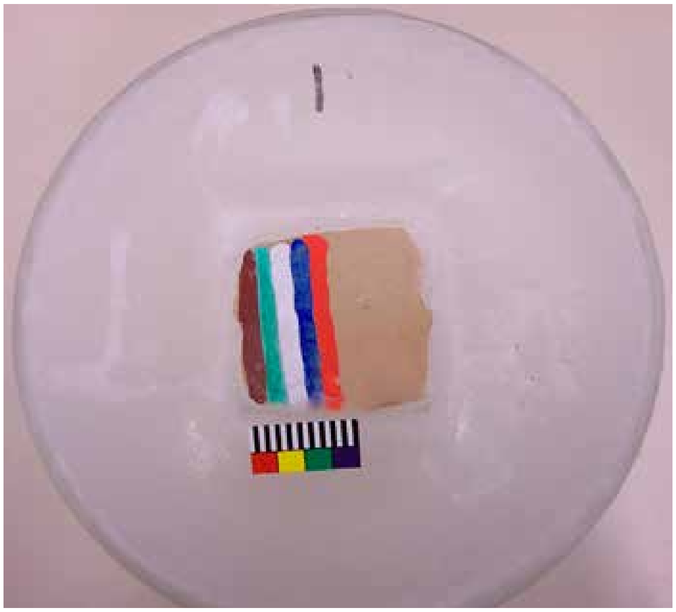

Fig. 16.17 Sodium chloride migration experiments on the conglomerate with a layer of clay plaster and half painted with the range of pigments used in wall paintings at Mogao.

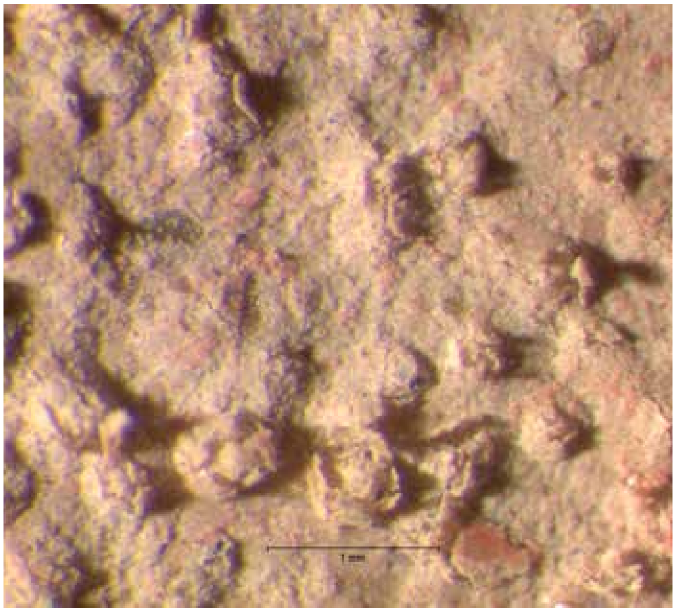

Fig. 16.18 Salt eruption on the unpainted clay plaster.

The greater abundance of fine material in the conglomerate may enhance capillary transport, while the larger pores in the sandstone allow rapid penetration of humid air and distribution of salt. Total porosity and pore size distribution are yet to be determined for conglomerate and sandstone. It would be informative to know whether sandstone lenses occur on the west wall of Cave 85; however, this is not possible to determine because of the large areas of surviving plaster. Sandstone would transport less salt to the surface but is more permeable to water vapor migration into the bulk of the rock, thereby potentially mobilizing more salt from the subsurface zone of enrichment.

Another similar laboratory test was conducted but this time with conglomerate samples overlaid with clay plaster and paint, replicating the stratigraphy of the paintings in the cave (fig. 16.17). Results showed the ability of salts to move through the conglomerate and up to the surface of the painted plaster under the same high and low RH cycling, though it took about 20 days in the laboratory to equilibrate across the sample. Sodium chloride was found to erupt on the clay plaster just below the paint layer, causing lifting of paint flakes and disruption of the plaster (fig. 16.18). Under examination euhedral crystals of sodium chloride were observed (fig. 16.19). Only in one instance, after five cycles, did deterioration to the paint layer occur. The resulting surface deterioration on these samples was similar to that observed on the wall paintings in the cave.

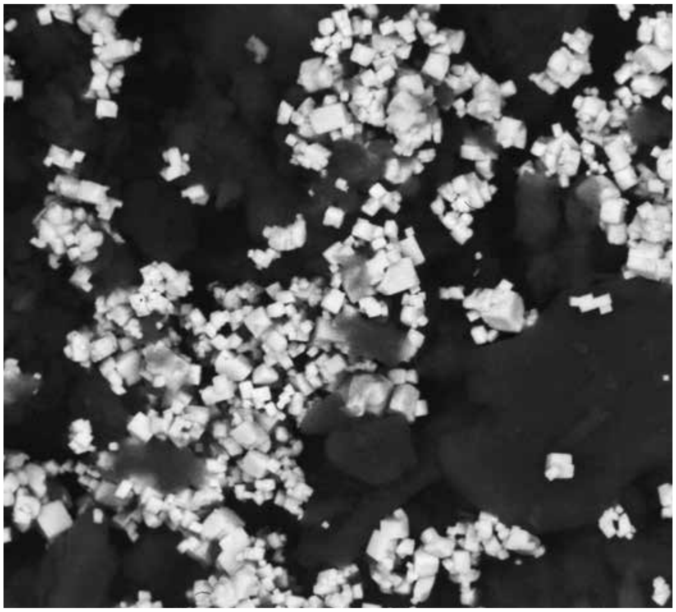

Fig. 16.19 Well-formed cubic crystals of sodium chloride below the paint layer (also at the clay-conglomerate interface).

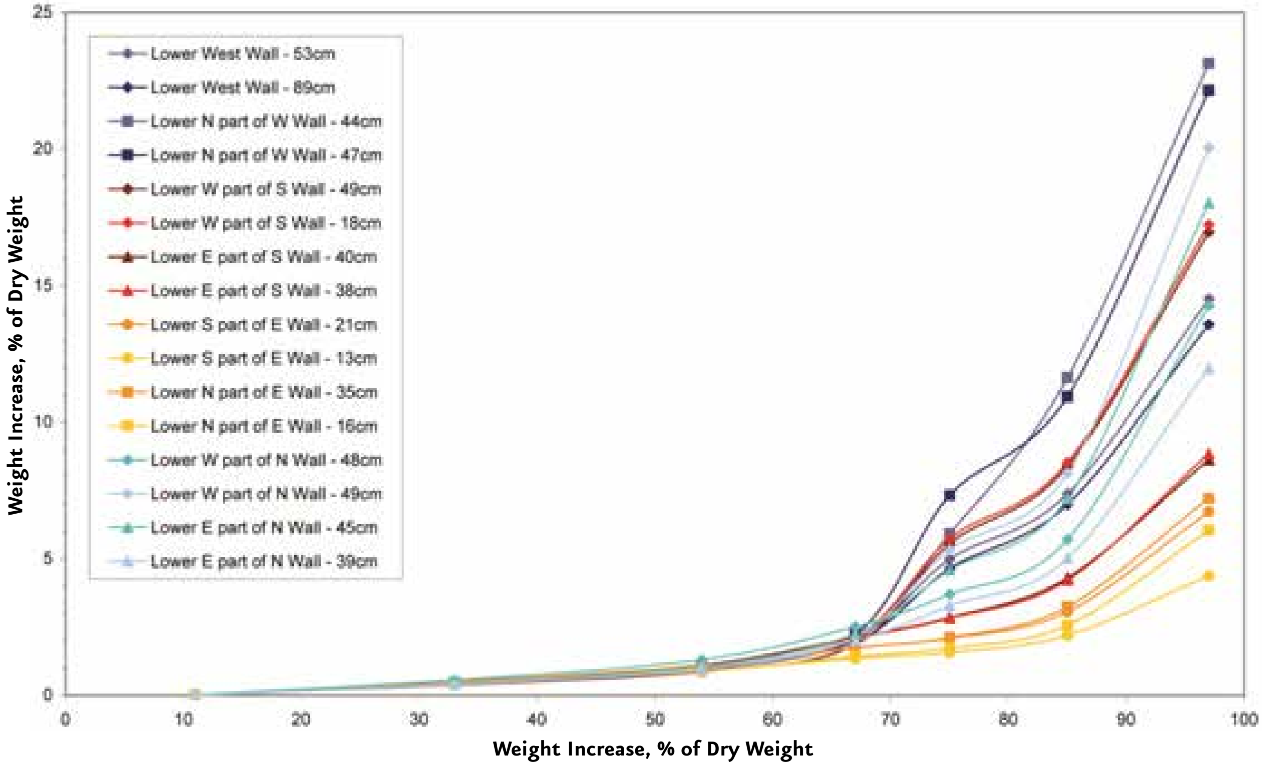

Fig. 16.20 Isotherms of plaster samples taken from Cave 98. The moisture uptake of samples from the western end of the cave was 50% to 100% more than that of samples from the east wall at 67% RH and 100% to 300% more at 75% RH.

Moreover, accumulation of salt at the conglomerate-plaster interface was also observed. In the cave this is a probable contributor to plaster detachment because of disaggregation and fretting of the rock from cycles of deliquescence and recrystallization. In other words, the conglomerate may recede behind the plaster by salt-induced fretting.

These experiments show that gradients in relative humidity alone, without the presence of liquid water, can transport sodium chloride from the internal face of the conglomerate through plaster to the painted surface. It is probable that over the centuries this phenomenon caused salt enrichment of the plaster walls in Cave 85.

Isotherms of Earthen Plaster from Caves 98 and 85

Sixteen samples of the earthen plaster were collected from Cave 98 (comparable to Cave 85 in its ground-level location, date of construction, size and geometry, and the type and distribution of deterioration). The samples, ranging from 10 to 17 grams, were crushed into a fine powder and divided into two sets, for isotherm measurements and anion and cation analysis, respectively.

In the isotherm measurement, samples were first placed in an oven kept at 105°C for three days, then cooled in desiccators. Samples were weighed and placed in a sealed humidity chamber maintained at 11% RH by use of saturated solutions of lithium chloride at 20°C. Samples were weighed daily. When each sample had reached equilibrium, indicated by no further weight increase, it was moved to a chamber at 33% RH using saturated solutions of magnesium chloride. The procedure was repeated using the humidity chamber at 54% RH (magnesium nitrate), 67% (potassium iodide), 75% (sodium chloride), 85% (potassium chloride), and 97% (potassium sulfate), and the resulting data were plotted (fig. 16.20).

All samples responded similarly below 54% RH. However, samples from the east wall absorbed less moisture than those from other locations in environments above 67% RH. Moisture absorption rates of the east wall samples were nearly linear up to 75%, when the rates increased slightly at 85% RH. Samples

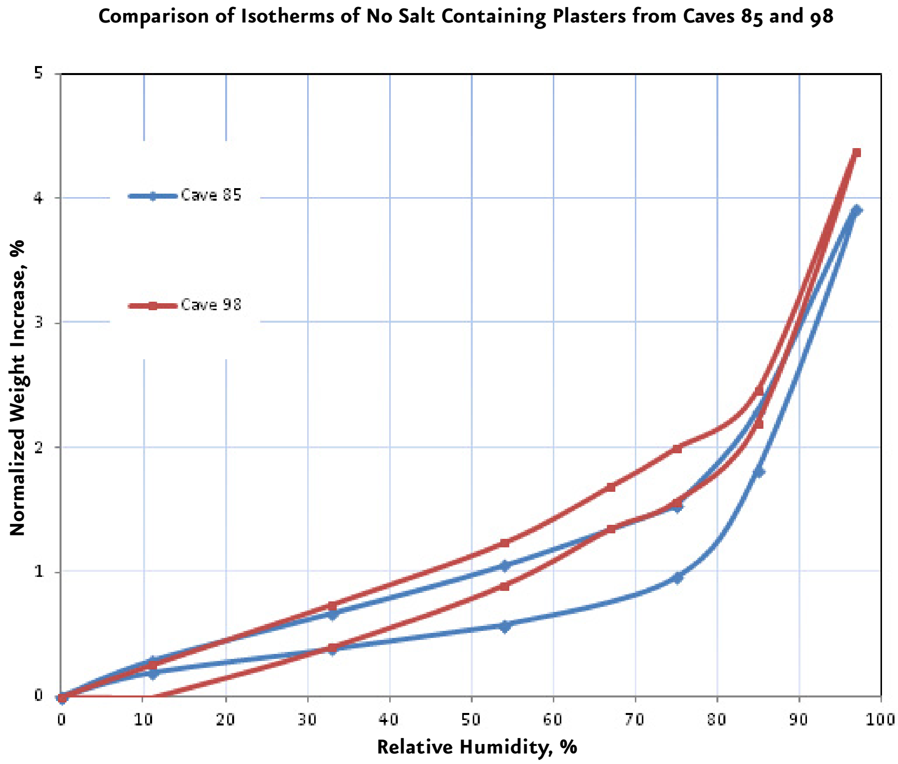

Fig. 16.21 Hysteresis isotherms of plaster samples that do not contain salt (less than 0.02% by weight) from Caves 85 (blue) and 98 (red). The absorption (lower line) and desorption (higher line) lines are plotted for each sample. The two caves showed similar moisture absorption/desorption characteristics at the tested range of relative humidity. The absorption rate was low and nearly constant to 75% RH. Absorbed amounts of moisture were 1–2% and 1.5–2.5% of their dry weights.

from the west wall and western portions of the north and south walls started to absorb more moisture than other samples at 67% RH. The moisture uptake of samples from the western side of the cave was 50% to 100% more than those from the east wall at 67% RH. And the uptake differences expanded to 100% to 300% at 75% RH environment. The difference increased exponentially at higher humidity environments.

Ion analysis of the plaster samples from Cave 98 found high levels of Na+, Cl- , and $SO_4$2- among samples from the western portion of the cave. Results indicated high concentrations of NaCl and Na_2SO_4 salts known to deliquesce at less than 75% RH (the RHeq of NaCl). The isotherm measurement of the salt mixture from Cave 85 also containing NaCl and Na_2SO_4 deliquesced at 67% RH. Higher concentrations of salt mixtures were present in the west wall. Larger amounts of moisture are absorbed by earthen plasters with higher concentrations of salts; the moisture absorption significantly increases at 67% RH. However, the absorption is not significant until the relative humidity reaches higher than 85% RH if a mud plaster does not contain a significant amount (less than 0.02% by weight) of salts.

The hysteresis isotherms of plaster samples from Caves 85 and 98 without salt have absorption (lower line) and desorption (higher line) lines plotted for each plaster (fig. 16.21). The two plasters showed similar moisture absorption/desorption characteristics. The absorption rate was low and nearly constant to 75% RH. Absorbed amounts of moisture were only 1–2% and 1.5–2.5% of their dry weights. This indicates that wall plasters are stable and absorb/desorb to 85% RH, if the salt content is less than 0.02% of their weight.

A fragment of painted plaster from the west slope of Cave 85 was also tested to measure the possible resulting expansion and contraction associated with humidity variation. The plaster, composed of 36% sand, 45% silt, and 19% clay, was derived from Daquan River alluvial sediment and contains, in the clay fraction, 30% swellable clays (illite/smectite) (see chap. 13). Laboratory experiments show detectable mass increase in salt-laden plaster after approximately three hours at 85% RH (fig. 16.22). The results illustrated a rather small displacement, 0.11%, occurring in two phases that can be attributed respectively to the clay component of the plaster and to the

a

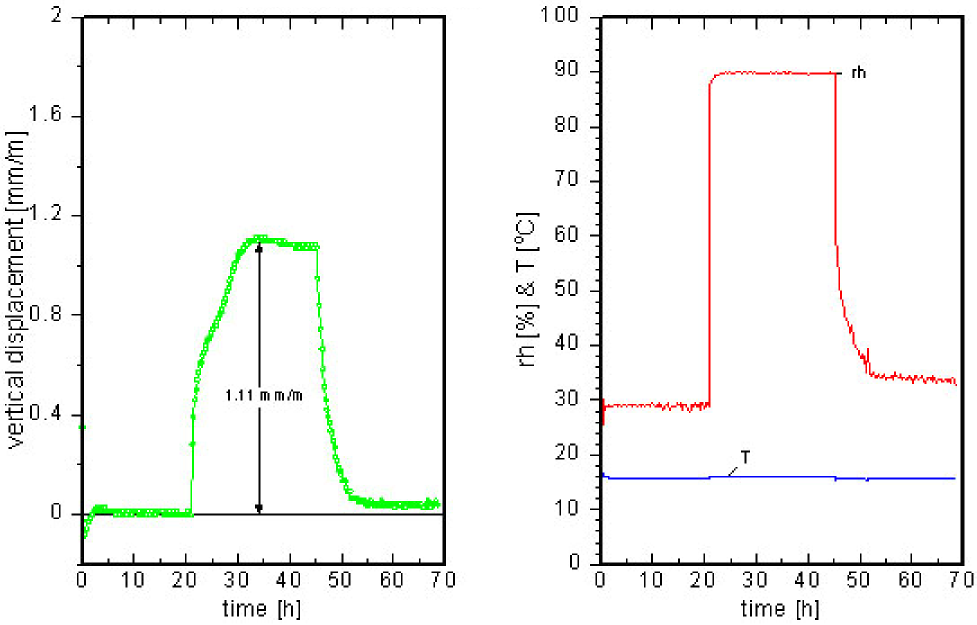

Fig. 16.22 Only a 0.11% maximum expansion of the earthen plaster was measured in response to RH (30% - 93% - 34%) at 15.8°C. The shape of the curve indicates that the expansion occurred in two phases that can be attributed respectively to the clay component of the plaster and to the hygroscopic salts present.

Fig. 16.23 Area of loss from the west ceiling slope of Cave 85 that occurred in 1996 after a period of rain.

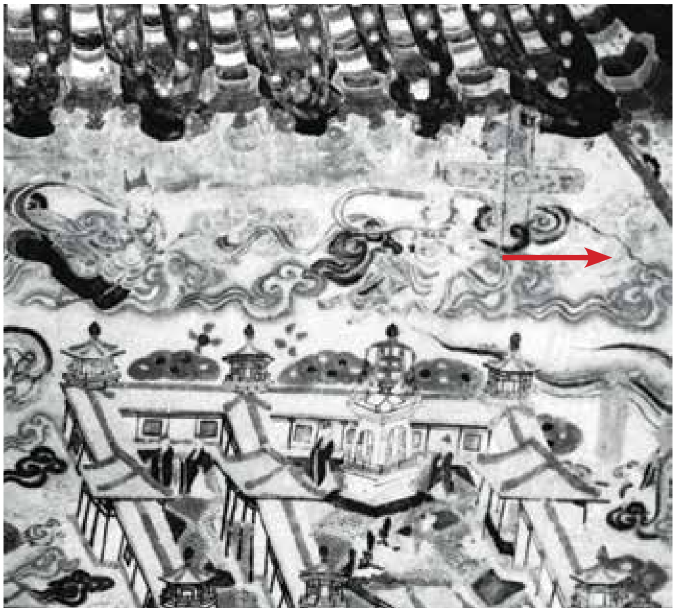

Fig. 16.24 A large crack is visible on the west ceiling slope in this photograph from 1989. Despite the insertion of the cross-brace in the 1970s to treat the detaching plaster, the area around the brace collapsed in July 1996.

hygroscopic salts present. The small expansion therefore probably does not play a significant role in the detachment of plaster.

Risk of Continued Plaster Loss

A latent catastrophic threat in Cave 85 is detachment of painted plaster. Extensive areas of plaster have separated from the conglomerate, and over time many segments have fallen under their own weight, most recently in the summer of 1996 (fig. 16.23). Detachment or separation of the plaster from the conglomerate is probably inherent, to some extent, from the time of construction of the cave (see chap. 15) but is exacerbated by cycles of deliquescence and crystallization of salts at the interface between the rock and the plaster (Agnew et al. 2010).

The loss occurred near a cross-brace that had been inserted into the painting on the west ceiling slope in 1974 to treat the long-standing problem of detaching plaster. A photograph of the area with the cross-brace, before the loss occurred, shows the presence of cracks, indicating that this area was still detached and therefore vulnerable to collapse (fig. 16.24).

A combined plot of the rainfall, relative humidity of outside air, and relative humidity inside Cave 85 between July 15 and August 2, 1996, demonstrates the impact of the exterior climate on the interior microclimate (fig. 16.25). The normal humidity in the cave in summer is 40–50% RH. On July 20, before a measurable rainfall event, the humidity in the cave rose from 42% to 75% RH as the outside humidity rose to 90% RH. This indicated that a large volume of the humid outside air had infiltrated into the cave. Although the outside relative humidity reduced to less than 65% for the three days following the rainfall, the cave's interior relative humidity did not. Because of the hysteresis effect, once hygroscopic materials absorb the moisture it takes longer for them to give off the moisture and return to ambient relative humidity. A continuous rain event on July 26–27 coupled with the humid outside conditions preceding and following the rain kept the cave's relative humidity above 75%. Although the total precipitation was low, the rainy condition continued until July 31. After nearly 11 continuous days of the cave's relative humidity above 65%, and with RH continuously above 75% inside the cave for 6 of those days, the humid inside air had deliquesced salts. This caused the large ceiling fragment of painted plaster to collapse, reported on July 30. This event demonstrates the relationship between extended humid or rain events with prolonged elevated humidity above 65% RH and damage to the cave walls.

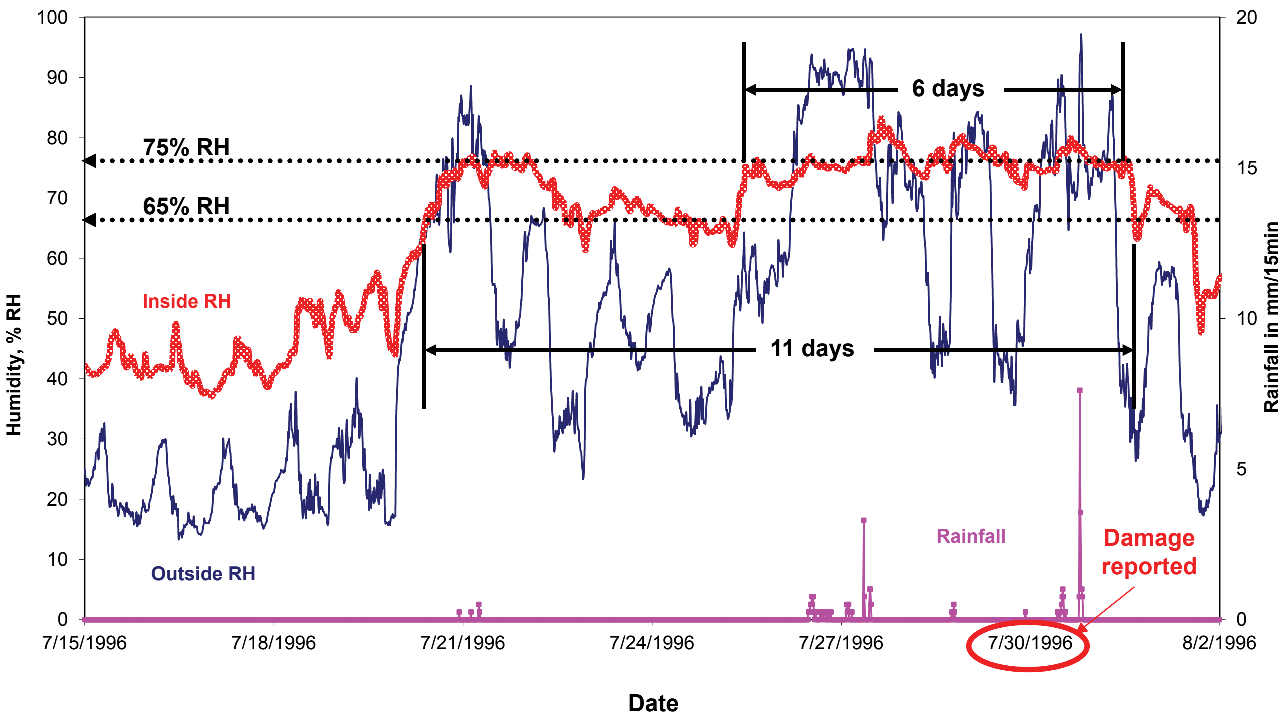

Fig. 16.25 Prolonged humidity in Cave 85 during the summer of 1996 led to collapse of a fragment of ceiling plaster.

Summary

The high content of hygroscopic salts (mainly NaCl) in the clay-based plaster is the predominant cause for the ongoing deterioration of the painted plaster in Cave 85. These salts are activated by fluctuations in humidity during summer rain events if intrusion of humid air occurs.

The cave moisture survey, undertaken as part of the environmental investigation, showed no evidence of liquid water but significant fluctuations in conditions of the cave environment when humid air intrudes (see chap. 14). Hygroscopic salts have destructive action on the paintings due to their hydration state changes or deliquescence and crystallization cycles activated by water vapor in the cave environment.

As atmospheric drying takes place salts move by the phenomenon of creep from within the bedrock to the plaster. Given the age of the cave (1,100-plus years), evidence of past flooding, and periods of extended rainfall, the conditions and time required for salt migration and enrichment at and near the surface have been met. Laboratory investigations have shown that the low concentrations of natural salts in the conglomerate can move to and become concentrated close to the wall paintings, mainly at the rock–plaster interface by the interplay of water vapor from the rock body and meteorological humidity.

The findings are pertinent both to how the salt has migrated and accumulated mainly at the west end of the cave and at what interfaces it accumulates, that is, conglomerate to clay plaster, clay plaster to paint layer. But questions still remain, and the discussion above has been simplified by considering only sodium chloride in the lab experiments, whereas analysis of the salt species present at Mogao indicates a range of other ionic types (mainly sulfate), which contribute to a lowering of the deliquescence RH but may also contribute to accelerated deterioration.

The complex interactions between water vapor (from both the atmosphere and the rock body) and hygroscopic salts (in the conglomerate and painted plaster), as well as painting technique and previous treatment (PVAc and PVA), have led to the deterioration seen today. Discussion of the cause and effect of the phenomena is clearly provisional, and research at a fundamental physicochemical level is needed. For effective preservation of the wall paintings at the Mogao Grottoes a combination of environmental controls and treatment and salt reduction techniques (see chap. 17) must depend on a complete understanding and diagnosis of all the deterioration mechanisms, their causes and rates. But for now the cave environment must be kept below 67% RH to avoid damage. Thus, at least the doors must remain closed to limit intrusion of humid air during periods of high external humidity. Further field investigations on salt profiles, water vapor sources, and subsurface zones of salt enrichment are needed to corroborate (or refute) the mechanisms proposed here and the debate regarding the origins of moisture.

Notes

1. Certain crystalline salts contain different, discrete numbers of molecules of water, known as the "water of crystallization." Depending upon conditions of humidity and temperature some salts, notably sodium sulfate, may change their hydration state with consequent volume change in the crystalline state. "Hydration" refers to a transition from one state to another, and occurs via an intermediary step in which the salt dissolves and the more hydrated phase crystallizes from the solution. The incorporation of additional water in the crystalline structure of the higher hydration state necessarily results in an increase in volume.
2. The physics of water and salt transport in porous media is exceedingly complex, as indeed is the mechanism of deterioration of stone by salts. Many studies have been undertaken, and the literature is extensive (Ginell 2005). The work of Pühringer (2002b) has been mentioned. Other useful papers appear in the volume edited by Charola (2005). In the past decade or so new tools have been applied to the problem, particularly nuclear magnetic resonance (see, e.g., Petković 2005). Other work of relevance, though technical, has been published by Dullien (1992). Camuffo (1995) provides a concise overview of stone weathering; more accessible to the conservator is the paper by Bionda (2004). Most published work in the conservation literature has been concerned with mechanisms of deterioration of stone by salts and to a much lesser degree with the salt enrichment process at the surface and subsurface. A generalized, nontechnical explanation of conditions under which salts enrichment occurs for particular rock types, salt mixtures, environmental conditions, and so forth is necessary to aid conservation practitioners in diagnosis and the development of remedial and preventive measures.
3. Merckoquant® sulfate test strips were used.
4. Soluble salts were extracted with warm deionized water and recrystallized by evaporating the solutions until dry.
5. Analysis was carried out by XRD.
6. As part of this project the use of aqueous extraction as a quick salt spot test to measure surface sodium chloride content was investigated (Chen et al. 2010).
7. Ion chromatography (IC) is a technique used to identify soluble salts, such as cations and anions. The samples must be pretreated by crushing into a homogeneous mixture. Procedures: Weigh sample on balance, transfer to a 50 ml polypropylene conical tube. Add Millipore water (18.2 megohms/cm) that is at least twice the volume of the sample. Agitate for 30 seconds and let sit at room temperature for 24 hours. Filter through a 0.2 µm ion chromatograph acrodisc. Transfer to a 1 ml polypropylene vial and inject into IC. Quantitative analysis of the soluble salts was performed on a Dionex DX-500 Chromatograph. An IonPac #CS12A analytical 4 mm column was used for the separation of cations. The eluent was 22 mN of H2SO4 with a flow rate of 1 ml/min, and a CSRS-ULTRA 4 mm was used as the suppressor. A mixture of cations and anions was used for calibration. Identified soluble salts were reported as parts per million and converted to mass percent.
8. Gravimetric measurements to determine water content of these samples were not accurate because of the inhomogeneity of the conglomerate, which contained pebbles.
9. These results do not include the ion content for micro-core samples taken from areas of flood damage at the base of the wall, which contain higher levels of soluble salts, including sulfate.
10. "Geology in Dunhuang," presentation by Wang Xudong at Round Table Discussion on Hypotheses of Deterioration, held at the Dunhuang Academy, Conservation Institute, 30–31 March 2000.
11. The RHeq is the equilibrium relative humidity value generated in a closed vessel by a saturated aqueous solution of a pure salt at a given temperature, and thus is the RH at which the salt deliquesces at that temperature.
12. In the Dynamic Vapor Sorption (DVS) technique, a micro-balance, capable of measuring a few grams of sample with microgram accuracy, is used to measure weight increase or decrease due to changes in moisture content. Small samples can be used, thereby achieving fast equilibrium weights. Both the sample and the micro-balance are in a chamber purged with a carrier gas, normally air or nitrogen, that is conditioned to a particular relative humidity. Since both the sample exposure and the weighing are continuously performed in the chamber, weighing errors are minimized. The conditioned carrier gas, produced by mixing dry gas and water vapor–saturated gas or by controlling the dew point temperature, allows the exposure of samples in a range from 0% to 98% RH at increments of less than 1%.
13. RUNSALT© 2002-2005 Davide Bionda.
14. Further research on this topic has been undertaken by the GCI and the DA as part of the Visitor Carrying Capacity Study for the site (Agnew et al. forthcoming).
15. This was a static air experiment in a closed chamber.
16. See also Lubelli et al. 2006.

CHAPTER 17

Preventive Measures and Treatment

Fig. 17.1 Plaster detachment was the most serious condition in Cave 85. Development and implementation of stabilization treatments in the form of injection grouting with an earth-based grout was the main focus of the conservation work.

Conservation of Cave 85 included both remedial stabilization treatment of the paintings and sculpture to prevent further losses and environmental control measures to slow deterioration. This was achieved through an understanding of the nature of deterioration and the history and present condition of the cave, followed by systematic treatment design and testing. The susceptibility of the earthen-based painted plaster and the widespread occurrence of salts in the rock and plaster posed challenges to the development of effective conservation treatments. Recurrence of plaster detachment, disruption, and exfoliation of wall paintings following earlier treatments indicated that preemptive remedial treatments taken without arresting the causes of deterioration are at best temporary and at worst extremely damaging (see chap. 15). Moreover, the previous interventions, including widespread consolidation with PVA and PVAc and the use of anchor braces to secure detached plaster, exacerbated persistent deterioration problems (see chap. 9). The instability of a high percentage of the painted plaster—in particular those areas of severe detachment—warranted remedial intervention in the form of injection grouting as the main focus of the conservation work (fig. 17.1).

Fig. 17.2 The conservation approach avoided the addition of new plaster repairs, which could cause redistribution of salts from the introduction of water from the wet plaster. Instead, areas of loss, such as at the base of the walls, were left with the conglomerate exposed.

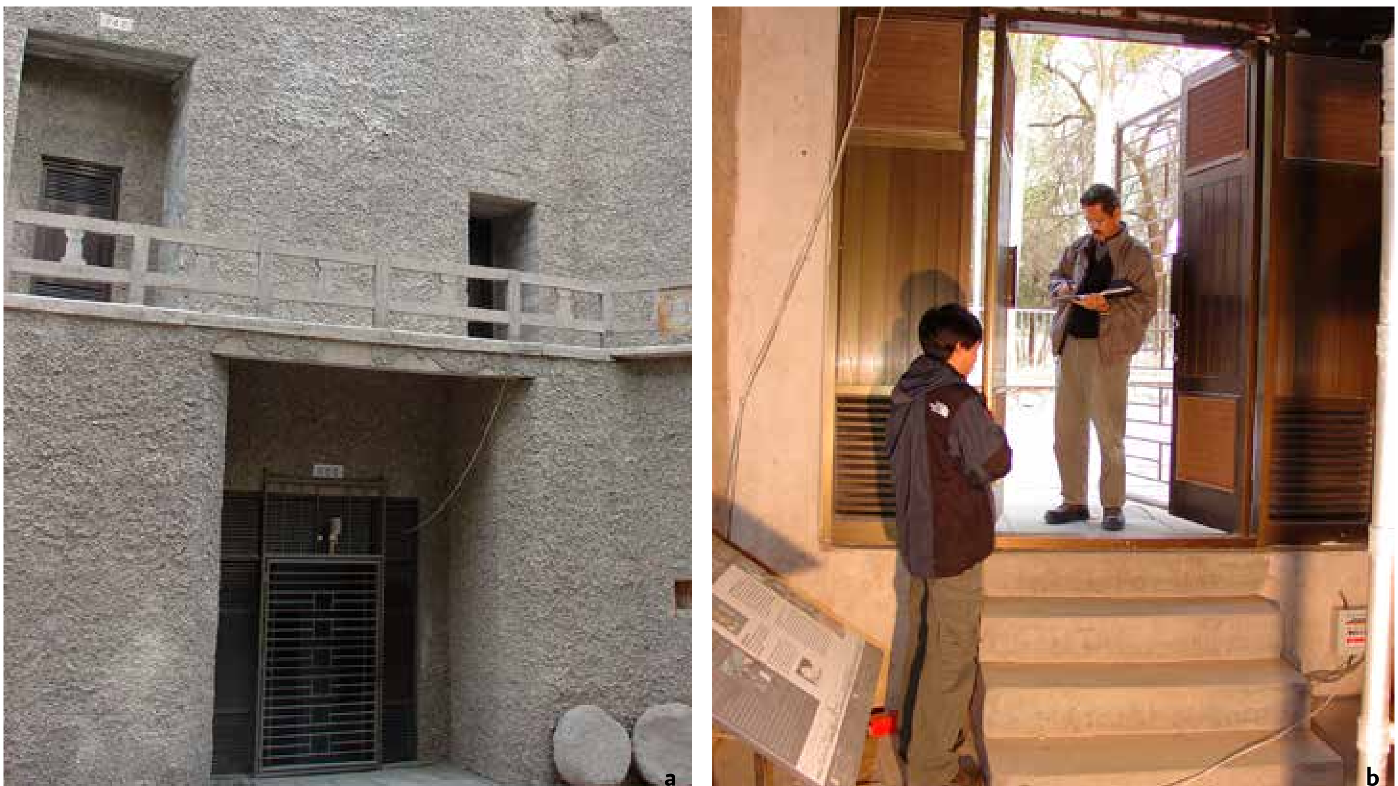

Fig. 17.3 Preventive measures such as environmental control are important. Recommended measures include closing the cave during periods of high external humidity. Environmental investigations show that keeping the door closed prevents the intrusion of humid air into the cave. This simple measure is essential for maintaining stable humidity conditions, thus preventing further salt deterioration.

Remedial Treatment Development and Testing

Conservation treatments in Cave 85 required an understanding of the cause-and-effect relationship between humidity and hygroscopic salts, including research on moisture-mediated deterioration in salt-enriched substrates (Agnew et al. 2010) (see chap. 16). The overall treatment favored minimal intervention with a focus on stabilization to prevent further loss. The goal was also to minimize unwanted side effects evident in past treatments and to not preclude the possibility of retreatment in the future. Thus, large plaster repairs from earlier work were not removed, and new plaster additions were generally avoided. Instead the conglomerate was left exposed in order to avoid adding water and to prevent the redistribution of soluble salts within the painted plaster (fig. 17.2).

Given the constraints of a salt-rich environment, treatment testing focused on the selection of materials and application methods for paintings on earthen supports. Materials typically used for lime-based paintings were not generally applicable. Material selection was thus based on compatibility with original materials and testing of suitable working properties and performance characteristics for each intervention.

Investigation into materials and application methodologies, including laboratory and in situ testing, was undertaken in the following areas: salt reduction from painted plaster; grouting to stabilize areas of plaster detachment; adhesive testing for paint flake relaying and consolidation of areas of powdering plaster and paint; plaster repairs; cleaning; and treatment of the altar platform.[1]

Salt Reduction of Painted Plaster

A common approach to treating salt problems in wall paintings is to attempt salt reduction through aqueous extraction.[2] Much previous research and practice on this topic exists but relates to lime-based plasters.[3] Patterns of moisture transfer and salt phase transitions in earthen plasters are as yet poorly understood. Attempts at desalination of plasters in general have not always been effective for a variety of reasons (Larsen and Bøllingtoft 1999); salt reduction in plasters by aqueous means is potentially damaging and can cause adverse effects to water-sensitive and water-soluble original materials. For Cave 85, this includes both animal glue and plant gum media in the paint and ground layers and the earthen materials in the plaster. Additionally, moisture can contribute to the alteration of copper and lead-based pigments. Aqueous extraction can also lead to the redistribution of salts within the porous plaster, while selective extraction of the more soluble salts may result in the concentration of less soluble salts, with unknown longer-term consequences. Interruptions in capillary continuity at the layers of a wall painting can cause accumulation of salts at these interfaces within the painting stratigraphy, leading to enhanced deterioration (Cather 2003).

Given the water sensitivity of the Cave 85 wall paintings and the fragility of areas of unstable plaster detachment, large-scale aqueous methods of salt extraction were not possible. Limited, localized areas of salt reduction were undertaken, out of necessity, in conjunction with treatments—namely grouting—to deal with the mobilization of salts (see Grouting section in this chapter).

Environmental Control

Environmental control plays a central role in preventive conservation by maintenance of a stable microclimate (Arnold and Zehnder 1991). In Cave 85 this includes inhibiting phase changes of salts—crystallization, hydration, and dissolution—which result in salt enrichment at the painted surface and physical damage over time (see chap. 16).[4] The extent to which environmental control can reduce the damage from salts in porous materials is still unclear and has been the focus of much research (Price 2000; Nunberg and Charola 2001; Sawdy 2003). Inhibiting salt phase changes through climate control is complicated as it assumes an understanding of the specific salts present, their relative proportions, and location and assumes that control of the environment will produce the desired conditions within the porous material where salts are present (Cather 2003).

As a rule, however, in order to minimize salt damage the environment must be maintained below the relative humidity level at which the salts absorb moisture from the air. This can be determined experimentally. Investigations in Cave 85 have demonstrated that salts and moisture are its primary causes of ongoing deterioration. Therefore, maintaining stable conditions—controlling the relative humidity—is necessary for long-term preservation. Recommended measures include keeping the

Fig. 17.4 Anchoring and pinning of detached areas of plaster were undertaken in the 1970s. This often led to increased deterioration as the pinning concentrated stress on already weakened plasters (a). Most of the anchors were removed after completion of the stabilization work in the cave (b).

RH below 62% by installation of a tight-fitting door to lessen the interchange of air between the exterior and the interior of the cave and closing the cave to visitors during rain or periods of high external humidity (Demas et al. 2010; Maekawa et al. 2010) (fig. 17.3) (see chap. 14).

Grouting

The most prevalent and serious problem in Cave 85 and at Mogao is the detachment and collapse of clay plasters from the conglomerate rock. Detachment typically stems from the creation of the paintings, such as shrinkage of the plasters upon drying and their poor adhesion to the conglomerate. Salt-related deterioration further complicates these inherent faults. Past treatments to solve this problem have included pinning the plaster to the rock with anchor braces and—in extreme cases—the detachment and transferral of paintings. Pinning has been problematic as it concentrates stress on already weakened plasters, leading ultimately to more damage (fig. 17.4).[5] The second approach is also discredited based on recognition of the irreparable harm caused by detachment and transfer.[6]

Injection grouting is now the treatment of choice for tackling the critical issue of plaster separation from the rock. The treatment introduces an adhesive material with bulking properties. Grouting research, mostly related to lime-based wall paintings, spans the past two decades.[7] A systematic methodology for development and testing has only quite recently been established, however, through the work of Griffin at the Courtauld Institute (Griffin 1997, 2004).[8] For earthen wall paintings—more difficult to treat than lime-based paintings, owing to their susceptibility to a wider range of deterioration phenomena—grouting research options were limited. Further work provided a substantive basis for testing and development of fully compatible earthen grouts (Griffin 1999).[9] Drawing on this research, the project required the design of a clay-based grout for large-scale application.[10]

Earthen Grout Design and Testing: Performance Characteristics and Working Properties

Development and testing of the Cave 85 grout were based on assessment of the performance characteristics and working properties of various grout formulations. Performance characteristics

Fig. 17.5 Laboratory testing was an essential component of the development of an injectable grout to be used to readhere areas of plaster detachment.

relate to the long-term performance of a treatment. For grouts they include minimal physical or chemical alteration to the painting, minimal volume change on drying, no introduction of soluble salts, good adhesion, durability and chemical stability, microbiological resistance, light weight, and retreatability (since grouting is irreversible); and in regard to the plaster, similar dry porosity, water vapor permeability, mechanical strength, and hygrothermal behavior.

Working properties are concerned with short-term behavior while a grout is in a liquid state and include the following: injectability, viscosity, tack (initial adhesion), reasonable setting time, and low toxicity (Griffin 1999, 11). For the wall paintings of Cave 85, two other working properties of the liquid grout were important because of the known high soluble salt content present in the cave: minimal water content and slow drying time (slow water release).

Quantitative and replicable laboratory tests on grout formulations were performed to assess performance characteristics (figs. 17.5, 17.6).[11] The testing methodology was developed on the basis of available American Standards for Testing Materials (ASTM) and Chinese Standards for Testing Materials (CSTM), as well as testing procedures used by Griffin (1997, 1999) and procedures developed specifically for the project.

Basic performance characteristics (linear shrinkage, density, and water vapor permeability) and working properties (wet density, drying time, water content, and rate of water release) were evaluated initially. Grout mixtures that did not reach appropriate requirements were omitted from further testing. Over 80 grout formulations were trialed, but only a small number were subjected to the full range of testing, culminating in specific strength tests such as uniaxial compression, yield strength, Young's modulus, and modulus of rupture. The final components of the grout-development program involved a series of in situ tests and artificial aging trials (fig. 17.7).

In situ trials included measuring shear resistance and direct adhesion of test panels grouted onto the exposed conglomerate at the base of the cave (fig. 17.8). Artificial aging of grouted plaster replicas, some contaminated with 2% NaCl, involved cycling these at 100% RH for 48 hours, followed by drying at 25°C for 20 hours (fig. 17.9).

Fig. 17.6 Lab testing included quantitative and empirical experiments to assess working properties and performance criteria of different grouts. This included rate of water release of grouts (a) and strength tests (b).

Fig. 17.7 In situ tests were also undertaken on the exposed conglomerate at the base of the wall (a). Adhesive strength of different grouts was evaluated using a simple pull test developed during the project (b).

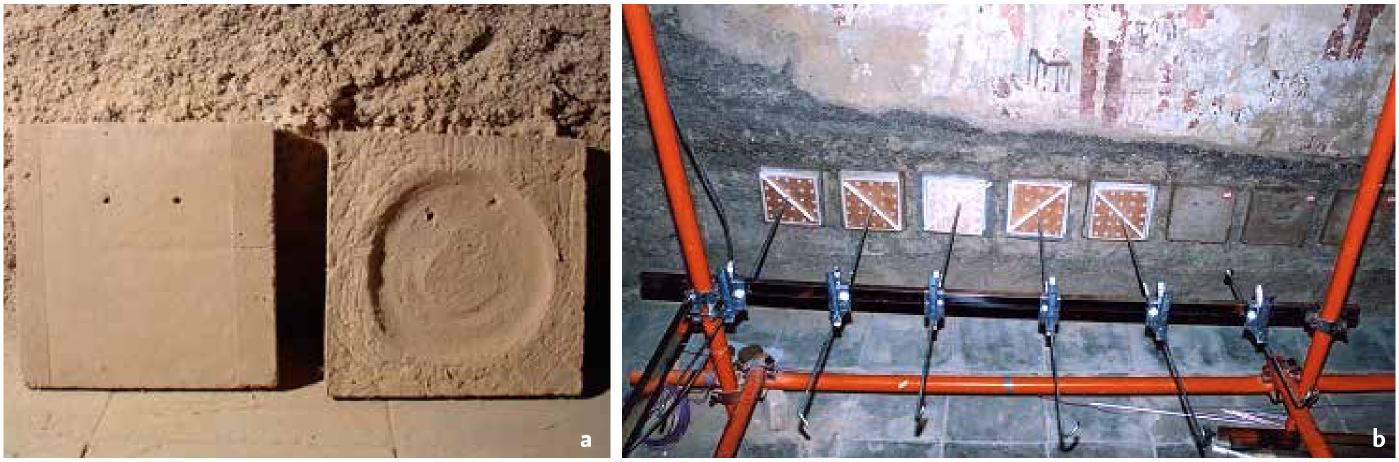

Fig. 17.8 In situ tests were undertaken to develop procedures for grouting. Plaster replica panels with a hollowed out back were attached to the wall and then grouted (a). This helped to develop the steps necessary for grouting such as application of an absorbent press to the replica panel as the grout dried (b).

With compatibility between rock, grout, and plaster a primary concern, it was essential to relate the results from laboratory testing to the original plaster. As already mentioned, however, differences in application and function between an original plaster and an injected grout make comparison difficult. In addition, it is often not possible to obtain sufficient amounts of original plaster for comparable testing. There are no clear-cut solutions to these problems, and approximation is unavoidable. For Cave 85, a replica plaster was prepared as a comparative base. Its components, 36% sand, 45% silt, 19% clay, and added straw, were derived from analysis of the earthen materials of original plaster samples (see table 17.1). The replica plaster was then tested in the same way as the grout mixtures, to provide a set of comparative values (see Appendix 17.B).

Fig. 17.9 The grout was subjected to artificial aging in a "sandwich test" whereby the grout was applied between two squares of replica plaster containing 2% NaCl (to simulate conditions of the original painted plaster). The sandwich was then cycled under conditions of high and low RH. The sample on the left is before aging and the one on the right after aging. After several cycles, the plaster was severely deteriorated, but the grout itself was still intact.

Basic qualitative and semiquantitative tests were designed to assess a range of working properties. Since the painted plaster in Cave 85 is water-sensitive, these included tests to compare and assess both the water content and the rate of water release of the grout mixtures.[12]

All testing was carried out at Mogao, apart from compressive strength, tensile strength, and three-point loading, which were undertaken at Lanzhou University (see Appendix 17.C).[13]

Constraints and Issues

At the start of the project condition assessment revealed much of the 350 m^2 of plaster in Cave 85 was dangerously separating from the conglomerate rock, particularly at the west end of the cave, most critically on the ceiling slopes. Due to the weight of the plaster, cracking and bulging were typical, and collapses had occurred in recent years, illustrating the unpredictable and high-risk condition. On the west wall itself, approximately 70% of the 57 m^2 of plaster was separated from the rock (see chap. 12). Huge risks were posed by the typically large size of individual areas of plaster separation, some extending over 1–2 m^2, with a gap between the plaster and the rock of up to 4 cm.

The treatment mandate therefore required not only the development and testing of an appropriate grout but also the development of an efficient salt-reduction system because of the migration of salts caused by the water-based grout.

Assessment of the painted plaster before, during, and after grouting was constrained by the concealed nature of the

PARTICLE-SIZE DISTRIBUTION			
	SAND (0.06–2 mm)	SILT (0.002–0.06 mm)	CLAY (<0.002 mm)
RIVERBED MUD	1%	71%	28%
CAVE 85 PLASTER	36%	45%	19%
CAVE 85 PLASTER (CALCULATED WITHOUT ADDED SAND)	0%	70.3%	29.7%

MINERALOGY OF CLAY-SIZE FRACTION					
	KAOLIN	ILLITE	CHLORITE	SMECTITE	MIXED ILLITE/SMECTITE
RIVERBED MUD	-	50%	40%	-	10%
CAVE 85 PLASTER	-	40%	30%	-	30%

Table 17.1 Earthen Materials Analysis

detachment and its treatment (Griffin 1997, 3).[14] Almost 300 liters of grout were injected in Cave 85 over the course of the project. The largest area of plaster separation was injected with 22 liters alone. This scale of treatment surpasses all other conservation interventions in terms of the quantity of materials applied. Grouting, moreover, is completely irreversible: a set grout becomes a nonextractable part of the wall painting.

Due to the weight of the plaster in Cave 85, cracking and bulging were typical, and the risk of collapse was acute (fig. 17.10). Caution was essential. Importantly, the purpose of grouting was not to fill all voids. Many large voids were only partly filled, to avoid adding excessive weight. In such cases, the aim of grouting was to break up the volume of the voids and to provide strategic areas of "anchoring" of plaster to rock. This also provided the possibility to retreat the paintings in the future.[15]

Compatibility

Because a grout becomes an integral part of a wall painting—and retreatment may be difficult—it must be composed of materials that are as similar as possible to those of the original plaster, so that original and added materials behave the same and are compatible in the long term.

Differences in application and function between an original plaster and a grout mean, however, that compatibility must be qualified. Earthen plasters, in which clay or earth acts as the binder, generally include aggregates (e.g., sand) and organic fibers, added to counter shrinkage and improve strength. In the original plaster, a high aggregate-to-binder ratio (4:1), and added plant fiber, helped to reduce shrinkage. Fiber also adds mechanical strength, countering the poor packing geometry of rounded sand particles. Unfortunately, fibers are not injectable. In the grout, fillers therefore needed to compensate for omission of fibers by providing improved particle-size distribution. They also needed to have low wet and dry densities, as the condition of the plaster could not support excessive added weight.

Since physical compatibility of the grout with the original materials can only be approximated, chemical compatibility is crucial. The clay fraction of an earthen plaster must be replicated in the grout. However, perceived drawbacks of earth, such as excessive shrinkage and low strength, have led to its avoidance as a grout binder (Griffin 1999).[16] Instead, earthen wall paintings are routinely injected with lime-based grouts,[17] or when earth is used, it is typically mixed with synthetic adhesives, possibly compromising its natural binding function. The development of a grout that relied entirely on earth as its binder was decided upon for the Cave 85 Project.

Earthen Materials Analysis

The main components of an earthen grout are shown in table 17.2, together with their functions and potential disadvantages. To be able to overcome any deficiencies, the mineralogical and

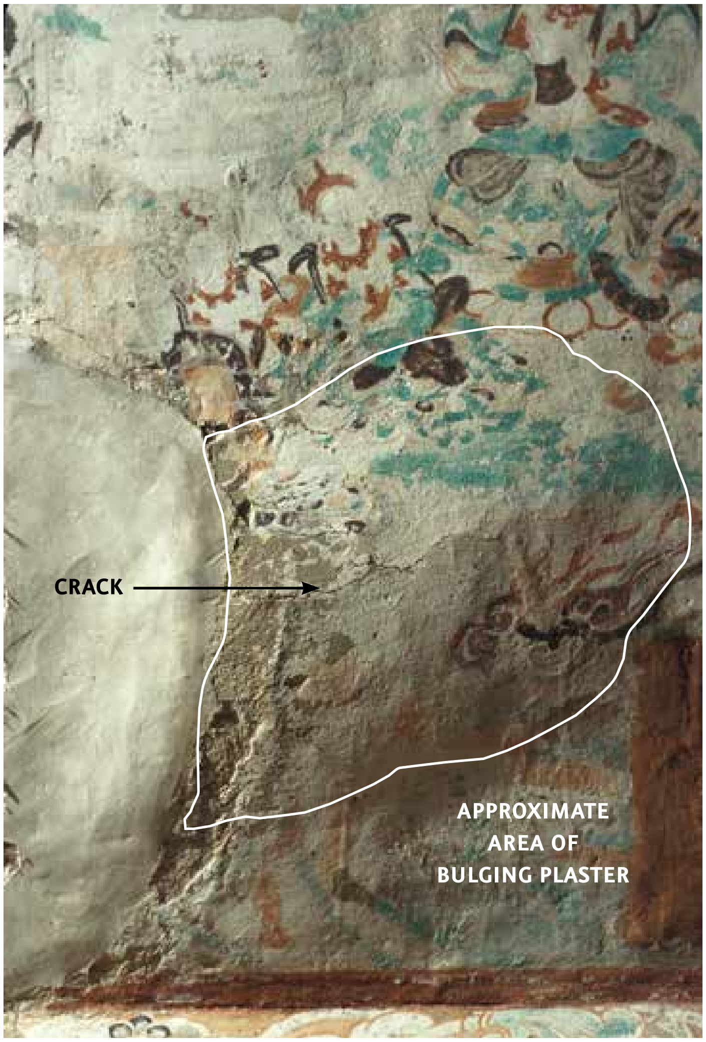

Fig. 17.10 Cracking and bulging of the painted plaster was typical of the severe plaster detachment. This type of condition has led to a number of areas of loss such as that seen on the western end of the north ceiling slope. The fragility of the plaster in an area such as this made the intervention of grouting particularly challenging. Injecting added weight into a ceiling area could increase the likelihood of collapse of the painting. Therefore, grouting had to be undertaken with caution.

GROUT COMPONENT	FUNCTION	POTENTIAL DISADVANTAGES
BINDER	• binds the components of the grout mixture • adheres plaster to the rock conglomerate	• high wet and dry densities • long drying time • high shrinkage
FILLER	• provides bulk and enhances internal cohesion • counters shrinkage on drying • improves porosity and water vapor permeability • reduces density • improves injectability • increases drying rate	• may affect compatibility • may result in too low or too high strength
FLUIDIZER	• fluidizes the solid • improves injectability	• damage to water-sensitive/soluble plasters and paint materials • activates salts
ADDITIVE	• modifies above grout properties including further improving injectability and adhesion and reducing density	• may affect compatibility

Table 17.2 Earthen Grout Components: Their Function and Potential Disadvantages

clay characteristics of the earth component must be known. With this data, an informed selection of the other material components can be made.

Mud collected from the bed of the Daquan River and plaster samples taken from Cave 85 were shown to be mineralogically nearly identical (see table 17.1). The only difference being that the plaster contains sand (see Appendix 17.B).

Thus, the riverbed mud was selected as the grout binder (fig. 17.11). The mud is characterized by its high silt content (71%), relatively low swelling clays (28%), and near-absence of sand (1%). For earthen materials to function well an equal distribution of silt, sand, and clay is desirable. Too much silt, for example, produces a material prone to shrinkage and cracking. Sand added by the artisans when formulating the original plaster reduced its silt proportion to approximately 45%, and the clay to 19%.

For the grout, testing therefore focused on characterizing and selecting fillers that would, like the sand and plant fibers in the original plaster, modify its performance (reduce shrinkage, provide internal cohesion) while also imparting necessary properties.

Characterization of Fillers

Given the wide range of available filler materials, an informed preselection was made, predicated on the known deficiencies of the earth binder and on the modifying role of the other components in the original plaster.[18] These requirements were too demanding of one material alone, and at least two fillers were necessary. Pretrial selection was based on visual and microscopic characterization and on basic qualitative and semiquantitative laboratory tests (fig. 17.12). Parameters examined included particle size and morphology, wet and dry densities, amount of water absorption and desorption, drying times, and expansion and contraction. Chemical characteristics such as pH and soluble salts content were also determined (see Appendix 17.D).

Cave 85 Grout Formulation

The selected grout formulation is shown in table 17.3. Key performance data for the grout and the replica plaster are shown in table 17.4.

The largest component of the grout is glass microspheres, widely employed as inert lightweight fillers in conservation, and their usefulness as a grout component is well recognized.[19]

Fig. 17.11 Mud from the Daquan River, used in the original plastering of the cave and now as the main binder component of the grout, was washed to remove salts and then laid out to dry.

Being nonabsorbent, microspheres have the outstanding advantage over porous fillers of maintaining very low wet and dry densities. Their spherical morphology, regular surface texture, and extremely small particle size also promote good viscosity and injectability; their buoyancy contributes to the suspension of other grout components in the fluid mixture.

However, their spherical morphology contributes to poor packing geometry, reducing internal cohesion: grout formulations tested with a higher proportion of glass microspheres were too weak (fig. 17.13).[20] Pumice filler provided a counterbalance to this problem. Added as a small proportion of the overall grout formulation, its variable and larger particle size, and angular morphology, helped internal cohesion. At the same time, the pumice has low density compared with other fillers, such as sand.[21]

Two properties are necessary for adhesion: initial wet adhesion (tack) when the grout is injected; and lasting adhesion once it has set. Synthetic adhesives have been added to earthen grouts to fulfill these demands, at risk of reducing the earth's natural binding function. Research has demonstrated the adhesive and strengthening properties of egg white as an additive: it augments clay binding properties and promotes tack and adhesion, increases plastic and liquid limits, and increases uniaxial compressive strength and modulus of rupture.[22] Egg white was therefore used for the Cave 85 grout, by whipping and folding it into the mixture as a lightweight, air-entraining foam (fig. 17.14).[23] This also improved viscosity and injectability and prevented sedimentation. The egg white also made up part of the fluidizer, allowing a reduced volume of water and slowing the rate of water release from the grout. Thus, the egg component of the grout was critical for a number of reasons. Artificial aging was undertaken to confirm the stability of the egg white and its low potential for microbiological growth.

Grouting Presses and System for Salt Extraction

Water as fluidizer in the grout dissolves soluble salts in the plaster.[24] Control of salt crystallization and localized salt reduction was therefore required as an adjunct of grouting.

Usual techniques for salt extraction rely on the moisture content and contact time of a wet poultice. For Cave 85, the moisture was instead the water released from the grout into a dry poultice. Testing focused on the use of highly absorbent tissue that could be incorporated while dry into presses placed against the plaster after grouting to absorb moisture from the grout.[25] Conformability to the surface and light weight were required. Tests were devised to assess amounts and rates of moisture uptake by the tissue when placed against a wet substrate (see

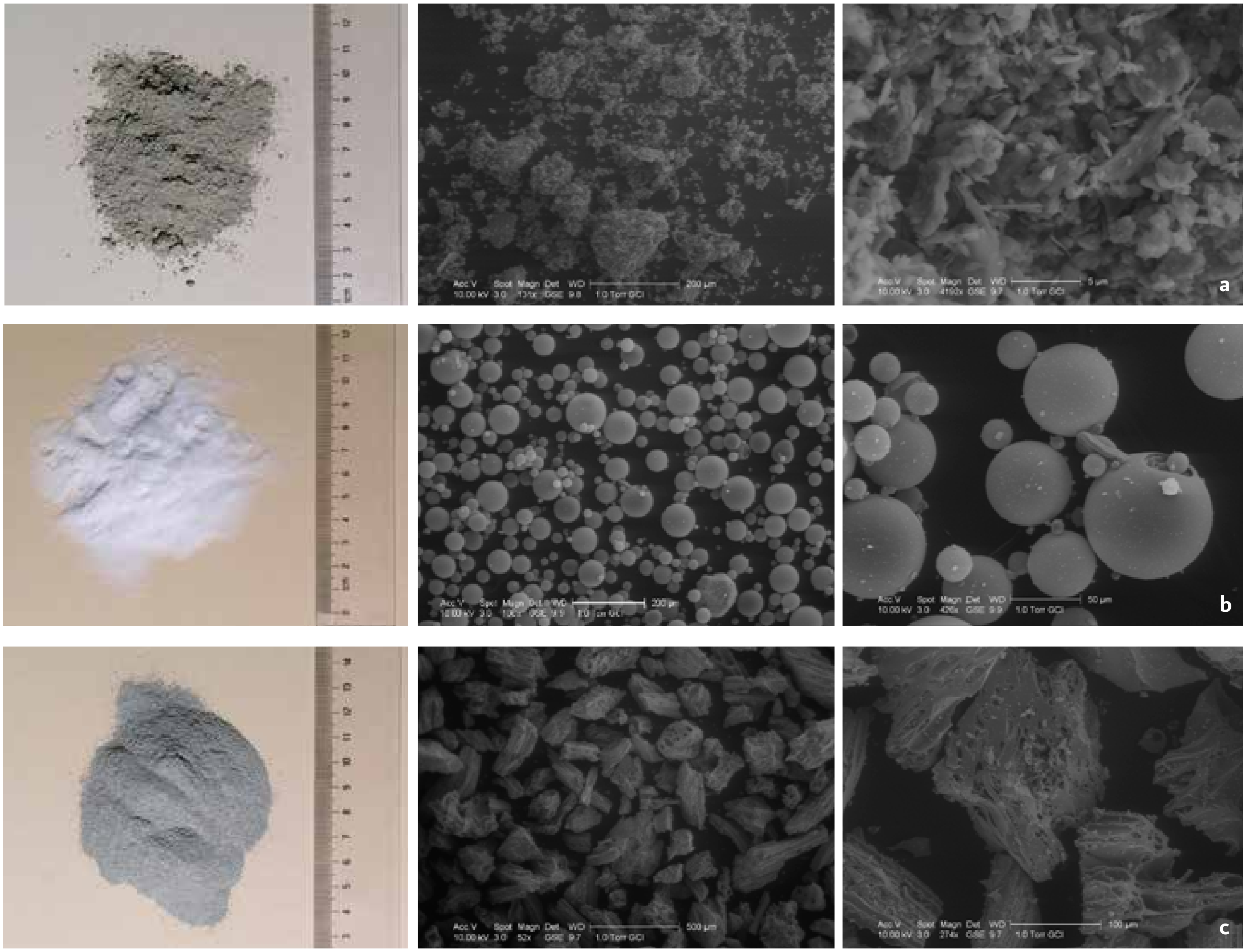

Fig. 17.12 Components of the Cave 85 grout as viewed under ESEM: riverbed mud (a); glass microspheres (b), selected because they are nonabsorbent and have extremely low density because their spherical morphology, regular surface texture, and small particle size also promote good viscosity and injectability; and pumice (c), selected for its low density, angular morphology, and variable and larger particle size compared to the glass microspheres.

COMPONENT	MATERIAL SELECTED	PARTICLE SIZE	VOLUME
BINDER	Crushed riverbed mud (soluble salts removed after soaking in water)	<300 µm	1
FILLER 1	Glass microspheres (Scotchlite K1®)	<75 µm	2
FILLER 2	Washed and sieved pumice	150 µm–75 µm	1
FLUIDIZER	Distilled water	–	0.66 (+ more as required for fluidity)
ADDITIVE	Egg white (whipped)	–	5% (by volume of dry components)

Table 17.3 Cave 85 Grout Components

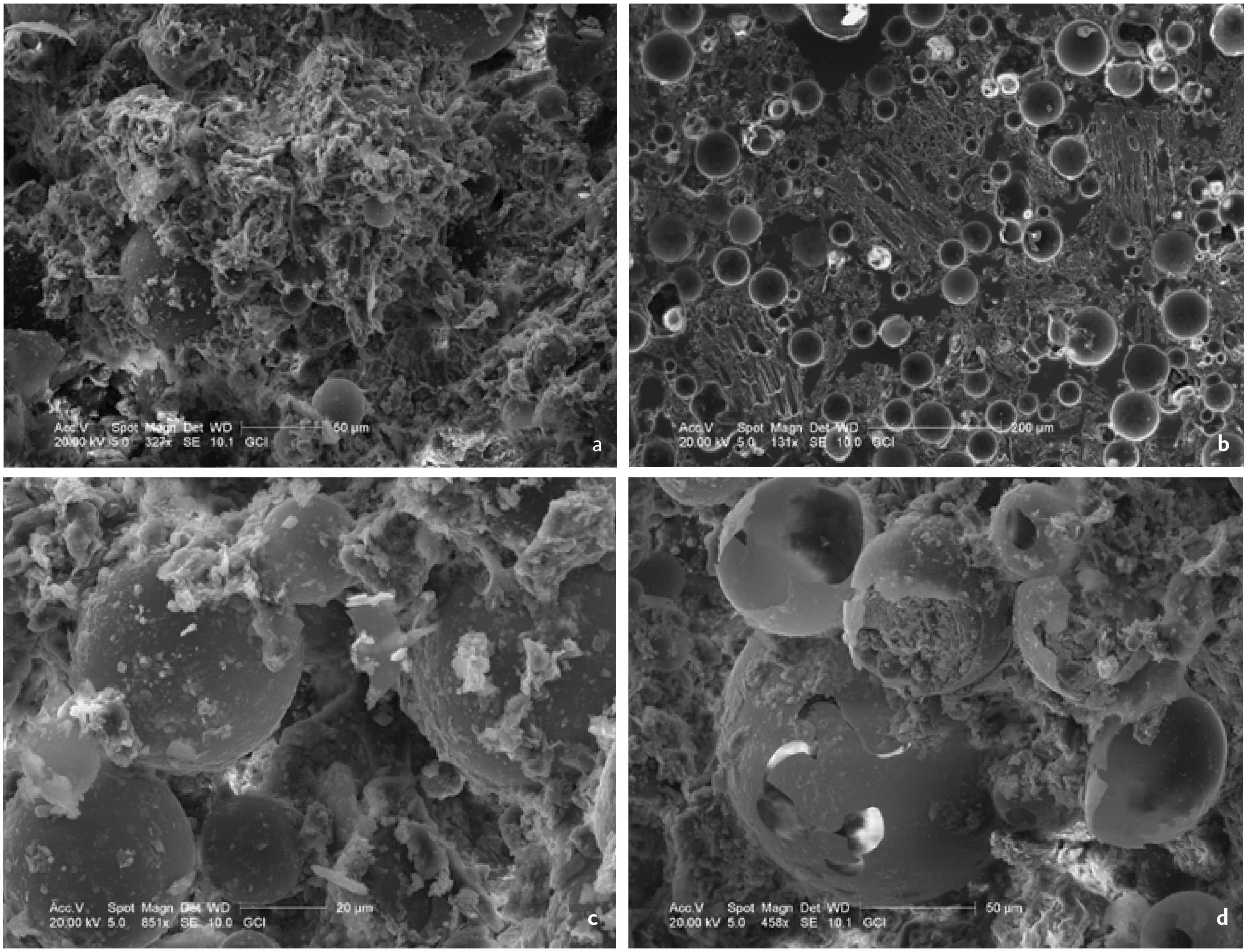

Fig. 17.13 Final grout formulation selected for Cave 85 under ESEM. Polished cross section of the grout shows good packing of pumice and glass microspheres bound together with clay (a, b). Detail showing glass microspheres (c); and, broken glass microspheres filled with clay (d).

	WET WEIGHT (g)	DRY WEIGHT (g)	SHRINKAGE (%)	WATER VAPOR PERMEABILITY (ml/m^{2}s)	UNIAXIAL COMPRESSION (MPa)	THREE-POINT LOAD (MPa)
CAVE 85 GROUT	101	59.4	2.2	5x10^{-4}	1.168	0.456
CAVE 85 REPLICA PLASTER	124.6	86.5	2.4	4x10^{-4}	1.553	0.354

Table 17.4 Key Performance Data of Grout

Fig. 17.14 Whipped egg white was added to the grout to augment clay binding properties and to improve viscosity and injectability and prevent sedimentation.

Fig. 17.15 Absorbent presses were applied after grouting in order to absorb moisture released from the grout and to prevent salt crystallization on the surface of the painting. Pressure rods were used to hold the presses in place and maintain good contact with the painted surface.

MOGAO GROTTOES

Cave 85

West Wall: GROUT AREA 1:

Results of micro-core sampling before & after grouting and poulticing

WEST WALL

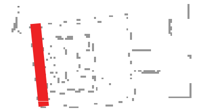

Description of area prior to grouting:
Relatively large area of plaster detachment (≈0.30m^2) both in size and volume (incorporating a detachment gap between the plaster and conglomerate of up to 2cm).

AREA 1

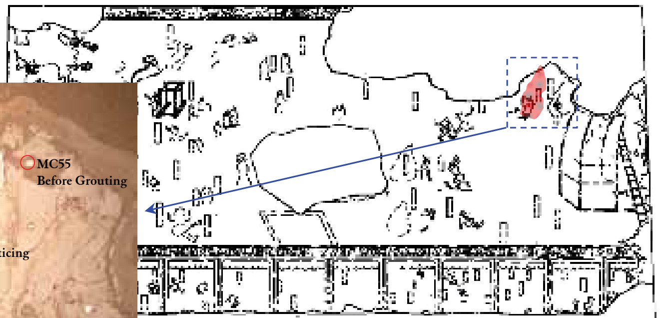

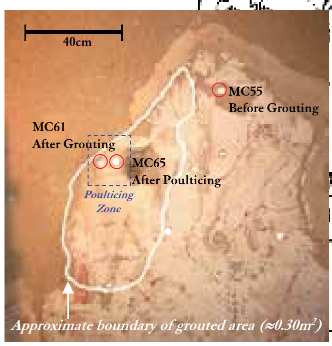

Approximate Incremental Depths (mm)	Before Grouting (g/100g)	After Grouting (g/100g)	After Poulticing (g/100g)
0-2	3.63	0.96	0.73
2-5 *(2-4)	3.55	1.09*	0.63*
5-7 #(4-8)	2.17	1.29 #	0.83#
8-15	n/a	1.20	1.13
15-25	n/a	0.83	0.93
25-36	n/a	0.96	0.73
Average Salt Content	**3.05**	**1.01**	**0.87**

GROUT AREA 1

(see Grouting Log for detailed information)

Procedures:

1. **Grouting:** Area grouted and dry absorbent layers applied. Area monitored carefully, wetted layers changed regularly with dry replacement layers

Quantity of grout injected:
2000ml grout diluted with 315ml distilled water

Absorbent layers applied:
-1x Japanese tissue
-1 or 2x KC-X70
-1x KC-X70 with clay

Drying Time:
Approximately 14 days

2. **Poulticing for Further Salt Extraction:** After drying of grout area, damp absorbent layers applied and removed (still damp) after a few minutes. Dry layers of Japanese tissue and KC-X70 applied and removed after 24 hours.

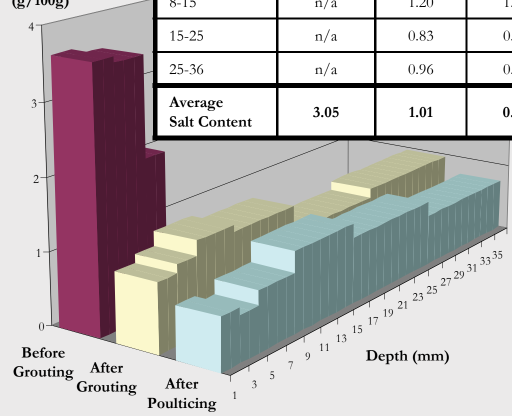

Analysis by the DA using a chloride ion specific electrode. NaCl concentration (g/100g) was calculated from this value.

Grouting was carried out during the Spring Campaign 2002

Fig. 17.16 Soluble salt content of plaster was analyzed before and after grouting to assess salt reduction and possible redistribution. After grouting, an absorbent press system was applied to the surface to absorb any moisture and salts in solution. In this example, from Area 1 on the west wall, additional poulticing was done to further reduce surface salt content. Results show a significant decrease in salt content and a slight reduction following secondary poulticing.

Fig. 17.17 Examination (a) and documentation (b) of plaster voids was an essential first step of the assessment before grouting.

Fig. 17.18 Tissue paper facing applied with 1% Tylose MH-300 was used as a temporary stabilization measure to protect fragile areas before grouting.

Fig. 17.19 Standardized procedures for mixing grout in the laboratory were developed to maintain quality control. Small quantities were mixed as needed.

Appendix 17.E). Since for extraction of moisture the time span for safe and effective absorption is limited, it was anticipated that frequent replacement of the absorbent layers would be necessary to avoid reverse migration.[26]

The presses had a lightweight wood backing with polyurethane foam padding to provide firm but conformable support to grouted areas of plaster. Over the foam padding were placed two layers of absorbent tissue (Kimberly-Clark Wypall X60®). A layer of the absorbent tissue was also impregnated with dried, local riverbed mud, which acted as an additional means of holding absorbed moisture. At the front of the press, lens tissue was incorporated to prevent adhesion to the wall painting. The press was applied to the wall with the aid of pressure rods mounted on the scaffolding (fig. 17.15). The efficacy of this system was dependent on monitoring and timing, and involved teamwork between the conservators and conservation scientists.

Chloride ion analysis, used as an indicator of soluble salts, of the removed absorbent materials was undertaken to evaluate extraction rates during the time the poultice was applied to a grouted area.[27] To evaluate the redistribution of remaining salts in the wall painting, micro-core samples were taken before and after grouting (in areas of unpainted plaster). Salt accumulation at internal interfaces—between the paint layer, ground, plaster, injected grout, and conglomerate—was a concern, and samples were therefore collected at depths corresponding to these strata (fig. 17.16).

Results were variable, reflecting difficulties of sampling and interpreting data from the heterogeneous stratigraphy of the wall paintings.[28] Broadly, however, they pointed to a general lowering of salt levels in areas of grouting, particularly at interfaces within the wall painting. Maximum extraction occurred immediately after grouting, with a decline thereafter as the grouted plaster slowly dried. Based on these findings, the absorbent layers were changed up to three times a day in the first few days after grouting and reduced to twice a day for much of the remainder of the drying period. Only in the final stages of drying were the presses left in place for longer periods.

Grouting: Step-by-Step Process

1. Pretreatment Assessment

The location and extent of plaster voids to be grouted were determined by visual and acoustic (tapping) methods. A rigorous assessment of these areas by graphic documentation, photography, and written logs was undertaken prior to grouting (fig. 17.17). Particular concerns were the gap between the plaster and the rock conglomerate (whether the plaster was flat or bulging or both); the condition of the plaster; the extent and configuration of plaster cracks; and the perimeter of the area of separation. Aspects of condition, such as areas of paint flaking and plaster decohesion, were also recorded in order to decide on stabilization treatments required before grouting and determine appropriate injection points.

Fig. 17.20 A large press being prepared before grouting. Planning was necessary to ensure the correct size was used. The press needed to be large enough to accommodate lateral moisture movement in the plaster.

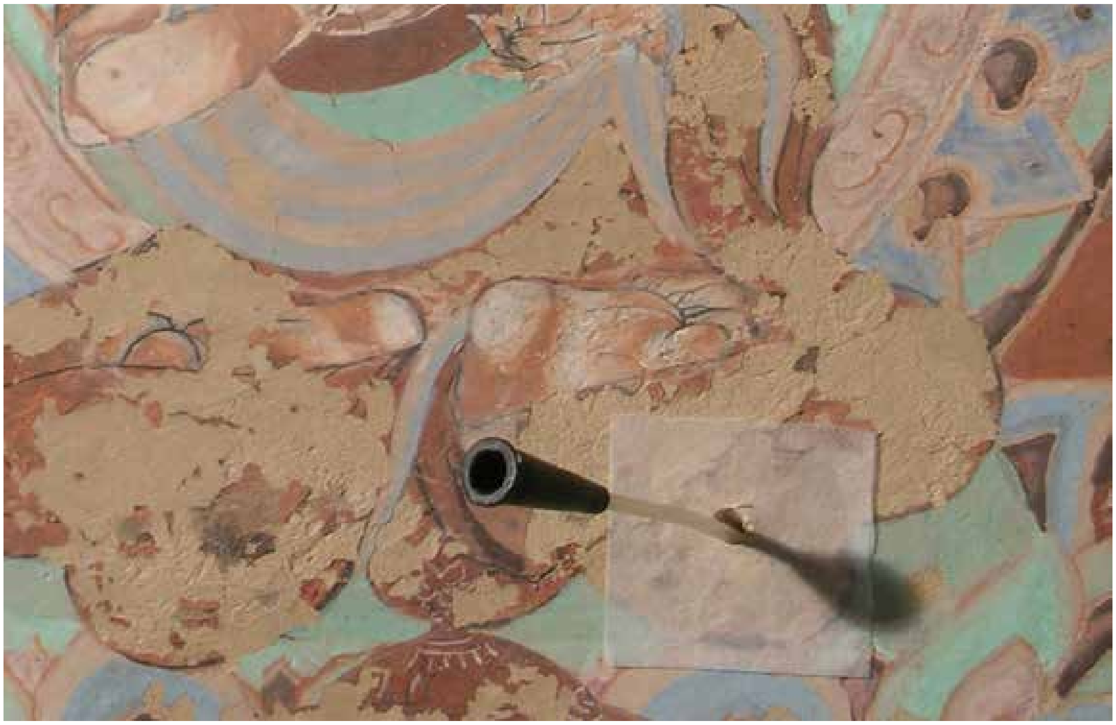

Fig. 17.21 On rare occasions new holes were drilled to provide access points for syringes and catheter tubes. They were done in areas of paint loss.

Fig. 17.22 Teamwork was essential during grouting.

Temporary and emergency stabilization measures were implemented for the worst areas of detachment. Areas with concentrated cracking were faced with tissue paper using a 1% Tylose® MH-300[29] solution in deionized water (fig. 17.18). Gauze bandages were also used to secure vulnerable areas of bulging detached plaster. The bandages were strapped across the painting and secured onto areas of repair plaster or losses in the original plaster with a 20% solution of Paraloid™ B-72 in acetone.[30] Paraloid was found to cause staining of the plaster, and its use was therefore kept to a minimum.

2. Grout Preparation

The final grout formulation was a product of considerable refinement regarding proportions of components, range of particle sizes, and particle morphology (see table 17.3). To maintain quality control, standardized laboratory preparation was necessary, particularly of individual materials before they were mixed. Small quantities (2–3 liters) were produced to ensure consistency (fig. 17.19). Given the relatively fast initial setting of the grout, this protocol also ensured that the mixture was used in its optimal working state.

Fig. 17.23 Temperature measurements of grouted areas were taken when press layers were changed to monitor the drying of the grout.

Fig. 17.24 The absorbent layers were changed regularly up to three times a day immediately after grouting and twice a day until the painted plaster and grout were dry.

Fig. 17.25 An ultrasonic humidifier ("Preservation Pencil") was used to further reduce surface salt following grouting (a). A fine mist of heated water was applied to the surface to dissolve salts, which were then removed by tamping with a sponge through an absorbent tissue (b).

Fig. 17.26 Detail of area of painting from the west wall showing salt efflorescence (a). Detail of same area after removal of surface salts with the ultrasonic humidifier (b).

3. In Situ Preparations

The combined treatment procedures required logistical preparation and coordination. Evaluating individual areas for grouting was essential for determining the size of the presses that would be placed against the plaster. Press dimensions had to be large enough to cover lateral moisture movement in the plaster (fig. 17.20).

Other in situ measures included preparing injection points, applying temporary facings, localized consolidation, and fixing of paint flakes. Where possible, existing holes in the plaster were used as entry points for catheters and needles; on occasion, new holes had to be drilled that were carefully made through plaster in areas of paint loss (fig. 17.21).

Usually four conservators were involved in the grouting of a single area, two preparing the grout and syringes with flexible catheter tubes, one delivering the grout, and one manually checking and supporting the plaster (fig. 17.22). Effective communication among team members was key. Treatment logs recording the amount of injected grout and the quantities of water added to fluidize the basic grout mixture in response to differing grouting situations were kept (see Appendix 17.F).

4. Post-Treatment

Post-treatment assessment of the grouted areas was intensive over the three- to four-week drying period. During this time, a daily regimen was established for changing the absorbent layers in the presses, preparing the absorbent materials in the laboratory, changing them in situ, and logging the frequency of changes. An infrared thermometer was used to monitor drying rates by comparing spot measurements of treated (damp) and adjacent untreated (dry) areas until the same temperature was reached (see sidebar on thermography) (fig. 17.23).

Checking and care of grouted areas coincided with the press changes, both measures requiring detection of early signs of salt-related and other forms of deterioration. To prevent salt crystallization on or immediately below the surface of the paintings, it was necessary that the absorbent presses be replaced quickly to reestablish capillary continuity with the painted plaster (fig. 17.24).

After complete drying of grouted areas, post-treatment care continued in other forms. Residual surface salts posed risks that were partly remedied by use of an ultrasonic humidifier that projected a fine mist of heated water at 50°C onto the surface of the treated areas to dissolve the salts, which were then removed by tamping with absorbent tissues (figs. 17.25, 17.26).[31] This technique provided control by limiting the amount of moisture added. As with the main salts-reduction procedures, these additional measures were monitored by tracking chloride ion levels in the used absorbent tissues and by sampling the plaster to check salt redistribution patterns (Chen et al. 2010). Results indicated that this treatment reduced surface salts.

A ThermaCAM® B2 infrared camera[1] was used to monitor the drying of grouted areas and to evaluate its potential to be used as a noninvasive examination tool to detect plaster detachment. The camera is a portable, noncontact tool that measures surface temperature and images the emitted infrared radiation of a wall surface.[2]

Assessment of the drying of wall surfaces using the infrared camera following grouting is based on the fact that water in the grout migrates through the painted plaster to the surface, where it evaporates. Evaporation decreases surface temperature. Temperature differences between a dry surface (outside the grouted area) and a moist surface (the grouted zone) were between 1°C and 1.5°C. With the infrared camera it was possible to visualize the area of evaporation associated with grouting. Recording was done over the period of drying of the grout (approximately 3–4 weeks) when the presses were changed (initially 2–3 times a day). It was important to know the area of evaporation in order to apply an appropriate size of absorbent materials to the surface to avoid crystallization of salts on the surface. The infrared image of the evaporation area is also a record of the area grouted (including the lateral diffusion of water in the plaster beyond the area where the grout actually reached) and therefore is useful for the long-term monitoring of the paintings (see chap. 18).

Evaluating the infrared camera's potential for detecting voids is based on the idea that grouted areas of plaster cool slower (having more mass) than voided areas. A temperature difference was observed, but the rate of cooling of the two areas was not great enough to clearly identify the void.

NOTES

1. The infrared camera is produced by FLIR Systems™.
2. The camera has a 2.5" color LCD screen and an infrared lens (25°). Images are downloaded to a PC using FLIR Systems ThermaCAM QuickView software. The radiation measured is a function of the surface temperature of an object and its emissivity. Emissivity was set to 0.9, which falls in the emissivity range of most building materials.

Fig. 17.27 Tests were carried out with an infrared camera to monitor the drying of a grouted area. A test was undertaken on a replica panel. The panel was grouted with a room temperature grout (a); water from the grout then wet the plaster surface (b). Images were taken with the infrared camera over several days as the grout dried (c).

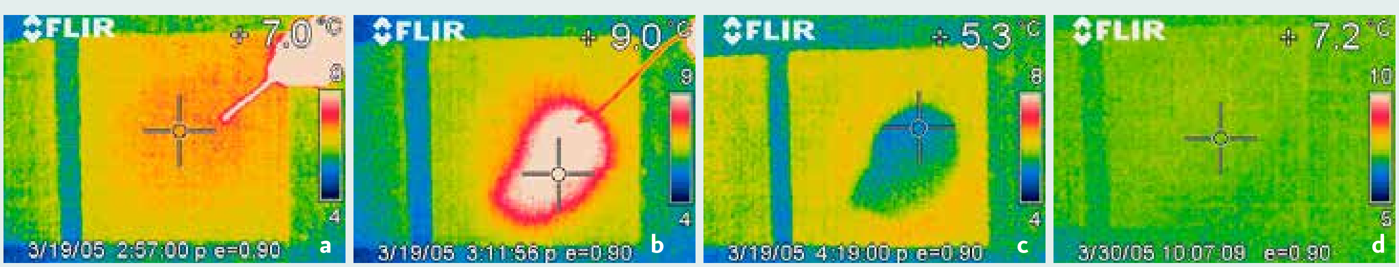

Fig. 17.28 Infrared images taken of the panel before grouting (a): the surface of the panel is 7°C; during grouting (b): the surface of the newly wet plaster area warms to 9°C; approximately one hour after grouting (c): the surface of the wet plaster area has cooled to 5.3°C; and eleven days after grouting (d). The surface of the plaster is dry as the temperature has returned to 7°C, and no temperature difference was noted across the panel.

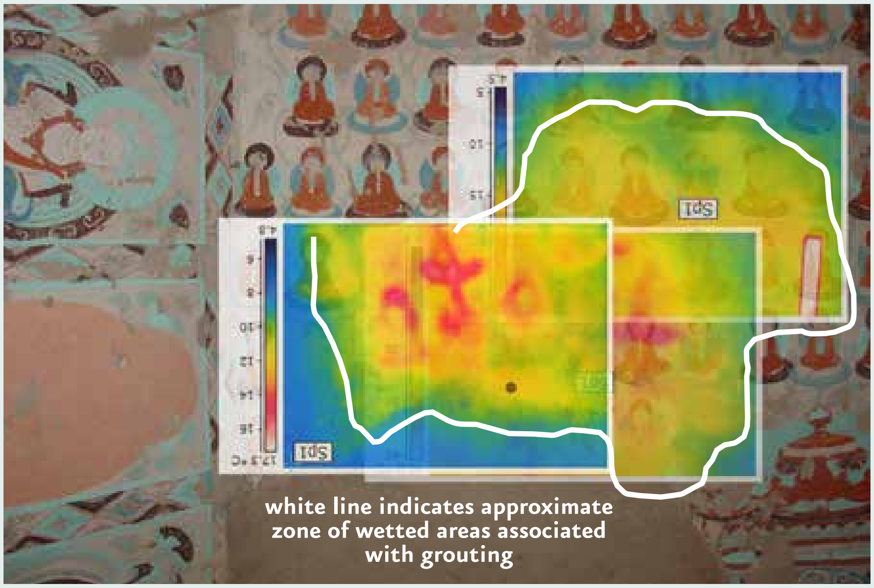

Fig. 17.29 The infrared camera was tested on a grouted area on the corridor ceiling. Results of the test gave a rough impression of the area grouted (area in red, yellow, and green). The area outside of the grouting is in blue. Because the scaffolding was already positioned the camera could not be placed far enough away to capture the whole area. Instead, multiple images had to be mosaiced together.

Fig. 17.30 Tests were carried out with an infrared camera to detect voids and areas of plaster detachment. A replica panel that had been partially grouted (with the left half of the panel removed in order to see the void)(a) was heated with a lamp (b) and then infrared images taken as the panel cooled.

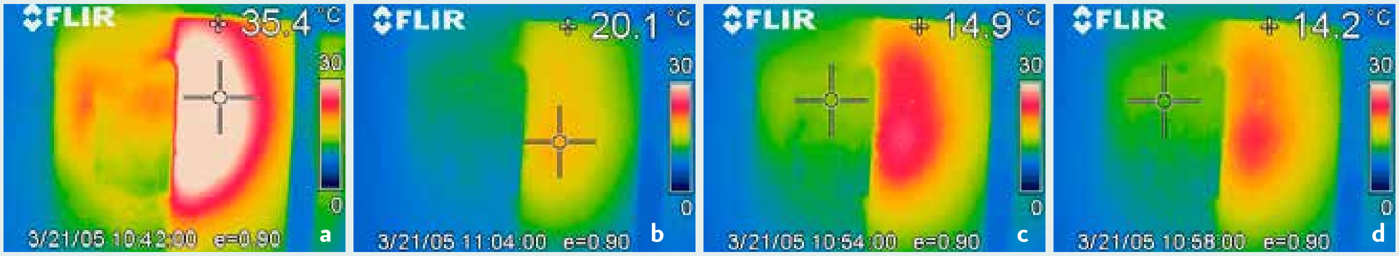

Fig. 17.31 Infrared images of the grouted panel were taken as it cooled. The idea was that grouted areas would cool slower than voided areas. A temperature difference was observed, but there was not enough resolution to clearly define the void.

Fig. 17.32 Example of flaking of the wall paintings in Cave 85 shown before (a) and after (b) treatment.

Adhesive and Consolidation Testing

Flaking and powdering of the paint layer is a problem in many of the caves at Mogao and has long been a concern of the Dunhuang Academy (fig. 17.32).[32] In Cave 85, following flaking treatment with PVA and PVAc emulsions in 1974 (see chap. 9), painting at the east end of the cave, where there are few salt-related conditions, remained stable, with only small localized areas of flaking recurring. In contrast, the high salt environment of much of the west end of the cave caused a worsening of condition in the form of widespread paint exfoliation (see sidebar, Emergency Treatment of Exfoliation), and powdering of both paint and upper plaster. This demonstrated the need for rethinking treatment for these problems, as the use of a vinyl emulsion was not suitable for the conditions in this cave. In order to determine a suitable and compatible adhesive/consolidant, performance characteristics were identified. These were good adhesive/cohesive performance over time; resistance and durability to a high salt environment; absence of optical change to painted plaster (including discoloration, staining, saturation, gloss); no effect on water vapor permeability of painted plaster; and microbiological resistance.

In addition, working properties specified were good adhesive/cohesive capabilities on initial contact (tackiness); good depth of penetration; ease of preparation and use on site; and low toxicity.

Materials Selected for Testing

Based on the desired performance characteristics and working properties a range of adhesives/consolidants was selected for testing. Because of the problems caused by PVA and PVAc, vinyl adhesives were only initially tested for comparative purpose.[33] Gums and glues, detected in the paint and ground layers of the painting (see chap. 13), and other similar traditional organic adhesives were considered compatible materials to test.[34]

The following adhesives were tested: gelatin, hide glue, bone glue, gum tragacanth, PVAc, and Primal™ AC-33.

Testing Procedures

The six materials were evaluated based on the tests shown in table 17.5. Results are presented in table 17.6.

TEST	PURPOSE	EVALUATION METHODS
ADHESIVE STRENGTH	To evaluate capacity of adhesive to readhere paint layer onto earthen plaster layer.	After drying of adhesive: visual examination and comparison with before-treatment photographs to evaluate changes.
COHESIVE STRENGTH	To evaluate capacity of material to consolidate decohesive paint and earthen plaster layers.	After drying of adhesive: visual examination and comparison with before-treatment photographs to evaluate changes.
ARTIFICIAL AGING	To assess stability and durability of adhesive in a salt-contaminated environment after repeat cycling of relative humidity.	After artificial aging: visual examination and comparison with before-treatment photographs to evaluate changes.
OPTICAL CHANGE	To evaluate visual effects of the solution applied on the painted plaster (including discoloration, staining, saturation, gloss).	After drying of adhesive: visual examination and comparison with before-treatment photographs and untreated sample to evaluate changes.
WATER VAPOR PERMEABILITY (WVP)	To assess changes to the water vapor permeability of the painted plaster following application of material.	Following ASTM E 96: Standard test method for water vapor transmission of materials and NORMAL 21/85, water vapor permeability.

Table 17.5 Adhesive and Consolidant Testing

Results of Adhesive/Cohesive Tests

Based on initial results, PVAc and Primal™ AC-33 were eliminated as possible treatment materials, while gelatin, hide glue, bone glue, and gum tragacanth were tested further in varying concentrations: gelatin (2% and 1%), hide glue (2% and 1%), bone glue (2% and 1%) and gum tragacanth (1% and 0.5%).[35] Artificial aging tests were also performed on prepared replicas (fig. 17.33). Gelatin was selected as the most appropriate material (fig. 17.34).

Treatment was carried out with gelatin solutions in concentrations varying from 1 to 2% in deionized water depending on variable conditions of areas of flaking and powdering throughout the cave. It was necessary to warm the gelatin to maintain low viscosity and to provide good penetration (fig. 17.35). The gelatin solution was applied behind paint flakes and fed through cracks in the paint layer, or applied directly to areas of powdering, using a syringe. The paint layer was then gently pressed back with a silk and cotton ball and a wooden spatula through a layer of Japanese tissue to protect the painted surface.

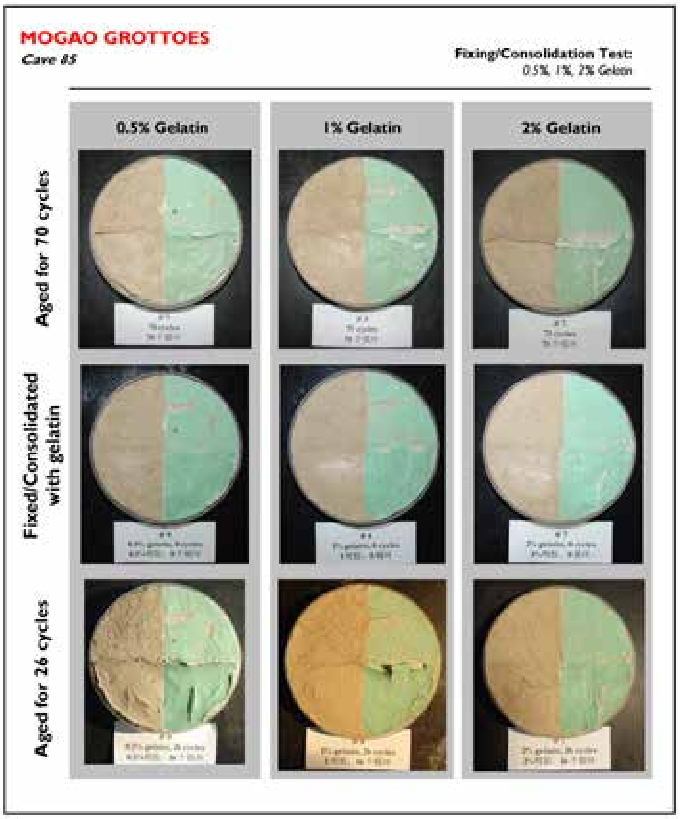

Fig. 17.33 In artificial aging tests painted replicas were aged for 70 cycles of low and high RH (1 cycle = 48 hrs at 100% RH followed by 24 hrs at ambient RH). Flaking and consolidation of the painted surface was then undertaken with gelatin at 0.5%, 1%, and 2%; and treated replicas were aged for 26 cycles.

MATERIALS TESTED (3% IN WATER)	PROS	CONS
GELATIN	• Compatible with original materials • Good adhesive strength • Good cohesive strength • Maintains adhesive and cohesive strength after aging, stable in high RH conditions • Little change in optical properties • Minimal or no film formation • Good WVP, does not inhibit passage of salts and moisture. • Good adhesive capabilities on initial contact • Low viscosity and good penetration	
HIDE GLUE	• Compatible with original materials • Good adhesive strength • Good cohesive strength • Maintains adhesive and cohesive strength after aging, stable in high RH conditions • Minimal or no film formation • Good WVP, does not inhibit passage of salts and moisture • Good adhesive capabilities on initial contact • Low viscosity and good penetration	• Initial glossy surface but lost during aging
BONE GLUE	• Compatible with original materials • Good adhesive strength • Good adhesive capabilities on initial contact • Good WVP, does not inhibit passage of salts and moisture • Low viscosity and good penetration	• Poor cohesive strength • Contraction of paint film on aging • Surface skin formation (film forming) • Initial glossy surface but lost during aging
GUM TRAGACANTH	• Compatible with original materials • Good adhesive strength • Good WVP, does not inhibit passage of salts and moisture • Good adhesive capabilities on initial contact	• Poor cohesive strength • Contraction of plaster on aging • Viscous, poor penetration • Not completely soluble and difficult to prepare
PVAc	• Good adhesive strength • Good adhesive capabilities on initial contact	• Not compatible with original materials • Poor cohesive strength • Contraction of paint film on aging • Surface skin formation (film forming) • Poor WVP, inhibits passage of salts and moisture • Severe color change
PRIMAL™ AC-33	• Good adhesive strength • Fair adhesive capabilities on initial contact	• Not compatible with original materials • Poor cohesive strength • Contraction of paint film on aging • Surface skin formation (film forming) • Poor WVP, inhibits passage of salts and moisture • Color change

Table 17.6 Results of Adhesive and Consolidant Tests

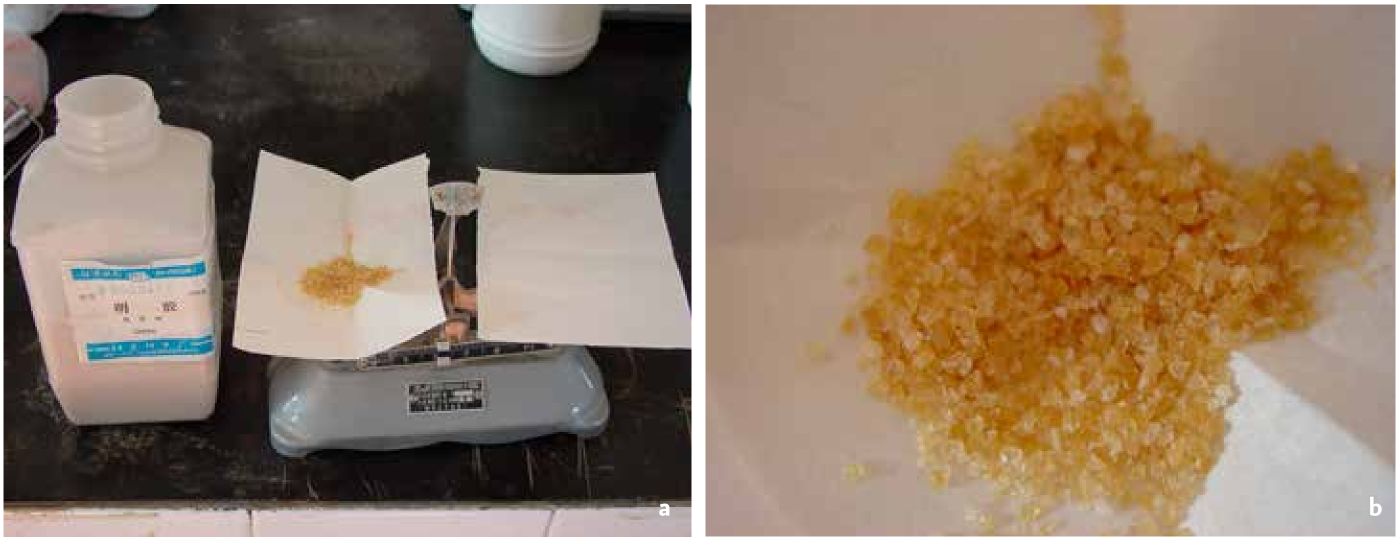

Fig. 17.34 Chinese lab reagent grade gelatin used in concentrations varying from 1–2% in water was selected as the most appropriate adhesive for fixing flakes and treating powdering plaster in Cave 85.

Fig. 17.35 Warming the gelatin in a hot water bath before use helped to keep a low viscosity for good penetration (a); using a syringe to inject gelatin solution behind flakes (b); pressing back the lifted flakes with a wooden spatula through a layer of Japanese tissue (c).

Emergency Treatment of Exfoliation

Fig. 17.36 Areas of exfoliation before (a) and after (b) treatment.

Areas of flaking had been treated with PVA and PVAc in 1974. Since then flaking at the west end of the cave has recurred in worsened form. The impregnation of paint and ground layers with vinyl emulsion in areas of salt deterioration has led to a different and severer type of flaking, exfoliation—the lifting of the paint layer, ground, and some fine plaster (see chaps. 9, 12).

In 1999, a sudden occurrence of widespread exfoliation, most likely caused by unusually severe fluctuations in RH, required emergency treatment. A treatment was developed to readhere the lifted layers and bulk out areas of underlying powdering plaster. Decohesion of the plaster layer, caused by deliquescence and recrystallization of salts, was otherwise found to lead to deformed and depressed surfaces upon readhesion of the exfoliated layer.

Treatment was carried out by injecting an earth-based slurry (riverbed mud and deionized water) behind exfoliated layers in order to consolidate the powdery earthen plaster and to provide bulking and adhesive properties. This was followed by gently pressing down the surface through absorbent tissue, which in addition helped to reduce any dissolved salts.

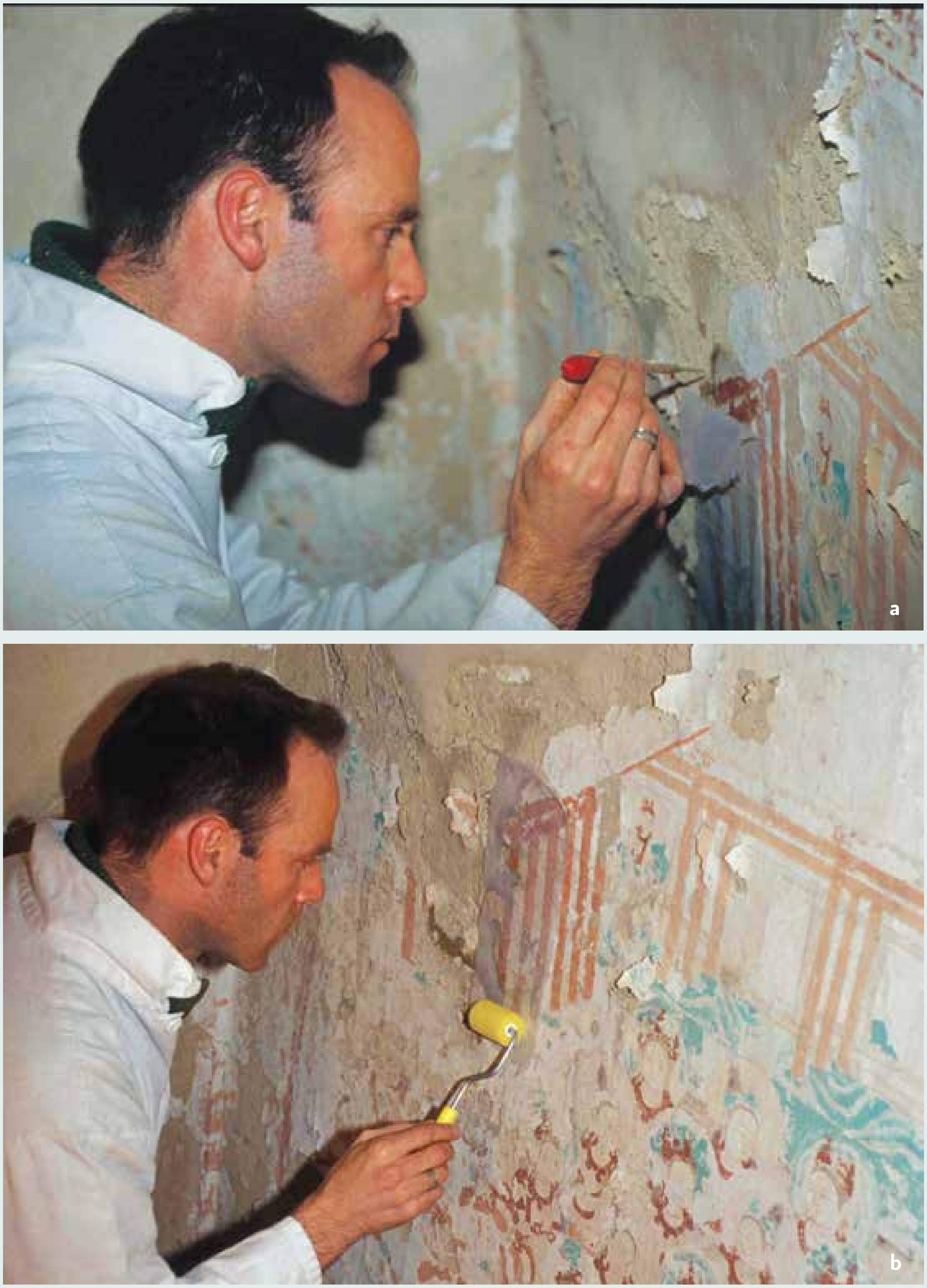

Fig. 17.37 A bulking adhesive consisting of riverbed mud and deionized water was used to readhere areas of exfoliation. It was applied behind lifted areas using a pipette (a). Large flakes were pressed back with a soft sponge roller through a layer of Japanese tissue (b). The tissue helped to absorb moisture and reduce any dissolved salts on the painted surface.

Fig. 17.38 The repair plaster used in Cave 85 is based on the composition of the original plaster and contains riverbed mud, sand, and chopped straw.

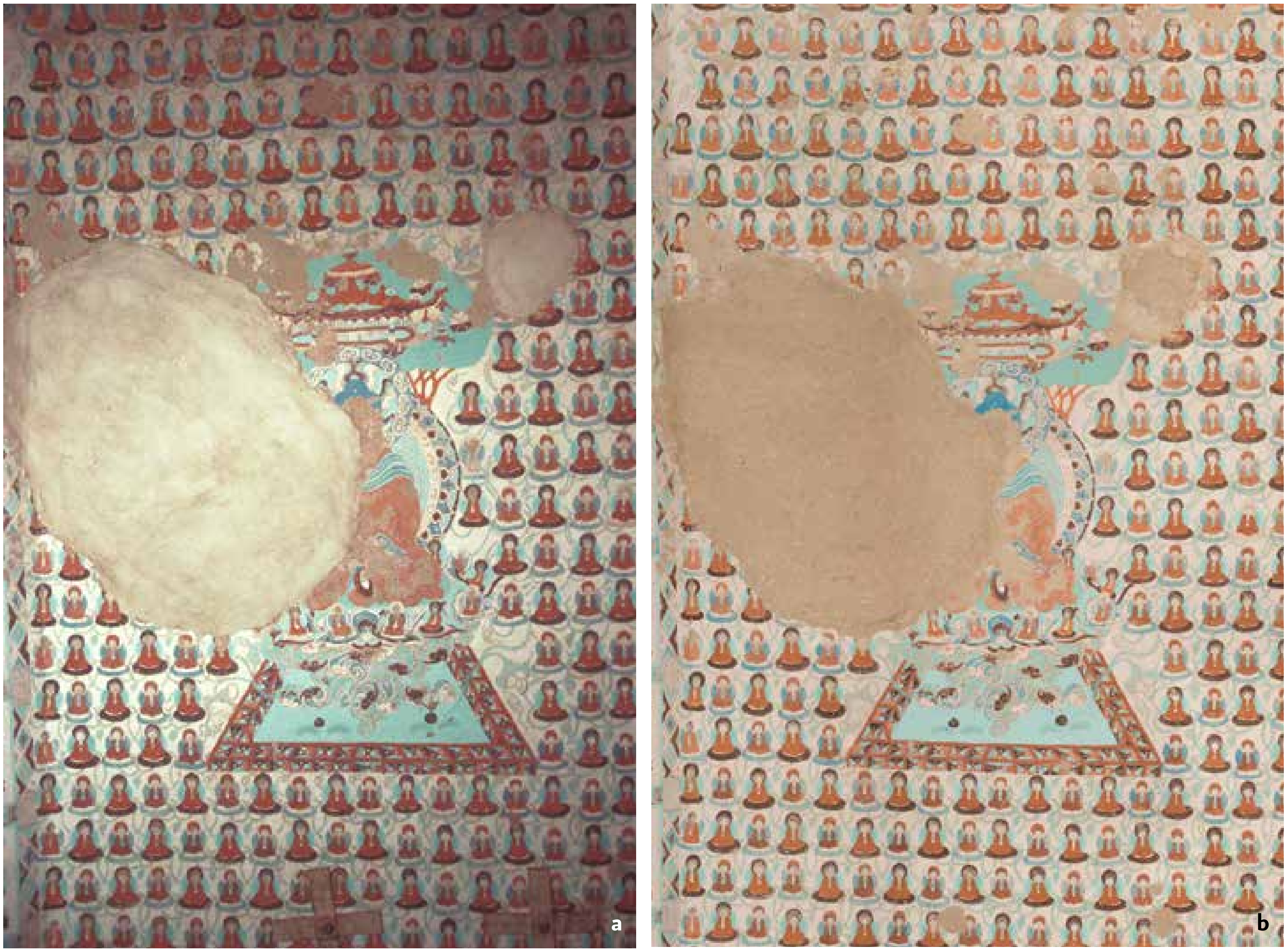

Fig. 17.39 Old plaster fills were sometimes left in place rather than replaced in order to avoid introducing water. In some cases, such as this example from the corridor ceiling, the plaster surface was partially removed in order to make the repair more aesthetically acceptable. Only the hard, white, smooth plaster skim repair was removed.

Fig. 17.40 To stabilize fragile edges of the painting, plaster repairs were made. Necessary precautions were taken to minimize the amount of water used, and absorbent presses were applied to areas to prevent salt crystallization on the surface of the painting.

Repair Plaster

Based on the composition of the original plaster (see table 17.1), a repair plaster was made with 64% riverbed mud (soluble salts removed by soaking in water), 36% local sand (washed and sieved, <425 μm), and chopped straw cut to 0.5–1 cm (fig. 17.38) (see Appendix 17.B).

The high soluble salt content in the original rock and plaster and the introduction of water from existing previous repair plaster had led to salt crystallization on surrounding areas of painting. In order to prevent salt-related deterioration, new repairs were kept to a minimum. In general, large areas of loss were not filled, while existing previous repairs were kept or were cut back to make them aesthetically acceptable (fig. 17.39). Where repairs were necessary, precautionary measures were taken, for example, to minimize the width of edging plaster, to avoid or reduce prewetting of the original plaster, to reduce the amount of water in the repair plaster, and to use an absorbent press system on all treated areas during drying to absorb salts dissolved by the repair mixture (fig. 17.40).

In two areas where there were particularly large and deep holes in the conglomerate, a decision was made to cover the areas with repair plaster. In order to do this, pieces of bamboo were placed over the void and the areas then plastered. This method significantly reduced the amount of plaster needed and also minimized the quantity of water introduced into the painting (fig. 17.41).

Fig. 17.41 A large, deep void in the conglomerate was filled by placing vertical pieces of cut bamboo over it and then applying plaster.

Fig. 17.42 Gentle dry cleaning of the corridor paintings was undertaken with soft brushes to remove dust, surface deposits, and smears of paint and dirt (a). Figure on the south wall of the corridor before cleaning (b). Figure after dry cleaning with brushes (c).

Fig. 17.43 Fragments of the original altar platform were uncovered during treatment. Painted and modeled fragments (upper part of image) had been reused as building blocks to reconstruct the shape of the altar base during a previous restoration.

Fig. 17.44 Selective plaster repairs were made to the altar platform for stabilization purposes and to preserve the physical evidence of the original modeled features (a). Partial uncovering of better-preserved areas of the original plaster was also undertaken (b).

After drying, the areas of repairs were inspected and found to have low shrinkage, good color, and an open texture; no salts appeared in adjacent areas.

Cleaning

Cleaning of the painted surface was not a major component of treatment. In the main chamber, gentle brushing to remove dust, webs, and other surface deposits was carried out mainly in preparation for grouting. Only in the entrance corridor, where proximity to the door had resulted in greater dust deposition on the painting, was more cleaning done. Past cleaning attempts have led to paint smearing; these may have been acts of deliberate defacement or to hide incised graffiti, or the result of misguided cleaning methods (see chap. 12) (fig. 17.42).

Cleaning options for the corridor painting were limited due to vulnerable conditions and technology. A floral decoration in the background survives as a faint impression, easily mistaken for dust rather than original paint. Areas of altered lead pigment similarly have a dusty, gray appearance, also difficult to distinguish from deposited dust. Conditions such as these meant that most cleaning had to be partial and/or selective. Superficial dust was removed or reduced by gentle mechanical (dry) methods, where trials indicated that such cleaning was possible. Cleaning was not attempted in other areas. No chemical (wet) cleaning was possible because of the sensitivity of the painting.

Treatment of Altar Platform

Treatment of the altar platform was limited, aimed at modifying previous existing repairs in order to reveal concealed original features. Damage to the altar base was considerable, probably as a result of past flooding (see chap. 12). Previous treatment had involved plastering over nearly all the remaining original plaster. Retreatment included the partial exposure of better-preserved areas, followed by their repair and consolidation. During this process, a large number of original painted plaster fragments were discovered reused as blocks for reconstructing the shape of the base (fig. 17.43). These ranged in size from a few centimeters to as large as 50 cm in length.

The exposed original plaster was usually very damaged and eroded. Repairs were applied selectively and sparingly to preserve physical evidence of the original modeled features (fig. 17.44). The repair plaster was the same as that used for repairs to the wall painting. No remodeling was done. Much of the previous repair plaster was also left to provide a stable surround to the newly exposed areas. The level of this plaster was reduced and modified to make it more visually sympathetic yet distinguishable from the original plaster.

Strengthening of areas of decayed earthen plaster was also necessary. This was undertaken using a 1% solution of gelatin applied by pipette or syringe or sprayed onto the surface. Prewetting with a mixture of alcohol and water (1:1) was necessary in order to allow sufficient penetration of the consolidant into the plaster. Without prewetting, loose clay particles limited penetration of the consolidant, leaving the plaster below weak and unconsolidated.

Summary

Given the complexity of the conservation problems, limited stabilization treatments were designed to meet the specific conditions and constraints. In particular, the formulation of a grout that relied entirely on the clay fraction of the earth component for its binding ability was a core accomplishment. The development of a combined grouting and salts-reduction treatment also provided an important model for the way in which treatment must be approached: particular circumstances of original technique, condition, and deterioration must be reflected in the final design. In addition, simple environmental control measures that reduce the intrusion of moist air into the cave must be implemented to ensure the efficacy of treatments over the long term and to prevent further deterioration of the wall paintings.

Notes

1. Treatment of the sculpture was undertaken by the Dunhuang Academy (see Appendix 17.A).
2. Alternatively, other methods of desalination have also been explored, including passivation and manipulation of crystallization (Cather 2003). Passivation aims to reduce the risk of potentially harmful phase changes by isolating the salt with a material of lower solubility (Matteini 2001), and efforts to manipulate crystallization have explored the use of inhibitors (Selwitz and Doehne 2002; Rodríguez Navarro et al. 2000) and altering interfacial forces (Scherer et al. 2001; Houck and Scherer 2006).
3. An aqueous poultice removes salts from a wall painting in two stages: a wetting or penetration stage, whereby the poultice introduces water into the wall painting; and a drying stage with the poultice, when the poultice provides an absorption layer into which water and dissolved salts migrate, before both the poultice and the salts are discarded (Tinzl 1994, 16, 18, 23). For a recent collection of papers on salt contamination of lime-based wall paintings and approaches to salts-reduction treatments, see Leitner et al. 2003.
4. Environmental control has been successful at several historic sites including the church of Zillis in Switzerland, where climate control measures allowed for the suppression of damaging fungi in the 12th-century painted wooden ceiling (Bläuer-Böhm et al. 2001).
5. Although this problem has been little studied, see Leitner 2000 for research into the dynamics of structural failure associated with pinning painted plaster to suspended wooden ceilings.
6. For a discussion of the detrimental effects of wall painting detachment and transfer, see Brajer 2002.
7. See, for example, Ferragni et al. 1984, 110–16; Botticelli et al. 1986, 177–79; Baglioni et al. 1997, 43–54; Barcellona et al. 1993, 637–43; Teutonico et al. 1994; and Peroni et al. 1982, 63–99.
8. Most of the conservation literature on grouts is primarily concerned with its laboratory-based development and testing (see again, for example, Ferragni et al. 1984, 110–16; Botticelli et al. 1986, 177–79; Baglioni et al. 1997, 43–54; Barcellona et al. 1993, 637–43). A significant precedent for the Cave 85 project was the collaborative project of the Courtauld Institute of Art and the Valletta Rehabilitation Project to conserve the late-16th-century frescoes by Filippo Paladini in the Chapel of the Grandmaster, Magisterial Palace, Valletta (Malta), undertaken from 1998 to 2004. Based on research of grouting at the Courtauld Institute (Griffin 1999, 2004), this project also focused on the development of a grout (lime-based), followed by its large-scale implementation.
9. Additional research on earth-based grouts has also been undertaken by the historic preservation graduate program at the University of Pennsylvania.
10. See also Rickerby et al., "Implementation," 2010; and Rickerby et al., "Development and Testing," 2010.
11. See, for example, Griffin 1999, Appendix D.
12. The testing standards that exist have mostly been developed for cement-based mortars. Tests for performance characteristics and working properties carried out during the development of the Cave 85 grout were based on those of Griffin (1997, 1999, 2004) and on ASTM and CSTM procedures. No standards have been specifically formulated for conservation grouts. Work undertaken by the GCI's Injection Grouts for the Conservation of Architectural Surfaces: Research and Evaluation project has begun to fill this gap. Information can be found at: http://www.getty

.edu/conservation/field_projects/grouts/grouts_component2.html.

13. The development and testing of the injection grouting and salts-reduction treatments of Cave 85 were conducted from 1998 to 2002.
14. Although manual acoustic methods (tapping) remain the norm for detecting, recording, and, to some extent, evaluating the risk posed by plaster voids in wall paintings, various nondestructive instrumental techniques have also been used, including 3D laser scanning and modeling for documenting spatial deformations (see, for example, Casciu et al. 2000, 208–19); ultrasonic pulse vibration and measurement (see, for example, Gosálbez et al. 2006, 492–97); and infrared thermography (see, for example, Grinzato et al. 1994, 257–74). Thermography in Cave 85 was attempted but proved unsuccessful (see Thermography sidebar in this chapter).
15. Graphic documentation of grouted areas is found in Appendix 17.G.
16. Griffin 1999 also found that some earthen grouts shrank less than lime-based grouts, because they required lower water content to achieve the same consistency.
17. Inherently poor adhesion between lime- and earth-based materials has been noted by Griffin 1999, 13, 60; and Cather 2003, 169.
18. Since fillers primarily alter the physical properties of a grout, they are usually selected for their chemical inertness. The possibility of using chemically reactive fillers in earthen grouts was not explored. Materials such as calcite, silica, and ferric oxide, for example, have been shown to act as cementing agents in earth mixtures, forming chemical bridges between clay micelles that may reduce swelling (Foth 1990, 31).
19. For a discussion of filler materials used in conservation, including glass microspheres, see Smith 2000.
20. Although SEM micrographs of glass microspheres show breakage of individual spheres, this does not occur on a sufficient scale to improve their overall packing geometry and thus better cohesion.
21. Pumice is also a natural pozzolana, though no pozzolanic reaction occurs in the Cave 85 grout mixture due to the absence of calcium hydroxide.
22. Proteins and amino acids react with clays to cause clay flocculation (Griffin 1999, 21–22). Amino acids are present in some quantity in egg white (Mills and White 1987, 76). Griffin found that egg white used as an additive in earthen grouts was beneficial (Griffin 1999, 24–31, 35, 39–42, 44–45, 51–60, 63–65, 69).
23. Egg white also has a long tradition of use as an additive to lime plasters and mortars because of its adhesive properties (Sickels 1982, 27, 37), and it is still similarly employed by conservators in Austria (pers. comm. Prof. Heinz Leitner). Partly based on these precedents, it was also used in the lime-based grout to conserve the wall paintings in the Chapel of the Grandmaster in the Magisterial Palace, Valletta, Malta. The preparation of the egg white in this grout influenced its use in the development of the Cave 85 grout.
24. Salt investigations indicate that the soluble salts content in the plaster at the west end of the cave can be up to 4% (expressed by weight) and that the most common ions are sodium and chloride (see chap. 16).
25. Materials tested were highly absorbent tissues, manufactured from cellulose fibers bonded to nonwoven polypropylene fabric. These were also tested after impregnation with dried riverbed mud, to enhance their absorbency.
26. During aqueous extraction, an equilibrium is established between the filled capillaries of the substrate and those of the applied absorbent. At this point, reverse migration may occur, due to greater capillary attraction of the substrate (see Grüner and Grasseger 1996).
27. Since sodium chloride was the major salt species present in Cave 85, monitoring of salt in the absorbent layers used in the presses, and in the original plaster before and after treatment, was carried out with a chloride ion electrode on aqueous extracts. For a fuller discussion of the salt contamination in Cave 85, see chapter 16.
28. For the difficulties of salt sampling in terms of characterizing topographic and stratigraphic distribution, see Cather 2003, 168.
29. Tylose® MH-300 is a water-soluble methylhydroxyethyl cellulose produced by SE Tylose GmbH & Co. KG.
30. Paraloid™ is a thermoplastic acrylic resin produced by Rohm and Haas.
31. The ultrasonic humidifier was a Preservation Pencil® produced by Preservation Equipment Ltd. The absorbent tissues (paper-pulp fibers bonded to nonwoven polypropylene fabric) were manufactured by Kimberley Clark (Kimberly-Clark KayDry EX-L®).
32. The Dunhuang Academy has a long history of testing both organic and inorganic adhesives to strengthen areas of flaking, exfoliation, and disrupted plaster. Testing of polyvinyl acetate (PVAc), peach gum, and isinglass was carried out by DA conservator Li Yunhe in Cave 474. Animal glues and plant gums were also tested as possible adhesives by the DA in Cave 130. Results were mixed: in some cases the flaking returned; in others drying of the glue and the thickness of its application caused contraction, flaking, and loss of the paint layer. The DA sought outside assistance on this issue, and in 1956 a Czech conservation consultant recommended the use of an adhesive material similar in appearance to clay. This powder, the identity of which is unknown, when mixed with water produced a pastelike consistency that could be applied behind the paint layer to act as an adhesive. This material was only tested in Cave 474 and was ruled unsatisfactory because the flaking returned and the material left the surface of the paintings shiny. In 1962, a Chinese student who studied conservation in Poland brought back PVA and PVAc, which has since been used not only as a fixative but also as an additive to grout mixtures and to consolidate paint and plaster layers. Despite some good results organic natural adhesives were rejected, and the use of synthetic adhesives was favored as they were at the time thought to be more stable materials. A paper on the suitability of PVAc and PVA for fixing paint flaking at Mogao was published in 1990 (Li et al. 1990). A subsequent article focused on the stability of these materials under artificial aging cycling of RH and T. Wrinkling and blistering of paint surfaces was recorded at 60% RH and above (Li et al. 1992).
33. Paraloid™ B-72 and methylcellulose were also included in the initial round of testing but were discounted early on as initial adhesion testing at 8% did not yield satisfactory results.
34. Inorganic consolidants such as lithium, potassium, and ethyl silicates were not tested. Lithium and potassium silicate have been previously tested by the Dunhuang Academy in 3% solutions with multiple applications with mixed results. Lithium silicate was not considered effective as an adhesive; potassium silicate was tested as a consolidant for plasters but led to the formation of soluble salts, caused undesirable color change, and created a hydrophobic surface after treatment. Ethyl silicate was not tested.
35. Glues and gum tragacanth were locally obtained, and laboratory grade gelatin was also purchased in China.

CHAPTER 18

Condition Monitoring

The nature and extent of the treatment program in Cave 85 require the implementation of a post-treatment condition monitoring plan. The principal remedial treatments of the wall paintings, injection grouting and soluble-salt reduction, were undertaken on a large scale, reflecting pretreatment conditions of extensive areas of plaster detachment and widespread salt contamination of the plaster and rock substrate (see chaps. 16, 17). The scale of the interventions was matched by their high-risk nature. Grouting is both an invasive and an imprecise intervention. Similarly, the reduction of soluble salts is also potentially hazardous, risking the redistribution of soluble salts, particularly in the case of earthen plasters. Moreover, remedial treatment was not a means of halting the complex and diverse range of environmental deterioration processes in the cave. Thus, a condition monitoring strategy must also reflect the continuing vulnerability of the plaster and paint materials and anticipate all other aspects of potential future deterioration.

Fig. 18.1 Monitoring salt activity can be difficult as efflorescence, such as seen here on the west wall, is visible only under certain environmental conditions.

Fig. 18.2 Alteration of lead pigments, visible as darkening of white lead, on the east slope of the ceiling is a gradual process.

Condition monitoring in Cave 85 must consider both the short term, the months and years immediately following completion of treatment, and the long term. The former assesses the direct effects and consequences of treatment, while the long term evaluates the overall state of preservation as a result of exposure to environmental conditions over time. However, recognizing change can be challenging. Conditions such as salt deterioration and color change (alteration of inorganic pigments and fading of organic colorants) can be both gradual and barely perceptible—occurring slowly over the course of many years (figs. 18.1, 18.2). In order to be able to perceive change, one must be familiar with the condition of the paintings at the start of monitoring. This requires an intimate knowledge of the paintings, including materials and techniques of execution, previous conditions and treatment, and a photographic record. Without this information it is not possible to undertake accurate monitoring. Furthermore, monitoring is a subjective process. It is difficult to maintain consistency in monitoring

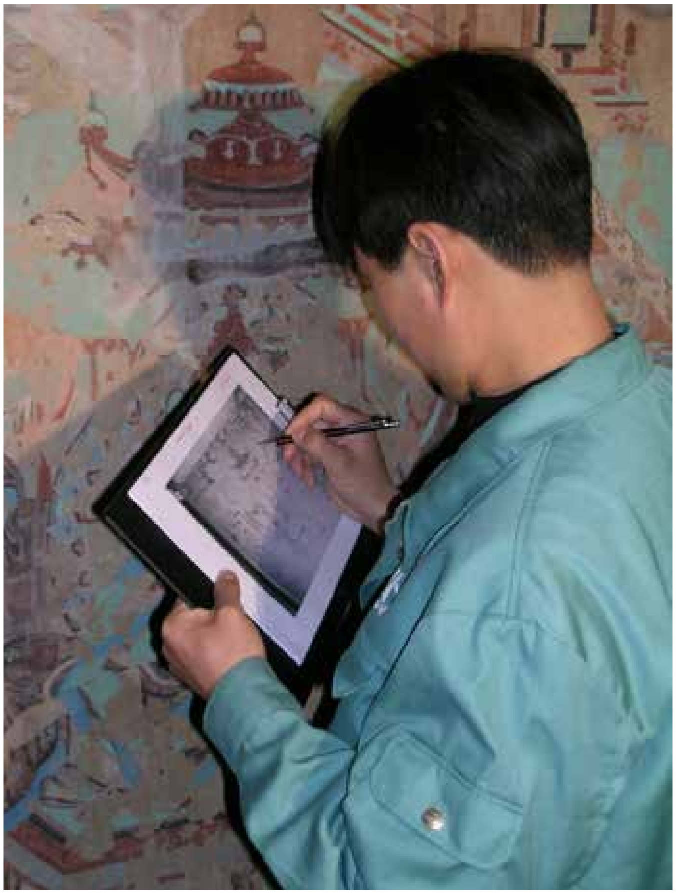

Fig. 18.3 Undertaking condition monitoring in the cave.

as it is based on individual perception of change that might differ from person to person. Good documentation of post-treatment condition is therefore needed in order to minimize this subjectivity.

Monitoring Strategy

In order to maximize the effectiveness and accuracy of monitoring, a number of requirements and constraints were considered in the selection of areas to be monitored and in determining a strategy. The first of these was to identify representative conditions. The large size of the cave dictated that monitoring be based on surveillance of selected physical conditions. It was therefore important that these should anticipate all potential deterioration concerns, relating both to treatment interventions and to deterioration issues, principally salt activity and the susceptibility of original materials to various forms of environmentally induced deterioration.

Given the range of conditions that required monitoring in both treated and untreated areas, it was recognized that visual inspection could not be limited simply to the more accessible parts of the cave. Major zones of grouting, for example, were located both on the ceiling slopes and along the tops of the walls. Moreover, the ceiling slopes represent areas of high risk and cannot be excluded from monitoring. Therefore, in addition to representative conditions, the monitoring strategy needed to cover topographic distribution throughout the cave.

These requirements of the monitoring strategy need to be maintainable over the long term. In this context, it was decided that the "low-tech" methods of replicable visual inspection and recording using photographs and assessment were preferable, though other techniques should not be ruled out given the range of physical conditions that exist and the tendency of much deterioration to occur at a barely perceptible rate. Although the majority of the selected monitoring areas are not readily accessible, all can be inspected by achievable means. Use of a remote inspection camera would be adequate to record a number of areas. For areas where physical contact and inspection are necessary, lightweight scaffolding can be used. Finally, the sustainability of the monitoring strategy depends on continuity of personnel at the Dunhuang Academy, their proficiency in assessing deterioration phenomena, and the ability to transfer monitoring procedures readily and accurately to others when the need arises (fig. 18.3).

Implementation

A monitoring strategy was implemented based on simple photographic recording of representative condition phenomena throughout the cave. Fourteen monitoring areas were selected by the conservation team following completion of treatment (figs. 18.4–18.17). Visual inspection using both incident and raking light was undertaken by the conservation team, whose members participated in the treatment campaigns and were familiar with the paintings, including in particular their past condition and recent treatment history.

For each area, baseline recording and information have been produced on a single sheet to guide monitoring. Each sheet contains location information, baseline photographs (context and, if necessary, macro images), and written comments summarizing condition and treatment history. Instructions are given highlighting specific conditions, how monitoring should be carried out (e.g., lighting conditions), and how frequently.

Conclusions and Recommendations

While exact forms of deterioration are impossible to predict, the fourteen selected monitoring areas provide a broad basis for assessing the diverse changes that could affect the cave. The circumstances and issues represented by the monitoring areas include treated and untreated areas in good condition, since it is essential to know that these areas remain in a stable state; treated areas representing all the problems that were addressed and the procedures and materials employed (injection grouting, salt reduction procedures, paint layer fixing, and exfoliation treatment), in order to assess long-term conditions; treated areas showing particular circumstances and conditions of high risk (e.g., large grouting areas, high salt contamination); inorganic and organic paint changes, in varying states of alteration; salt-related deterioration in its various forms and in different parts of the cave; areas where historical deterioration problems relating to failure of the original materials have been identified (e.g., plaster detachment along plaster joins); areas where persistent deterioration problems occur and continue to present problems (e.g., flaking of flesh-colored paint on the west wall); areas where previous treatments remain on the surface of the paintings (fixatives, consolidants) or penetrate the plaster stratigraphy (pins and anchors), indicative of areas of previous risk and future risk; and localized areas where conditions are known to have been particularly adverse (e.g., the northwest corner).

Signs of change in any of these areas should provide warning that wider deterioration could be occurring elsewhere. This raises the question of what should be done in response. While it is impossible to prescribe specific responses, recommendations are as follows: instances of emergent deterioration should be assessed on a case-by-case basis; conservation options should favor preventive measures rather than remedial interventions; and, specifically, more improved monitoring should be one of the immediate responses in order to establish better data on the nature and rate of deterioration and to inform conservation decisions.

Considering the wide range of physical conditions that have affected the paintings—a number of which could recur if unfavorable environmental conditions prevail—there is a need to develop and implement more sophisticated monitoring and recording tools in the future and to direct these improvements, as appropriate, at specific areas of concern. A particular issue is the concealed or barely perceptible nature of a number of the deterioration conditions in Cave 85. These include assessment of both plaster detachment and grouted areas; nature and rate of inorganic and (especially) organic color changes; nature and rate of salt phase transitions; and nature and rate of paint flaking and exfoliation.

The current strategy is therefore a basic starting point for monitoring and maintaining the future condition of Cave 85. While the selected areas may be considered a sufficient and representative monitoring base, improved monitoring procedures and techniques should be considered as part of the care of the wall paintings. In addition to the designated monitoring areas, general inspection of all areas of painting and sculpture should be undertaken on an annual basis. The opening of the cave to visitation, even if limited (i.e., closure during periods of high humidity), may affect the rate of deterioration of the paintings. In particular, the installation of lighting is something that must be considered in future monitoring (see chap. 19). It is therefore also important that condition monitoring is carried out as a corollary of continuing environmental monitoring.

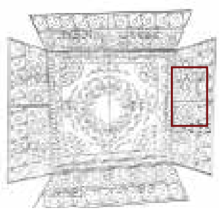

Cave 85, Mogao

Ceiling, East Side

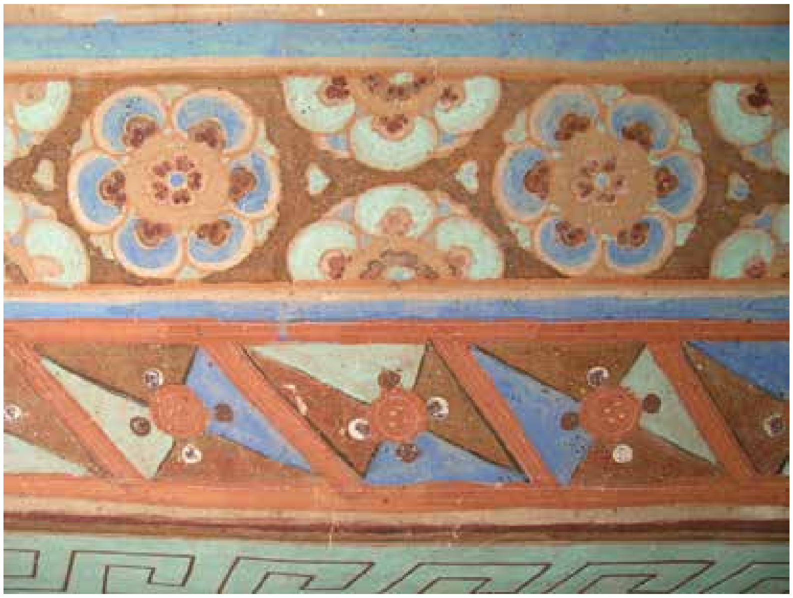

Fig. 18.4 Area 1; Ceiling, east side: Having been isolated relative to the other areas from light exposure and salt activity, the painting on this part of the ceiling is in an excellent state of preservation. In particular, a number of organic colorants and lead pigments, as well as azurite, survive in unaltered form, whereas in most other parts of the cave they have undergone various degrees of fading, deterioration, and/or chemical change. Monitoring of this area may therefore also serve as a benchmark for assessing potential color changes throughout the cave. Imaging for the purpose of future monitoring should include a standard color scale to facilitate accurate visual comparison. This area should be monitored annually in the first three to five years after the installation of cave lighting. Thereafter, monitoring intervals could be less frequent depending on recorded findings.

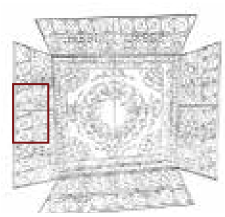

Cave 85, Mogao

Ceiling, West Side

Fig. 18.5 Area 2; Ceiling, west side: Selected as a contrast to Area 1, this area on the west side of the ceiling shows identical patterning and decoration and therefore the same range of inorganic and organic colorant materials but in radically altered and/or faded state, due to its different environmental exposure. Given limited knowledge regarding the long-term progress of such paint alterations, it cannot be assumed that change is not continuing. Monitoring is therefore necessary. Change in this area would also provide a warning signal for similar change elsewhere in the cave. Considering the advanced state of the observable color change and the difficulty of visually detecting future change, monitoring requires macro-imaging. It is further recommended that specific color measurements be undertaken to facilitate more accurate comparative monitoring.

In addition to color change, this area of painting was previously affected by widespread paint flaking, which was relaid and fixed during the current treatment program. Monitoring should therefore also take account of these factors. Considering issues of both paint alteration and flaking, this area should be monitored annually in the first three to five years after the installation of cave lighting. Thereafter, monitoring intervals could be longer depending on recorded findings.

Cave 85, Mogao

West Slope, South Side

Fig. 18.6 Area 3; West slope, south side: selected for monitoring because the area combines a number of critical conditions and circumstances. This is formerly an area of major plaster detachment on a ceiling slope, representing a particularly high-risk situation. An anchor and cross-brace were inserted in the 1970s as a means of stabilization, but serious plaster cracking since developed, indicating a continuing and possibly exacerbated condition at the start of the GCI/DA conservation project. Large-scale grouting was undertaken during the conservation program, and the anchor and cross-brace were left in situ.

Given all these factors, the area should be visually monitored based on photographic comparison, checking in particular the nature and formation of cracks as indicators of change. While gentle tapping of the surface may also be possible, detailed photography of specific cracks would provide more objective data by which to assess change. Annual checking is advisable, though there is no need to repeat the initial photographic base if no visual change is apparent.

Fig. 18.7 Area 4; West slope, north side: selected for reasons similar to those in Area 3, with the additional circumstance that this area had witnessed failure in the recent past (1996) involving substantial plaster collapse and loss. As with Area 3, this area should be visually monitored based on the photographic record, checking in particular the nature and formation of cracks as indicators of change.

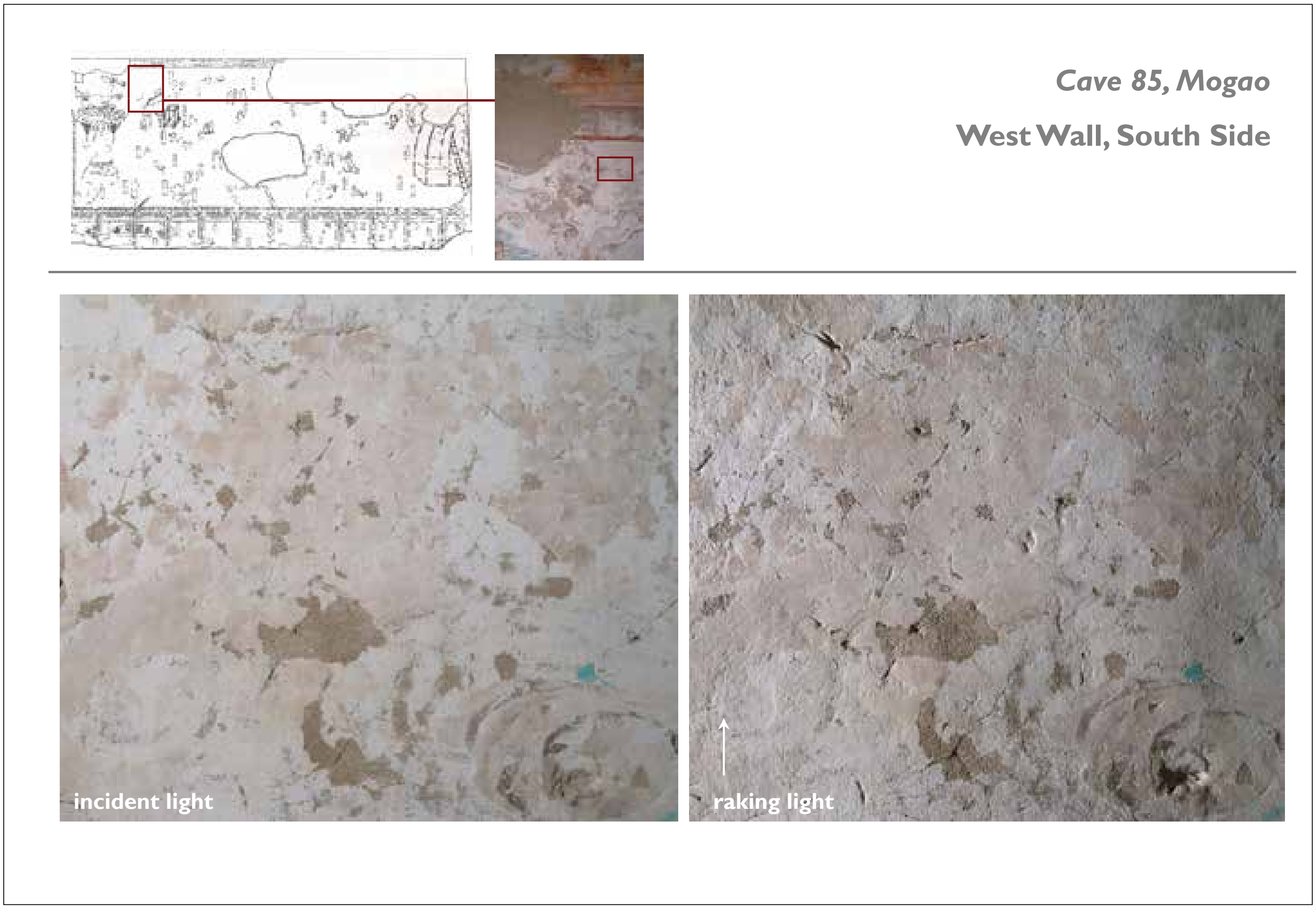

Fig. 18.8 Area 5; West wall, south side: As a region of persistent salt activity and intensive treatment intervention, the west wall as a whole is prone to future deterioration. A number of phenomena require monitoring. The selected area has been identified as having a high salt content and was the focus of extensive grouting and salt-reduction treatments, including post-grouting efforts to reduce surface salts. The main objective of monitoring this area is to detect the reemergence of salt-related deterioration, manifesting as small-scale salt pustules and/or lifting of the paint layer. Examination should be made in normal and raking light. Annual checking is advisable, and further macro-photography may be required to record small-scale salt activity. There is no need to repeat the initial photographic base record if no visual change is apparent.

Fig. 18.9 Area 6; West wall, south side: Untreated painting on the west wall affected by surface salt deterioration, which has resulted in densely concentrated punctate losses in the paint layer. As an area of plaster that has remained well attached to the rock substrate, this specific deterioration appears to have been facilitated by capillary continuity of the wall painting stratigraphy. Since, as elsewhere, the status of the deterioration is uncertain, monitoring is required. The punctate losses provide a distinctive comparative base for assessing any future deterioration. Annual monitoring is advisable, and further macro-photography may be required to record small-scale salt activity or other change.

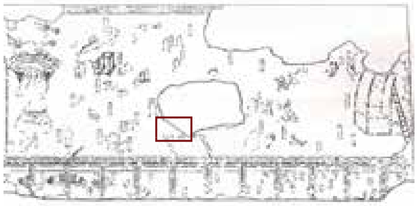

Cave 85, Mogao

West Wall, Middle

Fig. 18.10 Area 7; West wall, middle: One of the few areas on the west wall where a substantial layer of flesh-colored paint survives, which is highly susceptible to flaking and loss. The monitoring area has exhibited persistent flaking and has been treated to reduce surface salts and then fixed with gelatin. Even after these treatments, the paint layer remains fragile. Future assessment of condition will therefore require careful consideration of risk, based on photographic comparison. Macro-photography may be necessary to record small-scale flaking and facilitate accurate comparison and interpretation. Annual checking is advisable given the fragile nature of the paint layer and its history of flaking.

Cave 85, Mogao

West Wall, North Side

Fig. 18.11 Area 8; West wall, north side: selected for monitoring because the area combines a number of critical conditions and circumstances. Pretreatment condition comprised large-scale plaster detachment, cracked and decohesive plaster, and copious salt activity. The area was extensively destabilized by intersecting plaster cracks, many of which appear quite new, indicating continuing problems. Plaster failure corresponds with the location of original plaster joins, indicating an area of inherent weakness.

This area also required the largest quantity of grout to be injected on the west wall. Annual checking is therefore advisable. The area should be visually monitored based on photographic comparison, checking in particular the nature and formation of cracks. While monitoring by gentle tapping (only in the area demarcated by the white box) may also be possible, detailed photography of specific cracks is advisable, to provide objective assessment data. There is no need to repeat the initial photographic base if no visual change is apparent.

Fig. 18.12 Area 9; West wall, north side: selected for monitoring because the area exhibited a number of critical conditions, including severe pretreatment conditions of plaster detachment and cracking, paint layer flaking and powdering, salt eruptions, and other salt-related deterioration. This area was grouted during the current project, and, as it is an area of high salt content, annual checking is advisable. The area should be visually monitored based on photographic comparison, checking in particular the nature and formation of cracks. More detailed photography of specific cracks is advisable (and easily achievable given its near-ground-level location), to provide objective data. There is no need to repeat the initial photographic base if no visual change is apparent.

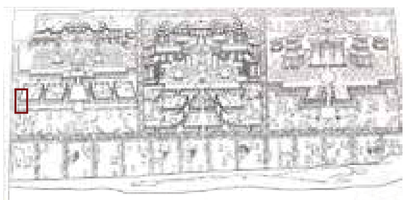

Cave 85, Mogao

North Wall, West Side

Fig. 18.13 Area 10; North wall, west side: The northwest corner of the cave has a history of specific deterioration, treatment, and retreatment. In 1999, for example, following an incident of sudden exfoliation and loss, the area was heavily retreated with aqueous PVAc emulsion. Conditions over time have shown a tendency for deleterious conditions to occur in this area. Given these circumstances, annual checking is advisable. Further macro-photography may be required to record any small-scale deterioration phenomena.

Fig. 18.14 Area 11; North wall, middle: selected for monitoring because the area combines a number of critical conditions and circumstances. This was an area of major grouting where the high-quality figurative painting survives in generally good condition. The area exhibited various forms of both incipient and more advanced paint layer deterioration, such as salt-related punctate loss, salt pustules, and lifting of paint edges. The deterioration phenomena, though small-scale, are distinctive, and any change in their appearance can be taken as a warning signal. Annual checking is therefore advisable. The area should be visually monitored based on photographic comparison, checking in particular the specific deterioration phenomena. More detailed photography of the individual phenomena is advisable, to provide more objective assessment. There is no need to repeat the initial photographic base if no visual change is apparent.

Cave 85, Mogao

North Wall, Middle

Fig. 18.15 Area 12; North wall, middle: selected for monitoring because the area combines a number of critical conditions and circumstances. This was an area of pretreatment plaster failure that corresponds with location of an original plaster join, indicating an area of inherent weakness. Major grouting was undertaken in this area where the high-quality figurative painting survives in generally good condition. Although the grouted area has a lower salt content than other walls at the west end of the cave, the grouting resulted in the formation of a salt-induced ridge at its perimeter. Although this was partly remedied by use of an ultrasonic humidifier to dissolve the salts, which were then removed by tamping with absorbent tissues (see also chap. 17), a concern is that residual salts could cause future deterioration. Annual checking is therefore advisable. The area should be visually monitored based on photographic comparison, checking in particular for the emergence of deterioration around the perimeter of the grouted area. If new deterioration does occur, additional salt-reduction treatment may be necessary.

Fig. 18.16 Area 13; East wall, north side: This was the largest area of plaster detachment in the cave and was consequently injected with the greatest amount of grout (approximately 21 liters). Plaster detachment on the east side of the cave is rare, and there is evidence that the particular problems here were historic, related to inherent weakness at plaster joins and to the thickness of the plastering. Annual checking is advisable. The area should be visually monitored based on photographic comparison, checking any changes in the distinctive network of intersecting cracks. While monitoring by gentle tapping (only in area demarcated by white box) may also be possible, more detailed photography of specific cracks is advisable, to provide a more accurate monitoring base.

Fig. 18.17 Area 14; East wall, south side: The east wall of the cave was treated with aqueous PVAc emulsion in 1974 to readhere flaking paint. Although there has been no recurrence of this problem, monitoring is advisable on an annual basis for a three- to five-year period. Thereafter, monitoring intervals could be less frequent depending on findings.

CHAPTER 19

Presentation and Visitation

Fig. 19.1 Guides continue to use flashlights in Cave 85 (as in unlit caves) after installation of lighting in order to direct the attention of visitors to areas being described, in this case, the small vignettes on the ceiling panels.

After completion of conservation treatment in 2005 the scaffolding was left in place to afford ease of access for post-treatment monitoring and documenting the condition of the wall paintings. At this time the GCI and the DA began discussing how best to present and interpret the cave to the public and develop an appropriate visitation policy. With the decision, in principle, to open the cave to visitation and with due consideration of the inherent risk from salt-induced deterioration during periods of high humidity, work began on developing a comprehensive approach to presentation and interpretation that would address the need for lighting in the cave, a method for preventing direct contact of visitors with the paintings while providing unimpeded viewing of the art, and a method for conveying a conservation message to the visiting public.

Lighting in the Cave

There has long been debate among DA staff about the need for lighting in the caves, some of which receive ambient light from outside when the doors are open and some of which are larger and remain dark even with open doors. Visitors see the paintings in the caves with the use of flashlights carried by guides. Over the years the quality of flashlights has improved somewhat, and large, clumsy D-size battery torches with poor light have been replaced by slimmer, more powerful versions with longer battery life. Guides find flashlights useful in directing the attention of visitors to the scenes being described (fig. 19.1), but alternatives such as laser pointers are being considered, and rechargeable flashlights are being investigated to reduce battery consumption and disposal.

Fig. 19.2 Testing of 200-watt tungsten light (a) and 3600 K LEDs (b) mounted on scaffolding.

Even with this improvement, there remain significant problems with viewing the paintings by flashlight. A flashlight illuminates only the specific details of the sutra or jataka stories being narrated by the guides, leaving the viewer literally in the dark about the larger context of the scenes and unable to grasp the overall composition and beauty of the paintings. Visitor perceptions of lighting were first gauged in 2002 when the DA undertook a comprehensive visitor survey. Among the questions asked were those addressing visitors' attitudes about lighting. These initial surveys were fairly evenly split in their responses. Forty-seven percent of respondents indicated a preference for lighting in the caves to illuminate the wall paintings. The remaining 53%, however, believed that it would not be appropriate to install lighting as it might negatively affect the wall paintings. These somewhat ambivalent responses in the surveys were better understood when placed in the context of the DA guides', informal conversations with visitors over the years. The responses reflect, on the one hand, a lack of understanding about the effects of lighting and a desire to experience the caves as they may have been seen originally (in low light) counterbalanced, on the other hand, by a desire to see the paintings clearly.

There is plentiful evidence of natural light–induced color change in the mineral pigments of the wall paintings at Mogao, and a number of studies have been published (Li and Michalski 1989; Li et al. 1990; Shen et al. 1990). Nonetheless, color change, the alteration and darkening of inorganic pigments or fading of organic colorants, has not been shown to have come to an end, and artificial lighting in the caves may induce further change; indeed, preliminary studies by accelerated testing using a microfadometer have shown this to be the case (Druzik 2010) (see chap. 15). Thus, caution is mandated in lighting of the caves, and specifications for light sources must be based on internationally accepted standards used in museums. Monitoring of any impact of lighting over the long term is essential.

Lighting criteria were based on considerations of aesthetics, conservation (no further change in both pigments and organic colorants), and easy maintenance (see table 19.1).

Tests were undertaken in Cave 85 to compare various LED sources with tungsten and fluorescent lamps (fig 19.2). Meeting the specified criteria meant the elimination of fluorescent sources (on the basis of UV emission, efficiency, disposal issues related to mercury, and generally cool color temperatures) and incandescent lamps (heat emission, short life, and high power consumption).

COLOR TEMPERATURE	Color temperature is measured in degrees K (the unit of absolute temperature, the Kelvin). In practical terms, it may be understood as the color of the light source: warm white (2,600–3,200 K), bright white (3,200–4,500 K), and daylight (4,500–6,500 K). This range covers the red to blue ends of the visible spectrum. Based on trials of different color temperatures in the cave, it was decided that light sources should have a warm color temperature (around 3,000 K or slightly lower). The appearance of the paintings was best at this color temperature; higher color temperatures created an unpleasing, "cool," artificial effect.
COLOR RENDERING INDEX	Color rendering index (CRI) is used in the lighting industry. It measures, on a scale of 100, the ability of a light source to reproduce the colors of objects faithfully in comparison to an ideal or natural light source. While it is generally agreed that a CRI of 85 is suitable for museum display, the best white LEDs measure above 90 when evaluated against a 3,000 K incandescent reference source.
AESTHETIC EFFECT	Uniform lighting of the walls and ceiling was not necessarily desirable since the cave would not have been created, viewed, or used originally under even illumination; however, mitigating areas of high illumination, especially at the lower areas of the walls, was important to achieve.
UV AND IR EMISSION	No UV and little IR.
LUX LEVELS	Lux is a measure of the illuminance at the surface of an object. Formally, it is the illuminance occurring when 1 lumen falls on a square meter of surface. Based on research in museums, 50 lux is an accepted standard for viewing of light-sensitive materials. Illumination levels of 70–100 lux were specified since the cave will only be intermittently lit for special tours.
LUMINOUS OUTPUT	Luminous output, measured in the unit lumen, is the amount of visible light produced per watt of electrical power consumed by a light source. A white LED typically has an output in the range of 30–15 lm/watt, which is more efficient than incandescent or fluorescent sources.
HEAT EMISSION FROM THE LIGHT SOURCE	Negligibly low.
LONGEVITY	Care and maintenance of lighting is an important management issue. It was essential that the light source be long-lived and easy to replace.
POWER CONSUMPTION	Low electrical power consumption.

Table 19.1 Lighting Criteria

LED sources were favored, and have the additional advantage of stable output over the life of the lamp (Druzik and Michalski 2011; Brodrick 2011). The final installation comprised several low-voltage LED sources to illuminate the walls and ceiling of the main chamber. The Peking University Center for Wide Gap Semiconductor Research was contracted by the DA to design, supply, and install LED sources. A remote control is used by guides to turn on selected lights to illuminate either particular areas or the entire chamber during visitation. The sources comply with the specified criteria and have a projected life of 50,000 hours and power consumption in the range of 8–30W/10V direct current.

Long-term monitoring of the stability of the wall painting pigments and colorants is being undertaken using International Organization for Standardization (ISO) blue scales textile fading cards[1] and a lux data logger (fig. 19.3) (see Appendix 19.A).[2]

In addition to color temperature, which is the most important criterion for aesthetics, the installation sought to avoid shadows and hot spots and to prevent light from striking visitors' eyes when they entered the cave through the corridor (fig. 19.4). The results are largely successful, but shadows cast by statues (fig. 19.5) and transitions, especially at the wall and the sloped ceiling, could not be fully avoided.

Physical Barriers

Existing physical barriers to prevent visitors from touching the paintings are heavy glass screens in aluminum framing, with

Fig. 19.3 Light monitoring set up on the north wall with two blue scales textile fading cards and a lux sensor.

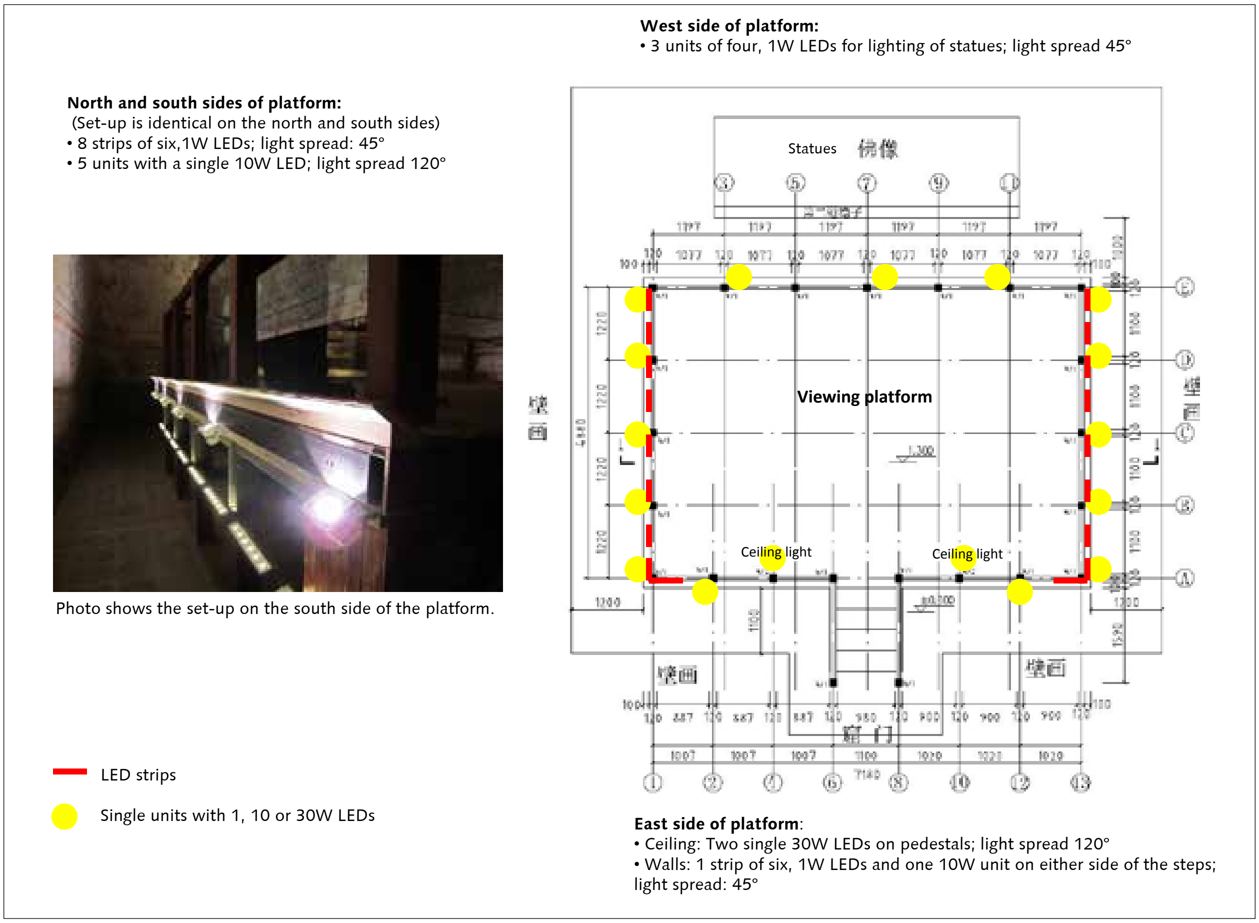

Fig. 19.4 Viewing platform with lighting setup and specifications.

Fig. 19.5 Lights installed on the platform to illuminate statues cast shadows on the wall, which were reduced but not eliminated.

wheeled bases. Based on observational studies by DA staff during high periods of visitation, 3.9% of visitors were recorded touching the walls in areas where glass screens did not provide protection. Over the course of a year, this small percentage equates to thousands of instances of direct contact. The glass screens therefore serve an important protective function against both deliberate and inadvertent contact with the wall paintings, but they are cumbersome, take up unnecessary space within the caves, and are a visual intrusion on the interior; experimentation with alternative railings systems has not been successful (fig. 19.6). Moreover, the glass accumulates dust and is frequently flawed by surface irregularities. A better method of isolating the walls has been, and still is, needed for the majority of caves. Visitor surveys on perceptions of the barriers found an ambivalence similar to that for lighting, with visitors recognizing that some form of barrier is required to protect the paintings but disliking the visual impediment that existing barriers pose.

Cave 85 has a large floor area, which enabled a different solution. A wooden railing system at 1.10–1.20 m from the wall prevents visitors from touching the walls but allows an unobstructed view of the paintings (see fig. 19.1). Because of the cave's size, this still allows a large viewing area for visitors.

Platform Concept and Design

An additional consideration was to provide a better view of the art from a raised platform in adequate light. While the large size of Cave 85 is an advantage for solving the barrier problem, it is an impediment to viewing the upper areas of the walls and pyramidal ceiling with its central panel, which is at a height of 13 m from the floor. In particular, the many small vignette paintings (for example, a butcher and his dogs and an acrobat) (see figs. 8.26, 10.8b) on the ceiling slopes are one of the delights of the Cave 85 paintings but are very difficult to see from floor level (see chaps. 8, 10). They introduce a human element, in contrast to the formal sutra paintings that dominate, and tell visitors something of the whimsy of the ancient artist. A further

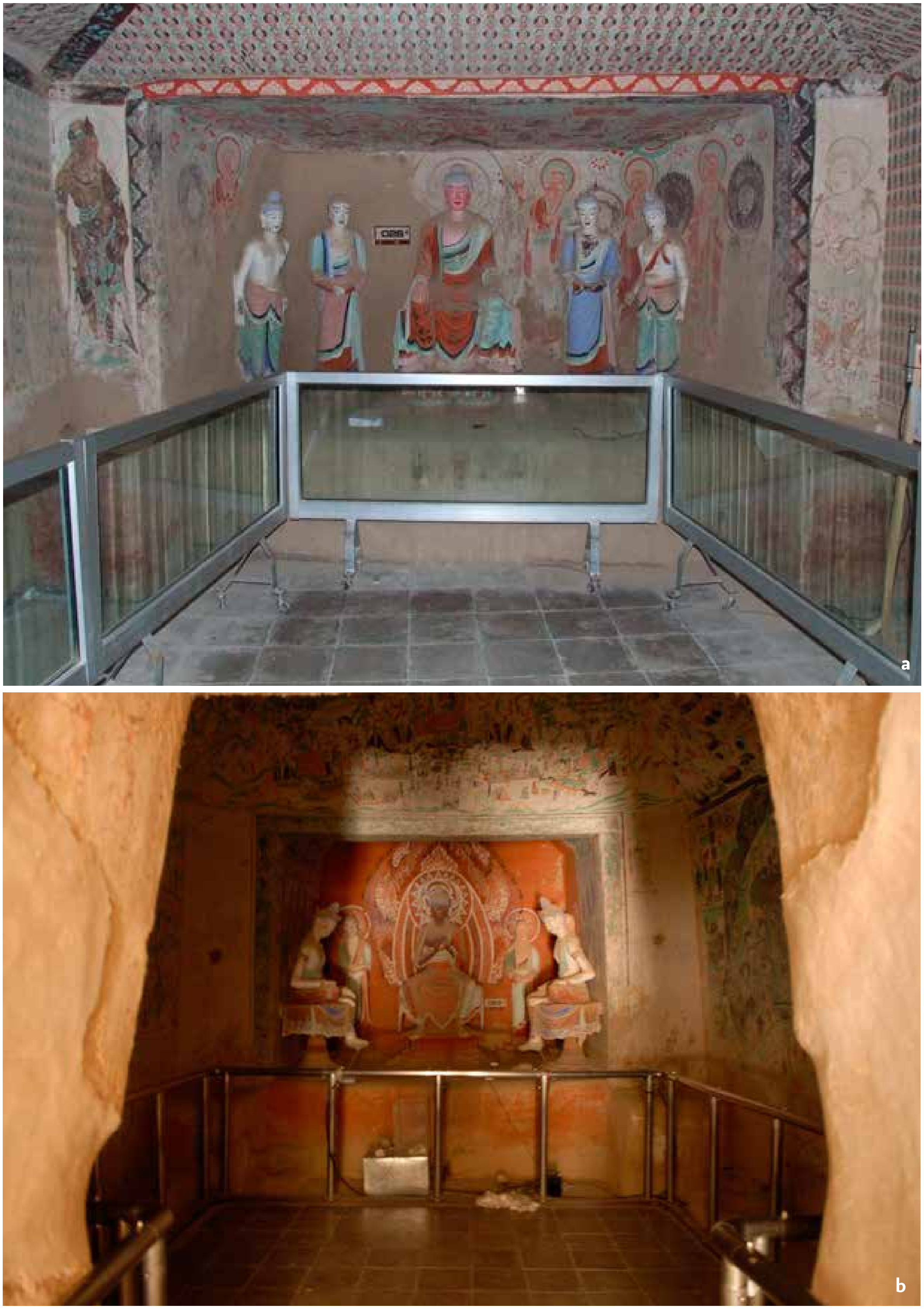

Fig. 19.6 Examples of existing glass and aluminum barriers in caves (most caves must employ taller barriers to prevent visitors from touching the walls) (a, Cave 26) and alternative tubular railing (b, Cave 23). Both caves are small and receive some ambient light from the outside with doors open.

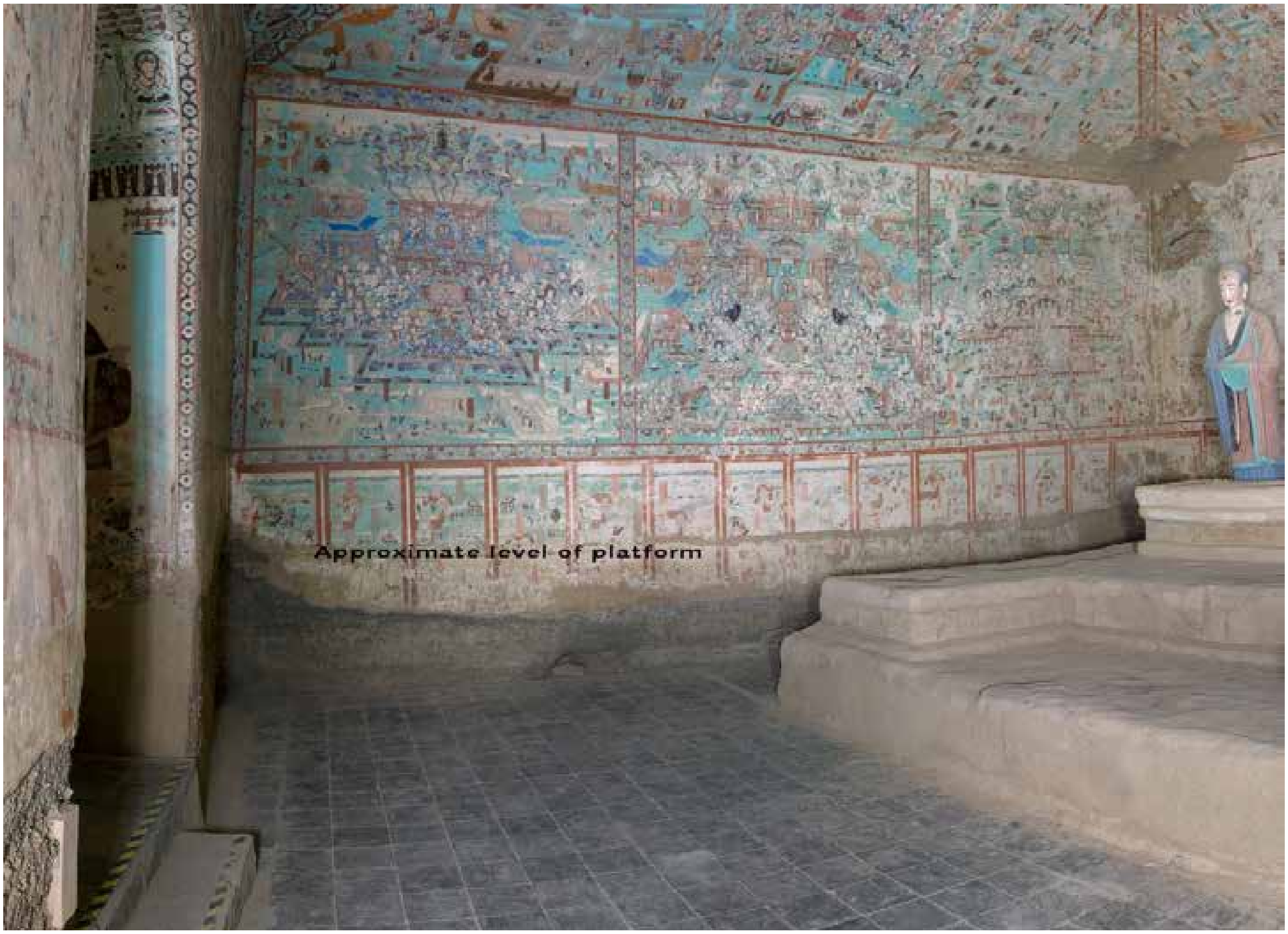

Fig. 19.7 Loss and deterioration of painting at the base of walls in Cave 85, with level of platform indicated.

consideration in favor of a viewing platform is the complete loss or deterioration of paintings in the lower parts of the walls from historical floodwater that had intruded, which means the visitor is confronted mainly with loss and deterioration when viewing the cave at eye level from the floor (fig. 19.7).

Thus, the idea of a viewing platform that would raise the visitor above the floor level was conceived. When it was time to remove the scaffold from the cave, a series of experiments were conducted utilizing the scaffolding at different heights to assess the impact of such an intervention (fig. 19.8). The optimal height of the platform was determined to be 1.30 m above floor level. This corresponds with the lost painting of much of the lower register, yet allows for the statuary group to be seen unimpeded from the doorway and corridor. The steel structure of the platform and its steps rests on the cave floor (fig.19.9); the surface is wood and is carpeted. The railings, which incorporate a tempered glass panel, define a platform space of 7.18 × 4.88 m. The platform also serves to carry the LED lighting system and interpretive panels, which were mounted in the four corners.

Interpretation

Multiple objectives may be served by opening the cave to visitors. Foremost was the desire of the DA to convey a conservation message and enhance an understanding of what conservation entails and how it is done by creating a special experience. Visitors to the site generally recognize the fragility of the art and are beginning to be aware of the impacts of burgeoning tourism in China on cultural sites, but they have only a rudimentary understanding of deterioration processes and how they may be mitigated by a systematic conservation, management, and monitoring program.

Fig. 19.8 Scaffolding, partially dismantled after completion of conservation, was used to determine the height of the viewing platform.

Fig. 19.9 Welded steel substructure of the final platform rests on the floor of the cave; altar base is on right.

To this end, five interpretive panels were created for the cave; four on the platform and one in the entry corridor (see Appendix 19.B). They focus especially on conservation issues and messages and therefore supplement the normal tour provided by the DA guides, which is principally related to history and iconography (although the guides are increasingly being provided with conservation information to incorporate into all their tours). The guides were asked for input on both content and location of panels (fig. 19.10). The panels have photos, graphics, and written content (in Chinese and English) related to the Cave 85 conservation project objectives, materials and techniques of the wall paintings and sculpture, condition and causes of deterioration, conservation of the cave, and prevention and future monitoring (fig. 19.11).

Cave 85 Visitation Policy

The results of a multiyear study by the GCI and the DA on establishing a sustainable visitor carrying capacity for the Mogao Grottoes served as the basis for the visitor policy for Cave 85 (Agnew et al. forthcoming). Restricting conditions were established for caves open to visitation. These are: CO_2 not to exceed 1,500 ppm (which relates to visitor health and safety) and RH not to exceed 62% (applicable to caves at risk from salt-induced deterioration, of which Cave 85 is one). RH is influenced mainly by intrusion of outside air through open doors and not by visitors' exhalation. Thus, during high humidity periods Cave 85 must remain closed to visitors. Humidity control through management practices is therefore essential for safe and sustainable visitation of the cave.

Cave 85, as presented, interpreted and visited (fig. 19.12) is not an option for all the caves though the basic design elements and lighting specifications are applicable and will be used as the baseline for other caves. For several reasons the cave can only be visited by selected groups: its susceptibility to salt-related deterioration during high summer humidity periods; and because a visit requires a considerably longer time than to the other unlit, uninterpreted caves, which are allotted only 6–8 minutes per cave in a tour of 10 caves.

Until further monitoring is undertaken, management systems for controlling visitation put in place, and interpretation strategies further developed, visitation to Cave 85 will be restricted to special groups and used to explain the conservation problems and solutions that have been developed through the Cave 85 project. Once the requisite systems have been established the cave can be opened to more general visitation, subject to the restrictions noted above, and the conservation message can thus be disseminated more widely.

Fig. 19.10 Discussion with DA guides on lighting, platform, and interpretation during the testing phase.

Notes

1. Blue scales (986–1000), also known as "blue wool" cards, are produced by University Products. Each card features pieces of wool cloth dyed with blue dyes of different degrees of fastness that are used as lightfastness standards. Eight blue wool standards are included that have increasing resistance to fading when exposed to light and are numbered accordingly. The numbers range from 1 (very poor resistance to light) to 8 (excellent resistance to light). To achieve a similar degree of fading on standard 2 as on standard 1 requires approximately twice the exposure time, standard 3 takes approximately twice as long as standard 2 to fade to the same degree, and so on to 8. Intermediary ratings (e.g., 5–6) can be given if the degree of change of the test specimen falls between the two blue wool standards. They allow one to monitor the net exposure to light of objects on display and to alert conservation managers to adjust intensity of illumination.
2. Lux data logger (ML4701) is produced by Hanwell Instruments Ltd.

a

Fig. 19.11 Example of interpretive panels installed in the cave.

Fig. 19.12 View of the main chamber with platform railing (a) and one of the two pedestal lighting fixtures for illumination of the ceiling during a visit by a group (b).

CHAPTER 20

Concluding Remarks

In 1996, after the first phase of collaboration between the Dunhuang Academy and the Getty Conservation Institute for conservation work at the Mogao Grottoes, it was jointly determined to confront the problems of deterioration of wall paintings at the site by a systematic and methodological conservation process. Cave 85 was chosen for this purpose, and it was agreed that an extensive phase of research and testing would precede any intervention. Among the objectives of the project were enhanced training of DA staff and dissemination of the results. At the same time, the State Administration of Cultural Heritage of China, the GCI, and the Australian Heritage Commission, with the participation of DA leadership, began development of national guidelines or principles for the conservation and management of heritage sites in China. The China Principles, issued by China ICOMOS in 2000, base conservation decisions, processes, implementation, and management on a site's cultural value and significance. They were used as the guiding precepts in the Cave 85 project.

The China Principles follow a sequence of bibliographical background research on a site, development of a significance statement, condition documentation, investigation and analysis of original materials and techniques, study of causes of deterioration, environmental monitoring, and testing—all undertaken before a conservation plan is decided upon. For Cave 85, some of the steps were done sequentially, others in parallel, where expedient to do so. Before treatment began, a panel of experts convened by SACH reviewed and approved the proposal.

What follows summarizes the key findings of the project in relation to future preservation and use of Cave 85. All of the work cannot be presented here. Supplementary data and results are given in the appendixes; images, environmental findings, test procedures, and so forth, are archived at the DA, with duplicate material held by the GCI. The structure of the present report follows the procedural sequence of the China Principles.

As in many caves at Mogao, one notices almost immediately on entering Cave 85 the extensive areas of complete loss of painted plaster. At various times over the centuries, plaster fragments have fallen from the ceiling and walls, most recently in 1996 after a period of sustained rain and high humidity in the cave. Careful examination of the wall paintings revealed extensive areas of detachment with separation of the decorated earthen plaster from the underlying conglomerate.

This detachment, invisible generally to the eye, is the greatest hidden threat to the wall paintings. Fragile plaster does not survive a fall from the ceiling or walls, nor can the shattered fragments found on the cave floor be feasibly reassembled in situ. Two precipitating factors cause collapse: seismic events and high humidity, the latter resulting from deliquescence of hygroscopic salts in the plaster and interface with the conglomerate. Salts at a humidity less than their deliquescence humidity act as a strong cementing agent, but as they undergo dissolution their strength diminishes to the point where they cannot act in this way and collapse of the plaster results. Thus, a focus of testing and implementation of the Cave 85 project was stabilization of the detached plaster by grouting using lightweight compatible materials.

What is strikingly obvious in Cave 85 is the extent of deterioration of the painted surface, particularly in the west and northwest areas of the main chamber. Friable earthen plaster and flaking and exfoliating layers are characteristics of this deterioration, in areas of both detached and separated plaster. Analysis revealed polyvinyl acetate (PVAc) in fallen paint flakes (applied in the 1970s) and enrichment of hygroscopic salts, principally sodium chloride, on the surface and in the plaster. Again, it is these salts that, through cycles of deliquescence and recrystallization, cause damage. Unfortunately, no practicable method exists for the safe extraction of the salts to levels at which they will not cause further damage. Having developed treatment methodologies for flaking and exfoliating layers, it was possible, during implementation, to reduce to some extent the surface salts, but the threat remains, and only by means of control of the cave's microclimate will it be possible to suppress further deterioration. The critical relative humidity (RH) for onset of absorption of water vapor from the atmosphere was established as 67%. For public visitation to Cave 85 a not to be exceeded humidity of 62% was determined to be a safe level. In practice, this requires keeping doors closed during periods of external humidity higher than this value in order to significantly slow the natural air exchange with the outside, and that, in turn, means no visitation to the cave. In general, avoiding sudden fluctuations in RH inside the cave is desirable, given not only the salts but also the presence of PVAc from past treatments that can cause surface layers to lift.

Monitoring of the condition of the wall paintings is an important measure to ensure their preservation. A protocol and schedule was developed for implementation by the Dunhuang Academy.

It would be unwise to state that there is now complete understanding of the many afflictions seen in Cave 85, or indeed at Mogao itself. The original materials and techniques that were used to create the art are complex, and the deterioration has occurred over many centuries and at different rates. More needs to be known about the art, in greater depth. Progress has been substantial, however. The Cave 85 project led to an understanding of many technical problems of wall paintings applied to earthen plaster; detachment or separation of the earthen support from the underlying conglomerate rock; the nearly ubiquitous salts; flaking, exfoliation, and disruption of the painted surface by deliquescent salts; migration of these soluble salts from the rock body under the influence principally of water vapor; binding media research; and importantly, the development of compatible materials for treatment. In tandem, the direct impact of visitors on the cave's environment was evaluated, as was the intrusion of air from the outside when the doors were opened. This research formed part of a much larger effort to determine the safe visitor capacity of the cave and other visited caves at the site.

Questions remain. What is the nature and origin of the organic colorants used both in combination with mineral pigments and as colored washes over certain areas, apparently to create a subtle effect? Why in some instances is there analytical evidence for carbohydrates as well as protein in the binding medium? What is the contribution of intrusive atmospheric moisture compared with that of humidity emanating through the rock body? Investigation and discussion will lead eventually to comprehensive and irrefutable understanding of these questions, which dictates further research for the Conservation Institute of the Dunhuang Academy to undertake.

With the completion of conservation treatment, it has been possible to turn to the way in which the cave could be presented and interpreted to visitors such that both the art and iconography and a conservation message are conveyed. While visitors are guided with narration by Dunhuang Academy Reception Department staff, as they are to all visited caves, there are unique features of the presentation as finally decided upon for Cave 85. These features are a raised viewing platform in the main chamber, LED illumination of "warm" color temperature to match the probable way in which the cave was lit in the Tang dynasty, and conservation-related interpretive panels. Visitor acceptability and comment have been favorable. Combined microclimatic monitoring is being undertaken, and effects, if any, of the low-level LED lighting on the wall paintings are being monitored by standard blue wool cards.

The successful outcomes of the Cave 85 project have been possible through the long-established collaboration of the Dunhuang Academy and the Getty Conservation Institute. The collaboration has been based on a common purpose: the preservation and management of the Mogao site. Allocation of resources to the project by both institutions, sustained effort with work campaigns in spring and fall, discussions and debate, staff exchanges, and training workshops have contributed to the endeavor. Obstacles of language barrier and cultural perspectives have been overcome through mutual understanding and the involvement of consultant interpreters as team members. The Cave 85 project, as part of the larger collaborative initiative of the GCI in China, under the auspices and with the support of the State Administration of Cultural Heritage, can stand as a successful model of international collaboration.

References

Agnew, Neville, ed. 1997. *Conservation of Ancient Sites on the Silk Road: Proceedings of an International Conference on the Conservation of Grotto Sites*. Los Angeles: Getty Conservation Institute. http://getty.edu/conservation/publications/pdf_publications/silkroad.html.

———, ed. 2010. *Conservation of Ancient Sites on the Silk Road: Proceedings of the Second International Conference on the Conservation of Grotto Sites, Mogao Grottoes, Dunhuang, People's Republic of China, June 28–July 3, 2004*. Los Angeles: Getty Conservation Institute.

Agnew, Neville, and Martha Demas, eds. 2002. *Principles for the Conservation of Heritage Sites in China*. Los Angeles: Getty Conservation Institute.

Agnew, Neville, Martha Demas, Shin Maekawa, and Lorinda Wong. 2012. A systematic methodology for sustainable visitation at the Mogao Grottoes, China. Unpublished final report. Getty Conservation Institute.

Agnew, Neville, and Huang Kezhong. 1997. Projects of the Getty Conservation Institute and the State Bureau of Cultural Relics: The Mogao and Yungang Grottoes. In *Conservation of Ancient Sites on the Silk Road: Proceedings of an International Conference on the Conservation of Grotto Sites, Dunhuang, People's Republic of China, June 28–July 3, 2004*, edited by Neville Agnew, 23–27. Los Angeles: Getty Conservation Institute.

Agnew, Neville, Shin Maekawa, and Shuya Wei. 2010. Causes and mechanisms of deterioration and damage in Cave 85. In *Conservation of Ancient Sites on the Silk Road: Proceedings of the Second International Conference on the Conservation of Grotto Sites, Mogao Grottoes, Dunhuang, People's Republic of China, June 28–July 3, 2004*, edited by Neville Agnew, 412–20. Los Angeles: Getty Conservation Institute.

Agnew, Neville, Po-Ming Lin, Li Zuixiong, and Wang Xudong. 1999. A lightweight composite panel for the repair of cave roofs at the Mogao Grottoes, China. *Conservation and Management of Archaeological Sites* 3 (3): 135–44.

Arnold, Andreas, and Konrad Zehnder. 1991. Monitoring wall paintings affected by soluble salts. In *The Conservation of Wall Paintings: Proceedings of a Symposium Organized by the Courtauld Institute of Art and the Getty Conservation Institute, London, July 13–16, 1987*, edited by Sharon Cather, 103–35. Los Angeles: Getty Conservation Institute.

Baglioni, Piero, Luigi Dei, Francesca Piqué, Giuseppi Sarti, and Enzo Ferroni. 1997. New autogenous lime-based grouts used in the conservation of lime-based wall paintings. *Studies in Conservation* 42 (1): 43–54.

Barcellona, Salvatore, Ulderico Santamaria, Ernesto Borrelli, and Marisa Laurenzi Tabasso. 1993. Evaluation of injection grouting for structural strengthening of ancient buildings. In *Conservation of Stone and Other Materials: Proceedings of the International RILEM/UNESCO Congress "Conservation of Stone and Other Materials: Research-Industry-Media," Held at UNESCO Headquarters, Paris, June 29–July 1, 1993*, edited by M.-J. Thiel, 637–43. London: E. & F. N. Spon.

Barnhart, Richard M., James Cahill, Wu Hung, Yang Xin, Nie Chongzheng, and Lang Shaojun. 1997. *Three Thousand Years of Chinese Painting, Culture & Civilization of China*. New Haven: Yale University Press.

Bell, Stephen E. J., Elsa S. O. Bourguignon, Andrew C. Dennis, John A. Fields, John J. McGarvey, and Kenneth R. Seddon. 2000. Identification of dyes on ancient Chinese paper samples using the subtracted shifted Raman spectroscopy method. *Analytical Chemistry* 72 (1): 234–39.

Bionda, Davide. 2004. *Salt Deterioration and Microclimate in Historical Buildings: Intermediary Report of the Project "Sustained Care of Sensitive Historical Monuments."* Zürich: Institut für Denkmalpflege, Forschungsstelle Technologie und Konservierung, ETH Zürich. http://e-collection.ethbib.ethz.ch/show?type=bericht&nr=374.

Birstein, Vadim J. 1975. On the technology of Central Asian wall paintings: The problem of binding media. *Studies in Conservation* 20 (1): 8–19.

Bisbing, Richard E. 2006. Analytical report on fibers from render layers, Mogao Cave 85. Unpublished report. McCrone Associates, Inc.

Bläuer-Böhm, Christine, Konrad Zehnder, Heinz Domeisen, and Andreas Arnold. 2001. Climate control for the passive conservation of the Romanesque painted wooden ceiling in the church of Zillis (Switzerland). *Studies in Conservation* 46 (4): 251–68.

Botticelli, Guido, Mauro Matteini, Arcangelo Moles, and Giancarlo Lanterna. 1986. A mineral expansive material for readhesion operations on mural paintings. In *Scientific Methodologies Applied to Works of Art: Proceedings of the Symposium, Florence, Italy, 2–4 May 1984*, edited by Paolo L. Parrini, 177–79. Milan: Montedison Progetto cultura.

Brajer, Isabelle. 2002. *The Transfer of Wall Paintings: Based on Danish Experience*. London: Archetype Publications.

Brodrick, James. 2011. Can museums measure up? *Lighting Design + Application: LD + A* (July): 50–55.

Bukantis, Mark. 2002. Microscopical analysis of two fiber samples from Tang dynasty earthen plaster. Unpublished report. McCrone Associates, Inc.

Camuffo, Dario. 1995. Physical weathering of stones. *Science of the Total Environment* 167 (1–3): 1–14.

Casciu, Stefano, Giuseppe A. Centauro, and Massimo Chimenti. 2000. The archival documentation system: The computerized heart of the restored *History of the True Cross* by Piero della Francesca. In *GraDoc: Graphic Documentation Systems in Mural Painting Conservation: Research Seminar, Rome 16–20 November 1999*, edited by Werner Schmid, 208–19. Rome: ICCROM.

Cather, Sharon. 2003. Aqueous extraction of soluble salts from porous materials: Alternatives and contra-indications. In *Mauersalze und Architekturoberflächen*, edited by Heinz Leitner, Steffen Laue, and Heiner Siedel, 167–72. Dresden: Hochschule für Bildende Künste.

Cennini, Cennino. 1960. *The Craftsman's Handbook: The Italian "Il libro dell'arte."* Translated by Daniel V. Thompson. New York: Dover.

Charola, A. Elena, guest ed. 2005. Selected papers on salt damage and desalination. Special issue, *Internationale Zeitschrift für Bauinstandsetzen und Baudenkmalpflege* (Restoration of Buildings and Monuments: An International Journal) 11 (6).

Chen Gangquan. 2010. The analysis of the source of water causes the blister on the wall paintings of cave 351 of Mogao Grottoes. In *Proceedings of International Symposium on Conservation of Ancient Sites 2008 & ISRM-Sponsored Regional Symposium*, edited by Li Zuixiong and Wang Xudong, 129–35. Beijing: Science Press.

Chen Gangquan, Michael R. Schilling, Li Yanfei, Joy Mazurek, Yu Zhongren, and Lisa Shekede. 2010. A rapid means of measuring residual salt after grouting and poulticing wall paintings. In *Conservation of Ancient Sites on the Silk Road: Proceedings of the Second International Conference on the Conservation of Grotto Sites, Mogao Grottoes, Dunhuang, People's Republic of China, June 28–July 3, 2004*, edited by Neville Agnew, 488–93. Los Angeles: Getty Conservation Institute.

Chen Juxia. 2008. Study on the Zhai family of Dunhuang. Ph.D. diss., Lanzhou University.

China Architectural Design Academy, Getty Conservation Institute, Australian Heritage Commission, and Dunhuang Academy. 2010. Dunhuang Mogao Grottoes Conservation Master Plan (2006–2025).

Clunas, Craig. 1997. *Art in China*. Oxford History of Art. Oxford: Oxford University Press.

Colombini, Maria Perla, Roger Fuoco, Ambrogio Giacomelli, and Beatrice Muscatello. 1998. Characterization of proteinaceous binders in wall painting samples by microwave-assisted acid hydrolysis and GC-MS determination of amino acids. *Studies in Conservation* 43 (1): 33–41.

Colombini, Maria Perla, Francesca Modugno, Marina Giacomelli, and Sandro Francesconi. 1999. Characterisation of proteinaceous binders and drying oils in wall painting samples by gas chromatography–mass spectrometry. *Journal of Chromatography A* 846 (1–2): 113–24.

Conservation Institute of the Dunhuang Academy. *Cave 85 Documentation Book* [In Chinese].

Dei, Luigi, Andreas Ahle, Piero Baglioni, Daniela Dini, and Enzo Ferroni. 1998. Green degradation products of azurite in wall paintings: Identification and conservation treatment. *Studies in Conservation* 43 (2): 80–88.

Demas, Martha, Shin Maekawa, Jonathan Bell, and Neville Agnew. 2010. Sustainable visitation at the Mogao Grottoes: A methodology for visitor carrying capacity. In *Conservation of Ancient Sites on the Silk Road: Proceedings of the Second International Conference on the Conservation of Grotto Sites, Mogao Grottoes, Dunhuang, People's Republic of China, June 28–July 3, 2004*, edited by Neville Agnew, 160–69. Los Angeles: Getty Conservation Institute.

Douglass, David L., Chichang Shing, and Ge Wang. 1992. The light-induced alteration of realgar to pararealgar. *American Mineralogist* 77 (11–12): 1266–74.

Druzik, James R. 2010. Evaluating the light sensitivity of paints in selected wall paintings at the Mogao Grottoes: Caves 217, 98, and 85. In *Conservation of Ancient Sites on the Silk Road: Proceedings of the Second International Conference on the Conservation of Grotto Sites, Mogao Grottoes, Dunhuang, People's Republic of China, June 28–July 3, 2004*, edited by Neville Agnew, 457–63. Los Angeles: Getty Conservation Institute.

Druzik, James R., and Stefan W. Michalski. 2011. *Guidelines for Selecting Solid-State Lighting for Museums*. Los Angeles: Getty Conservation Institute. http://www.getty.edu/conservation/our_projects/science/lighting/lighting_component8.html.

Duan Xiuye. 1988. Study of the productive materials of the Mogao Grottoes. [In Chinese]. *Dunhuang yan jiu* (Dunhuang Research) (16): 41–59.

Duan Xiuye, Li Jun, Guo Hong, and Li Teichao. 1993. Report on the analyses of pigments found in Caves no. 232 and no. 35 at the Mogao Grottoes, Dunhuang. [In Chinese]. In vol. 2 of *Dunhuang yan jiu wen ji. Shi ku bao hu pian*, 307–8. Lanzhou: Gansu min zu chu ban she.

Dullien, Francis A. L. 1992. *Porous Media: Fluid Transport and Pore Structure*. 2nd ed. San Diego: Academic Press.

Dunhuang wen wu yan jiu suo. 1980–82. *Tonko Bakukokutsu*. 5 vols. Tokyo: Heibonsha.

Englekirk, Robert E. 1997. Geotechnical issues in the conservation of sites. In *Conservation of Ancient Sites on the Silk Road: Proceedings of an International Conference on the Conservation of Grotto Sites*, edited by Neville Agnew, 147–58. Los Angeles: Getty Conservation Institute.

Fan Jinshi. 1997. Fifty years of protection of the Dunhuang Grottoes. In *Conservation of Ancient Sites on the Silk Road: Proceedings of an International Conference on the Conservation of Grotto Sites*, edited by Neville Agnew, 12–22. Los Angeles: Getty Conservation Institute.

Fan Jinshi and Liu Yongzeng. 2007. *Appreciation of Dunhuang Grottoes: A Selection of 50 Caves from the Mogao Grottoes, Yulin Grottoes and Western Thousand Buddha Grottoes*. Nanjing: Jiangsu Fine Arts Publishing House.

Fan Jinshi and Zhao Shengliang. 2009. *The Art of Mogao Grottoes in Dunhuang: A Journey into China's Buddhist Shrine*. 1st English ed. Paramus, NJ: Homa & Sekey Books.

Ferragni, Daniela, Massimo Forti, Joseph Malliet, Paolo Mora, Jeanne Marie Teutonico, and Giorgio Torraca. 1984. Injection grouting of mural paintings and mosaics. In *Adhesives and Consolidants: Preprints of the Contributions to the Paris Congress, 2–8 September 1984*, edited by Norman S. Brommelle, 110–16. London: International Institute for Conservation of Historic and Artistic Works.

FitzHugh, Elisabeth West. 1986. Red lead and minium. In *Artists' Pigments: A Handbook of Their History and Characteristics,* vol. 1, edited by Robert L. Feller, 109–39. Washington, DC: National Gallery of Art.

———. 1997. Orpiment and realgar. In *Artists' Pigments: A Handbook of Their History and Characteristics,* vol. 3, edited by Elisabeth West FitzHugh, 47–79. Washington, DC: National Gallery of Art.

Foth, Henry D. 1990. *Fundamentals of Soil Science*. 8th ed. New York: Wiley.

Fraser, Sarah Elizabeth. 1996. Régimes of production: The use of pounces in temple construction. *Orientations* 27 (10): 60–69.

———. 2004. *Performing the Visual: The Practice of Buddhist Wall Painting in China and Central Asia, 618–960*. Stanford, CA: Stanford University Press.

Gao, Dexiang, and Jacques Giès. 2008. Trésors des grottes de Dunhuang: Mille ans d'art bouddique, 4ème–15ème siècles. Exposition organisée par le Centre culturel de Chine à Paris en collaboration avec le Musée national des Arts asiatiques Guimet, du 18 novembre au 28 février 2009. Paris: Centre culturel de Chine.

Gautier, Gwénaëlle, and Maria Perla Colombini. 2007. GC-MS identification of proteins in wall painting samples: A fast clean-up procedure to remove copper-based pigment interferences. *Talanta* 73 (1): 95–102.

Gettens, Rutherford J., Hermann Kühn, and W. Thomas Chase. 1993. Lead white. In *Artists' Pigments: A Handbook of Their History and Characteristics,* vol. 2, edited by Ashok Roy, 67–81. Washington, DC: National Gallery of Art.

Gettens, Rutherford J., and George L. Stout. [1942] 1966. *Painting Materials: A Short Encyclopaedia*. Reprint. New York: Dover.

Gibbs, Peter J., and Kenneth R. Seddon. 1998. The in situ identification of ancient dyes. In *Conservation des manuscrits de Dunhuang et d'Asie centrale*, edited by Monique Cohen, 131–42. Paris: Bibliothèque nationale de France.

Ginell, William S. 2005. Salt migration in the Mogao Caves. Unpublished report. Getty Conservation Institute.

Giovannoni, Sabino, Mauro Matteini, and Arcangelo Moles. 1990. Studies and developments concerning the problem of altered lead pigments in wall painting. *Studies in Conservation* 35 (1): 21–25.

Gosálbez, Jorge, Addisson Salazar, Ignacio Bosch, Ramón Miralles, and Luis Vergara. 2006. Application of ultrasonic nondestructive testing to the diagnosis of consolidation of a restored dome. *Materials Evaluation* 64 (5): 492–97.

Gosudarstvennyĭ Ėrmitazh (Russia). 1997–2005. *Eluosi guo li Ai'ermitashi bo wu guan cang Dunhuang yi shu pin* (Dunhuang Art Relics Collected in the State Heritage Museum of Russia). 6 vols. Shanghai: Shanghai gu ji chu ban she.

Green, Lorna. 2001. Colour transformations of ancient Egyptian pigments. In *Colour and Painting in Ancient Egypt*, edited by W. Vivian Davies, 43–48. London: British Museum Press.

Griffin, Isobel. 1997. Pozzolanas as additives for grouts: An investigation of their use in wall painting conservation. Postgraduate Diploma diss., Courtauld Institute of Art.

———. 1999. Earthen grouts in wall painting conservation: An investigation of their working properties and performance characteristics. M.A. thesis, Courtauld Institute of Art.

———. 2004. Pozzolanas as additives for grouts: An investigation of their working properties and performance characteristics. *Studies in Conservation* 49 (1): 23–34.

Grinzato, Ermanno, Paolo Bison, Sergio Marinetti, and Vladimir Vavilov. 1994. Nondestructive evaluation of delaminations in fresco plaster using transient infrared thermography. *Research in Nondestructive Evaluation* 5 (4): 257–74.

Grüner, Friedrich, and Gabriele Grassegger. 1993. Der Einfluß der Kompressentrocknung auf den Entsalzungseffekt: Laborversuche zur quantitativen Erfassung. *WTA-Berichte* 9: 75–86.

Guo Hong. 1997. Dunhuang Academy Conservation Institute internal report on mineral pigment identification [In Chinese].

Guo Hong, and Duan Xiuye. 1993. Report on the study of various pigments to be used for copying work at the Mogao Grottoes, Dunhuang. [In Chinese]. In vol. 2 of *Dunhuang yan jiu wen ji. Shi ku bao hu pian*, 304–5. Lanzhou: Gansu min zu chu ban she.

Guo Qinglin, Wang Xudong, Xue Ping, Zhang Guobin, Hou Wenfang, and Zhang Zhengmo. 2010. Preliminary research on salinity and moisture content inside the rock structure of cave 98, Mogao Grottoes. [In Chinese]. In *Proceedings of International Symposium on Conservation of Ancient Sites 2008 & ISRM-Sponsored Regional Symposium*, edited by Li Zuixiong and Wang Xudong, 163–69. Beijing: Science Press.

He Shizhe. 1980. The collection of inscriptions of attendants on wall paintings at the Mogao caves. [In Chinese]. *Zhongguo shi yan jiu* (Journal of Chinese Historical Studies) 3: 25–42.

Houck, Jason, and George W. Scherer. 2006. Controlling stress from salt crystallization. In *Fracture and Failure of Natural Building Stones: Applications in the Restoration of Ancient Monuments*, edited by Stavros K. Kourkoulis, 299–312. Dordrecht: Springer.

Huang Kezhong. 1991. The effect of earthquakes on Mogao Grottoes and the concrete façade. [In Chinese]. *Dunhuang yan jiu* (Dunhuang Research) (28): 107–12.

Ippolito, Jean Marie. 1985. Chinese paint pigments and their classification, with an examination of four Ming dynasty paintings at the Seattle Art Museum. M.A. thesis, University of Washington.

Jin Weiruo. 1959. Study of the names and quantity of caves and niches at the Mogao Grottoes. [In Chinese]. *Wen wu* (Cultural Relics) 5: 50–54, 61.

Kerber, Gabrielle, Manfred Koller, and Franz Mairinger. 1972. Studies of blue-green alterations into Austrian medieval wall painting. In *ICOM Committee for Conservation, Madrid, 1972: Preprints*. Paris: International Council of Museums.

Kuchitsu, Nobuaki, and Duan Xiuye. 1993. Salt crystallization and deterioration of mural paintings in the Dunhuang Mogao Grottoes, Gansu Province, China. [In Japanese]. *Hozon kagaku* (Science for Conservation) (32): 28–34.

———. 1997. Geological environment of the Mogao Grottoes at Dunhuang. In *Conservation of Ancient Sites on the Silk Road: Proceedings of an International Conference on the Conservation of Grotto Sites, Dunhuang, People's Republic of China,* 3–8 October 1993, edited by Neville Agnew, 244–48. Los Angeles: Getty Conservation Institute.

Larsen, Poul Klenz, and Peder Bøllingtoft. 1999. Desalination of a painted brick vault in Kirkerup Church. In *12th Triennial Meeting, Lyon, 29 August–3 September 1999: Preprints*, edited by Janet Bridgland, 473–77. London: James & James.

Leitner, Heinz. 2000. Brittle and flexible: The structural stabilisation of painted plaster on suspended wooden ceilings. *Zeitschrift für Kunsttechnologie und Konservierung* 14 (1): 97–138.

Leitner, Heinz, Steffen Laue, and Heiner Siedel, eds. 2003. *Mauersalze und Architekturoberflächen*. Dresden: Hochschule für Bildende Künste.

Li Qiaoping. 1948. *The Chemical Arts of Old China*. Easton, PA: Journal of Chemical Education.

Li Shi. 1993. A preliminary understanding of binding media in the Dunhuang murals. [In Chinese]. *Dunhuang yan jiu* (Dunhuang Research) (34): 108–17.

———. 1995. Quantitative analysis of binding media of the Dunhuang murals. [In Chinese]. *Dunhuang yan jiu* (Dunhuang Research) (45): 29–46.

Li Shi, Li Yunhe, Li Tiechao, and Xiang Xiaomei. 1992. Results of light aging tests using polyvinyl alcohol and polyvinyl acetate under controlled environments. [In Chinese]. *Dunhuang yan jiu* (Dunhuang Research) (33): 61–77.

Li Yongning. 1981. The compilation of inscriptions on steles at the Mogao Grottoes and their problems. [In Chinese]. *Dunhuang yan jiu* (Dunhuang Research) 1: 56–79.

Li Yunhe, Li Shi, Li Tiechao, and Xiang Xiaomei. 1990. Research in the application of polyvinyl alcohol and polyvinyl acetate on the restoration of mural paintings. [In Chinese]. *Dunhuang yan jiu* (Dunhuang Research) (24): 95–106.

Li Zuixiong. 1992. A study of the red pigments used in the Mogao frescoes and the mechanism of their discoloration. [In Chinese]. *Dunhuang yan jiu* (Dunhuang Research) (32): 41–54.

Li Zuixiong and Stefan W. Michalski. 1989. Effects of light and humidity on the three pigments of hematite, vermilion, and red lead. [In Chinese]. *Dunhuang yan jiu* (Dunhuang Research) (20): 80–85.

Ling Yuquan, Qu Jianjun, Fan Jinshi, and Li Yunhe. 1997. Research into the control of damage by windblown sand at the Mogao Grottoes. In *Conservation of Ancient Sites on the Silk Road: Proceedings of an International Conference on the Conservation of Grotto Sites, Dunhuang, People's Republic of China,* 3–8 October 1993, edited by Neville Agnew, 213–26. Los Angeles: Getty Conservation Institute.

Liu Qingzhu. 1980. Preliminary discussion on the art of the wall paintings of the no. 3 palace building in the ruins of the Qin capital, Xianyang, Shaanxi Province. [In Chinese]. *Kao gu yu wen wu* (Archaeology and Cultural Relics) 2: 98–99.

Lu Hongnian. 1956. Notes on the methods of painting walls in China. [In Chinese]. *Wen wu can kao zi liao* 8: 15–17.

Lubelli, Barbara, Rob P. J. van Hees, and Caspar J. W. P. Groot. 2006. The effect of environmental conditions on sodium chloride damage: A step in the development of an effective weathering test. *Studies in Conservation* 51 (1): 41–56.

Ma De. 1989. The "family cave" and its construction of the Monk-supervisor. [In Chinese]. *Dunhuang yan jiu* (Dunhuang Research) (21): 54–58.

———. 1996. *Dunhuang Mogao ku shi yan jiu* (Research on the History of the Mogao Grottoes at Dunhuang). Lanzhou: Gansu jiao yu chu ban she.

Ma Shichang. 1995. Buddhist cave-temples and the Cao Family at Mogao Ku, Dunhuang. *World Archaeology* 27 (2): 303–17.

Maekawa, Shin. 1994. Preventive strategies for reducing the impact of visitors on the microenvironment of caves at the Mogao Grottoes. In *Preventive Conservation Practice, Theory and Research: Preprints of the Contributions to the Ottawa Congress, 12–16 September 1994*, edited by Ashok Roy and Perry Smith, 76–79. London: International Institute for Conservation of Historic and Artistic Works.

Maekawa, Shin, Liu Gang, Xue Ping, Guo Qinglin, and Hou Wenfang. 2010. Origins of moisture affecting the wall paintings in Cave 85. In *Conservation of Ancient Sites on the Silk Road: Proceedings of the Second International Conference on the Conservation of Grotto Sites, Mogao Grottoes, Dunhuang, People's Republic of China, June 28–July 3, 2004*, edited by Neville Agnew, 464–70. Los Angeles: Getty Conservation Institute.

Maekawa, Shin, Zhan Yongjun, Wang Baoyi, Fu Wenli, and Xue Ping. 1997. Environmental monitoring at the Mogao Grottoes. In *Conservation of Ancient Sites on the Silk Road: Proceedings of an International Conference on the Conservation of Grotto Sites, Dunhuang, People's Republic of China,* 3–8 October 1993, edited by Neville Agnew, 301–13. Los Angeles: Getty Conservation Institute.

Matteini, Mauro. 2001. Künstliches oxalat bei der konservierung von wandmalereien und künstwerken aus kalkstein. In *Konservierung von Wandmalerei: Reaktive Behandlungsmethoden zur Bestandserhaltung: Beiträge einer Fortbildungsveranstaltung der Restaurierungswerkstätten des Bayerischen Landesamtes für Denkmalpflege am 9. Dezember 1994,* edited by Jürgen Pursche, 53–66. Munich: Bayerisches Landesamt für Denkmalpflege.

Mills, John S., and Raymond White. 1987. *The Organic Chemistry of Museum Objects*. London: Butterworths.

Murray, Julia K. 1994. The evolution of Buddhist narrative illustration in China after 850. In *Latter Days of the Law: Images of Chinese Buddhism, 850–1850*, edited by Marsha Smith Weidner, 125–49. Lawrence: Spencer Museum of Art, University of Kansas.

Naumova, M. M., and S. A. Pisareva. 1994. A note on the use of blue and green copper compounds in paintings. *Studies in Conservation* 39 (4): 277–83.

Needham, Joseph. 1976. *Chemistry and Chemical Technology*. Vol. 5 of *Science and Civilisation in China*. Cambridge: Cambridge University Press, 1954–.

Ning Qiang. 2004. *Art, Religion, and Politics in Medieval China: The Dunhuang Cave of the Zhai Family*. Honolulu: University of Hawai'i Press.

Nunberg, Sarah, and A. Elena Charola. 2001. Salts in ceramic bodies. II. Deterioration due to minimal changes in relative humidity. *Internationale Zeitschrift für Bauinstandsetzen und Baudenkmalpflege* (Restoration of Buildings and Monuments: An International Journal) 7 (2): 131–46.

Pan Yunhe and Fan Jinshi. 2003. *Dunhuang zhen shi yu xu ni* (Dunhuang Real and Virtual). Hangzhou: Zhejiang da xue chu ban she.

Pan Yushan and Ma Shichang. 1985. *Mogao ku ku qian dian tang yi zhi* (Ruins of Frontal Buildings Added to the Mogao Grottoes). Beijing: Wen wu chu ban she: Xin hua shu dian Beijing fa xing suo fa xing.

Pelliot, Paul. 1983. *Grottes 73 à 111a*. Vol. 3 of *Grottes de Touen-houang: Carnet de notes de Paul Pelliot: Inscriptions et peintures murales*. Paris: Collège de France, Instituts d'Asie, Centre de Recherche sur l'Asie Centrale et la Haute Asie.

Peng Jinzhang and Wang Jianjun. 2000. *Dunhuang Mogao ku bei qu shi ku* (Northern Grottoes of Mogaoku, Dunhuang). 3 vols. Beijing: Wen wu chu ban she.

Peroni, Simonetta, C. Tersigni, Giorgio Torraca, Stefano Cerea, Massimo Forti, Federico Guidobaldi, Paola Rossi-Doria, A. De Rege, Daniela Picchi, F. J. Pietrafitta, and G. Benedetti. 1982. Lime based mortars for the repair of ancient masonry and possible substitutes. In *Mortars, Cements and Grouts Used in the Conservation of Historic Buildings*, 63–99. Rome: ICCROM.

Petković, Jelena. 2005. Moisture and ion transport in layered porous building materials: A nuclear magnetic resonance study. Ph.D. thesis, Technische Universiteit Eindhoven.

Piqué, Francesca. 1997. Scientific examination of the sculptural polychromy of Cave 6 at Yungang. In *Conservation of Ancient Sites on the Silk Road: Proceedings of an International Conference on the Conservation of Grotto Sites, Mogao Grottoes, Dunhuang, People's Republic of China,* 3–8 October 1993, edited by Neville Agnew, 348–61. Los Angeles: Getty Conservation Institute.

Po-Ming Lin, Neville Agnew, Li Yunhe, and Wang Wanfu. 1997. Desert-adapted plants for control of windblown sand. In *Conservation of Ancient Sites on the Silk Road: Proceedings of an International Conference on the Conservation of Grotto Sites, Mogao Grottoes, Dunhuang, People's Republic of China,* 3–8 October 1993, edited by Neville Agnew, 227–34. Los Angeles: Getty Conservation Institute.

Price, Clifford A., ed. 2000. *An Expert Chemical Model for Determining the Environmental Conditions Needed to Prevent Salt Damage in Porous Materials: Protection and Conservation of the European Cultural Heritage*. European Commission Research Report no. 11. London: Archetype.

Price, Clifford A., and Peter Brimblecombe. 1994. Preventing salt damage in porous materials. In *Preventive Conservation Practice, Theory and Research: Preprints of the Contributions to the Ottawa Congress, 12–16 September 1994*, edited by Ashok Roy and Perry Smith, 90–93. London: International Institute for Conservation of Historic and Artistic Works.

Pühringer, Josef. 1983. *Salt Disintegration: Salt Migration and Degradation by Salt, a Hypothesis*. Swedish Council for Building Research Document D15:1983. Stockholm: Swedish Council for Building Research.

———. 2002a. Hygrothermic deterioration of materials by salts: A technical approach. *Internationale Zeitschrift für Bauinstandsetzen und Baudenkmalpflege* (Restoration of Buildings and Monuments: An International Journal) 8 (4): 349–70.

———. 2002b. Deterioration of materials by salt precipitation: Technical aspects of "crystallisation/hydration." *Internationale Zeitschrift für Bauinstandsetzen und Baudenkmalpflege* (Restoration of Buildings and Monuments: An International Journal) 8 (5): 512–36.

Rickerby, Stephen, Lisa Shekede, Fan Zaixuan, Tang Wei, Qiao Hai, and Yang Jinjian. 2010. Implementation of grouting and salts-reduction treatments of Cave 85 wall paintings. In *Conservation of Ancient Sites on the Silk Road: Proceedings of the Second International Conference on the Conservation of Grotto Sites, Mogao Grottoes, Dunhuang, People's Republic of China, June 28–July 3, 2004*, edited by Neville Agnew, 480–87. Los Angeles: Getty Conservation Institute.

Rickerby, Stephen, Lisa Shekede, Fan Zaixuan, Tang Wei, Qiao Hai, Yang Jinjian, and Francesca Piqué. 2010. Development and testing of the grouting and soluble-salts reduction treatments of Cave 85 wall paintings. In *Conservation of Ancient Sites on the Silk Road: Proceedings of the Second International Conference on the Conservation of Grotto Sites, Mogao Grottoes, Dunhuang, People's Republic of China, June 28–July 3, 2004*, edited by Neville Agnew, 471–79. Los Angeles: Getty Conservation Institute.

Rodríguez Navarro, Carlos, Eric Doehne, and Eduardo Sebastián. 2000. Influencing crystallization damage in porous materials through the use of surfactants: Experimental results using sodium dodecyl sulfate and cetyldimethylbenzylammonium chloride. *Langmuir* 16 (3): 947–54.

Rong Xinjiang. 1996. *Guiyijun shi yanjiu: Tang Song shidai Dunhuang lishi kaosu* (Studies in the History of the Return to Allegiance Army: Dunhuang during the Tang and Song). Shanghai: Shanghai guji chubanshe.

Sawdy, Alison. 2003. The role of environmental control for reducing the rate of salt damage in wall paintings. In *Conserving the Painted Past: Developing Approaches to Wall Painting Conservation: Post-Prints of a Conference Organised by English Heritage, London, 2–4 December, 1999*, edited by Robert Gowing and Adrian Heritage, 95–109. London: James & James.

Schafer, Edward H. 1955. Orpiment and realgar in Chinese technology and tradition. *Journal of the American Oriental Society* 75 (2): 73–89.

Scherer, George W., Robert Flatt, and George Wheeler. 2001. Materials science research for the conservation of sculpture and monuments. *MRS Bulletin* 26 (1): 44–50.

Schilling, Michael R. 2000. Extraction of vinyl polymers from samples of wall plaster from Cave 85. Unpublished report. Getty Conservation Institute, Los Angeles, CA.

———. 2001. Experiment to measure the movement of salt through conglomerate rock. Unpublished report. Getty Conservation Institute, Los Angeles, CA.

———. 2005. Paint media analysis. In *Scientific Examination of Art: Modern Techniques in Conservation and Analysis*, 186–205. Washington, DC: National Academies Press.

Schilling, Michael R., and Herant P. Khanjian. 1996a. Gas chromatographic analysis of amino acids as ethyl chloroformate derivatives. Part 2. Effects of pigments and accelerated aging on the identification of proteinaceous binding media. *Journal of the American Institute for Conservation* 35 (2): 123–44.

———. 1996b. Gas chromatographic analysis of amino acids as ethyl chloroformate derivatives. III. Identification of proteinaceous binding media by interpretation of amino acid composition data. In *11th Triennial Meeting, Edinburgh, Scotland, 1–6 September, 1996: Preprints (ICOM Committee for Conservation)*, edited by Janet Bridgland, 211–19. London: Earthscan.

Schilling, Michael R., Joy Mazurek, David Carson, Su Bomin, Fan Yuquan, and Ma Zanfeng. 2010. Analytical research in Cave 85. In *Conservation of Ancient Sites on the Silk Road: Proceedings of the Second International Conference on the Conservation of Grotto Sites, Mogao Grottoes, Dunhuang, People's Republic of China, June 28–July 3, 2004*, edited by Neville Agnew, 438–49. Los Angeles: Getty Conservation Institute.

Selwitz, Charles M., and Eric Doehne. 2002. The evaluation of crystallization modifiers for controlling salt damage to limestone. *Journal of Cultural Heritage* 3 (3): 205–16.

Shekede, Lisa, Fan Zaixuan, Francesca Piqué, and Lorinda Wong. 2010. The role of in situ examination in the technical investigation of the Cave 85 paintings. In *Conservation of Ancient Sites on the Silk Road: Proceedings of the Second International Conference on the Conservation of Grotto Sites, Mogao Grottoes, Dunhuang, People's Republic of China, June 28–July 3, 2004*, edited by Neville Agnew, 430–37. Los Angeles: Getty Conservation Institute.

Shen Fenling, Li Zuixiong, and Fan Zaixuan. 1990. Humidity is the main cause for color change of minium. [In Chinese]. *Dunhuang yan jiu* (Dunhuang Research) (25): 98–102.

Shi Pingting. 1990. Research on illustration painting of Suvarna-prabhasa Sutra. [In Chinese]. In *Dunhuang shi ku yan jiu guo ji tao lun hui wen ji. Shi ku kao gu bian* (Proceedings of the 1987 International Conference on Dunhuang Grottoes), edited by Duan Wenjie, Zhao Min, Fan Jinshi and Liang Weiying, 414–55. Shenyang: Liaoning mei shu chu ban she.

Shi Zhangru. 1996. *Mogao ku xing.* [Section and Plan Measurements of the Mogao Grottoes: Field Project Report no. 3]. 3 vols. Taipei: Zhong yang yan jiu yuan li shi yu yan yan jiu suo.

Sickels, Lauren-Brook. 1982. Organics vs. synthetics: Their use as additives in mortars. In *Mortars, Cements and Grouts Used in the Conservation of Historic Buildings*, 25–52. Rome: ICCROM.

Smith, Allyson. 2000. Characterisation of fillers. Postgraduate Diploma diss., Courtauld Institute of Art.

Stein, Aurel, Sir. 1921. *Serindia: Detailed Report of Explorations in Central Asia and Westernmost China*. Vol. 2. Oxford: Clarendon Press.

Sun Rujian. 1997. Review of stabilization projects at the Mogao Grottoes. In *Conservation of Ancient Sites on the Silk Road: Proceedings of an International Conference on the Conservation of Grotto Sites, Mogao Grottoes, Dunhuang, People's Republic of China,* 3–8 October 1993, edited by Neville Agnew, 159–69. Los Angeles: Getty Conservation Institute.

Takahashi, Hidenori, and Sadatoshi Miura. 1997. Climate of Dunhuang area, China. In *The Conservation of Dunhuang, Mogao Grottoes, and Related Studies: International Symposium on the Conservation and Restoration of Cultural Property, Nara, February 1–3, 1996*, 41–50. Tokyo: Tokyo National Research Institute of Cultural Properties.

Tan Chung, ed. 1994. *Dunhuang Art: Through the Eyes of Duan Wenjie*. New Delhi: Indira Gandhi National Centre for Arts; Abhinav Publications. http://www.igna.nic.in/ks_19.htm.

Tang Yumin and Sun Rujian. 1988. Exploring the causes of color change in the Mogao Grottoes wall paintings. [In Chinese]. *Dunhuang yan jiu* (Dunhuang Research) (16): 18–27.

Tanimoto, Chikaosa, Chunze Piao, Keigo Koizumi, Shuichi Iwata, Tadashi Masuya, Li Zuixiong, Wang Xudong, and Guo Qinglin. 2005. Application of satellite remote sensing of fault distribution and groundwater in Mogao, Dunhuang. In *Alaska Rocks 2005: Proceedings: Rock Mechanics for Energy, Mineral and Infrastructure Development in the Northern Regions: June 25–29, University of Alaska–Anchorage*, edited by Gang Chen, 805–65. Alexandria, VA: ARMA.

———. 2010. Geology and hydrogeology at the Mogao Grottoes, Dunhuang. In *Conservation of Ancient Sites on the Silk Road: Proceedings of the Second International Conference on the Conservation of Grotto Sites, Mogao Grottoes, Dunhuang, People's Republic of China, June 28–July 3, 2004*, edited by Neville Agnew, 189–95. Los Angeles: Getty Conservation Institute.

Teutonico, Jeanne Marie, Iain McCaig, and John Ashurst. 1994. The Smeaton project: Factors affecting the properties of lime-based mortars. *APT Bulletin* 25 (3–4): 32–49.

Tinzl, Christoph. 1994. Removal of salts from lime plaster by means of poulticing. Postgraduate Diploma diss., Courtauld Institute of Art.

Verri, Giovanni, Alfredo Aldrovandi, Giuseppe Centauro, Catia Clementi, Daniela Comelli, Costanza Miliani, Marcello Picollo, Francesca Piqué, and Lucia Toniolo. 2005. Evaluation of non-invasive techniques for the detection of organic material in wall painting. In *8th International Conference on "Non-Destructive Investigations and Microanalysis for the Diagnostics and Conservation of the Cultural and Environmental Heritage": Lecce (Italy), 15–19 May 2005*, edited by Concetto Parisi, Giancarlo Buzzanca, and Alessandra Paradisi. Brescia: Associazione italiana prove non distruttive monitoraggio diagnostica.

Verri, Giovanni, Catia Clementi, Daniela Comelli, Sharon Cather, and Francesca Piqué. 2008. Correction of ultraviolet-induced fluorescence spectra for the examination of polychromy. *Applied Spectroscopy* 62 (12): 1295–1302.

Verri, Giovanni, Daniela Comelli, Sharon Cather, David Saunders, and Francesca Piqué. 2008. Post-capture data analysis as an aid to the interpretation of ultraviolet-induced fluorescence images. In *Computer Image Analysis in the Study of Art: San Jose, CA, 28–29 January 2008: Proceedings of SPIE—The International Society for Optical Engineering,* vol. 6810, edited by David G. Stork and Jim Coddington, article no. 681002. Bellingham, WA; Springfield, VA: SPIE, IS&T.

Vincent, Irene Vongehr. 1953. *The Sacred Oasis: Caves of the Thousand Buddhas, Tun Huang*. Chicago: University of Chicago Press.

Wainwright, Ian N. M., Elizabeth A. Moffatt, P. Jane Sirois, and Gregory S. Young. 1997. Analysis of wall painting fragments from the Mogao and the Bingling Temple Grottoes. In *Conservation of Ancient Sites on the Silk Road: Proceedings of an International Conference on the Conservation of Grotto Sites*, *Mogao Grottoes, Dunhuang, People's Republic of China,* 3–8 October 1993, edited by Neville Agnew, 334–340. Los Angeles: Getty Conservation Institute.

Walker, Matt. 1999. Arsenic and old paint. *New Scientist* 162 (2188): 20.

Wallert, Arie. 1984. Orpiment and realgar: Some pigment characteristics. *Maltechnik Restauro* 90 (4): 45–57.

Wang Jinyu. 2003. The producing area of Hecuba Juno application of pigment on Dunhuang Grottoes art. [In Chinese]. *Wen wu bao hu yu kao gu ke xue* (Sciences of Conservation & Archaeology) 15 (3): 47–56.

———. 2010. The significance of Cave 85. In *Conservation of Ancient Sites on the Silk Road: Proceedings of the Second International Conference on the Conservation of Grotto Sites, Mogao Grottoes, Dunhuang, People's Republic of China, June 28–July 3, 2004*, edited by Neville Agnew, 399–405. Los Angeles: Getty Conservation Institute.

Wang Jinyu and Wang Jincong. 1999. The manufactures and applications of verdigris pigment of the minority nationalities in northwestern China. [In Chinese]. *Guangxi minzu xueyuan xuebao. Ziran kexue ban* 141–43.

Whitfield, Roderick. 1995. *Dunhuang: Caves of the Singing Sands: Buddhist Art from the Silk Road*. 2 vols. London: Textile & Art Publications.

Whitfield, Roderick, Susan Whitfield, and Neville Agnew. 2000. *Cave Temples of Mogao: Art and History on the Silk Road*. Los Angeles: Getty Conservation Institute.

Whitfield, Susan. 1999. *Life along the Silk Road*. London: John Murray.

Whitmore, Paul M., Xun Pan, and Catherine Bailie. 1999. Predicting the fading of objects: Identification of fugitive colorants through direct nondestructive lightfastness measurements. *Journal of the American Institute for Conservation* 38 (3): 395–409.

Wong, Lorinda. 1997. Condition recording in the field of wall painting conservation. Postgraduate Diploma diss., Courtauld Institute of Art.

Wouters, Jan. 1985. High performance liquid chromatography of anthraquinones: Analysis of plant and insect extracts and dyed textiles. *Studies in Conservation* 30 (3): 119–28.

———. 1994. Dye analysis of Chinese and Indian textiles: With special emphasis on the recognition of *Miscanthus tinctorius* and *Sophora japonica* and the composition of green and blue colours. *Dyes in History and Archaeology* (12): 12–22.

Wouters, Jan, and Cecily M. Grzywacz. 2006. A contribution to the characterisation of ancient Chinese colorants. Unpublished report. Getty Conservation Institute.

Wu Hung. 1992. Reborn in paradise: A case study of Dunhuang sutra painting and its religious, ritual and artistic context. *Orientations* 23 (5): 52–60.

Wu Mangong. 1959. Arrangement for lanterns in caves and niches on December 8 (lunar calendar) at the Mogao Grottoes. [In Chinese]. *Wen wu* (Cultural Relics) 5: 49.

Xiao Mo. 1989. *Dunhuang jian zhu yan jiu* (Architectural Research of Dunhuang Grottoes). Beijing: Wen wu chu ban she.

Xu Weiye, Zhou Guoxin, and Li Yunhe. 1983. A report of an X-ray analysis on the inorganic pigments in the murals and sculptures of Mogao Grottoes. [In Chinese]. *Dunhuang yan jiu* (Dunhuang Research) 3: 187–97.

Yao Zeng, Zhou Zhonghua, and Li Weitang 1993. Elastic dynamic characteristics of adjoining rock of Mogao at Dunhuang. [In Chinese]. In vol. 1 of *Dunhuang yan jiu wen ji. Shi ku bao hu pian*, 1:376–82. Lanzhou: Gansu min zu chu ban she.

Ye Yun, Lynn G. Salmon, and Glen R. Cass. 2000. The ozone fading of traditional Chinese plant dyes. *Journal of the American Institute for Conservation* 39 (2): 245–57.

Yin Guangming. 2001. Changes of themes of Raudraksa's battle with Sariputra and argument between Buddhism and Taoism. [In Chinese]. *Dunhuang yan jiu* (Dunhuang Research) (68): 4–13.

Yu Feian. 1988. *Chinese Painting Colors: Studies of Their Preparation and Application in Traditional and Modern Times*. Translated by Jerome Silbergeld and Amy McNair. Seattle: University of Washington Press.

Zhang Minquan. 2000. Hypotheses of deterioration: Round table discussion at the Dunhuang Academy, March 30–31, 2000.

Zhuang Jiayi and Nie Chongzheng. 2000. *Traditional Chinese Paintings: Silent Poems in Praise of Nature and Human Life*. Translated by Chen Gengtao. China Basics Series. Beijing: China Intercontinental Press.

Appendixes

Note to reader: Appendixes are numbered based on the chapters to which they refer.

APPENDIX 2.A

Cave 85 Project Team Members

DUNHUANG ACADEMY		
WANG XUDONG	Supervision	1997–2010
SU BOMIN	Supervision	1997–2010
MA XIWU AND STAFF	Administration	2001–2010
WANG XIAOWEI	Documentation	1999–2010
XU SHUQING	Documentation	1997–2010
ZHU WANYI	Documentation	1997–2010
LIU RUI	Documentation	2003–2005
SUN SHENGLI	Documentation	2005–2010
CHAI BOLONG	Documentation	2002–2010
MA JIANHONG	Documentation	1997–2010
WANG JINYU	Documentation	1997–2005
TANG AILING	Documentation	1997–2005
SUN HONGCAI	Photography	1997–2010
FAN ZAIXUAN	Conservation	1997–2010
QIAO HAI	Conservation	1999–2010
YANG JINGJIAN	Conservation	2000–2006
CUI QIANG	Conservation	2003–2006
ZHAO HONGLIANG	Conservation	2004–2006
LIU TAO	Conservation	1999–2001
TANG WEI	Conservation	2001–2006
YIN ZHIHONG	Conservation	2004–2006
FU YOUXU	Conservation	1997–1999
LIU GANG	Environmental	1997–2002
XUE PING	Environmental	1997–2010
ZHANG GUOBIN	Environmental	2002–2010
ZHANG ZHENGMO	Environmental	2005–2010
HOU WENFANG	Environmental	1997–2010
FAN YUQUAN	Analytical	1999–2010
ZHAO LINYI	Analytical	2000–2010
CHEN GANGQUAN	Analytical	2002–2010
LI YANFEI	Analytical	2001–2010
YU ZONGREN	Analytical	2000–2010
MA ZANFENG	Analytical	1997–2002
GUO HONG	Analytical	1997–2002
LI PING	Interpretation and Presentation	2007–2010
SUN YIHUA	Presentation – Platform (Architecture)	2007–2010
XU HONGSHENG	Presentation – Platform (Engineering)	2007–2010

GETTY CONSERVATION INSTITUTE		
NEVILLE AGNEW	Supervision	1997–2010
MARTHA DEMAS	Interpretation and Presentation	2007–2010
SHIN MAEKAWA	Environmental	1997–2010
MICHAEL SCHILLING	Analytical	1997–2010
FRANCESCA PIQUÉ	Conservation, Documentation and Analytical	1997–2010
LORI WONG	Conservation, Documentation and Analytical	2001–2010
LESLIE RAINER	Conservation	1997–1999
PO-MING LIN	Facilitation and Translation	1997–2010
PETER BARKER	Translation	1997–2010
STEPHEN RICKERBY	Conservation	1997–2010
LISA SHEKEDE	Conservation and Analytical	1999–2010
CHINESE ACADEMY OF CULTURAL HERITAGE		
ZHENG JUN	Conservation and Documentation	1997–2002
CHEN QING	Conservation	2003–2005

APPENDIX 12.A

Documentation Area Grid References

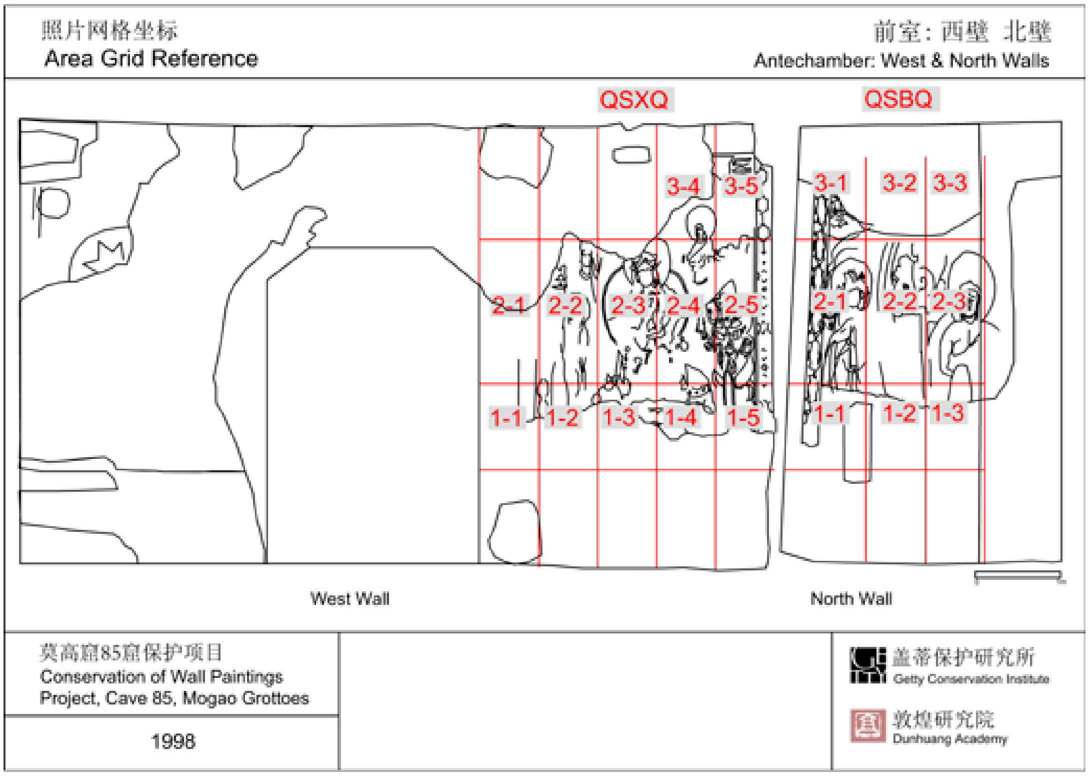

照片网格坐标
Area Grid Reference

藻井
Ceiling

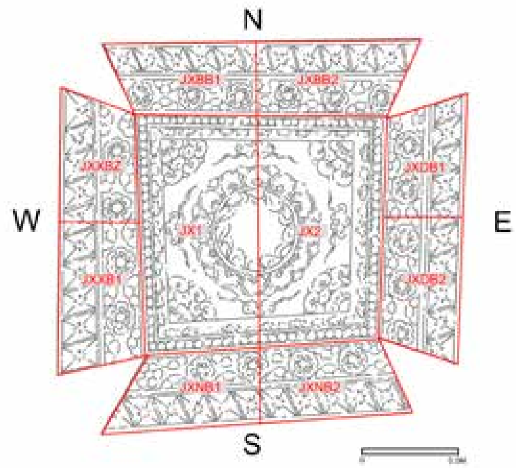

莫高窟85窟保护项目
Conservation of Wall Paintings Project
Cave 85, Mogao Grottoes

1998

盖蒂保护研究所
Getty Conservation Institute

敦煌研究院
Dunhuang Academy

照片网格坐标
Area Grid Reference

甬道
Corridor

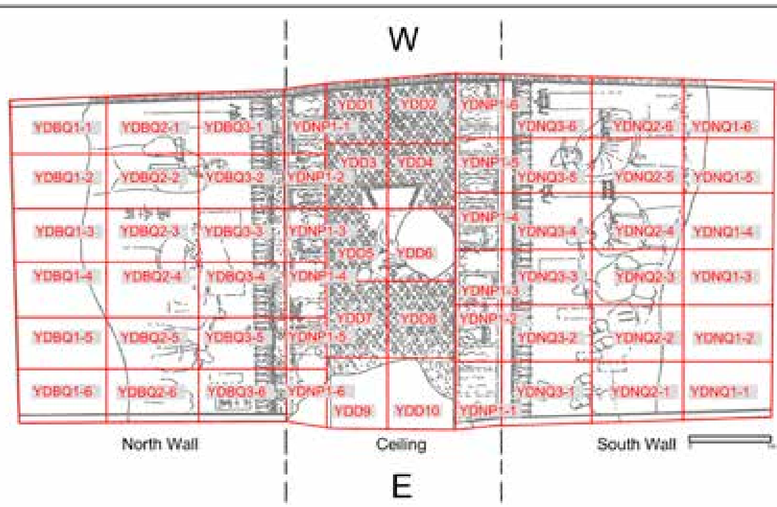

莫高窟85窟保护项目
Conservation of Wall Paintings Project
Cave 85, Mogao Grottoes

1998

盖蒂保护研究所
Getty Conservation Institute

敦煌研究院
Dunhuang Academy

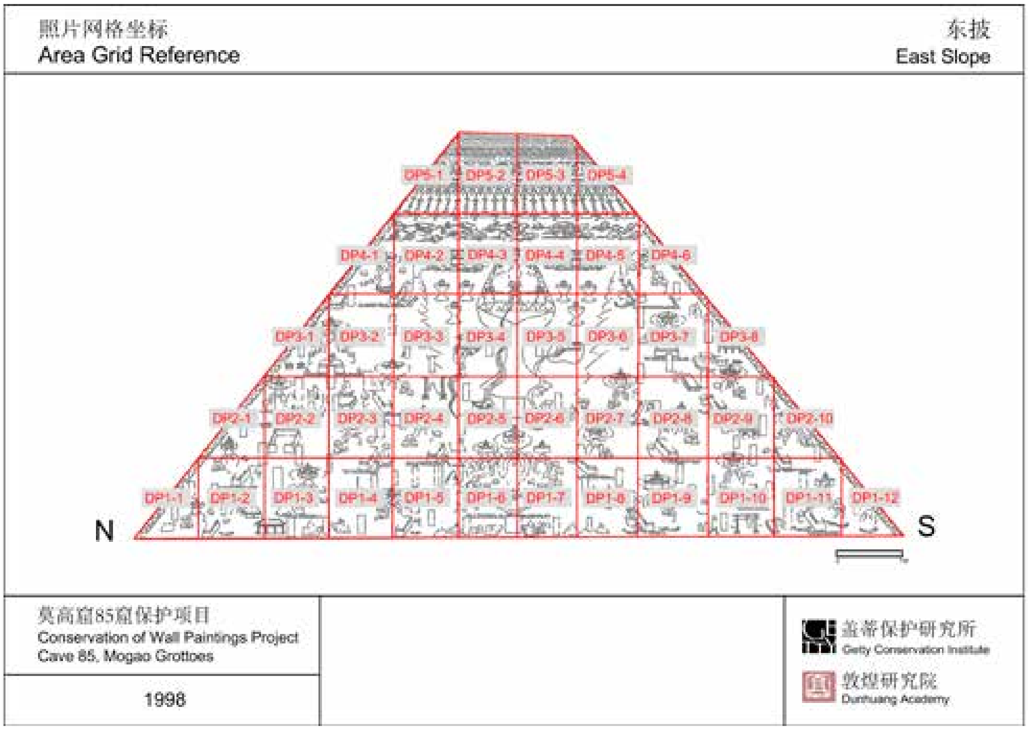
照片网格坐标
Area Grid Reference
东披
East Slope
DP5-1 DP5-2 DP5-3 DP5-4
DP4-1 DP4-2 DP4-3 DP4-4 DP4-5 DP4-6
DP3-1 DP3-2 DP3-3 DP3-4 DP3-5 DP3-6 DP3-7 DP3-8
DP2-1 DP2-2 DP2-3 DP2-4 DP2-5 DP2-6 DP2-7 DP2-8 DP2-9 DP2-10
DP1-1 DP1-2 DP1-3 DP1-4 DP1-5 DP1-6 DP1-7 DP1-8 DP1-9 DP1-10 DP1-11 DP1-12
N
S
莫高窟85窟保护项目
Conservation of Wall Paintings Project
Cave 85, Mogao Grottoes
1998
盖蒂保护研究所
Getty Conservation Institute
敦煌研究院
Dunhuang Academy

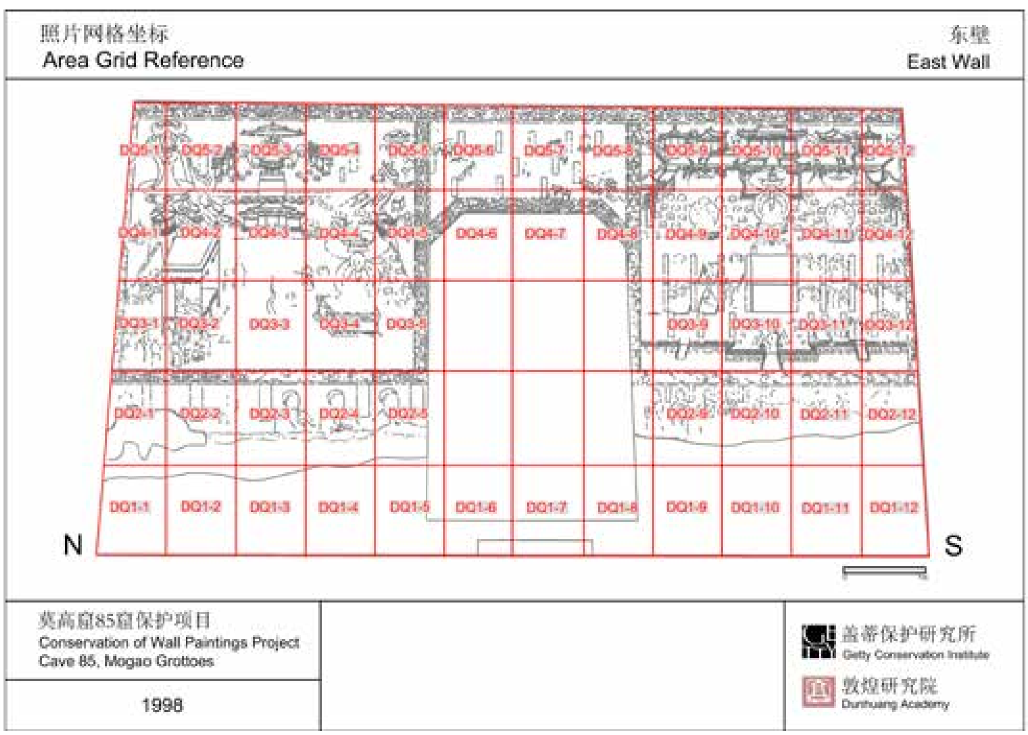
照片网格坐标
Area Grid Reference
东壁
East Wall
DQ5-1 DQ5-2 DQ5-3 DQ5-4 DQ5-5 DQ5-6 DQ5-7 DQ5-8 DQ5-9 DQ5-10 DQ5-11 DQ5-12
DQ4-1 DQ4-2 DQ4-3 DQ4-4 DQ4-5 DQ4-6 DQ4-7 DQ4-8 DQ4-9 DQ4-10 DQ4-11 DQ4-12
DQ3-1 DQ3-2 DQ3-3 DQ3-4 DQ3-5 DQ3-9 DQ3-10 DQ3-11 DQ3-12
DQ2-1 DQ2-2 DQ2-3 DQ2-4 DQ2-5 DQ2-9 DQ2-10 DQ2-11 DQ2-12
DQ1-1 DQ1-2 DQ1-3 DQ1-4 DQ1-5 DQ1-6 DQ1-7 DQ1-8 DQ1-9 DQ1-10 DQ1-11 DQ1-12
N
S
莫高窟85窟保护项目
Conservation of Wall Paintings Project
Cave 85, Mogao Grottoes
1998
盖蒂保护研究所
Getty Conservation Institute
敦煌研究院
Dunhuang Academy

照片网格坐标
Area Grid Reference

北披
North Slope

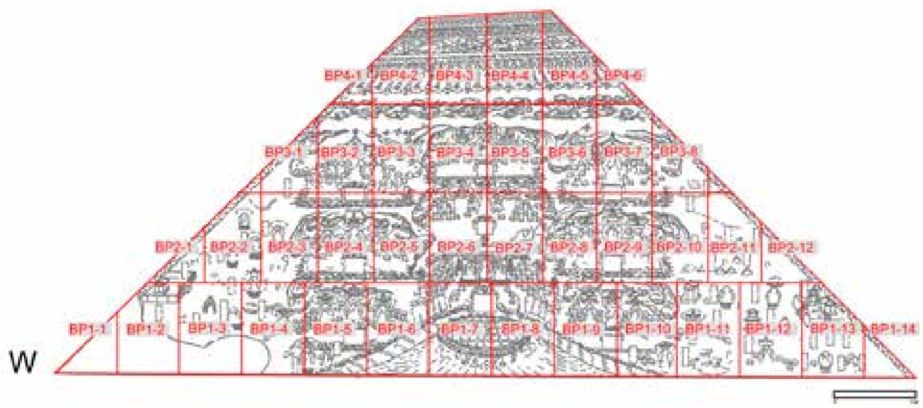

莫高窟85窟保护项目
Conservation of Wall Paintings Project
Cave 85, Mogao Grottoes

1998

盖蒂保护研究所
Getty Conservation Institute

敦煌研究院
Dunhuang Academy

照片网格坐标
Area Grid Reference

北壁
North Wall

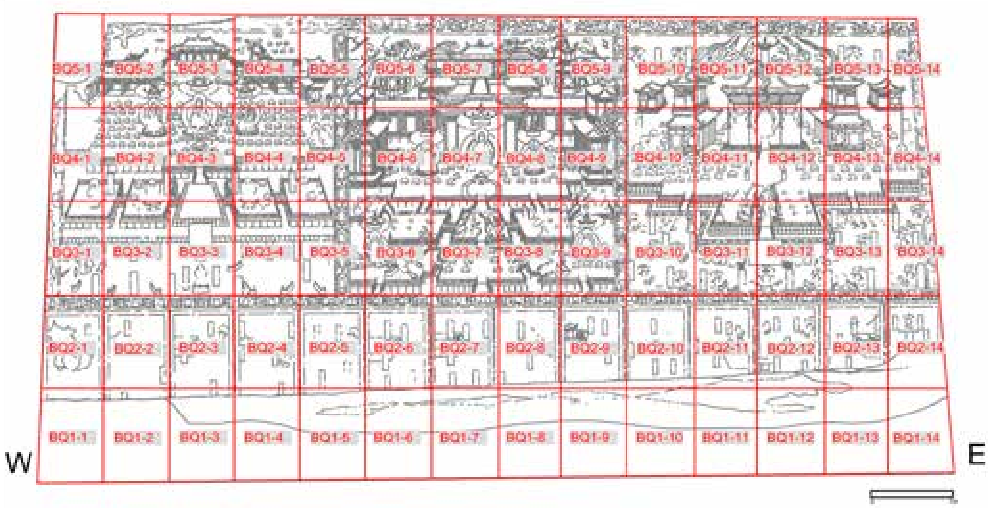

莫高窟85窟保护项目
Conservation of Wall Paintings Project
Cave 85, Mogao Grottoes

1998

盖蒂保护研究所
Getty Conservation Institute

敦煌研究院
Dunhuang Academy

照片网格坐标
Area Grid Reference

南披
South Slope

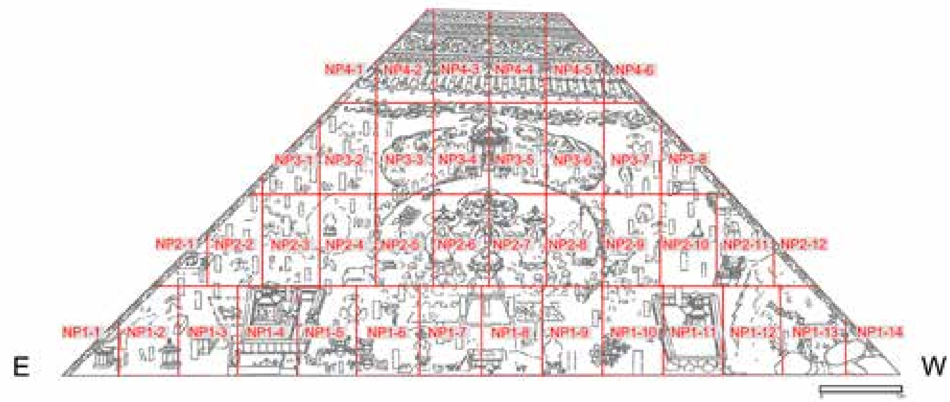

莫高窟85窟保护项目
Conservation of Wall Paintings Project
Cave 85, Mogao Grottoes

1998

盖蒂保护研究所
Getty Conservation Institute

敦煌研究院
Dunhuang Academy

照片网格坐标
Area Grid Reference

南壁
South Wall

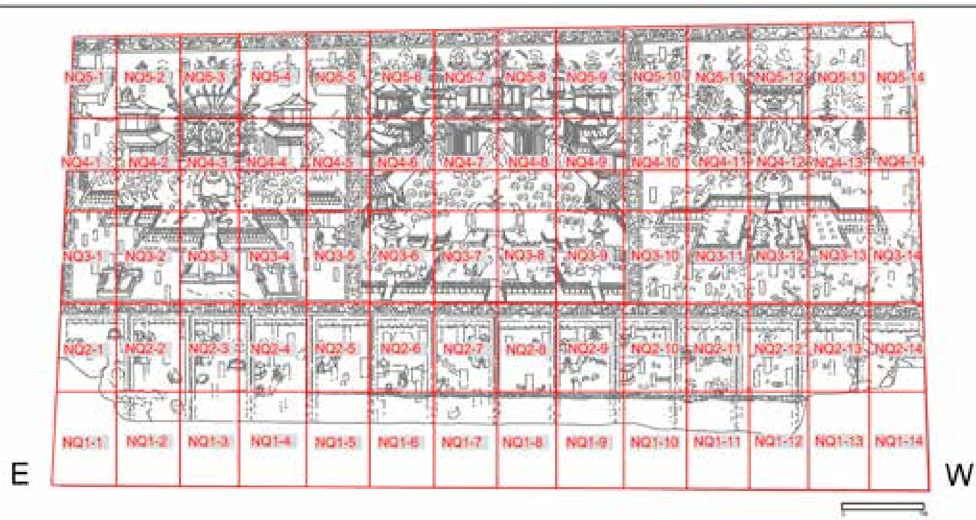

莫高窟85窟保护项目
Conservation of Wall Paintings Project
Cave 85, Mogao Grottoes

1998

盖蒂保护研究所
Getty Conservation Institute

敦煌研究院
Dunhuang Academy

照片网格坐标
Area Grid Reference

西披
West Slope

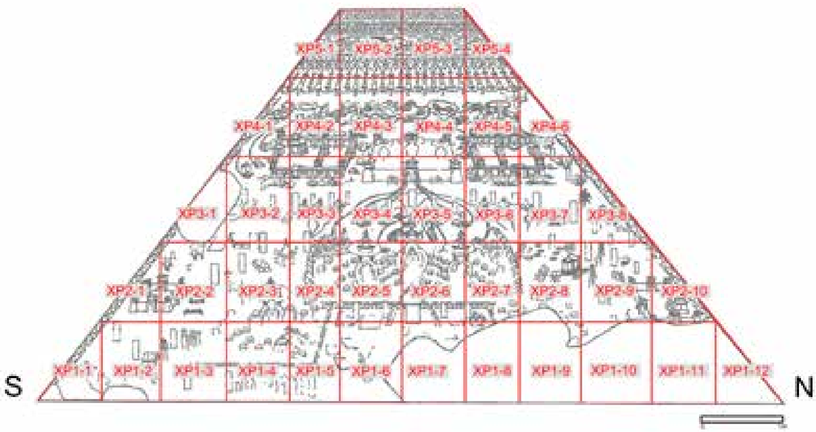

莫高窟85窟保护项目
Conservation of Wall Paintings Project
Cave 85, Mogao Grottoes

1998

盖蒂保护研究所
Getty Conservation Institute

敦煌研究院
Dunhuang Academy

照片网格坐标
Area Grid Reference

西壁
West Wall

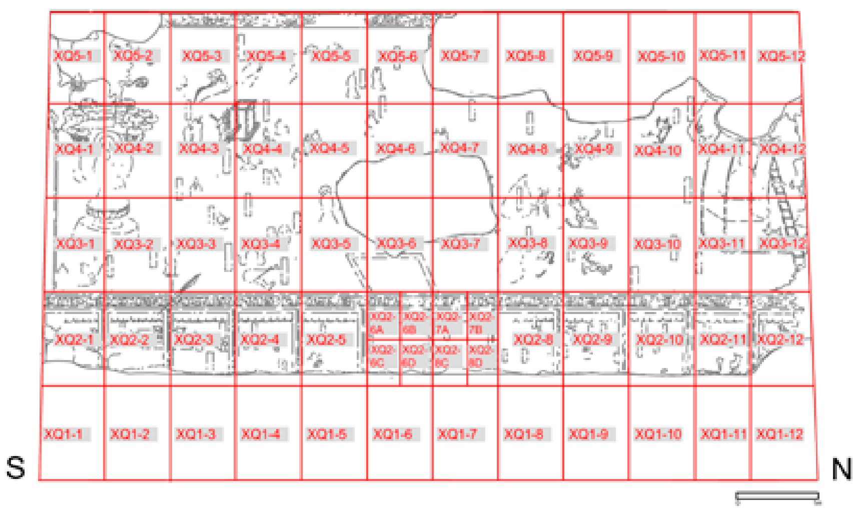

莫高窟85窟保护项目
Conservation of Wall Paintings Project
Cave 85, Mogao Grottoes

1998

盖蒂保护研究所
Getty Conservation Institute

敦煌研究院
Dunhuang Academy

APPENDIX 12.B

Graphic Documentation: Previous Treatment and Current Conditions of Plaster

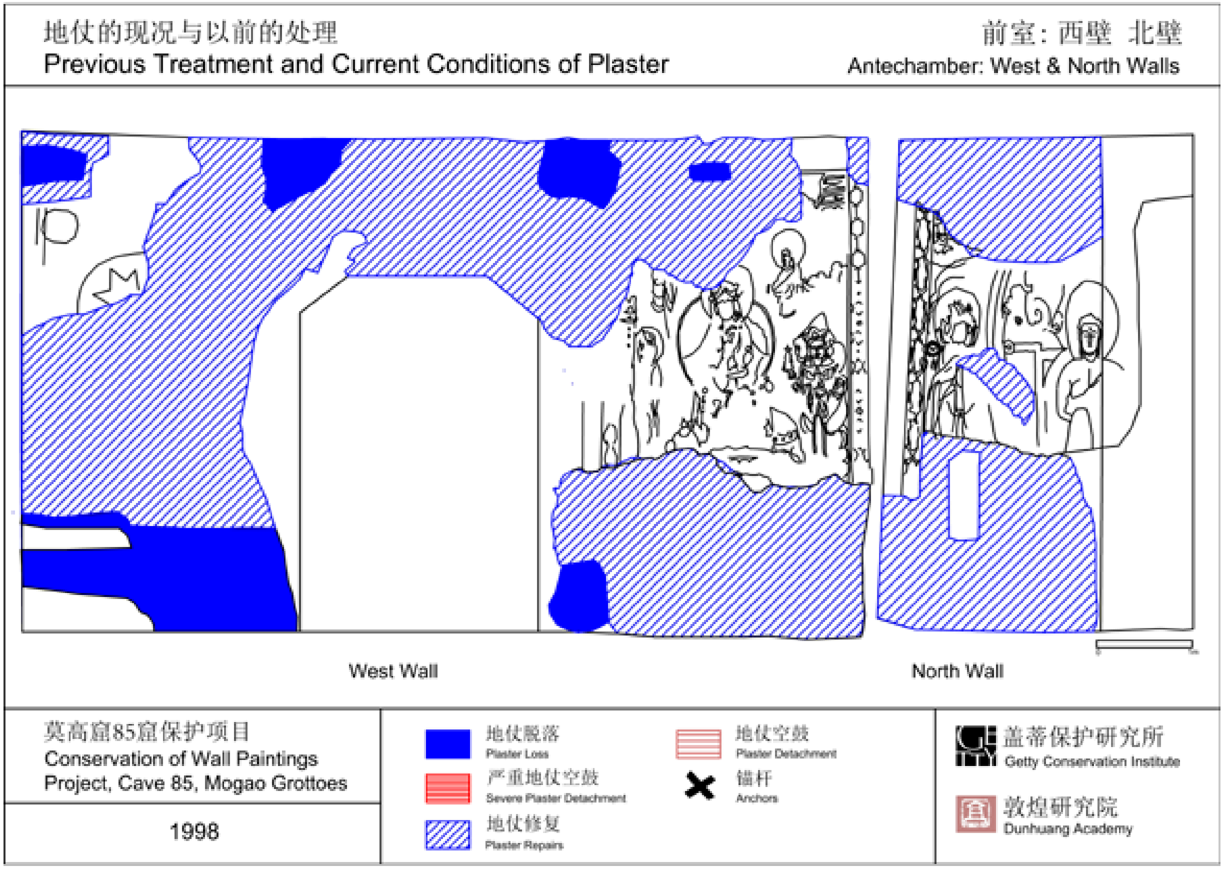

地仗的现况与以前的处理
Previous Treatment and Current Conditions of Plaster

藻井
Ceiling

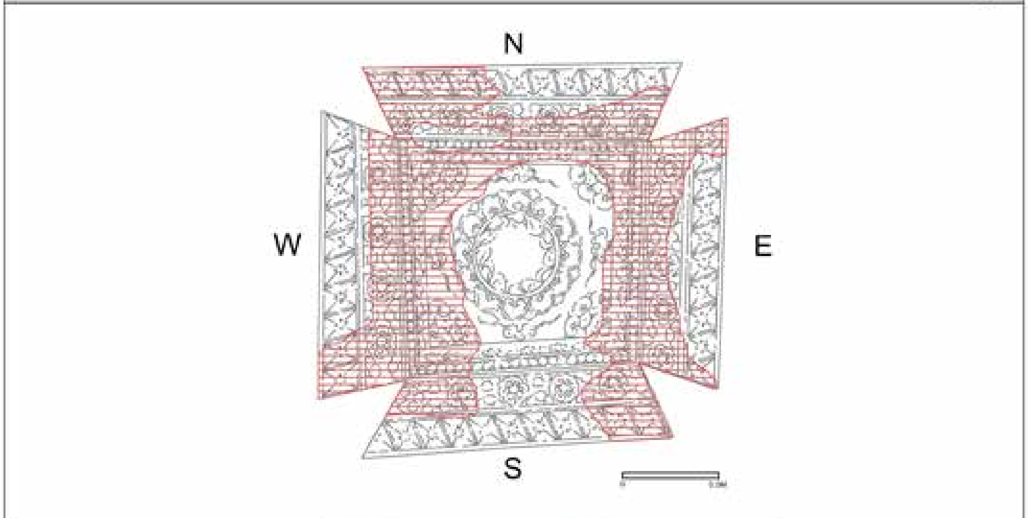

莫高窟85窟保护项目
Conservation of Wall Paintings Project
Cave 85, Mogao Grottoes

1998

地仗脱落 Plaster Loss
严重地仗空鼓 Severe Plaster Detachment
地仗修复 Plaster Repairs
地仗空鼓 Plaster Detachment
锚杆 Anchors

盖蒂保护研究所 Getty Conservation Institute
敦煌研究院 Dunhuang Academy

地仗的现况与以前的处理
Previous Treatment and Current Conditions of Plaster

甬道
Corridor

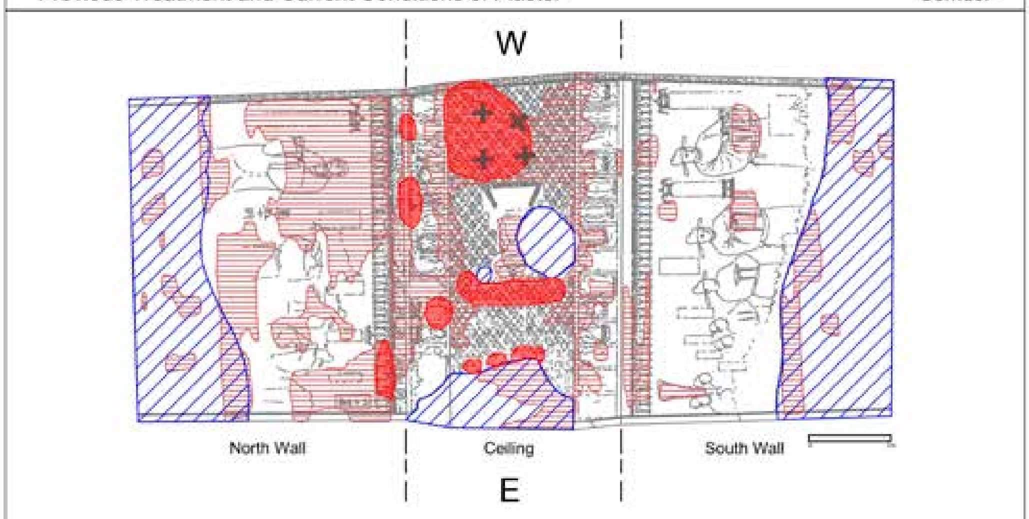

莫高窟85窟保护项目
Conservation of Wall Paintings Project
Cave 85, Mogao Grottoes

1998

地仗脱落 Plaster Loss
严重地仗空鼓 Severe Plaster Detachment
地仗修复 Plaster Repairs
地仗空鼓 Plaster Detachment
锚杆 Anchors

盖蒂保护研究所 Getty Conservation Institute
敦煌研究院 Dunhuang Academy

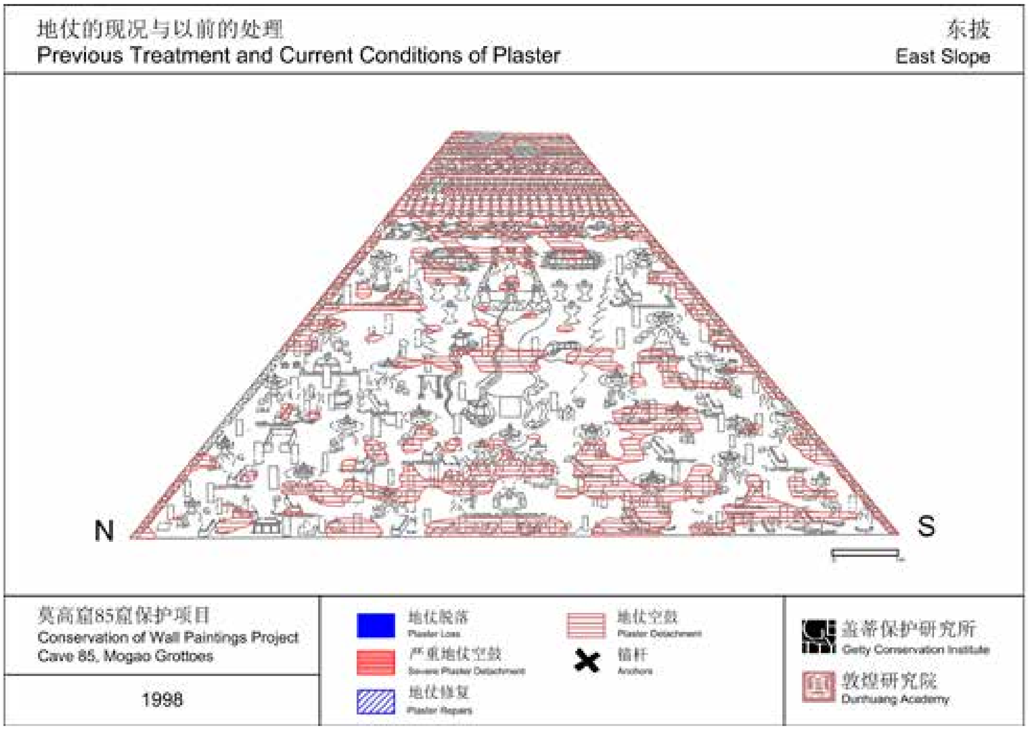
地仗的现况与以前的处理
Previous Treatment and Current Conditions of Plaster
东披
East Slope
N
S
莫高窟85窟保护项目
Conservation of Wall Paintings Project
Cave 85, Mogao Grottoes
1998
地仗脱落
Plaster Loss
严重地仗空鼓
Severe Plaster Detachment
地仗修复
Plaster Repairs
地仗空鼓
Plaster Detachment
锚杆
Anchors
盖蒂保护研究所
Getty Conservation Institute
敦煌研究院
Dunhuang Academy

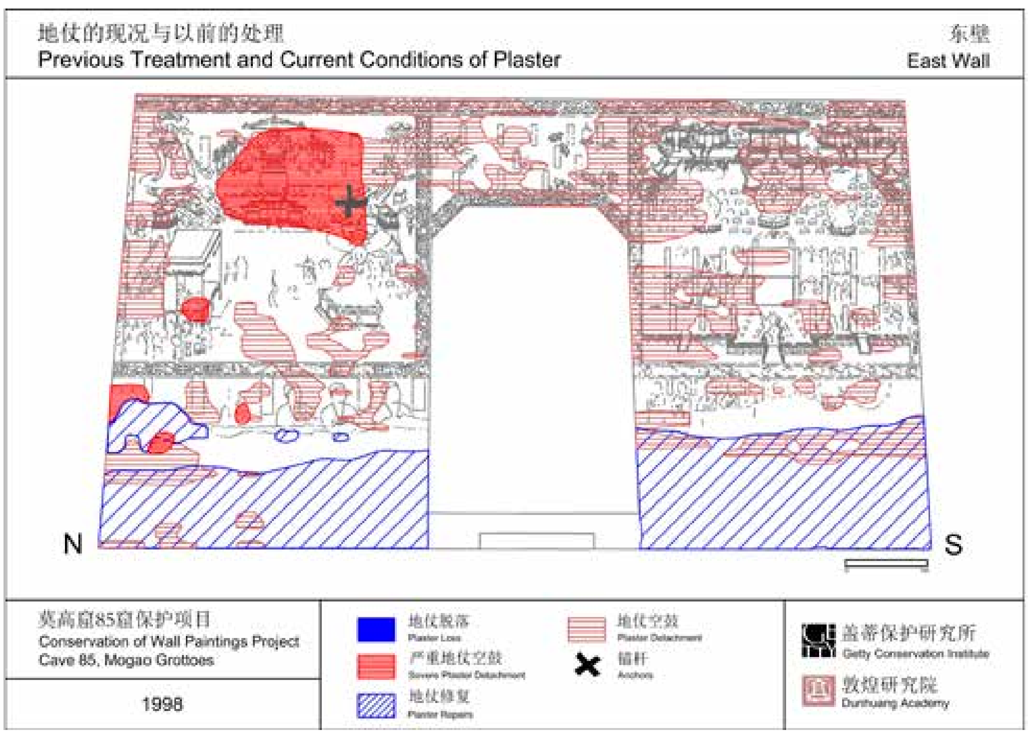
地仗的现况与以前的处理
Previous Treatment and Current Conditions of Plaster
东壁
East Wall
N
S
莫高窟85窟保护项目
Conservation of Wall Paintings Project
Cave 85, Mogao Grottoes
1998
地仗脱落
Plaster Loss
严重地仗空鼓
Severe Plaster Detachment
地仗修复
Plaster Repairs
地仗空鼓
Plaster Detachment
锚杆
Anchors
盖蒂保护研究所
Getty Conservation Institute
敦煌研究院
Dunhuang Academy

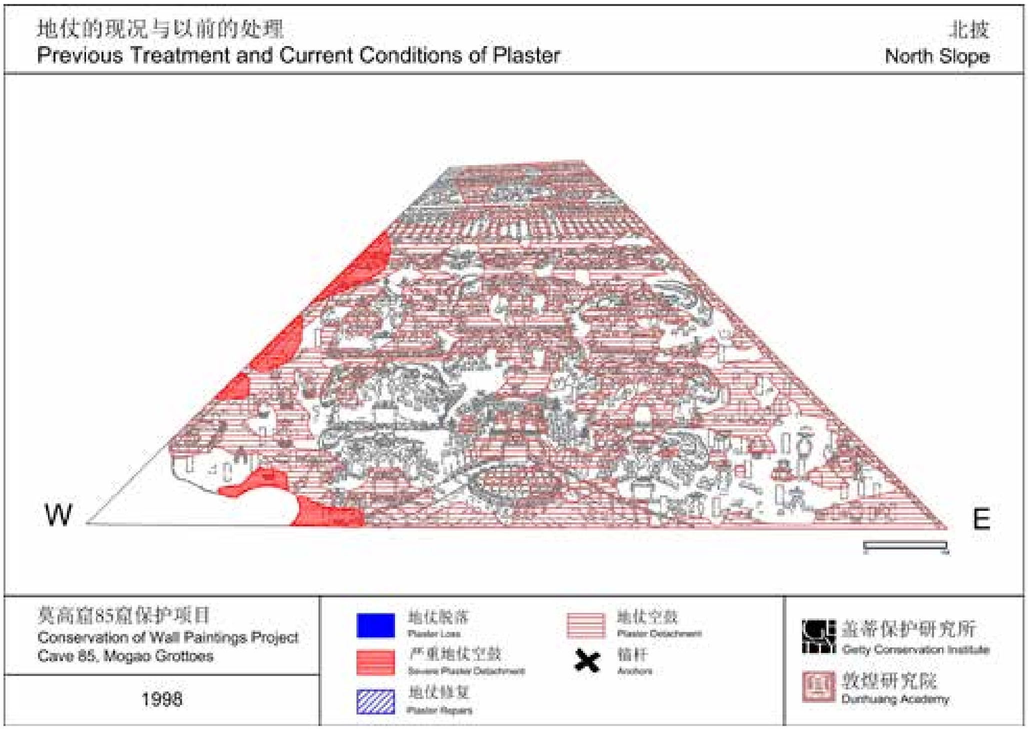
地仗的现况与以前的处理
Previous Treatment and Current Conditions of Plaster
北披
North Slope
W
E
莫高窟85窟保护项目
Conservation of Wall Paintings Project
Cave 85, Mogao Grottoes
1998
地仗脱落
Plaster Loss
严重地仗空鼓
Severe Plaster Detachment
地仗修复
Plaster Repairs
地仗空鼓
Plaster Detachment
锚杆
Anchors
盖蒂保护研究所
Getty Conservation Institute
敦煌研究院
Dunhuang Academy

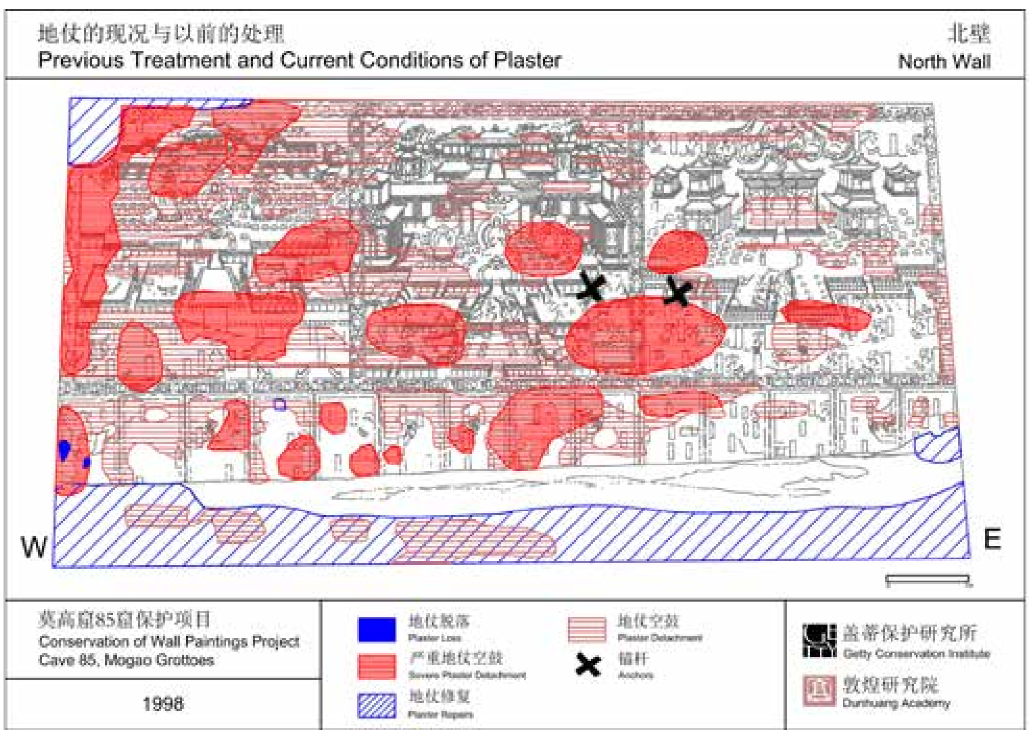
地仗的现况与以前的处理
Previous Treatment and Current Conditions of Plaster
北壁
North Wall
W
E
莫高窟85窟保护项目
Conservation of Wall Paintings Project
Cave 85, Mogao Grottoes
1998
地仗脱落
Plaster Loss
严重地仗空鼓
Severe Plaster Detachment
地仗修复
Plaster Repairs
地仗空鼓
Plaster Detachment
锚杆
Anchors
盖蒂保护研究所
Getty Conservation Institute
敦煌研究院
Dunhuang Academy

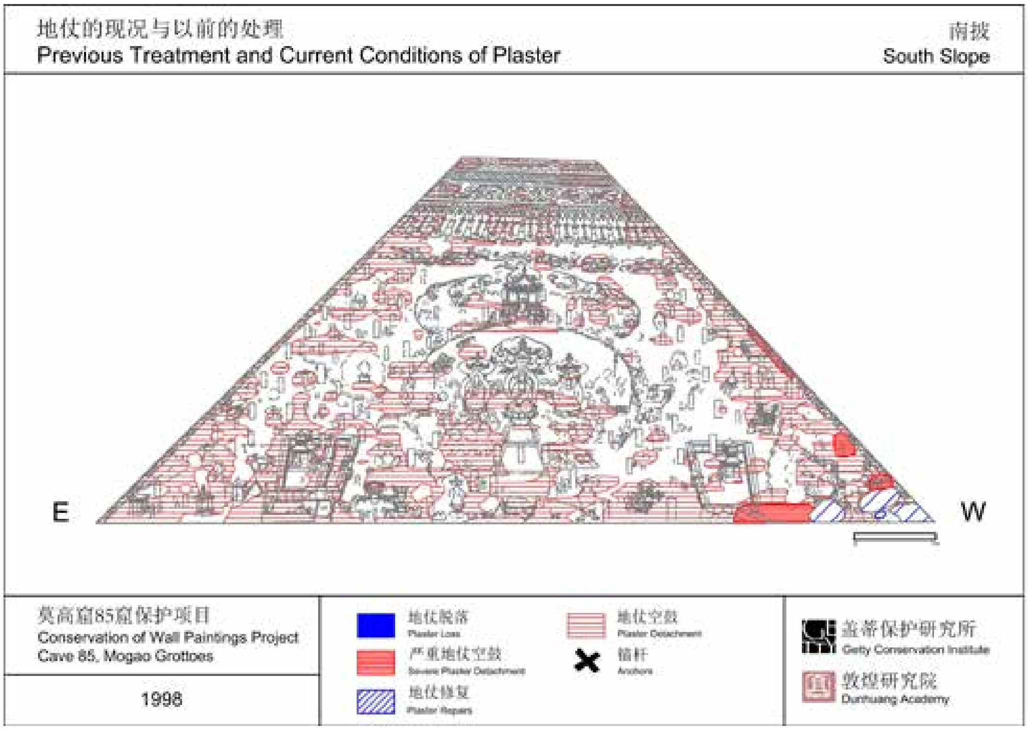
地仗的现况与以前的处理
Previous Treatment and Current Conditions of Plaster
南披
South Slope
E
W
莫高窟85窟保护项目
Conservation of Wall Paintings Project
Cave 85, Mogao Grottoes
1998
地仗脱落
Plaster Loss
严重地仗空鼓
Severe Plaster Detachment
地仗修复
Plaster Repairs
地仗空鼓
Plaster Detachment
锚杆
Anchors
盖蒂保护研究所
Getty Conservation Institute
敦煌研究院
Dunhuang Academy

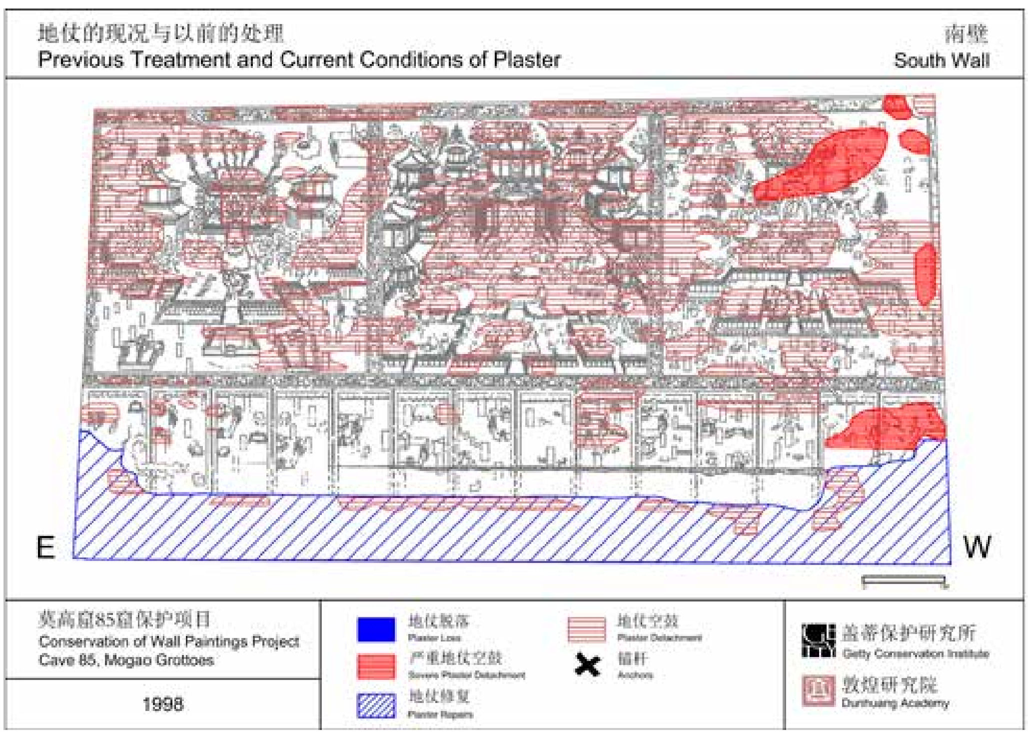
地仗的现况与以前的处理
Previous Treatment and Current Conditions of Plaster
南壁
South Wall
E
W
莫高窟85窟保护项目
Conservation of Wall Paintings Project
Cave 85, Mogao Grottoes
1998
地仗脱落
Plaster Loss
严重地仗空鼓
Severe Plaster Detachment
地仗修复
Plaster Repairs
地仗空鼓
Plaster Detachment
锚杆
Anchors
盖蒂保护研究所
Getty Conservation Institute
敦煌研究院
Dunhuang Academy

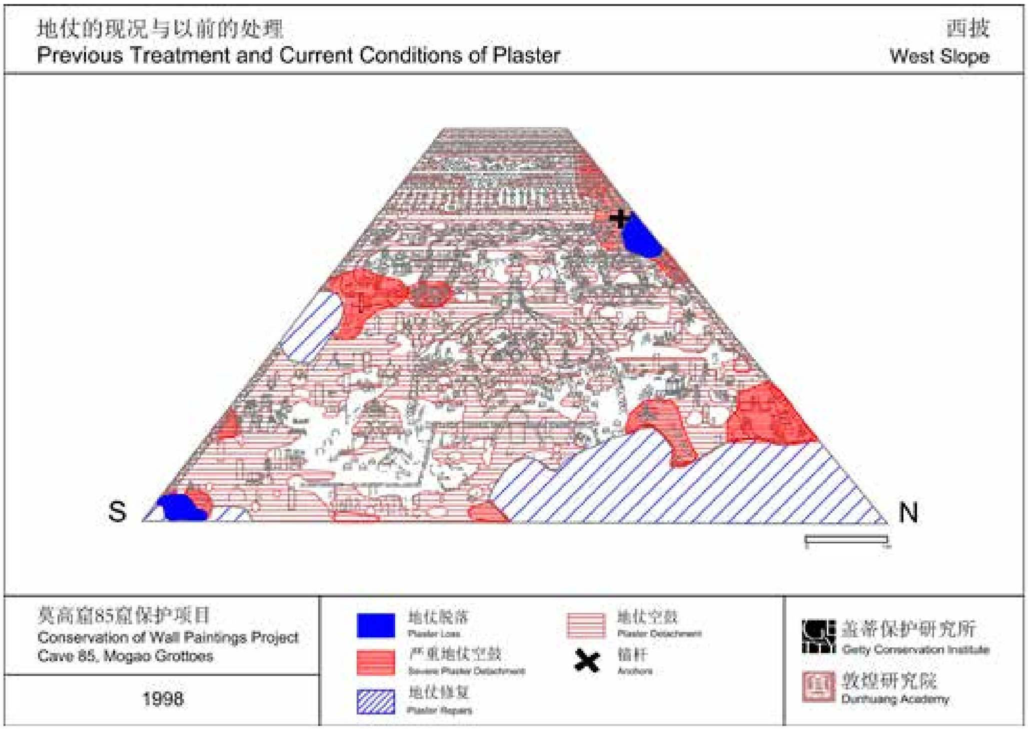

地仗的现况与以前的处理
Previous Treatment and Current Conditions of Plaster
西披
West Slope
S
N
莫高窟85窟保护项目
Conservation of Wall Paintings Project
Cave 85, Mogao Grottoes
1998
地仗脱落
Plaster Loss
严重地仗空鼓
Severe Plaster Detachment
地仗修复
Plaster Repairs
地仗空鼓
Plaster Detachment
锚杆
Anchors
盖蒂保护研究所
Getty Conservation Institute
敦煌研究院
Dunhuang Academy

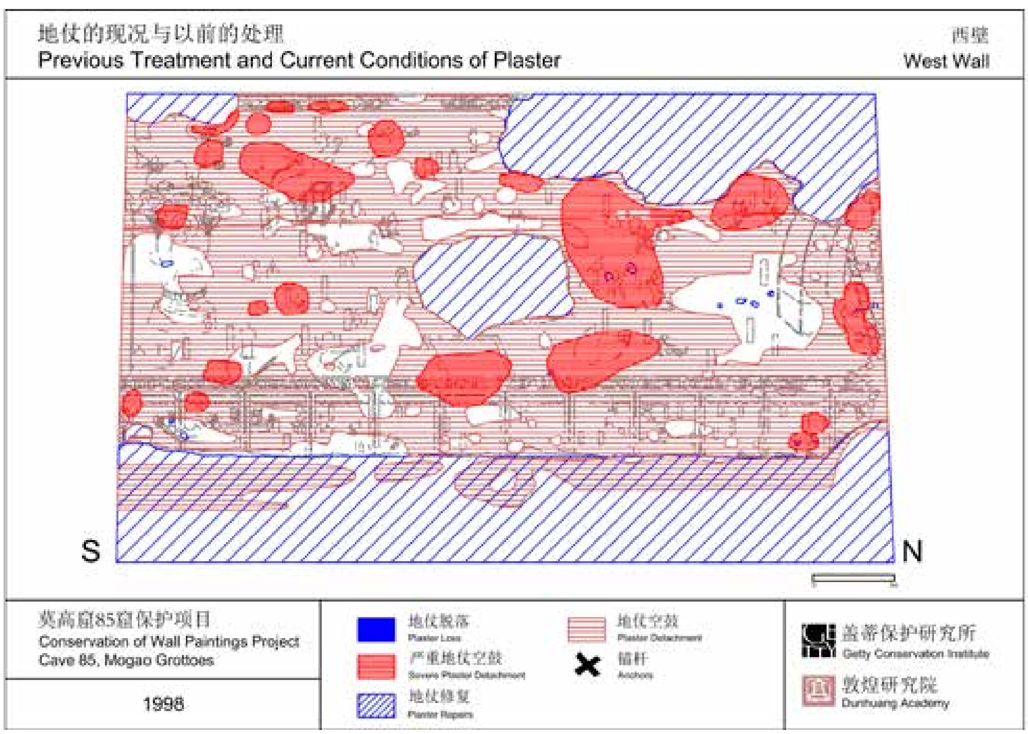

地仗的现况与以前的处理
Previous Treatment and Current Conditions of Plaster
西壁
West Wall
S
N
莫高窟85窟保护项目
Conservation of Wall Paintings Project
Cave 85, Mogao Grottoes
1998
地仗脱落
Plaster Loss
严重地仗空鼓
Severe Plaster Detachment
地仗修复
Plaster Repairs
地仗空鼓
Plaster Detachment
锚杆
Anchors
盖蒂保护研究所
Getty Conservation Institute
敦煌研究院
Dunhuang Academy

APPENDIX 12.C

Illustrated Condition Terminology

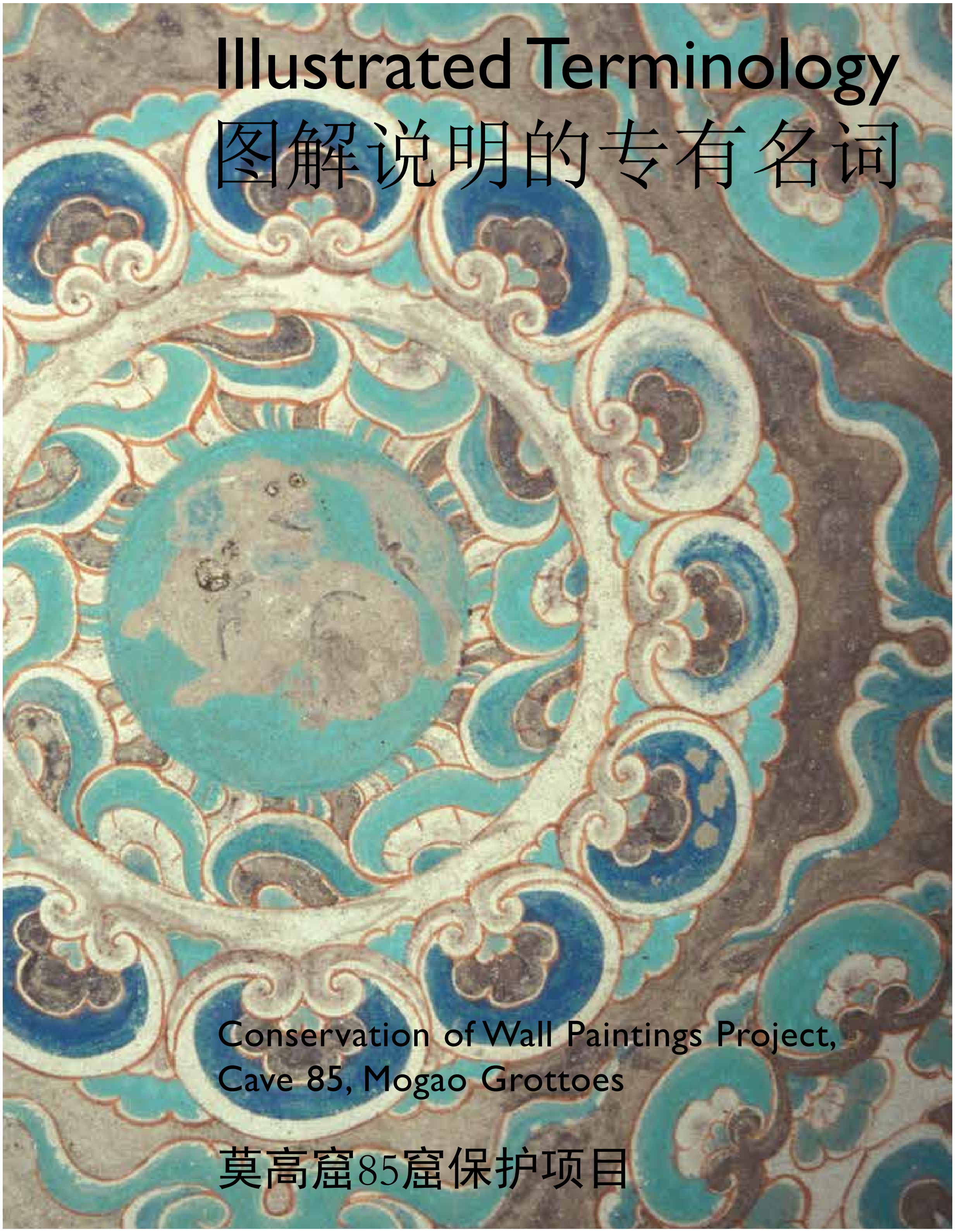

Introduction

The objective of this Illustrated Terminology is to establish a common language for the recording, communication, and interpretation of information generated during the conservation of wall paintings project in Cave 85 at Mogao. The terminology incorporates existing usage by the Dunhuang Academy. A written definition is included for each term. Images and diagrams are included as necessary to further illustrate the written definition. Where appropriate, additional information is provided to expand on the term defined, giving the distribution of condition phenomena within the cave and background to aid in the interpretation of the detailed graphic documentation.

The Cave 85 terminology reflects the specific technique of execution of the Late Tang dynasty paintings and the particular condition phenomena and treatment interventions present in Cave 85. If used in other caves at Mogao and at other sites this terminology should be adapted as necessary.

现状

常见病害名词

Condition

general condition

Cave 85 Definition　85 窟项目定义

deep loss
地仗脱落

Area where the entire stratigraphy is missing through to the conglomerate
壁画所有结构层脱落露出沙砾岩

West slope 西斜披 (XP 4-6)

Cave 85 Definition 85 窟项目定义

plaster detachment
空鼓

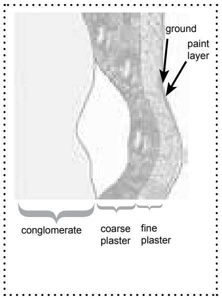

Lack of adhesion between the coarse plaster and the conglomerate
粗泥层与沙砾岩之间粘结力丧失

West slope 西斜披 (XP ?-?)

unstable plaster detachment
严重空鼓

Also referred to as "prioritized detachment"

Detachment where the plaster has lost its overall cohesiveness and is often severely cracked and deformed.
空鼓部分的地仗丧失了整体的内聚力并拌有严重裂缝和变形

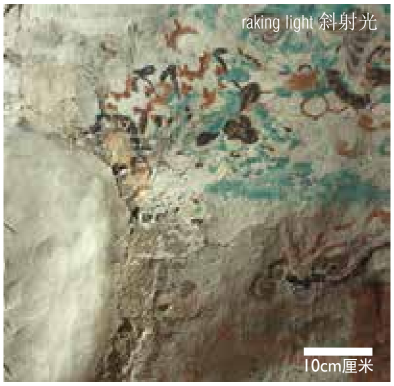

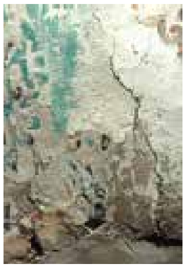

North slope 北斜披 (BP 1-4)

现状

常见病害名词

Condition

general condition

Cave 85 Definition 85 窟项目定义

cracks

裂缝

While most cracks have occurred over time, some resulted as the plaster dried and the paint layer was applied over them (see upper image).

Fissures that occur through any or all of the layers of the painting stratigraphy

穿过壁画结构中任何一层或所有层的裂隙

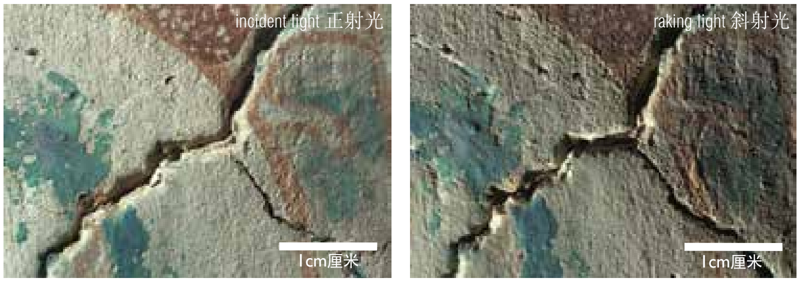

North wall, middle tier 北壁， 中层 (BQ 3-9)

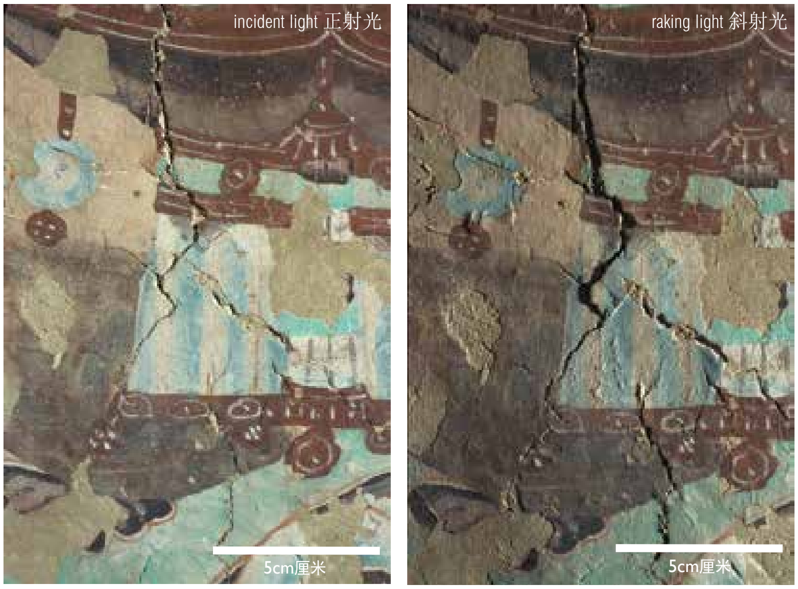

East wall, south side, middle tier 东壁， 南边， 中层 (DP 3-4)

Cave 85 Definition　85 屈项目定义

mechanical damage
机械损伤

Physical harm inflicted on a painting which is either accidental or intentional
无意或有意（如刻画涂写）造成的壁画的物理损伤

West wall, middle tier 西壁，中层 (XQ 3-3)

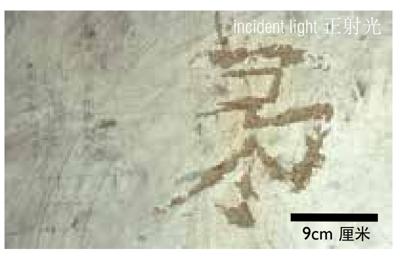

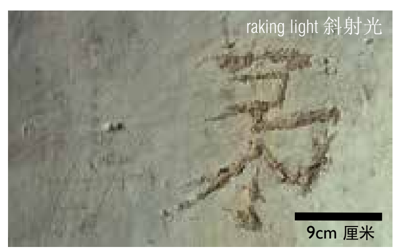

Corridor, North wall (YDBQ 2-3)

现状
常见病害名词

Condition
general condition

Cave 85 Definition 85 窟项目定义

disruption
酥碱

General term used to describe areas of usually salt-related deterioration where the painted plaster exhibits partial loss of cohesion within any or all of the layers.
任何一个或多个结构层内部内聚力部分丧失

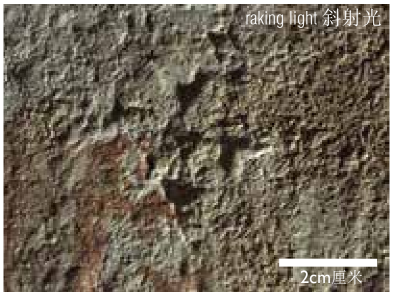

West wall, center 西壁, 中心 (XQ 3-9)

现状
地仗层

Condition
plaster layer

Cave 85 Definition　85窟项目定义

crater eruption & loss
火山口状鼓起与脱落

Bulges (from 0.5cm to 1cm in diameter) in the paint, ground and fine plaster layers leading to crater-shaped losses, containing small $CaSO_4$ inclusions
画层，底色层和细泥层中小范围起鼓（直径0.5至1厘米）导致火山口状的脱落，脱落部分留有硫酸钙硬核

Crater-shaped eruptions and losses (2 mm–1 cm in diameter) are found sporadically around the cave, though in particular on the west slope.

East slope 东斜披 (DP 2-5)

West slope 西斜披 (XP 2-3)

现状
地仗层

Condition
plaster layer

Cave 85 Definition　85 窟项目定义

exfoliation
酥碱起甲

Combined lifting of the paint layer, ground, and some fine plaster associated with the loss of cohesion of the plaster below the paint and ground layers.
画层，底色层和部分地仗起翘

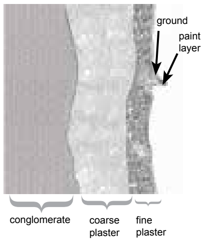

Exfoliation was recorded predominantly on the west end of the main chamber.

South wall 南壁 (NQ 5-13)

现状
粉层

Condition
ground layer

Cave 85 Definition　85 窟项目定义

ground loss
粉层脱落

Recorded as “Remaining areas of ground” to facilitate the manual graphic recording process.

Loss of the ground and paint layers
粉层脱落

East wall, north side 东壁， 北边 (DQ 3-4/DQ 4-4)

现状
粉层

Condition
ground layer

Cave 85 Definition　85 窟项目定义

punctate loss
点状脱落

Punctate losses are found predominantly on the west end of the main chamber. These occur along the base of the walls and are concentrated in areas of attached plaster, eventually leading to total loss of the paint layer and ground in the most extreme situations.

Rounded losses (less than 1mm in diameter) of the paint and ground layer
画层和底色层直径小于1毫米的圆形脱落

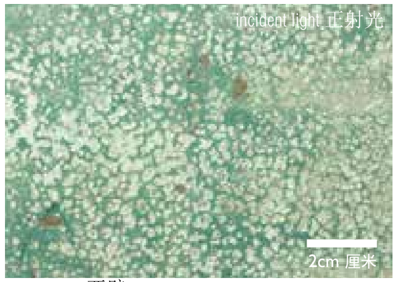

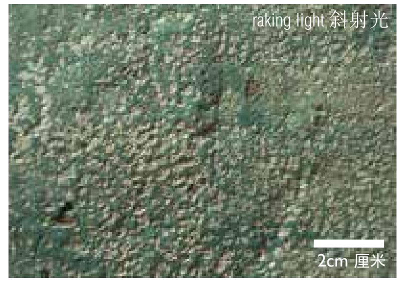

West wall 西壁 (XQ 4-6)

North wall, middle tier 北壁，中层 (BQ 3-8)

现状
画层

Condition
paint layer

Cave 85 Definition　85 窟项目定义

paint loss
画层脱落

Recorded as “Remaining areas of paint” to facilitate the manual graphic recording process.

Loss of the paint layer reveaing the ground below
画层脱落

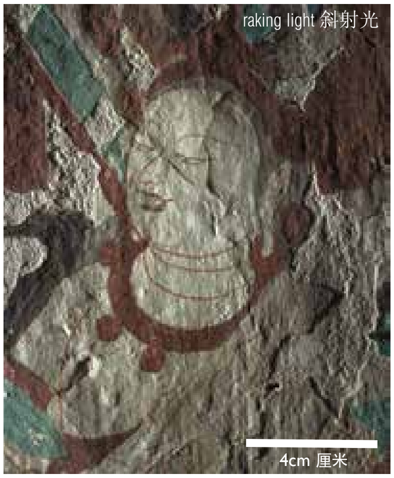

North wall 北壁 (BQ 3-8)

现状
画层

Condition
paint layer

Cave 85 Definition　85 窟项目定义

flaking
起甲

Fracturing and lifting of the ground and/or paint layer(s)
底色层，画层，表面涂层起翘并拌有破损

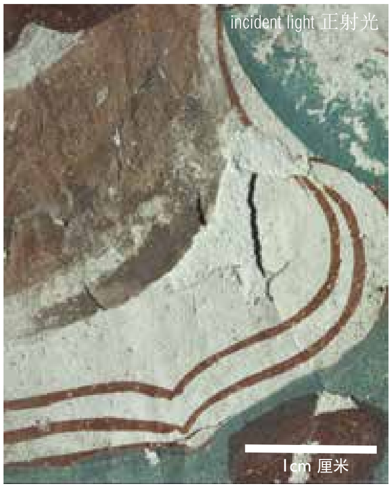

South wall 南壁 (NQ 4-11)

现状
画层

Condition
paint layer

Cave 85 Definition　85 窟项目定义

blistering
泡状起甲

Bubbling deformation and detachment of the ground and/or paint and/or coating layer(s) leading to loss.
底色层，画层，表面涂层气泡变形导致脱落

Loss of paint due to this type of deterioration is documented separately as “Blistering loss” in the manual graphic documentation.

This phenomenon occurs mainly on the cave ceiling.

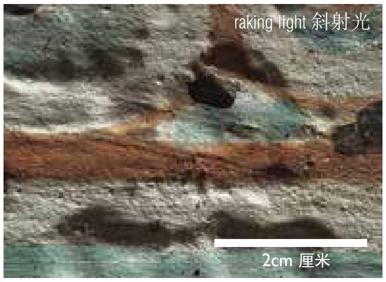

Ceiling, West panel (JXXB 1/JXXB 2)

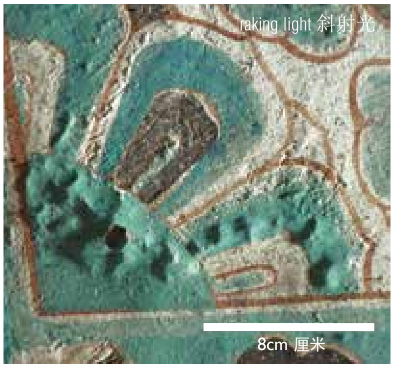

Ceiling, northwest corner (JX 1)

现状
画层

Condition
paint layer

Cave 85 Definition　85 窟项目定义

pigment alteration/ colorant fading
颜料变色/

Alteration of mineral pigments or fading of organic colorants

South slope 南斜披 (NP 2-3)

West slope 西斜披 (XP 5-2)

East slope 东斜披 (DP 5-2)

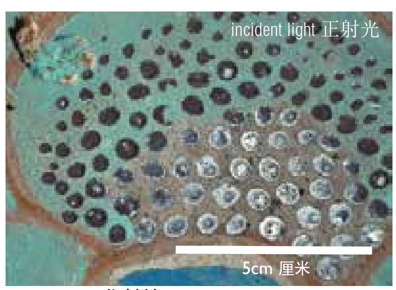

North slope 北斜披 (BP 4-5)

Cave 85 Definition 85 窟项目定义

insect excreta
昆虫排泄物

Black, shiny expelled waste material of an insect
昆虫黑色有光泽排泄物

South slope 南斜披 (NP-23)

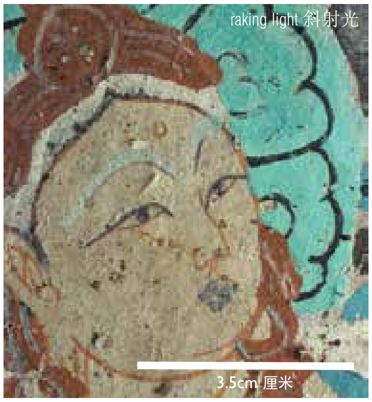

East slope 东斜披 (DP 1-6)

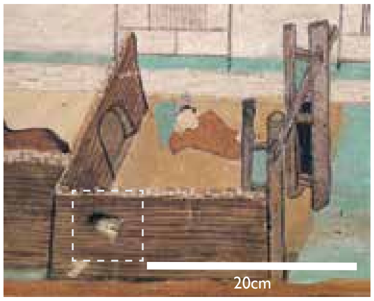

South slope 南斜披 (NP1-4)

APPENDIX 12.D

Graphic Documentation: Sculpture and Altar Platform Condition

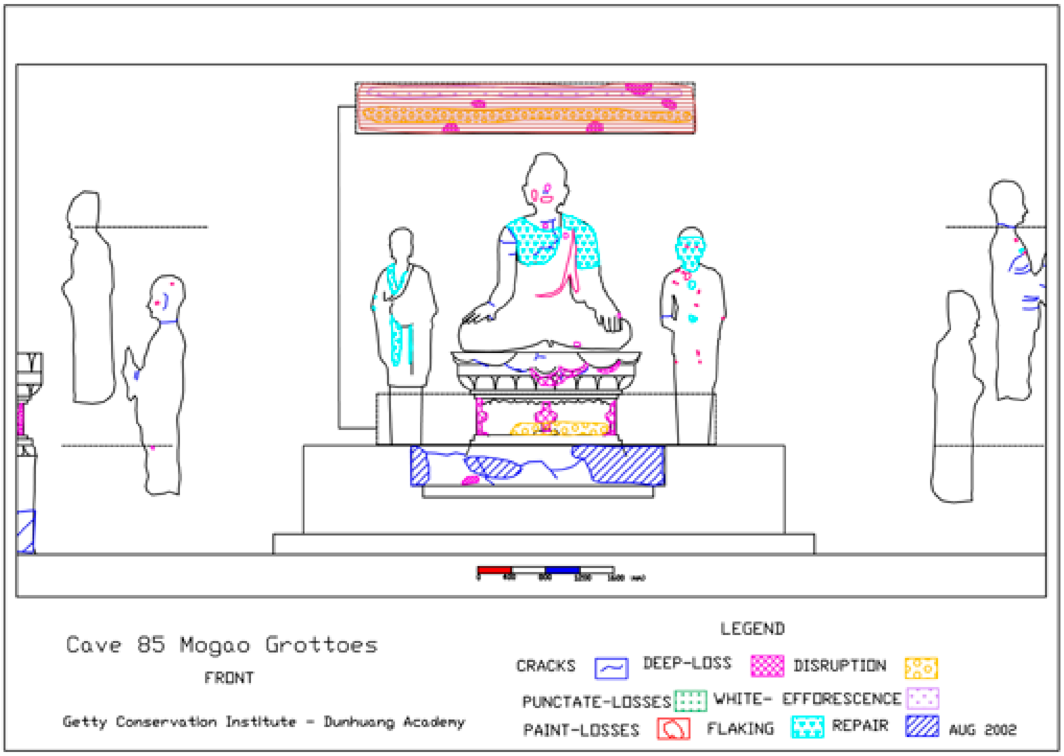

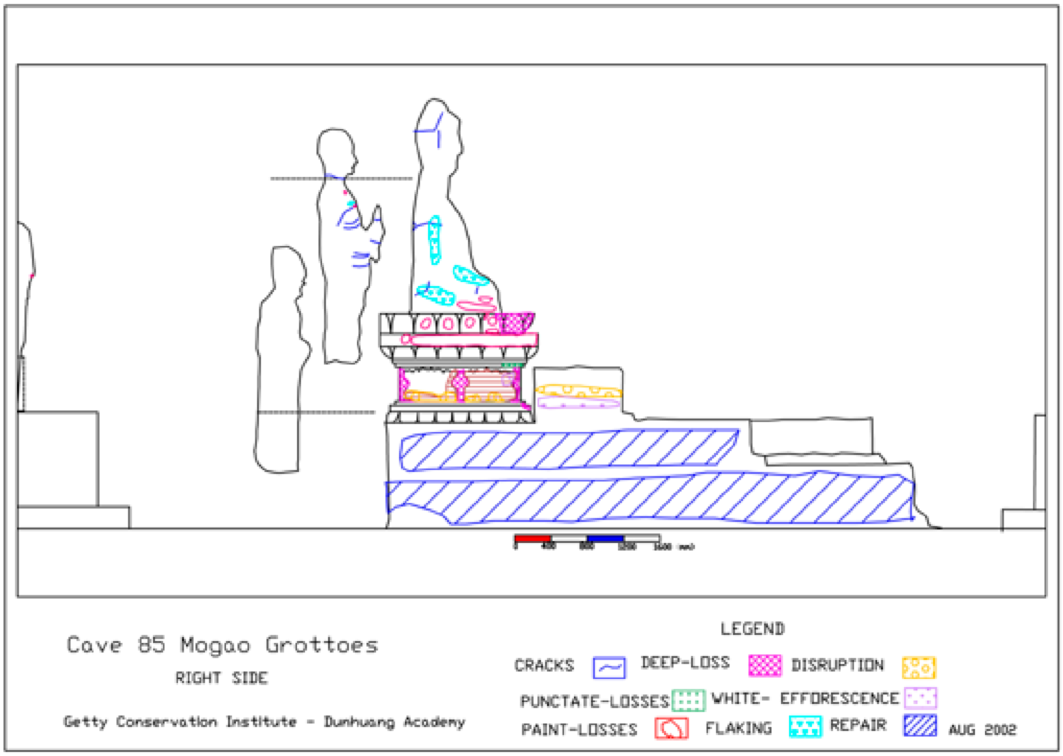

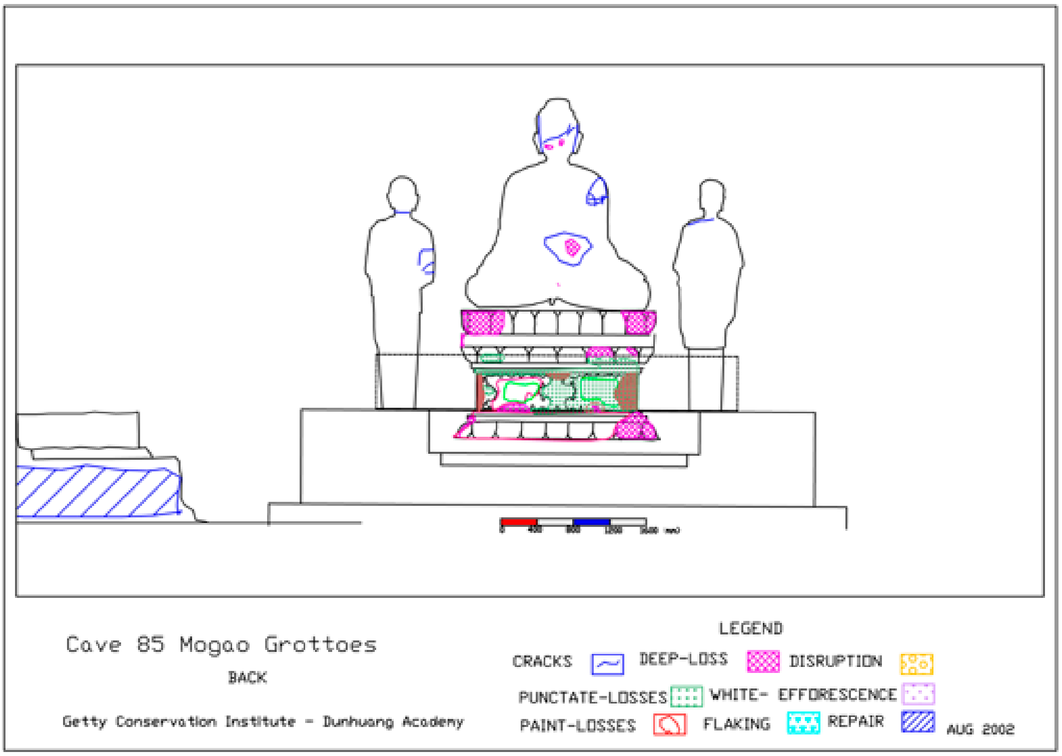
LEGEND
Cave 85 Mogao Grottoes
BACK
CRACKS
DEEP-LOSS
DISRUPTION
PUNCTATE-LOSSES
WHITE- EFFORESCENCE
Getty Conservation Institute - Dunhuang Academy
PAINT-LOSSES
FLAKING
REPAIR
AUG 2002

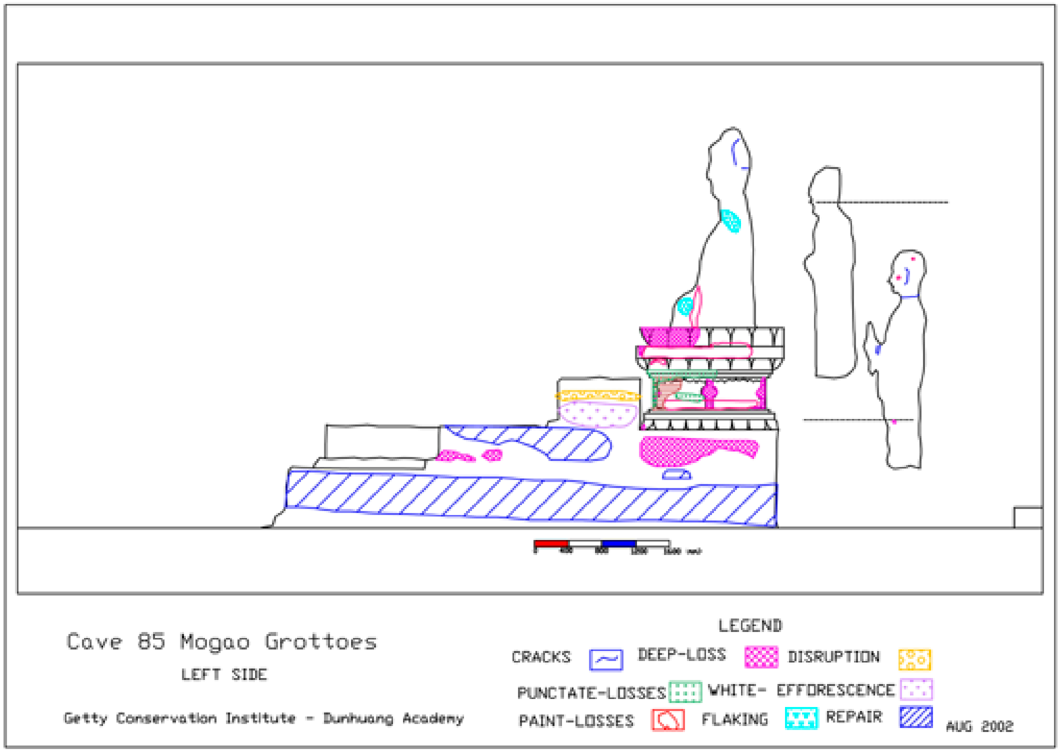
LEGEND
Cave 85 Mogao Grottoes
LEFT SIDE
CRACKS
DEEP-LOSS
DISRUPTION
PUNCTATE-LOSSES
WHITE- EFFORESCENCE
Getty Conservation Institute - Dunhuang Academy
PAINT-LOSSES
FLAKING
REPAIR
AUG 2002

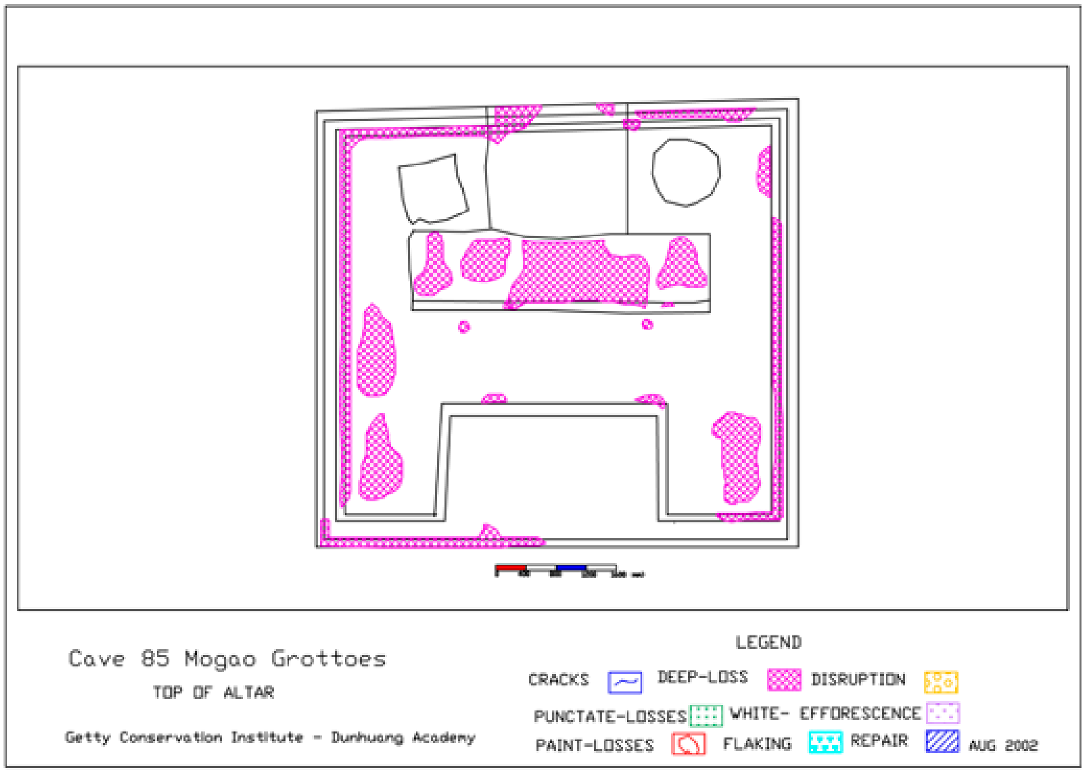
Cave 85 Mogao Grottoes
TOP OF ALTAR
Getty Conservation Institute - Dunhuang Academy
LEGEND
CRACKS
DEEP-LOSS
DISRUPTION
PUNCTATE-LOSSES
WHITE- EFFORESCENCE
PAINT-LOSSES
FLAKING
REPAIR
AUG 2002

APPENDIX 13.A

Literary Evidence of the Use of Organic Colorants in Chinese Painting during the Tang Dynasty at Mogao

There is a considerable amount of literary evidence to support the use of organic colorants in Chinese painting during the Tang dynasty. The Tang dynasty writer Zhang Yanyuan refers to the use of "ant ore," which is almost certainly the red organic colorant lac (*Coccus laccal;* Pinyin: *chong jiao*). This was produced beyond China's southwestern borders and is known to have been imported into the country from an early date (Yu 1988, 12). Safflower (*Carthamus tinctorius;* Pinyin: *hong-hua/honglanhua*), also widely used, produced an orange-red colorant when treated with an alkali (Gettens and Stout [1942] 1966, 154). Its use at Mogao has been documented in Library Cave documents, which record donors offering "honglan" for use in the decoration of the caves.[1] Madder (*Rubia tinctorum/ Rubia cordifolia;* Pinyin: *qian cao*) grew wild across northwestern China, from which a rich pink dye was extracted (Yu 1988, 11). These three plant dyes were the most common components in the preparation of "rouge," which was used both as a cosmetic and as a painting material (Yu 1988, 12). Such compounds are known to have been available at Mogao, through the presentation of "eight jins of good quality rouge" from a Dunhuang military commander to a local Uighur chief, documented in Library Cave documents.[2] Logwood (synonym: sappanwood; *Caesalpinia sappan;* Pinyin: *su mu*) produced a purple-red dye (Li 1948, 141; Ye et al. 2000, 248; Yu 1988, 13), and a further purple dye was extracted from gromwell (*Lithospermum erythrorhizon;* Pinyin: *zi cao*) (Ye et al. 2000, 246).

Numerous yellow dyes were available to Tang dynasty artists. Safflower produced not only a red dye but also a golden yellow when prepared on an alum mordant (Yu 1988, 11). One of the yellow colorants on the Tang dynasty Diamond Sutra has been identified as amur corkwood (*Phellodendron amurense;* Pinyin: *huang bai*), a bright yellow bark extract originating in Sichuan Province (Bell et al. 2000, 234). Rattan (synonym: gamboge; *Garcinia hamburyi/Garcinia Morella;* Pinyin: *teng huang*), a colorant indigenous to India, Sri Lanka, and Thailand, was known to have been imported to China before the Tang dynasty (Gettens and Stout [1942] 1966, 114–15; Yu 1988, 13). The pagoda tree (*Sophora japonica;* Pinyin: *huai hua*), known to have been in cultivation from the fifth century, yielded a yellow dye that was used with malachite for the specific purpose of improving its adhesion (Ippolito 1985, 89–90; Li 1948, 141). According to the Yuan dynasty author Li Kan, two separate decoctions were prepared from its buds and the petals and used to add luster to different grindings of the pigment. Other available organic yellows include gardenia seed extracts (*Gardenia jasminoides;* Pinyin: *zhizi*) (Yu 1988, 14; Ye et al. 2000, 246).

Notes

1. Wang Jinyu, Dunhuang Academy, pers. comm.
2. Wang Jinyu, Dunhuang Academy, pers. comm.

APPENDIX 13.B

Graphic Documentation: Sampling Locations

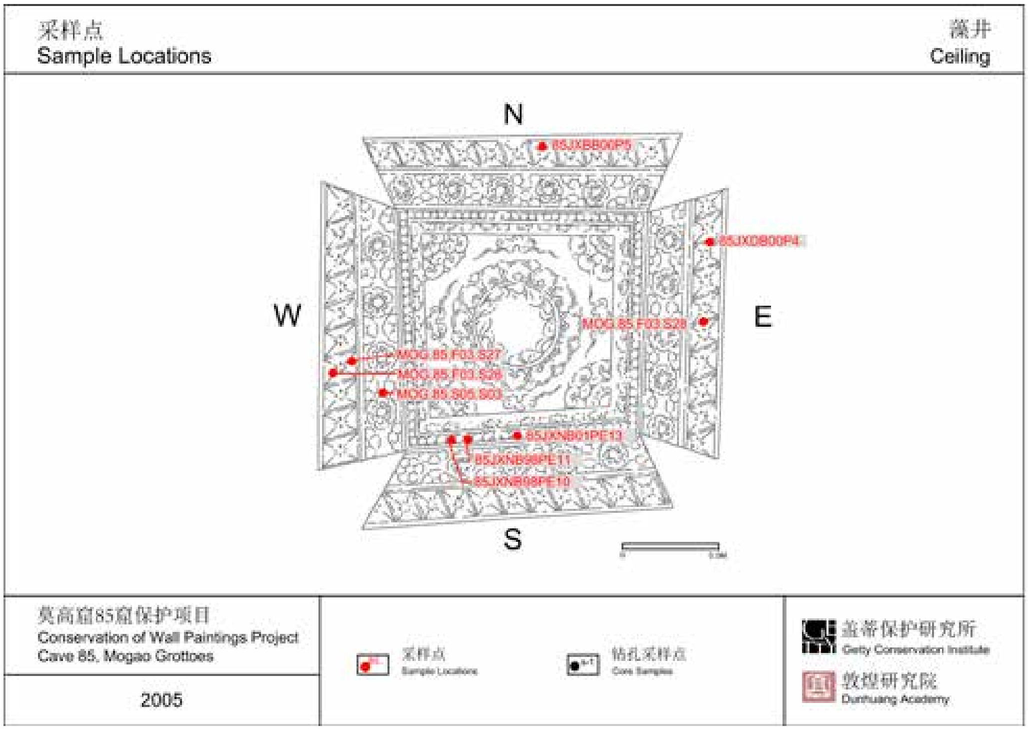

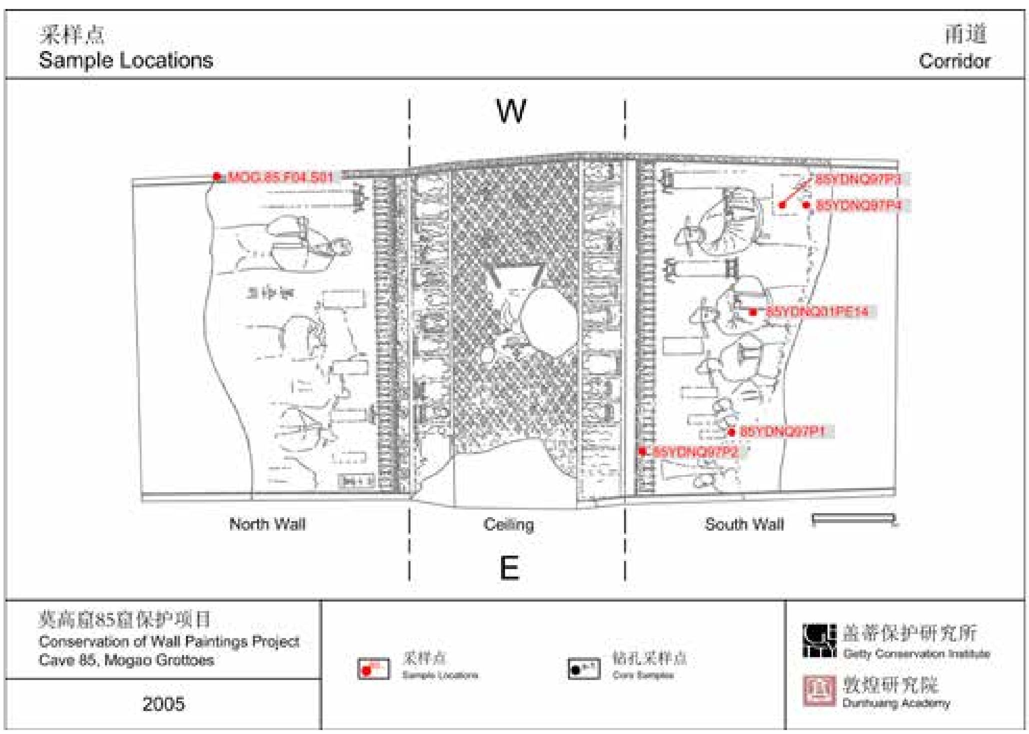

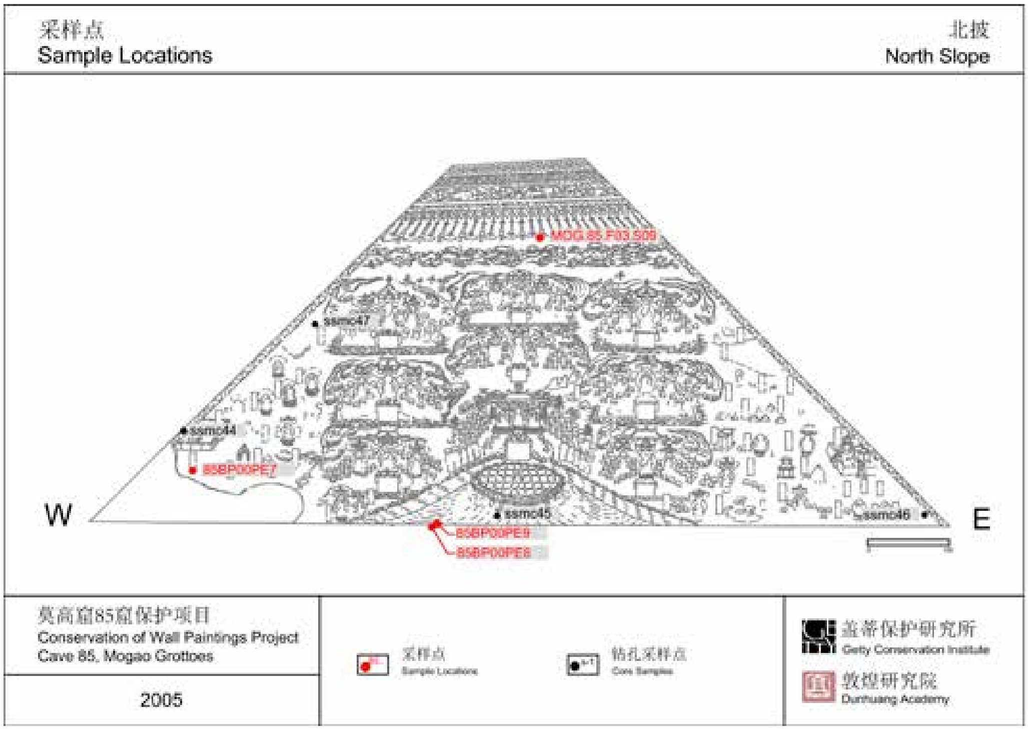

采样点
Sample Locations
北披
North Slope
MOG.85.F03.S09
ssmc47
ssmc44
85BP00PE7
W
ssmc45
ssmc46
E
85BP00PE9
85BP00PE8
莫高窟85窟保护项目
Conservation of Wall Paintings Project
Cave 85, Mogao Grottoes
2005
采样点
Sample Locations
钻孔采样点
Core Samples
盖蒂保护研究所
Getty Conservation Institute
敦煌研究院
Dunhuang Academy

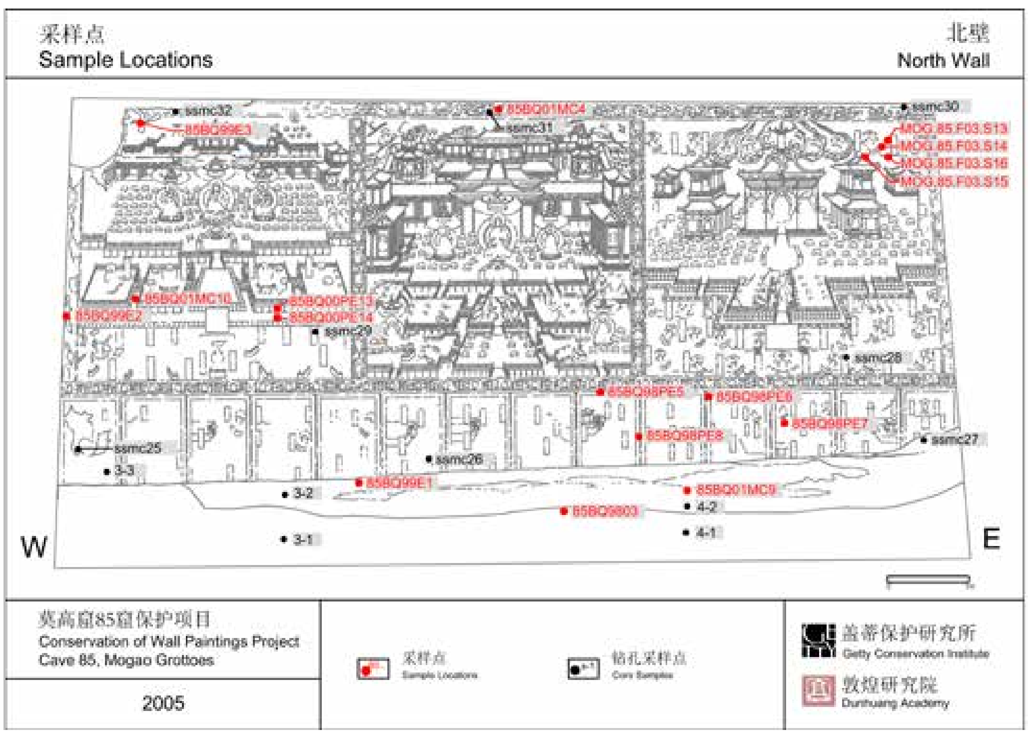

采样点
Sample Locations
北壁
North Wall
ssmc32
85BQ99E3
85BQ01MC4
ssmc31
ssmc30
MOG.85.F03.S13
MOG.85.F03.S14
MOG.85.F03.S16
MOG.85.F03.S15
85BQ01MC10
85BQ00PE13
85BQ00PE14
85BQ99E2
ssmc29
ssmc28
85BQ98PE5
85BQ98PE6
85BQ98PE7
85BQ98PE8
ssmc27
ssmc25
3-3
ssmc26
3-2
85BQ99E1
85BQ01MC9
85BQ9803
4-2
3-1
4-1
W
E
莫高窟85窟保护项目
Conservation of Wall Paintings Project
Cave 85, Mogao Grottoes
2005
采样点
Sample Locations
钻孔采样点
Core Samples
盖蒂保护研究所
Getty Conservation Institute
敦煌研究院
Dunhuang Academy

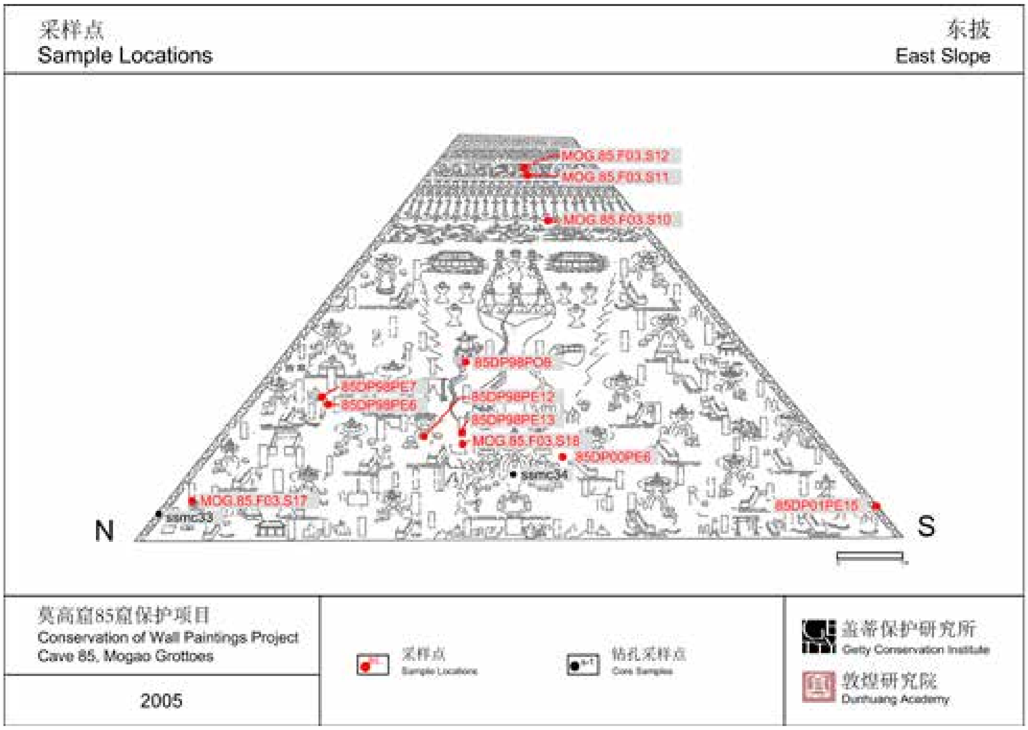

采样点
Sample Locations
东披
East Slope
MOG.85.F03.S12
MOG.85.F03.S11
MOG.85.F03.S10
85DP98PO8
85DP98PE7
85DP98PE6
85DP98PE12
85DP98PE13
MOG.85.F03.S18
85DP00PE6
ssmc34
MOG.85.F03.S17
ssmc33
85DP01PE15
N
S
莫高窟85窟保护项目
Conservation of Wall Paintings Project
Cave 85, Mogao Grottoes
2005
采样点
Sample Locations
钻孔采样点
Core Samples
盖蒂保护研究所
Getty Conservation Institute
敦煌研究院
Dunhuang Academy

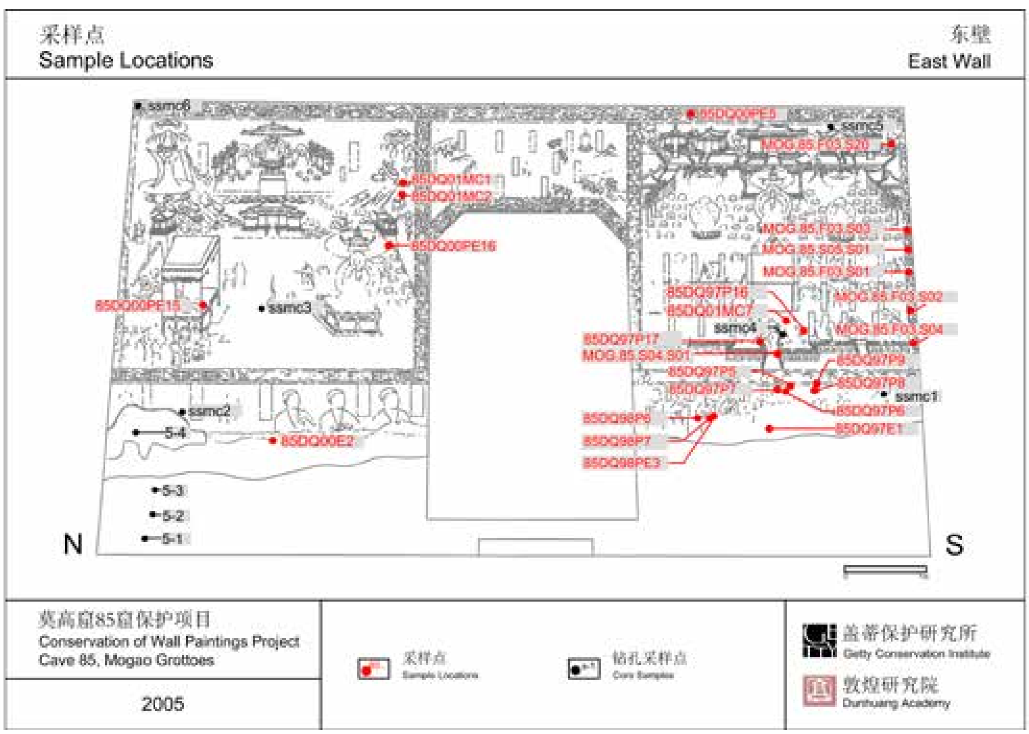

采样点
Sample Locations
东壁
East Wall
ssmc6
85DQ00PE5
ssmc5
MOG.85.F03.S20
85DQ01MC1
85DQ01MC2
85DQ00PE16
MOG.85.F03.S03
MOG.85.S05.S01
MOG.85.F03.S01
85DQ97P16
85DQ01MC7
MOG.85.F03.S02
85DQ00PE15
ssmc3
ssmc4
MOG.85.F03.S04
85DQ97P17
MOG.85.S04.S01
85DQ97P9
85DQ97P5
85DQ97P8
85DQ97P7
ssmc1
85DQ97P6
ssmc2
5-4
85DQ00E2
85DQ98P6
85DQ97E1
85DQ98P7
85DQ98PE3
5-3
5-2
5-1
N
S
莫高窟85窟保护项目
Conservation of Wall Paintings Project
Cave 85, Mogao Grottoes
2005
采样点
Sample Locations
钻孔采样点
Core Samples
盖蒂保护研究所
Getty Conservation Institute
敦煌研究院
Dunhuang Academy

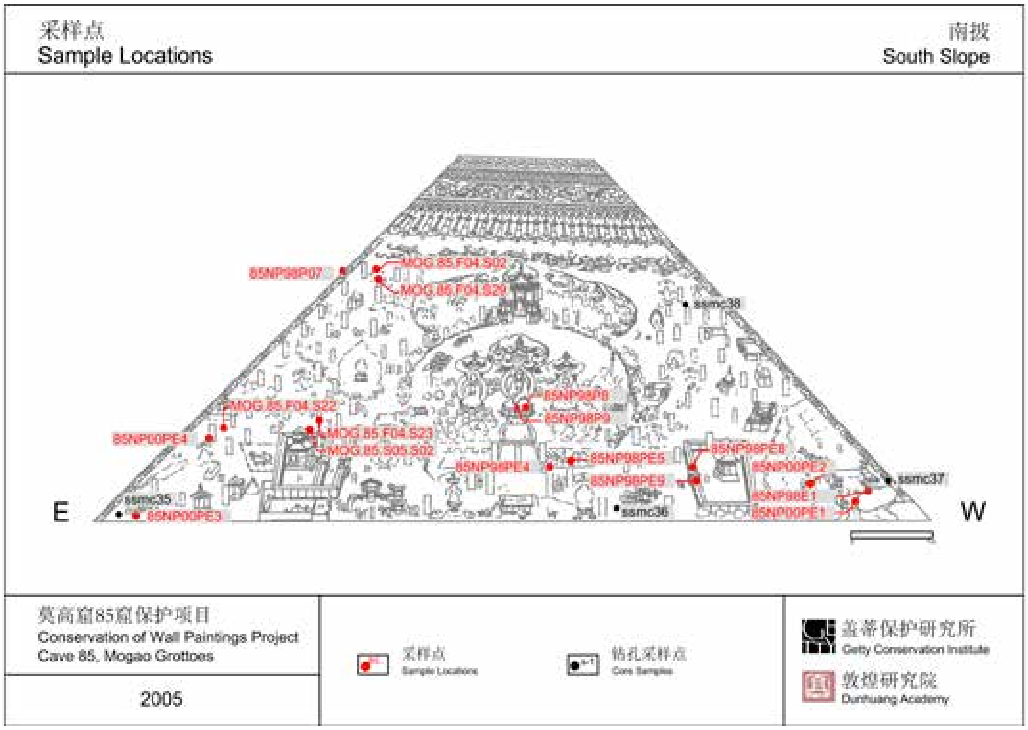
采样点
Sample Locations
南披
South Slope
85NP98P07
MOG.85.F04.S02
MOG.85.F04.S29
ssmc38
85NP98P8
85NP98P9
MOG.85.F04.S22
85NP00PE4
MOG.85.F04.S23
MOG.85.S05.S02
85NP98PE4
85NP98PE5
85NP98PE8
85NP00PE2
85NP98PE9
ssmc37
85NP98E1
85NP00PE1
ssmc35
85NP00PE3
ssmc36
E
W
莫高窟85窟保护项目
Conservation of Wall Paintings Project
Cave 85, Mogao Grottoes
2005
采样点
Sample Locations
钻孔采样点
Core Samples
盖蒂保护研究所
Getty Conservation Institute
敦煌研究院
Dunhuang Academy

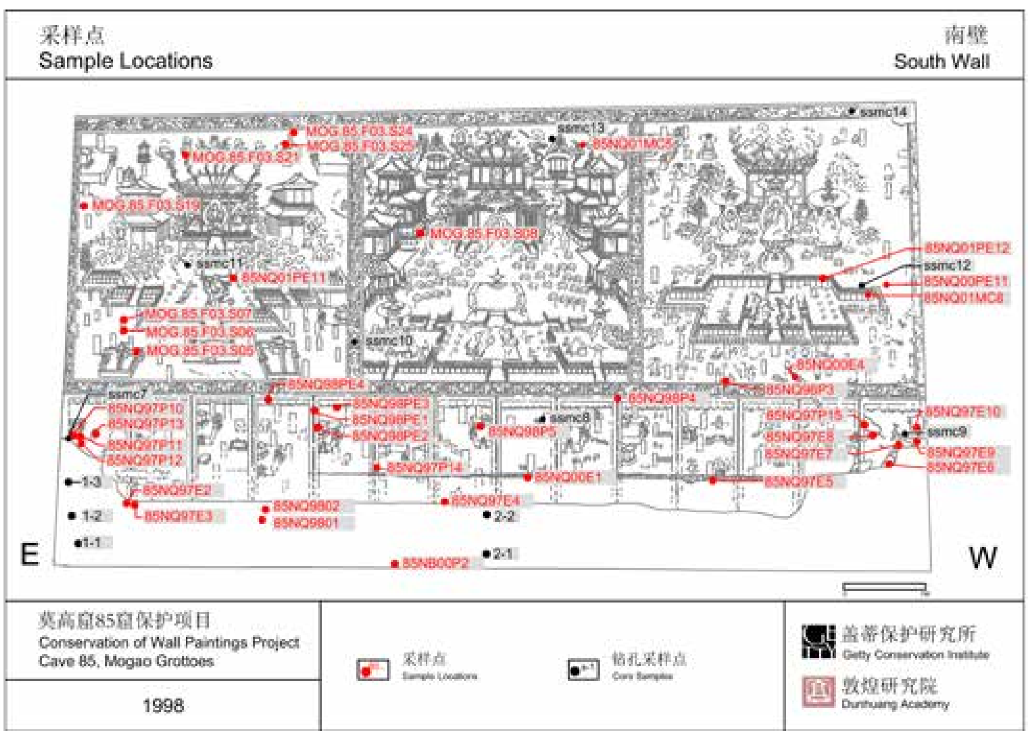
采样点
Sample Locations
南壁
South Wall
ssmc14
MOG.85.F03.S24
MOG.85.F03.S25
ssmc13
85NQ01MC8
MOG.85.F03.S21
MOG.85.F03.S19
MOG.85.F03.S08
85NQ01PE12
ssmc11
85NQ01PE11
ssmc12
85NQ00PE11
85NQ01MC8
MOG.85.F03.S07
MOG.85.F03.S06
MOG.85.F03.S05
ssmc10
85NQ00E4
ssmc7
85NQ98PE4
85NQ98P3
85NQ97P10
85NQ98PE3
85NQ98P4
85NQ97E10
85NQ97P13
85NQ98PE1
ssmc8
85NQ97P15
ssmc9
85NQ97P11
85NQ98PE2
85NQ98P5
85NQ97E8
85NQ97P12
85NQ97E7
85NQ97E9
85NQ97P14
85NQ97E6
1-3
85NQ97E2
85NQ00E1
85NQ97E5
85NQ9802
85NQ97E4
1-2
85NQ97E3
85NQ9801
2-2
1-1
E
2-1
W
85NB00P2
莫高窟85窟保护项目
Conservation of Wall Paintings Project
Cave 85, Mogao Grottoes
1998
采样点
Sample Locations
钻孔采样点
Core Samples
盖蒂保护研究所
Getty Conservation Institute
敦煌研究院
Dunhuang Academy

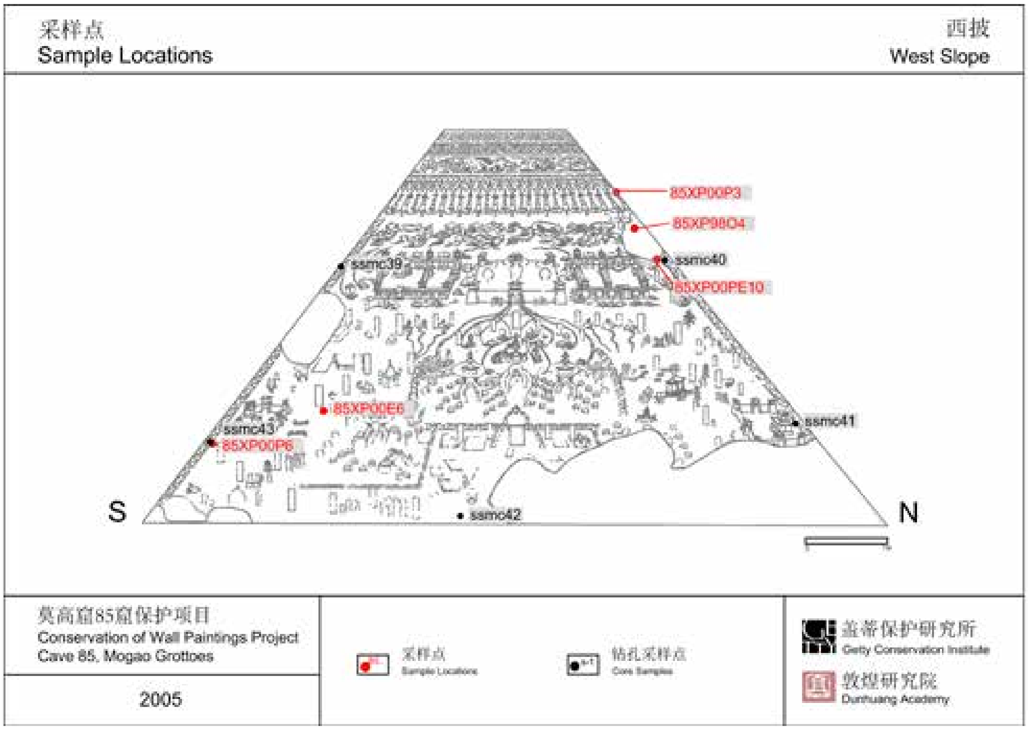
采样点
Sample Locations
西披
West Slope
85XP00P3
85XP98O4
ssmc39
ssmc40
85XP00PE10
85XP00E6
ssmc43
85XP00P6
ssmc41
S
N
ssmc42
莫高窟85窟保护项目
Conservation of Wall Paintings Project
Cave 85, Mogao Grottoes
2005
采样点
Sample Locations
钻孔采样点
Core Samples
盖蒂保护研究所
Getty Conservation Institute
敦煌研究院
Dunhuang Academy

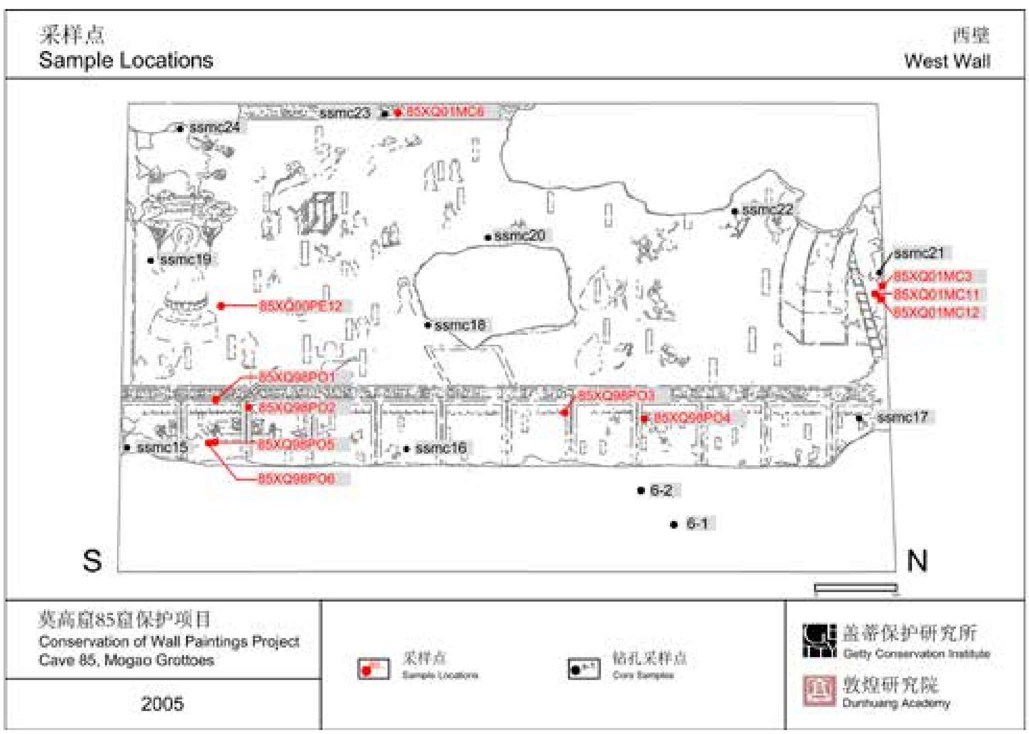
采样点
Sample Locations
西壁
West Wall
ssmc23
85XQ01MC6
ssmc24
ssmc22
ssmc20
ssmc21
ssmc19
85XQ01MC3
85XQ01MC11
85XQ01MC12
85XQ00PE12
ssmc18
85XQ98PO1
85XQ98PO3
85XQ98PO2
85XQ98PO4
ssmc17
ssmc15
85XQ98PO5
ssmc16
85XQ98PO6
6-2
6-1
S
N
莫高窟85窟保护项目
Conservation of Wall Paintings Project
Cave 85, Mogao Grottoes
2005
采样点
Sample Locations
钻孔采样点
Core Samples
盖蒂保护研究所
Getty Conservation Institute
敦煌研究院
Dunhuang Academy

APPENDIX 14.A

Psychrometry and Psychrometric Chart

While it can be applied to any gas-vapor system, psychrometry is most commonly employed to examine mixtures of water vapor and air. It describes the processes that air containing water vapor undergoes as a function of temperature at a specified atmospheric pressure. Air in normal situations contains a water vapor component. The ratio of the two for a given air mass can be specifically described by such variables as temperature, relative humidity, and humidity ratio.

A visual depiction of the psychrometric processes of moist air is provided by what is known as a psychrometric chart. Printed for a specific barometric pressure (to account for changes in air density), the graph relates thermophysical properties of an air mass. The properties typically included are

- Dry-bulb temperature (x-axis in units of °C): temperature recorded by a typical thermometer.
- Humidity ratio (y-axis in units of g of water/kg of dry air): measures actual moisture content in air; also known as absolute humidity, specific humidity, moisture content, or mixing ratio.
- Relative humidity (lines curving upward from right to left in units of %): the percent ratio of water vapor pressure to the vapor pressure of air saturated with water vapor at a given temperature and pressure.

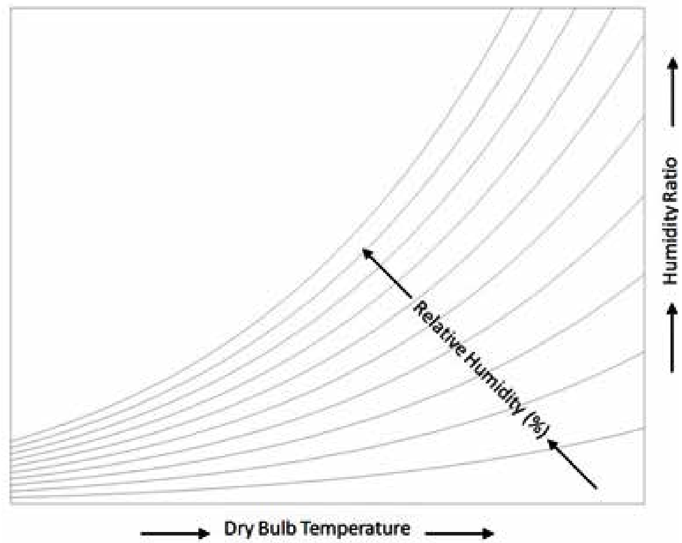

Fig. 1 Simplified form of a psychrometric chart depicting axis for dry bulb temperature and humidity ratio as well as indicator lines for relative humidity.

APPENDIX 14.B

Description of Air Change (ACH) Rate Measurements

There are several ways to measure the air change rate of enclosures such as display cases, rooms, buildings, caves, and tombs. The method used at the Mogao Grottoes was the tracer gas dilution method. In this technique a tracer gas, such as sulfur hexafluoride (SF_6) or carbon dioxide (CO_2), is released in a cave, and the rate of its dilution as a result of the infiltration of the outside air is measured using a trace gas analyzer designed specifically for the gas. The concentration of the tracer gas is recorded as a function of the time from the start of the measurement, t_0. Time for the original concentration of tracer gas, CO_2 to reach half its starting value, 0.5^*C_0, is called the "half-time." This presupposes perfect mixing of air in the cave. This is the time, usually measured in hours, for one air change. After two air changes the tracer gas concentration will be reduced to one quarter that of CO_2; after three air changes, to one-eighth, and so on.

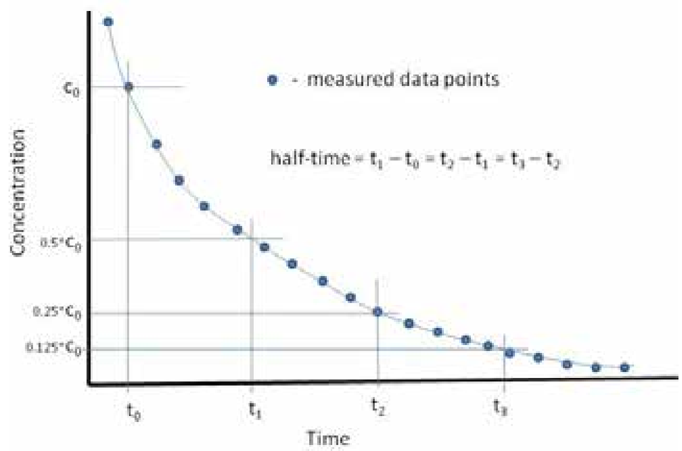

Fig. 1 The concentration of the tracer gas is measured as a function of time.

The air change rate is normally expressed as the number of half-times occurring in one hour. There is no single fixed value for a cave's ACH. The range of ACH values for a particular cave depends on whether the entrance doors are open or closed; the temperature difference between exterior and interior; exterior wind speed and direction; and cave characteristics such as size, architectural configuration, and area of door opening. The ACH value can vary within a day and from day to day. Thus a range of values is always found. ACH values drop markedly when cave doors are closed or when visitors block the entryway.

Prior to 2007, ACH rate measurements were conducted with CO_2 as a tracer gas due to the availability of CO_2 monitors at the Mogao Grottoes. Although CO_2 provided reasonable measurement accuracy, it is a constituent (approximately 350 parts per million) of normal air and limits measurements to vacant caves because of safety concerns for those inside as its safety limit is 5,000 ppm. In 2007 a trace gas analyzer for SF_6 gas was used. Its advantages were that it requires a minute amount (less than 1 ppm) of SF_6 for each measurement; unlike CO_2, SF_6 gas is not a constituent of air, and being chemically inert, its permissible exposure limit for human safety is 1,000 ppm. The analyzer allowed the ACH rate measurement of a large number of large caves with and without visitors.

APPENDIX 16.A

Salt Investigation: Chloride and Sulfate Content of Conglomerate

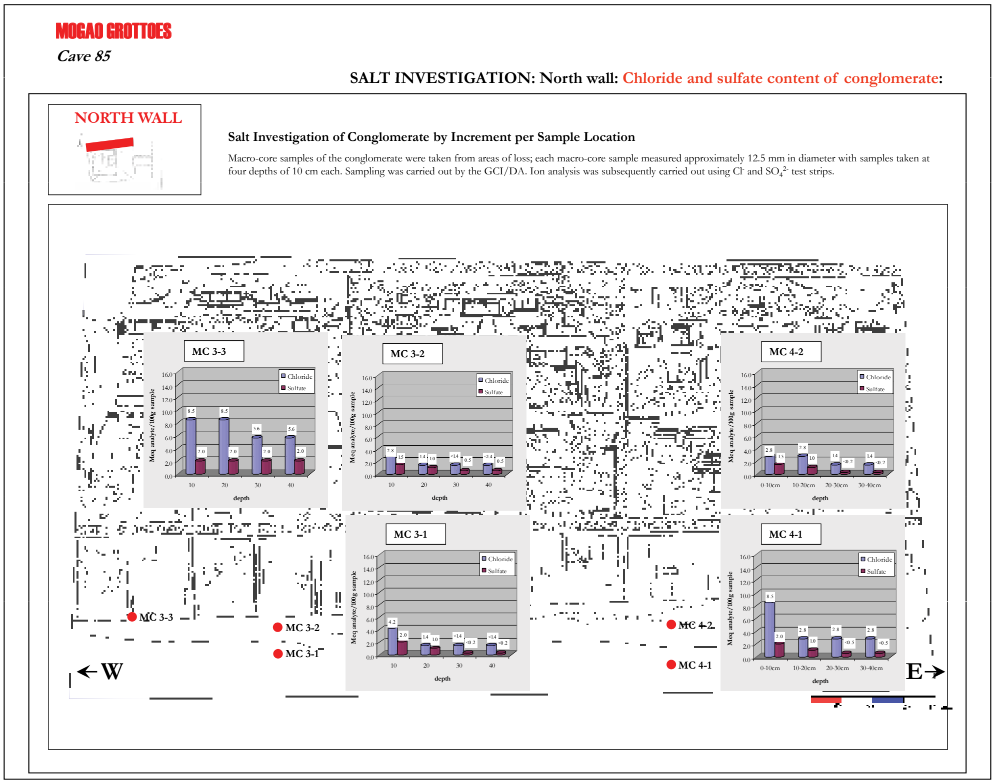

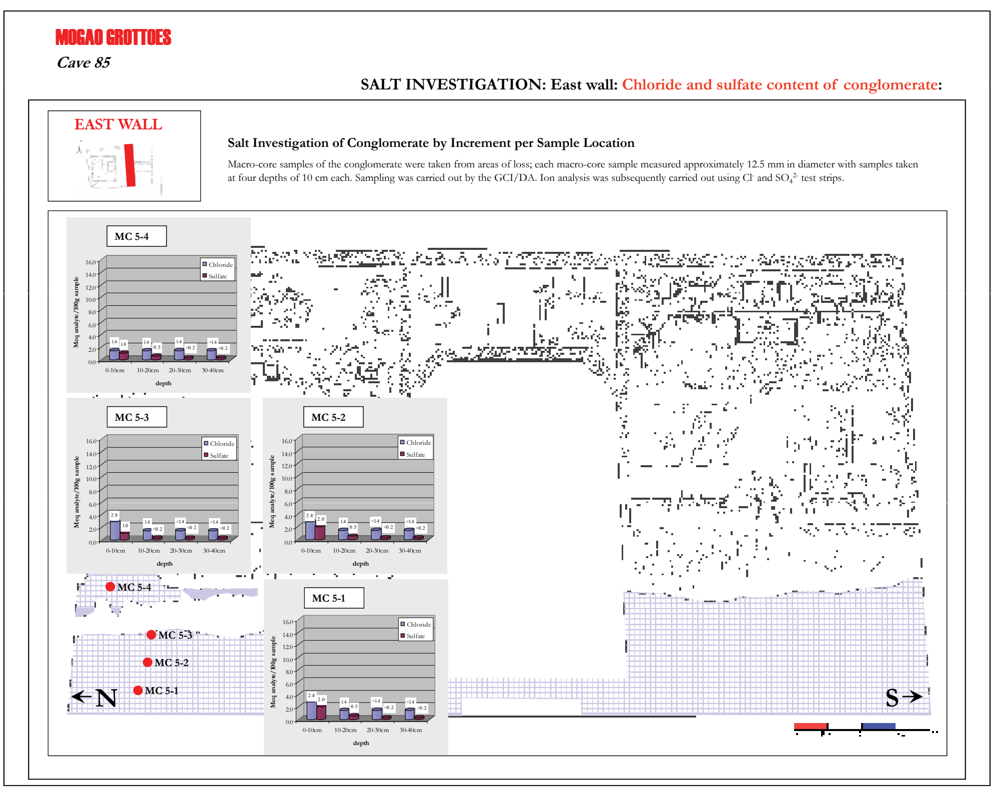

MOGAO GROTTOES

Cave 85

SALT INVESTIGATION: South wall: Chloride and sulfate content of conglomerate:

SOUTH WALL

Salt Investigation of Conglomerate by Increment per Sample Location

Macro-core samples of the conglomerate were taken from areas of loss; each macro-core sample measured approximately 12.5 mm in diameter with samples taken at four depths of 10 cm each. Sampling was carried out by the GCI/DA. Ion analysis was subsequently carried out using Cl^- and SO_4^{2-} test strips.

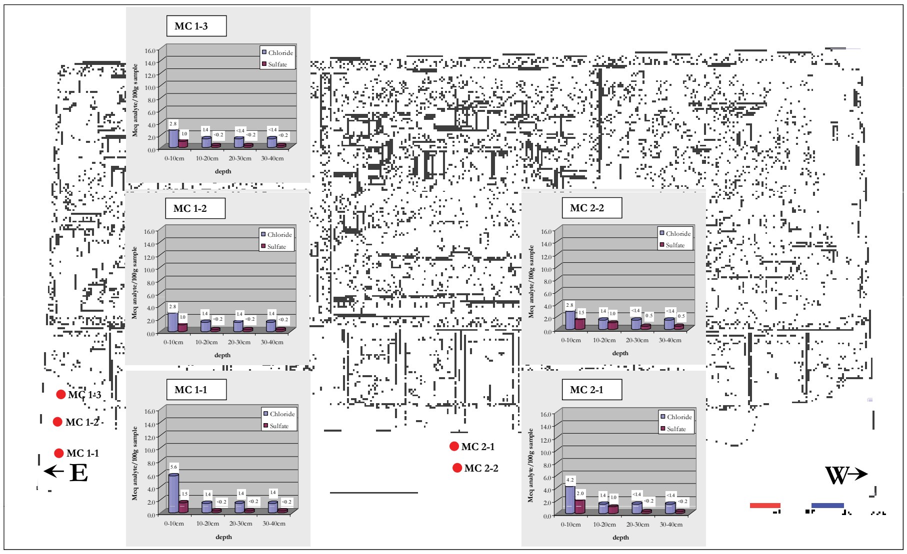

MOGAO GROTTOES

Cave 85

SALT INVESTIGATION: West wall: Chloride and sulfate content of conglomerate:

WEST WALL

Salt Investigation of Conglomerate by Increment per Sample Location

Macro-core samples of the conglomerate were taken from areas of loss; each macro-core sample measured approximately 12.5 mm in diameter with samples taken at four depths of 10 cm each. Sampling was carried out by the GCI/DA. Ion analysis was subsequently carried out using Cl^- and SO_4^{2-} test strips.

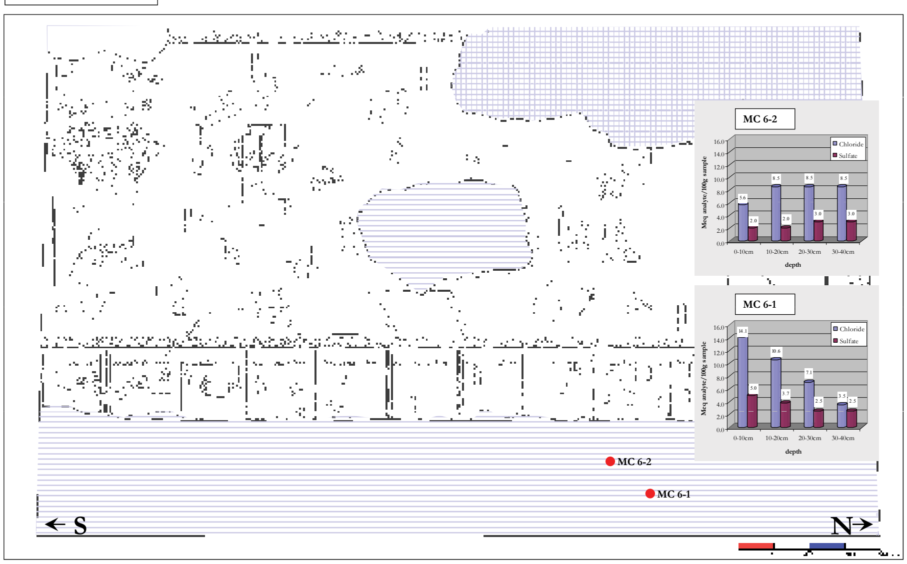

APPENDIX 16.B

Salt Survey of Plaster: Total Content of Ions per Sample Location

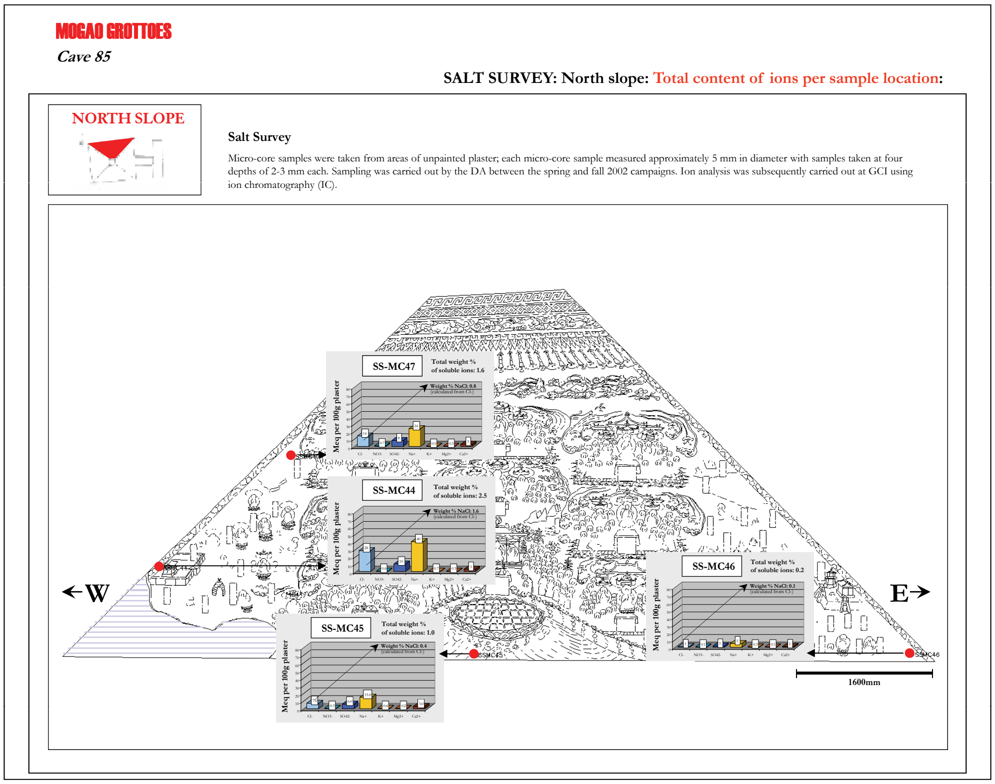

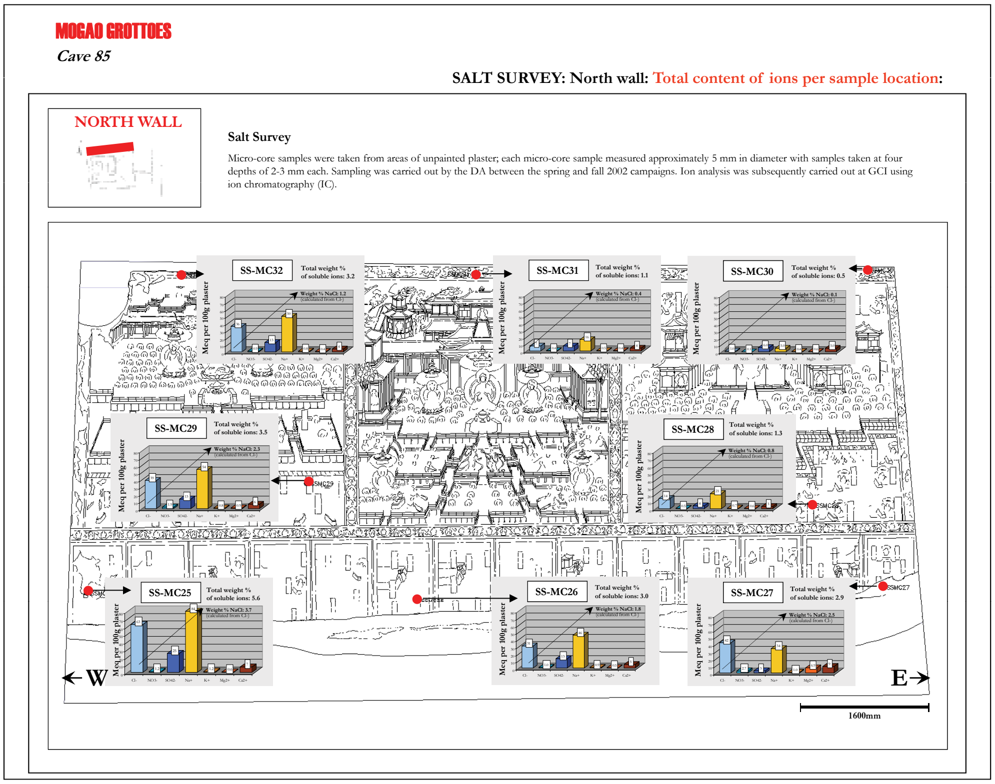

MOGAO GROTTOES

Cave 85

SALT SURVEY: East slope: Total content of ions per sample location:

EAST SLOPE

Salt Survey

Micro-core samples were taken from areas of unpainted plaster; each micro-core sample measured approximately 5 mm in diameter with samples taken at four depths of 2-3 mm each. Sampling was carried out by the DA between the spring and fall 2002 campaigns. Ion analysis was subsequently carried out at GCI using ion chromatography (IC).

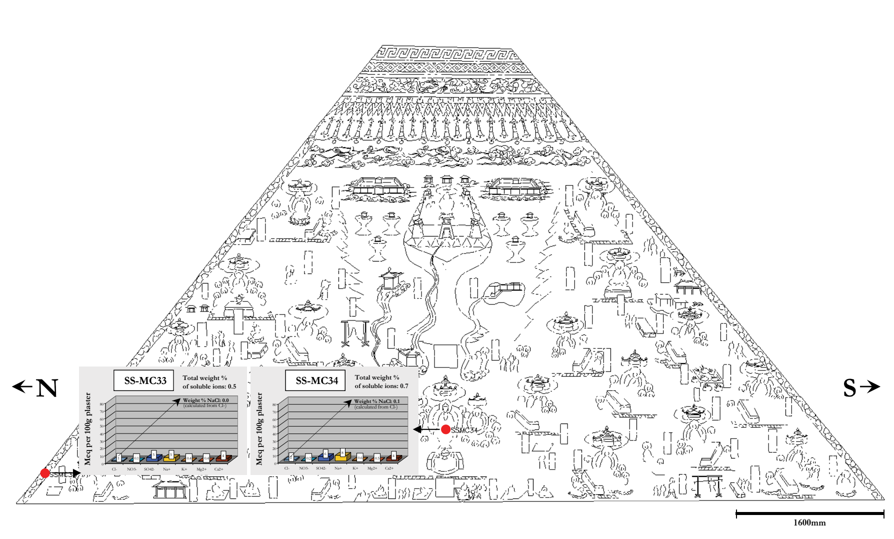

MOGAO GROTTOES

Cave 85

SALT SURVEY: East wall: Total content of ions per sample location:

EAST WALL

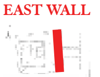

Salt Survey

Micro-core samples were taken from areas of unpainted plaster; each micro-core sample measured approximately 5 mm in diameter with samples taken at four depths of 2-3 mm each. Sampling was carried out by the DA between the spring and fall 2002 campaigns. Ion analysis was subsequently carried out at GCI using ion chromatography (IC).

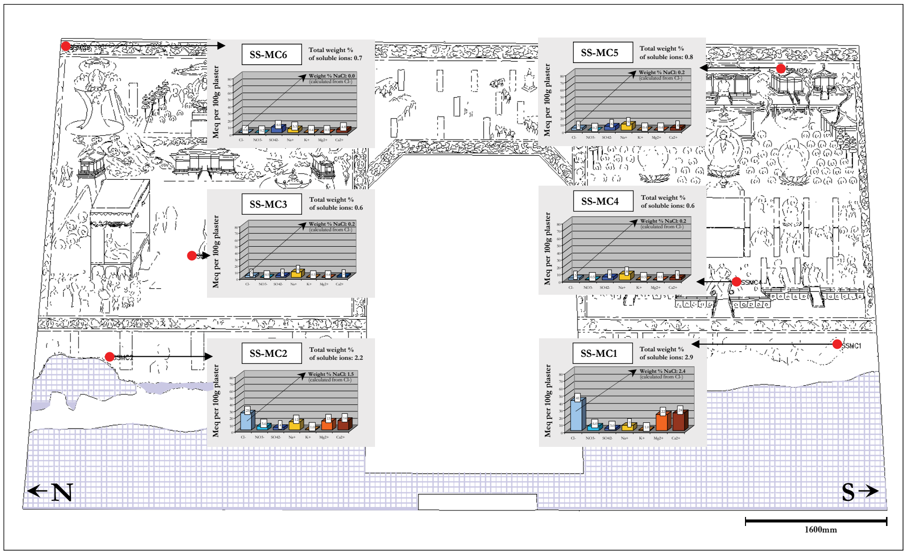

MOGAO GROTTOES

Cave 85

SALT SURVEY: South slope: Total content of ions per sample location:

SOUTH SLOPE

Salt Survey

Micro-core samples were taken from areas of unpainted plaster; each micro-core sample measured approximately 5 mm in diameter with samples taken at four depths of 2-3 mm each. Sampling was carried out by the DA between the spring and fall 2002 campaigns. Ion analysis was subsequently carried out at GCI using ion chromatography (IC).

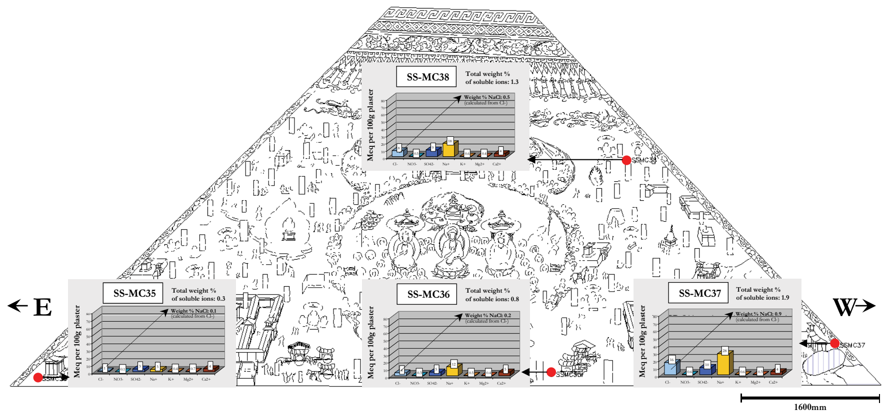

MOGAO GROTTOES

Cave 85

SALT SURVEY: South wall: Total content of ions per sample location:

SOUTH WALL

Salt Survey

Micro-core samples were taken from areas of unpainted plaster; each micro-core sample measured approximately 5 mm in diameter with samples taken at four depths of 2-3 mm each. Sampling was carried out by the DA between the spring and fall 2002 campaigns. Ion analysis was subsequently carried out at GCI using ion chromatography (IC).

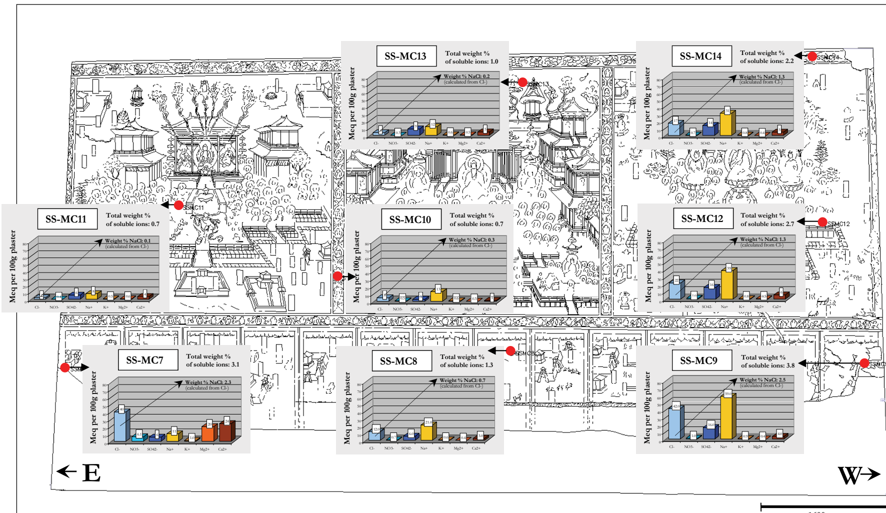

MOGAO GROTTOES

Cave 85

SALT SURVEY: West slope: Total content of ions per sample location:

WEST SLOPE

Salt Survey

Micro-core samples were taken from areas of unpainted plaster; each micro-core sample measured approximately 5 mm in diameter with samples taken at four depths of 2-3 mm each. Sampling was carried out by the DA between the spring and fall 2002 campaigns. Ion analysis was subsequently carried out at GCI using ion chromatography (IC).

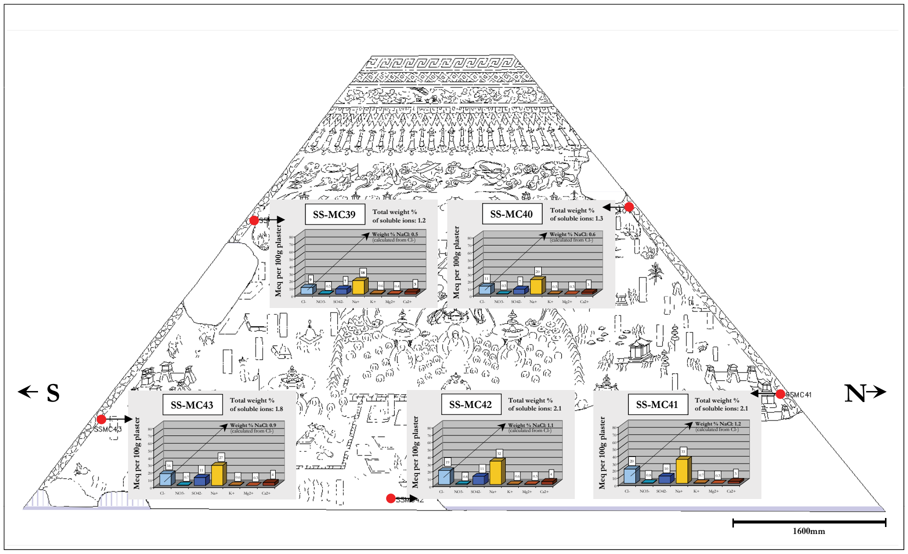

MOGAO GROTTOES

Cave 85

SALT SURVEY: West wall: Total content of ions per sample location:

WEST WALL

Salt Survey

Micro-core samples were taken from areas of unpainted plaster; each micro-core sample measured approximately 5 mm in diameter with samples taken at four depths of 2-3 mm each. Sampling was carried out by the DA between the spring and fall 2002 campaigns. Ion analysis was subsequently carried out at GCI using ion chromatography (IC).

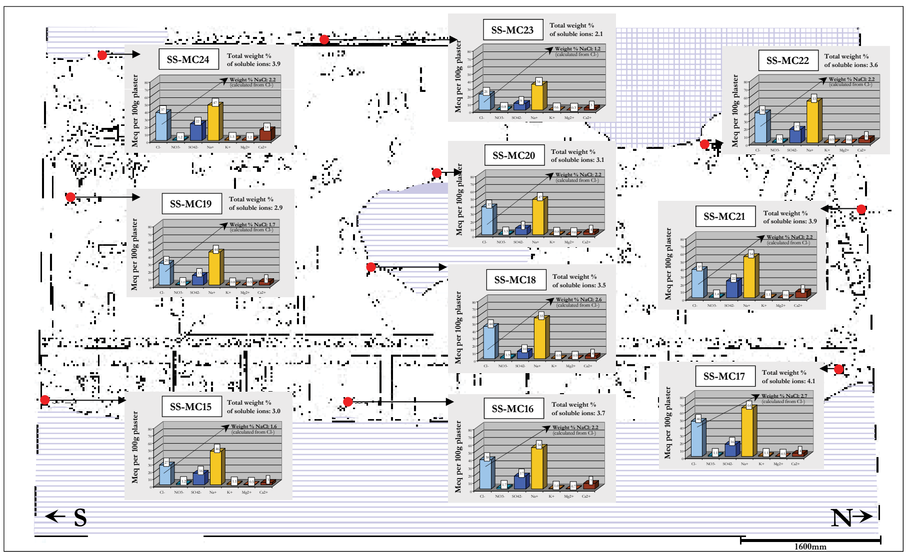

APPENDIX 16.C

Salt Survey of Plaster: Total Content of Ionic Species per Micro-Core Sampling Increment

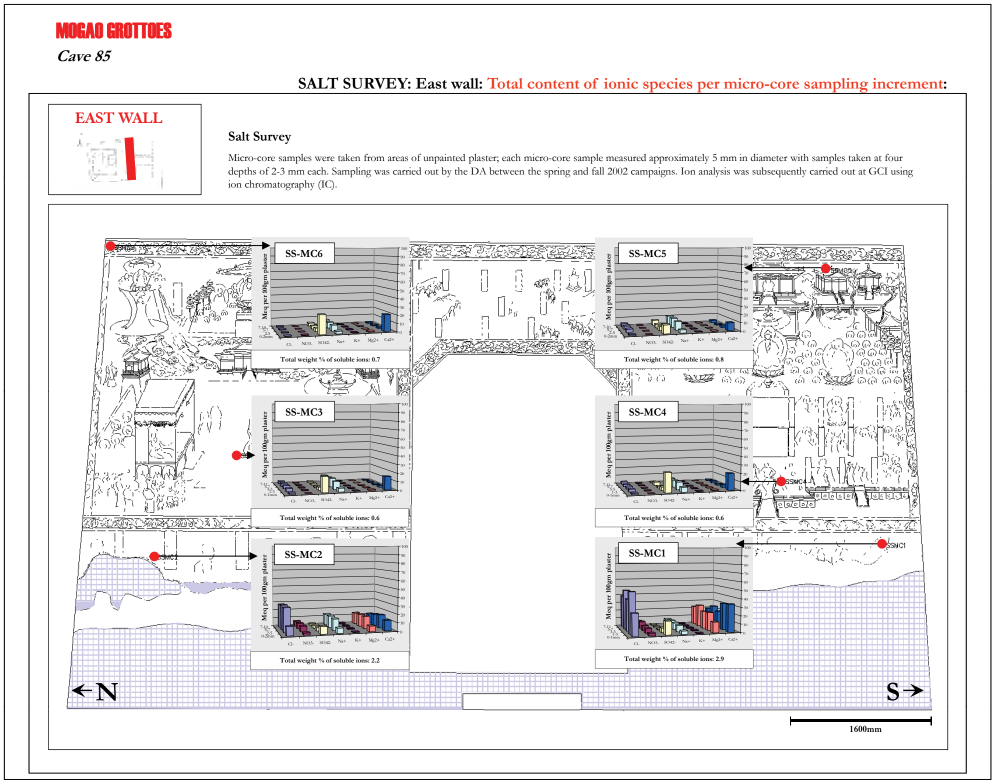

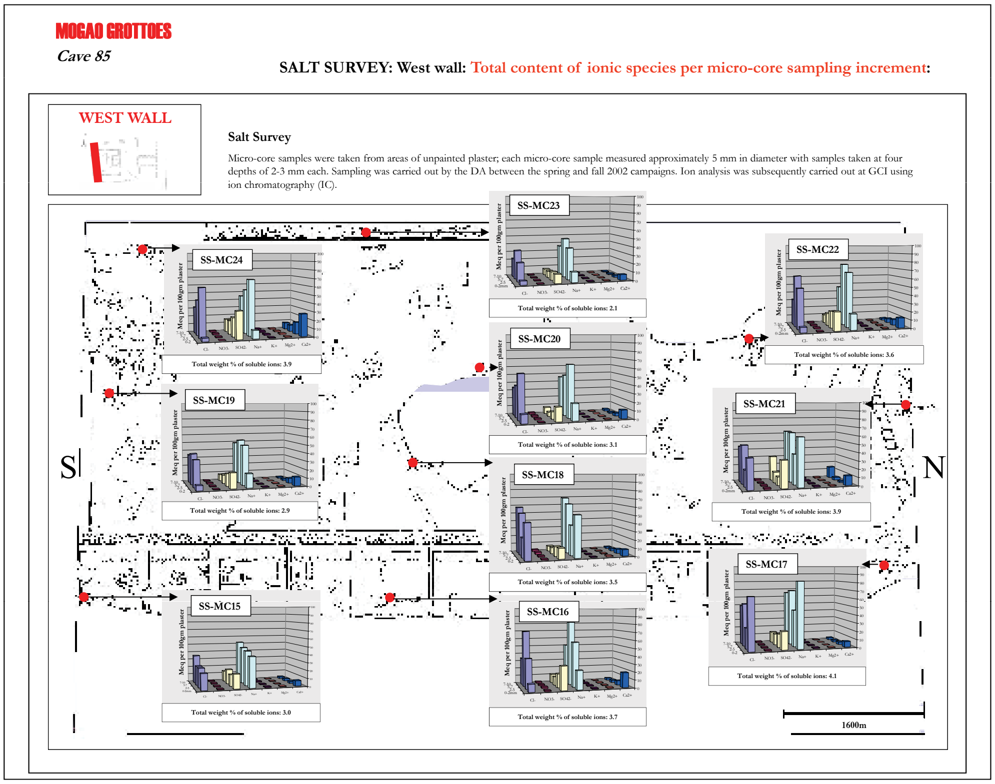

APPENDIX 16.D

Cave 61 Salt Survey of Plaster: Total Content of Ions per Sample Location

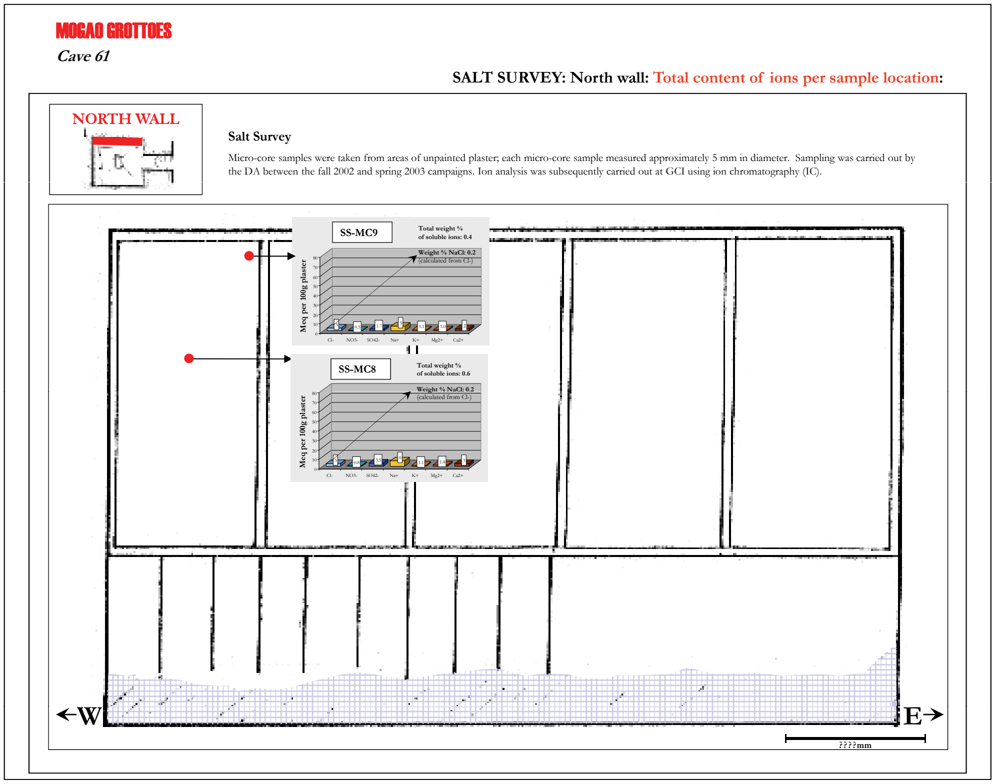

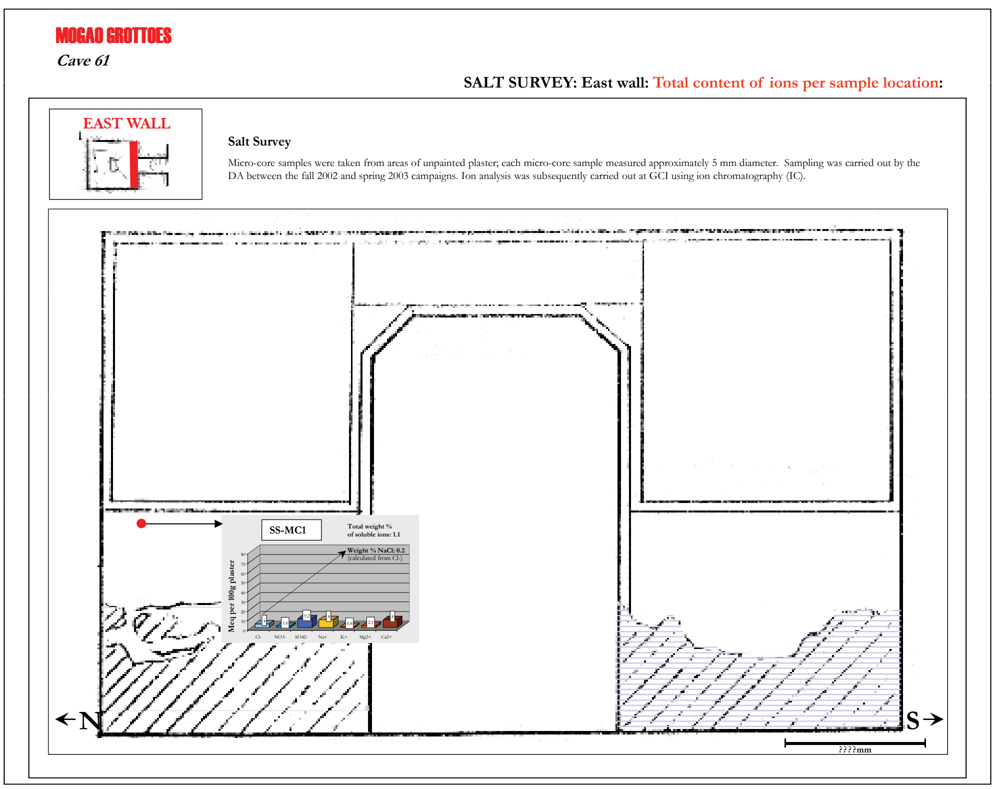

MOGAO GROTTOES

Cave 61

SALT SURVEY: South wall: Total content of ions per sample location:

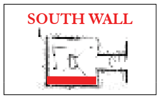

Salt Survey

Micro-core samples were taken from areas of unpainted plaster; each micro-core sample measured approximately 5 mm in diameter. Sampling was carried out by the DA between the fall 2002 and spring 2003 campaigns. Ion analysis was subsequently carried out at GCI using ion chromatography (IC).

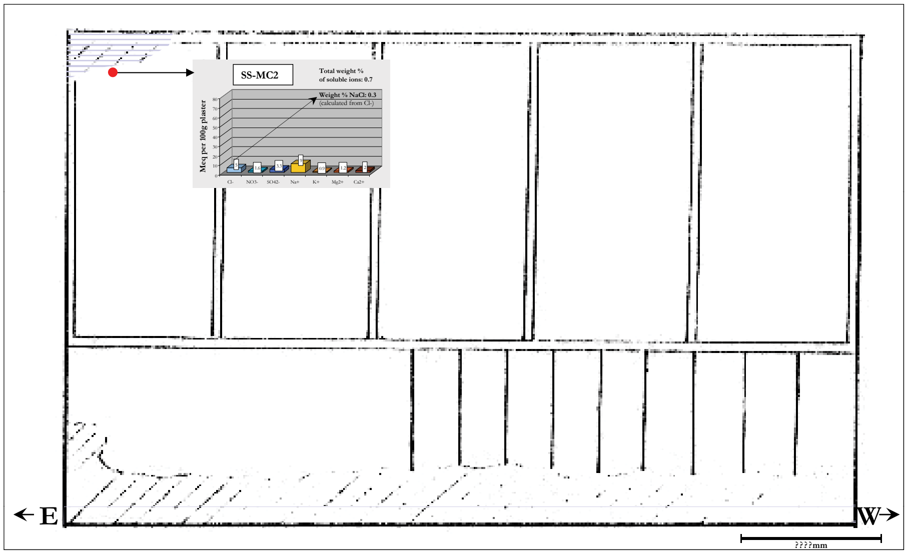

MOGAO GROTTOES

Cave 61

SALT SURVEY: West wall: Total content of ions per sample location:

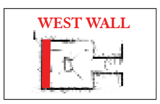

Salt Survey

Micro-core samples were taken from areas of unpainted plaster; each micro-core sample measured approximately 5 mm in diameter. Sampling was carried out by the DA between the fall 2002 and spring 2003 campaigns. Ion analysis was subsequently carried out at GCI using ion chromatography (IC).

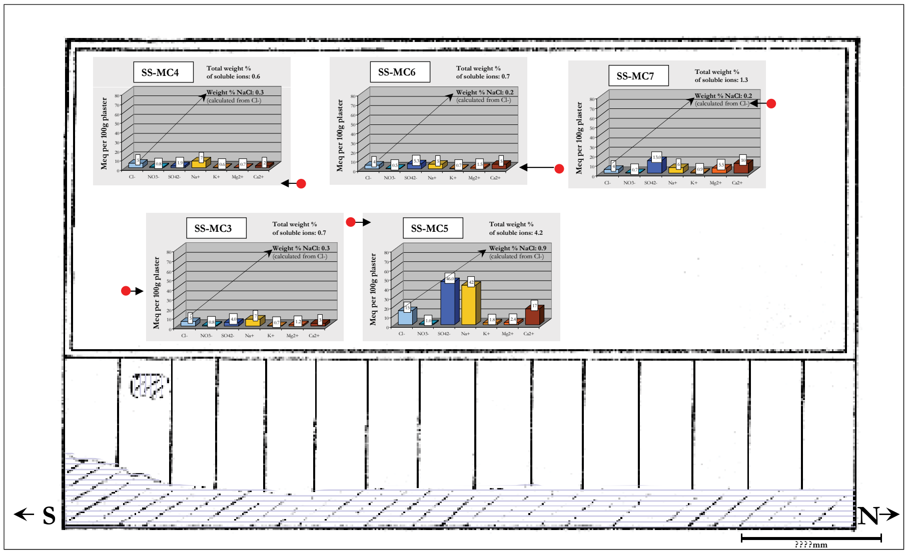

MOGAO GROTTOES

Cave 61

SALT SURVEY: West slope: Total content of ions per sample location:

WEST SLOPE

Salt Survey

Micro-core samples were taken from areas of unpainted plaster; each micro-core sample measured approximately 5 mm in diameter. Sampling was carried out by the DA between the fall 2002 and spring 2003 campaigns. Ion analysis was subsequently carried out at GCI using ion chromatography (IC).

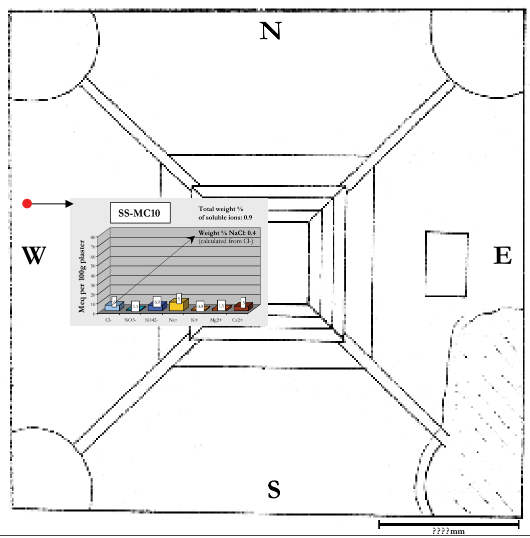

APPENDIX 16.E

Cave 98 Salt Survey of Plaster: Total Content of Ions per Sample Location

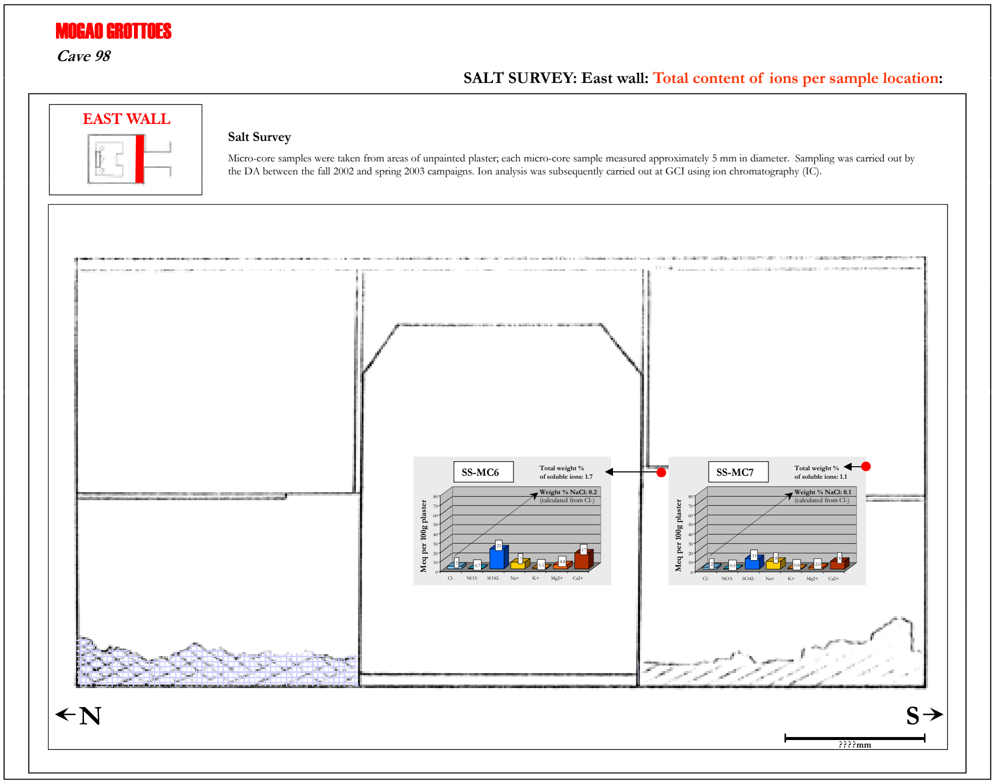

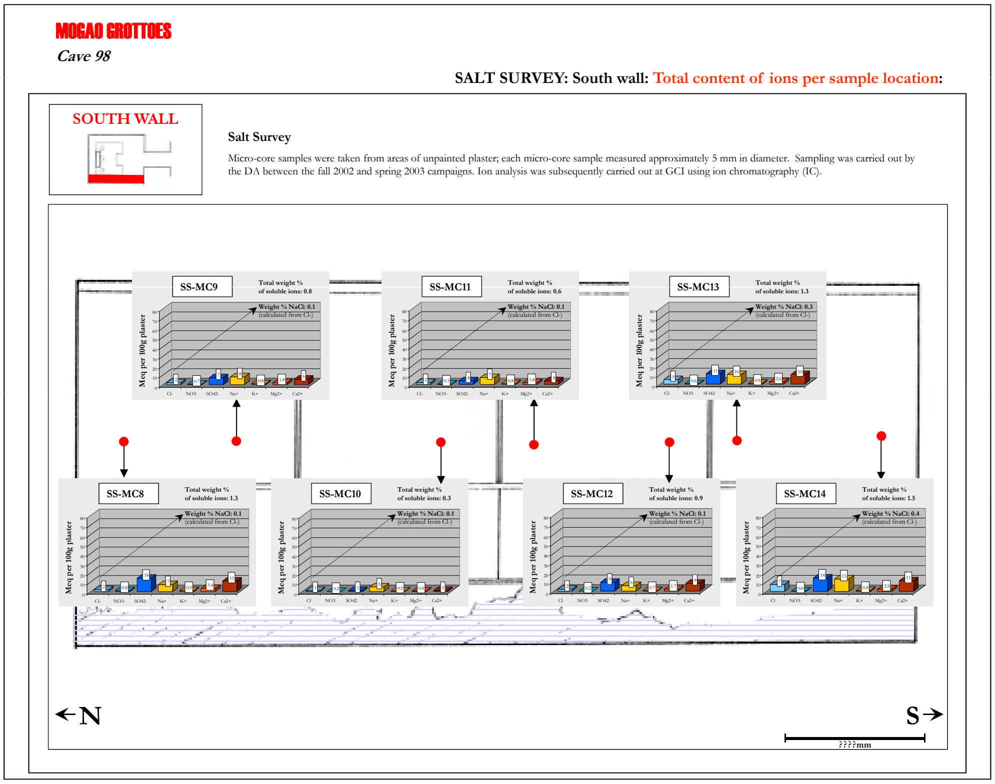

MOGAO GROTTOES

Cave 98

SALT SURVEY: West wall: Total content of ions per sample location:

WEST WALL

Salt Survey

Micro-core samples were taken from areas of unpainted plaster; each micro-core sample measured approximately 5 mm in diameter. Sampling was carried out by the DA between the fall 2002 and spring 2003 campaigns. Ion analysis was subsequently carried out at GCI using ion chromatography (IC).

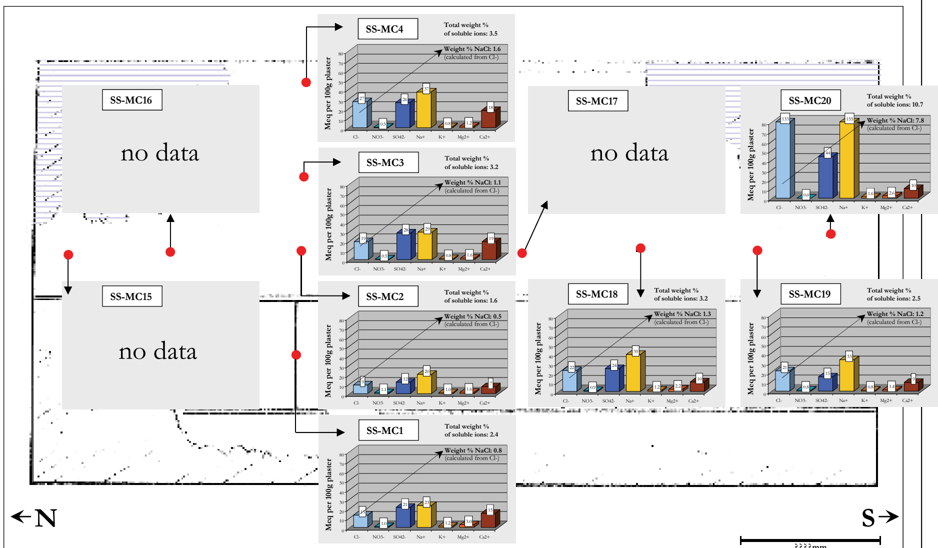

MOGAO GROTTOES

Cave 98

SALT SURVEY: West slope: Total content of ions per sample location:

WEST SLOPE

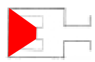

Salt Survey

Micro-core samples were taken from areas of unpainted plaster; each micro-core sample measured approximately 5 mm in diameter. Sampling was carried out by the DA between the fall 2002 and spring 2003 campaigns. Ion analysis was subsequently carried out at GCI using ion chromatography (IC).

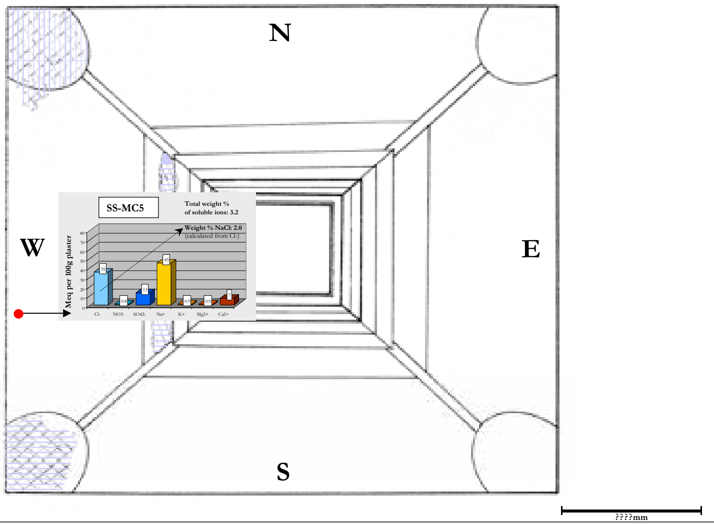

APPENDIX 17.A

Report on the Conservation of Cave 85 Statuary by the Dunhuang Academy

Cave 85 was originally constructed during the Late Tang and had periods of partial redecoration during the Five Dynasties and the Yuan and Qing dynasties. There is a central altar platform on which three sculptures are still extant. The main Buddha sculpture (Sakyamuni) and Kasyapa were made during the Late Tang; the Ananda sculpture was entirely replaced during the Qing dynasty (fig. 1). Conservation of the sculptures was undertaken by the Dunhuang Academy Conservation Institute between May and June 2010.

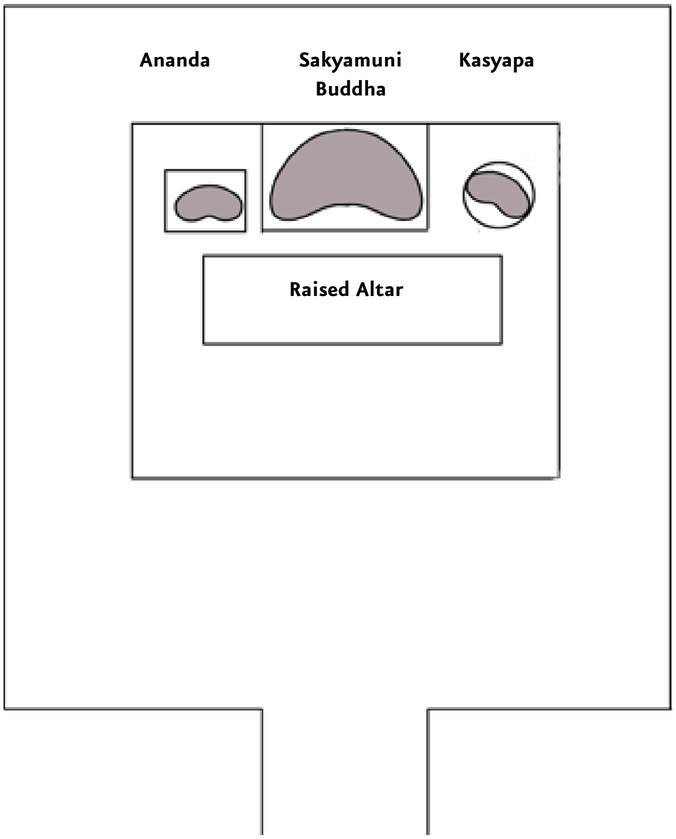

Fig. 1 Plan of altar platform showing location of statuary and raised altar.

Investigation and Analytical Research on Deterioration of the Statuary

Deterioration of the Statuary

Detailed in situ investigation showed that each of the three sculptures suffered from different types of deterioration (see chap. 12). The Sakyamuni Buddha had flaking of the paint layer, damage to the nose, cracking on the neck, and partial loss of the lotus seat base (figs. 2, 3). The sculpture of Kasyapa was tilted forward, the right elbow/wrist had cracks, and there was flaking paint in the chest area (figs. 4, 5). The Ananda statue had cracking on the neck and some loss (fig. 6). This sculpture, which had been replaced in the Qing, was positioned on a square pedestal that was different from the bases of the two other statues, which were constructed during the Late Tang. There was also a slight difference in the direction that the Ananda statue was facing in relation to Kasyapa.

Surface depressions were observed on the top of the raised altar bed that sits directly in front of the statues; research showed that originally five bases with statues that were constructed during the Five Dynasties were located there. The statues are no longer extant. As treatment of the altar bed could affect future archaeological research damaged sections were not repaired.

Fig. 2 Losses on the lotus seat of the Sakyamuni Buddha statue.

Fig. 3 Flaking paint on the leg of the Sakyamuni Buddha.

Fig. 4 Flaking paint on the chest of Kasyapa.

Fig. 5 Crack in the arm of Kasyapa.

Fig. 6 Loss in the neck of Ananda.

Analytical Research on the Mechanism of Deterioration

Investigation and research showed that the main types of deterioration to the statuary are flaking of the paint layer, tilting of the statuary, and cracking and loss of the mud plaster layer. The flaking on the statuary is similar to that found on the wall paintings at the site, which is caused in part by the aging of the binding media in the paint layer. The tilting problem is mainly due to natural gravitational forces; and the cracking and loss of the mud plaster, to vibration and gravitational forces.

Selection of Conservation Materials and Techniques

Conservation Materials

Conservation efforts took into consideration that the sculptures were constructed during different periods and therefore required different restoration materials. Flaking of the paint layer occurs mainly on the main sculpture (Sakyamuni) and Kasyapa, which were both constructed during the Late Tang, at the same time as the wall paintings in the main chamber. Gelatin was selected as the adhesive, and a repair plaster similar to that used on the wall paintings was also employed (see Adhesive and Consolidation Testing and Repair Plaster sections in this chapter). In some cases six-gauge iron wire was used for extra support, for example, during stabilization of the broken right arm and shoulder of Kasyapa. Since the inserted iron wire will be completely sealed oxidation of the metal will be less likely to occur. As the Ananda sculpture was constructed during the Late Qing, the base was reconstructed using a repair plaster with cut straw (1:0.12 mud plaster to cut straw).

Conservation Techniques

The technique for flake fixing on the statues is similar to that used on the wall paintings. The damaged sections of Sakyamuni's lotus seat were conserved by adding repair plaster and shaping the material to its original lotus shape. For the sculpture of Kasyapa, the tilting was corrected, the broken and cracked right arm was returned to the correct position, and cracks were filled. According to the decision of the DA Conservation Institute, the base of the sculpture of Ananda was reconstructed in the same style as the lotus seat of Kasyapa and the angle of the sculpture adjusted. The cracks and areas of loss were repaired with plaster and shaped to the original form.

Implementation

After the survey phase had been completed restoration was undertaken based on the results of analytical research on the mechanism of deterioration and the materials and techniques for conservation.

Areas of Flaking

- A soft wool brush and a bulb aspirator was used to gently clean behind flakes;
- A syringe was used to inject 1.5% gelatin solution behind flakes;
- Cotton balls were used to press back flakes.

Tilting (figs. 14, 15)

- The degree of tilting was calculated, the correct position was found, a reference point was determined, and the sculpture was fixed in place temporarily;
- The lotus seat was opened up according to the design plan and the foundation cleaned;
- The reference point was used to show the correct position of the sculpture, and the sculpture was turned to its corrected position and fixed and stabilized in place;
- The statue was returned to its original position and cracks and damaged areas repaired.

Areas of Loss

- Cleaned areas damaged due to loss;
- Used a mud repair plaster, keeping the surface of the newly plastered areas recessed by 2 mm to differentiate it from the intact original sculpture layer.

Conservation of the Sakyamuni Buddha (figs. 7, 8)

- Dust removal;
- 1% acrylic emulsion was applied twice, and salt was reduced in areas of deterioration;
- A mud plaster was used to return the statue base to its original form; the surface of the newly plastered areas was recessed by 2 mm to differentiate it from the intact original sculpture layer.

Conservation of the Kasyapa Statue (figs. 9, 10, 11)

- An opening was made under the right elbow (4 cm × 6 cm);

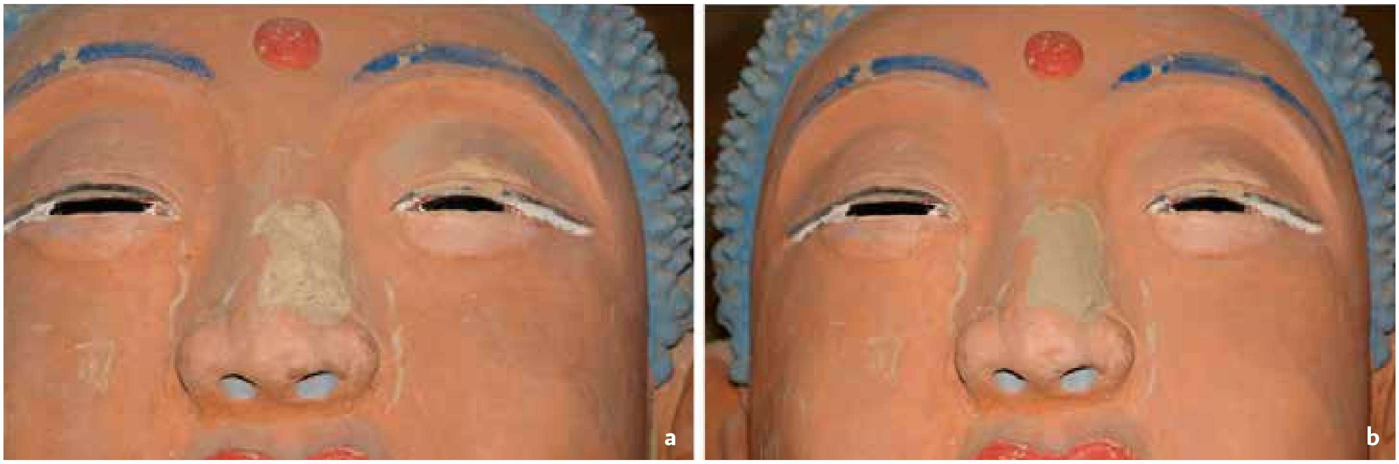

Fig. 7 Nose of the Sakyamuni Buddha before (a) and after (b) conservation.

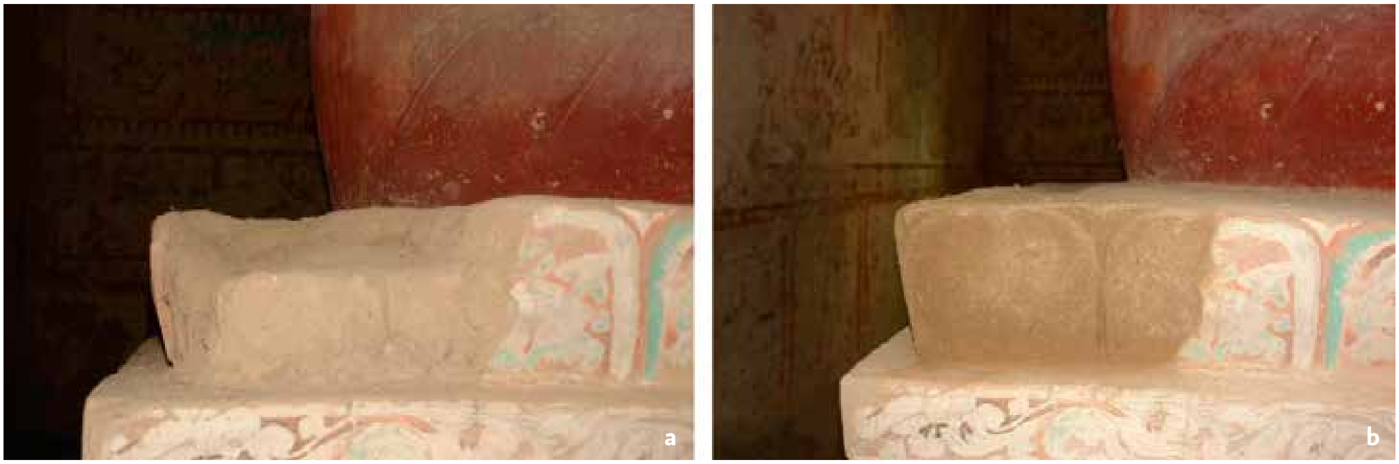

Fig. 8 Lotus seat of the Sakyamuni Buddha before (a) and after (b) conservation.

- A six-gauge iron wire was used to fix the elbow to the inner support by wrapping the wire around;
- Four strands of wire (approximately two upper arm lengths) were inserted from the bottom to the top of the arm through the inner straw core and around the lateral frame of the shoulder;
- Gaps and cracks were filled with mud and straw mixture;
- The repaired parts were painted with mineral pigment.

Conservation of the Ananda Statue (figs.12, 13)
As this work required re-creation of the lotus pedestal and re-adjustment of the statue's angle the base had to be opened up.

- The sculpture was stabilized with a scaffolding system;
- The square base of the sculpture was removed, and the foundations were cleaned;
- The angle of the sculpture of Ananda was adjusted to match that of Kasyapa;
- Mud plaster was used to mold the lotus seat;
- Cracks on the neck and other areas of damage were repaired.

Conservation of the Raised Bed
Investigation and research confirmed that the raised offering bed on the altar platform contained seats for five Buddha sculptures constructed during the Five Dynasties (no longer extant). Stabilization was undertaken only on areas in danger of collapse with a 1% acrylic emulsion.

After conservation was completed the work was reviewed and approved by an experts committee from the Dunhuang Academy Conservation Institute that included Wang Xudong, Su Bomin, and Fan Zaixuan.

Fig. 9 Flaking paint on the chest of Kasyapa before (a) and after (b) conservation.

Fig. 10 Arm of Kasyapa before (a) and after (b) conservation.

Fig. 11 Foot of Kasyapa before (a) and after (b) conservation.

Fig. 12 Base of the Ananda statue before (a) and after (b) modification.

Fig. 13 Neck of Ananda before (a) and after (b) conservation.

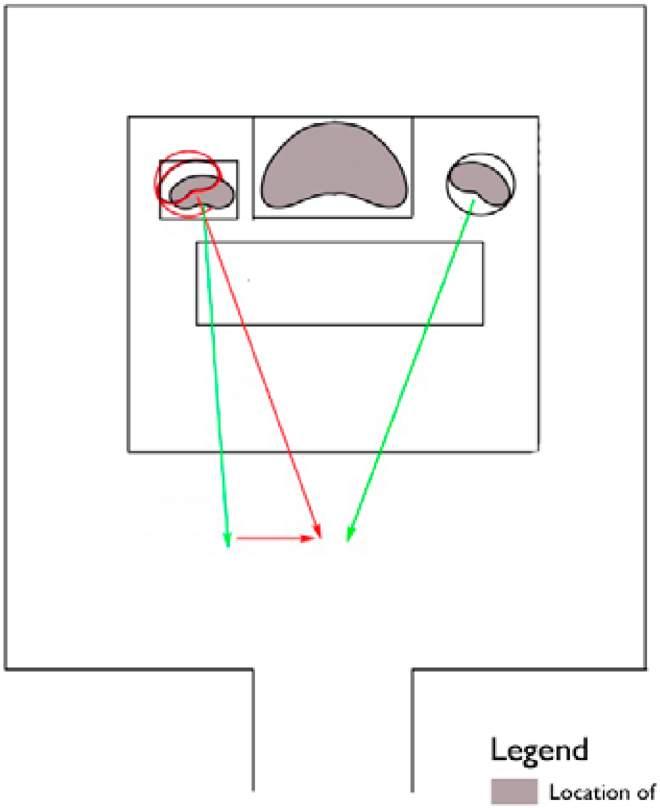

Fig. 14 Plan showing how the Ananda statue was adjusted to correct the tilt.

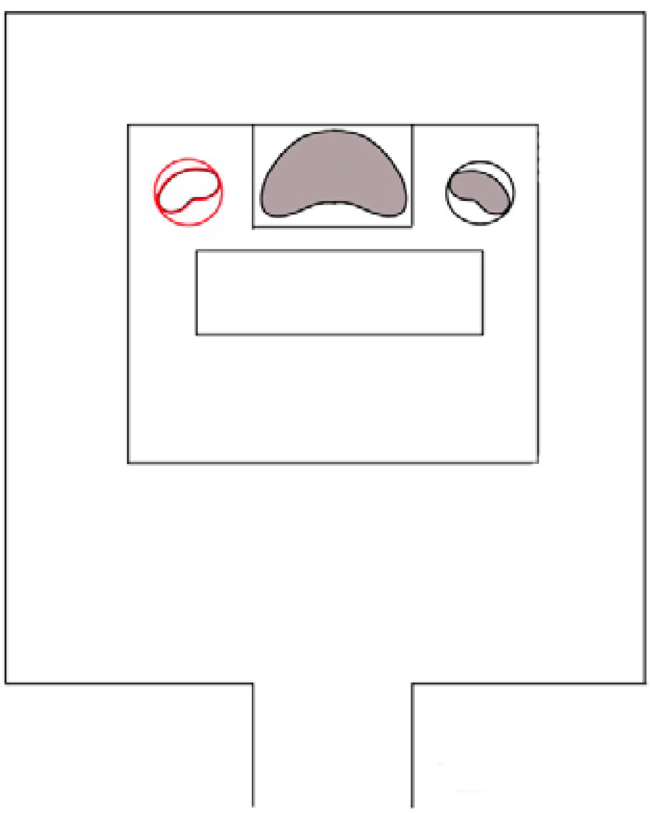

Fig. 15 Plan showing the modifications to the Ananda statue and base (shown in red).

APPENDIX 17.B

Properties of Original and Added Earthen Materials

COMPONENTS AND PROPORTIONS

MATERIAL	CONSTITUENT PARTS	PARTICLE SIZE	TOTAL VOLUME (ml)	TOTAL MASS (g)
CAVE 85 GROUT (75–150μM PUMICE)	• Crushed, washed and dried riverbed mud • Sieved pumice • Scotchlite K1® glass microspheres • Distilled water • Whisked egg white	<600 μm 75–150 μm <75μm N/A N/A	18.2 18.2 36.4 23.6 3.6	33.4 20.4 3.5 37.0 5.7
CAVE 85 PLASTER (REPLICA)	• Crushed, washed and dried riverbed mud • Local desert sand • Chopped straw • Distilled water	< 4.25 μm < 4.25 μm 1–2 cm lengths N/A	51.4 20.6 N/A 28.0	48.4 27.4 2.3 21.9
DAQUAN RIVERBED MUD	• Crushed, washed and dried riverbed mud • Distilled water	<4.25 μm N/A	64.8 35.2	68.4 31.6

pH AND SOLUBLE ION CONTENT

MATERIAL	pH	Cl^- (g/100 g solid)	SO_4^{2-} (g/100 g solid)	NO_3^- (g/100 g solid)	Mg^{2+} (g/100 g solid)	Ca^{2+} (g/100 g solid)	Na^+ (g/100 g solid)
CAVE 85 GROUT (75–150 μM PUMICE)	9.2	0.02	0.05	0.001	0.004	0.02	0.06
CAVE 85 PLASTER (REPLICA)	9.0	0.03	0.05	–*	–	0.03	0.03
DAQUAN RIVERBED MUD (UNWASHED)	8.7	0.04	0.20	0.01	0.01	0.05	0.06
DAQUAN RIVERBED MUD (WASHED)	–	0.05	0.15	0.001	0.01	0.04	0.05

HYGRAL BEHAVIOR

MATERIAL	INITIAL WATER RELEASE (time [s] to reach 2.5 cm circle)	INITIAL WATER RELEASE (time [s] to reach 3.1 cm circle)	INITIAL WET WEIGHT (g/100 ml)	FINAL (DRY) WEIGHT (g/100 ml)	DRYING TIME (hrs)	DRY DENSITY (g/cm^3)	DIAMETRIC SHRINKAGE (%)	WATER VAPOR PERMEABILITY (g/cm^2h)
CAVE 85 GROUT (75–150 μM PUMICE)	330	655	101	59.4	72.5	1.05	2.2	6.3×10^{-4}
CAVE 85 PLASTER (REPLICA)	--	--	124.6	86.5	--	1.72	2.4	4.0×10^{-4}
DAQUAN RIVERBED MUD	185	372	161.1	110.3	50.2	1.65	6.4	4.74×10^{-4}

DENSITY AND POROSITY

MATERIAL	DIAMETER (mm)	SPECIFIC GRAVITY (g/cm^3)	APPARENT DENSITY METHOD 1 (g/cm^3)	APPARENT DENSITY METHOD 2 (g/cm^3)	BULK POROSITY (% vol)	ULTRASONIC VELOCITY (km/s)
CAVE 85 GROUT (75–150 μM PUMICE)	79.00	2.538	--	0.75	--	1.05
CAVE 85 PLASTER (REPLICA)	79.71	2.641	1.602	1.48	39.33	0.98
DAQUAN RIVERBED MUD	76.14	2.629	1.661	1.60	36.816	1.01

ADHESION AND STRENGTH

MATERIAL	SHEAR RESISTANCE (SMOOTH CLIFF FACE) (N)	SHEAR RESISTANCE (ROUGH CLIFF FACE) (N)	UNIAXIAL STRENGTH (MPa)	THREE-POINT LOAD (MPa)	DENSITY (g/cm^3)	SHEAR STRENGTH (KPa)	INTERNAL FRACTION ANGLE (°)
CAVE 85 GROUT (75–150 µM PUMICE)	381.9	350.9	1.608	0.30	0.84	58.2	28.5
CAVE 85 PLASTER (REPLICA)	>400	>400	1.553	0.25	1.34	56.2	25.8
DAQUAN RIVERBED MUD	358.5	385.7	–	–	–	–	–

NOTES

*"–" indicates when a test was not run.

APPENDIX 17.C

Grout Formulation Testing

Definitions, Rationale, and Procedures

Initial Water Release (min, sec)

Definition: A comparative test of loss of water from a grout as measured by the time and distance water migrated by capillarity on an absorbent surface.

Testing rationale: During grouting it is important to minimize both the amount of water (while still ensuring sufficient fluidity) and the rate of migration from grout into salt-enriched, aged, and decoherent earthen plasters. Earthen plasters may deform or collapse through the loss of strength and weight increase following the introduction of water. Excess water also mobilizes salts. Initial water release testing of grout formulations is therefore a method for evaluating these risks.

Procedures: A series of concentric circles of fixed diameter are drawn on filter paper (for the tests presented in the grout formulation tables, three circles of 5 cm, 6.4 cm, and 7.7 cm diameter were used; for the tests presented in the properties of original and added earthen materials tables, two circles of 2.5 cm and 3.1 cm diameter were used). A fixed quantity (5 ml) of grout formulation is then released by syringe into the center of the circles, and the time taken for water released from the grout to reach each of the circles is recorded in minutes and seconds.

Drying Time (hr)

Definition: The time (hours) required for a grout to reach constant weight at a constant T.

Testing rationale: For the same reasons as those set out for initial water release testing, a rapid drying time minimizes risks associated with the introduction of water during grouting.

Procedures (based on ASTM C266–89 and C191–82): In this comparative test of different formulations a series of 70 ml petri dishes were weighed, filled with grout, and reweighed to obtain the wet weight. The dishes were placed in an oven maintained at 30°C and the time and date recorded. The dishes were weighed twice daily until constant mass was reached. The number of hours between the start and end of the procedure is the drying time.

Water Loss on Drying (%)

Definition: The amount of water retained in a dry grout formulation calculated as a percentage by recording mass change on drying to constant weight.

Testing rationale: Porosity, particle-size distribution, and morphology affect the amount of water required to produce a grout with optimal fluidity. The amount of water used to achieve fluidity affects initial water release, drying time, and shrinkage, as well as factors discussed in relation to initial water release, so determining the percentage water loss is useful for evaluating the hygral properties of grout formulations.

Procedures (after I. Griffin): A series of 70 ml petri dishes were weighed, filled with wet grout, and reweighed to obtain the wet weight (M_1). The dishes were then placed in an oven maintained at 30°C and the time and date recorded. The dishes were weighed twice daily until constant mass was reached, providing the dry weight (M_2). Water loss was then obtained by difference. $(M_1 - M_2) \times 100/M1$ gives the result as a percentage.

Diametric Shrinkage (%)

Definition: Dimensional decrease of a disc of grout after water loss, obtained by measuring the diameter before and after drying to constant mass, expressed as a percentage of the original diameter.

Testing rationale: As the purpose of a grout is to stabilize voids by reestablishing adhesion between the plaster and the support, contact must be maintained between the two surfaces not only on initial application but also after drying. Minimal shrinkage is therefore an important performance requirement for grouts.

Procedures (after Griffin): A series of 70 ml petri dishes were filled with newly prepared grout formulations, and the diameter of the petri dish measured with vernier calipers to provide the wet diameter (D_1). The dishes were then placed in an oven maintained at 30°C and weighed twice daily until constant mass was reached. The diameter of the dried grout formulation was measured to provide the dry diameter (D_2). Shrinkage was then obtained by difference. $(D_1\text{-}D_2) \times 100/D_1$ gives the results as a percentage.

Dry Density (g/cm^3)

Definition: Dry density is equal to the dry mass of the sample divided by its volume.

Testing rationale: For long-term stability the grout must respond to its environment in a similar way to that of the earthen plaster by having similar values for density, porosity, water vapor permeability, etc. It is important that the density of the grout should be similar to and not exceed that of the original. Dry density of the original plaster was calculated as 1.72; the chosen grout formulation was between 1.05 and 1.16.

Procedures: A series of 70 ml petri dishes were weighed, filled with newly prepared grout formulations, and placed in an oven maintained at 30°C. The dishes were then weighed twice daily until constant mass was reached (M_2). The dry volume (V_2) was obtained from the dry diameter (D_2) and dry height (H_2) using the formula

$$H_2 \times (D_2/2)^2 \times 3.14$$

Density was then calculated using the formula

$$M_2/ V_2$$

Water Vapor Permeability (g/cm^2·h)

Definition: The rate of water evaporation through a dried disc of grout formulation of known area and height at constant RH and T.

Testing rationale: For long-term stability the grout must respond to its environment in a similar way to that of the earthen plaster by having similar values for density, porosity, water vapor permeability, etc. It is important that the water vapor permeability of the grout be similar to or greater than that of the earthen plaster to reduce the formation of salts crystals at stratigraphic interfaces. Water vapor permeability of the original plaster was 4.0×10^{-4}; that of the chosen grout was 6.3×10^{-4} g/cm^2·h.

Procedures (based on ASTM E 96–95): The diameter and thickness of a series of dried discs of grout formulation were measured. They were then placed over beakers containing a set volume of water. The space between the disc and the beaker was then sealed with wax to ensure that water could only evaporate through the disc. The combined mass of the beaker, disc, wax, and water was then recorded before placing into an incubator set at 30°C and 50% RH. They were weighed twice daily and the mass recorded over time as water vapor diffused through the disk of grout.

Shear Resistance

Definition: Force required to shear the bond between grouted test panels of earthen plaster of known area and thickness from the conglomerate rock surface.

Testing rationale: Future movement between plaster and rock support cannot be precluded, in the event of which the grout, and not the original painted plaster, should fail. It is therefore important that adhesion and shear resistance of the grout should be similar to that of the original but not exceed it.

Procedures: Two sets of replica plaster panels 8 × 8 cm and 0.5 cm thick were applied wet to the conglomerate surface, one set on a very rough surface and one on a smoother surface. Four more sets of the same size were made in molds with a round depression of constant area and depth in one side. These were dried and applied to the two rock faces using wet replica plaster. The concave sides were applied to face the rock so that a void existed between the plaster and the rock. Five ml of water were injected into the voids through a hole in each block. Between 20 and 45 ml of grout formulation number 81 were injected into half of the panels and the same amount of riverbed mud injected into the others so that it was evenly distributed inside the void. All the panels were allowed to dry. Shear testing was conducted by bonding a metal plate to the surface of each panel, from which a cradle of known weight was suspended. Weights were added gradually until the grout failed and the panel was pulled from the wall. The force (N) was then calculated from the data (1 Kg = 9.8 N).

Soluble Salt Content

Definition: The amount of soluble salts contained in grout component materials and formulations.

Testing rationale: Soluble salts are dissociated in an aqueous solution. The cations and anions are not necessarily representative of the crystalline salts present, but identification of the ionic species and the amounts present provides useful guidance when considering salt-related deterioration. Cations of relevance in analysis of soluble salts are Na^+, K^+, Ca^{2+}, Mg^{2+}; anions are Cl^-, SO_4^{2-}, NO_3^-, CO_3^{2+}.

Procedures: Analysis of soluble ionic species in samples was undertaken using ion chromatography in the laboratory or on-site using ion-specific test strips and a chloride ion–specific electrode. Microequivalents per gram were reported (mass % divided by molecular weight and charge of ion).

Bulk Porosity (% vol)

Definition: The volume of voids in a solid expressed as a percentage of the total volume of a mass of the solid. Voids, or pores, may be interconnected, which allows diffusion of gases and permeability of water in the liquid phase.

Testing rationale: The pore structure of some grouts contain distinct individual closed pores not interconnected as well as open channels, which permits the diffusion of water vapor. Whipped egg white as a component of the grout significantly affects the quantity and size of the pores, resulting in fewer and smaller pores than the same grout but without the addition of egg white. This reduction in porosity improves bonding and water resistance of the grout.

Procedures: A number of standard techniques are used to determine bulk porosity including mercury intrusion porosimetry and various gas methods such as helium.

The following tests were conducted in 2002 by the Dunhuang Academy at Lanzhou University.

Uniaxial Strength (MPa)

Definition: Unidirectional load applied to a standard size of solid sample of grout. The stress recorded at the load that causes failure is a measure of its compressive strength.

Testing rationale: Designed to give a semiquantitative indicator of strength. Ideally the mechanical strength of a grout should be slightly less than that of the original materials to ensure that the grout will fail first but also strong enough to provide strength and support to the plaster.

Procedures (after Griffin; tests performed by DA at Lanzhou University): Syringes with approximate lengths of 5 cm and diameter of 2.5 cm (2:1 ratio) were filled with grout and allowed to dry initially within the syringe and then under ambient conditions after their removal. Dry samples were tested with uniaxial compression in a laboratory vice, and values were recorded at each incremental increase (tightening) of the vice.

Three-Point Load (MPa)

Definition: Modulus of rupture or the flexural breaking load (bending strength) of the material.

Testing rationale: Designed to give a semiquantitative indicator of strength. Ideally the mechanical strength should be slightly less than that of the original to ensure that the grout will fail first but also strong enough to provide strength and support to the painted plaster. A more useful strength test than uniaxial testing in that it provides a more realistic measure of how a solid fails.

Procedure (tests performed by DA at Lanzhou University): Test blocks of dry grout were prepared and tested.

Table 1. Selected Grout Formulations: Arranged by Component Type and Proportions

Grout no.	Components & proportions	Initial water release: circle 1 (min/sec)	Initial water release: circle 2 (min/sec)	Initial water release: circle 3 (min/sec)	Drying time to constant mass (hr)	Wet weight (g)	Dry weight (g)	Water loss on drying (%)	Diametric shrinkage (%)	Dry density (g/cm^3)	Water vapor permeability ($g/cm^2 \cdot h$)	Comments
G53	Earth	1' 15"	2' 40"	5' 46"	54	104	66	36.5	5.37	3.89	4.74×10^{-4}	disadvantages: high weight and shrinkage
G54	Earth:2 Scotchlite:1	1' 10"	2' 37"	6' 02"	45	86	55	36.05	5.12	3.15	4.4×10^{-4}	advantages: the addition of Scotchlite reduces weight, shrinkage, and drying time; disadvantages: reduces water vapor permeability
G55	Earth:2 Scotchlite:1 Egg white 5%	2' 11"	3' 45"	8' 33"	44	87	55	36.78	5.12	3.15	4.31×10^{-4}	advantages: egg white inhibits rapid water release; disadvantages: slight reduction in water vapor permeability
G27	Earth:2 Scotchlite:1 Black coal ash: 1	1' 10"	2' 30"	5' 55"	72	84	57	32.14	3.64	2.9	4.22×10^{-4}	advantages: coal ash reduces shrinkage; disadvantage: increases drying time and reduces water vapor permeability
G28	Earth:2 Scotchlite:1 Black coal ash: 1 Egg white 5%	2' 03"	4' 48"	8' 10"	54	83	54	34.94	3.89	3.13	4.03×10^{-4}	as 55
G47	Earth:2 Scotchlite:1 Brick dust: 1	0' 46"	1' 37"	3' 28"	47	80	50	37.50	4.14	2.77	4.4×10^{-4}	advantages: replacing coal ash with brick dust reduces drying time and weight, increases water vapor permeability; disadvantages: increases water release and shrinkage
G48	Earth:2 Scotchlite:1 Brick dust: 1 Egg white 5%	1' 48"	4' 08"	9' 00"	51	77	47	38.96	5.12	2.57	4.8×10^{-4}	as 55
G60	Earth:2 Scotchlite:1 Harborlite: 1	1' 33"	3' 02"	4' 67"	47	81	49	39.51	4.38	2.83	6.08×10^{-4}	advantages: replacing brick dust with Harborlite slows water release and greatly improves water vapor permeability; disadvantages: increases shrinkage
G61	Earth:2 Scotchlite:1 Harborlite: 1 Egg white 5%	1' 35"	3' 40"	7' 37"	50	83	55	39.76	5.12	2.76	6.06×10^{-4}	as 55
G66	Earth:1 Scotchlite: 2 Sand: 1 Egg white 5%	4' 42"	6" 16"	9' 00"	64	93	66	30.3	4.74	1.25	4.78×10^{-4}	advantages: reversing quantities of earth and Scotchlite retards initial water release and shrinkage disadvantages; sand increases weight
G71	Earth:1 Scotchlite: 2 Sand: 0.3 Harborlite: 0.2 Egg white 5%	5' 14"	6' 57"	not recorded	144	83.5	53.1	38.1	4.06	1.12	5.28×10^{-4}	advantages: addition of Harborlite perlite increases WVP, slows water release, and reduces shrinkage; disadvantages: increases drying time
G75	Earth:1 Scotchlite: 2 Sand: 0.3 Black coal ash: 0.2 Egg white 5%	5' 36"	6' 35"	not recorded	78	75	46.8	37.6	4.38	1.04	6.13×10^{-4}	advantages: replacement of Harborlite perlite with coal ash reduces drying time, but weight and water vapor permeability results may not be reliable
G81	Earth:1 Scotchlite: 2 Pumice: 1 Egg white 5%	7' 10"	11' 15"	not reached	41	77	41.6	38.7	3.18	1.17	6.3×10^{-4}	advantages: use of pumice retards water release, increases water vapor permeability, and reduces drying time and weight

Table 2. Selected Grout Formulations: Arranged in Order of Optimum Water Release Performance

Grout no.	Components & proportions	Initial water release: circle 1 (min/sec)	Initial water release: circle 2 (min/sec)	Initial water release: circle 3 (min/sec)	Drying time to constant mass (hr)	Wet weight (g)	Dry weight (g)	Water loss on drying (%)	Diametric shrinkage (%)	Dry density (g/cm^3)	Water vapor permeability ($g/cm^2 \cdot h$)
G81	EA:1; SC:2; PU:1; EGG 5%	7' 10"	11' 15"	not reached	41	77	41.6	38.7	3.18	1.17	6.3×10^{-4}
G75	EA:1; SC:2; SA:0.3; CO:0.2; EGG: 5%	5' 36"	6' 35"	not recorded	78	75	46.8	37.6	4.38	1.04	6.13×10^{-4}
G71	EA:1; SC: 2; SA: 0.3; H: 0.2; EGG: 5%	5' 14"	6' 57"	not recorded	144	83.5	53.1	38.1	4.06	1.12	5.28×10^{-4}
G66	EA:1; SC:2; SA:1; EGG:5%	4' 42"	6" 16"	9' 00"	64	93	66	30.3	4.74	1.25	4.78×10^{-4}
G55	EA:2; SC:1; EGG: 5%	2' 11"	3' 45"	8' 33"	44	87	55	36.78	5.12	3.15	4.31×10^{-4}
G28	EA:2; SC:1; CO:1; EGG: 5%	2' 03"	4' 48"	8' 10"	54	83	54	34.94	3.89	3.13	4.03×10^{-4}
G48	EA:2; SC:1; BR:1; EGG: 5%	1' 48"	4' 08"	9' 00"	51	77	47	38.96	5.12	2.57	4.8×10^{-4}
G61	EA:2; SC:1; H:1; EGG: 5%	1' 35"	3' 40"	7' 37"	50	83	55	39.76	5.12	2.76	6.06×10^{-4}
G60	EA:2; SC:1; H:1	1' 33"	3' 02"	4' 67"	47	81	49	39.51	4.38	2.83	6.08×10^{-4}
G53	EA	1' 15”	2’ 40”	5' 46"	54	104	66	36.5	5.37	3.89	4.74×10^{-4}
G54	EA:2; SC:1	1' 10"	2' 37"	6' 02"	45	86	55	36.05	5.12	3.15	4.4×10^{-4}
G27	EA:2; SC:1; CO:1	1' 10"	2' 30"	5' 55"	72	84	57	32.14	3.64	2.9	4.22×10^{-4}
G47	EA:2; SC:1; BR: 1	0' 46"	1' 37"	3' 28"	47	80	50	37.50	4.14	2.77	4.44×10^{-4}

Abbreviations: EA=Daquan riverbed mud; SC=Scotchlite KI® glass microspheres; PU=Pumex® pumice; SA=local desert sand; CO=local black coal ash; BR=brick dust; H=Harborlite 20x20® perlite; EGG=whisked egg white.

Table 3. Selected Grout Formulations: Arranged by Optimum Drying Time

Grout no.	Components & proportions	Initial water release: circle 1 (min/sec)	Initial water release: circle 2 (min/sec)	Initial water release: circle 3 (min/sec)	Drying time to constant mass (hr)	Wet weight (g)	Dry weight (g)	Water loss on drying (%)	Diametric shrinkage (%)	Dry density (g/cm^3)	Water vapor permeability ($g/cm^2 \cdot h$)
G81	EA:1; SC:2; PU:1; EGG 5%	7' 10"	11' 15"	not reached	41	77	41.6	38.7	3.18	1.17	6.3×10^{-4}
G55	EA:2; SC:1; EGG: 5%	2' 11"	3' 45"	8' 33"	44	87	55	36.78	5.12	3.15	6.14×10^{-4}
G54	EA:2; SC:1	1' 10"	2' 37"	6' 02"	45	86	55	36.05	5.12	3.15	6.06×10^{-4}
G47	EA:2; SC:1; BR: 1	0' 46"	1' 37"	3' 28"	47	80	50	37.50	4.14	2.77	4.84×10^{-4}
G60	EA:2; SC:1; H:1	1' 33"	3' 02"	4' 67"	47	81	49	39.51	4.38	2.83	6.08×10^{-4}
G61	EA:2; SC:1; H:1; EGG: 5%	1' 35"	3' 40"	7' 37"	50	83	55	39.76	5.12	2.76	6.06×10^{-4}
G48	EA:2; SC:1; BR:1; EGG: 5%	1' 48"	4' 08"	9' 00"	51	77	47	38.96	5.12	2.57	4.88×10^{-4}
G28	EA:2; SC:1; CO:1; EGG: 5%	2' 03"	4' 48"	8' 10"	54	83	54	34.94	3.89	3.13	4.94×10^{-4}
G53	EA	1' 15”	2’ 40”	5' 46"	54	104	66	36.5	5.37	3.89	6.06×10^{-4}
G66	EA:1; SC:2; SA:1; EGG:5%	4' 42"	6" 16"	9' 00"	64	93	66	30.3	4.74	1.25	4.78×10^{-4}
G27	EA:2; SC:1; CO:1	1' 10"	2' 30"	5' 55"	72	84	57	32.14	3.64	2.9	5.9×10^{-4}
G75	EA:1; SC:2; SA:0.3; CO:0.2; EGG: 5%	5' 36"	6' 35"	not recorded	78	75	46.8	37.6	4.38	1.04	6.13×10^{-4}
G71	EA:1; SC: 2; SA: 0.3; H: 0.2; EGG: 5%	5' 14"	6' 57"	not recorded	144	83.5	53.1	38.1	4.06	1.12	5.28×10^{-4}

Abbreviations: EA=Daquan riverbed mud; SC=Scotchlite KI® glass microspheres; PU=Pumex® pumice; SA=local desert sand; CO=local black coal ash; BR=brick dust; H=Harborlite 20x20® perlite; EGG=whisked egg white.

Table 4. Selected Grout Formulations: Arranged in Order of Optimum Wet Weight

Grout no.	Components & proportions	Initial water release: circle 1 (min/sec)	Initial water release: circle 2 (min/sec)	Initial water release: circle 3 (min/sec)	Drying time to constant mass (hr)	Wet weight (g)	Dry weight (g)	Water loss on drying (%)	Diametric shrinkage (%)	Dry density (g/cm^3)	Water vapor permeability ($g/cm^2 \cdot h$)
G75	EA:1; SC:2; SA:0.3; CO:0.2; EGG: 5%	5' 36"	6' 35"	not recorded	78	75	46.8	37.6	4.38	1.04	6.13×10^{-4}
G81	EA:1; SC:2; PU:1; EGG 5%	7' 10"	11' 15"	not reached	41	77	41.6	38.7	3.18	1.17	6.3×10^{-4}
G48	EA:2; SC:1; BR:1; EGG: 5%	1' 48"	4' 08"	9' 00"	51	77	47	38.96	5.12	2.57	4.8×10^{-4}
G47	EA:2; SC:1; BR: 1	0' 46"	1' 37"	3' 28"	47	80	50	37.50	4.14	2.77	4.4×10^{-4}
G60	EA:2; SC:1; H:1	1' 33"	3' 02"	4' 67"	47	81	49	39.51	4.38	2.83	6.08×10^{-4}
G28	EA:2; SC:1; CO:1; EGG: 5%	2' 03"	4' 48"	8' 10"	54	83	54	34.94	3.89	3.13	4.03×10^{-4}
G61	EA:2; SC:1; H:1; EGG: 5%	1' 35"	3' 40"	7' 37"	50	83	55	39.76	5.12	2.76	6.06×10^{-4}
G71	EA:1; SC: 2; SA: 0.3; H: 0.2; EGG: 5%	5' 14"	6' 57"	not recorded	144	83.5	53.1	38.1	4.06	1.12	5.28×10^{-4}
G27	EA:2; SC:1; CO:1	1' 10"	2' 30"	5' 55"	72	84	57	32.14	3.64	2.9	4.22×10^{-4}
G54	EA:2; SC:1	1' 10"	2' 37"	6' 02"	45	86	55	36.05	5.12	3.15	4.4×10^{-4}
G55	EA:2; SC:1; EGG: 5%	2' 11"	3' 45"	8' 33"	44	87	55	36.78	5.12	3.15	4.31×10^{-4}
G66	EA:1; SC:2; SA:1; EGG:5%	4' 42"	6" 16"	9' 00"	64	93	66	30.3	4.74	1.25	4.78×10^{-4}
G53	EA	1' 15"	2' 40"	5' 46"	54	104	66	36.5	5.37	3.89	4.74×10^{-4}

Abbreviations: EA=Daquan riverbed mud; SC=Scotchlite KI® glass microspheres; PU=Pumex® pumice; SA=local desert sand; CO=local black coal ash; BR=brick dust; H=Harborlite 20x20® perlite; EGG=whisked egg white.

Table 5. Selected Grout Formulations: Arranged in Order of Optimum Dry Weight

Grout no.	Components & proportions	Initial water release: circle 1 (min/sec)	Initial water release: circle 2 (min/sec)	Initial water release: circle 3 (min/sec)	Drying time to constant mass (hr)	Wet weight (g)	Dry weight (g)	Water loss on drying (%)	Diametric shrinkage (%)	Dry density (g/cm^3)	Water vapor permeability ($g/cm^2 \cdot h$)
G81	EA:1; SC:2; PU:1; EGG 5%	7' 10"	11' 15"	not reached	41	77	41.6	38.7	3.18	1.17	6.3×10^{-4}
G75	EA:1; SC:2; SA:0.3; CO:0.2; EGG: 5%	5' 36"	6' 35"	not recorded	78	75	46.8	37.6	4.38	1.04	6.13×10^{-4}
G48	EA:2; SC:1; BR:1; EGG: 5%	1' 48"	4' 08"	9' 00"	51	77	47	38.96	5.12	2.57	4.8×10^{-4}
G60	EA:2; SC:1; H:1	1' 33"	3' 02"	4' 67"	47	81	49	39.51	4.38	2.83	6.08×10^{-4}
G47	EA:2; SC:1; BR: 1	0' 46"	1' 37"	3' 28"	47	80	50	37.50	4.14	2.77	4.4×10^{-4}
G71	EA:1; SC: 2; SA: 0.3; H: 0.2; EGG: 5%	5' 14"	6' 57"	not recorded	144	83.5	53.1	38.1	4.06	1.12	5.28×10^{-4}
G28	EA:2; SC:1; CO:1; EGG: 5%	2' 03"	4' 48"	8' 10"	54	83	54	34.94	3.89	3.13	4.03×10^{-4}
G61	EA:2; SC:1; H:1; EGG: 5%	1' 35"	3' 40"	7' 37"	50	83	55	39.76	5.12	2.76	6.06×10^{-4}
G54	EA:2; SC:1	1' 10"	2' 37"	6' 02"	45	86	55	36.05	5.12	3.15	4.4×10^{-4}
G55	EA:2; SC:1; EGG: 5%	2' 11"	3' 45"	8' 33"	44	87	55	36.78	5.12	3.15	4.31×10^{-4}
G27	EA:2; SC:1; CO:1	1' 10"	2' 30"	5' 55"	72	84	57	32.14	3.64	2.9	4.22×10^{-4}
G66	EA:1; SC:2; SA:1; EGG:5%	4' 42"	6" 16"	9' 00"	64	93	66	30.3	4.74	1.25	4.78×10^{-4}
G53	EA	1' 15"	2' 40"	5' 46"	54	104	66	36.5	5.37	3.89	4.74×10^{-4}

Abbreviations: EA=Daquan riverbed mud; SC=Scotchlite KI® glass microspheres; PU=Pumex® pumice; SA=local desert sand; CO=local black coal ash; BR=brick dust; H=Harborlite 20x20® perlite; EGG=whisked egg white.

Table 6. Selected Grout Formulations: Arranged in Order of Optimum Shrinkage Performance

Grout no.	Components & proportions	Initial water release: circle 1 (min/sec)	Initial water release: circle 2 (min/sec)	Initial water release: circle 3 (min/sec)	Drying time to constant mass (hr)	Wet weight (g)	Dry weight (g)	Water loss on drying (%)	Diametric shrinkage (%)	Dry density (g/cm^3)	Water vapor permeability ($g/cm^2 \cdot h$)
G81	EA:1; SC:2; PU:1; EGG 5%	7' 10"	11' 15"	not reached	41	77	41.6	38.7	3.18	1.17	6.3×10^{-4}
G27	EA:2; SC:1; CO:1	1' 10"	2' 30"	5' 55"	72	84	57	32.14	3.64	2.9	4.22×10^{-4}
G28	EA:2; SC:1; CO:1; EGG: 5%	2' 03"	4' 48"	8' 10"	54	83	54	34.94	3.89	3.13	4.03×10^{-4}
G71	EA:1; SC: 2; SA: 0.3; H: 0.2; EGG: 5%	5' 14"	6' 57"	not recorded	144	83.5	53.1	38.1	4.06	1.12	5.28×10^{-4}
G47	EA:2; SC:1; BR: 1	0' 46"	1' 37"	3' 28"	47	80	50	37.50	4.14	2.77	4.44×10^{-4}
G75	EA:1; SC:2; SA:0.3; CO:0.2; EGG: 5%	5' 36"	6' 35"	not recorded	78	75	46.8	37.6	4.38	1.04	6.13×10^{-4}
G60	EA:2; SC:1; H:1	1' 33"	3' 02"	4' 67"	47	81	49	39.51	4.38	2.83	6.08×10^{-4}
G66	EA:1; SC:2; SA:1; EGG:5%	4' 42"	6" 16"	9' 00"	64	93	66	30.3	4.74	1.25	4.78×10^{-4}
G55	EA:2; SC:1; EGG: 5%	2' 11"	3' 45"	8' 33"	44	87	55	36.78	5.12	3.15	4.31×10^{-4}
G48	EA:2; SC:1; BR:1; EGG: 5%	1' 48"	4' 08"	9' 00"	51	77	47	38.96	5.12	2.57	4.8×10^{-4}
G61	EA:2; SC:1; H:1; EGG: 5%	1' 35"	3' 40"	7' 37"	50	83	55	39.76	5.12	2.76	6.06×10^{-4}
G54	EA:2; SC:1	1' 10"	2' 37"	6' 02"	45	86	55	36.05	5.12	3.15	4.4×10^{-4}
G53	EA	1' 15”	2’ 40”	5' 46"	54	104	66	36.5	5.37	3.89	4.74×10^{-4}

Abbreviations: EA=Daquan riverbed mud; SC=Scotchlite KI® glass microspheres; PU=Pumex® pumice; SA=local desert sand; CO=local black coal ash; BR=brick dust; H=Harborlite 20x20® perlite; EGG=whisked egg white.

Table 7. Selected Grout Formulations: Arranged in Order of Optimum Water Vapor Permeability

Grout no.	Components & proportions	Initial water release: circle 1 (min/sec)	Initial water release: circle 2 (min/sec)	Initial water release: circle 3 (min/sec)	Drying time to constant mass (hr)	Wet weight (g)	Dry weight (g)	Water loss on drying (%)	Diametric shrinkage (%)	Dry density (g/cm^3)	Water vapor permeability (g/cm^2·h)
G81	EA:1; SC:2; PU:1; EGG 5%	7' 10"	11' 15"	not reached	41	77	41.6	38.7	3.18	1.17	6.3×10^{-4}
G75	EA:1; SC:2; SA:0.3; CO:0.2; EGG: 5%	5' 36"	6' 35"	not recorded	78	75	46.8	37.6	4.38	1.04	6.13×10^{-4}
G60	EA:2; SC:1; H:1	1' 33"	3' 02"	4' 67"	47	81	49	39.51	4.38	2.83	6.08×10^{-4}
G61	EA:2; SC:1; H:1; EGG: 5%	1' 35"	3' 40"	7' 37"	50	83	55	39.76	5.12	2.76	6.06×10^{-4}
G71	EA:1; SC: 2; SA: 0.3; H: 0.2; EGG: 5%	5' 14"	6' 57"	not recorded	144	83.5	53.1	38.1	4.06	1.12	5.28×10^{-4}
G48	EA:2; SC:1; BR:1; EGG: 5%	1' 48"	4' 08"	9' 00"	51	77	47	38.96	5.12	2.57	4.8×10^{-4}
G66	EA:1; SC:2; SA:1; EGG:5%	4' 42"	6" 16"	9' 00"	64	93	66	30.3	4.74	1.25	4.78×10^{-4}
G53	EA	1' 15”	2’ 40”	5' 46"	54	104	66	36.5	5.37	3.89	4.74×10^{-4}
G54	EA:2; SC:1	1' 10"	2' 37"	6' 02"	45	86	55	36.05	5.12	3.15	4.4×10^{-4}
G47	EA:2; SC:1; BR: 1	0' 46"	1' 37"	3' 28"	47	80	50	37.50	4.14	2.77	4.4×10^{-4}
G55	EA:2; SC:1; EGG: 5%	2' 11"	3' 45"	8' 33"	44	87	55	36.78	5.12	3.15	4.31×10^{-4}
G27	EA:2; SC:1; CO:1	1' 10"	2' 30"	5' 55"	72	84	57	32.14	3.64	2.9	4.22×10^{-4}
G28	EA:2; SC:1; CO:1; EGG: 5%	2' 03"	4' 48"	8' 10"	54	83	54	34.94	3.89	3.13	4.03×10^{-4}

Abbreviations: EA=Daquan riverbed mud; SC=Scotchlite KI® glass microspheres; PU=Pumex® pumice; SA=local desert sand; CO=local black coal ash; BR=brick dust; H=Harborlite 20x20® perlite; EGG=whisked egg white.

APPENDIX 17.D

Selected Grout Fillers

Table 1. Selected Grout Fillers: Comparative Mass and Hygral Properties

Material no.	Material description	Container M_1(g)	Dry sample V_1 (ml)	M_1 + dry sample M_2 (g)	Dry sample $M_2 - M_1$ (g)	Vol H_2O added V_2 (ml)	M_1 + wet sample M_3 (g)	Wet sample $M_3 - M_1$ (g)	Vol H_2O-saturated sample V_3 (ml)	Comments
F1	Daquan riverbed mud (<600 μm)	52	80	142	90	33	175	123	80	Very fine particles with high wet and dry mass compared with other materials. Does not require sieving to exclude larger fraction. Water slow to penetrate, with low/moderate quantities required for saturation.
F2	Local desert sand (unsieved)	52	80	189	137	25	214	162	80	Fine, rounded grains and fragments of mixed geological origin. Very high wet and dry mass compared to other materials tested. Water penetrated quickly. Particles dense and nonabsorbent, with low quantities of water required for saturation.
F3	Local desert sand (75-300 μm)	52	80	180	128	28	208	156	80	Finer particles of F3 have slightly lower mass than F2. Smaller particles required slightly more water for saturation.
F4	Jilin Perlite (unsieved)	52	80	62	10	50	112	60	80	Compared to other materials tested, extremely low-mass, low-density, highly absorbent light gray rounded particles and small dark impurities. Material absorbed 5x its volume of water quickly, without volume change.
F5	Jilin Perlite (75-300 μm)	52	80	78	26	50	128	76	75	Water penetrated with more difficulty than F4. Smaller particles in F5 have greater mass than F4. Darker in color than F4 and contained more dark impurities. Loss of volume accompanied addition of water. % water loss after 4 days @ 40^{O}C = 48.
F6	Harborlite 20x20®Perlite (unsieved)	52	80	58	6	47	105	53	80	Lower mass, lighter color, more homogeneous than F4 & F5, with none of the dense dark impurities found in this material. Required less water for saturation.
F7	Harborlite 20x20®Perlite (75-300 μm)	52	80	58	6	51	109	57	70	Not darker in color than F6, unlike differences found in F4 & F5, but water absorption similar to F5. As with F5, volume loss accompanied addition of water.
F8	Local black coal ash (unsieved)	52	80	112	60	44	158	104	92	Comparatively moderate-/ high-mass spherical particles, fragments and dust. Water absorption fairly rapid, accompanied by marked volume increase, which was maintained following drying. Wetted particles immediately clumped together to form a "cake" and emitted a tarry smell.
F9	Local black coal ash (75-300 μm)	52	80	142	90	33	175	123	78	Mass increased markedly following sieving, as many of the larger, porous spherical particles were excluded. Water penetrated much more slowly than F8 but also formed a "cake," surprisingly, instead of the marked volume increase on wetting of F8. Addition of water was accompanied by a slight volume decrease. Tarry smell.
F10	Local gray coal ash (unsieved)	52	80	119	67	55	174	122	87	Moderate/high mass compared with other tested materials, slightly higher than F8. Water absorption fairly rapid, with accompanying "caking" and volume increase, somewhat lower than with F8. Tarry smell.
F11	Local gray coal ash (75-300 μm)	52	80	108	56	60	168	116	85	Unlike F9, finer fraction has lower mass than that of the unsieved material. Water absorbed easily, requiring more water for saturation than F8, F9 or F10, accompanied by volume increase and "caking." Tarry smell.

F12	Local white coal ash (unsieved)	52	80	135	83	39	172	120	82	Very fine particles, initially hydrophobic, with very slow water penetration accompanied by slight volume increase and "caking." Compared to other tested materials, mass is moderate/high.
F13	Local white coal ash (75-300 μm)	52	80	100	48	53	154	102	84	A great deal of material had to be sieved to obtain a sufficient amount for testing. Much of the finer fraction was black. Like F11, the finer fraction is lower in mass than the unsieved material. Addition of water accompanied by volume increase and "caking."
F14	Pumex pumice grade 1/ON® (unsieved)	52	80	128	76	38	166	114	80	Sharp, well-graded particles with excellent potential for improving geometric packing of grout. Water absorption fairly slow. Rapid evaporation: water loss after 4 days @ 40°C = 64.8%. Unlike coal ash, no "caking."
F15	Pumex pumice grade 1/ON® (75-300 μm))	52	80	110	58	50	158	106	80	Finer fraction considerably lower in mass than unsieved material. Sharp, well-graded particles remained separated and did not "cake." The morphology, particle range, water absorption and water release properties of F15 make it very suitable for use as a grout filler.
F16	Silvaperl Vermolite VO® vermiculite	52	80	68	14	50	116	64	80	Large particles with lamellar structure that could not be easily sieved or crushed into a usable size (no particles <450 μm so cannot be injected). Water penetrated easily and evaporated slowly. % water loss after 4 days @ 40°C = 45.5.
F17	OMYA Wollastonite NYAD G® (unsieved)	52	80	100	48	62	161	109	80	Acicular particle shape potentially useful for geometric packing but problematic to inject. High water absorbency and very low evaporation rate are unwanted characteristics. % water loss after 4 days @ 40°C = 38.
F18	Perspex Distribution Ltd. Lucite Perspex VA® ground perspex	52	80	67	15	39	106	54	80	Angular, low-mass material but almost all particles >450 μm so cannot be injected and cannot be crushed. Initially hydrophobic, but subsequently water penetrated with ease. Unsure if totally inert.
F19	Sovitec SA microfine G3® ground glass	52	80	178	126	29	207	155	80	Mass greater than many other materials tested with properties very similar to F2 & F3.
F20	3M Scotchlite KI® glass microspheres	52	80	56.5	4.5	N/A	N/A	N/A	N/A	Extremely low-mass material, which makes it a useful bulking filler. However, its very fine particle size, poor grading, and spherical shape must be counteracted by an additional, angular and well-graded component.

APPENDIX 17.E

Sorbent and Separation Layer Testing

Definitions, Rationale, and Procedures

Vertical Capillary Absorption

Definition: Measurement of the capillary absorption rate, capacity, and sorbency ratio of sorbent layer materials of constant area when vertically suspended over a water source.

Testing rationale: To minimize disruption to the paint surface caused by the mobilization of salts and moisture during grouting, the occurrence of moisture evaporation and salts crystallization at the paint surface needs to be prevented. Measuring the capacity of sorbent materials to absorb moisture in a range of conditions informs selection of those with optimum properties for this task.

Procedure: A series of squares of fixed area (15 × 15 cm) were cut from each test sorbent, and the dry weight was obtained. Each square was then suspended over a container of water with the lower edge touching the surface of the water. Capillary rise was measured after 3 minutes, and the squares were weighed again. The squares were then suspended again over the water until capillary saturation was obtained. The time taken to achieve saturation was recorded for each material, and the final weight was obtained. The sorbency ratio was then calculated using the following:

$$(M_3 - M_1)\ M_1$$

% weight gain following 3 mins was calculated using the following:

$$(100/M_1) \times M_2 - 100$$

% weight gain on saturation was calculated using the following:

$$(100/M_1) \times M_3 - 100$$

Parallel Capillary Absorption

Definition: Measurement of the capillary absorption rate, capacity, and sorbency ratio by sorbent layer materials of constant area laid over a damp capillary mat with constant water source.

Testing rationale: To minimize disruption to the paint surface caused by the mobilization of salts and moisture during grouting, the occurrence of moisture evaporation and salts crystallization at the paint surface needs to be prevented. Measuring the capacity of sorbent materials to absorb moisture in a range of conditions informs selection of those with optimum properties for this task.

Procedure: A series of squares of fixed area (15 × 15 cm) were cut from each test sorbent, and the dry weight was obtained. Each square was then placed horizontally onto a dampened capillary mat fed at one end from a tray of water to ensure a constant moisture supply. A glass plate was then applied over each square to simulate an impermeable press. The squares were removed once uniform surface wetting was observed through the glass plate, or after 1 hour if this did not occur. The wet weights were obtained, and sorbency and % weight gain were calculated as above.

Spray Absorption

Definition: Measurement of saturation capacity and sorbency ratio of sorbent layer materials of constant area suspended vertically and sprayed with water until saturation occurs.

Testing rationale: To minimize disruption to the paint surface caused by the mobilization of salts and moisture during grouting, the occurrence of moisture evaporation and salts crystallization at the paint surface needs to be prevented. Measuring the capacity of sorbent materials to absorb moisture in a range of conditions informs selection of those with optimum properties for this task.

Procedure: A series of squares of fixed area (15 × 15 cm) were cut from each test sorbent, and the dry weight was obtained. Each square was then suspended vertically and sprayed until saturation was reached (i.e., when excess moisture dripped out of the sorbent). The wet weights were obtained, and sorbency and % weight gain were calculated as above.

Table 1a. Sorbent and Separation Layer Materials: Vertical Capillary Absorption Capacity

No.	Manufacturer & name	Dry wt M_1 (g)	Cap rise after 3 mins (cm)	Wet wt after 3 mins M_2 (g)	Wt gain after 3 mins (%)	Wet wt after capillary saturation M_3 (g)	Wt gain after capillary saturation (%)	Capillary saturation time (min)	Sorbency ratio after capillary saturation	Description and comments
S1	Rocky Mountain Environmental Ltd. Grey universal pad	4.86	4	16.53	240.12	N/A	N/A	N/A	N/A	tough gray dimpled pad with perforated outer skin containing recycled fibers. Water collected at bottom and dripped out if lifted up. No capillary rise above 4 cm.
S2	3M Multiformat M-B2001®	5.65	4.5	20.92	270.26	N/A	N/A	N/A	N/A	tough polypropylene/polyester fiber dimpled sheet with perforated outer skin. No capillary rise above 4.5 cm.
S3	Robinson best no. 6® cotton wool	5.11	<0.5	17.02	233.07	N/A	N/A	N/A	N/A	thick multiple layers of cotton wool fibers. No capillary absorption.
S4	Gardman 70000® capillary mat	7.06	8.5	24.47	246.6	31.03	339.51	12	3.39	non-woven polyester fiber matting with acrylate binder. Very good capillarity.
S5	Tesco sponge cloth	10.36	5	29.62	185.9	N/A	N/A	N/A	N/A	dimpled foam household sponge. Max capillarity of 9 cm reached after 60 mins.
S6	Contec/Cravenmount Foamtec®	2.53	0	2.53	0	N/A	N/A	N/A	N/A	yellow porous reticulated polyurethane foam. No capillary absorption.
S7	Contec/Cravenmount PR-89 Procel ®	2.09	6.5	6.64	217.7	N/A	N/A	N/A	N/A	thin (<1 mm) tough white cellulose sheet thermally bonded between two layers of polypropylene fabric. Max capillarity of 10.5 cm reached after 80 mins.
S8	Contec/Cravenmount C2®	1.48	9	3.91	164.19	5.21	252.02	19	2.52	thin (<1 mm) tough white cellulose/polyester sheet with smooth striated texture. Very good capillarity.
S9	Kimberley-Clark Wypall x70 cloth 8384	1.89	9.5	6.58	248.15	8.55	352.38	7	3.52	thin (<1 mm) tough white sheet of paper pulp fiber bonded to tough non-woven polypropylene fabric. Excellent capillarity and wet strength.
S10	Kimberley-Clark Wypall x60 cloth 8371	1.6	8.5	5.08	217.5	6.97	335.62	22	3.35	thin (<1 mm) tough white sheet of paper pulp fiber bonded to tough nonwoven polypropylene fabric. Good capillarity and wet strength.
S11	Kimberley-Clark Wypall x80 cloth 8373	2.71	7	7.39	172.69	11.83	336.53	42	3.36	thin (<1 mm) tough white sheet of paper pulp fiber bonded to tough nonwoven polypropylene fabric. Similar to S10 but slower capillary absorption.
S12	Zecchi Japanese tissue 502	0.17	2.5	0.41	141.17	N/A	N/A	N/A	N/A	extremely thin handmade tissue long-fiber paper. Poor capillarity.
S13	Zecchi Japanese tissue 508	0.34	<0.5	0.39	14.7	N/A	N/A	N/A	N/A	very thin hand-made tissue long-fibre paper. Poor capillarity
S14	Qian Long gongzhi Chinese laid paper	0.49	3	0.8	63.26	N/A	N/A	N/A	N/A	thin (<1 mm) laid paper. Max capillary rise of 5 cm reached after 60 mins.

Table 1b. Sorbent and Separation Layer Materials: Vertical Capillary Absorption Capacity Arranged in Order of Optimum Sorbency

No.	Manufacturer & name	Dry wt M_1 (g)	Cap rise after 3 mins (cm)	Wet wt after 3 mins M_2 (g)	Wt gain after 3 mins (%)	Wet wt after capillary saturation M_3 (g)	Wt gain after capillary saturation (%)	Capillary saturation time (min)	Sorbency ratio after capillary saturation	Description and comments
S9	Kimberley-Clark Wypall x70 cloth 8384	1.89	9.5	6.58	248.15	8.55	352.38	7	3.52	thin (<1 mm) tough white sheet of paper pulp fiber bonded to tough non-woven polypropylene fabric. Excellent capillarity and wet strength.
S4	Gardman 70000® capillary mat	7.06	8.5	24.47	246.6	31.03	339.51	12	3.39	nonwoven polyester fiber matting with acrylate binder. Very good capillarity.
S11	Kimberley-Clark Wypall x80 cloth 8373	2.71	7	7.39	172.69	11.83	336.53	42	3.36	thin (<1 mm) tough white sheet of paper pulp fiber bonded to tough nonwoven polypropylene fabric. Similar to S10 but slower capillary absorption.
S10	Kimberley-Clark Wypall x60 cloth 8371	1.6	8.5	5.08	217.5	6.97	335.62	22	3.35	thin (<1 mm) tough white sheet of paper pulp fiber bonded to tough nonwoven polypropylene fabric. Good capillarity and wet strength.
S8	Contec/Cravenmount C2®	1.48	9	3.91	164.19	5.21	252.02	19	2.52	thin (<1 mm) tough white cellulose/polyester sheet with smooth striated texture. Very good capillarity.
S1	Rocky Mountain Environmental Ltd. Grey universal pad	4.86	4	16.53	240.12	N/A	N/A	N/A	N/A	tough gray dimpled pad with perforated outer skin containing recycled fibers. Water collected at bottom and dripped out if lifted up. No capillary rise above 4 cm.
S2	3M Multiformat M-B2001®	5.65	4.5	20.92	270.26	N/A	N/A	N/A	N/A	tough polypropylene/polyester fiber dimpled sheet with preforated outer skin. No capillary rise above 4.5 cm.
S3	Robinson best no. 6® cotton wool	5.11	<0.5	17.02	233.07	N/A	N/A	N/A	N/A	thick multiple layers of cotton wool fibers. No capillary absorption.
S5	Tesco sponge cloth	10.36	5	29.62	185.9	N/A	N/A	N/A	N/A	dimpled foam household sponge. Max capillarity of 9 cm reached after 60 mins.
S6	Contec/Cravenmount Foamtec®	2.53	0	2.53	0	N/A	N/A	N/A	N/A	yellow porous reticulated polyurethane foam. No capillary absorption.
S7	Contec/Cravenmount PR-89 Procel ®	2.09	6.5	6.64	217.7	N/A	N/A	N/A	N/A	thin (<1 mm) tough white cellulose sheet thermally bonded between two layers of polypropylene fabric. Max capillarity of 10.5 cm reached after 80 mins.
S12	Zecchi Japanese tissue 502	0.17	2.5	0.41	141.17	N/A	N/A	N/A	N/A	extremely thin handmade tissue long-fiber paper. Poor capillarity.
S13	Zecchi Japanese tissue 508	0.34	<0.5	0.39	14.7	N/A	N/A	N/A	N/A	very thin handmade tissue long-fiber paper. Poor capillarity.
S14	Qian Long gongzhi Chinese laid paper	0.49	3	0.8	63.26	N/A	N/A	N/A	N/A	thin (<1 mm) laid paper. Max capillary rise of 5 cm reached after 60 mins.

Table 2a. Sorbent and Separation Layer Materials: Parallel (Surface Contact) Capillary Absorption Capacity

No.	Manufacturer & name	Dry wt M_1 (g)	Wet wt after max capillary absorption M_2 (g)	Wt gain after max capillary absorption (%)	Time to reach max capillary absorption (min)	Sorbency ratio after capillary absorption	Description and comments
S1	Rocky Mountain Environmental Ltd. Grey universal pad	4.91	N/A	N/A	N/A	N/A	tough gray dimpled pad with perforated outer skin containing recycled fibwrs. Very low parallel capillary absorption as poor surface conformance. Removed after 60 mins following minimal uptake. Wt after removal: 5.72 g.
S2	3M Multiformat M-B2001®	5.69	N/A	N/A	N/A	N/A	tough polypropylene/polyester fiber dimpled sheet with perforated outer skin. Similar, slightly better absorption capacity than S1. Removed after 60 mins following minimal uptake. Wt after removal: 11.76 g.
S3	Robinson best no. 6® cotton wool	6.28	N/A	N/A	N/A	N/A	thick multiple layers of cotton wool fibers. Removed after 60 mins following minimal uptake. Wt after removal: 6.84 g.
S4	Gardman 70000® capillary mat	7.06	N/A	N/A	N/A	N/A	nonwoven polyester fiber matting with acrylate binder. Removed after 60 mins following minimal uptake. Wt after removal: 8.97 g.
S5	Tesco sponge cloth	5.63	14.49	157.37	60	1.57	dimpled foam household sponge. Slow uptake. Removed just prior to visible saturation.
S6	Contec/Cravenmount Foamtec®	2.53	N/A	N/A	N/A	N/A	yellow porous reticulated polyurethane foam. No capillary absorption after 60 mins.
S7	Contec/Cravenmount PR-89 Procel ®	2.13	3.48	63.38	53	0.63	thin (<1 mm) tough white cellulose sheet thermally bonded between two layers of polypropylene fabric. Slow, patchy absorption starting at edges.
S8	Contec/Cravenmount C2®	1.54	4.3	179.22	3.3	1.79	thin (<1 mm) tough white cellulose/polyester sheet with smooth striated texture. Rapid absorption.
S9	Kimberley-Clark Wypall x70 cloth 8384	2.02	6.28	210.89	1.45	2.1	thin (<1 mm) tough white sheet of paper pulp fiber bonded to tough nonwoven polypropylene fabric. Rapid absorption and high sorbency ratio. Actual capacity per area higher than S10.
S10	Kimberley-Clark Wypall x60 cloth 8371	1.6	5.02	213.75	2.15	2.13	thin (<1 mm) tough white sheet of paper pulp fiber bonded to tough nonwoven polypropylene fabric. Rapid absorption and high sorbency ratio. Actual capacity per unit area fairly high.
S11	Kimberley-Clark Wypall x80 cloth 8373	3.13	8.69	177.63	3	1.77	thin (<1 mm) tough white sheet of paper pulp fiber bonded to tough nonwoven polypropylene fabric. Rapid absorption. Actual absorption capacity per area higher than S10 and S9.
S12	Zecchi Japanese tissue 502	0.19	0.54	184.21	4	1.84	extremely thin hand-made tissue long-fiber paper. Rapid absorption initially, then slowed down. Actual absorption capacity per unit area very low.
S13	Zecchi Japanese tissue 508	0.26	0.69	165.38	35	1.65	very thin handmade tissue long-fiber paper. Unexpectedly slow absorption, starting at edges. Actual absorption capacity per unit area very low.
S14	Qian Long gongzhi Chinese laid paper	0.55	1.85	236.36	1	2.36	thin (<1 mm) laid paper. Rapid absorption and high sorbency ratio, but actual capacity per unit area is low.

Table 2b. Sorbent and Separation Layer Materials: Parallel (Surface Contact) Capillary Absorption Capacity Arranged in Order of Optimum Sorbency

No.	Manufacturer & name	Dry wt M_1 (g)	Wet wt after max capillary absorption M_2 (g)	Wt gain after max capillary absorption (%)	Time to reach max capillary absorption (min)	Sorbency ratio after capillary absorption	Description and comments
S14	Qian Long gongzhi Chinese laid paper	0.55	1.85	236.36	1	2.36	thin (<1 mm) laid paper. Rapid absorption and high sorbency ratio, but actual capacity per unit area is low.
S10	Kimberley-Clark Wypall x60 cloth 8371	1.6	5.02	213.75	2.15	2.13	thin (<1 mm) tough white sheet of paper pulp fiber bonded to tough nonwoven polypropylene fabric. Rapid absorption and high sorbency ratio. Actual capacity per unit area fairly high.
S9	Kimberley-Clark Wypall x70 cloth 8384	2.02	6.28	210.89	1.45	2.1	thin (<1 mm) tough white sheet of paper pulp fiber bonded to tough nonwoven polypropylene fabric. Rapid absorption and high sorbency ratio. Actual capacity per area higher than S10.
S12	Zecchi Japanese tissue 502	0.19	0.54	184.21	4	1.84	extremely thin hand-made tissue long-fiber paper. Rapid absorption initially, then slowed down. Actual absorption capacity per unit area very low.
S8	Contec/Cravenmount C2®	1.54	4.3	179.22	3.3	1.79	thin (<1 mm) tough white cellulose/polyester sheet with smooth striated texture. Rapid absorption.
S11	Kimberley-Clark Wypall x80 cloth 8373	3.13	8.69	177.63	3	1.77	thin (<1 mm) tough white sheet of paper pulp fiber bonded to tough nonwoven polypropylene fabric. Rapid absorption. Actual absorption capacity per area higher than S10 and S9.
S13	Zecchi Japanese tissue 508	0.26	0.69	165.38	35	1.65	very thin handmade tissue long-fiber paper. Unexpectedly slow absorption, starting at edges. Actual absorption capacity per unit area very low.
S5	Tesco sponge cloth	5.63	14.49	157.37	60	1.57	dimpled foam household sponge. Slow uptake. Removed just prior to visible saturation.
S7	Contec/Cravenmount PR-89 Procel ®	2.13	3.48	63.38	53	0.63	thin (<1 mm) tough white cellulose sheet thermally bonded between two layers of polypropylene fabric. Slow, patchy absorption starting at edges.
S1	Rocky Mountain Environmental Ltd. Grey universal pad	4.91	N/A	N/A	N/A	N/A	tough gray dimpled pad with perforated outer skin containing recycled fibers. Very low parallel capillary absorption as poor surface conformance. Removed after 60 mins following minimal uptake. Wt after removal: 5.72 g.
S2	3M Multiformat M-B2001®	5.69	N/A	N/A	N/A	N/A	tough polypropylene/polyester fibre dimpled sheet with preforated outer skin. Similar, slighly better absorption capacity to S1. Removed after 60 mins following minimal uptake. Wt after removal: 11.76 g
S3	Robinson best no. 6® cotton wool	6.28	N/A	N/A	N/A	N/A	thick multiple layers of cotton wool fibers. Removed after 60 mins following minimal uptake. Wt after removal: 6.84 g.
S4	Gardman 70000® capillary mat	7.06	N/A	N/A	N/A	N/A	non-woven polyester fiber matting with acrylate binder. Removed after 60 mins following minimal uptake. Wt after removal: 8.97 g.
S6	Contec/Cravenmount Foamtec®	2.53	N/A	N/A	N/A	N/A	yellow porous reticulated polyurethane foam. No capillary absorption after 60 mins.

Table 3a. Sorbent and Separation Layer Materials: Spray Absorption Capacity

No.	Manufacturer & name	Dry wt M_1 (g)	Wet wt after spray saturation M_2 (g)	Wt gain after spray saturation (%)	Sorbency ratio after spray saturation	Description and comments
S1	Rocky Mountain Environmental Ltd. Grey universal pad	4.86	37.06	662.55	6.62	tough gray dimpled pad with perforated outer skin containing recycled fibers. Very good spray absorption capacity but pad stiffens .
S2	3M Multiformat M-B2001®	5.65	41.36	632.03	6.32	tough polypropylene/polyester fiber dimpled sheet with perforated outer skin. Similar absorption capacity to S1. but pad does not stiffen.
S3	Robinson best no. 6® cotton wool	5.11	N/A	N/A	N/A	thick multiple layers of cotton wool fibers. Water drips from outer fibers without penetration of water into the mass of cotton fibers.
S4	Gardman 70000® capillary mat	7.06	45.19	540.08	5.4	nonwoven polyester fiber matting with acrylate binder. Very good spray absorption capacity.
S5	Tesco sponge cloth	10.36	57.27	452.79	4.53	dimpled foam household sponge. Good absorption in terms of area, but poor in relation to overall mass.
S6	Contec/Cravenmount Foamtec®	2.53	22.17	776.28	7.76	yellow porous reticulated polyurethane foam. No capillary absorption, but very good absorption when sprayed.
S7	Contec/Cravenmount PR-89 Procel ®	2.09	12.9	517.22	5.17	thin (<1 mm) tough white cellulose sheet thermally bonded between two layers of polypropylene fabric. Average/good spray absorption capacity.
S8	Contec/Cravenmount C2®	1.48	8.47	472.29	4.72	thin (<1 mm) tough white cellulose/polyester sheet with smooth striated texture. Average/good spray absorption capacity.
S9	Kimberley-Clark Wypall x70 cloth 8384	1.89	11.21	493.12	4.93	thin (<1 mm) tough white sheet of paper pulp fiber bonded to tough nonwoven polypropylene fabric. Average/good spray absorption capacity.
S10	Kimberley-Clark Wypall x60 cloth 8371	1.6	10.63	564.37	5.64	thin (<1 mm) tough white sheet of paper pulp fiber bonded to tough nonwoven polypropylene fabric. Average/good spray absorption capacity.
S11	Kimberley-Clark Wypall x80 cloth 8373	2.71	16.58	511.8	5.12	thin (<1 mm) tough white sheet of paper pulp fiber bonded to tough nonwoven polypropylene fabric. Average/good spray absorption capacity.
S12	Zecchi Japanese tissue 502	0.17	1.45	752.94	7.53	extremely thin hand-made tissue long-fiber paper. Compromised result as point prior to saturation difficult to gauge.
S13	Zecchi Japanese tissue 508	0.25	1.41	464	4.64	very thin handmade tissue long-fiber paper. Compromised result as point prior to saturation difficult to gauge.
S14	Qian Long gongzhi Chinese laid paper	0.52	2.25	332.69	3.33	thin (<1 mm) laid paper. Poor spray absorption.

Table 3b. Sorbent and Separation Layer Materials: Spray Absorption Capacity Arranged in Order of Optimum Sorbency

No.	Manufacturer & name	Dry wt M_1 (g)	Wet wt after spray saturation M_2 (g)	Wt gain after spray saturation (%)	Sorbency ratio after spray saturation	Description and comments
S6	Contec/Cravenmount Foamtec®	2.53	22.17	776.28	7.76	yellow porous reticulated polyurethane foam. Poor capillary absorption but very good absorption when sprayed.
S12	Zecchi Japanese tissue 502	0.17	1.45	752.94	7.53	extremely thin handmade tissue long-fiber paper. Compromised result as point prior to saturation difficult to gauge.
S1	Rocky Mountain Environmental Ltd. Grey universal pad	4.86	37.06	662.55	6.62	tough gray dimpled pad with perforated outer skin containing recycled fibers. Very good spray absorption capacity, but pad stiffens.
S2	3M Multiformat M-B2001®	5.65	41.36	632.03	6.32	tough polypropylene/polyester fiber dimpled sheet with perforated outer skin. Similar absorption capacity to S1, but pad does not stiffen.
S10	Kimberley-Clark Wypall x60 cloth 8371	1.6	10.63	564.37	5.64	thin (<1 mm) tough white sheet of paper pulp fiber bonded to tough nonwoven polypropylene fabric. Average/good spray absorption capacity.
S4	Gardman 70000® capillary mat	7.06	45.19	540.08	5.4	nonwoven polyester fiber matting with acrylate binder. Very good spray absorption capacity.
S7	Contec/Cravenmount PR-89 Procel ®	2.09	12.9	517.22	5.17	thin (<1 mm) tough white cellulose sheet thermally bonded between two layers of polypropylene fabric. Average/good spray absorption capacity.
S11	Kimberley-Clark Wypall x80 cloth 8373	2.71	16.58	511.8	5.12	thin (<1 mm) tough white sheet of paper pulp fiber bonded to tough nonwoven polypropylene fabric. Average/good spray absorption capacity.
S9	Kimberley-Clark Wypall x70 cloth 8384	1.89	11.21	493.12	4.93	thin (<1 mm) tough white sheet of paper pulp fiber bonded to tough nonwoven polypropylene fabric. Average/good spray absorption capacity.
S8	Contec/Cravenmount C2®	1.48	8.47	472.29	4.72	thin (<1 mm) tough white cellulose/polyester sheet with smooth striated texture. Average/good spray absorption capacity.
S13	Zecchi Japanese tissue 508	0.25	1.41	464	4.64	very thin handmade tissue long-fiber paper. Compromised result as point prior to saturation difficult to gauge.
S5	Tesco sponge cloth	10.36	57.27	452.79	4.53	dimpled foam household sponge. Good absorption in terms of area, but poor in relation to overall mass.
S14	Qian Long gongzhi Chinese laid paper	0.52	2.25	332.69	3.33	thin (<1 mm) laid paper. Poor spray absorption.
S3	Robinson best no. 6® cotton wool	5.11	N/A	N/A	N/A	thick multiple layers of cotton wool fibrrs. Water drips from outer fibers without penetration of water into the mass of cotton fibers.

APPENDIX 17.F

Grout Log Examples

Grouting Log

Dunhuang Academy: Cave 85

Grout area number: ___10___ **Void dimensions (cm):** __40 x 40 cm

Grout area location: Wall/slope; level: _______W wall 2nd lift south
(NB: attach print-out of grout location image and mark on void area)

Condition of plaster prior to grouting: (severity of delamination; cohesion of plaster, etc.) Bulging and delamination associated with vertical crack from top of wall, previously patched during the original painting intervention. Problem is an old one reasserting itself. Plaster is lacking in cohesion, particularly around the crack and hole associated with it.
Condition of painting prior to grouting: (punctate eruptions; paint loss; discoloration; etc.) Fair amount of painting survives in this area. Quite a lot of green landscape background, some figures, but upper layers lost. Only tenacious colors – red, green, and black survive.

Date	Time	Grout quantity (ml)	Added water (ml)	No. holes made	No. holes used	Additional information (problems encountered, etc.)
12/08/03	am	*515*	*65*	2	1	First grout area to be undertaken entirely by members of DA team. Press applied and changed twice daily, top layers only.
14/08/03	am					First appearance of moisture on the surface.
18/08/03	am					First small ridge formed in the exposed upper plaster to right of the vertical crack, pressed down successfully using tissue and silk ball.
21/08/03	am					First ridge formed again but diminished. Pressed down with gelatin and spatula through tissue. Second, soft ridge formed at base of vertical crack to the left and at upper edge on right. Treated with gelatin and pressed back with wooden spatula.
23/08/03	am					Ridge is no longer forming, but the area has a slightly uneven appearance due to indenting of the friable plaster surface using the wooden spatula.
25/08/03	am					No further changes to surface appearance. Press only changed 1 time daily from now on.
05/09/03	am					No temperature difference between grouted and adjacent areas. Press not changed but left in place over the weekend.
08/09/03	am					Press removed.
10/09/03	am					Area completely dry and stable.

Drying time	29 days
Total amount of grout	515 ml
Total amount of water added	65 ml (12.6%)

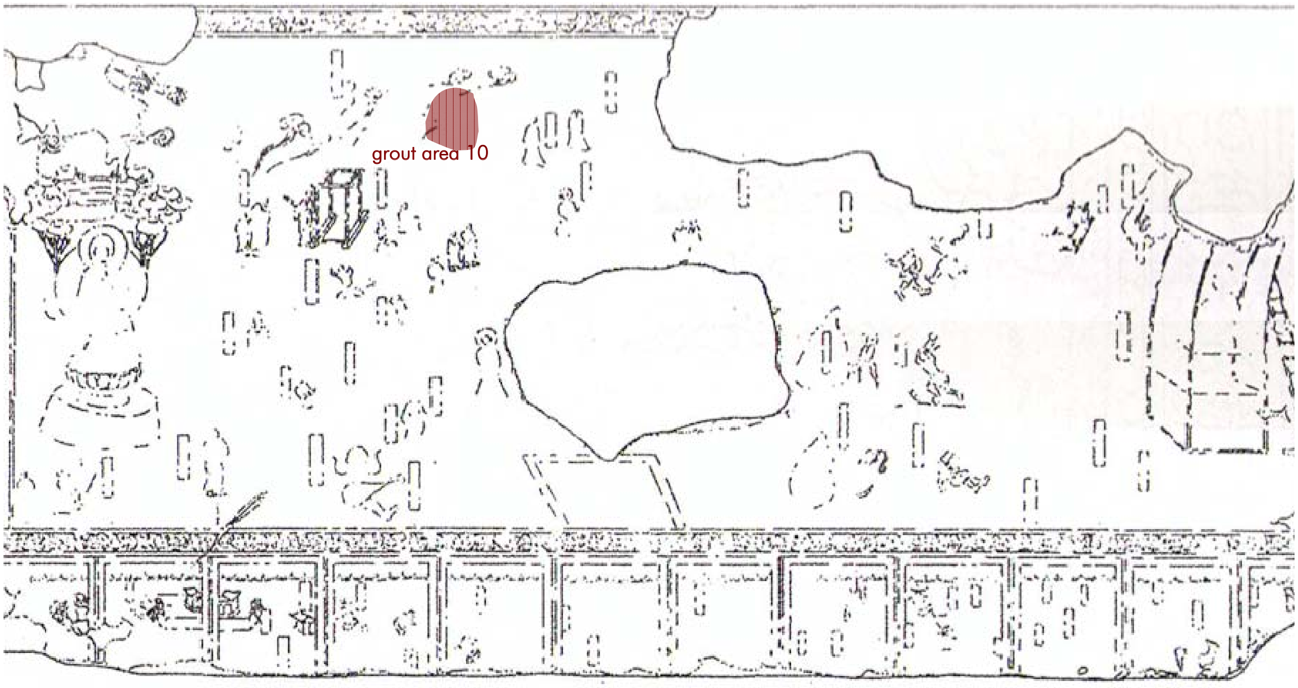

Grouting Log

Dunhuang Academy: Cave 85

Grout area number: ___12___ **Void dimensions (cm):** __60 x 80 cm

Grout area location: Wall/slope; level: _______N slope 2nd lift west side
(NB: attach print-out of grout location image and mark on void area)

Condition of plaster prior to grouting: (severity of delamination; cohesion of plaster; etc.) Cohesive in appearance. Grout area is located at edge of large loss to left of bulge. This links up to the large loss adjacent to grout area 11. Around the perimeters of the loss, the plaster is cracked and bulging, particularly to the right of the loss.	
Condition of painting prior to grouting: (punctate eruptions; paint loss; discoloration; etc.) Above and to the right of the loss considerable paint loss down to the upper plaster layer, in entire corner, but particularly in immediate vicinity of the loss. Otherwise more painting left than on any place on the west wall.	

Date	Time	Grout quantity (ml)	Added water (ml)	No. holes used	No. holes made	Additional information (problems encountered, etc.)
18/08/03	am pm	*320* *630*	*25* *50*	3	3	Second area to be grouted on slope.
19/08/03	am	*665*	*45*			Area of detachment of upper plaster layer temporarily separated after grouting but was faced up using thick tissue and water, pressed, and was ok next day.
21/08/03	am					Surface very wet in appearance, and superficial salts efflorescences visible around the plaster loss in which the original access hole had been made. This was faced with water and thick tissue in an attempt to mobilize the salts into the tissue. Press then replaced.
25/08/03						Fairly severe ridge formed at top of grout area at interface with remaining void, which was a bit unstable. A proposal to conduct further grouting in this area to stabilize was decided as unnecessary and potentially dangerous given the position of the void, so no further grouting was conducted.
29/08/03						Some paint flaking occurring on the west side of the void area. A further application of water and thick tissue was applied to mobilize salts into the tissue. Press then replaced.
26/09/03						Grout area completely dry and stable.

Drying time	40 days
Total amount of grout	1,615 ml
Total amount of water added	120 ml

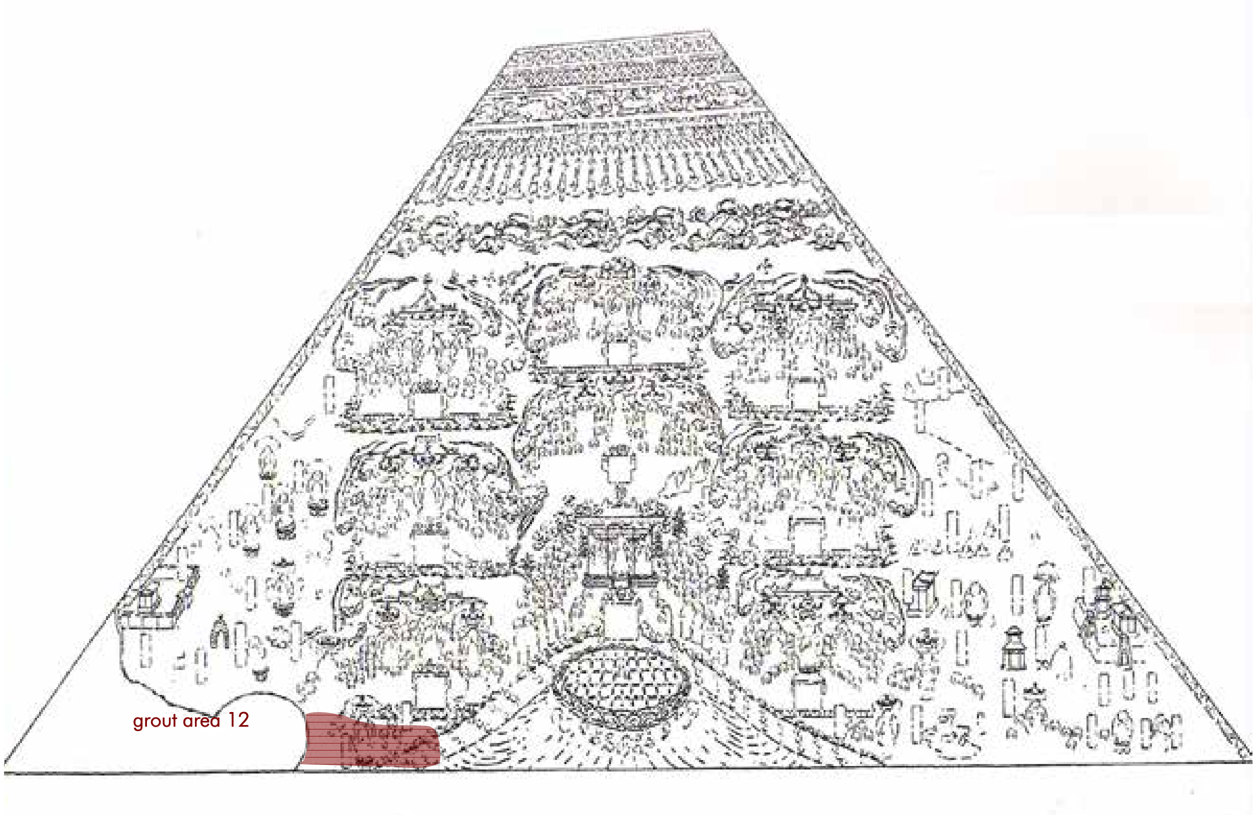

Grouting Log

Dunhuang Academy: Cave 85

Grout area number: 21 **Void dimensions (cm):** approx. 200 x 200 cm

Grout area location: Wall/slope; level: E wall N side 1st and 2nd lifts
(NB: attach print-out of grout location image and mark on void area)

Condition of plaster prior to grouting: (severity of delamination; cohesion of plaster, etc.)

Plaster in some places is extremely thick – probably up to 2 cm. Generally good condition, with good cohesion on surface and at depth. Very little evidence of salts disruption. However, plaster is severely delaminating across a wide area, associated with severe cracking reappearing along lines of original stress cracks formed during drying of original plaster. Some years ago (Fan Tou was around) a metal anchor was cement-bedded 30-40 cm into the wall in an area of the severest plaster cracking and delamination.

Condition of painting prior to grouting: (punctate eruptions; paint loss; discoloration; etc.)

Paint condition generally good, with entire stratigraphy surviving over much of the area, but flaking down to the plaster layer is widespread.

Date	**Time**	**Grout quantity** (ml)	**Added water (ml)**	**No. holes made**	**No. holes used**	**Additional information** (problems encountered, etc.)
25-03-04	11-00	2125	85	**6**	**4**	Grouting initiated and press put in place following grouting.
26-03-04	10.00 14-40	1665 1865	95 115			AM press changed – all layers as damp down to clay layer. Existing holes used.
27-03-04	10.20 14.20	985 1270	75 40	**3**	**3**	AM press changed – all layers as damp down to clay layer. Existing and new holes used.
28-03-04						Sunday – press changed once at 10.00 am.
29-03-04	11.00	2880	155			AM press changed – all layers as damp down to clay layer. Pause in grouting to allow drying. Existing holes used.
30-03-04		-	-			AM press changed – all layers as damp down to clay layer. Pause in grouting to allow drying.
31-03-04		-	-			AM press changed – all layers as damp down to clay layer. Pause in grouting to allow drying.
01-04-04	10.30	1620 2000	25 40	3	2	AM press changed – all layers as damp down to clay layer. Resumed grouting. Existing and new holes used.
02-04-04	09-30 2.00	3,350 3,145	30 0			AM press changed – all layers as damp down to clay layer. Some wrinkling of the paint layer on the surface of the very damp and most recently grouted areas. Resumed grouting further to left of this area. Existing holes used.
03-04-04		-	-			AM press changed – all layers as damp down to clay layer. Some wrinkling of the paint layer on the surface of the very damp and most recently grouted areas.
04-04-04						Press changed (Sunday).
05-04-04						AM & PM press changed –all layers as damp down to clay layer.
06-04-04	9.30	800	50	3	3	AM press changed. Last pockets at upper right grouted. Press replaced.
07-04-04						AM & PM press changed – top layers only. Every day for next few days 16.
16-04-04						Top layers still being replaced twice daily.

Drying time	Completed after end campaign
Total amount of grout	21,705 ml
Total amount of water added	710 ml (3.3%)

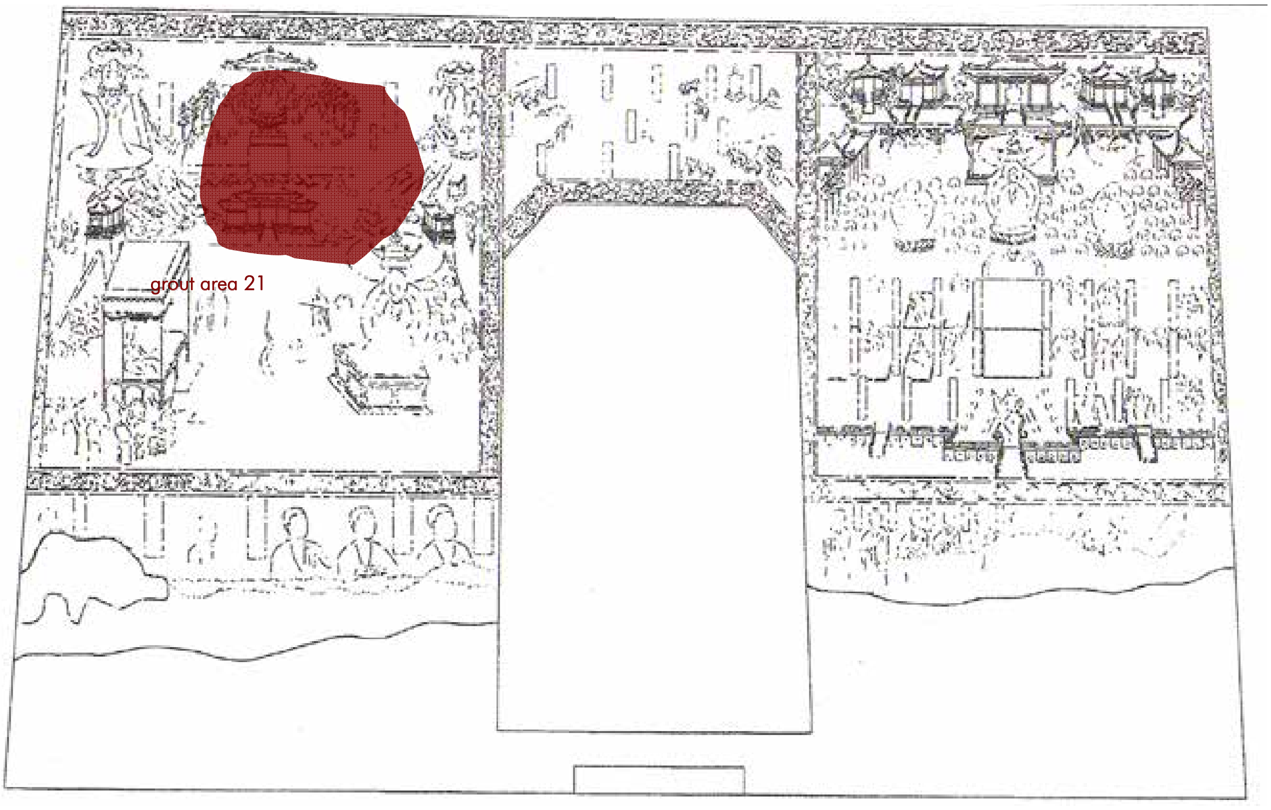

APPENDIX 17.G

Graphic Documentation—Treatment: Grouting

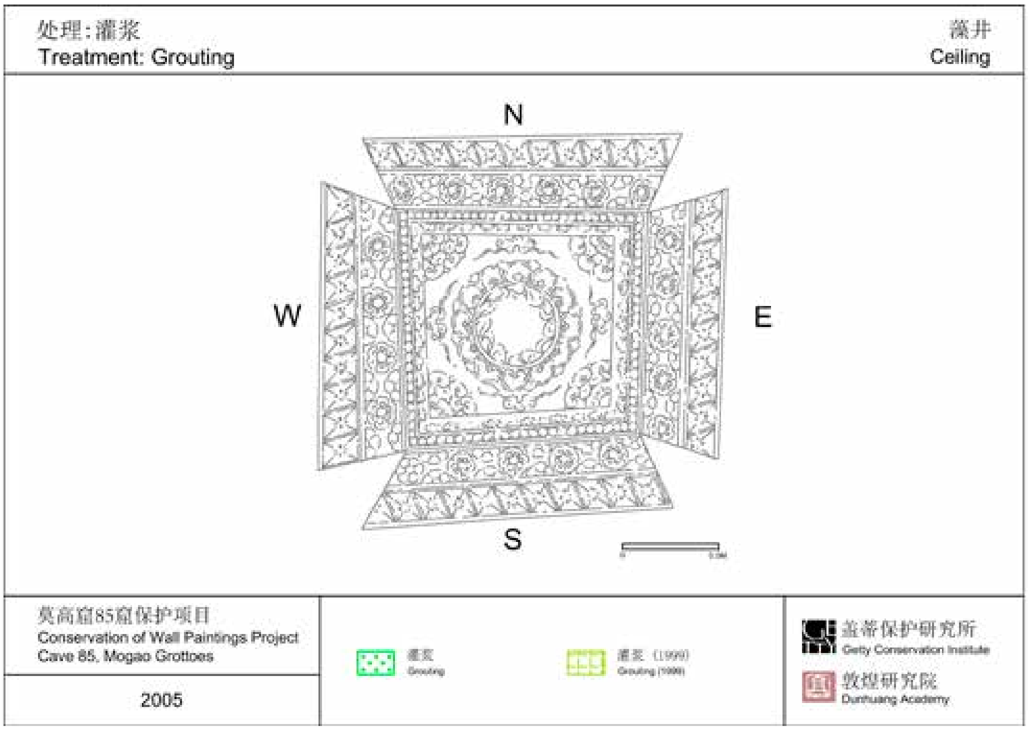

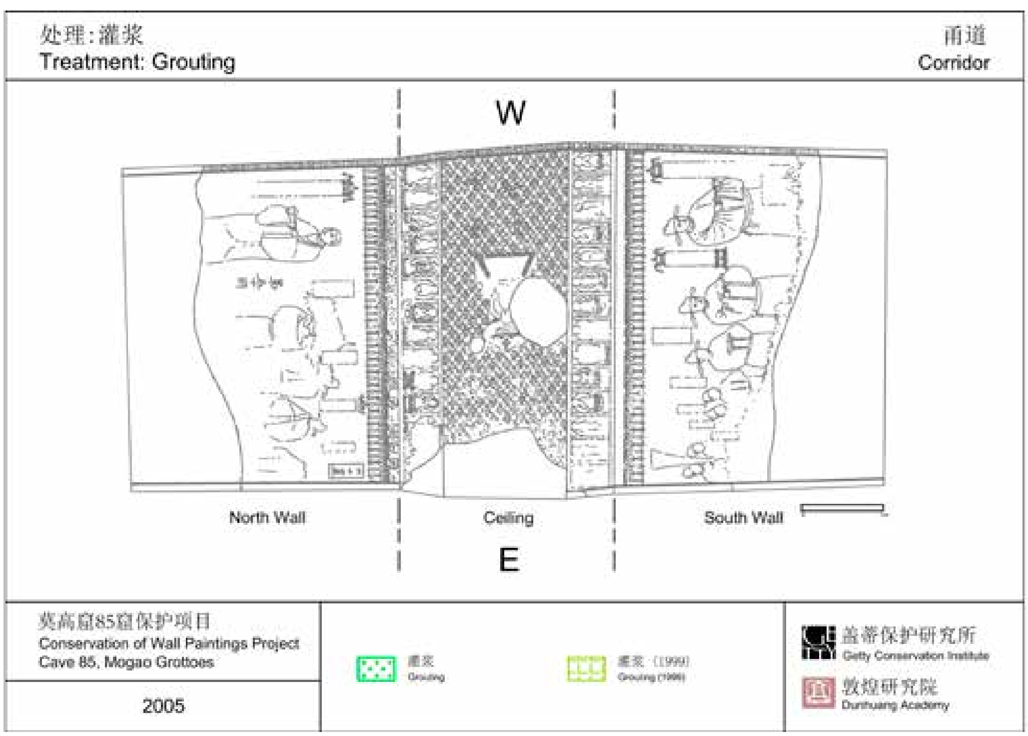

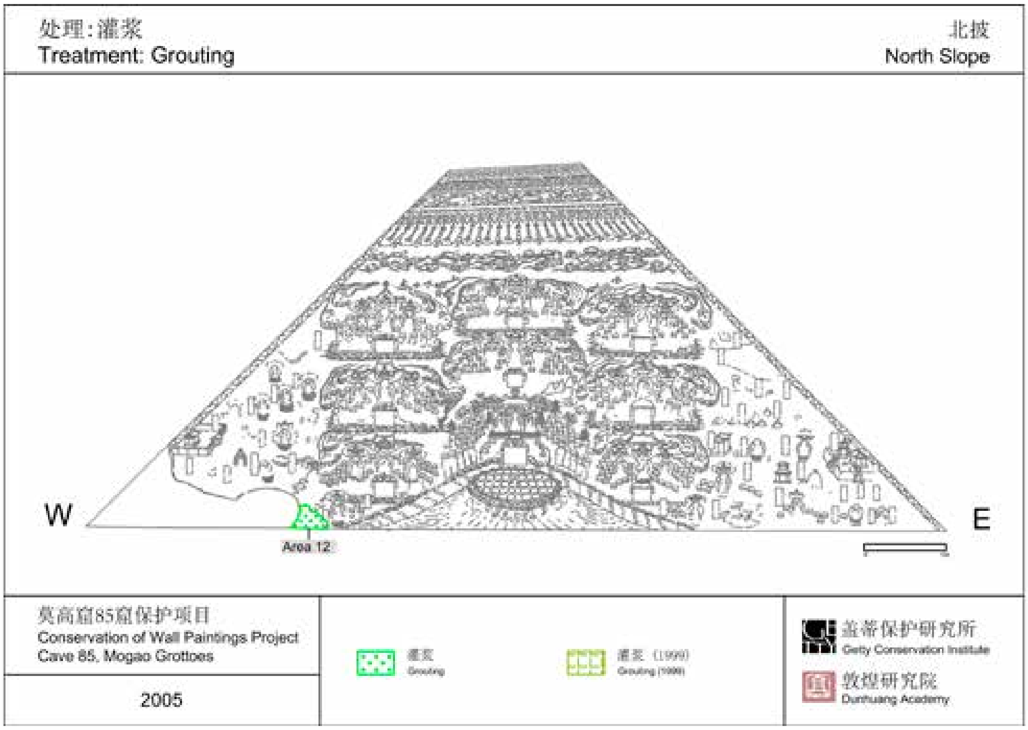
处理:灌浆
Treatment: Grouting
北披
North Slope
W
E
Area 12
莫高窟85窟保护项目
Conservation of Wall Paintings Project
Cave 85, Mogao Grottoes
2005
灌浆
Grouting
灌浆（1999）
Grouting (1999)
盖蒂保护研究所
Getty Conservation Institute
敦煌研究院
Dunhuang Academy

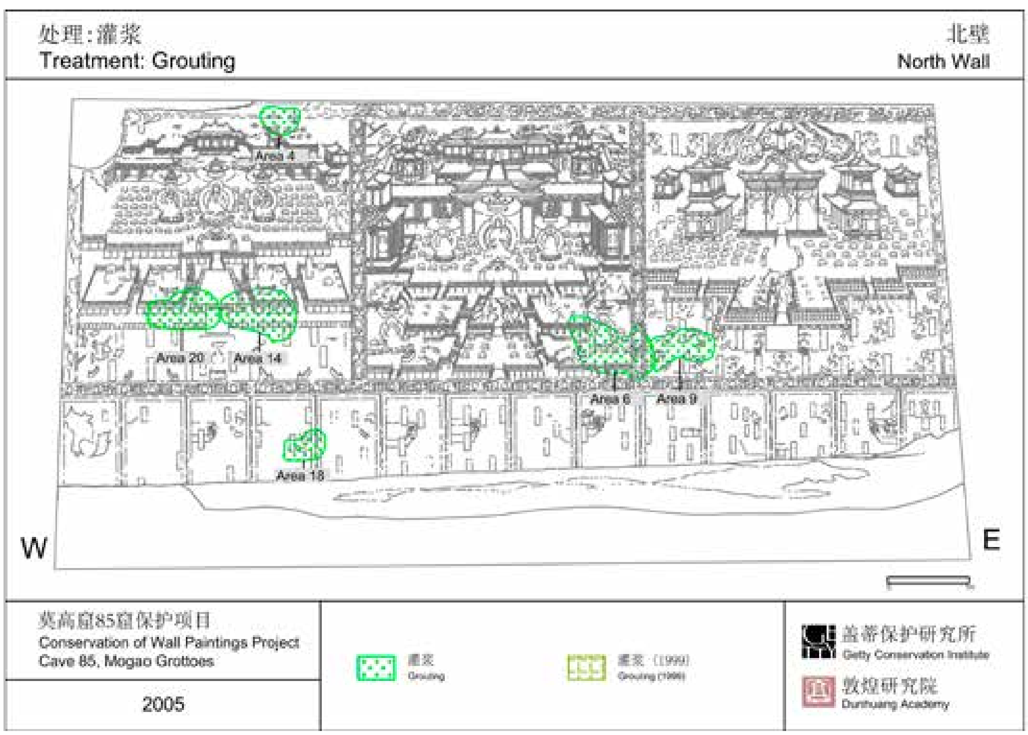
处理:灌浆
Treatment: Grouting
北壁
North Wall
Area 4
Area 20
Area 14
Area 6
Area 9
Area 18
W
E
莫高窟85窟保护项目
Conservation of Wall Paintings Project
Cave 85, Mogao Grottoes
2005
灌浆
Grouting
灌浆（1999）
Grouting (1999)
盖蒂保护研究所
Getty Conservation Institute
敦煌研究院
Dunhuang Academy

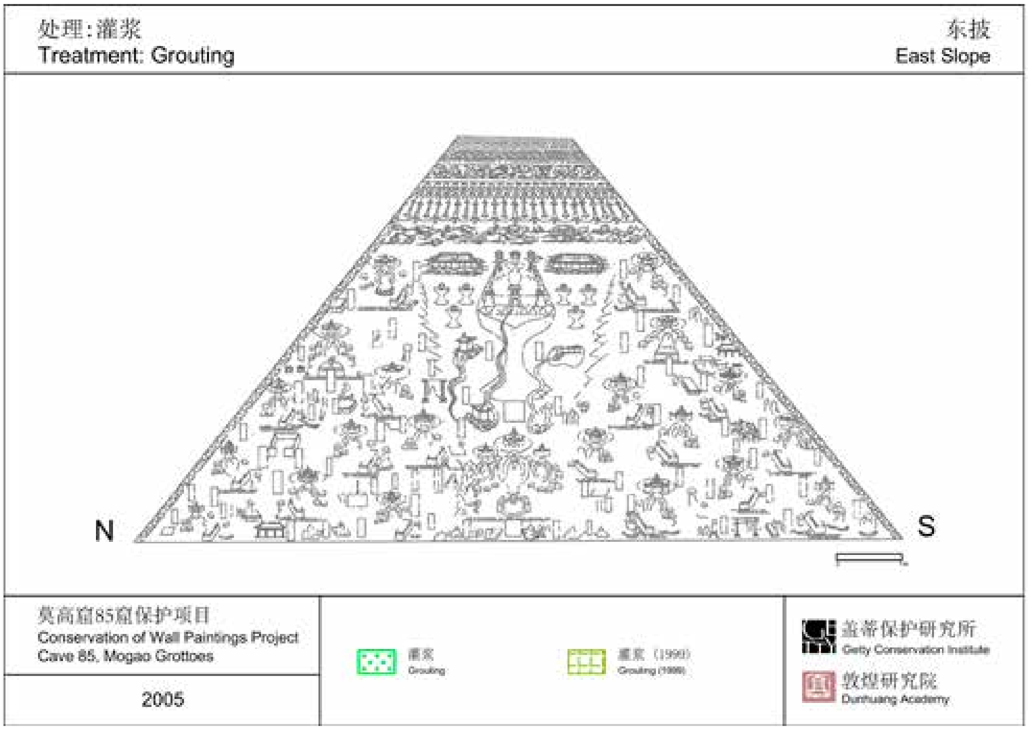
处理:灌浆
Treatment: Grouting
东披
East Slope
N
S
莫高窟85窟保护项目
Conservation of Wall Paintings Project
Cave 85, Mogao Grottoes
2005
灌浆
Grouting
灌浆（1999）
Grouting (1999)
盖蒂保护研究所
Getty Conservation Institute
敦煌研究院
Dunhuang Academy

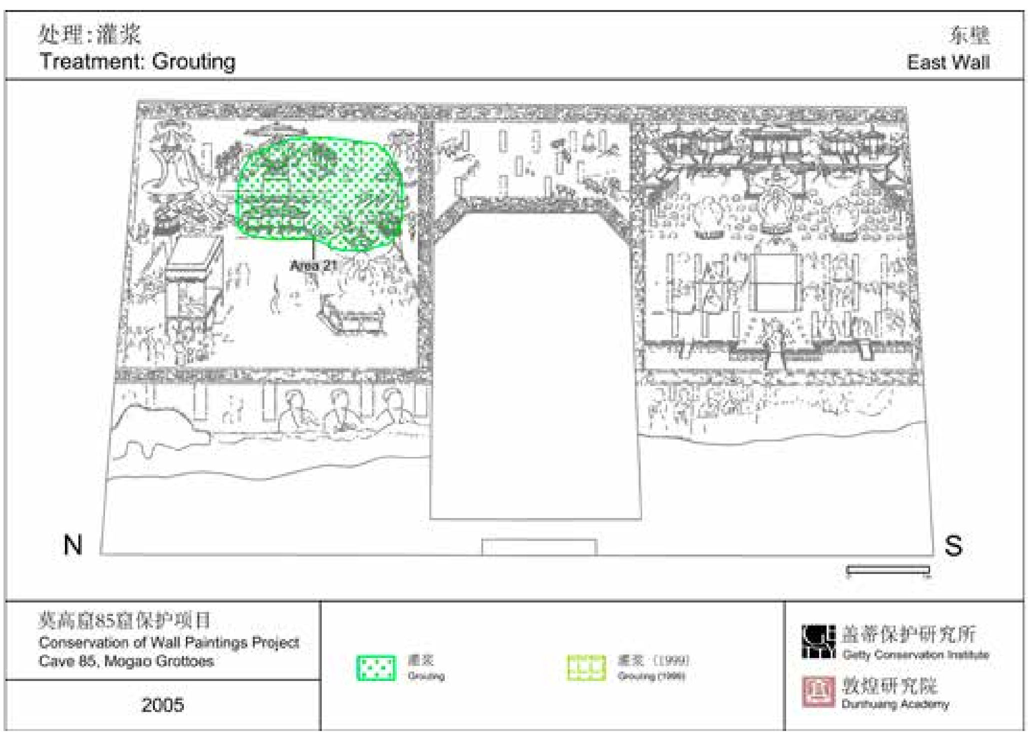
处理:灌浆
Treatment: Grouting
东壁
East Wall
Area 21
N
S
莫高窟85窟保护项目
Conservation of Wall Paintings Project
Cave 85, Mogao Grottoes
2005
灌浆
Grouting
灌浆（1999）
Grouting (1999)
盖蒂保护研究所
Getty Conservation Institute
敦煌研究院
Dunhuang Academy

处理:灌浆
Treatment: Grouting

南披
South Slope

莫高窟85窟保护项目
Conservation of Wall Paintings Project
Cave 85, Mogao Grottoes

2005

灌浆
Grouting

灌浆 (1999)
Grouting (1999)

盖蒂保护研究所
Getty Conservation Institute

敦煌研究院
Dunhuang Academy

处理:灌浆
Treatment: Grouting

南壁
South Wall

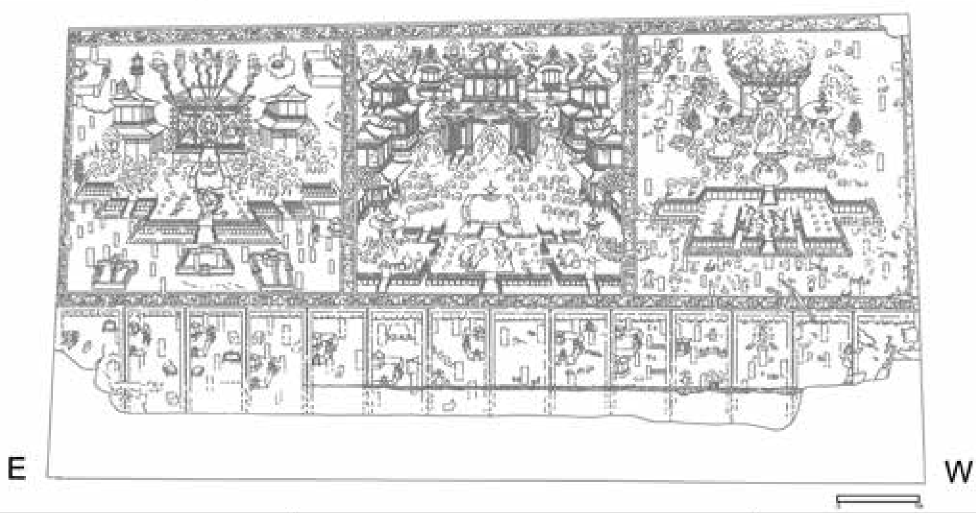

莫高窟85窟保护项目
Conservation of Wall Paintings Project
Cave 85, Mogao Grottoes

1998

灌浆
Grouting

灌浆 (1999)
Grouting (1999)

盖蒂保护研究所
Getty Conservation Institute

敦煌研究院
Dunhuang Academy

处理：灌浆
Treatment: Grouting

西披
West Slope

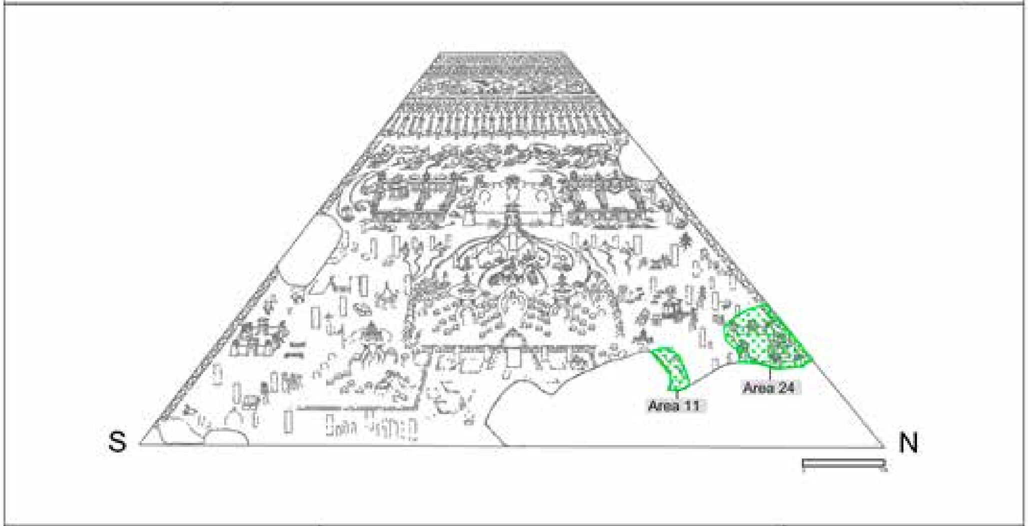

莫高窟85窟保护项目
Conservation of Wall Paintings Project
Cave 85, Mogao Grottoes

2005

灌浆 Grouting

灌浆 (1999) Grouting (1999)

盖蒂保护研究所
Getty Conservation Institute

敦煌研究院
Dunhuang Academy

处理：灌浆
Treatment: Grouting

西壁
West Wall

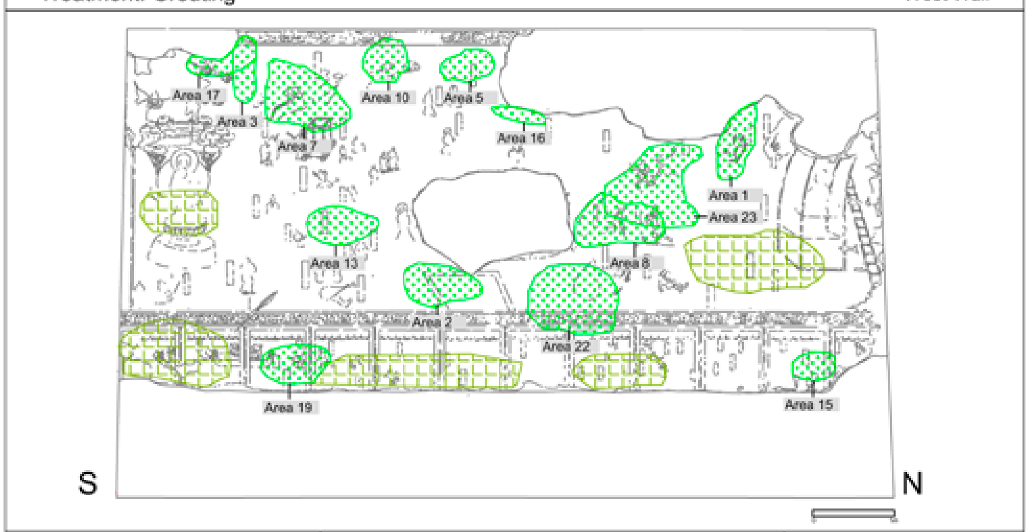

莫高窟85窟保护项目
Conservation of Wall Paintings Project
Cave 85, Mogao Grottoes

2005

灌浆 Grouting

灌浆 (1999) Grouting (1999)

盖蒂保护研究所
Getty Conservation Institute

敦煌研究院
Dunhuang Academy

APPENDIX 19.A

Light Monitoring

莫高窟**85**窟照明监测

Light Monitoring in Cave 85, Mogao Grottoes

85窟主室东壁勒克斯（烛光）强度的测绘图
勒克斯强度由曝光值计算出来的，曝光值由 Sekonic 测光仪测出来的（Multimaster L-408）.

Mapping of Lux Levels on East Wall of Main Chamber
Lux levels were calculated from exposure values (Ev) measured with a Sekonic exposure meter (Multimaster L-408).

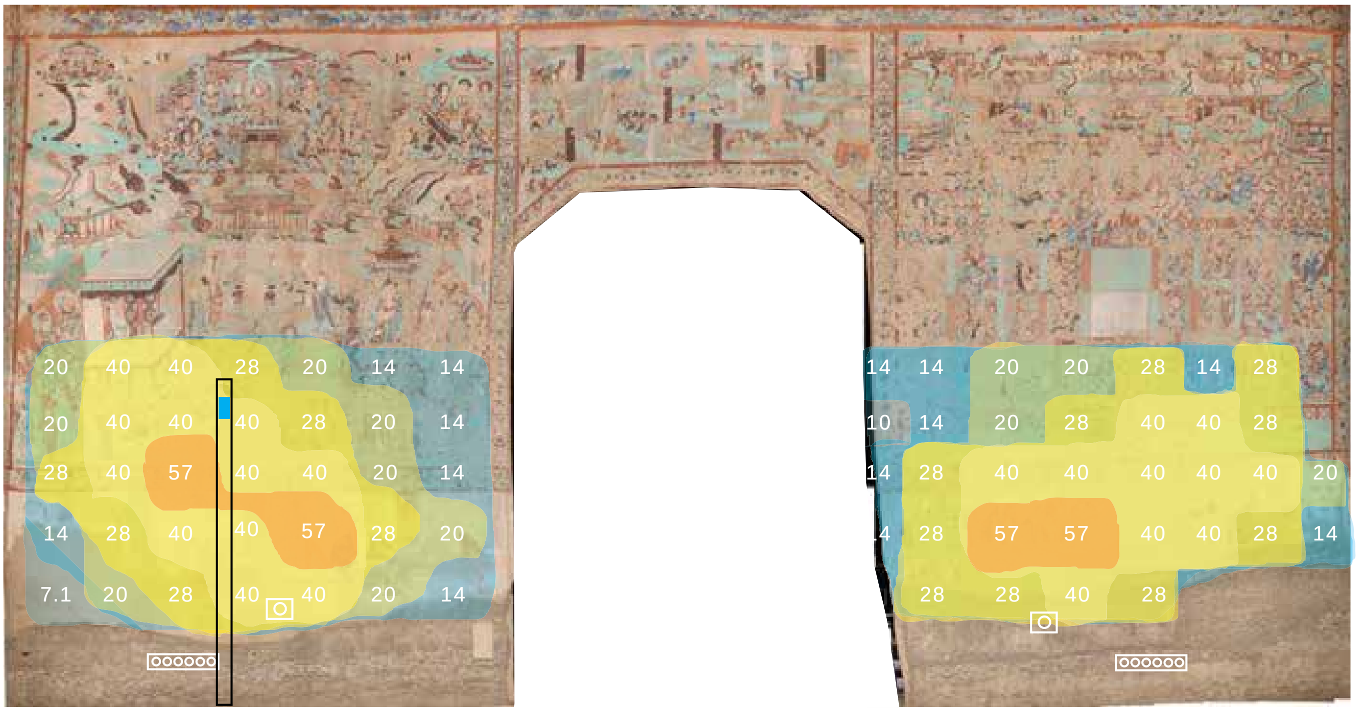

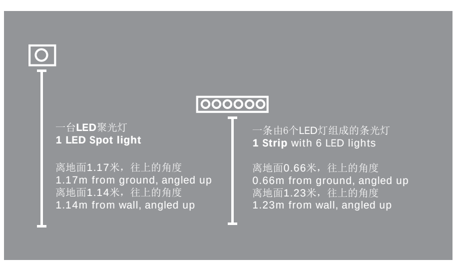

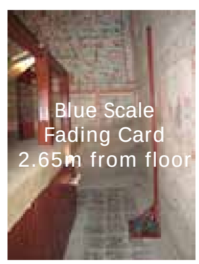

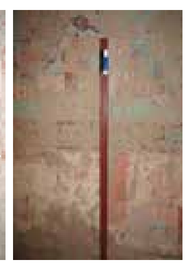

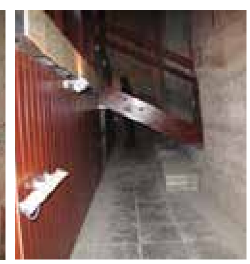

莫高窟85窟照明监测

85窟主室北壁勒克斯（烛光）强度的测绘图
勒克斯强度由曝光值计算出来的，曝光值由 Sekonic 测光仪测出来的（Multimaster L-408）.

Light Monitoring in Cave 85, Mogao Grottoes

Mapping of Lux Levels on North Wall of Main Chamber
Lux levels were calculated from exposure values (Ev) measured with a Sekonic exposure meter (Multimaster L-408).

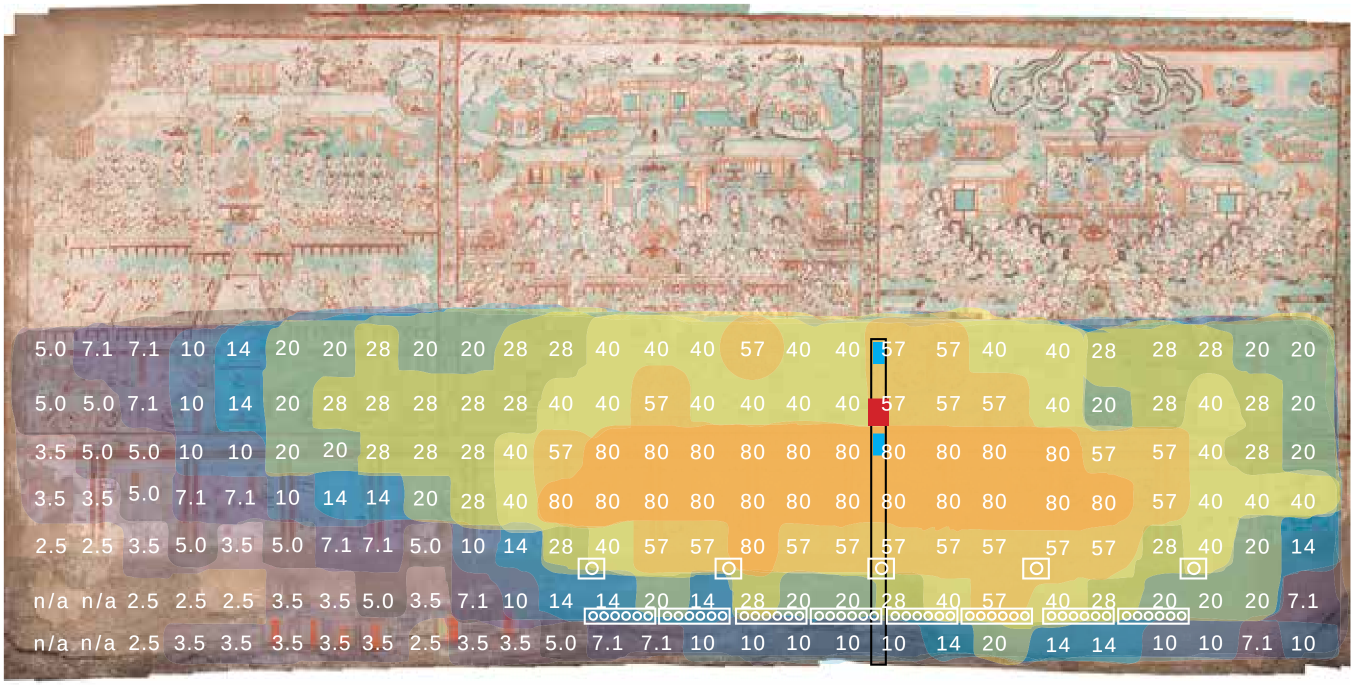

五台**LED**聚光灯
5 LED Spot light

离地面1.17米，往上的角度
1.17m from ground, angled up
离地面1.20米，往上的角度
1.20m from wall, angled up

八条由6个LED灯组成的条光灯
8 Strip with 6 LED lights

离地面0.67米，往上的角度
0.67m from ground, angled up
离地面1.28米，往上的角度
1.28m from wall, angled up

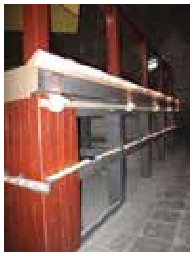

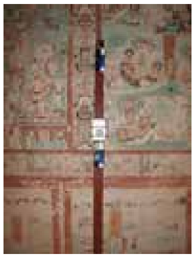

莫高窟**85**窟照明监测

85窟主室南壁勒克斯（烛光）强度的测绘图
勒克斯强度由曝光值计算出来的，曝光值由 Sekonic 测光仪测出来的（Multimaster L-408）.

Light Monitoring in Cave 85, Mogao Grottoes

Mapping of Lux Levels on South Wall of Main Chamber
Lux levels were calculated from exposure values (Ev) measured with a Sekonic exposure meter (Multimaster L-408).

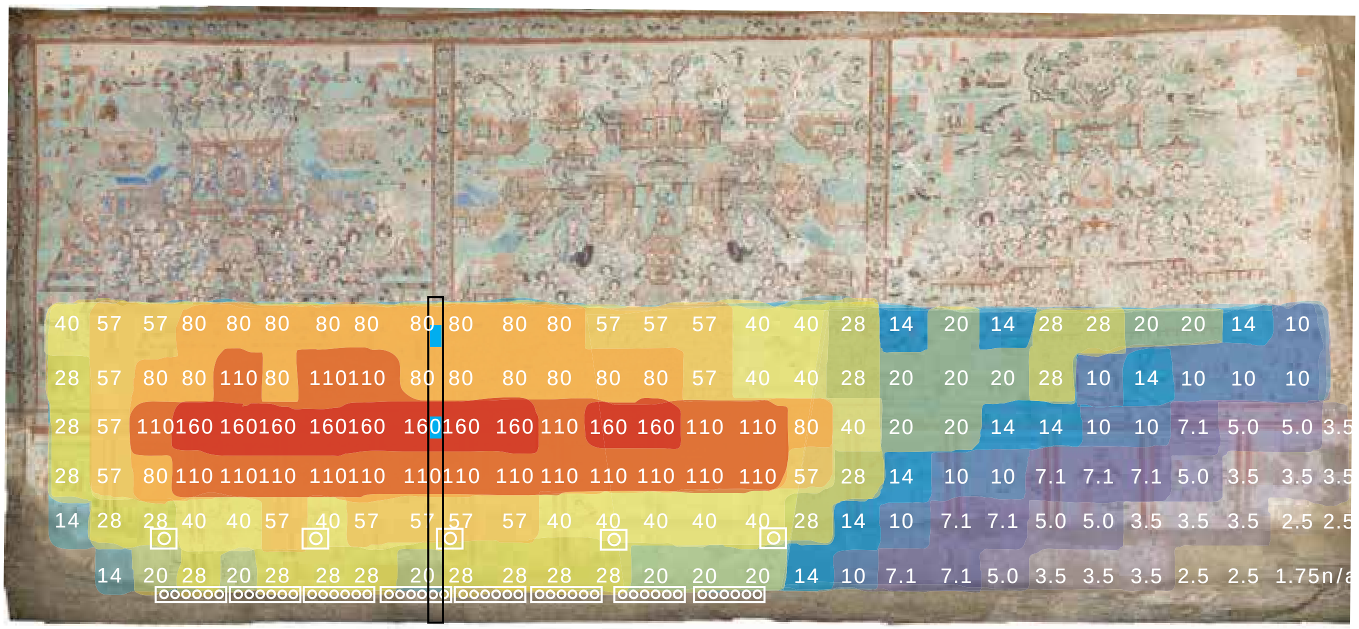

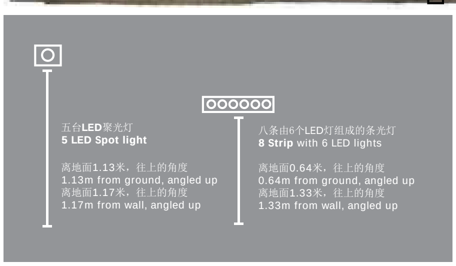

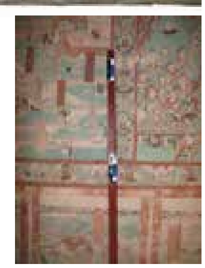

莫高窟**85**窟照明监测

Light Monitoring in Cave 85, Mogao Grottoes

85窟主室西壁勒克斯（烛光）强度的测绘图
勒克斯强度由曝光值计算出来的，曝光值由 Sekonic 测光仪测出来的（Multimaster L-408）.

Mapping of Lux Levels on West Wall of Main Chamber
Lux levels were calculated from exposure values (Ev) measured with a Sekonic exposure meter (Multimaster L-408).

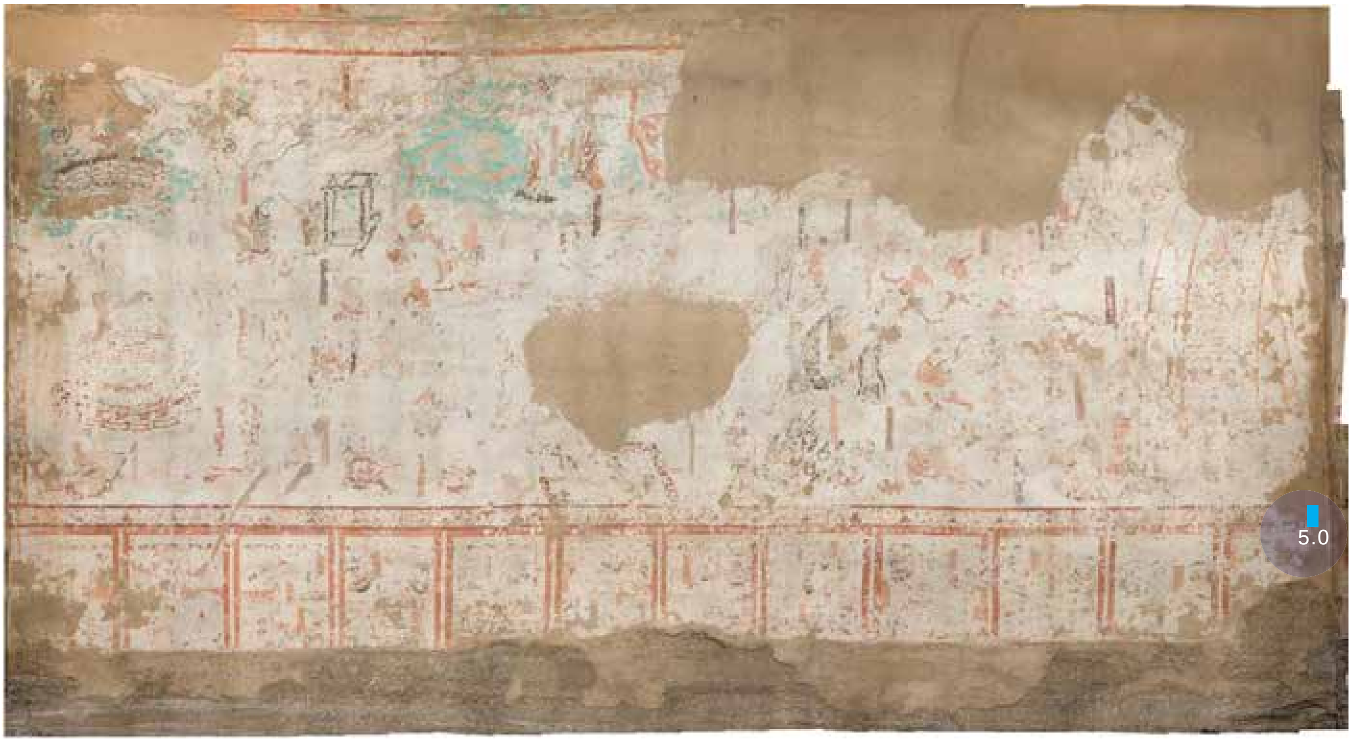

三台**LED**聚光灯
3 LED Spot light

Postioned to light statues, angled up

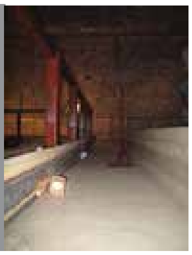

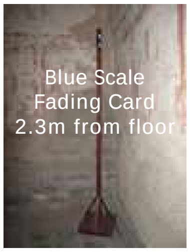

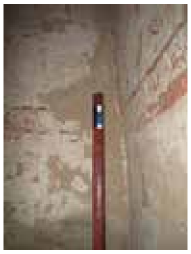

APPENDIX 19.B

Interpretive Panels

壁画和塑像

Wall Painting and Sculpture

第85窟绘有350平方米的壁画。主要壁画绘制于晚唐(公元848-公元907)时期，后经五代(公元907-公元979)与元代(公元1279-公元1368)两次局部重修。大佛坛上的塑像群也为晚唐之作，20世纪初大量重修。

Cave 85 is decorated with 350 square meters of wall painting. The main scheme of painting dates from the construction of the cave during the Late Tang dynasty (848-907 CE). There are two later periods of localized redecoration from the Five Dynasties (907-979) and the Yuan dynasty (1279-1368). A sculpture group on a large altar platform also dates from the Late Tang but was extensively restored in the early 20th century.

第85窟主室北壁三幅大型经变画。
The north wall of the main chamber of Cave 85 depicts three large sutras.

此窟绘有代表莫高窟晚唐时期最高艺术水平的一些壁画，主要包括17幅绘制精美的佛教经变画。
The cave contains some of the highest quality painting of the Late Tang dynasty at Mogao, significant for their refined representation of seventeen Buddhist sutras.

释迦牟尼佛坐于带有装饰的佛座上，大弟子迦叶和小弟子阿难分立左右。
The Sakyamuni Buddha sits on a decorated pedestal with a standing figure of Kasyapa (older disciple) to his left and Ananda (younger disciple) to his right.

绘画材料与技术

Painting Materials and Technique

莫高窟开凿于由松散砂砾岩层的崖壁上，壁画的制作工艺为:用粘土、细砂和植物纤维的混合物做为壁画地仗，涂抹于开凿石窟的四壁和窟顶，使壁面平整便于作画，之后在地仗层上敷以薄底色层；在底色层上以红黑线条勾勒出线描草图，用天然矿物颜料和有机颜料在壁面上作画，有时会有多层壁画。

The cave temples of Mogao were hewn in the cliff face of soft conglomerate rock. The rock cut walls and ceilings were then plastered and smoothed over with a mixture of clay, sand and plant fiber. The paintings were initially drawn out as line drawings in black and red ink on a thin ground layer which covered the earthen plaster; the line drawings were then filled in with washes of natural mineral pigments and organic colorants, sometimes applied in multiple layers.

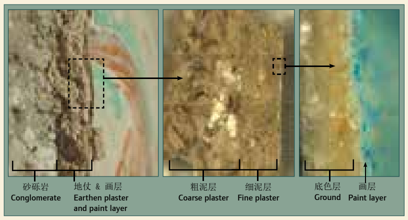

第85窟壁画结构剖面。
Cross-section of painted plaster in Cave 85.

第85窟的壁画出现很多唐代日常生活的方方面面，比如在主室东披上的肉铺。
The paintings of Cave 85 show many aspects of daily life in the Tang period such as this butcher shop on the east slope of the main chamber.

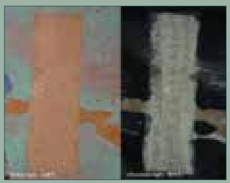

第85窟内有数以千计的榜题引导修行者观看每个叙事场面。
There are hundreds of cartouches throughout the cave containing sutra texts to guide the practitioner through each narrative.

第85窟的壁画可称为唐代的图画百科全书，内容包括服装、武器、工具、交通、乐器以及建筑等方面的信息。
The paintings comprise what has been termed a pictorial encyclopedia of the Tang era including information on costumes, weapons, tools, transportation, architecture, and musical instruments.

莫高窟壁画层位。
The layers of the Mogao wall painting.

塑像的制作使用了与制作壁画地仗层相同的方法，即在以芦苇包裹的木头骨架上涂抹泥层，塑造成型，然后再加以绘画（图示例子不是第85窟的）。
Sculpture was created using the same plaster as the wall paintings on an armature of wooden sticks and bundled reeds, modeled and then painted (example shown is not from Cave 85).

Image credit: From the exhibition catalog Trésors des grottes de Dunhuang: Mille ans d'art bouddhique IVème-XVème siècles
(Exposition organisée par le Centre culturel de Chine à Paris en collaboration avec le Musée national des Arts asiatiques Guimet)
du 18 novembre 2009 au 28 février 2009

病害状况与成因

Condition and Causes of Deterioration

壁画病害包括盐害、起甲、地仗层与砂砾岩层之间失去粘结力后造成的空鼓脱落等。后者为最严重的病害。在85窟发现大量的壁画空鼓有脱落的危险。最近一次壁画脱落发生在1996年，有一大片壁画从主室西披脱落。

The paintings suffered from salt deterioration, flaking, and loss of adhesion between the conglomerate rock and the earthen plaster. The latter problem was the most serious, as substantial areas of the painted plaster were found to be detached and susceptible to collapse. Most recently, a large piece of painted plaster fell from the west slope in 1996.

85窟后部区域盐害造成颜料层的点状脱落。
Salt deterioration is the cause of the small point-like losses in the paint layer in areas toward the back of the cave.

颜料层起甲与酥碱起甲。
Flaking and exfoliation of the paint layer.

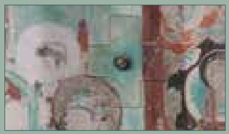

20世纪70年代，为防止壁画脱落进行了壁画锚固。上图显示仍然保留在主室北壁的锚固与垫板。
Anchors and bolts were inserted into the walls in the 1970's to secure areas of detachment. The anchor shown above was left in place on the north wall of the main chamber.

锚固只是用来对付壁画仍然继续脱落的一个权宜之计。1996年的残片脱落是在一段时间的高湿度之后发生的。
The anchors were only a temporary solution as areas of painted plaster continued to be lost. These fragments fell in 1996 after a period of high humidity.

主室窟顶壁画脱落发生在1996年的区域。
This area of collapse of painted plaster occurred on the ceiling of the main chamber in 1996.

病害调查与诊断

Investigation and Diagnosis

对以前壁画处理与状况的记录和历史照片进行了研究。病害趋势显示，此窟壁画病害自东向西加重，洞窟后部（西部）的病害最严重。合作组对壁画的病害成因、病害机理以及劣化速度进行了调查与诊断。

Study of historic photographs, recording of previous treatment and condition were undertaken. Patterns of deterioration showed an east-west distribution with condition worsening toward the rear (west end) of the cave. The causes, activation mechanisms, and rates of deterioration of the wall paintings were then investigated and diagnosed.

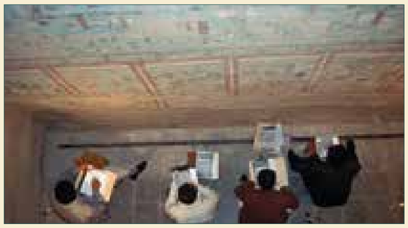

项目开始时进行的状况调查记录。
Condition recording was undertaken at the start of the project.

莫高窟在被废弃后的数百年里，洞窟一直暴露在外，崖面风化、风沙和水的侵蚀是壁画和塑像产生病害的主要原因。
The cave was open to the exterior for many centuries after the abandonment of the site. Erosion of the cliff face, windblown sand and water were responsible for much of the deterioration of the cave wall paintings and sculpture.

壁画大量脱落是由于四壁下部遭到湿气侵入及上层地仗层的坍塌。
The paintings have suffered large losses at the base of all walls from moisture ingress and collapse of upper areas of plaster.

85窟病害分布3维模型显示了85窟的病害模式。壁画脱落区域（黄色）集中于四壁下部和后部，窟顶角落；壁画空鼓区域（红色）在整窟都有发现，但主要集中于石窟后部。
A 3D cave model shows patterns of deterioration found throughout the cave. Areas of loss of painted plaster (yellow) were concentrated at the base of walls and toward the rear, upper corners of the cave; areas of detachment (red) were found throughout but were also concentrated toward the back of the cave.

图解形式显示85窟以前的处理与状况。图例是西壁病害状况图。蓝色阴影部分为脱落区域，红色部分为大面积地仗层空鼓。
Records of previous treatment and condition were graphically displayed. This example of the west wall shows areas of loss (blue hatching) and large areas of plaster detachment (red).

病害成因

Causes of Deterioration

过去洞窟内病害的原因有立即性的与逐渐性的：湿气侵入四壁下部导致原来材料发生物理化学性变化以及盐份的活动导致病害发生。我们可以减低大部分的病害原因，但是无法移除壁画中的所有盐份。因此，了解盐害发生的过程，制订预防性与保护性的措施，是降低病害发展速度的基本手段。

Past causes of deterioration in the cave have been both immediate and gradual: moisture ingress at the base of walls, physicochemical changes of the original materials, and deterioration caused by salts. We can reduce most of these causes, however, we cannot remove all of the salts present in the painted plaster. Therefore, understanding the processes of salt deterioration was the basis for developing conservation and preventive measures to slow the rate of deterioration.

壁画层的剖面图（左上）和高倍放大的氯化钠（普通食盐）的晶体推挤颜料层（右上）。盐是大部分病害的主要原因，诸如造成颜料层脱落、地仗层酥碱以及壁画空鼓等。
A cross-section of painted plaster (above, left) and a highly magnified image of NaCl (ordinary table salt) crystals pushing through the paint layer (above, right). Salt is responsible for much of the deterioration such as loss of the paint layer, disruption of the plaster, as well as contributing to detachment of the painted plaster.

保护

Conservation

以前，莫高窟的保护操作专注于实际的修复，较少注意壁画病害的成因。结果，20世纪70年代已经治理过的一些病害，如起甲和地仗层空鼓有复发的现象并导致了进一步的劣化与脱落。

因此，对保护材料与病害治理的研究及测试成为本保护项目的主要内容。

In the past, conservation practice focused on repair rather than addressing the causes of deterioration. Consequently, some conditions such as flaking and plaster detachment of the wall paintings—both previously treated in the 1970s—recurred causing progressive deterioration and loss.

As a result, research and testing of appropriate conservation materials and treatments became a large part of the project.

在病害治理前仔细检查每个区域。
Each area was carefully examined before treatment.

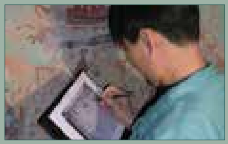

所有的区域在治理前后都有记录并且建立档案。
All areas were documented before and after treatment.

用注射器将浓度1-2%的明胶溶液注入起甲的壁画层，使之重新粘结。
Flaking paint was readhered with a 1-2% gelatin solution injected with a syringe.

使用木质工具（图示）或丝绸包裹的软球体轻柔地将起甲的壁画压回原位。
The paint flakes were then gently pressed back into place using a wooden tool (shown) or a soft silk covered ball.

正在主室东壁进行保护工作。
Conservation work in progress on the east wall of the main chamber.

研究与测试
Research and Testing

根据所了解的病害成因和机理，遵循最小干预、相容性和可再处理的原则，对85窟进行了保护干预 。选择与配置保护材料并且对其进行严格的测试，以评估其性能。

Conservation interventions followed the principles of minimal intervention, compatibility, and retreatability and were based on knowledge of the causes and mechanisms of deterioration. Treatment materials were selected and formulated and then rigorously tested to evaluate their performance.

在筛选出加固壁画层的灌浆材料之前在实验室内对 80 多种不同配比的灌浆材料进行测试。
More than 80 different grout mixtures were tested in the laboratory before a material was selected to reattach areas of painted plaster.

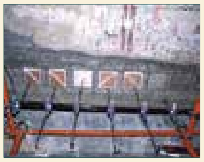

在第85窟内四壁下部的砂砾岩层（没有颜料层的区域）上粘结新的模拟地仗试块进行灌浆材料试验。
Testing of grout mixtures was undertaken in Cave 85 at the base of walls (in unpainted areas) by adhering modern plaster panels to the conglomerate.

第85窟筛选出来的灌浆材料包括本地清洗过的粘土、玻璃微珠(Scotchlite K1®)、碾碎过的浮石、搅拌好的蛋清和蒸馏水。
The adhesive grout formulated for Cave 85 included local washed clay, glass microspheres (Scotchlite K1®), crushed pumice, whipped egg white and distilled water.

对整窟大面积的壁画层进行了灌浆处理。
Large areas of painted plaster were injected with the grout mixture throughout the cave.

使用注射器和导管在壁画层后进行灌浆处理。
Injection of the grout mixture behind the painted plaster was done using syringes and catheter tubes.

在灌浆之后，立即用有吸水能力的顶板顶住壁画一直到灌浆材料干燥为止。这一关键步骤减低了含水灌浆材料所造成的可溶盐运移并且避免盐分在壁画表面结晶。
Immediately after grouting an absorbent press was applied and kept in place as the grout dried. This key step reduced soluble salts mobilized by water in the grout which would crystallize on the surface of the wall painting.

实施保护措施
Treatment Implementation

第85窟的主要治理措施包括灌浆：用灌浆材料重新粘合已经与砂砾岩层分离的壁画地仗层，并且使用一种明胶溶液加固起甲的颜料层。改进壁画保护所用的材料与工艺是本项目的一个主要目标。

Principal remedial treatments in Cave 85 included grouting—the reattachment of separated plaster from the rock conglomerate with an adhesive grout—and fixing of flaking paint with a gelatin solution. Improving the techniques and materials for conserving wall paintings on earthen plasters was a major aim of the project.

治理后的窟顶西披。没有对脱落的区域重绘，最小限度地添加新的地仗泥层，以避免人为增加水分 （来自潮湿的地仗层），因为水分会造成可溶盐在壁画层内运移。保留了早期保护工作中对地仗层的修复区域以及近年来因壁画脱落使砾岩裸露的区域（如1996年脱落的区域）。
The west ceiling slope after conservation treatment. Areas of loss were not repainted and new plastering was kept to a minimum in order to avoid the addition of water (from the wet plaster) which could redistribute soluble salts within the painted plaster. Instead, plaster repairs from earlier conservation work were left in place and recent areas of loss (such as the area of collapse from 1996) were left unfilled with the conglomerate exposed.

第85窟的保存

Preserving Cave 85

由于无法完全消除一些引起病害的因素，因此对壁画进行加固时，还必须采取其他的措施减缓病害的发生。如果不采取这些措施，保护处理最终将会失效，壁画也将继续劣化。

在第85窟，病害的主要因素是可溶盐。它仍然存在于壁画中，而控制窟内的湿度就可以减缓盐害对壁画的影响。

As it is not possible to eliminate some causes of deterioration, efforts to slow decay are needed in addition to stabilization treatments. Without such measures treatments will eventually fail and the paintings will continue to deteriorate.

In the case of Cave 85, the principal cause of deterioration—soluble salts—is still present and mitigation of their effects is based on control of humidity in the cave.

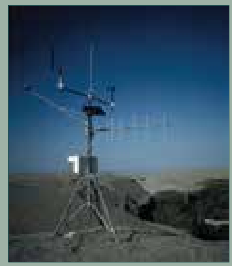

莫高窟崖顶设置有全自动气象站可监测降雨强度与雨量、空气温度、相对湿度、风速和风向等气象因子。
A weather station at the top of the cliff measures rainfall intensity and amount, air temperature, relative humidity, and wind speed and direction.

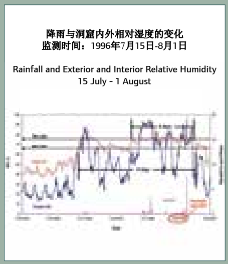

1996年在一段时期的降雨后，第85窟窟顶壁画脱落（图上底部的粉红色线条显示了降雨强度）。降雨对相对湿度的影响很大。比较一段时期的降雨前后相对湿度的变化。
Collapse of painted plaster from the ceiling in 1996 followed a period of rainfall (pink lines at base of graph indicate rainfall intensity). The effect of rain on the relative humidity (RH) is dramatic. Compare the RH before and after the major period of rain.

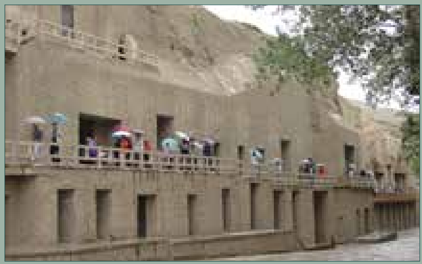

尽管莫高窟处于沙漠的环境中，当地还是会降雨。降雨虽然罕见，还是会使窟内相对湿度升高至危险的阶段。相对湿度的突然升高会激活盐分，引发壁画病害。
Despite the desert setting it does rain at the site. These rain events, though rare, can cause the relative humidity to rise to dangerous levels inside the caves. The rise in relative humidity can activate salts leading to deterioration of the wall paintings.

预防措施

Preventive Measures

环境控制措施可以有效地减缓与盐分有关的病害发生。特别是在降雨期间，关闭洞窟的门可以减低窟内外空气的交换率，从而保持窟内湿度的稳定。

Environmental control measures are effective in slowing salt-related deterioration. Keeping the door to the cave closed reduces air exchange between the interior and the outside climate, thus maintaining stable humidity conditions in the cave, particularly during periods of rain.

第85 窟入口。
The entrance door to Cave 85.

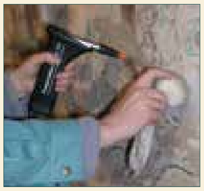

鉴于泥质地仗的脆弱状况和壁画对水的高度敏感，降低可溶盐只能限于局部选定的区域。使用超声波加湿器配合吸水棉纸可以用来吸收表面及表面下的盐分。
Reduction of soluble salts was limited to select areas given the fragile condition of the earthen plaster and the water sensitive painting. An ultrasonic humidifier was used with absorbent tissue to absorb surface and subsurface salts.

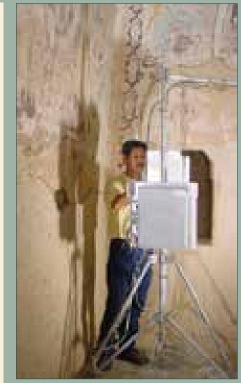

在第85窟内部也监测温度和相对湿度。相对湿度高于67%时，壁画中的盐分就会从空气中吸收水分，因此将窟内相对湿度保持在该数值以下是保存洞窟的关键。
Monitoring of temperature and relative humidity was also undertaken inside the cave. Above 67% relative humidity salts absorb moisture from the air. Keeping the humidity below this value is key to preserving the cave.

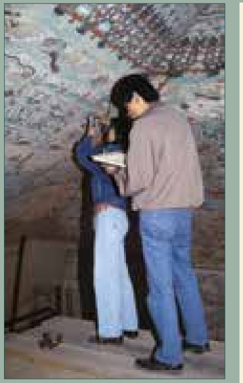

定期下载洞窟内不同位置监测探头所收集的数据。
Data was regularly downloaded from monitoring probes at various locations throughout the cave.

现状监测

Condition Monitoring

在完成第85窟的保护工作之后，进行定期监测壁画状况。因为引起病害的因素不能完全消除，现状监测就显得非常重要。

Following completion of conservation treatments in the cave, the condition of the wall painting is regularly inspected. Condition monitoring is important because the causes of deterioration cannot be completely eliminated.

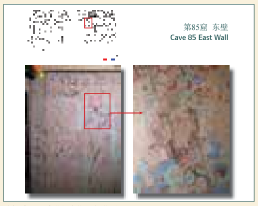

选择壁画区域进行定期现状监测。
Areas of the wall painting were selected for regular monitoring of condition.

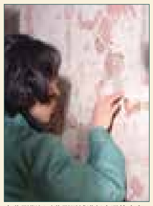

在监测期间对监测区域进行肉眼检查和拍照。
Areas are checked and photographed during these periods of monitoring.

About the Editors

Lori Wong is a wall painting conservator and project specialist at the Getty Conservation Institute. Neville Agnew, senior principal project specialist at the GCI, is the coauthor of *Cave Temples of Mogao: Art and History on the Silk Road*, and the editor of *Conservation of Ancient Sites on the Silk Road: Proceedings of the First International Conference on the Conservation of Grotto Sites* (1997), and *Conservation of Ancient Sites on the Silk Road: Proceedings of the Second International Conference on the Conservation of Grotto Sites* (2010).

Illustration Credits

© Bibliothèque nationale de France: Figs. 8.6, 8.7, 13.26

© The British Library Board. Photo 392/27(589): Fig. 5.9

© The British Library Board. Photo 392/56 (86): Fig. 10.2

© The British Library Board. Photo 392/56 ((689): Fig. 9.3

© The British Library Board. Photo 393/26 (327): Fig. 5.8

© The British Library Board. Photo: Or. 8210/P.2: Fig. 13.22a

© The Trustees of the British Museum: Figs. 13.51a, 13.51b, 13.52a, 13.52b

Lois Connor: frontispiece, Fig. 1.2

Courtesy of the Dunhuang Academy: Figs. 1.3a, 1.3b, 1.4, 5.4, 6.6, 6.7, 6.10, 8.1, 8.2, 8.3, 8.5, 8.12, 8.13, 8.14, 8.15, 8.16, 8.17, 8.19, 8.20, 8.24, 9.2, 9.6b, 9.7b, 9.8, 9.10, 9.14, 9.16, 9.17, 9.18, 9.19, 9.20, 9.22, 9.24, 9.26, 9.27, 9.28b, 9.30, 11.2, 13.23, 13.27a, 13.50, 15.3, 16.24, back cover

Elevation, Cave 85, from Sarah E. Fraser, *Performing the Visual: The Practice of Buddhist Wall Painting* (Stanford, 2004), p. 237: Fig. 8.23

The Lo Archive: Figs. 9.13, 9.23a, 9.28a

Courtesy Musée national des arts asiatiques Guimet: Figs. 9.1b, 9.1c

From Zhongguo dizhen redu quhuatu, Diyiban [China seismic intensity zoning map, First Series] 中国地震烈度区划图 (1956) 第一版, Beijing, National Earthquake Bureau: Fig. 15.4

The Needham Research Institute: Fig. 12.18b

© RMN-Grand Palais/Art Resource, New York: Figs. 9.1a, 9.7a

Copy photo: Thierry Ollivier. Musée des Arts Asiatiques-Guimet, Paris, France. © RMN-Grand Palais/Art Resource, New York: Fig. 9.4

© Richard Ross: Front cover, p. xiii, Fig. 8.30

The State Hermitage Museum, St. Petersburg: Figs. 9.5, 9.11, 9.12, 12.18a

By permission of University of Chicago Press: 9.6a, 9.9, 9.15

USGS Landsat: Figs. 5.3, 6.1

THE GETTY CONSERVATION INSTITUTE

The Mogao Grottoes, a World Heritage Site near the town of Dunhuang in northwestern China, are located on the edge of the Gobi Desert, along the ancient caravan routes—collectively known as the Silk Road—that once linked China with the West. Founded by a Buddhist monk in the late fourth century, Mogao flourished over the following millennium, as monks, local rulers, and travelers commissioned hundreds of cave temples in a mile-long rock cliff, and adorned them with vibrant murals portraying scenes from Buddhist scripture, portraits of local rulers, and richly detailed scenes of everyday life. Today there remain 492 decorated grottoes, which contain thousands of sculptures and some 45,000 square meters of wall painting, making Mogao one of the world's most significant sites of Buddhist art.

Over the centuries these beautiful artworks have suffered deterioration of many kinds, from floods and earthquakes to flaking of the paint layer and the collapse of wall paintings. In 1997 the Getty Conservation Institute, which had been working with the Dunhuang Academy at Mogao since 1989, began a case study, in collaboration with the DA, using the large, Late Tang dynasty Cave 85 in an initiative to develop a conservation methodology that would solve a number of hitherto intractable problems in the conservation treatment of earthen-based wall paintings, which are ubiquitous at similar sites in China and Central Asia. This abundantly illustrated volume is the definitive report on this signature project, which was completed in 2010.

Getty Publications
(800) 223-3431
www.getty.edu/publications

ISBN 978-1-60606-157-2
90000
9 781606 061572

Printed in the U.S.A.